

## ENCLOSURE 3

NEDO-33869 Revision11  
September 2022

Non-Proprietary Information – Class I (Public)



Global Nuclear Fuel

NEDO-33869  
Revision 11  
September 2022

*Non-Proprietary Information*

## **RAJ-II Safety Analysis Report**

*Copyright 2022 Global Nuclear Fuel - Americas, LLC  
All Rights Reserved*



## **INFORMATION NOTICE**

This is a non-proprietary version of the document NEDE-33869P, Revision 11, which has the proprietary information removed. Portions of the document that have been removed are indicated by open and closed brackets as shown here [[        ]].

## **IMPORTANT NOTICE REGARDING CONTENTS OF THIS REPORT PLEASE READ CAREFULLY**

The information contained in this document is furnished for the purpose of obtaining NRC approval of the RAJ-II radioactive material transport package. The use of this information by anyone other than that for which it is intended is not authorized.

NEDO-33869 Revision 11  
Non-Proprietary Information

### Revision Summary

Revision	Description
0	Initial Issue
7.1	Revised to incorporate administrative updates to align the SAR to the current Certificate of Compliance, provide clarifications, and correct minor errors.
8	Withdrawn
9	Modified to reflect changes to the GNF 10x10 fuel.
10	Revised to incorporate changes in response to Revision 9 requests for additional information 1.0 and 7.0.
11	Revision affecting all chapters to provide safety analysis results for LEU+ (Low-Enriched Uranium (=8 wt% U-235))

## Revision 11 Detailed Revision Summary

Location	Description of Change
<b>Chapter 1</b>	
Chapter 1	Incorporation of new 8.0 wt% U-235 contents throughout chapter.
Table 1-3 Section 1.2.2.1	Incorporation of new 8.0 wt% U-235 contents.
Section 1.1 Section 1.2.2.4.1 Section 1.2.2.4.2	Incorporation of 8.0 wt% U-235 contents CSI values.
Section 1.2.1	Incorporation of aluminum honeycomb material throughout section.
Section 1.2.2.7	Incorporation of 8.0 wt% U-235 maximum decay heat.
Appendix 1.3	Incorporation of latest drawing revisions.
<b>Chapter 2</b>	
Chapter 2	Administrative and grammatical updates throughout chapter.
Section 2.1 Section 2.2 Table 2-3 Section 2.12.2.2	Incorporated aluminum as possible honeycomb construction material.
Section 2.1.2.4.3 Section 2.3.2 Section 2.7.1	Removed paper description of honeycomb.
Section 2.1.4	Included 8.0 wt% U-235 LEU+ fuel content.
Section 2.7.1.3 Section 2.12.2.3 Section 2.12.3.2 Table 2-12 Table 2-13 Figure 2-44 Figure 2-45 Figure 2-46 Figure 2-47	Corrected GNF-J corner drop test orientation description.
<b>Chapter 3</b>	
Chapter 3	Administrative and grammatical updates throughout chapter.
Section 3.1.1	Clarified location of alumina silicate within inner container.
Section 3.1.3	Clarified NCT inner container maximum temperatures. Clarified temperatures are based on analysis with paper honeycomb material.
Figure 3-1	Removed paper description of honeycomb.
Section 3.2.1	Incorporated aluminum as possible honeycomb construction material.
Section 3.3	Clarified the maximum NCT temperature of the inner container is the starting point for the HAC.
Table 3-5 Table 3-6	Updated table titles to clarify data is based on analysis with paper honeycomb material.

NEDO-33869 Revision 11  
Non-Proprietary Information

Location	Description of Change
Table 3-8	
Section 3.5.3	Added statement about aluminum honeycomb material for the analysis. Clarified the maximum temperature within the inner container during NCT.
Table 3-8	Corrected column header to clarify T thru IC Outer Shell.

Chapter 4	
Chapter 4	Administrative and grammatical updates throughout chapter. Incorporation of new 8.00 wt% U-235 enriched contents throughout chapter.
Table 4-2 Table 4-3 Table 4-5	Updated tables to incorporate 8.00 wt% U-235 contents.  Added new Table 4-5
Section 4.5.1.1 Section 4.5.1.2 Section 4.5.1.3 Section 4.5.1.4	Incorporated calculation of 8.00 wt% U-235 contents.
Chapter 5	
Chapter 5	Administrative updates throughout chapter. Incorporation of new 8.00 wt% U-235 enriched contents throughout chapter.
Table 5-1	Updated per LEU+ analysis Added “* Transport index may not exceed 10.”
Section 5.2.1	2 <sup>nd</sup> paragraph changed “3.73E+10” to “3.89E+10” per LEU+ analysis Updated Reference
Table 5-2	Updated per LEU+ analysis
Section 5.2.2	1 <sup>st</sup> paragraph - Changed “9.94E+03,” “5.74E+03,” and “4.20E+03” to “9.77E+03,” “5.56E+03,” and “4.21E+03,” respectively per LEU+ analysis 2 <sup>nd</sup> paragraph - Changed “0.7095” to “less than 0.95” 3 <sup>rd</sup> paragraph - Changed “1.99E+05” to “1.95E+05”
Section 5.4.4	Changed “93%” to “92%” and added “with the limiting result being one meter from the top of the package surface under NCT” in the last sentence.
Reference 5-1	Changed “C996-15” to “C996-20” (latest revision)
Chapter 6	
Section 6.1	Addition of definitions of LEU and LEU+.Addition of general description of Ch. 6 Revision 11 change methodology.
Table 6-1	Addition of LEU+ CSI designations and new LEU+ gadolinia rod requirements.
Table 6-2	Formatting changes and GNF 10x10 enrichment update.
Table 6-3	Addition of Fuel Assembly and Fuel Rod Package NCT and HAC results.
Section 6.1.3	Addition of CSI information for LEU+.
Section 6.2	Addition of LEU+ isotopics.

NEDO-33869 Revision 11  
Non-Proprietary Information

Section 6.3.1.1 Section 6.3.4.8 Section 6.3.4.11 Section 6.6.1	Addition of LEU+ PCF Thickness.
Section 6.3.1.1.2	Rewording of LEU enrichment and gadolinia description. Addition of LEU+ enrichment and gadolinia description.
Section 6.3.1.2.2	Addition of LEU+ HAC array size.
Section 6.3.1.3	Addition of LEU+ enrichment.
Section 6.3.1.3.4	Updated the worst case fuel rod to include LEU+.
Table 6-8	Addition of LEU+ UO <sub>2</sub> and UO <sub>2</sub> -Gd <sub>2</sub> O <sub>3</sub> atomic densities.
Section 6.3.3	Addition of a description of which standard composition is used to model the polyethylene in the RAJ-II KENO files. This is included to resolve concerns regarding a SCALE User notice regarding h-poly.
Section 6.3.4	Addition of a brief description of the intent of Revision 11. Addition of an assurance statement that scoping calculations were performed to support the justifications and information in Revision 11.
Figure 6-25	Addition of the gadolinia-uranium fuel rod loading for 13 – 22 gadolinia rods.
Section 6.3.4.8	Addition of fuel channel conclusion, see SAR Section 6.6.2.
Section 6.4 Section 6.5 Section 6.6	Addition of LEU+ enrichment and gadolinia description.
Section 6.6.2	Addition to the HAC Channel Sensitivity study conclusion and the addition of Table 6-23
Section 6.7.1	Reiteration that criticality studies have been repeated for LEU+ loose fuel rods. Addition of LEU+ peak reactivity moderator density. Rephrased the specific rod pitch value to ‘constant’ to encompass differences in limiting pitch and emphasize the difference between the two studies. Addition of USL for LEU+ fuel.
Table 6-24 Table 6-25	Addition of LEU+ results.
Section 6.7.3	Addition of details on transporting LEU+ loose rods in a stainless steel pipe.
Section 6.7.5 Section 6.7.6 Section 6.7.7	Reiteration that GNF 10x10 LEU+ is considered a limiting design, along with GNF 8x8.
Section 6.9	Addition of LEU+ HAC package array size.
<b>Chapter 7</b>	
	No changes to Chapter 7 except header revision number
<b>Chapter 8</b>	
Section 8.2.5	Removed paper description of honeycomb.

## Table of Contents

	<b>Page</b>
<b>1.0 General Information .....</b>	<b>1-1</b>
1.1 Introduction.....	1-1
1.2 Package Description.....	1-6
1.2.1 Packaging.....	1-6
1.2.2 Contents .....	1-10
1.2.3 Special Requirements for Plutonium .....	1-15
1.2.4 Operational Features .....	1-15
1.3 Appendix.....	1-16
1.3.1 RAJ-II General Arrangement Drawings .....	1-16
1.3.2 References.....	1-16
<b>2.0 Structural Evaluation .....</b>	<b>2-1</b>
2.1 Description of Structural Design.....	2-1
2.1.1 Discussion .....	2-1
2.1.2 Design Criteria .....	2-2
2.1.3 Weights and Centers of Gravity.....	2-4
2.1.4 Identification of Codes and Standards for Package Design.....	2-4
2.2 Materials.....	2-7
2.2.1 Material Properties and Specifications.....	2-7
2.2.2 Chemical, Galvanic, or Other Reactions.....	2-10
2.2.3 Effects of Radiation on Materials .....	2-11
2.3 Fabrication and Examination .....	2-11
2.3.1 Fabrication .....	2-11
2.3.2 Examination .....	2-11
2.4 General Requirements for All Packages .....	2-11
2.4.1 Minimum Package Size.....	2-11
2.4.2 Tamper-Indicating Feature.....	2-11
2.4.3 Positive Closure .....	2-11
2.5 Lifting and Tie-Down Standards for All Packages.....	2-12
2.5.1 Lifting Devices.....	2-13
2.5.2 Tie-Down Devices .....	2-24
2.6 Normal Conditions of Transport .....	2-34
2.6.1 Heat .....	2-35
2.6.2 Cold.....	2-38
2.6.3 Reduced External Pressure.....	2-38
2.6.4 Increased External Pressure .....	2-38
2.6.5 Vibration .....	2-38
2.6.6 Water Spray.....	2-39
2.6.7 Free Drop .....	2-39
2.6.8 Corner Drop .....	2-40
2.6.9 Compression.....	2-40
2.6.10 Penetration .....	2-43
2.7 Hypothetical Accident Conditions .....	2-44
2.7.1 Free Drop .....	2-44

2.7.2	Crush .....	2-47
2.7.3	Puncture .....	2-47
2.7.4	Thermal .....	2-48
2.7.5	Immersion – Fissile Material .....	2-49
2.7.6	Immersion – All Packages .....	2-49
2.7.7	Deep Water Immersion Test (for Type B Packages Containing More than $10^5$ A <sub>2</sub> ) .....	2-49
2.7.8	Summary of Damage.....	2-49
2.8	Accident Conditions for Air Transport of Plutonium .....	2-52
2.9	Accident Conditions for Fissile Material Packages for Air Transport.....	2-52
2.10	Special Form .....	2-52
2.11	Fuel Rods .....	2-53
2.12	Appendix.....	2-53
2.12.1	References.....	2-53
2.12.2	Certification Tests .....	2-54
2.12.3	GNF-J Certification Tests .....	2-73
2.12.4	Outer Container Gasket Sealing Capability .....	2-82
<b>3.0</b>	<b>Thermal Evaluation .....</b>	<b>3-1</b>
3.1	Description of Thermal Design.....	3-1
3.1.1	Design Features.....	3-1
3.1.2	Content's Decay Heat .....	3-2
3.1.3	Summary Tables of Temperatures .....	3-2
3.1.4	Summary Tables of Maximum Pressures .....	3-2
3.2	Material Properties and Component Specifications.....	3-4
3.2.1	Material Properties.....	3-4
3.2.2	Component Specifications .....	3-6
3.3	Thermal Evaluation Under Normal Conditions of Transport .....	3-7
3.3.1	Heat and Cold.....	3-7
3.3.2	Maximum Normal Operating Pressure .....	3-8
3.4	Thermal Evaluation Under Hypothetical Accident Conditions .....	3-8
3.4.1	Initial Conditions.....	3-9
3.4.2	Fire Test Conditions.....	3-9
3.4.3	Maximum Temperatures and Pressure.....	3-12
3.4.4	Maximum Thermal Stress.....	3-13
3.4.5	Accident Conditions for Fissile Material Packages for Air Transport .....	3-14
3.5	Appendix.....	3-19
3.5.1	References.....	3-19
3.5.2	ANSYS Input File Listing.....	3-20
3.5.3	NCT Transient Analysis.....	3-29
<b>4.0</b>	<b>Containment .....</b>	<b>4-1</b>
4.1	Description of the Containment System .....	4-1
4.2	Containment Under Normal Conditions of Transport .....	4-2
4.3	Containment Under Hypothetical Accident Conditions .....	4-3
4.4	Leakage Rate Tests for Type B Packages .....	4-4
4.5	Appendix.....	4-5

NEDO-33869 Revision 11  
Non-Proprietary Information

	4.5.1	Determination of Allowable Leak Rates.....	4-5
	4.5.2	Summary .....	4-12
	4.5.3	References .....	4-12
<b>5.0</b>	<b>Shielding Evaluation .....</b>		<b>5-1</b>
5.1	Description of the Shielding Design .....		5-1
	5.1.1	Design Features.....	5-1
	5.1.2	Summary Table of Maximum Radiation Levels.....	5-1
5.2	Source Specification.....		5-3
	5.2.1	Gamma Source .....	5-3
	5.2.2	Neutron Source .....	5-4
5.3	Shielding Model .....		5-5
	5.3.1	Configuration of Source and Shielding.....	5-5
	5.3.2	Material Properties .....	5-6
5.4	Shielding Evaluation .....		5-7
	5.4.1	Methods.....	5-7
	5.4.2	Input and Output Data.....	5-7
	5.4.3	Flux-to-Dose Rate Conversion.....	5-8
	5.4.4	External Radiation Levels .....	5-9
5.5	References .....		5-10
<b>6.0</b>	<b>Criticality Evaluation .....</b>		<b>6-1</b>
6.1	Description of Criticality Design .....		6-1
	6.1.1	Design Features.....	6-5
	6.1.2	Summary Table of Criticality Evaluation .....	6-5
	6.1.3	Criticality Safety Index .....	6-9
6.2	Fissile Material Contents .....		6-10
6.3	General Considerations .....		6-11
	6.3.1	Model Configuration.....	6-11
	6.3.2	Material Properties .....	6-32
	6.3.3	Computer Codes and Cross-Section Libraries .....	6-39
	6.3.4	Demonstration of Maximum Reactivity .....	6-37
6.4	Single Package Evaluation.....		6-96
	6.4.1	Configuration .....	6-96
	6.4.2	Results.....	6-96
6.5	Evaluation of Package Arrays Under NCT.....		6-99
	6.5.1	Configuration .....	6-99
	6.5.2	Results.....	6-99
6.6	Package Arrays Under HAC .....		6-100
	6.6.1	Configuration .....	6-100
	6.6.2	Results.....	6-100
6.7	Fuel Rod Transport in the RAJ-II .....		6-104
	6.7.1	Freely Loose Fuel Rod Study.....	6-104
	6.7.2	Fuel Rods Strapped Together.....	6-107
	6.7.3	Fuel Rods Transported in 5-Inch Stainless Steel Pipe .....	6-107
	6.7.4	Fuel Rods Transported in Stainless Steel Protective Case.....	6-110
	6.7.5	Single Package Fuel Rod Transport Evaluation.....	6-110
	6.7.6	Evaluation of Package Arrays with Fuel Rods Under NCT .....	6-113



NEDO-33869 Revision 11  
Non-Proprietary Information

6.7.7	Fuel Rod Transport Package Arrays Under HAC.....	6-115
6.8	Fissile Material Packages for Air Transport .....	6-118
6.9	Conclusion .....	6-119
6.10	Benchmark Evaluations .....	6-120
6.10.1	SCALE 4.4a and GEMER.....	6-120
6.10.2	KENO-VI .....	6-120
6.11	Appendix .....	6-126
6.11.1	Single Package NCT Input.....	6-126
6.11.2	Single Package HAC Input .....	6-130
6.11.3	Package Array NCT Input.....	6-133
6.11.4	Package Array HAC Input .....	6-137
6.11.5	Single Package Loose Rods NCT Input.....	6-134
6.11.6	Single Package Loose Fuel Rods HAC Input .....	6-137
6.11.7	Package Array Loose Fuel Rods NCT Input .....	6-146
6.11.8	Package Array Loose Fuel Rods HAC Input .....	6-149
6.11.9	Data Tables for Figures in Chapter 6 .....	6-153
6.11.10	Summary of Experiments .....	6-171
6.12	References .....	6-187
<b>7.0</b>	<b>Package Operations .....</b>	<b>7-1</b>
7.1	Package Loading .....	7-1
7.1.1	Preparation for Loading .....	7-1
7.1.2	Loading of Contents .....	7-2
7.1.3	Preparation for Transport .....	7-5
7.2	Package Unloading.....	7-5
7.2.1	Receipt of Package from Carrier.....	7-5
7.2.2	Removal of Contents.....	7-5
7.3	Preparation of Empty Package for Transport.....	7-6
7.4	Other Operations .....	7-6
7.5	Appendix .....	7-6
<b>8.0</b>	<b>Acceptance Tests and Maintenance Program .....</b>	<b>8-1</b>
8.1	Acceptance Tests.....	8-1
8.1.1	Visual Inspections and Measurements .....	8-1
8.1.2	Weld Examinations .....	8-1
8.1.3	Structural and Pressure Tests .....	8-1
8.1.4	Leakage Tests.....	8-1
8.1.5	Component and Material Tests .....	8-2
8.1.6	Shielding Tests.....	8-2
8.1.7	Thermal Tests.....	8-2
8.1.8	Miscellaneous Tests .....	8-2
8.2	Maintenance Program .....	8-3
8.2.1	Structural and Pressure Tests .....	8-3
8.2.2	Leakage Tests.....	8-3
8.2.3	Component and Material Tests .....	8-3
8.2.4	Thermal Tests.....	8-3
8.2.5	Miscellaneous Tests .....	8-3
8.3	Appendix .....	8-5

NEDO-33869 Revision 11  
Non-Proprietary Information

8.3.1	References .....	8-5
-------	------------------	-----

## List of Tables

	<b>Page</b>
Table 1-1	Weights and Outer Dimensions of the Package ..... 1-8
Table 1-2	Maximum Weight of Uranium Dioxide Pellets per Fuel Assembly ..... 1-11
Table 1-3	Maximum Concentrations ..... 1-11
Table 1-4	Example of Fuel Structural Materials ..... 1-11
Table 1-5	Density of Structural Materials ..... 1-12
Table 2-1	RAJ-II Weight ..... 2-6
Table 2-2	Representative Mechanical Properties of Series 300 Stainless Steel Components ..... 2-8
Table 2-3	Mechanical Properties of Typical Components ..... 2-9
Table 2-4	Properties of Series 300 Stainless Steel ..... 2-12
Table 2-5	Material Properties ..... 2-35
Table 2-6	Thermal Contraction at -40°C ..... 2-37
Table 2-7	Thermal Expansion at 800°C ..... 2-37
Table 2-8	Temperatures ..... 2-43
Table 2-9	Summary of Tests for RAJ-II ..... 2-50
Table 2-10	Test Unit Weights ..... 2-56
Table 2-11	Testing Summary ..... 2-58
Table 2-12	GNF-J CTU Test Series Summary ..... 2-76
Table 2-13	GNF-J CTU Test Series Results ..... 2-77
Table 3-1	Summary of Maximum Pressures ..... 3-2
Table 3-2	Material Properties for Structural / Thermal Components ..... 3-5
Table 3-3	Material Properties for Air ..... 3-6
Table 3-4	IC Structural and Packing Materials Melting Points ..... 3-7
Table 3-5	Convection Coefficients for Post-Fire Analysis ..... 3-15
Table 3-6	Calculated Temperatures for Different Positions on the Walls of the Inner Container ..... 3-15
Table 3-7	Material Properties ..... 3-31
Table 3-8	NCT Temperatures Through the Package Thickness ..... 3-32
Table 4-1	RAJ-II Content Radionuclide Maximum Concentrations ..... 4-5
Table 4-2	RAJ-II Content Radionuclide A <sub>2</sub> , Specific Activity, Mass, and Activity ..... 4-6
Table 4-3	A <sub>2</sub> Effective for RAJ-II Content Mixture ..... 4-7
Table 5-1	Summary Table of External Radiation Levels ..... 5-2
Table 5-2	Gamma Source Terms ..... 5-4
Table 5-3	Shielding Model Input Parameters ..... 5-7
Table 5-4	Gamma Flux-to-Dose Rate Conversion Factors (ANSI/ANS-6.1.1 1977) ..... 5-8
Table 5-5	Neutron Flux-to-Dose Rate Conversion Factors (ANSI/ANS-6.1.1 1977) ..... 5-9
Table 6-1	RAJ-II Fuel Assembly Loading Criteria ..... 6-2
Table 6-2	RAJ-II Fuel Rod Loading Criteria ..... 6-4
Table 6-3	Criticality Evaluation Summary ..... 6-6

NEDO-33869 Revision 11  
Non-Proprietary Information

Table 6-4	Nominal vs. Worst Case Fuel Parameters for the RAJ-II Criticality Analysis.....	6-7
Table 6-5	Uranium Isotopic Distribution .....	6-9
Table 6-6	RAJ-II Fuel Rod Transport Model Fuel Parameters .....	6-25
Table 6-7	Dimensional Tolerances.....	6-31
Table 6-8	Material Specifications for the RAJ-II.....	6-32
Table 6-9	RAJ-II NCT Model Fuel Parameters .....	6-34
Table 6-10	RAJ-II NCT Model Fuel Parameters for Determining the Polyethylene Wrap Dimensions.....	6-34
Table 6-11	Fuel Assembly Parameters for Polyethylene Mass Calculations.....	6-37
Table 6-12	Polyethylene Mass and Volume Fraction Calculations .....	6-37
Table 6-13	RAJ-II Array HAC Fuel Assembly Orientation .....	6-41
Table 6-14	RAJ-II Shipping Container 14x2x16 Array with Gadolinia-Urania Fuel Rods .....	6-47
Table 6-15	RAJ-II Sensitivity Analysis for Channeled Fuel Assemblies .....	6-51
Table 6-16	RAJ-II Array HAC Worst Case Parameter Fuel Designs .....	6-58
Table 6-17	RAJ-II Array HAC Part Length Fuel Rod Calculations .....	6-76
Table 6-18	Relative Reactivity of Fuel Designs with As-Built Part Length Rod Locations.....	6-80
Table 6-19	RAJ-II Inner Container Thermal Insulator Region and Polyethylene Foam Material Study.....	6-86
Table 6-20	RAJ-II Inner Container Partially Filled with Moderator.....	6-88
Table 6-21	RAJ-II Array Spacing Sensitivity Study .....	6-90
Table 6-22	HAC Channel Sensitivity (10x1x10) .....	6-98
Table 6-23	HAC Channel Sensitivity (8x1x8) .....	6-99
Table 6-24	BWR UO <sub>2</sub> Fuel Rod Pitch Sensitivity Study Results .....	6-101
Table 6-25	BWR UO <sub>2</sub> Fuel Rod Maximum Quantity at Reduced Moderator Densities.....	6-102
Table 6-26	Results for 8x1x8 HAC Array of Containers with Fuel Rods in Stainless Steel Pipe .....	6-113
Table 6-27	AOA – LEU Heterogeneous Systems with Gadolinia .....	6-118
Table 6-28	Data for Figure 6-29 RAJ-II Array HAC Polyethylene Sensitivity .....	6-147
Table 6-29	Data for Figure 6-30 RAJ-II Fuel Rod Pitch Sensitivity Study .....	6-149
Table 6-30	Data for Figure 6-31 RAJ-II Array HAC Pellet Diameter Sensitivity Study .....	6-150
Table 6-31	Data for Figure 6-32 RAJ-II Array HAC Fuel Rod Clad ID Sensitivity Study .....	6-151
Table 6-32	Data for Figure 6-33 RAJ-II Array HAC Fuel Rod Clad OD Sensitivity Study .....	6-152
Table 6-33	Data for Figure 6-41 Moderator Density Sensitivity Study for the RAJ-II HAC Worst Case Parameter Fuel Design .....	6-153
Table 6-34	Data for Figure 6-44 RAJ-II Single Package NCT Results .....	6-154
Table 6-35	Data for Figure 6-45 RAJ-II Single Package HAC Results .....	6-155
Table 6-36	Data for Figure 6-46 RAJ-II Package Array Under NCT Results .....	6-156
Table 6-37	Data for Figure 6-47 RAJ-II Package Array HAC Results, Inner Container Moderation Study .....	6-157

NEDO-33869 Revision 11  
Non-Proprietary Information

Table 6-38	Data for Figure 6-48 RAJ-II Package Array HAC Results, Outer Container Moderation Study .....	6-158
Table 6-39	Data for Figure 6-51 RAJ-II BWR UO <sub>2</sub> Fuel Rod Transport in Stainless Steel Pipe .....	6-159
Table 6-40	Data for Figure 6-52 RAJ-II BWR UO <sub>2</sub> Fuel Rod Single Package Under NCT .....	6-160
Table 6-41	Data for Figure 6-53 RAJ-II BWR UO <sub>2</sub> Fuel Rod Transport Single Package HAC .....	6-161
Table 6-42	Data for Figure 6-55 RAJ-II Package Array Under NCT with BWR UO <sub>2</sub> Loose Fuel Rods .....	6-162
Table 6-43	Data for Figure 6-57 RAJ-II BWR UO <sub>2</sub> Fuel Rod Transport Under HAC .....	6-163
Table 6-44	Summary of Information for Experiment .....	6-165
Table 6-45	Parameters for Benchmark Cases for SCALE 4.4a 44 Group Cross-Section Set.....	6-166
Table 6-46	Parameters for Benchmark Cases for SCALE 4.4a 238 Group Cross-Section Set.....	6-167
Table 6-47	Urania Gadolinia Experiment Summary .....	6-168
Table 6-48	Experimental Parameters for Calculating U-235 and H Atom Densities .....	6-169
Table 6-49	Urania Gadolinia Critical Experiment Trending Data .....	6-170
Table 6-50	Urania Gadolinia Benchmark $k_{eff}$ Data .....	6-171
Table 6-51	Close Proximity Experiment Summary .....	6-172
Table 6-52	Close Proximity Experiment Trending Data.....	6-173
Table 6-53	Close Proximity Experiment $k_{eff}$ Data .....	6-174
Table 6-54	Tightly Packed Configuration Experiment Summary.....	6-175
Table 6-55	Tightly Packed Configuration Experiment Trending Data .....	6-176
Table 6-56	Tightly Packed Configuration Experiment $k_{eff}$ Data.....	6-177
Table 6-57	Reduced Density Moderation Experiments Summary and Trending Parameters .....	6-178
Table 6-58	Reduced Density Moderation Experiments Trending Data and $k_{eff}$ Data .....	6-179
Table 7-1	Recommended Packaging Component Torques .....	7-1

## List of Figures

	<b>Page</b>
Figure 1-1	RAJ-II Package Assembly ..... 1-2
Figure 1-2	Cross-Section of Inner Container..... 1-3
Figure 1-3	Inner Container..... 1-4
Figure 1-4	Inner and Outer Container..... 1-5
Figure 1-5	Shock Absorber Geometry ..... 1-7
Figure 1-6	Example Fuel Rod (Primary Containment)..... 1-9
Figure 1-7	Fuel Assembly with Optional Packing Materials..... 1-13
Figure 2-1	Center of Gravity of Package Components..... 2-7
Figure 2-2	Inner Container Sling Locations ..... 2-29
Figure 2-3	Sling Attachment Plate Details ..... 2-30
Figure 2-4	Lifting Configuration of Inner Container..... 2-30
Figure 2-5	Center of Gravity of Loaded Inner Container ..... 2-31
Figure 2-6	Hooking Bar of Sling Fitting ..... 2-31
Figure 2-7	Perforated Plate of Sling Fitting..... 2-32
Figure 2-8	Sling Fitting Weld Geometry for Attachment to Support Plate..... 2-32
Figure 2-9	Loads on Sling Fitting..... 2-33
Figure 2-10	Welds for Support Plate Attachment to Body..... 2-33
Figure 2-11	Tie-Down Configuration..... 2-34
Figure 2-12	Vibrational Test Experimental Set-Up..... 2-39
Figure 2-13	Stacking Arrangement..... 2-44
Figure 2-14	Slap-Down Orientation ..... 2-51
Figure 2-15	Puncture Pin Orientation..... 2-51
Figure 2-16	End Drop 90° Orientation ..... 2-52
Figure 2-17	Inner Container Being Prepared to Receive Mockup Fuel and Added Weight..... 2-59
Figure 2-18	Partial Fuel Assemblies in CTU 1..... 2-60
Figure 2-19	Top End Fittings on Fuel in CTU 1 ..... 2-60
Figure 2-20	Contents of CTU 2 ..... 2-61
Figure 2-21	Outer Container without Inner Container ..... 2-61
Figure 2-22	Inner Container Secured in Outer Container..... 2-62
Figure 2-23	CTU 2 Prior to Testing..... 2-62
Figure 2-24	Addition of Tare Weight to CTU 1 ..... 2-63
Figure 2-25	Addition of Tare Weight to CTU 2 ..... 2-63
Figure 2-26	CTU 1 Positioned for 15° 9 m (30 ft) Slap-Down Drop..... 2-64
Figure 2-27	Alignment for Oblique Puncture..... 2-64
Figure 2-28	Position for Puncture Test..... 2-65
Figure 2-29	Position for End Drop ..... 2-65
Figure 2-30	Primary Impact End Slap-Down Damage..... 2-66
Figure 2-31	Secondary Impact End Damage ..... 2-66
Figure 2-32	Puncture Damage ..... 2-67
Figure 2-33	Close Up of Puncture Damage..... 2-67
Figure 2-34	End Impact ..... 2-68
Figure 2-35	Damage from End Impact (Bottom and Side)..... 2-68

NEDO-33869 Revision 11  
Non-Proprietary Information

Figure 2-36	End Impact Damage (Top and Side).....	2-69
Figure 2-37	Damage Inside Outer Container to CTU 1.....	2-69
Figure 2-38	Internal Damage to Outer Container CTU 1 .....	2-70
Figure 2-39	Lid Crush on CTU 1.....	2-70
Figure 2-40	Damage to Fuel in CTU 1 .....	2-71
Figure 2-41	Internal Damage to CTU 2.....	2-71
Figure 2-42	Fuel Damage CTU 2 .....	2-72
Figure 2-43	Fuel Prior to Leak Testing CTU 2 .....	2-72
Figure 2-44	CTU 1 J 9-m CG-Over-Bottom Corner Free Drop: View of Impacted Corner.....	2-78
Figure 2-45	CTU 1J 9-m CG-Over-Bottom Corner Free Drop: View of Opposite Corner.....	2-78
Figure 2-46	CTU 1J 9-m CG-Over-Bottom Corner Free Drop: View of Bottom .....	2-79
Figure 2-47	CTU 1J 9-m CG-Over-Bottom Corner Free Drop: Close-Up View of Top Corner .....	2-79
Figure 2-48	CTU 1J 9-m Vertical End Drop: Close-Up Side View of Bottom Damage .....	2-80
Figure 2-49	CTU 1J 9-m Vertical End Drop: Overall View of Damage.....	2-80
Figure 2-50	CTU 2J 9-m Horizontal Free Drop: Close-Up Side View of Damage .....	2-81
Figure 2-51	CTU 2J 9-m Horizontal Free Drop: Overall Side View of Damage.....	2-81
Figure 3-1	Overall View of RAJ-II Package .....	3-3
Figure 3-2	Transverse Cross-Sectional View of the Inner Container.....	3-4
Figure 3-3	Calculated Temperature Evolution During HAC Transient.....	3-16
Figure 3-4	Calculated Isotherms at the End of Fire Phase (1,800 s) .....	3-16
Figure 3-5	Calculated Isotherms at 100 s After the End of Fire.....	3-17
Figure 3-6	Calculated Isotherms at 1,468 s After the End of Fire.....	3-17
Figure 3-7	Calculated Isotherms at 12 hr After the End of Fire .....	3-18
Figure 3-8	Vertical Face Model.....	3-29
Figure 3-9	Comparison Between Energy Equation Solution with a Sine Wave Equation .....	3-33
Figure 5-1	MCNP Model and Tally Locations .....	5-6
Figure 6-1	RAJ-II Outer Container NCT Model .....	6-10
Figure 6-2	RAJ-II Inner Container NCT Model.....	6-11
Figure 6-3	RAJ-II Container Cross-Section NCT Model.....	6-12
Figure 6-4	Polyethylene Insert (FANP Design).....	6-16
Figure 6-5	Polyethylene Cluster Separator Assembly (GNF Design).....	6-17
Figure 6-6	RAJ-II Outer Container HAC Model.....	6-18
Figure 6-7	RAJ-II Inner Container HAC Model.....	6-19
Figure 6-8	RAJ-II Cross-Section HAC Model .....	6-20
Figure 6-9	RAJ-II HAC Model with Fuel Assembly Orientation 1 .....	6-21
Figure 6-10	RAJ-II HAC Model with Fuel Assembly Orientation 2 .....	6-21
Figure 6-11	RAJ-II HAC Model with Fuel Assembly Orientation 3 .....	6-22
Figure 6-12	RAJ-II HAC Model with Fuel Assembly Orientation 4 .....	6-22
Figure 6-13	RAJ-II HAC Model with Fuel Assembly Orientation 5 .....	6-23
Figure 6-14	RAJ-II HAC Model with Fuel Assembly Orientation 6 .....	6-23
Figure 6-15	RAJ-II HAC Model with Fuel Assembly Orientation 7 .....	6-24

NEDO-33869 Revision 11  
Non-Proprietary Information

Figure 6-16	RAJ-II HAC Model with Channels.....	6-24
Figure 6-17	RAJ-II BWR UO <sub>2</sub> Fuel Rod Transport Single Package NCT Model .....	6-26
Figure 6-18	RAJ-II BWR UO <sub>2</sub> Fuel Rod Transport Single Package HAC Model.....	6-27
Figure 6-19	RAJ-II UC and Generic PWR UO <sub>2</sub> Fuel Rod Transport Single Package HAC Model .....	6-27
Figure 6-20	RAJ-II BWR UO <sub>2</sub> Fuel Rod Transport Package Array NCT Model .....	6-28
Figure 6-21	RAJ-II BWR UO <sub>2</sub> Fuel Rod Transport Package Array HAC Model.....	6-30
Figure 6-22	RAJ-II UC and Generic PWR UO <sub>2</sub> Fuel Rod Transport Package Array HAC Model .....	6-31
Figure 6-23	Visual Representation of the Clad/Polyethylene Smeared Mixture versus Discrete Modeling.....	6-36
Figure 6-24	Quadrants of a 10x10 Lattice .....	6-43
Figure 6-25	Gadolinia-Urania Fuel Rod Loading Pattern for GNF 10x10.....	6-44
Figure 6-26	Gadolinia-Urania Fuel Rod Placement Pattern for 10x10 Fuel Assemblies at 5.0 wt% <sup>235</sup> U .....	6-48
Figure 6-27	Gadolinia-Urania Fuel Rod Placement Pattern for 9x9 Fuel Assemblies at 5.0 wt% <sup>235</sup> U .....	6-49
Figure 6-28	Gadolinia-Urania Fuel Rod Placement Pattern for 8x8 Fuel Assemblies at 5.0 wt% <sup>235</sup> U .....	6-50
Figure 6-29	RAJ-II Array HAC Polyethylene Sensitivity .....	6-52
Figure 6-30	RAJ-II Fuel Rod Pitch Sensitivity Study .....	6-53
Figure 6-31	RAJ-II Array HAC Pellet Diameter Sensitivity Study .....	6-54
Figure 6-32	RAJ-II Array HAC Fuel Rod Clad ID Sensitivity Study .....	6-56
Figure 6-33	RAJ-II Array HAC Fuel Rod Clad OD Sensitivity Study .....	6-57
Figure 6-34	Gadolinia-Urania Fuel Rod Placement Pattern for 10x10 Fuel Assemblies .....	6-60
Figure 6-35	Gadolinia-Urania Fuel Rod Placement Pattern for 9x9 Fuel Assemblies .....	6-67
Figure 6-36	Gadolinia-Urania Fuel Rod Placement Pattern for 8x8 Fuel Assemblies .....	6-72
Figure 6-37	FANP 10x10 Worst Case Fuel Parameters Model with Part Length Fuel Rods .....	6-81
Figure 6-38	GNF 10x10 Worst Case Fuel Parameters Model with Part Length Fuel Rods .....	6-82
Figure 6-39	FANP 9x9 Worst Case Fuel Parameters Model with Part Length Fuel Rods .....	6-83
Figure 6-40	GNF 9x9 Worst Case Fuel Parameters Model with Part Length Fuel Rods .....	6-84
Figure 6-41	Moderator Density Sensitivity Study for the RAJ-II HAC Worst Case Parameter Fuel Design .....	6-85
Figure 6-42	Polyethylene Foam Thickness Sensitivity Study, HAC 10x1x10 (2N=100).....	6-87
Figure 6-43	RAJ-II Inner Container Fuel Compartment Flooding Cases.....	6-89
Figure 6-44	RAJ-II Single Package NCT Results .....	6-93
Figure 6-45	RAJ-II Single Package HAC Results.....	6-94
Figure 6-46	RAJ-II Package Array Under NCT Results .....	6-95



NEDO-33869 Revision 11  
Non-Proprietary Information

Figure 6-47	RAJ-II Package Array HAC Results, Inner Container Moderation Study .....	6-97
Figure 6-48	RAJ-II Package Array HAC Results, Outer Container Moderation Study .....	6-98
Figure 6-49	BWR UO <sub>2</sub> Fuel Rod Pitch Sensitivity Study .....	6-101
Figure 6-50	RAJ-II with BWR UO <sub>2</sub> Fuel Rods in 5-Inch Stainless Steel Pipes for Transport .....	6-104
Figure 6-51	RAJ-II BWR UO <sub>2</sub> Fuel Rod Transport in Stainless Steel Pipe.....	6-105
Figure 6-52	RAJ-II BWR UO <sub>2</sub> Fuel Rod Single Package Under NCT .....	6-107
Figure 6-53	RAJ-II BWR UO <sub>2</sub> Fuel Rod Transport Single Package HAC .....	6-108
Figure 6-54	RAJ-II UC and Generic PWR UO <sub>2</sub> Fuel Rod Transport Single Package HAC .....	6-109
Figure 6-55	RAJ-II Package Array Under NCT with BWR UO <sub>2</sub> Loose Fuel Rods.....	6-110
Figure 6-56	RAJ-II Package Array Bounding NCT with UC and Generic PWR UO <sub>2</sub> Loose Fuel Rods .....	6-111
Figure 6-57	RAJ-II BWR UO <sub>2</sub> Fuel Rod Transport Under HAC.....	6-112
Figure 6-58	USL as a Function of Enrichment.....	6-117

## ACRONYMS

Term	Definition
2-D	Two-Dimensional
ACEL	Atomic Energy of Canada Limited
AFG	Average Energy Group causing Fission
AMS	Additional Margin to Subcriticality
ANS	American Nuclear Society
ANSI	American National Standards Institute
AOA	Area of Applicability
ASME	American Society of Mechanical Engineers
ASNT	American Society for Non-destructive Testing
ASTM	American Society for Testing and Materials
B&PVC	Boiler and Pressure Vessel Code
BWR	Boiling Water Reactor
CANDU	Canada Deuterium-Uranium
CE	Combustion Engineering
CFR	Code of Federal Regulations
CG	Center of Gravity
CSI	Criticality Safety Index
CTU	Certification Test Unit
EALF	Energy of the Average Lethargy causing Fission
FANP	Framatome Advanced Nuclear Power
Gd	Gadolinium
GNF-A / GNF	Global Nuclear Fuel – Americas, LLC
GNF-J	Global Nuclear Fuel – Japan
HAC	Hypothetical Accident Condition(s)
HDPE	High Density Polyethylene
H/U	Hydrogen to Uranium
H/X	Hydrogen to Fissile Material
IAEA	International Atomic Energy Agency
IC	Inner Container
ID	Inner Diameter
IC Inner Thermal Insulator (Aluminum Silicate)	The alumina silicate thermal insulation between the inner and outer walls of IC container to provide added margin to criteria set forth for HAC fire condition in 10 CFR 71.73(c)(4).
IC Lid	The lid of the inner container.

NEDO-33869 Revision 11  
Non-Proprietary Information

Term	Definition
IC Body	The body of the inner container consisting of the outer wall the thermal insulation, the inner wall, the polyethylene liner, and the shock absorbing system along with the fuel securement system.
JIS	Japanese Industrial Standard
JSNDI	Japanese Society for Non-destructive Inspection
LDPE	Low Density Polyethylene
LEU	Low-Enriched Uranium ( $\leq 5$ wt% U-235)
LEU+	LEU Plus, industry term for 5-10 wt% U-235 but for GNF-A meaning up to 8.0 wt% U-235.
LWR	Light Water Reactor
MS	Margin of Safety
NCT	Normal Conditions of Transport
NDIS	Non-destructive Inspection Society
NRC	Nuclear Regulatory Commission
OC	Outer Container
OD	Outer Diameter
OC Body	The assembly consisting of the OC lower wall, and the internal shock absorbing material.
OC Lid	The lid for the outer container.
Packaging	The assembly of components necessary to ensure compliance with packaging requirements as defined in 10 CFR 71.4. Within this SAR, the packaging is denoted as the RAJ-II packaging.
Package	The packaging with its radioactive contents, as presented for transportation as defined in 10 CFR 71.4. Within this SAR, the package is denoted as the RAJ-II package.
Payload	Unirradiated fuel assemblies and fuel rods.
PC	Personal Computer
PNL	Pacific Northwest Laboratories
PWR	Pressurized Water Reactor
QA	Quality Assurance
RAM	Radioactive Material
SAR	Safety Analysis Report
SS	Stainless Steel
SSLTL	Single-Sided Lower Tolerance Limit
UC	Uranium Carbide
UO <sub>2</sub>	Uranium Dioxide
USL	Upper Subcritical Limit

NEDO-33869 Revision 11  
Non-Proprietary Information

Term	Definition
wt%	Weight Percent
W/F	Water to Fuel

## **1.0 GENERAL INFORMATION**

This chapter of the Safety Analysis Report (SAR) presents an introduction and general description of the RAJ-II package. The major components comprising the RAJ-II package are presented in Figure 1-1 through Figure 1-4. Terminology and acronyms used throughout this document are presented in the Acronyms table. This package is intended to be used to transport unirradiated Boiling Water Reactor (BWR) fuel assemblies, BWR fuel rods, CANDU fuel rods, and Pressurized Water Reactor (PWR) fuel rods, containing Type B fissile material. The fissile material can be in the form of uranium dioxide or uranium carbide enriched up to 5.0 weight percent (wt%) U-235, referred to as LEU for the purposes of this report, or up to 8.0 weight percent (wt%) U-235, referred to as LEU+ for the purposes of this report.

### **1.1 INTRODUCTION**

The model RAJ-II package number USA/9309/B(U)F-96, under docket 71-9309, has been developed to transport Type B fissile material. The analyses are performed under an NRC-approved quality assurance program documented in NEDO-11209-A, Revision 16 (Reference 1-1), which specifically complies with Title 10 of the Code of Federal Regulations, Part 50 (10 CFR 50) Appendix B requirements and is adopted to meet the requirements of 10 CFR 71, Subpart H for transportation of radioactive material.

The integrity of the fuel is maintained by the protective outer package, the insulated inner package and the fuel rod cladding through both Normal Conditions of Transport (NCT) and Hypothetical Accident Condition (HAC) deformations. A variety of full-scale engineering development tests were included as part of the certification process. Ultimately, two full-scale Certification Test Units (CTUs) were subjected to a series of free drops and puncture drops. The inner and outer containers provide both thermal protection as well as mechanical protection from drops or accident conditions.

Fuel rod cladding and welded end plugs form the containment vessel of the radioactive material contents transported in the RAJ-II package. The RAJ-II package is designed for shipment by truck, ship, or rail as a Type B fissile material package per the definition in 10 CFR 71.4 and 49 CFR 173.403. The requirements of Type B packages are demonstrated in Chapter 4 where the effective  $A_2$  and allowable leakage rates are provided in Section 4.5.

The payload within each RAJ-II package consists of a maximum of two unirradiated BWR fuel assemblies or individual rods (BWR, uranium carbide, or generic PWR) contained in a 5-inch stainless steel pipe, protective case or strapped together and positioned in one or both sides of the inner container. See Table 6-1 and Table 6-2 for the fuel loading criteria. The shielding and criticality assessments are provided in Chapter 5.0 and Chapter 6.0. The Transport Index (TI) for this package is based on the shielding assessments described in Chapter 5.0. The Criticality Safety Index (CSI) for the RAJ-II package is defined in Chapter 6.0. Section 6.1.3 provides the calculation of the CSI, where the CSI for 5.0 wt % LEU fuel assemblies is 1.0 and the CSI for 5.0 wt% fuel rods is 1.6. The CSI for 8.0 wt% LEU+ fuel assemblies and fuel rods is 1.6.

NEDO-33869 Revision 11  
Non-Proprietary Information

RAJ-II package dimensions identified in the text, tables, and figures of this SAR are intended to be nominal. The drawings provided in Section 1.3.1 contain the dimensions and the tolerances.

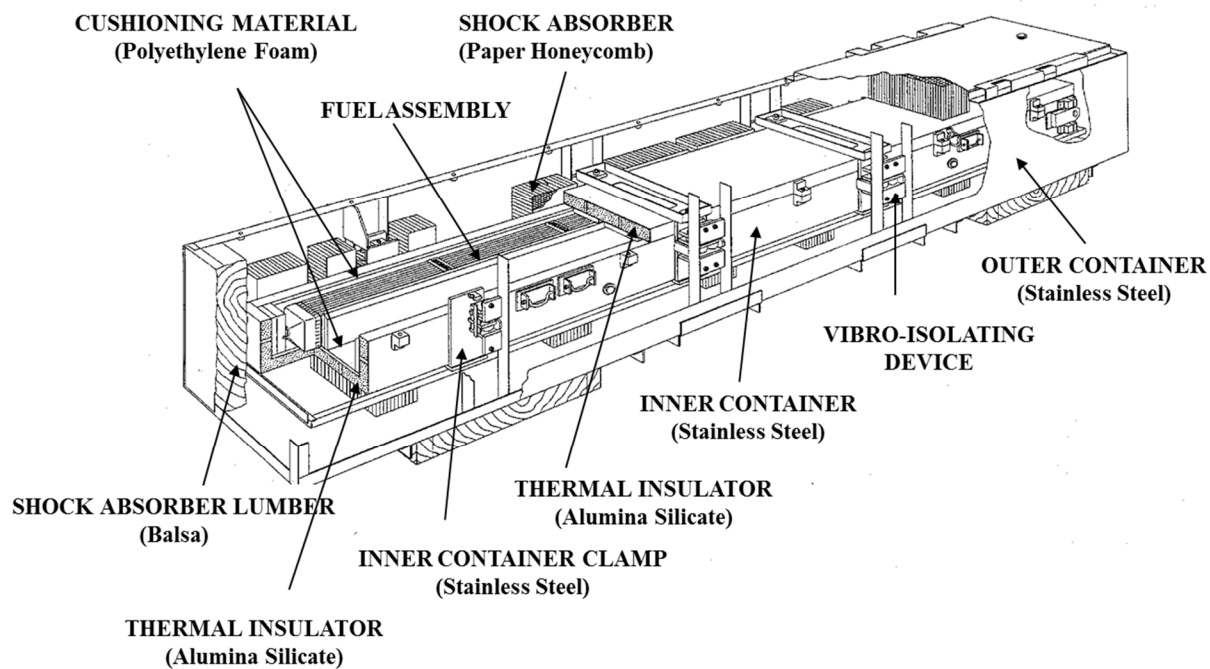


**Figure 1-1 RAJ-II Package Assembly**

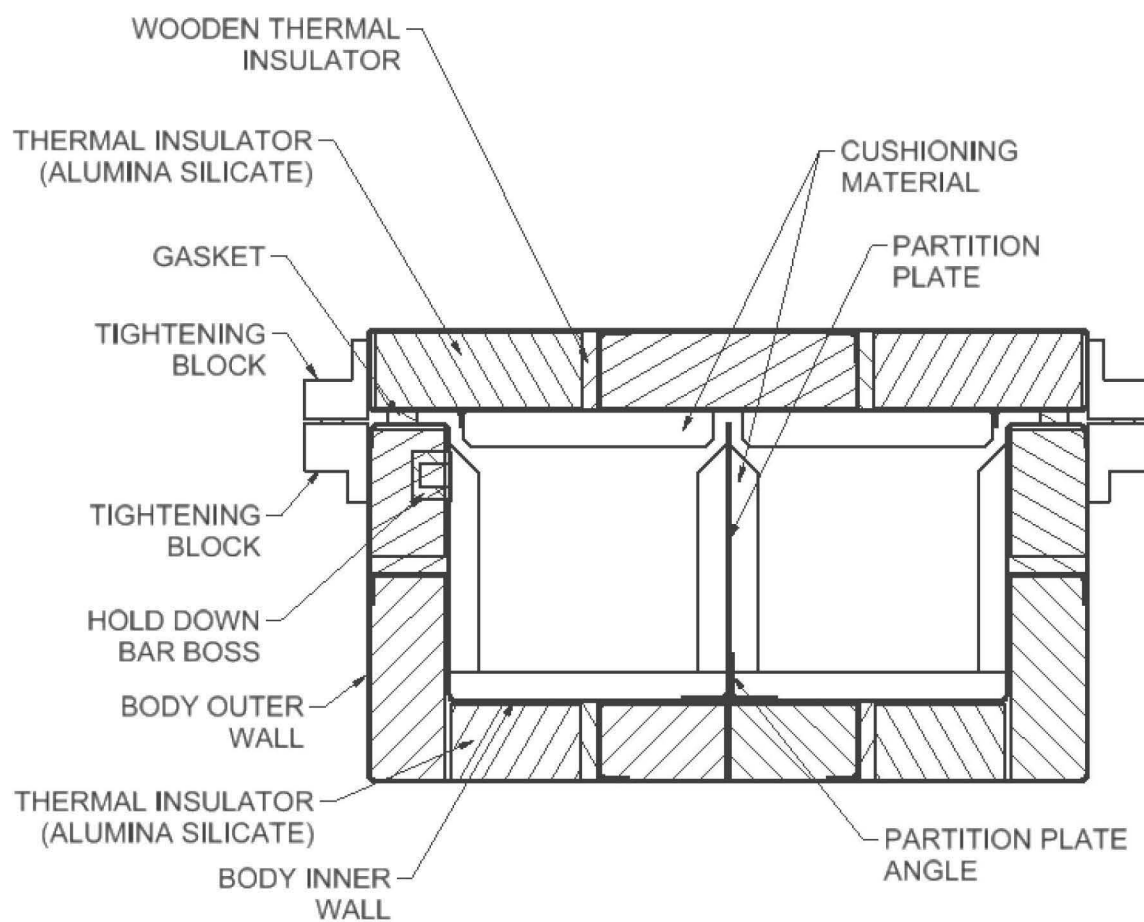
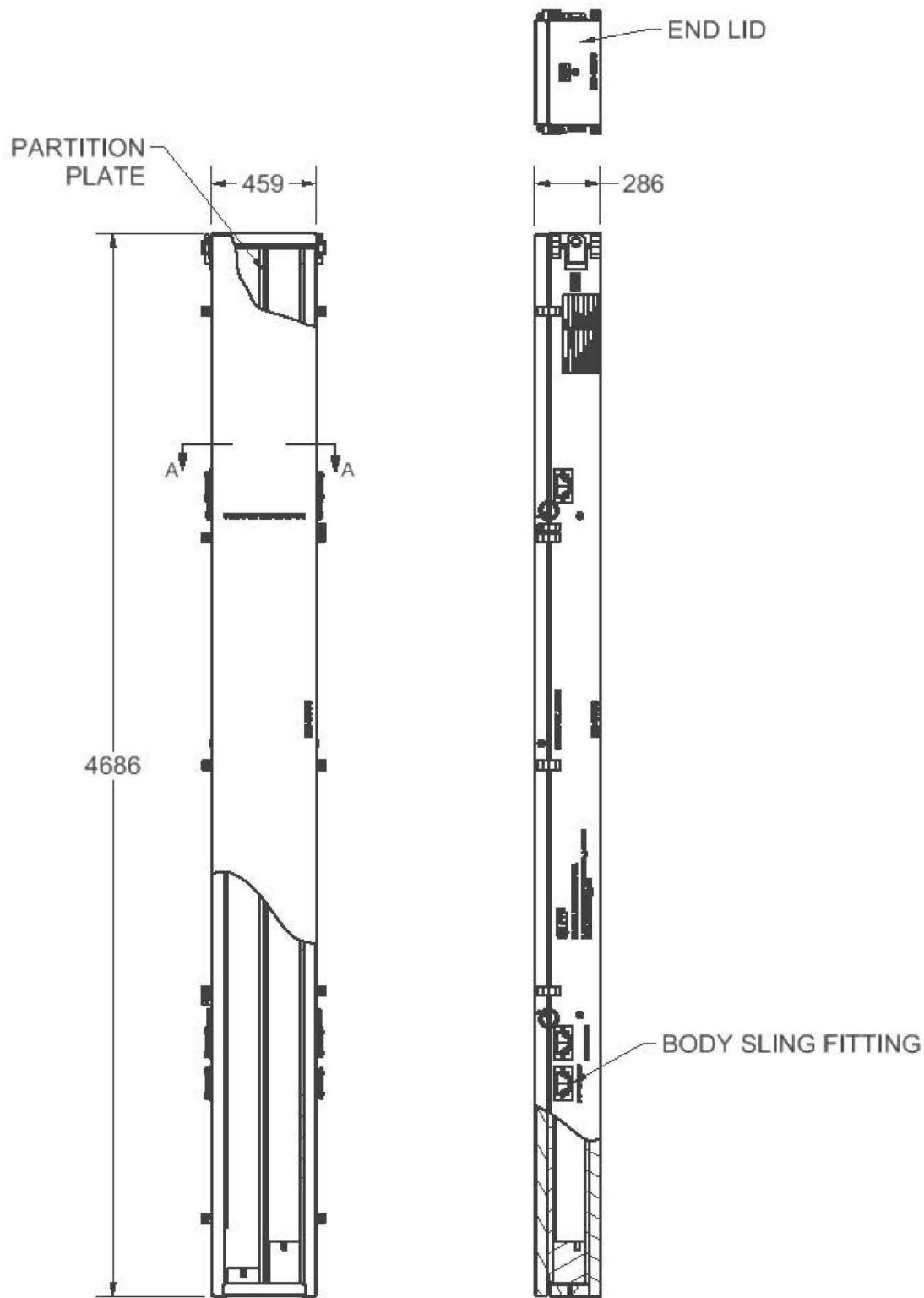


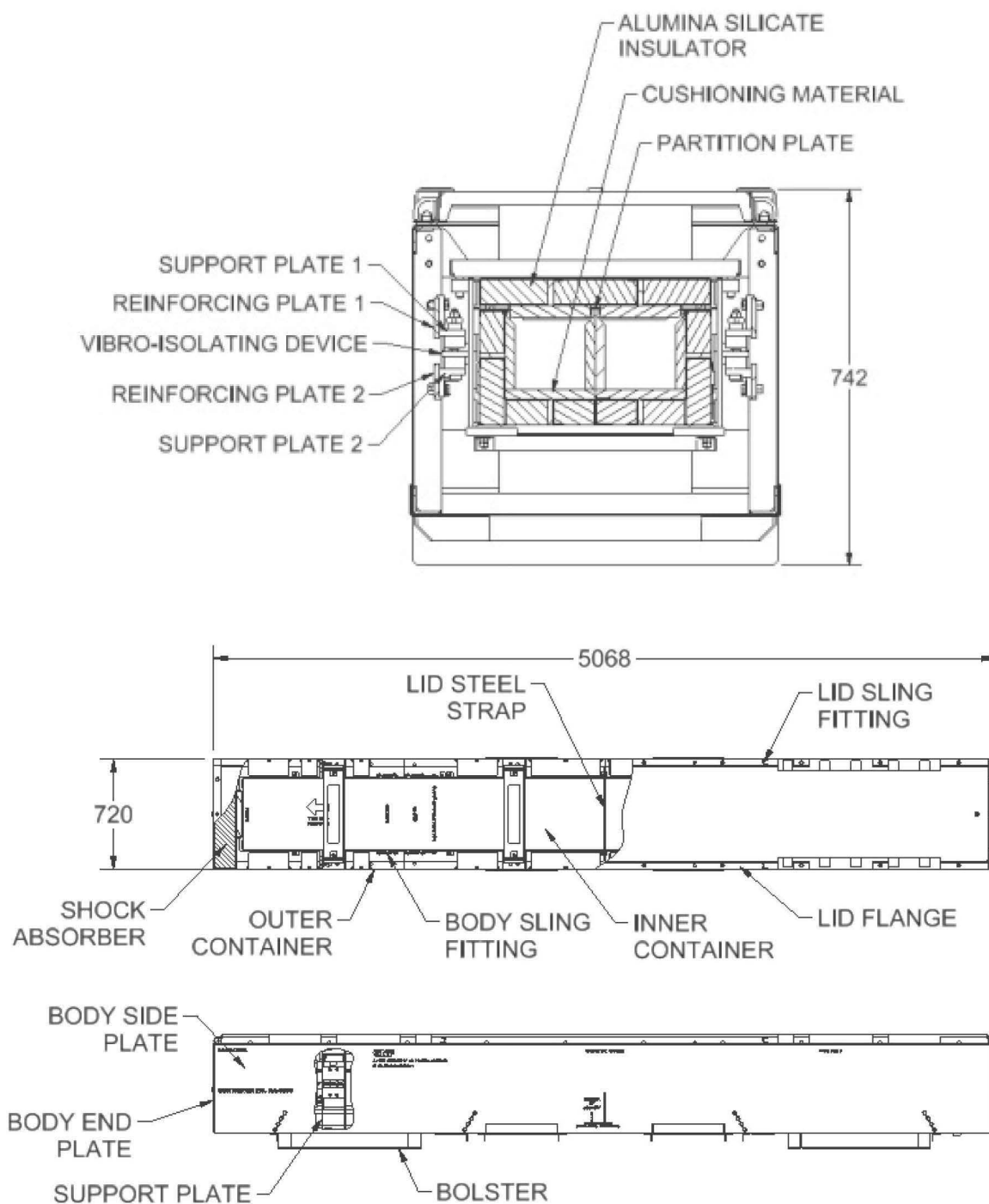
**Figure 1-2 Cross-Section of Inner Container**



Dimensions are in *mm*

**Figure 1-3 Inner Container**





Dimensions are in *mm*

**Figure 1-4 Inner and Outer Container**

## **1.2 PACKAGE DESCRIPTION**

This section presents a basic description of the RAJ-II package.

### **1.2.1 Packaging**

The packaging is comprised of one inner container and one outer container both made of stainless steel. The inner container is comprised of a double-wall stainless steel sheet structure with alumina silicate thermal insulator filling the gap between the two walls to reduce the flow of heat into the contents in the event of a fire. Foam polyethylene cushioning material is placed on the inside of the inner container for protection of the fuel assembly. The outer container is comprised of a stainless steel angular framework covered with stainless steel plates. Inner container clamps are installed inside the outer container with a vibro-isolating device to alleviate vibrations during transportation. Additionally, wood and a honeycomb resin impregnated craft paper or aluminum (hereinafter called "honeycomb") are placed as shock absorbers to reduce shock due to a drop of the package. In addition to the packaging described above, the fuel rod cladding and welded end plugs provide primary containment of the radioactive material.

#### **1.2.1.1 General Packaging Description**

##### **1.2.1.1.1 Inner Container**

The structure of the inner container is shown in Figure 1-2 and Figure 1-3. The inner container is comprised of three main parts: an inner container body, an inner container end lid (removable), and an inner container top lid (removable). These components are fastened together by bolts made of stainless steel through tightening blocks. The inner container body is fitted with six sling fittings and the inner container lid is fitted with four sling fittings as shown in Figure 2-2. The inner container body has a double wall structure made of stainless steel. Its main components are an outer wall, inner wall and alumina silicate thermal insulator.

The outer wall is made of a 1.5 mm (0.0591 in) thick stainless steel sheet formed to a U-shape that constitutes the bottom and sides of the inner container body. A total of 14 stainless steel tightening blocks are attached on the sides of the outer wall, seven per side, to fasten the inner container lid and the inner container end lid by bolts.

The inner wall of the inner packaging is formed into a U-shape with a 1.0 mm (0.0391 in) thick stainless steel sheet. The inner packaging is partitioned down the center with a 2.0 mm (0.0787 in) thick stainless steel sheet welded to the bottom of the packaging. Foam polyethylene is placed on the inner surface of the inner wall where the fuel assemblies are seated. The void space between the outer and inner steel sheeting is filled with an alumina silicate thermal insulation 48 mm (1.89 in) thick.

##### **1.2.1.1.2 Outer Container**

The structure of the outer container is shown in Figure 1-4. The outer container is comprised of three parts: a container body, a container lid and inner container hold clamps made of stainless steel and fastened together using steel bolts.

Two tamper-indicating device attachment locations are provided, one on each end, of the outer container.

#### 1.2.1.1.2.1 Outer Container Body

The outer container is made from a series of stainless steel angles (50mm x 50mm x 4mm) (1.97 inch x 1.97 inch x 0.157 inches) that make the framework. Welded to the framework are a bottom plate and side plates made of 2 mm (0.079 inch) thick stainless steel.

Sling holding angles for handling with a crane and protective plates for handling with a forklift are welded on the outside of the container body.

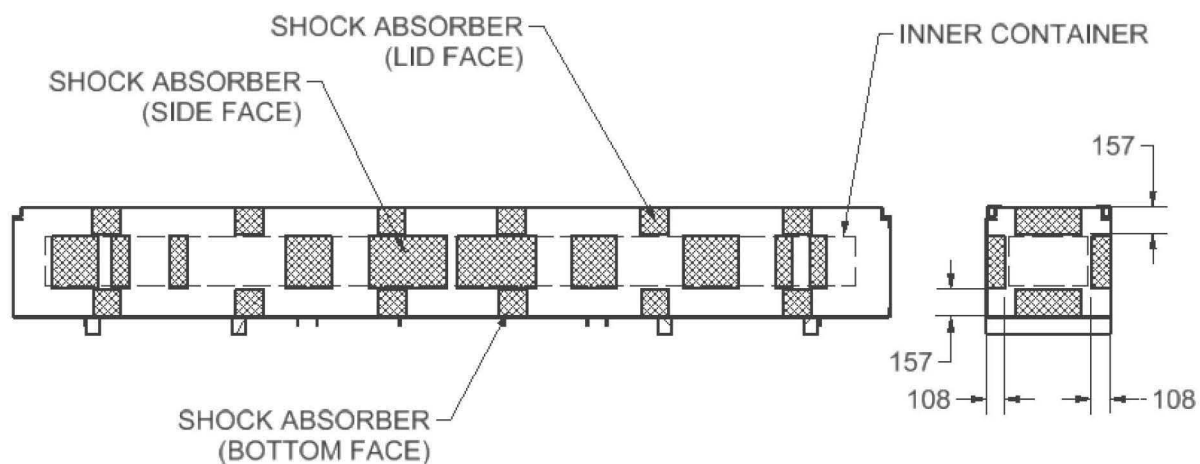
A total of eight sets of support plates are welded on the inside of the outer container body for installing the inner container hold clamps. Shock absorbers made of 146 mm (5.75 in) wood are attached to each end and paper or aluminum honeycomb shock absorbers are attached to the bottom and sides for absorbing shock due to a drop. The geometry of the shock absorber is shown in Figure 1-5. The shock absorbers are 157 mm (6.18 in) thick and 108 mm (4.25 in) thick.

#### 1.2.1.1.2.2 Outer Container Lid

The outer container lid is comprised of a lid flange and a lid plate made of stainless steel.

Stainless steel lid sling fittings are welded in four places on the top surface of the outer container lid. A paper or aluminum honeycomb shock absorber, 157 mm (6.18 in) thick by 160 mm (6.30 in) wide and 380 mm (14.96 in) long is attached to the bottom side of the lid similar to the attachment at the bottom of the container.

The outer container lid has holes for bolts in its flange so that it can be fastened to the outer container body by the stainless steel bolts.



Dimensions are in mm

**Figure 1-5 Shock Absorber Geometry**

### 1.2.1.1.2.3 Inner Container Hold Clamp (Located on Outer Container)

The inner container hold clamp consists of an inner container receptacle and a vibro-isolating device.

The inner container receptacle consists of an inner container support plate, a support frame, a bracket and an inner container hold clamp fastener made of steel. The receptacle guides the inner container to the correct position. The inner container receptacle is fitted with the vibro-isolating device through the gusset attached to the bracket.

The vibro-isolating material is attached on the upper and lower side of the gusset. Shock mount fastening bolts go through the center of each piece of vibro-isolating material. The bolts at both ends are tightened so that the vibro-isolating material pieces press the gusset.

There are four sets (eight pieces) of vibro-isolating devices mounted on the outer container.

Finally, a variety of stainless steel fasteners are used as specified in Section 1.3.1.

### 1.2.1.1.3 Gross Weight and Dimensions

A summary of the major component weights and outside dimensions of the RAJ-II package are given in Table 1-1. A summary of overall component weights is delineated in Table 2-1.

**Table 1-1      Weights and Outer Dimensions of the Package**

Item	Weight and Outer Dimensions
Maximum gross shipping weight	1,614 kg (3,558 lbs)
Maximum weight of inner container	308 kg (679 lbs)
Maximum weight of outer container	622 kg (1,371 lbs)
Maximum weight of packaging	930 kg (2,050 lbs)
Loose rods pipe nominal mass per component	106 kg (234 lbs)
Protective case nominal mass per component	87 kg (192 lbs)
Dimensions of inner container	Length: 4,686 mm (184.49 in) Width: 459 mm (18.07 in) Height: 286 mm (11.26 in)
Dimensions of outer container	Length: 5,068 mm (199.53 in) Width: 720 mm (28.35 in) Height 742 mm (29.21 in) (including bolsters)

### 1.2.1.2 Containment Features

The containment system components are identified above in Section 1.2.1 and in the accompanying figures. The primary containment boundary of this package is the fuel rod cladding together with the welded end plugs as shown in the example in Figure 1-6. The fuel rod is

constructed by loading the uranium dioxide pellets into a cladding tube. The tubes are pressurized with helium and end plugs are welded to the tube which effectively seals and contains the radioactive material. Welds of the fuel rods are verified for integrity by such means as X-ray inspection, ultrasonic testing, or process control. The RAJ-II package cannot be opened unintentionally. Both the inner container and outer container lids are attached to their respective bodies with socket-headed cap screws. There are twenty-four bolts holding the outer lid in place. There are no other openings in the outer container. The inner container has ten bolts holding the main lid in place and four bolts holding the end closure in place. Thus, the requirements of 10 CFR 71.43(c) are satisfied.



**Figure 1-6 Example Fuel Rod (Primary Containment)**

There are no pressure relief systems included in the RAJ-II package design to relieve pressure from within either the inner or outer containers or the fuel rod. Fire-consumable fusible plugs are used on the exterior surface of both the outer and inner containers to prevent pressure build up from the insulating and shock absorbing material during a fire event. These fusible plugs may be made of plastic. Two plugs are installed in the outer container body and two in the outer container lid. Four are installed in the inner container body, one in the end lid and two in the main lid.

#### **1.2.1.3 Shielding Features**

Due to the nature of the unirradiated fuel payload, neutron and gamma shielding is not necessary nor provided by the RAJ-II packaging. Due to insignificant decay heat of unirradiated fuel, payload personnel barriers are not necessary.

#### **1.2.1.4 Criticality Control Features**

The RAJ-II package does not require specific design features to provide neutron moderation and absorption for criticality control. The contents of the package rely on gadolinia loading for criticality control based on enrichment. Gadolinia loading requirements are provided in Table 6-1. There are no spacers required for criticality control. Fissile materials in the payload are limited to an amount that ensures safely sub-critical packages for both NCT and HAC. Further discussion of criticality control features is provided in Chapter 6.0.

#### **1.2.1.5 Structural Features**

The RAJ-II package design features for impact limiting and internal supporting/positioning functions are described in Section 1.2.1.1.

##### **1.2.1.5.1 Protrusions**

The only significant protrusions on the RAJ-II packaging exterior are those associated with the lifting features on the outer container exterior. These are the sling holding angles and the bolsters at the bottom of the packaging. The bolsters protrude a maximum of 80 mm (3.15 in).

The only significant protrusions on the inner container exterior are the lifting sling fittings and the tightening blocks that are used for securing the lid. There are lifting sling fittings on the body and the main lid. Each of the sling fittings fold down so they protrude only the thickness of the lifting rod or bail.

#### **1.2.1.5.2 Lifting and Tie-Down Devices**

The lifting devices for the RAJ-II consist of the sling holding angles on the outer container which keep the slings from moving when used to sling the container during handling. The loaded outer container is designed to use two slings under the container. The empty container is also handled with two slings. The package may also be handled by the use of a forklift. The sling holding angles are designed so that even if they failed it would not affect the performance of the package.

The inner container is handled by the use of a series of lifting sling fittings. They are attached in a manner that even if they fail it will not compromise the performance of the inner container. On both the inner and outer containers, the lid lifting devices are marked to ensure proper use. A detailed discussion of lifting and tie-down designs, with corresponding structural analyses, is provided in Sections 2.4.1 and 2.4.2.

#### **1.2.1.6 Heat Transfer Features**

Unirradiated fuel has insignificant decay heat; therefore, the RAJ-II package is not designed for dissipating heat. A more detailed discussion of the package thermal characteristics is provided in Chapter 3.0. Due to the passive design of the RAJ-II package with regard to heat transfer, there are no coolants utilized within the RAJ-II package.

#### **1.2.1.7 Packaging Markings**

The packaging will be marked with its model number, serial number, gross weight and also with the package identification number assigned by the Nuclear Regulatory Commission (NRC).

### **1.2.2 Contents**

This package is intended to be used to transport unirradiated BWR and PWR fuel assemblies, BWR fuel rods, CANDU fuel rods, and PWR fuel rods, containing Type B fissile material. The fissile material can be in the form of uranium dioxide or uranium carbide enriched up to 5.0 wt% U-235, referred to as LEU for the purposes of this report, or uranium dioxide up to 8.0 weight percent (wt%) U-235, referred to as LEU+ for the purposes of this report. Loading criteria and details for fuel assemblies are specified later in Table 6-1 and fuel rods in Table 6-2.

#### **1.2.2.1 Maximum Quantity of Fissile and Radioactive Materials**

The contents consist of enriched commercial grade uranium or enriched reprocessed uranium, as defined in ASTM C996-20, uranium oxide or uranium carbide fuel rods enriched to 5.0 wt% U-235 for LEU or uranium oxide fuel rods enriched to no more than 8.0 wt% U-235 for LEU+, with limits specified in Table 1-2 and Table 1-3. For the limits of Table 1-3, U-238 is considered the remainder. See Chapter 4 for the  $A_2$ —effective calculation.

**Table 1-2      Maximum Weight of Uranium Dioxide Pellets per Fuel Assembly for 5.0 wt% and 8.0 wt% U-235**

Type 8×8 Fuel Assembly	Type 9×9 Fuel Assembly	Type 10 x10 Fuel Assembly
235 kg	240 kg	275 kg

**Table 1-3      Maximum Concentrations**

Isotope	Maximum Content for 5.0 wt% U-235	Maximum Content for 8.0 wt% U-235
U-232	5.00E-08 g/gU	5.00E-08 g/gU
U-234	2.00E-03 g/gU	2.00E-03 g/gU
U-235	5.00E-02 g/gU	8.00E-02 g/gU
U-236	2.50E-02 g/gU	2.50E-02 g/gU
Np-237	1.66E-06 g/gU	1.66E-06 g/gU
Pu-238	6.20E-11 g/gU	6.20E-11 g/gU
Pu-239	3.04E-09 g/gU	3.04E-09 g/gU
Pu-240	3.04E-09 g/gU	3.04E-09 g/gU
Gamma Emitters	4.4E+05MeV-Bq/kgU	4.4E+05MeV-Bq/kgU

### 1.2.2.2      Chemical and Physical Properties

An example of the structural materials of the fuel assembly is shown in Table 1-4. Zirconium alloy, stainless steel and Ni-Cr-Fe alloy are chemically stable materials that are heat resistant and corrosion resistant. The density for the fuel assembly materials is presented in Table 1-5.

**Table 1-4      Example of Fuel Structural Materials**

Component Parts	Typical Structural Materials
Cladding tube	Zirconium alloy, metallic zirconium, stainless steel
Internal spring	Stainless steel
Getter	Zirconium alloy and stainless steel
Upper and Lower end plug	Zirconium alloy
Water rod	Zirconium alloy
Upper and Lower tie plate	Stainless steel
Spacer	Zirconium alloy and Ni-Cr-Fe alloy (Inconel X-750)
Finger spring	Ni-Cr-Fe alloy
Expansion spring	Ni-Cr-Fe alloy
Nut	Stainless steel

Locking tab washer	Stainless steel
--------------------	-----------------

**Table 1-5      Density of Structural Materials**

Main Structural Materials	Density
Zirconium alloy Metallic zirconium	Approximately 6.5 g/cm <sup>3</sup> (0.235 lb/in <sup>3</sup> )
Uranium dioxide pellet	Less than 10.74 g/cm <sup>3</sup> (0.376 lb/in <sup>3</sup> )
Stainless steel	Approximately 7.9 g/cm <sup>3</sup> (0.285 lb/in <sup>3</sup> )
Ni-Cr-Fe alloy	Approximately 8.5 g/cm <sup>3</sup> (0.307 lb/in <sup>3</sup> )

### 1.2.2.3      Nonfissile Materials: Neutron Absorbers or Moderators

As indicated in Section 1.2.1.4, the RAJ-II package does not require specific design features to provide neutron moderation and absorption for criticality control. Fuel is loaded with uranium dioxide mixed with gadolinium oxide (hereinafter gadolinia), and the pellets in the gadolinia fuel rods contain a minimum of 2.0 wt% gadolinia. The quantity of gadolinia specified in Table 6-1 is the primary means of criticality control for the fuel assemblies. For shipments of fuel rods, neutron absorbers are not required to maintain criticality safety.

A number of packing materials (e.g., cluster separators, and polyethylene bags) may be used to protect the fuel assembly. An example of the packing materials and their use is shown in Figure 1-7. These packing materials may contain hydrogenous compounds such as polyethylene that affect the criticality safety of the shipments. The amount of polyethylene allowed is provided in Tables 6-1 and Table 6-2. Use of polyethylene material or other plastics (e.g., cluster separators) is optional; polyethylene or plastic mass limits are determined in accordance with Section 6.3.2.2.



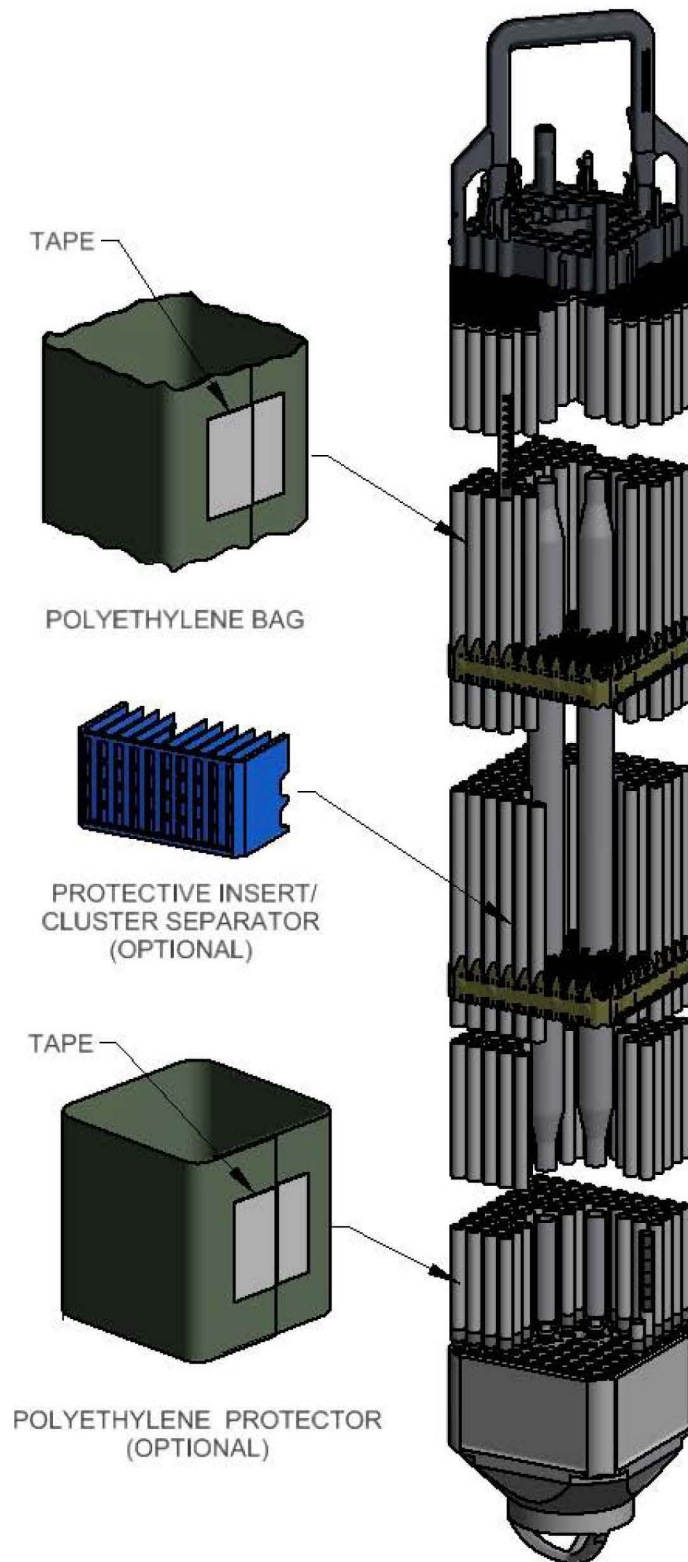


**Figure 1-7 Fuel Assembly with Optional Packing Materials**

#### **1.2.2.4 Physical Configuration**

##### **1.2.2.4.1 Fuel Assembly**

A maximum of two fuel assemblies are placed in each RAJ-II package, in either 8x8, 9x9 or 10x10 configurations as specified in Table 6-1. Fuel assemblies may also be shipped with a fuel channel. The nuclear fuel pellets located in rods and contained in the packaging are uranium oxides primarily as  $\text{UO}_2$ . The fuel lattice average enrichment is less than or equal to 5.0 wt% or 8.0 wt% U-235 (the fuel pellet maximum enrichment is less than or equal to 5.0 wt% or 8.0 wt% U-235). The CSI for fuel assembly shipments is 1.0 at 5.0 wt% U-235 and is 1.6 at 8.0 wt% U-235.

The configuration of typical fuel assemblies is shown in Figure 1-7. The fuel assemblies may be of various models and types as long as they meet the requirements listed in Table 6-1.

##### **1.2.2.4.2 Fuel Rods**

Fuel rod shipments must meet the maximum number of rods per compartment listed in Table 6-2 (two compartments per RAJ-II package). Fuel rods contain uranium oxide or uranium carbide with a maximum pellet enrichment of 5.0 wt% U-235 for LEU or uranium oxide with a maximum pellet enrichment of 8.0 wt% U-235 for LEU+. The CSI for fuel rod shipments is 1.6.

###### **1.2.2.4.2.1 Fuel Rods Freely Loose or Strapped Together**

Fuel rods may be shipped freely loose or strapped together and are limited to the quantity specified in Table 6-2. Fuel rods are fixed together using ring clamps. The criticality safety case for loose rods shows that fuel rods can be arranged in any configuration within the volume of the inner container. Based on this criticality safety analysis, the ring clamps are not relied on or needed for maintaining the configuration of the fuel rods.

###### **1.2.2.4.2.2 Fuel Rods in a 5-Inch Pipe**

Another physical configuration is the use of a 5-inch diameter schedule 40 stainless steel pipe. The physical configuration of the pipe is shown in drawing 0028B98. The number of fuel rods shipped in this configuration is limited by the quantities in Table 6-2. The quantities in Table 6-2 were determined based on sensitivity studies of optimum rod pitch (and thereby optimum moderator to fuel ratio) and the maximum array size which meets the criticality safety limits. For uranium carbide and generic PWR rods, the quantities in Table 6-2 represent dense packing of the rods within the pipe. In reality, fewer rods may be able to fit within the pipe due to manufacturing tolerances and use of packing materials.

###### **1.2.2.4.2.3 Fuel Rods in a Protective Case**

The protective case is a stainless steel box comprised of a body, lid, wood spacer absorber and end plate. Detailed drawings of the protective case are provided in Section 1.3.1. The protective case is surrounded by polyurethane foam cushioning material, which provides a snug fit within the inner container. Depending on the rod type, the protective case may be used to transport any authorized fuel rods as shown in Table 6-2.

#### **1.2.2.5 Maximum Normal Operating Pressure**

The maximum internal pressure of the fuel rods at room temperature and the maximum normal operating pressure of the contents are described in Section 3.3.2.

#### **1.2.2.6 Maximum Weight of the Contents**

The total weight of payload contents (fuel assemblies or fuel rods and rod shipping containers, and packing material) must not exceed is 684 kg (1,508 lbs). The maximum uranium payload is 484 kg (1069 lbs).

#### **1.2.2.7 Maximum Decay Heat**

The maximum decay heat based on 484 kg of uranium with the maximum radionuclide concentration provided in Table 4-1 is 0.217 watts for 5.0 wt% U-235 LEU and 0.218 watts for 8.0 wt% U-235 LEU+ per RAJ-II package, which are each insignificant.

#### **1.2.3 Special Requirements for Plutonium**

Consistent with 10 CFR 71.63, there are no special requirements for plutonium. Chapter 4 shows that the plutonium content is less than 0.74 TBq (20 Ci).

#### **1.2.4 Operational Features**

The RAJ-II package is not considered complex. Operational features are readily apparent from an inspection of the drawings provided in Section 1.3.1 and the previous discussions presented in Section 1.2.1. Operational procedures and instructions for loading, unloading, and preparing empty RAJ-II packages for transport are provided in Chapter 7.0.

## 1.3 APPENDIX

### 1.3.1 RAJ-II General Arrangement Drawings

This section presents the RAJ-II package general arrangement drawing consisting of 15 drawings entitled *RAJ-II SAR Drawing* listed in Section 1.3.1.1. Within the packaging general arrangement drawing, dimensions important to the packaging safety are dimensioned and toleranced. Other dimensions are provided as reference dimensions and are toleranced in accordance with the Japan Industrial Standard (JIS) B 0405. See Sections 2.1.4.1 and 2.1.4.2.

#### 1.3.1.1 Drawing List

##### Outer Container Drawings

Drawing Number	Sheet Number	Revision #	Name
105E3737	1	9	Outer/Inner Container Assembly Licensing Drawing
105E3738	1, 2, 3	11	Outer Container Main Body Assembly Licensing Drawing
105E3739	1	6	Outer Container Fixture Assembly Licensing Drawing
105E3740	1	7	Outer Container Fixture Assy Installation Licensing Drawing
105E3741	1	4	Outer Container Shock Absorber Assy Licensing Drawing
105E3742	1	5	Outer Container Bolster Assembly Licensing Drawing
105E3743	1	7	Outer Container Lid Assembly Licensing Drawing
105E3744	1	8	Outer Container Marking Licensing Drawing

##### Inner Container Drawings

Drawing Number	Sheet Number	Revision #	Name
105E3745	1, 2, 3, 4	11	Inner Container Main Body Assembly Licensing Drawing
105E3746	1	4	Inner Container Parts Assembly Licensing Drawing
105E3747	1	6	Inner Container Lid Assembly Licensing Drawing
105E3748	1	4	Inner Container End Lid Assembly Licensing Drawing
105E3749	1	8	Inner Container Marking Licensing Drawing

##### Contents Drawings

Drawing Number	Sheet Number	Revision #	Name
105E3773	1	2	RAJ-II Protective Case Licensing Drawing
0028B98	1	2	Shipping Container Loose Fuel Rods

### 1.3.2 References

- 1-1 GE Hitachi Nuclear Energy, "Quality Assurance Program Description," NEDO-11209-A, Revision 16, December 23, 2020.

## **2.0 STRUCTURAL EVALUATION**

This chapter presents evaluations demonstrating that the RAJ-II package meets applicable structural criteria. The RAJ-II packaging, consisting of unirradiated fuel rods that provide containment, an Inner Container (IC), and an Outer Container (OC) with honeycomb spacers, is evaluated and shown to provide adequate protection for the payload. Normal Conditions of Transport (NCT) and Hypothetical Accident Condition (HAC) evaluations, using analytic and empirical techniques, are performed to address 10 CFR 71 performance requirements.

Numerous tests were successfully performed on the RAJ-II package during its initial qualification in Japan that provided a basis for selecting the certification tests. RAJ-II certification testing involved two full-scale Certification Test Units (CTU) at Oak Ridge, TN. The RAJ-II CTUs were subjected to a series of free drop and puncture drop tests. The RAJ-II CTU protected the simulated fuel rods, which maintained a leak tight containment boundary throughout certification testing. Details of the certification test program are provided in Section 2.12.2.

### **2.1 DESCRIPTION OF STRUCTURAL DESIGN**

#### **2.1.1 Discussion**

A comprehensive discussion on the RAJ-II packaging design and configuration is provided in Chapter 1.0. Drawings provided in Section 1.3.1 show the construction of the RAJ-II and how it protects the fuel rods. The containment is provided by the fuel cladding and welded end fittings of the fuel rods. The fuel is protected by an IC that provides thermal insulation and cushioning foam that protects the fuel from vibration. The IC is supported by a vibration isolation system inside the OC that has shock absorbing blocks of balsa and honeycomb made of materials such as aluminum or resin impregnated kraft paper (hereinafter called "honeycomb"). Specific discussions relating to the aspects important to demonstrating the structural configuration and performance to design criteria for the RAJ-II packaging are provided in the following sections. Standard fabrication methods are used to fabricate the RAJ-II package.

Detailed drawings showing applicable dimensions and tolerances are provided in Section 1.3.1.

Weights for the various components and the assembled packaging are provided in Section 2.1.3.

##### **2.1.1.1 Containment Structures**

The primary containment for the radioactive material in the RAJ-II is the fuel rod cladding, which is manufactured to high standards for use in nuclear reactors. The fabrication standards for the fuel are in excess of what is needed to provide containment for shipping of the fuel. The fuel rod cladding is designed to provide containment throughout the life of the fuel, prior to loading, in transportation, and while used in the reactor where it operates at higher pressures and temperatures, and the cladding must contain fission products as well as the fuel itself.

The cladding tubes for the fuel are high quality seamless tubing. The clad fuel is verified leak tight before shipment.

### **2.1.1.2 Non-Containment Vessel Structures**

The RAJ-II is made up of two non-containment structures, the IC and the OC, that are designed to protect the fuel assemblies and clad rods which serve as the containment. The IC design provides some mechanical protection, although its primary function is to provide thermal protection. The OC consists of a metal wall with shock absorbing devices inside and vibration isolation mounts for the IC. Section 1.2.1 provides a detailed description of the IC and OC. Non-containment structures are fabricated in accordance with the drawings in Section 1.3.1.

Welds for the non-containment vessel walls are subjected to visual inspection as delineated on the drawings in Section 1.3.1.

### **2.1.2 Design Criteria**

Proof of performance for the RAJ-II package is achieved by a combination of analytic and empirical evaluations. The acceptance criteria for analytic assessments are in accordance with 10 CFR 71 and the applicable regulatory guides. The acceptance criterion for empirical assessments is a demonstration that both the IC and OC will protect the fuel assemblies and rods during the thermal event and the fuel itself is not damaged throughout the NCT and HAC certification testing. Package deformations obtained from certification testing are considered in subsequent thermal, shielding, and criticality evaluations.

#### **2.1.2.1 Analytic Design Criteria (Allowable Stresses)**

The allowable stress values used for analytic assessments of RAJ-II package structural performance come from the regulatory criteria such as yield strength or 1/3 of yield or from the American Society of Mechanical Engineers (ASME) Code (Reference 2-1) for the particular application. Material yield strengths, taken from the ASME Code, used in the analytic acceptance criteria,  $S_y$ , and ultimate strengths,  $S_u$ , are presented in Table 2-2.

#### **2.1.2.2 Containment Structures**

The fuel cladding provides the primary containment for the nuclear fuel.

#### **2.1.2.3 Non-Containment Structures**

For evaluation of lifting devices, the allowable stresses are limited to one-third of the material yield strength, consistent with the requirements of 10 CFR 71.45(a). For evaluation of tie-down devices, the allowable stresses are limited to the material yield strength, consistent with the requirements of 10 CFR 71.45(b).

#### **2.1.2.4 Miscellaneous Structural Failure Modes**

##### **2.1.2.4.1 Brittle Fracture**

By avoiding the use of ferritic steels in the RAJ-II packaging, brittle fracture concerns are precluded. Specifically, most primary structural components are fabricated of austenitic stainless steel. Because this material does not undergo a ductile-to-brittle transition in the temperature range of interest (above -40°F), it is safe from brittle fracture.

The closure bolts used to secure the inner and outer container lids are stainless steel, socket head cap screws ensuring that brittle fracture is not of concern. Other critical fasteners used in the RAJ-II packaging assembly provide redundancy and are made from stainless steel, again eliminating brittle fracture concerns.

#### **2.1.2.4.2 Extreme Total Stress Intensity Range**

Because the response of the RAJ-II package to HAC is typically evaluated empirically rather than analytically, the extreme total stress intensity range has not been quantified. Two full-scale CTUs (see Section 2.12.2) successfully passed free-drop and puncture testing. The CTUs were also fabricated in accordance with the drawings in Section 1.3.1, thus incurring prototypic fabrication induced stresses. Exposure to these conditions has demonstrated leak tight containment of the fuel, geometric configuration stability for criticality safety, and protection for the fuel. Thus the intent of the extreme total stress intensity range requirement has been met.

#### **2.1.2.4.3 Buckling Assessment**

Due to the small diameter of the containment boundary (the fuel rod cladding) and the fact that its radial deflection is limited by the internal fuel pellets, radial buckling is not a failure mode of concern for the containment boundary. Axial buckling deflection is also limited by the inner wall of the IC and lid. The applied axial load to the fuel is also limited by the wood at the end of the packaging. The limited horizontal movement of the fuel during an end drop limits the ability of the fuel to buckle as demonstrated in tests performed on CTU 2 (see Section 2.12.2).

It is also noted that 30-foot drop tests performed on full-scale models with the package in various orientations produced evidence of limited fuel buckling (see Section 2.12.2). Certification testing does not provide a specific determination of the design margin against buckling but is considered as evidence that buckling will be limited. In addition, buckling is a potential concern when ensuring adequate geometric configuration control of the post-accident package for criticality control. This involves not only the internal configuration of the package, but the potential spacing between packages as well. Deformation of the RAJ-II is limited by its redundant structure. The wall of the package acts to stiffen the support plates that carry the load of the IC via the vibration isolating mechanism. Part of the redundant system to minimize deformation of the fuel is the honeycomb that absorbs shocks that would impart side loading to the fuel. The IC, consisting of an inner wall separated from an outer wall by thermal insulation, is lined with cushioning material that supports the fuel. Regardless of the failure mechanism of the support plates, the total deformation is limited by the shock absorbers (honeycomb). These blocks immediately share the load. Hence, even if the support plates would buckle allowing the outer wall to plastically deform, the amount of deformation is limited by the shock absorbing material. This has been demonstrated by testing to only allow 118 mm (4.7 in) of deformation of the shock absorbing blocks. The redundant support system combined with the vibro-isolation and shock absorption system prevents the deformation of the IC and the fuel.

The axial deformation resulting from an end drop is controlled in a similar manner. The end of the OC has a wood shock absorber built in that carries the load from the IC to the outer wall after the vibro-isolation device deflects. This reduces the load carried by the outer wall and support

plates. It prevents large loads and deformations that could contribute to buckling of the fuel. The IC constrains the fuel from large deformations or buckling.

Therefore, the support system prevents buckling of the packaging or fuel that would affect criticality control or containment.

### **2.1.3 Weights and Centers of Gravity**

The maximum gross weight of a RAJ-II package, including a maximum payload weight of 684 kg (1,508 pounds), is 1,614 kg (3,558 pounds). A detailed breakdown of the RAJ-II package component weights is summarized in Table 2-1. The nominal horizontal shift in the Center of Gravity (CG) of the package is approximately 92 mm (3.62 in) from the centerline. The maximum vertical CG of the package is located 421 mm (16.57 in) above the bottom surface of the package when fully loaded. This is taken into account in the lifting and tie-down calculations presented in Section 2.5. Figure 2-1 shows the locations of the center of gravity for the major components and the location of the center of gravity for the assembled package.

### **2.1.4 Identification of Codes and Standards for Package Design**

The radioactive isotopic content of the fuel is primarily U-235 with small amounts of other isotopes that make it Type B. Using the isotopic content limits shown in Section 1.2.2, the package would be considered a Category II for 5.0 wt% U-235 LEU and 8.0 wt% U-235 LEU+. As such the applicable codes that would apply are the ASME Boiler and Pressure Vessel Code (BPVC) Section III, Subsection ND for the containment boundary, which is the fuel cladding, and Section III, Subsection NG for the criticality control structure and Section VIII for the non-containment components.

The fuel cladding, due to its service in the reactor and need for high integrity, is designed and fabricated to standards that exceed those required by ASME Section III Subsection ND. Chapter 6.0 demonstrates that the packaging remains sub-critical. The packaging capabilities are verified by testing and the codes used in fabrication are called out on the drawings in Section 1.3.1. The sheet metal construction of the packaging requires different joint designs and manufacturing techniques that would normally be covered by the above referenced codes.

#### **2.1.4.1 JIS/ASTM Comparison of Materials**

The CTUs were manufactured in Japan using material meeting Japanese Industrial Standards (JIS) specifications. The fuel cladding and pellets were manufactured in the United States (U.S.) to U.S. specifications. The future manufacturing of RAJ-II packages may be performed using U.S. standards (American Society for Testing and Materials (ASTM), or ASME) that are appropriate substitutes for the JIS specifications. To assure that the packaging manufactured in the future meets the performance requirements demonstrated for the RAJ-II CTUs a detailed review of the differences between the U.S. and Japanese standards was performed. The scope of the study included: stainless steel products, wood products, rubber, paper honeycomb, and polyethylene cushioning foam. The study concluded that U.S. standards are compatible to the JIS standards. Future manufacturing of these packages for domestic use may be to U.S. or Japanese specifications meeting the tolerances specified in the general arrangement drawings.



#### 2.1.4.2 JIS/ASME Weld Comparison

Based upon an evaluation, it is concluded that the following standards are equivalent for the purposes of fabrication of the RAJ-II container in the U.S.:

Japanese Specification	U.S. Specification
JIS Z 3821 Standard qualification procedure for welding technique of stainless steel (Reference 2-2)	ASME Section IX (Reference 2-1)
JIS Z 3140 Method of inspection for spot weld (Reference 2-3)	
JIS Z 3145 Method of bend test for stud weld (Reference 2-4)	

#### 2.1.4.3 JIS/JSNDI/ASNT Non-Destructive Examination Personnel Qualification and Certification Comparison

The following standards are considered equivalent for non-destructive examination personnel qualification and certification. Personnel with these qualifications and certifications are authorized to perform examinations of the fabrication inspection requirements for the RAJ-II container in the U.S. Although these documents cover other disciplines, this comparison only applies to liquid penetrant examination.

Japanese Specification <sup>1</sup>	U.S. Specification <sup>2</sup>
JIS Z 2305 Qualification & Certification for NDT Personnel (Reference 2-5)	SNT-TC-1A Recommended Practice (Reference 2-8)
Certification NDIS 0601 (Reference 2-6)	
Certification NDIS J001 (Reference 2-7)	

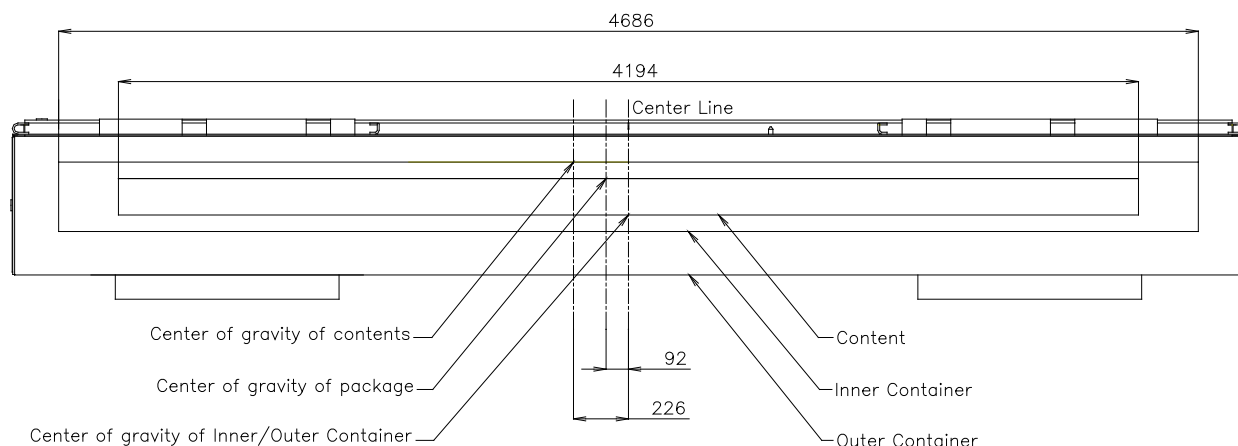
#### Notes:

1. NDIS = Non-destructive Inspection Standard, & JSNDI = Japanese Society for Non-Destructive Inspection.
2. SNT-TC = Society of Non-destructive Testing - Technical Council, & ASNT = American Society of Nondestructive Testing.

NEDO-33869 Revision 11  
Non-Proprietary Information

**Table 2-1      RAJ-II Weight**

Contents	Number of Assemblies per Package	Maximum 2 Assemblies
	Total weight	684 kg (1,508 lb)
Inner Container	Body	200 kg (441 lb) (including bolts)
	Lid	101 kg (223 lb)
	End lids	7 kg (15.4 lb)
	Total Weight	308 kg (679 lb)
Outer Container	Body	485 kg (1,069 lb) (including bolts)
	Lid	137 kg (302 lb)
	Total Weight	622 kg (1,371 lb)
Total Weight of Package		1,614 kg (3,558 lb)



(unit: mm)

**Figure 2-1 Center of Gravity of Package Components**

## 2.2 MATERIALS

### 2.2.1 Material Properties and Specifications

The major structural components (i.e., the OC and IC walls, supports, and attachment blocks) are fabricated from austenitic stainless steel. Other materials performing a structural function are lumber (bolster), balsa (shock absorber), honeycomb (shock absorber), alumina silicate (thermal insulator), polyethylene foam (cushioning material), and zirconium alloy (fuel rod cladding). The drawings presented in Section 1.3.1 delineate the specific material(s) used for each RAJ-II packaging.

The remainder of this section presents and discusses pertinent mechanical properties for the materials that perform a structural function. Both the materials that are used in the analytics and those whose function in the package is demonstrated by test such as the shock absorbing material are presented. In cases where alternate materials may be used, such as with the honeycomb, the critical characteristics of the alternate material are typically equivalent. Alternative materials and their equivalency are detailed out where appropriate. In general, the analytics covering the lifting and tie down capabilities of the package and some normal condition events are limited to the stainless steel structure of the packaging.

Table 2-2 presents the bounding mechanical properties for the Series 300 stainless steel used in the RAJ-II packaging. Each of the representative mechanical properties is those of Type 304 stainless steel and is taken from Section II, Parts A and D, of the ASME BPVC. These properties are applicable to packages that have been made to either JIS or ASME specifications. The density of stainless steel is taken as 0.29 lb/in<sup>3</sup> (8.03E3 kg/m<sup>3</sup>), and Poisson's Ratio is 0.3.

Table 2-3 presents the mechanical properties of the main non-stainless steel components of the package necessary for the structural analysis.

**Table 2-2      Representative Mechanical Properties of Series 300 Stainless Steel Components**

①		②	③	④	⑤
Minimum Elongation (%)	Temperature °C (°F)	Yield Strength, S <sub>y</sub> MPa (×10 <sup>3</sup> psi)	Ultimate Strength, S <sub>u</sub> MPa (×10 <sup>3</sup> psi)	Elastic Modulus, E GPa (×10 <sup>6</sup> psi)	Thermal Expansion Coefficient, α × 10 <sup>-6</sup> mm/mm/°C (×10 <sup>-6</sup> in/in/°F)
35	-29 (-20)	206.8 (30.0)	517.1 (75.0)	-----	-----
40	21 (70)	206.8 (30.0)	517.1 (75.0)	195.1 (28.3)	-----
30	38 (100)	206.8 (30.0)	517.1 (75.0)	-----	15.39 (8.55)
25	93 (200)	172.4 (25.0)	489.5 (71.0)	190.3 (27.6)	15.82 (8.79)
30	149 (300)	155.1 (22.5)	455.1 (66.0)	186.2 (27.0)	16.2 (9.00)
40	204 (400)	142.7 (20.7)	444.0 (64.4)	182.7 (26.5)	16.54 (9.19)
40 <sup>⑥</sup>	23°C <sup>⑥</sup>	205 MPa Min <sup>⑥</sup>	520 MPa Min <sup>⑥</sup>	-----	-----
40 <sup>⑦</sup>	21°C <sup>⑦</sup>	205 MPa Min <sup>⑦</sup>	515 MPa Min <sup>⑦</sup>	-----	-----

**Notes:**

- ① ASME Code, Section II, Part A, (Reference 2-1)
- ② ASME Code, Section II, Part D, Table Y-1, (Reference 2-1)
- ③ ASME Code, Section II, Part D, Table U, (Reference 2-1)
- ④ ASME Code, Section II, Part D, Table TM-1, Material Group G, (Reference 2-1)
- ⑤ ASME Code, Section II, Part D, Table TE-1, 18Cr-8Ni, Coefficient B, (Reference 2-1)
- ⑥ JIS Handbook Ferrous Materials and Metallurgy I, Sections G4303, G4304, G4305 Material Specifications, (Reference 2-9)
- ⑦ ASTM A240 (Reference 2-10), A666 (Reference 2-11), & A276 (Reference 2-12) Material Specifications

NEDO-33869 Revision 11  
Non-Proprietary Information

**Table 2-3 Mechanical Properties of Typical Components**

<b>Materials (Usage)</b>	<b>Yield Stress or Yield Strength</b>	<b>Tensile Strength</b>	<b>Compressive Strength</b>	<b>Bending Strength</b>	<b>Static Initial Peak Stress</b>	<b>Modulus of Longitudinal Elasticity</b>	<b>Density (g/cm<sup>3</sup>)</b>
Lumber (bolster)	56.3 MPa Nominal	—	50.5 MPa Nominal	72.0 MPa Nominal	—	7.85 GPa Nominal	0.53 Nominal
Balsa (shock absorber)	—	—	16 MPa Nominal	—	—	—	0.18 Nominal
Paper or aluminum honeycomb (shock absorber)	—	—	—	—	2.35 MPa Nominal	—	0.06 Nominal
Alumina Silicate (thermal insulator)	—	—	294 kPa Nominal	314 kPa Nominal	—	—	0.25 Nominal
Foam Polyethylene (cushioning foam)	—	—	Approx. 0.2MPa @ 50% strain	—	0.69 MPa Nominal	—	0.068 Nominal
Zirconium Alloy (fuel rods) ASTM B811 (Reference 2-13)	241 MPa (35,000psi)	413 MPa (60,000psi)	—	—	—	97.1 GPa Nominal	6.5 Nominal
Series 300 Stainless Socket Headed Cap Screw	241 MPa (35,000psi) (Min)	379 MPa (75,000psi) (Min)	—	—	—	—	—

## **2.2.2 Chemical, Galvanic, or Other Reactions**

The major materials of construction of the RAJ-II packaging (i.e., austenitic stainless steel, polyethylene foam, alumina thermal insulator, resin impregnated paper or aluminum honeycomb, lumber (hemlock and balsa), and natural rubber) will not have significant chemical, galvanic or other reactions in air, inert gas, or water environments, thereby satisfying the requirements of 10 CFR 71.43(d). These materials have been previously used, without incident, in Radioactive Material (RAM) packages for transport of similar payload materials. A successful RAM packaging history combined with successful use of these fabrication materials in similar industrial environments ensures that the integrity of the RAJ-II package will not be compromised by any chemical, galvanic, or other reactions.

The RAJ-II packaging is primarily constructed of Series 300 stainless steel. This material is highly corrosion resistant to most environments. The metallic structure of the RAJ-II packaging is composed entirely of this material and compatible Series 300 weld material. Because both the base and weld materials are Series 300 materials, they have nearly identical electrochemical potential thereby minimizing any galvanic corrosion that could occur.

The stainless steel within the IC cavity between the inner and outer walls is filled with a ceramic alumina silicate thermal insulator. This material is non-reactive with either the wood or the stainless steel, both dry or in water. The alumina silicate is very low in free chlorides to minimize the potential for stress corrosion of the IC structure.

The polyethylene foam that is used in the IC for cushioning material has been used previously and is compatible with stainless steel. The polyethylene foam is very low in free halogens and chlorides.

Resin impregnated paper or aluminum honeycomb are used in the RAJ-II packaging as cushioning material. The impregnated paper is resistant to water and break down. It is low in leachable halides. The aluminum construction is more susceptible to corrosion than the paper construction, but corrosion of the aluminum honeycomb material would only occur over time with repeated exposure to water. Per Chapter 7, section 7.1.1 inspections, which include checking for corrosion, are performed prior to loading the RAJ-II fuel.

The natural rubber that is used as a gasket for the lids and in the vibro-isolating system contains no corrosives that would adversely affect the RAJ-II packaging. This material is organic in nature and non-corrosive to the stainless steel boundaries of the RAJ-II packaging.

### **2.2.2.1 Content Interaction with Packaging Materials of Construction**

The materials of construction of the RAJ-II packaging are checked for compatibility with the materials that make up the contents or fuel rods that are to be shipped in the RAJ-II. The primary materials of construction of the fuel assembly that could come in contact with the packaging are the stainless steel and the zirconium alloy material that is used for the cladding of the fuel rods. Zirconium alloy (including metal zirconium), stainless steel, and Ni-Cr-Fe alloy, which form a passivated oxide film on the surface under normal atmosphere with slight moisture, are essentially stable. The contact of the above three kinds of metals with polyethylene is chemically stable.

These materials are compatible with the stainless steel, polyethylene, and natural rubber that could come in contact with the contents.

### **2.2.3 Effects of Radiation on Materials**

Because this is an unirradiated fuel package, the radiation to the packaging material is insignificant. Furthermore, the primary materials of construction and containment, austenitic stainless steel and the zirconium alloy cladding of the fuel, are highly resistant to radiation.

## **2.3 FABRICATION AND EXAMINATION**

### **2.3.1 Fabrication**

The RAJ-II is fabricated using standard fabrication techniques. This includes cutting, bending and welding the stainless steel sheet metal. As shown on the drawing the welding is done in accordance with the American Welding Society (AWS) D1.6 (Reference 2-14). The process may also be controlled by ASME Section IX or other international codes. The containment, the cladding of the fuel rods, is fabricated to standards that exceed the required Section VIII of the ASME BPVC due to the service requirements of the fuel in reactors.

### **2.3.2 Examination**

The primary means of examination to determine compliance of the RAJ-II to the design requirements is visual examination of each component and the assembled units. This includes dimensional verification as well as material and weld examination. The materials will also be certified to the material specifications. Shock absorbing material such as the honeycomb will also have verified material properties.

## **2.4 General Requirements for All Packages**

### **2.4.1 Minimum Package Size**

The RAJ-II package is a rectangular box that is 742 mm (29.21 in) high by 720 mm (28.35 in) wide by 5,068 mm (199.53 in) long. Thus, the requirement of 10 CFR 71.43(a) is satisfied.

### **2.4.2 Tamper-Indicating Feature**

Seal pins are provided at each end of the OC body and lid for the use of tamper indicating seals. A tamper indicating seal is attached at each end of the loaded OC by inserting the seal through the holes in the body and lid seal pins and securing the seal. The tamper indicating seal is not readily breakable and would provide evidence of tampering or opening by an unauthorized person. Thus, the requirement of 10 CFR 71.43(b) is satisfied.

### **2.4.3 Positive Closure**

The RAJ-II container is positively closed by means of high strength bolts which require use of tools and deliberate action to facilitate their removal. The number, type, and size of these bolts are provided on the drawings included in Section 1.3.1.

## 2.5 LIFTING AND TIE-DOWN STANDARDS FOR ALL PACKAGES

For analysis of the lifting and tie-down components of the RAJ-II packaging, material properties from Section 2.2 are taken at a temperature of 75°C (167°F) per Section 2.6.1.1. This is the maximum temperature that the container reaches when in the sun. Note that the difference in material properties between 75°C and that given in Section 2.6.1.1 of 77°C is inconsequential. The primary structural material is Series 300 stainless steel that is used in the OC.

A loaded RAJ-II package can be lifted using either a forklift or by slings. The gross weight of the package is a maximum of 1,614 kg (3,558 lb). Locating/protection plates for the forklift and locating angles for the sling locate the lift points for the package. In both cases the package is lifted from beneath. The failure of these locating/protective features would not cause the package to drop nor compromise its ability to perform its required functions.

The IC may be lifted empty or filled with the contents using the sling fittings that are attached at the positions shown in Figure 2-2. The details of the sling fittings are as shown in Figure 2-3 and Figure 2-4. Because the center of gravity depends on existence of the contents, the sling fittings for the filled container and the empty container are marked respectively as "Use When Loaded" and "Use When Empty" to avoid improper operations; see Figure 2-5. The sling fittings on the lid of the IC are marked as "Use for Lifting Lid" for lifting the lid only.

The sling devices are mechanically designed to be able to handle the package and the IC filled with the fuel assemblies in safety; they can lift three times the gross weight of the package, or three times the gross weight of the filled IC, respectively, so that they can withstand rapid lifting.

Properties of Series 300 stainless steel are summarized below in Table 2-4.

**Table 2-4 Properties of Series 300 Stainless Steel**

Material Property	Value	Reference
<b>At 75°C (167°F)</b>		
Elastic Modulus, E	191.7 GPa ( $27.8 \times 10^6$ psi)	Table 2-2
Yield Strength, $\sigma_y$	184.7 MPa (26,788 psi)	
Shear Strength, Equal to (0.6) $\sigma_y$	110.8 MPa (16,073 psi)	



### 2.5.1 Lifting Devices

This section demonstrates that the attachments designed to lift the RAJ-II package are designed with a minimum safety factor of three against yielding, per the requirements of 10 CFR 71.45(a).

The lifting devices on the OC lid are restricted to only lifting the OC lid, and the lifting devices in the inner lid are restricted to only lifting the IC lid. Although these lifting devices are designed with a minimum safety factor of three against yielding, detailed analyses are not specifically included herein because these lifting devices are not intended for lifting a RAJ-II package.

The OC can be handled by either forklift or slings in a basket hitch around the package, requiring no structural component whose failure could affect the performance of the package.

#### 2.5.1.1 Lifting of Inner Container

The IC is lifted when loaded with fuel from the OC with sling fittings attached to the body of the IC. Three pairs (six in total) of the sling fittings are attached to the IC as shown in Figure 2-2. The center of gravity depends upon whether the IC is filled. Because the six sling fittings are the same, the stress in the sling fittings are evaluated for the maximum weight condition that occurs when the IC is filled with fuel assemblies.

The stress on the sling fitting when lifting the IC filled with contents is evaluated by determining the maximum load acting on any given fitting.

The maximum load,  $P_v$ , (see Figure 2-9) acting on one of the sling fitting vertically when lifting is given by the following equation:

$$P_v = \frac{(W_2 + W_3)}{n} \cdot g$$

Where:

$P_v$ : maximum load acting to sling fitting in vertical direction	N
$W_2$ : mass of IC	308 kg (679 lb)
$W_3$ : mass of contents	684 kg (1,508 lb)
$n$ : number of sling fittings	4
$g$ : acceleration of gravity	9.81 m/s <sup>2</sup>

Accordingly, the maximum load acting on the sling fitting vertically is calculated as:

$$P_v = \frac{684 + 308}{4} \times 9.81 = 2.433 \times 10^3 \text{ N (546.9 lbf)}$$

The load,  $P$ , acting to the sling fitting when the sling is at a minimum angle of 60° is calculated as:

$$P = \frac{P_v}{\sin \theta} = \frac{2.433 \times 10^3}{\sin 60^\circ} = 2.809 \times 10^3 \text{ N (631 lbf)}$$

Also, the maximum load,  $P_H$ , acting on the sling fitting horizontally is calculated as:

$$P_H = \frac{P_v}{\tan \theta} = \frac{2.433 \times 10^3}{\tan 60^\circ} = 1.405 \times 10^3 \text{ N (316 lbf)}$$

Each sling fitting is made up of a hooking bar which is a 12 mm (0.47 in) diameter bent rod and a perforated plate that is made up of two pieces of angle that are welded together. The perforated plate of the sling fitting is welded to a support that is welded to the body of the IC.

The shearing stress in the hooking bar (see Figure 2-6) is given by the following equation:

$$\tau_N = \frac{P \times \phi}{A}$$

Where:

$\tau_N$ : shearing stress on hooking bar of sling fitting MPa

P: maximum load  $2.809 \times 10^3 \text{ N (631 lbf)}$

A: cross-section of hooking bar of sling fitting  $\pi/4 \times 12^2 = 113 \text{ mm}^2 (0.175 \text{ in}^2)$

$\phi$ : load factor 3

Accordingly, the shearing stress on the hooking bar of the sling fitting at its center is calculated as:

$$\tau_N = \frac{2.809 \times 10^3 \times 3}{113} = 74.58 \text{ MPa (10,820 psi)}$$

The yield stress for stainless steel is 184.7 MPa (26,790 psi) and the shear allowable is  $0.6 \times 184.7 = 110.8 \text{ MPa (16,070 psi)}$  at the maximum normal temperature, hence the Margin of Safety (MS) is:

$$MS = \frac{110.8}{74.58} - 1 = 0.48$$

Therefore, the sling fitting can withstand three times the load without yielding in shear.

The strength of the perforated plate of a sling fitting is evaluated for failure by shearing. The shear stress on a perforated plate (see Figure 2-7) of the sling fitting by the total load is given by the following equation:

$$\tau_N = \frac{P \cdot \phi}{A}$$

Where:

$\tau_N$ : shearing stress on the perforated plate of a sling fitting MPa

P: maximum load  $2.809 \times 10^3 \text{ N (631 lbf)}$

A: cross-section of the upper part of the perforated plate

$$2 \times \frac{50 - 14}{2} \times 6 = 216 \text{ mm}^2 (0.33 \text{ in}^2)$$

$\phi$ : load factor 3

Accordingly, the shearing stress,  $\tau_N$ , on the perforated plate of sling fitting is calculated as:

$$\tau_N = \frac{2.809 \times 10^3 \times 3}{216} = 39.01 \text{ MPa (5,658 psi)}$$

The allowable shearing stress for stainless steel is 110.8 MPa (16,073 psi). Then the margin of safety is:

$$MS = \frac{110.8}{39.01} - 1 = 1.84$$

Therefore, the shear strength of the plate meets the requirement of not yielding under three times the load.

Next, the strength of the welds of the sling fittings is evaluated for the torsional loads applied. Torsional loads are applied to the welds of the sling fittings per Figure 2-8.

The moment of inertia of area,  $I_P$ , to the welds of sling fittings is given by the following equation:

$$I_P = I_X + I_Y$$

$$I_X = I_{X2} - I_{X1}$$

$$I_Y = \sum I_{Yi}$$

Where:

$I_P$  : moment of inertia of area to welds  $\text{mm}^4$

$I_X$  : moment of inertia of area to welds for X-axis  $\text{mm}^4$

$I_Y$  : moment of inertia of area to welds for Y-axis  $\text{mm}^4$

$I_{X1}$  : moment of inertia of area to inside of weld for X-axis  $\text{mm}^4$

$I_{X2}$  : moment of inertia of area to outside of weld for X-axis  $\text{mm}^4$

$I_{Yi}$  : moment of inertia of area to each weld for Y-axis  $\text{mm}^4$

The moment of inertia of area,  $I$ , to a cross-sectional area of width,  $b$ , and height,  $h$ , is given by:

$$I = \frac{1}{12} b h^3$$

Conservatively only the outside welds, not including any corner wrap around, that attach the sling fitting to the support plate are considered. Thus, the moment of inertia of area,  $I_X$  and  $I_Y$  to the welds for X-axis and Y-axis are calculated as:

$$I_X = \left(\frac{1}{12} \times 88 \times 54^3\right) - \left(\frac{1}{12} \times 88 \times 50^3\right) = 2.38 \times 10^5 \text{ mm}^4 (0.57 \text{ in}^4)$$

$$I_Y = 2I_{Y1} = 2 \times \frac{1}{12} \times 2 \times 88^3 = 2.27 \times 10^5 \text{ mm}^4 (0.55 \text{ in}^4)$$

Accordingly, the moment of inertia of area,  $I_P$ , to the welds is calculated as:

$$I_P = (2.38 \times 10^5) + (2.27 \times 10^5) = 4.65 \times 10^5 \text{ mm}^4 (1.12 \text{ in}^4)$$

The shearing stress,  $S_d$ , on the weld due to the load acting on the sling fitting is given by the following equation:

$$S_d = \frac{P \cdot \phi}{A}$$

Where:

$S_d$ : shearing stress on welds due to the load to sling fitting	MPa
$P$ : maximum load acting to one of sling fitting	$2.809 \times 10^3 \text{ N (631 lbf)}$
$A$ : overall cross-section of welds	$2 \times 88 = 176 \text{ mm}^2 (0.273 \text{ in}^2)$
$\phi$ : load factor	3

Accordingly, the shearing stress on welds due to the load acting to the sling fitting is calculated as:

$$S_d = \frac{2.809 \times 10^3 \times 3}{176} = 47.9 \text{ MPa (6,950 psi)}$$

The maximum bending moment acting to the sling fitting is given by the following equation (see Figure 2-9):

$$M_{\max} = P \cdot l$$

Where:

$M_{\max}$ : maximum bending moment acting to sling fitting	N · mm
$P$ : maximum load acting to one of sling fitting	$2.809 \times 10^3 \text{ N (631 lbf)}$
$l$ : distance from fulcrum to load point	17 mm (0.67 in)

Therefore, the maximum bending moment acting to the sling fitting is calculated as:

$$\begin{aligned} M_{\max} &= 2.809 \times 10^3 \times 17 \\ &= 4.8 \times 10^4 \text{ N} \cdot \text{mm (424.8 in} \cdot \text{lbf)} \end{aligned}$$

NEDO-33869 Revision 11  
Non-Proprietary Information

The stress due to this bending moment is given by the following equation:

$$S_m = \frac{M_{\max} \cdot r \cdot \phi}{I_p}$$

Where:

$S_m$ : Stress acting to a point at  $r$  from center of gravity due to bending moment    MPa

$r$ : distance from center of gravity to end of welds     $\sqrt{44^2 + 25^2} = 50.6 \text{ mm (1.99 in)}$

$M_{\max}$ : maximum bending moment acting to sling fitting

$$4.8 \times 10^4 \text{ N}\cdot\text{mm (424.8 in}\cdot\text{lbf)}$$

$I_p$ : moment of inertia of area to welds     $4.65 \times 10^5 \text{ mm}^4 (1.12 \text{ in}^4)$

$\phi$ : load factor    3

From this equation, the maximum bending moment,  $S_m$ , acting to the sling fitting is calculated as:

$$S_m = \frac{4.8 \times 10^4 \times 50.6 \times 3}{4.65 \times 10^5} = 15.6 \text{ MPa (2,260 psi)}$$

In addition, the composite shearing stress,  $S$ , on the weld is given by the following equation:

$$S = \sqrt{S_d^2 + S_m^2 + 2S_d S_m \cos\theta}$$

Where:

$$\cos\theta = 25/50.6$$

From this equation, the composite shearing stress,  $S$ , is calculated as:

$$\begin{aligned} S &= \sqrt{47.9^2 + 15.6^2 + 2 \times 47.9 \times 15.6 \times 25/50.6} \\ &= 57.2 \text{ MPa (8,300 psi)} \end{aligned}$$

The allowable shearing stress for Series 300 stainless steel is 110.8 MPa (16,073 psi). Then the margin of safety is:

$$MS = \frac{110.8}{57.2} - 1 = 0.94$$

The welds are capable of carrying three times the expected load without yielding.

Likewise, the welds of the support plates for sling fittings are evaluated in the same manner. Because the welds of the support plates (see Figure 2-10) receive the same load as mentioned above in the case of the welds of the sling fittings, it is evaluated by same analytic method as mentioned above. The symbols used here shall have the same meaning. Note the support plate thickness of the sling fittings is 4 mm (0.16 in).

The moment of inertia of area,  $I_P$ , to the welds on the support plate is given by the following equation:

$$I_P = I_X + I_Y$$

Where:

$$I_X = I_{X2} - I_{X1}$$

$$I_Y = I_{Y2} - I_{Y1}$$

The moment of inertia of areas  $I_X$  and  $I_Y$  to the welds for X-axis and Y-axis are calculated as:

$$\begin{aligned} I_X &= \frac{1}{12} \times 153 \times 83^3 - \frac{1}{12} \times 150 \times 80^3 \\ &= 8.903 \times 10^5 \text{ mm}^4 (2.14 \text{ in}^4) \end{aligned}$$

$$\begin{aligned} I_Y &= \frac{1}{12} \times 83 \times 153^3 - \frac{1}{12} \times 80 \times 150^3 \\ &= 2.273 \times 10^6 \text{ mm}^4 (5.46 \text{ in}^4) \end{aligned}$$

Accordingly, the moments of inertia of areas to the welds for the support plates are calculated as:

$$\begin{aligned} I_P &= 8.903 \times 10^5 + 2.273 \times 10^6 \\ &= 3.163 \times 10^6 \text{ mm}^4 (7.60 \text{ in}^4) \end{aligned}$$

The overall cross-section,  $A$ , of welds of the support plate is:

$$\begin{aligned} A &= (153 \times 83) - (150 \times 80) \\ &= 699 \text{ mm}^2 (1.08 \text{ in}^2) \end{aligned}$$

The shearing stress,  $S_d$ , on the welds of the support plate for the sling fitting is calculated by a similar equation as the welds of the sling fitting.

$$S_d = \frac{2.809 \times 10^3 \times 3}{699} = 12.1 \text{ MPa (1,760 psi)}$$

The stress,  $S_m$ , on the welds of the support plate due to the bending moment is calculated as:

$$S_m = \frac{5.9 \times 10^4 \times 85 \times 3}{3.163 \times 10^6} = 4.76 \text{ MPa (690 psi)}$$

Where:

$$r = \sqrt{75^2 + 40^2} = 85 \text{ mm (3.35 in)}$$

$$M_{\max} = 2.809 \times 10^3 \times (17 + 4) = 5.9 \times 10^4 \text{ N}\cdot\text{mm (522.1 in}\cdot\text{lbf)}$$

The composite shearing stress  $S$  on the welds of support plate is calculated as:

$$S = \sqrt{S_d^2 + S_m^2 + 2S_d S_m \cos\theta}$$

Where:

$$\cos\theta = 40/85$$

$$\begin{aligned} S &= \sqrt{12.1^2 + 4.76^2 + (2 \times 12.1 \times 4.76 \times (40/85))} \\ &= 14.9 \text{ MPa (2,160 psi)} \end{aligned}$$

The allowable shearing stress for Series 300 stainless steel is 110.8 MPa (16,073 psi). Therefore, the margin of safety is:

$$MS = \frac{110.8}{14.9} - 1 = 6.4$$

Therefore, the support plate welds are capable of carrying three times the normal load and not yielding.

As indicated by the margins of safety calculated for each component, the hook bar has the lowest margin. Therefore, in case of an overload, the hook bar will fail prior to any other component. This ensures that, at failure, the rest of the packaging is capable of performing its function of protecting the fuel.

#### 2.5.1.1.1 Effect of Horizontal CG Offset

The nominal horizontal CG of the IC is approximately offset by 145 mm (5.71 in) from the centerline of the IC, as illustrated in Figure 2-5. This results in a small shift in the loading from one end of the package to the other. The stresses reported in Section 2.5.1.1 are linearly proportional to the load acting upon the sling. The hook bar is the limiting structural component when lifting the IC. The maximum allowable sling load satisfying the load factor of three is calculated as:

$$P_{\max} = \frac{110.8}{\phi} \cdot A = \frac{110.8}{3} \cdot \pi / 4 \cdot 12^2 = 4.177 \times 10^3 \text{ N (939.0 lbf)}$$

The corresponding maximum load acting on the sling fitting vertically is calculated as:

$$P_{v, \max} = P_{\max} \cdot \sin \theta = 4.177 \times 10^3 \cdot \sin 60^\circ = 3.617 \times 10^3 \text{ N (813.2 lbf)}$$

The maximum horizontal CG offset of the IC is calculated as:

$$CG_{\text{off}} = \frac{P_{v, \max} \cdot n/2}{(W_2 + W_3) \cdot g} \cdot (D_A + D_B) - D_B$$

Where:

$CG_{\text{off}}$ : maximum allowable horizontal CG offset of the IC mm (in)

$D_B$ : Minimum horizontal distance from IC sling fitting to nominal CG offset

$$1370-145 = 1225 \text{ mm (48.23 in)}$$

$D_A$ : Maximum horizontal distance for IC sling fitting to nominal CG offset

$$2630-1370+145 = 1405 \text{ mm (55.31 in)}$$

Accordingly, the maximum allowable horizontal CG offset of the IC is calculated as:

$$CG_{\text{off}} = \frac{3.617 \times 10^3 \cdot 4/2}{(684 + 308) \cdot 9.81} \cdot (1405 + 1225) - 1225 = 730 \text{ mm (28.75 in)}$$

The nominal horizontal CG offset of the IC of 145 mm (5.71 in) is less than the maximum allowable horizontal CG offset of 730 mm (28.75 in) required to satisfy a load factor of three on all IC lifting components. The magnitude of CG offset difference is more than a factor of five, and thus the structural effects are concluded as negligible.

#### **2.5.1.2 Package Lifting Using the Outer Container Lid Lifting Lugs**

The OC lid is lifted by four (4) Ø8 mm (Ø0.315 in) Type 304 stainless steel bars that are welded to the 50 × 50 × 4 stainless steel lid flange angle. Under a potential excessive loading condition, such as lifting the entire loaded package, these four lifting lugs are required to fail prior to damaging the OC lid structure.

The OC lid is also equipped with the four (4) Ø6 mm (Ø0.236 in) Type 304 stainless steel bar handles, which may be used to manually lift the lid. These bars are welded to the vertical leg of the lid flange angle with single-sided flare-bevel welds for an approximate length of 13 mm, as shown in View G-G on general arrangement drawing 105E3743 (Section 1.3.1). Because the handles have smaller cross-section (Ø6 mm vs. Ø8 mm), and have smaller and shorter attachment welds, the analysis of the lid lifting bars bounds the handles.

The four lifting bars will be used for this analysis with an assumed lifting angle of 45 degrees. From Table 2-1, the RAJ-II package weighs 1,614 kg [15,827 N] (3,558 lb). For the assumed lifting arrangement, the maximum load on the bar is:

$$F = 1/4 \left[ \frac{15,827}{\sin 45^\circ} \right] = 5,596 \text{ N (1,258 lbs)}$$



NEDO-33869 Revision 11  
Non-Proprietary Information

Assuming that the lift point is centered above the midpoint of the package (located 1,025 mm longitudinally and 318 mm laterally from lifting bar), the resultant forces on the lifting bar will be:

$$F_{\text{horizontal}} = F_{\text{vertical}} = F \cos 45^\circ = 3,957 \text{ N (890 lbs)}$$

$$F_{//} = F_{\text{horizontal}} \sin(\tan^{-1}\left(\frac{1,025}{318}\right)) = 3,779 \text{ N (850 lbs)}$$

$$F_{\perp} = F_{\text{horizontal}} \cos(\tan^{-1}\left(\frac{1,025}{318}\right)) = 1,173 \text{ N (264 lbs)}$$

Where:  $F_{\text{horizontal}}$  = Force in horizontal plane  
 $F_{//}$  = Force parallel to longitudinal axis of package  
 $F_{\perp}$  = Force perpendicular to longitudinal axis of package

These reaction loads will develop both bending and shear stresses in the bar, shear stresses in the attachment welds, and tensile stresses in the flange angle. Each of these stress components will be analyzed separately.

### **Bending of Bar**

The maximum reaction load on the lifting bar will be bending stresses in the bar. Treating the bar as a fixed-fixed beam, the maximum bending stress,  $\sigma_b$ , will be:

$$\sigma_b = \frac{M_{\text{max}}}{Z_{\text{bar}}}$$

Where:  $M_{\text{max}} = 1/8[(F_{\text{vertical}})^2 + (F_{//})^2]^{1/2}(l) = 1/8(5,472)(76) = 51,984 \text{ N-mm (460 lbf-in)}$   
 $Z_{\text{bar}} = \pi(d^3)/32 = \pi(8^3)/32 = 50.3 \text{ mm}^3 (0.003 \text{ in}^3)$   
 $l = 2(46-8) = 76 \text{ mm (2.99 in)}$  [assumed equal to bent free length of bar]

Substituting these values results in a maximum bending stress of 1,033 MPa (149,824 psi). The allowable bending stress for the Type 304 material is equal to  $S_y = 184.7 \text{ MPa (26,788 psi)}$ . Therefore, the margin of safety against yielding in bending is:

$$MS = \frac{184.7}{1,033} - 1.0 = -0.8$$

### **Shear of Bar**

The maximum reaction load on the lifting bar will result in shear stresses in the bar. For the shearing of the bar, the maximum shear stress will be:

$$\tau_{\text{bar}} = \frac{[(F_{\text{vertical}})^2 + (F_{//})^2]^{1/2}}{\text{Area}} = \frac{5,472}{(\pi/4)(8)^2} = 108.9 \text{ MPa (15,795 psi)}$$

NEDO-33869 Revision 11  
Non-Proprietary Information

The allowable shear stress for the Type 304 material is equal to  $0.6S_y = 0.6(184.7) = 110.8$  MPa (16,070 psi). Therefore, the margin of safety against yielding in shear is:

$$MS = \frac{110.8}{108.9} - 1.0 = +0.02$$

### **Tension in Bar**

Because the bending stress is well beyond the yield strength, the bar will bend until the reaction load will be reacted as pure tension in the bar. For this condition, the tensile stress,  $\sigma_{t\text{-bar}}$ , in the bar will be:

$$\sigma_{t\text{-bar}} = \frac{F}{2(\text{Area})} = \frac{5,596}{2[(\pi/4)(8^2)]} = 55.7 \text{ MPa (8,079 psi)}$$

The allowable tensile stress for the Type 304 material is equal to the minimum yield strength, 184.7 MPa (26,788 psi). The margin of safety for this condition is then:

$$MS = \frac{184.7}{55.7} - 1.0 = +2.3$$

### **Attachment Welds**

As shown in View F-F on general arrangement drawing 105E3743 (Section 1.3.1), the lifting bars are welded to the lid flange angle with double-sided flare-bevel welds for an approximate length of 28 mm (1.10 in) on each leg of the bar. The ends of the bar are welded with a seal fillet weld, which has minimal strength and hence, will be ignored. Because the bar is relatively small, the flare-bevel weld will be treated as an equivalent fillet weld with a 4 mm leg. For this assumption, the maximum primary shear stress,  $\tau_{\text{weld}}$ , in the weld will be:

$$\tau_{\text{weld}} = \frac{[(F_{\text{vertical}})^2 + (F_{\parallel})^2]^{1/2}}{\text{Shear area of welds}} = \frac{5,472}{4(4 \cos 45^\circ)(28)} = 17.3 \text{ MPa (2,509 psi)}$$

Due to the offset, there will also be a secondary (torsion) shear stress,  $\tau'_{\text{weld}}$ , component:

$$\tau'_{\text{weld}} = \frac{Mr}{J}$$

Where:

M = applied moment to weld group

$$= [(F_{\text{vertical}})^2 + (F_{\parallel})^2]^{1/2}(\text{distance from centroid} + \text{bend radius} + 1/2 \text{bar diameter})$$

$$= 5,472(14 + 8 + 4) = 142,272 \text{ N-mm (1,259 lbf-in)}$$

r = distance from centroid of weld group to farthest point in weld

$$= [(1/2(46-8))^2 + (14)^2]^{1/2} = 23.6 \text{ mm (0.929 in)}$$

J = second polar moment of inertia of weld group,  $\text{mm}^4$

NEDO-33869 Revision 11  
Non-Proprietary Information

Because the four flare-bevel welds are the same size and location, the second polar moment of inertia for the weld group is determined treating the welds as a line (Reference 2-15). For this case, the second polar moment of inertia is:

$$J = 0.707(h) \frac{d(3b^2 + d^2)}{6}$$

Where:  $h$  = leg length of weld = 4 mm

$d$  = length of weld = 28 mm

$b$  = distance between weld groups =  $(46^2 + 46^2)^{1/2} = 65.1$  mm

Substituting these values results in a secondary polar moment of inertia of 178,138 mm<sup>4</sup> (0.428 in<sup>4</sup>). The secondary shear stress then becomes:

$$\tau'_{\text{weld}} = \frac{(142,272)(23.6)}{178,138} = 18.8 \text{ MPa (2,727 psi)}$$

The total shear stress in the weld is then the square root of the sum of the squares of the primary shear and secondary shear:

$$\tau_{\text{total}} = \left[ (\tau_{\text{weld}})^2 + (\tau'_{\text{weld}})^2 \right]^{1/2} = 25.5 \text{ MPa (3,698 psi)}$$

The allowable shear stress for the Type 304 material is equal to 110.8 MPa (16,070 psi). Therefore, the margin of safety against yielding in shear for the welds is:

$$\text{MS} = \frac{110.8}{25.5} - 1.0 = +3.3$$

### **Shear Tearout of Base Metal**

Shear tearout of the 4 mm thick base metal is evaluated by conservatively considering only the area of a section equal to the weld length of the two welds. The 2 mm (0.08 in) thick sheet that is attached to the vertical leg of the flange angle is ignored for this calculation. The total shear area,  $A_{\text{shear}}$ , will be:

$$A_{\text{shear}} = 2[4(28)] = 224 \text{ mm}^2 (0.347 \text{ in}^2)$$

For this case, the shear stress of the base metal,  $\tau_{\text{basemetal}}$ , is:

$$\tau_{\text{base metal}} = \frac{F}{A_{\text{shear}}} = \frac{5,596}{224} = 25.0 \text{ MPa (3,624 psi)}$$

The allowable shear stress for the Type 304 material is equal to 110.8 MPa (16,070 psi). The margin of safety for this condition is then:

$$\text{MS} = \frac{110.8}{25.0} - 1.0 = +3.4$$

## **Summary**

As demonstrated by these calculations, the minimum margin of safety for the OC lid lifting lugs is -0.8, which results in failure of the bar in bending for lifting the complete loaded package. The largest positive margin of safety (+3.4) occurs in the base metal of the lid flange angle, which demonstrates that the OC lid structure would not fail in an excessive load condition. All other margins of safety in the load path are positive but are lower than the base metal. Therefore, potentially lifting the complete package by these lid lifting lugs will fail the lifting bar and have no detrimental effect on the effectiveness of the RAJ-II package.

### **2.5.2 Tie-Down Devices**

There are no tie-down features that are a structural part of the RAJ-II package. The packages are transported either in container vans or on flatbed trucks. When transported in container vans, blocking and bracing is provided that distributes any loads into the packages. This bracing and blocking is customized to address individual shipping configurations and the specific container van being used. When transported on a flatbed trailer, straps going over the package are used to secure it to the trailer. Therefore, the requirements of 10 CFR 71.45(b) are satisfied because no structural part of the package is used as a tie-down device.

An evaluation is performed on the ability of the package to withstand loadings of 2g vertical and 5g laterally when restrained by strapping. The worst-case loading situation for the packages is when they are stacked in groups of nine on a flatbed trailer and secured with a minimum of three straps. Although the packages may be shipped in other configurations such as 2x3 the greatest strap loading that would be applied to the package is when it is secured in a 3x3 configuration. Between each adjacent column of packages  $2 \times 4$  wood shoring may be placed where the straps will be applied. The evaluation below is conservatively performed without the  $2 \times 4$  shoring in place.

As a bounding evaluation, it is assumed that the outside corners of the top outside packages carry all the vertical loads that would result from the vertical acceleration and the vertical load required to resist the over-turning moment from the horizontal acceleration. The corners of all top packages would actually carry the vertical load. See Figure 2-11.

For modeling purposes, the matrix of nine packages is treated as a rigid body. By summing moments, the vertical force required to prevent the over-turning of the stack by the horizontal loads is determined. This load is conservatively applied to one edge of one container.

The key dimensions and weights for each package are:

Width	$w = 720 \text{ mm (28.3in)}$
Total height	$h = 742 \text{ mm (29.2in)}$
CG height	$cgy = 421 \text{ mm (16.6 in)}$
Mass of each package	$m = 1,614 \text{ kg (3,558 lb)}$
Gravitational acceleration	$g = 9.81 \text{ m/sec}^2$

NEDO-33869 Revision 11  
Non-Proprietary Information

Vertical acceleration factor  $g_v = 2$

Horizontal acceleration factor  $g_h = 5$

The vertical center of gravity of the 9-package matrix is:

$$CG_y = 3mg(2h + cgy)/9mg + 3mg(h + cgy)/9mg + 3mg(cgy)/9mg = 1.163 \times 10^3 \text{ mm (45.8 in)}$$

Summing the forces in the vertical direction due to the 2g loading, the strap load applied at the two locations can be determined for this load condition.

$$R_{st} = 9 g_v m g/2 = 1.425 \times 10^5 \text{ N (3.202} \times 10^4 \text{ lbf)}$$

Summing moments about one of the bottom corners of the stack will determine the strap force required to resist overturning due to the horizontal loading.

$$R_s = \frac{(g_h(CG_y)9mg)}{(3w)} = 3.835 \times 10^5 \text{ N (8.621} \times 10^4 \text{ lbf)}$$

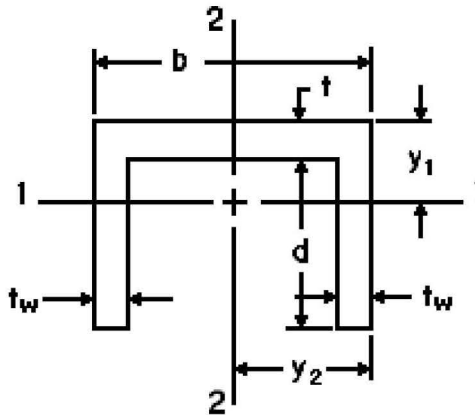
Total vertical strap load is:

$$R_t = R_{st} + R_s = 5.260 \times 10^5 \text{ N (1.182} \times 10^5 \text{ lbf)}$$

Checking the support plate carrying capability:

There are eight (8) 5 mm  $\times$  55 mm support plates in groups of two (2) that carry the vibro-isolation frame inside the OC. These are skip welded to the wall, plus have two thick (10 mm and 15 mm) by 80 mm and 70 mm wide plates welded between them. These plates are in addition to the body straps and the body struts (angles) in the corners that provide vertical stiffening to the side panels. On top of the side panel, there are two angles that make up the flange in both the body and the lid that provide load distribution capability to the side wall and the internal structure. In addition, these angles are stiffened at the ends by the bolster support angle that further distributes the end strap loads to the end structure of the package reducing load in the sides of the package.

Because the eight support plates are assembled together in groups of two with the reinforcement plates connecting the plates along with the welding to the wall, each two-plate section is considered as a column that is capable of carrying the tie-down loads. By addressing the support plates as a channel section, which is 140 mm wide and 57 mm deep, its properties can be determined.



Channel section

Length of web  $b = 140 \text{ mm (5.5 in)}$

Length of flange  $d = 55 \text{ mm (2.2 in)}$

Web thickness  $t = 2 \text{ mm (0.08 in)}$

Flange thickness  $t_w = 5 \text{ mm (0.2 in)}$

Area  $A = tb + 2t_w d = 830.3 \text{ mm}^2 (1.287 \text{ in}^2)$

Because there are four of these assemblies to a side the total area is:

$$A_{\text{spt}} = 4A = 3,321 \text{ mm}^2 (5.148 \text{ in}^2)$$

The compressive stress is:

$$\sigma_c = R_t / A_{\text{spt}} = 158.4 \text{ MPa (23.0 ksi)}$$

This is less than the yield stress of the Type 304 stainless steel  $S_y = 206.8 \text{ MPa (30.0 ksi)}$ .

The resistance of the plate to buckling is also evaluated. The equation to obtain the moments of inertia of areas of the support plate which are subject to buckling is:

$$y_1 = (bt^2 + 2t_w d(2t + d)) / (2(tb + 2t_w d)) = 19.9 \text{ mm (0.783 in)}$$

$$y_2 = b/2 = 70 \text{ mm (2.756 in)}$$

Moments of Inertia

$$I_1 = b(d+t)^3/3 + d^3(b-2t_w)/3 - A(d+t-y_1)^2 = 2.894 \times 10^5 \text{ mm}^4 (0.695 \text{ in}^4)$$

$$I_2 = (d+t)b^3/12 - d(b-2t_w)^3/12 = 2.110 \times 10^7 \text{ mm}^4 (7.122 \text{ in}^4)$$

The radius of gyration can then be calculated for each axis:

$$r_1 = \sqrt{\frac{I_1}{A}} = 18.7 \text{ mm (0.736 in)} \quad r_2 = \sqrt{\frac{I_2}{A}} = 59.7 \text{ mm (2.35 in)}$$

The minimum radius of gyration indicates the weakest orientation for buckling:

$$k = r_1 = 18.7 \text{ mm (0.736 in)}$$

$$\ell: \text{Length of support plate} = 160 \text{ mm (6.3 in)}$$

The slenderness ratio,  $\frac{\ell}{k}$ , is:

$$\frac{\ell}{k} = \frac{160}{18.7} = 8.6$$

As the ends are fixed, the coefficient “n” becomes 4, so the limit value of the slenderness ratio becomes:

$$85\sqrt{n} = 85\sqrt{4} = 170$$

Because the slenderness ratio of this material is less than the limit value slenderness ratio, Euler's equation is not applicable, and the secant formula for buckling is used. The equation to obtain the support plate's buckling strength is:

$$\frac{P}{A} = \frac{S_y}{1 + \frac{ec}{k^2} \sec \left[ \frac{C\ell}{2k} \sqrt{\frac{P}{AE}} \right]}$$

Where: P: Buckling strength (load) of support column

A: Area of column = 830.3 mm<sup>2</sup> (1.287 in<sup>2</sup>)

S<sub>y</sub>: Minimum yield strength of Type 304 stainless steel = 206.8 MPa (30.0 ksi)

C: Coefficient to the long support fixed at both ends = 1.2

E: Elastic modulus of Type 304 stainless steel = 1.95 × 10<sup>5</sup> MPa (Table 2-2)

e: Eccentricity (small because the strap load is centered) = 5 mm (0.2 in)

ℓ: Unsupported length of the support column = 160 mm (6.3 in)

c: Shortest distance to an outside side edge from the centroid = 19.9 mm (0.783 in)

Substituting these values in the above equation and solving for P iteratively results in a buckling strength of the support plate column of:

$$P = 1.332 \times 10^5 \text{ N (29,945 lbf)}$$

NEDO-33869 Revision 11  
Non-Proprietary Information

There are four support columns to a side, which results in the sidewall frame having a minimum capacity of:

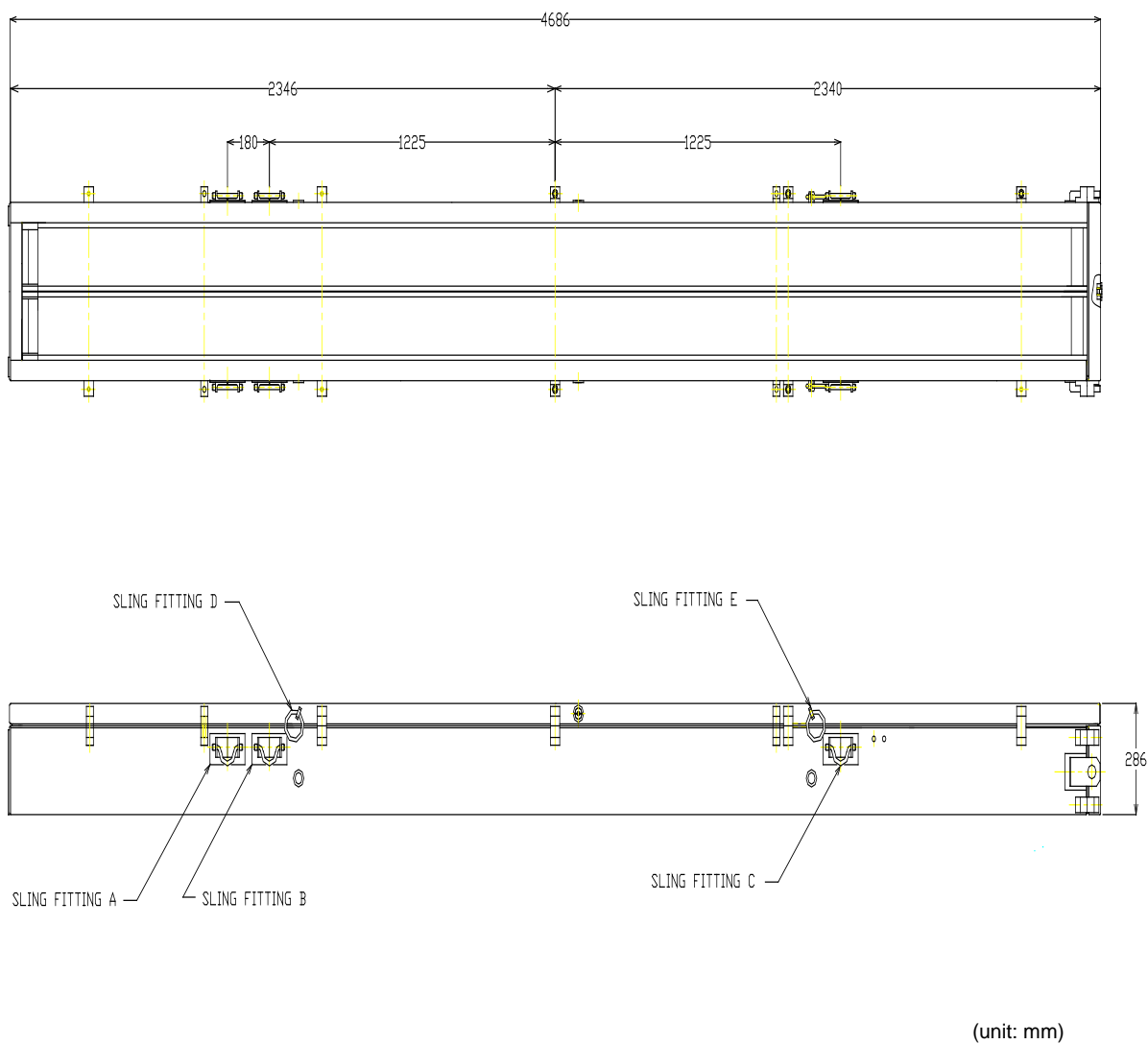
$$P_t = 4P = 5.328 \times 10^5 \text{ N (119,780 lbf)}$$

Because this load capacity is greater than the applied load ( $R_t = 5.259 \times 10^5 \text{ N (1.182} \times 10^5 \text{ lbf)}$ ), the supports will not buckle when the worst-case tie-down loads are applied to a package. This capacity approaches the force required to yield the columns in compression (i.e.,  $A_{spt}S_y = 6.868 \times 10^5 \text{ N (1.544} \times 10^5 \text{ lbf)}$ ).

By considering the stiffening of the support plates with the reinforcement plates used to carry the inner support frame, it has been demonstrated that the support plates have sufficient capacity to react the tie-down load if the package experiences a 5g lateral and a 2g vertical loading simultaneously. This evaluation does not take into consideration the large carrying capability of the ends of the package where there are corner angles, end plates, and wood overlay plates that further strengthen the package's buckling capability. The use of three or more straps ensures that the load is distributed along the package so that the load can be reacted by the support plates and other internal structure. The stiffness of the OC lid, when the bolster support angles are considered with the reinforced edge of the OC body, ensures that the load is distributed to the internal structure of the package.

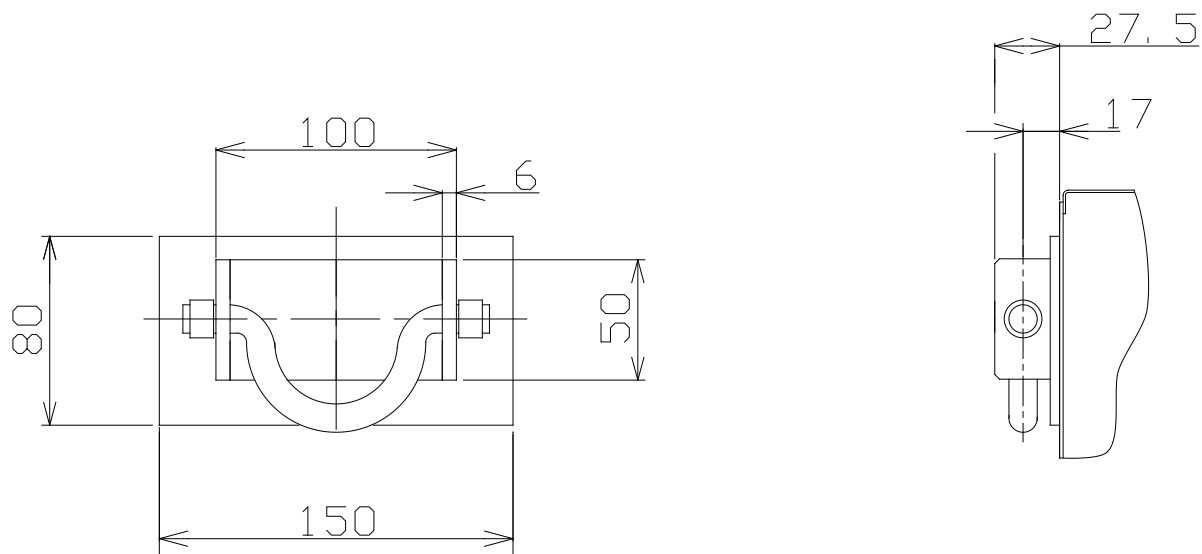


NEDO-33869 Revision 11  
Non-Proprietary Information



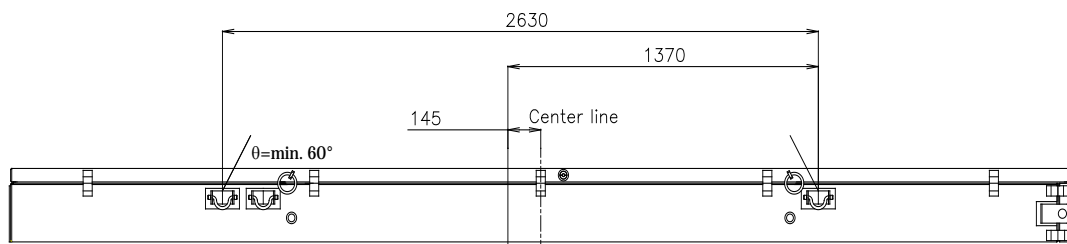
Combination of Sling Fitting	Used For
A and C	Lifting a Loaded Container
B and C	Lifting an Empty Container
D and E	Lifting a Lid

**Figure 2-2 Inner Container Sling Locations**



(unit: mm)

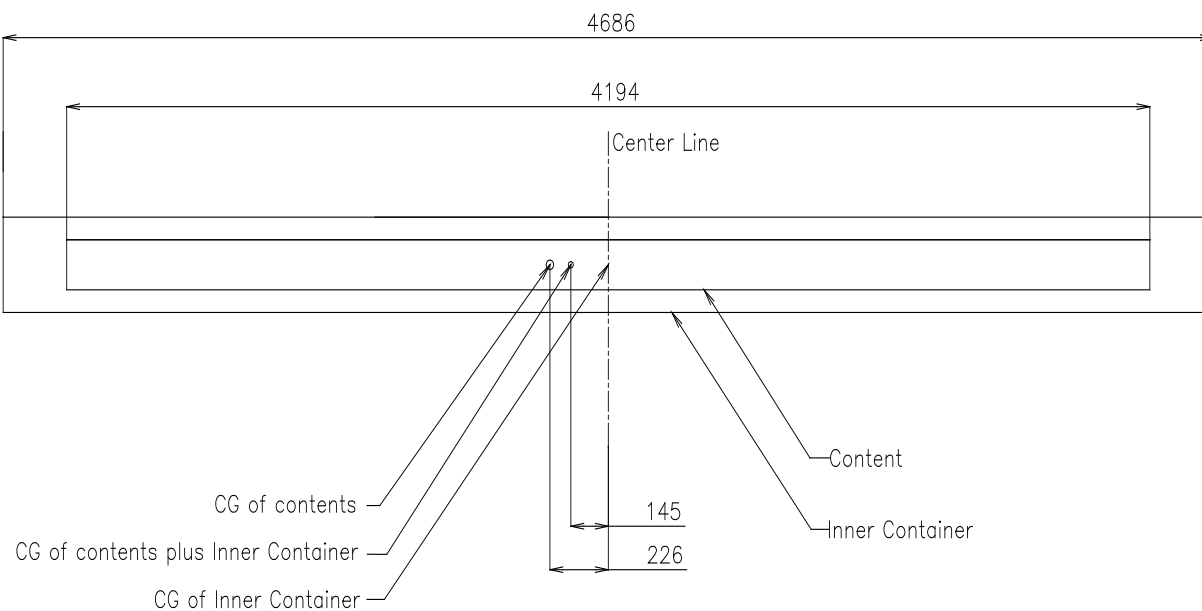
**Figure 2-3 Sling Attachment Plate Details**



(unit: mm)

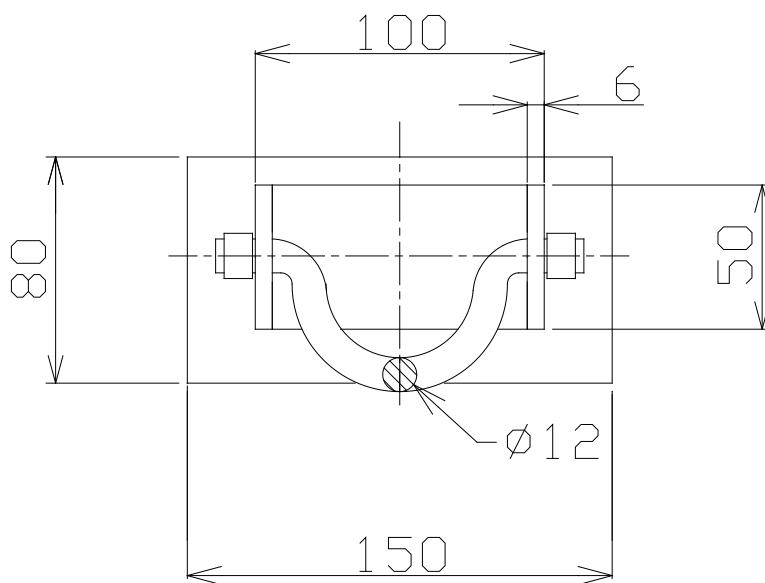
**Figure 2-4 Lifting Configuration of Inner Container**

NEDO-33869 Revision 11  
Non-Proprietary Information



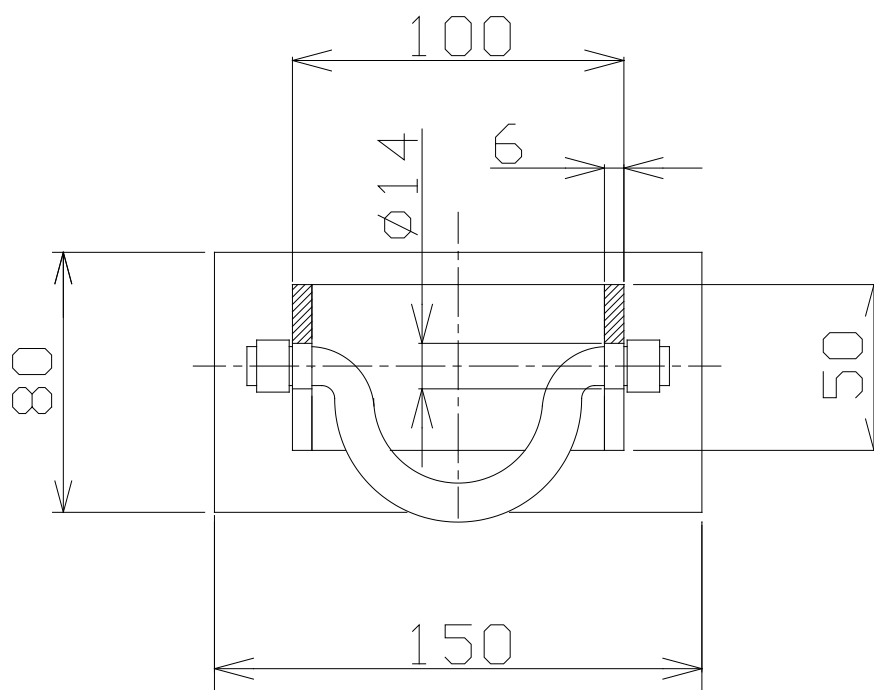
(unit: mm)

**Figure 2-5 Center of Gravity of Loaded Inner Container**



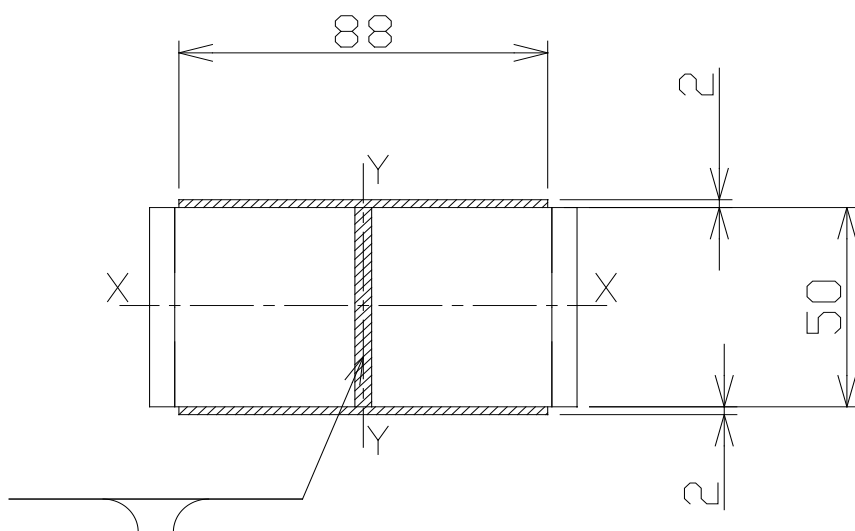
(unit: mm)

**Figure 2-6 Hooking Bar of Sling Fitting**



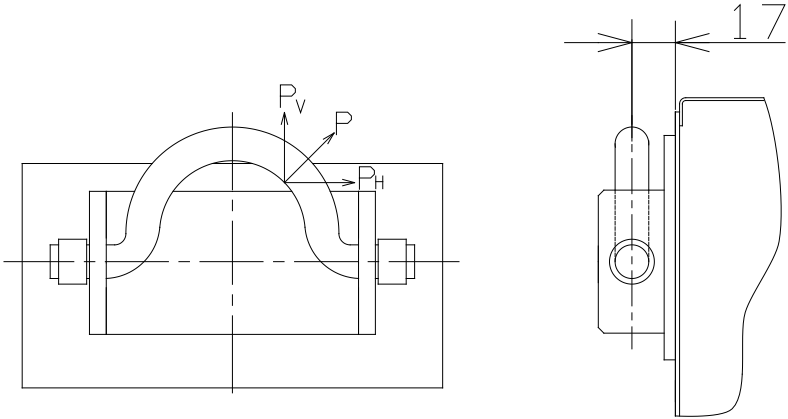
(unit: mm)

**Figure 2-7 Perforated Plate of Sling Fitting**



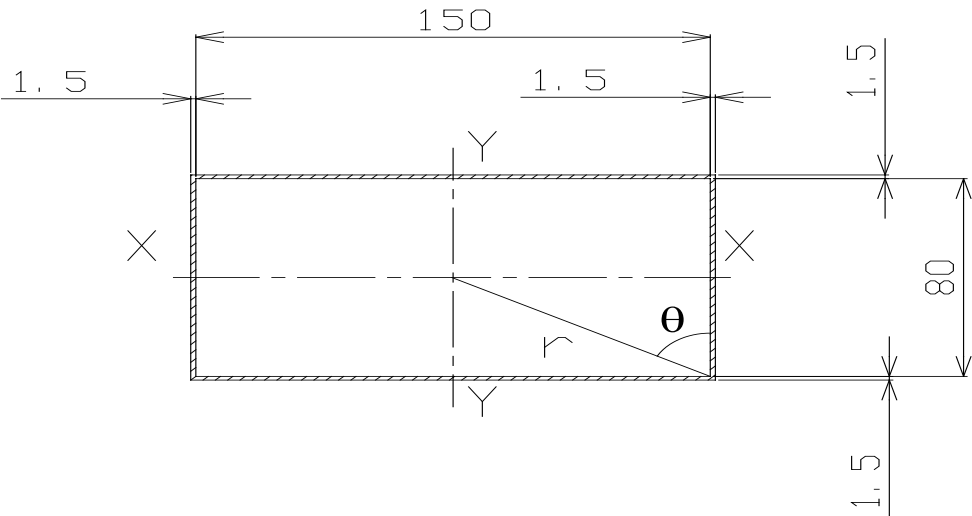
(unit: mm)

**Figure 2-8 Sling Fitting Weld Geometry for Attachment to Support Plate**



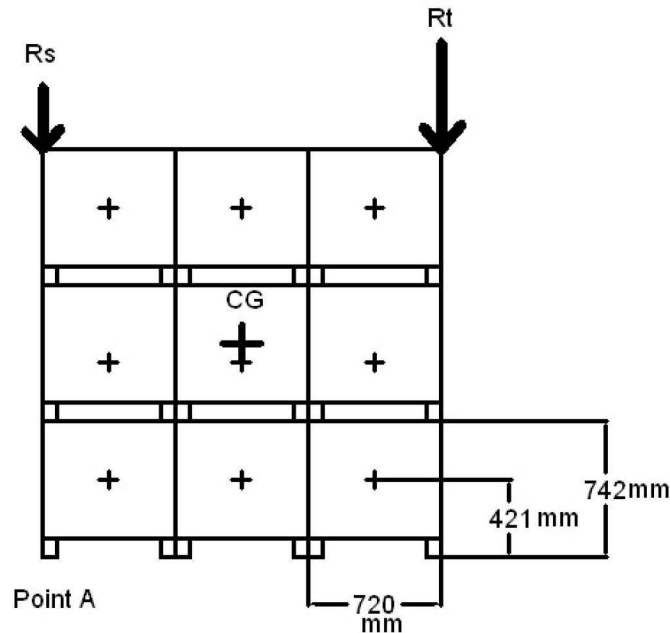
(unit: mm)

Figure 2-9    Loads on Sling Fitting



(unit: mm)

Figure 2-10    Welds for Support Plate Attachment to Body



**Figure 2-11 Tie-Down Configuration**

## 2.6 NORMAL CONDITIONS OF TRANSPORT

The RAJ-II package, when subjected to the NCT specified in 10 CFR 71.71, is shown to meet the performance requirements specified in Subpart E of 10 CFR 71. The NCT were evaluated by analysis and by comparison to the accident testing. The primary analysis was done for the compression loading. A static analysis was performed in Section 2.6.9. Because the NCT pressure and temperatures are well below the design conditions for the fuel cladding, no separate analysis was performed.

Regulatory Guide 7.6 (Reference 2-16) criteria are demonstrated as acceptable for NCT analytic evaluations presented in this section. Discussions regarding brittle fracture and fatigue are presented in Sections 2.1.2.4 and 2.6.5 and are shown not to be the limiting cases for the RAJ-II package design. The ability of the welded containment fuel rod cladding to remain leak-tight is documented in Chapter 4.0.

Properties of Type 304 stainless steel, as representative of those properties for Series 300 stainless steel, are summarized below in Table 2-5 based on published ASME properties.

**Table 2-5      Material Properties**

Material Property	Material Property Value <sup>①</sup>			Reference
	-40°C (-40°F)	21°C (70°F)	75°C (167°F)	
Type 304 Stainless Steel				
Elastic Modulus, E	198.6 GPa (28.8×10 <sup>6</sup> psi)	195.1 GPa (28.3×10 <sup>6</sup> psi)	191.7 GPa (27.8×10 <sup>6</sup> psi)	Table 2-2
Design Stress Intensity, S <sub>m</sub>	137.9 MPa (20,000 psi)	137.9 MPa (20,000 psi)	137.9 MPa (20,000 psi)	
Yield Strength, S <sub>m</sub>	206.8 MPa (30,000 psi)	206.8 MPa (30,000 psi)	184.7 MPa (26,788 psi)	
Tensile Strength	517.1 MPa (75,000 psi)	517.1 MPa (75,000 psi)	498.6 MPa (72,300 psi)	

**Notes:**

① Based on ASME Code properties (Reference 2-1).

The RAJ-II package's ability to survive HAC, a 30 ft free drop, a 40 in puncture drop, and a 30 minute thermal event also demonstrated the package's ability to also survive the NCT. Evaluations are performed, when appropriate, to supplement or expand on the available test results. This combination of analytic and test structural evaluations provides an initial configuration for NCT thermal, shielding and criticality performance. In accordance with 10 CFR 71.43(f), the evaluations performed herein successfully demonstrate that under NCT tests the RAJ-II package experiences "no substantial reduction in the effectiveness of the packaging". Summaries of the more significant aspects of the full-scale free drop testing are included in Section 2.6.7, with details presented in Section 2.12.2.

### 2.6.1 Heat

The NCT thermal analyses presented in Chapter 3.0, consist of exposing the RAJ -II package to direct sunlight and 100°F still air per the requirements of 10 CFR 71.71(b). Because there is negligible decay heat in the unirradiated fuel, the entire heating came from the solar insolation. Results are listed in Table 2-8. The maximum temperature of 77°C (171°F) was located on the lid of the OC.

### 2.6.1.1 Summary of Pressures and Temperatures

The fuel exhibits negligible decay heat. The RAJ-II package and internal components, when loaded with the required 10 CFR 71.71(c)(1) insulation conditions, develop a maximum temperature of 77°C (171°F). The resulting pressure at the maximum temperature is 1.33 MPa absolute (193 psia) for Boiling Water Reactor (BWR) fuel types, and up to 3.0 MPa absolute (435 psia) for all non-BWR fuel types (Pressurized Water Reactor (PWR) and CANDU).

### 2.6.1.2 Differential Thermal Expansion

With NCT temperatures throughout the packaging being relatively uniform (i.e., no significant temperature gradients), the concern with differential expansions is limited to regions of the RAJ-II packaging that employ adjacent materials with sufficiently different coefficients of thermal expansion. The IC is a double-walled, composite construction of alumina silicate thermal insulator between inner and outer walls of stainless steel. The alumina silicate thermal insulator is loosely packed between the two walls and does not stress the walls. Differential thermal expansion stresses are negligible in the OC for three reasons: 1) the temperature distribution throughout the entire OC is relatively uniform, 2) the OC is fabricated from only one type of structural material, and 3) the OC is not radially or axially constrained within a tight-fitting structure due to the relatively low temperature differentials and lack of internal restraint within the RAJ-II package.

The cladding of the fuel which serves as containment is not stressed due to differential thermal expansion because a gap remains between the fuel pellet and the cladding at both the cold temperature -40°C and the highest temperature the fuel could see due to the HAC is conservatively 800°C (see Chapter 3.0). This is demonstrated as follows:

At an ambient temperature of 20°C, a radial gap between the outer diameter of a fuel pellet and inner diameter of the cladding of at least [ ] is representative of general fuel types. Likewise, the maximum outer diameter of a general fuel pellet does not exceed [ ]. The strain due to thermal expansion or contraction in the zirconium alloy cladding is equal to (Reference 2-17):

$$\left(\frac{\Delta D}{D}\right)_{clad} = 7.4 \times 10^{-6} (\Delta T)$$

Where  $\Delta T$  is positive for an increase in temperature and negative for a decrease in temperature.

The strain due to thermal expansion or contraction in the fuel pellet is equal to (Reference 2-18):

$$\left(\frac{\Delta D}{D}\right)_{fuel} = -3.28 \times 10^{-3} + 1.179 \times 10^{-5} T - 2.429 \times 10^{-9} T^2 + 1.219 \times 10^{-12} T^3$$

Where T is the absolute final temperature in degrees Kelvin (K).

Table 2-6 summarizes the thermal strain in the cladding and pellets with a temperature change from 20 to -40°C ( $\Delta T = -60^\circ C, T = 233K$ ).



**Table 2-6 Thermal Contraction at -40°C**

	Strain at -40°C (-) $\left(\frac{\Delta D}{D}\right)$
<b>Pellet OD</b>	$-6.49 \times 10^{-4}$
<b>Cladding ID</b>	$-4.44 \times 10^{-4}$

The thermal contraction strain of the pellet is greater than that of the cladding and will result in an increased gap at -40°C.

Table 2-7 summarizes the thermal expansion in the cladding and pellets with a temperature change from 20°C to 800°C ( $\Delta T = 780^\circ\text{C}$ ,  $T = 1,073 \text{ K}$ ); all dimensions are expressed in centimeters. The ambient inner diameter of the cladding, of  $[[\text{ }]]$ , is based on the ambient pellet diameter (of  $[[\text{ }]]$ ) and radial gap (of  $[[\text{ }]]$ ). At 800°C the pellet thermal strain exceeds that of the cladding. However, a radial gap still remains between the pellet and cladding at 800°C.

**Table 2-7 Thermal Expansion at 800°C**

	Strain at 800°C (-) $\left(\frac{\Delta D}{D}\right)$	Thermal Expansion at 800°C (cm) $\left(\frac{\Delta D}{D}\right)D$	Dimension at 800°C (cm) $D + \left(\frac{\Delta D}{D}\right)D$
<b>Pellet OD</b>	$8.08 \times 10^{-3}$	$[[\text{ }]]$	
<b>Cladding ID</b>	$5.77 \times 10^{-3}$		$[[\text{ }]]$

At 800°C, a radial gap between the fuel pellet and cladding remains:

$$[[\text{ }]] - [[\text{ }]]$$

### 2.6.1.3 Stress Calculations

Because the temperatures and pressures generated under NCT are well below the design conditions for reactor fuel, no specific calculations were performed for the fuel containment.

#### **2.6.1.4 Comparison with Allowable Stresses**

The NCT are well below the operating conditions of the fuel. Therefore, no comparison to allowable stresses was performed.

#### **2.6.2 Cold**

The NCT cold condition consists of exposing the RAJ-II packaging to a steady-state ambient temperature of -40°F. Insolation and payload internal decay heat are assumed to be zero. These conditions will result in a uniform temperature throughout the package of -40°F. With no internal heat load (i.e., no contents to produce heat), the net pressure differential will only be reduced from the initial conditions at loading.

For the containment, the principal structural concern due to the NCT cold condition is the effect of the differential expansion of the fuel to the zirconium alloy tube. During the cool-down from 20°C to -40°C, the tube could shrink onto the fuel because of difference in the thermal expansion coefficient. However, the clearance between the fuel and the cladding is such that even if the fuel did not shrink, there would still be clearance. Differential thermal expansion stresses are negligible in the package for three reasons: 1) the temperature distribution throughout the entire package is relatively uniform, 2) the package is fabricated from only one type of structural material, and 3) the package is not radially or axially constrained.

Brittle fracture at -40°F is addressed in Section 2.1.2.4.1.

#### **2.6.3 Reduced External Pressure**

The effect of a reduced external pressure of 25 kPa (3.5 psia) per 10 CFR 71.71(c)(3) is negligible for the RAJ-II packaging. The RAJ-II package contains no pressure-tight seal and therefore cannot develop differential pressure. Therefore, the reduced external pressure requirement of 3.5 psia delineated in 10 CFR 71.71(c)(3) will have no effect on the package. Compared with the internal pressure in the fuel rods, a reduced external pressure of 3.5 psia will have a negligible effect on the fuel rods.

#### **2.6.4 Increased External Pressure**

The RAJ-II package contains no pressure-tight seal and, therefore, cannot develop differential pressure. Therefore, the increased external pressure requirement of 140 kPa (20 psia) delineated in 10 CFR 71.71(c)(4) will have no effect on the package. The pressure-tight cladding of the fuel rods is designed for much higher pressures in its normal service in a reactor and is not affected by the slight increase in external pressure.

The fuel rod cladding and welded end plugs form the containment. These tubes, designed for the conditions in an operating reactor, have the capability of withstanding the increased external pressure. The failure mode of radial buckling is not a plausible failure mode because the fuel pellets would prevent any significant deformation due to external pressure.

#### **2.6.5 Vibration**

The RAJ-II container contains an internal shock mount system to suppress vibratory stresses induced on the package's internal structures. The container has been extensively used over the

last decade by GNF for shipping fuel assemblies and rods. Visually examinations are performed for any potential damage after each use and prior to subsequent use.

The extensive usage experience is supplemented by vibrational testing of the RAJ-II container loaded with dummy fuel assemblies. The vibrational tests conducted covered longitudinal, horizontal, and vertical directions. In these tests, the RAJ-II was strapped down to two separate mounting plates, which were rigidly mounted to two vibration exciters. Photographs of the configuration for the horizontal and vertical tests are shown in Figure 2-12. It is noted that the straps hold the top corners of the test container in a manner similar to what a top corner container (in a 3x3 arrangement) would experience. The tests were conducted at ambient temperature. For the longitudinal orientation, the testing consisted of a sinusoidal sweep from 5 Hz to 99.25 Hz at 0.25 mm double amplitude displacement, and from 99.25 Hz to 100 Hz at 5g at a sweep rate of one octave per minute. For the horizontal orientation, the testing consisted of a sinusoidal sweep from 5 Hz to 14 Hz at 3.12 mm double amplitude displacement at one octave per minute, and from 13.99 Hz to 25.03 Hz at 3.12 mm double amplitude displacement and from 25.03 Hz to 100 Hz at 4g at one octave per minute. For the vertical orientation, the testing consisted of sinusoidal sweep from 5 Hz to 99.25 Hz at 0.25 mm double amplitude displacement, and from 99.25 Hz to 100 Hz at 5g at one octave per minute. Following the tests, no evidence of damage to the container was reported.



Configuration for testing in the horizontal orientation



Configuration for testing in the vertical orientation

**Figure 2-12 Vibrational Test Experimental Set-Up**

### **2.6.6 Water Spray**

The materials of construction of the RAJ-II package are such that the water spray test identified in 10 CFR 71.71(c)(6) will have a negligible effect on the package.

### **2.6.7 Free Drop**

Because the maximum gross weight of the RAJ-II package is 1,614 kg (3,558 lb), a 1.2-meter or 4-foot free drop is required per 10 CFR 71.71(c)(7). The HAC 9 m (30 ft) free drop test required in 10 CFR 71.73(c)(1) is substantially more damaging than the 1.2 m (4 ft) NCT free drop test. Section 2.7.1 demonstrates the RAJ-II package's survivability and bounds the free drop

requirements of 10 CFR 71.71(c)(7). Due to the relatively fragile nature of the fuel assembly payload in maintaining its configuration for operational use, any event that would come close to approximating the NCT free drop would cause the package to be removed from service and re-examined prior to continued use.

As part of the effort to obtain package certification in Japan by GNF-J, certification testing of the package, which included both an end drop and a lid-down horizontal drop, was performed. In each case a 0.3 m (1 ft) and a 1.2 m (4 ft) drop were performed prior to the 9 m (30 ft) drop. In both cases the RAJ-II was slightly damaged, but the damage had no significant effect on the performance of the package in relation to either the containment or the ability of the package to meet the requirements of 10 CFR 71. The GNF-J certification testing is discussed in Section 2.12.3.

Therefore, the requirements of 10 CFR 71.71(c)(7) are met.

### **2.6.8 Corner Drop**

This test does not apply because the package weight is in excess of 100 kg (220 lb) and the structural materials used in the RAJ-II are not primarily wood or fiberboard, as delineated in 10 CFR 71.71(c)(8).

### **2.6.9 Compression**

Because the package weighs less than 5,000 kg (11,000 lb), as delineated in 10 CFR 71.71(c)(9), the package must be able to support five times its weight without damage.

The load to be given as the test condition is the load ( $W_1$ ) times five of the weight of this package or the load ( $W_2$ ) which is obtained through multiplying the package's vertical projected area by 13 kPa, whichever is heavier. In the case of this package, the equations to obtain each load are:

$$W_1 = 5 \times m \times g$$

$$W_2 = 13 \text{ kPa} \times L \times B$$

Where:

m: Mass of package                      1,614 kg (3,558 lb)

g: Gravitational acceleration                      9.81 m/s<sup>2</sup>

L: Length of package                      5,068 mm (199.53 in)

B: Width of package                      720 mm (28.35 in)

From this:

$$W_1 = 5 \times 1,614 \times 9.81 = 79.16 \text{ kN (17,800 lbf)}$$

$$W_2 = 13 \times 10^{-3} \times 5,068 \times 720 = 47.4 \text{ kN (10,660 lbf)}$$

Therefore, as  $W_1 > W_2$ , the stacking load is assumed as  $W = 79.16 \text{ kN (17,800 lbf)}$ .

The stacking of these packages is as shown in Figure 2-13, so the OC only sustains the stacking load. In this case, it is assumed that loads are carried by a total of eight support plates positioned

NEDO-33869 Revision 11  
Non-Proprietary Information

in the center of the bolster out of sixteen support plates of the OC body positioned at the lowest layer. This assumption makes the load sustaining area smaller, so the evaluation is conservative. The compressive load given to the support plate is the above-mentioned stacking load plus the weight of the OC's lid.

The equation to obtain the support plate's compressive load is:

$$W_c = W_1 + W_3$$

$W_c$ : Compressive load N

$W_1$ : Stacking load 79.16 kN (17,800 lbf)

$W_3$ : Load by the OC's lid 1.34 kN (301 lbf)

$m_F$ : Mass of OC lid 137 kg (302 lb)

$g$ : Gravitational acceleration 9.81m/s<sup>2</sup>

From this,  $W_c = 80.5 \text{ kN (18,100 lbf)}$

When the fuel assemblies are packed, the center of gravity of the OC is shifted longitudinally, so the load acting on the support plate, which is closer to the center of gravity, becomes larger.

Therefore, the equation to obtain the vertical maximum load given to one support plate, which is closer to the center of gravity, is:

$$P = \frac{W \cdot \ell_2}{4 \cdot \ell_0}$$

Where:

$P$ : Maximum load acting on one support plate  
which is nearer to the center of gravity N

$W$ : Compressive load given to the support plate 80.5 kN (18,100 lbf)

$\ell_0$ : Longitudinal support plate space 3,510 mm (138.2 in)

$\ell_2$ : Distance from the package's center of gravity position  
to the support

$$\frac{3,510}{2} + 92 = 1,847 \text{ mm (73.76 in)}$$

From this, the maximum load  $P$  acted to one support plate, which is nearer to the center of gravity, is:

$$\begin{aligned} P &= \frac{80.5 \times 10^3 \times 1,847}{4 \times 3,510} \\ &= 10.6 \times 10^3 \text{ N (2,380 lbf)} \end{aligned}$$

The resistance of the plate to buckling is also evaluated. The equation to obtain the moment of inertia of area of the support plate which is subject to buckling is:

$$I_z = \frac{1}{12} hb^3$$

Where:

$I_z$ : Moment of inertia of area of support plate mm<sup>4</sup>

$b$ : Thickness of support plate 5 mm (0.2 in)

$h$ : Width of support plate 55 mm (2.2 in)

From this, the moment of inertia of area,  $I_z$ , of the support plate is:

$$I_z = \frac{1}{12} \times 55 \times 5^3 = 572.9 \text{ mm}^4 (1.376 \times 10^{-3} \text{ in}^4)$$

The equation to obtain the radius of gyration of the area of the support plate is:

$$k = \sqrt{\frac{I_z}{A}}$$

Where:

$k$ : Radius of gyration of area of support plate mm

$I_z$ : Moment of inertia of area of support plate 572.9 mm<sup>4</sup> (1.376x10<sup>-3</sup> in<sup>4</sup>)

$A$ : Cross-sectional area of support plate  $5 \times 55 = 275 \text{ mm}^2$  (0.426 in<sup>2</sup>)

$\ell$ : Length of support plate 559 mm (22.4 in)

From this, the radius of gyration of area  $k$  of the support plate is:

$$k = \sqrt{\frac{572.9}{275}} = 1.44 \text{ mm (0.0568 in)}$$

Also, the slenderness ratio  $\frac{\ell}{k}$  is:

$$\frac{\ell}{k} = \frac{559}{1.44} = 388$$

As the ends are fixed, the coefficient  $n$  becomes 4, so the limit value of the slenderness ratio becomes:

$$85\sqrt{n} = 85\sqrt{4} = 170$$

Because the slenderness ratio of this material, 388, exceeds the limit value of slenderness, Euler's equation is used. The equation to obtain the support plate's buckling strength is:

$$P_k = \frac{n\pi^2 EI_z}{\ell^2}$$

Where:

$P_k$ : Buckling strength (load) of support plate	N
$n$ : Coefficient to the long support fixed at both ends	4
$E$ : Longitudinal elasticity modulus of 304 stainless steel	$1.94 \times 10^5$ MPa (at 40°C)
$I_z$ : Moment of inertia of area of support plate	$572.9 \text{ mm}^4$ ( $1.376 \times 10^{-3} \text{ in}^4$ )
$\ell$ : Length of the support plate	559 mm (22.4 in)

From this, the buckling strength  $P_k$  of the support plate is:

$$P_k = \frac{4 \times 3.14^2 \times 1.94 \times 10^5 \times 572.9}{559^2} = 14.0 \times 10^3 \text{ N (3,050 lbf)}$$

Therefore,  $P_k > P$ , so the body support plate will not buckle.

#### 2.6.10 Penetration

The 1 m (40 in) drop of a 6 kg (13 lb), hemispherical-headed, 3.2 cm (1.3 in) diameter, steel cylinder, as delineated in 10 CFR 71.71(c)(10), is of negligible consequence to the RAJ-II package. This is because the RAJ-II package is designed to minimize the consequences associated with the much more limiting case of a 1 m (40 in) drop of the entire package onto a puncture bar as discussed in Section 2.7.3. The drop of the 6 kg bar will not penetrate the OC.

**Table 2-8      Temperatures**

Location	Maximum Temperature
Environment (Open Air)	38°C
Package's External Surface	77°C
Inner Container	< 77°C

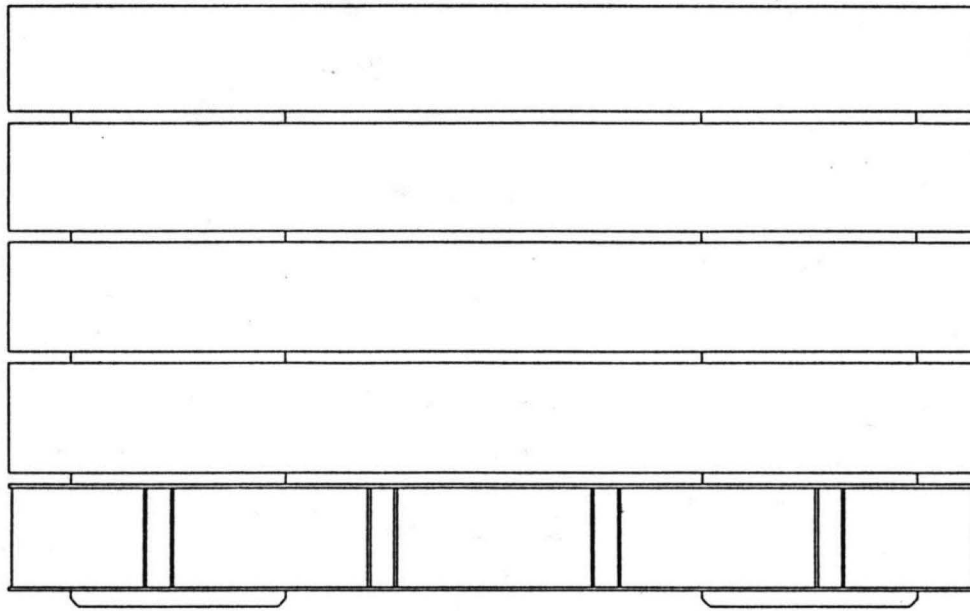


**Figure 2-13 Stacking Arrangement**

## **2.7 HYPOTHETICAL ACCIDENT CONDITIONS**

The RAJ-II package, when subjected to the sequence of HAC tests specified in 10 CFR 71.73 is shown to meet the performance requirements specified in Subpart E of 10 CFR 71. The primary proof of performance for the HAC tests is via the use of full-scale testing. A CTU was free dropped, and puncture tested to confirm that both the inner and outer containers protected the fuel and allowed containment to be maintained after a worst-case HAC sequence. Another CTU was free dropped from 9 meters on its end with the fuel maintaining containment after the drop. Observations from CTU testing confirm the conservative nature of the deformed geometry assumptions used in the criticality assessment provided in Chapter 6.0. Immersion is addressed by comparison to the design basis for the fuel.

Test results are summarized in Section 2.7.8, with details provided in Section 2.12.2.

### **2.7.1 Free Drop**

Subpart F of 10 CFR 71 requires performing a free drop test in accordance with the requirements of 10 CFR 71.73(c)(1). The free drop test involves performing a 30-foot, HAC free drop onto a flat, essentially unyielding, horizontal surface, with the package striking the surface in a position (orientation) for which maximum damage is expected. The ability of the RAJ-II package to adequately withstand this specified free drop condition is demonstrated via testing of four full-scale, CTUs.

To properly select a worst-case package orientation for the 30-foot free drop event, items that could potentially compromise containment integrity, shielding integrity, and/or criticality safety of the RAJ-II package must be clearly identified. For the RAJ-II packaging design, there are two primary considerations: 1) protect the fuel so that containment is maintained, and 2) ensure



sufficient structure is around the package to maintain the geometry used in the criticality safety evaluation. Shielding integrity is not a controlling case for the reasons described in Chapter 5.0. Criticality safety is conservatively evaluated based on measured physical damage to the containers from certification testing, as described in Chapter 6.0.

Because the containment is welded closed, the leak-tight capability of the containment may be compromised by two methods: 1) as a result of excessive deformation leading to rupture of the containment boundary, and/or 2) as a result of thermal degradation of the containment material itself in a subsequent fire event and rupture of the weld or the cladding tube by over-pressurization. Importantly, these methods require significant impact damage to the surrounding outer and inner container so that the fuel is either loaded externally or the fuel is directly exposed to the fire.

Additional items for consideration include the possibility of separating the OC lid from the OC body and buckling or deforming of the OC and/or IC from an end drop or horizontal drop.

For the above reasons, testing must include impact orientations that affect the lid and stability of the walls of the containers. In general, the energy absorbing capabilities of the RAJ-II are governed by the deformation of the stainless steel and honeycomb that is not significantly affected by temperature.

Sections 2.12.2 and 2.12.3 provide a comprehensive report of the certification test process and results. Discussions specific to CTU test orientations for free drop and puncture, including initial test conditions, are also provided.

The RAJ-II package has undergone extensive testing during its development. Testing has included 1.2 m (4 ft) drops on the end in the vertical orientation and the lid in the horizontal orientation. The package has been also dropped from 9 m (30 ft) in the same orientation demonstrating that the damage from the 1.2 m (4 ft) drops has little consequence on the performance of the package in 9 m (30 ft) drop. Based on these preliminary tests it was determined that the worst-case orientation for the 9 m (30 ft) drop test would be slap-down on the lid. The lid down drop demonstrated that the vibration isolation frame bolts would fail allowing the IC to come in contact with the honeycomb in the lid and partially crush the honeycomb. It was expected that the slap-down orientation would maximize the crush of this material minimizing the separation distance between the fuel assemblies in the post-accident condition.

A single “worst-case” 9 m (30 ft) free drop is required by 10 CFR 71.73(c)(1). Based on the above discussion and experience with other long slender packages similar to the RAJ-II, a 15 degree slap-down on the lid was chosen for the 9 m (30 ft) drop. Following that drop, a 25 degree oblique puncture drop on the damaged lid was performed. See Figure 2-14, Figure 2-15, and Section 2.12.2.

Other free drop orientations that were tested include vertical end and bottom corner. These tests demonstrated that the RAJ-II package contains the fuel assemblies without breaching the fuel cladding (containment boundary).

#### **2.7.1.1 End Drop**

Several 9 m (30 ft) end free drops were performed on GNF-J CTU 1J and GNF-A CTU 2; see Figure 2-16. The orientation was selected with the lower end of the fuel down to maximize the damage because the expansion springs in the fuel rods are located in the upper end. This orientation maximized the damage to the energy absorbing wood in the end of the RAJ-II and maximized the axial loading on the fuel assembly. Both tests resulted in deformations of the fuel, though cladding integrity was maintained. These tests demonstrated that the containment boundary was maintained after a 9 m (30 ft) end drop test. The change in fuel rod pitch, from normal, occurred within the lower 1,626 mm (64 in) of the test bundle and on average increased by no more than 4.1%. However, while test data supports an average lattice expansion of up to 4.1%, an additional structural analysis calculated [[ ]] as a conservative post-drop rod pitch for the limiting GNF 10x10 bundle (Reference 2-19).

#### **2.7.1.2 Side Drop**

No side drop testing was performed in this certification sequence. A side drop test was done in previous testing of the package. That testing resulted in the IC holding frame top bolts failing and allowing the IC to come in contact with the outer lid. The IC showed little damage and the fuel was not deformed. It was judged that the slapdown and the horizontal drop tests bounded the side drop orientation.

#### **2.7.1.3 Corner Drop**

A 9 m (30 ft) free drop on the OC upper end bottom corner was performed on GNF-J CTU 1J. The impact point previously sustained damage due to 0.3 m (1 ft) and 1.2 m (4 ft) free drops. The resultant cumulative deformation was approximately 163 mm (6 in). There was no loss of contents or significant structural damage to the OC as a result of this free drop. The maximum recorded impact acceleration was 203g. Refer to Section 2.12.3 for complete details of the corner free drop.

#### **2.7.1.4 Oblique Drops**

An orientation of 15 degrees from horizontal was tested with GNF-A CTU 1. Additional information regarding the selection of this angle is provided in Supplement 1, "Clarifications on the RAJ-II Selection of Slapdown and Puncture Orientations" (Reference 2-20). The IC holding frame was plastically deformed and only a portion of the bolts failed. The fuel and the IC were not significantly damaged. The damage sustained was bounded by the assumptions utilized in the criticality and thermal evaluations. The fuel was leak tested after the test and was demonstrated to have maintained containment boundary. Refer to Section 2.12.2 for complete details of the 15-degree oblique free drop.

#### **2.7.1.5 Horizontal Drop**

A 9 m (30 ft) horizontal free drop on the OC lid was performed on GNF-J CTU 2J. The impact resulted in a maximum deformation of 19 mm (0.8 in), which occurred in the OC lid. The side wall of the OC body bulged approximately 19 mm (0.8 in). Some localized weld failure of OC lid flange/OC lid interface occurred where the bolster angles attach to the lid. None of the OC lid bolts failed as a result of the impact. There was no loss of contents as a result of the free drop.

The maximum recorded impact acceleration was 146g. Refer to Section 2.12.3 for complete details of the horizontal free drop.

#### **2.7.1.6 Summary of Results**

Successful HAC free drop testing of the test units indicates that the various RAJ-II packaging design features are adequately designed to withstand the HAC 30 ft free drop event. The most important result of the testing program was the demonstrated ability of the fuel to maintain its containment capability as defined by American National Standards Institute (ANSI) N14.5 (Reference 2-21).

The RAJ-II also maintained its basic geometry required for nuclear criticality safety. Observed permanent deformations of the RAJ-II packaging were less than those assumed for the criticality evaluation.

The GNF-A mockup fuel assembly rods were leakage rate tested after the conclusion of the testing and were demonstrated to be leak tight, as defined in ANSI N14.5 (Reference 2-21).

A comprehensive summary of free drop test results is provided in Sections 2.12.2 and 2.12.3.

#### **2.7.2 Crush**

Subpart F of 10 CFR 71 requires performing a dynamic crush test in accordance with the requirements of 10 CFR 71.73(c)(2). Because the RAJ-II package weight exceeds 500 kg (1,100 pounds), the dynamic crush test is not required.

#### **2.7.3 Puncture**

Subpart F of 10 CFR 71 requires performing a puncture test in accordance with the requirements of 10 CFR 71.73(c)(3). The puncture test involves a 1 m (40 in) free drop of a package onto the upper end of a solid, vertical, cylindrical, mild steel bar mounted on an essentially unyielding, horizontal surface. The bar must be 150 mm (6 in) in diameter, with the top surface horizontal and its edge rounded to a radius of not more than 6 mm (0.25 in). The package is to be oriented in a position for which maximum damage will occur. The length of the bar used was approximately 1.5 m (60 in). The ability of the RAJ-II package to adequately withstand this specified puncture drop condition is demonstrated via testing of the full-scale RAJ-II CTUs.

To properly select a worst-case package orientation for the puncture test, items that could potentially compromise containment integrity and/or criticality safety of the RAJ-II package must be clearly identified. For the RAJ-II package design, the foremost item to be addressed is the ability of the containment to remain leak-tight. Shielding integrity is not a controlling case for the reasons described in Chapter 5.0. Criticality safety is conservatively evaluated based on measured physical damage to the OC and IC walls as described in Chapter 6.0.

Previous testing has shown that the 1 m drop onto the puncture bar did not penetrate the outer wall. Based on this previous testing and other experience, an oblique and horizontal puncture drop orientations centered over the fuel were chosen as the most damaging.

Sections 2.12.2 and 2.12.3 provide a comprehensive report of the certification test process and results. Discussions specific to the configuration and orientation of the test unit are provided.

The “worst-case” puncture drop as required by 10 CFR 71.73(c)(3) was performed on the package with the lid down and 25 degrees from horizontal. The angle was chosen based on experience with other packages and the RAJ-II. Additional information regarding the selection of this angle is provided in Supplement 1, “Clarifications on the RAJ-II Selection of Slapdown and Puncture Orientations” (Reference 2-20). The puncture bar was aimed at the CG of the package to maximize the energy imparted to the package.

The puncture pin did not penetrate the OC. It deformed the lid inward, and it contacted the IC lid and deformed it a small amount. The outer lid total deformation was less than 12 cm (4.7 in) and the IC lid deformed less than 5 cm (2.0 in).

#### **2.7.4 Thermal**

Thermal testing of the GNF-J CTU 2J was performed following the free drop and puncture drop tests (refer to Section 2.12.3). Although there was no failure of the containment boundary due to the thermal testing, the thermal evaluation of the RAJ-II package for the HAC heat condition as presented in Chapter 3.0, demonstrates regulatory compliance to 10 CFR 71.73(c)(4). Because the RAJ-II package does not contain pressure-tight seals, the HAC pressure for the OC and the IC is zero. The fuel exhibits negligible decay heat.

##### **2.7.4.1 Summary of Pressures and Temperatures**

The maximum predicted HAC temperature for the fuel is 648°C (921 K, 1,198°F) during the fire event. The various fuel rod types are designed to withstand a minimum temperature of 765°C (1,038 K, 1,409°F) without bursting. The pressure due to the accident conditions does not exceed the rupture pressure of the fuel rods as demonstrated in Chapter 3.0.

##### **2.7.4.2 Differential Thermal Expansion**

The cladding of the fuel, which serves as the containment, is not stressed due to differential thermal expansion between the pellet and cladding; see Section 2.6.1.2. The fuel cladding is not restricted by the packaging and hence cannot develop any significant differential thermal expansion stresses. The packaging itself is made of the same metal (austenitic stainless steel) eliminating any significant stresses due to differential thermal expansion.

##### **2.7.4.3 Stress Calculations**

Stress calculations for the controlling hoop stress for the fuel cladding that provides containment is provided in Chapter 3.0.

##### **2.7.4.4 Comparison with Allowable Stresses**

The allowable stress used in the analysis in Chapter 3.0 is based on empirical data from burst tests and analytical calculations. The allowed fuel cladding configurations for the RAJ-II have a positive margin of safety based on stresses required to fail the fuel.

### **2.7.5 Immersion – Fissile Material**

Subpart F of 10 CFR 71 requires performing an immersion test for fissile material packages in accordance with the requirements of 10 CFR 71.73(c)(5). The criticality evaluation presented in Chapter 6.0 assumes optimum hydrogenous moderation of the contents, thereby conservatively addressing the effects and consequences of water in-leakage.

### **2.7.6 Immersion – All Packages**

Subpart F of 10 CFR 71 requires performing an immersion test for packages in accordance with the requirements of 10 CFR 71.73(c)(6). Because the RAJ-II package is not sealed against pressure, there will not be any differential pressure with the water immersion loads defined in 10 CFR 71.73(c)(6). The water immersion will have a negligible effect on the container and the payload, consisting of the fuel rods that provide the containment. The fuel rods are designed to withstand differential pressures greater than 1,000 psi. Submergence is a normal design condition for the fuel rods and the evaluations are performed on that condition.

### **2.7.7 Deep Water Immersion Test (for Type B Packages Containing More than $10^5$ A<sub>2</sub>)**

Not applicable. The RAJ-II does not contain more than  $10^5$  A<sub>2</sub>.

### **2.7.8 Summary of Damage**

As discussed in the previous sections, the cumulative damaging effects of the free drops and a puncture drop were satisfactorily withstood by the RAJ-II packaging during certification testing. Table 2-9 summarizes the drop tests. Subsequent helium leak testing confirmed that containment was maintained within allowable leak rates defined in Chapter 4.0. The package was also successfully evaluated for maintaining containment during and after the fire event. The deformation of the package in the worst-case HAC did not exceed that which is evaluated for in Chapter 6.0. Therefore, the requirements of 10 CFR 71.73 have been satisfied.

**Table 2-9 Summary of Tests for RAJ-II**

Test No.	Test Description	Test Unit Angular Orientation		CTU Temperature	Remarks
		Axial <sup>①</sup>	Rotational		
1	9 m (30 ft) Slap Down	15°	Lid Down	Ambient	Top of package impacted first. OC lid crushed over 11 cm (4.3 in).
2	Puncture	25°	Lid Down	Ambient	Puncture pin crushed the OC lid down to the IC lid. It did not rupture the OC lid or significantly deform the IC lid or fuel.
3	9 m (30 ft) End Drop	90°	Lower End Down	Ambient	Crushed end wood impact absorber. Deformed the fuel assembly but did little damage to the rods.

**Notes:**

- ① Axial angle,  $\theta$ , is relative to horizontal (i.e., side drop orientation)

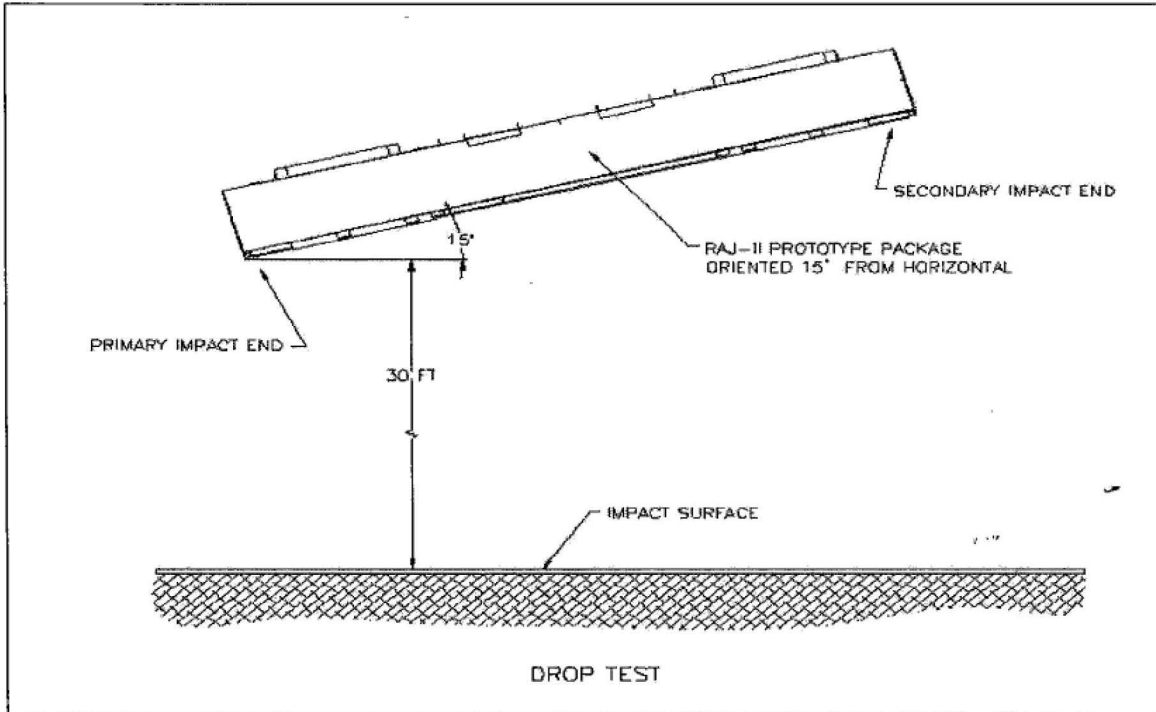


**Figure 2-14 Slap-Down Orientation**

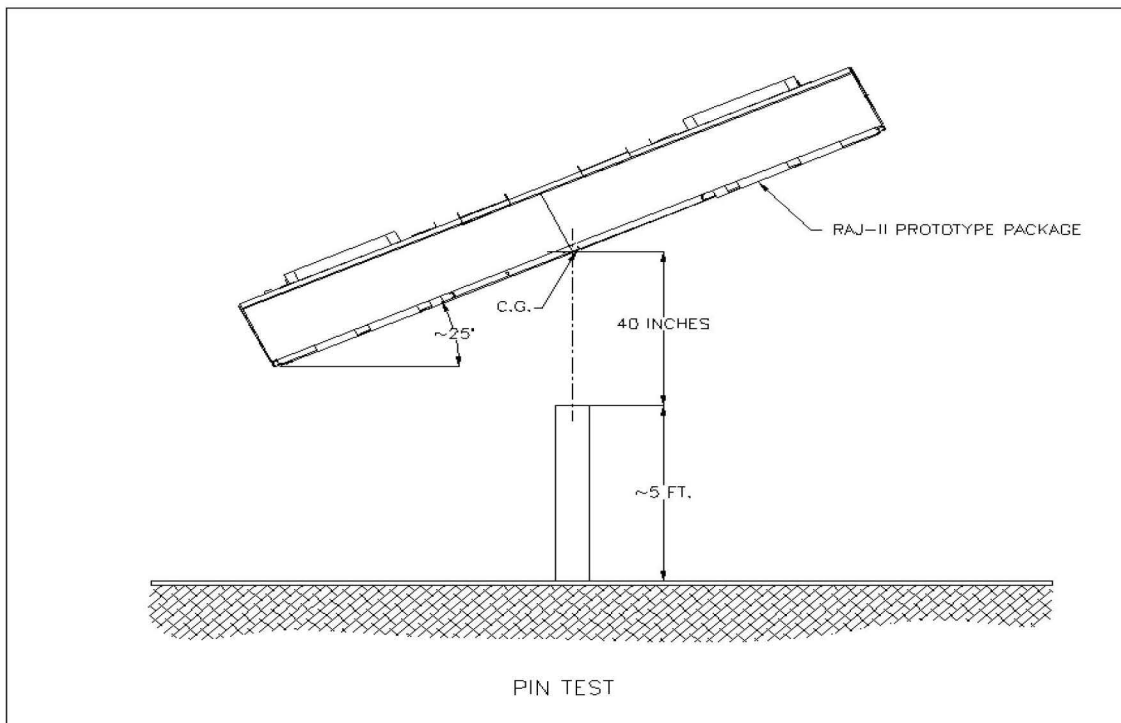


**Figure 2-15 Puncture Pin Orientation**

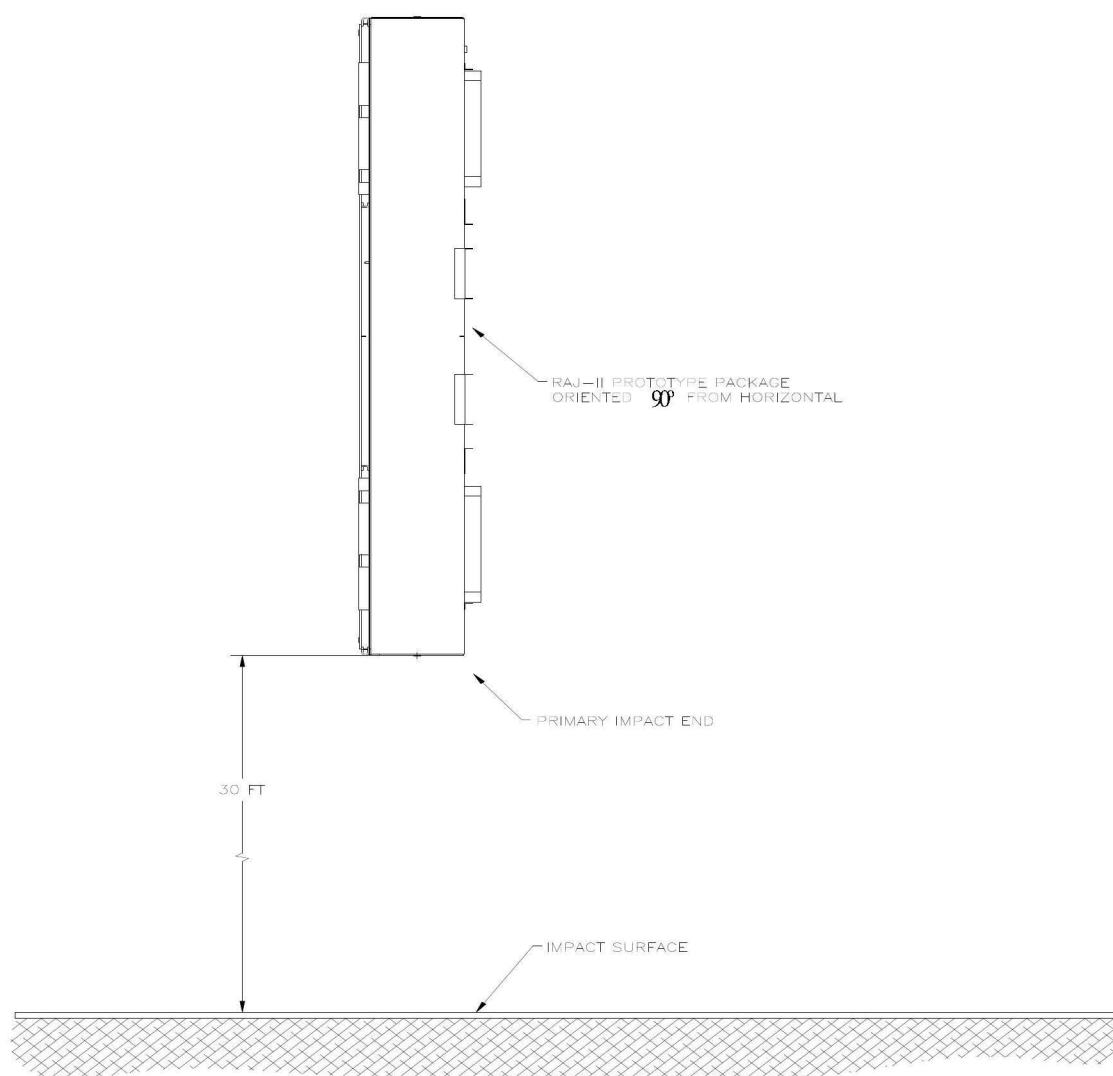


**Figure 2-16 End Drop 90° Orientation**

**2.8 ACCIDENT CONDITIONS FOR AIR TRANSPORT OF PLUTONIUM**

Not applicable. This package will not be used for the air transport of plutonium.

**2.9 ACCIDENT CONDITIONS FOR FISSILE MATERIAL PACKAGES FOR AIR TRANSPORT**

Not applicable. This package will not be used for the air transport of fissile material.

**2.10 SPECIAL FORM**

This section does not apply for the RAJ-II package because special form is not claimed.



## **2.11 FUEL RODS**

In each event evaluated above either by analysis or by test, the unirradiated fuel rods were protected by the RAJ-II package so that they sustained no significant damage. Fuel rod cladding is considered to provide containment of radioactive material under both normal and accident test conditions. Discussion of this cladding and its ability to maintain sufficient mechanical integrity to provide such containment is described in Section 1.2.1.2 and Chapter 4.0.

## **2.12 APPENDIX**

### **2.12.1 References**

- 2-1. American Society of Mechanical Engineers, ASME Boiler Pressure Vessel Code.
- 2-2. Japan Welding Engineering Society, JIS Z 3821, "Standard Qualification Procedure for Welding Technique of Stainless Steel."
- 2-3. Japan Welding Engineering Society, JIS Z 3140, "Method of Inspection for Spot Weld."
- 2-4. Japan Welding Engineering Society, JIS Z 3145, "Method of Bend Test for Stud Weld."
- 2-5. Japanese Society for Non-destructive Inspection, JIS Z 2305, "Non-destructive Testing – Qualification and Certification of NDT Personnel."
- 2-6. Japanese Society for Non-destructive Inspection, NDIS 0601, "Rule of Qualification and Certification of Non-destructive Testing Personnel."
- 2-7. Japanese Society for Non-destructive Inspection, NDIS J001, "Qualification and Certification of NDT Personnel."
- 2-8. American Society for Nondestructive Testing, SNT-TC-1A, "Personnel Qualification and Certification in Nondestructive Testing Recommend Practice."
- 2-9. Japanese Standards Association, JIS Handbook, "Ferrous Materials and Metallurgy."
- 2-10. American Society for Testing and Materials, A240, "Standard Specification for Chromium and Chromium-Nickel Stainless Steel Plate, Sheet, and Strip for Pressure Vessels and for General Applications."
- 2-11. American Society for Testing and Materials, A666, "Standard Specification for Annealed or Cold-Worked Austenitic Stainless Steel Sheet, Strip, Plate, and Flat Bar."
- 2-12. American Society for Testing and Materials, A276, "Standard Specification for Stainless Steel Bars and Shapes."
- 2-13. American Society for Testing and Materials, B811, "Standard Specification for Wrought Zirconium Alloy Seamless Tubes for Nuclear Reactor Fuel Cladding."
- 2-14. American Welding Society, D1.6, "Structural Welding Code - Stainless Steel."
- 2-15. Shigley, Joseph E., and Mischke, Charles R., "Mechanical Engineering Design," Fifth Edition, McGraw-Hill, Inc., 1989.

- 2-16. Regulatory Guide 7.6 Revision 1, “Design Criteria for the Structural Analysis of Shipping Cask Containment Vessels,” U.S. Nuclear Regulatory Commission, Washington, DC, March 1978.
- 2-17. Framatome ANP MOX Material Properties Manual 51-5010288-03.
- 2-18. Framatome ANP MOX Material Properties Manual 51-5010288-02.
- 2-19. Letter, Scott P. Murray (GNF) to Document Control Desk (NRC), “GNF-A Request for Letter Authorization to Use the RAJ-II Package,” SPM 14-030, July 30, 2014.
- 2-20. Letter, Charles M. Vaughan (GNF) to E. William Branch (NRC), “Response to NRC Questions Regarding Stress on Fuel, Basis for Selecting Container Orientation for Testing and Wording in SAR Relating to Damage During HAC Test,” CMV-04-045, October 28, 2004.
- 2-21. American National Standards Institute, N14.5-2014, “Radioactive Materials - Leakage Tests on Packages for Shipment.”
- 2-22. Global Nuclear Fuel - Japan (fka Japan Nuclear Fuel Co., Ltd), “Application for Approval of Packaging, Type RAJ II,” STO-M00-034, dated September 26, 2000.
- 2-23. Goodyear Tire & Rubber Company, “Handbook of Molded and Extruded Rubber,” Third Edition.
- 2-24. U.S. Department of Energy (DOE), “Safety Analysis Report for the TRUPACT-II Shipping Package,” USNRC Certificate of Compliance 71-9218, U.S Department of Energy, Carlsbad Field Office, Carlsbad, New Mexico.
- 2-25. ORD 5700A/US, “Parker O-ring Handbook,” 2001, Parker Hannifin Corporation, Lexington, KY.

## **2.12.2 Certification Tests**

### **2.12.2.1 Evaluation by Test**

The primary means of demonstrating that the package meets the regulatory HAC was by test. The package was tested by dropping four full-scale CTUs from 9 m (30 ft) in different orientations; two of the test units were dropped as part of the Japanese certification process. The weight of the units was maximized to provide bounding conditions.

Within the GNF-A CTUs, the fuel was mocked up by a metal boxed section that provided the representative weight in one fuel assembly shipping location. The steel section was segmented to prevent the mockup from adding unrealistic stiffness to the package. In the other fuel assembly shipping position, a mockup fuel assembly was used. This had the same cross-sectional properties of the actual fuel. The rods were filled with lead to represent the actual fuel. Weights were added alongside of the assembly to provide the correct mass for fuel that may be shipped with channels as well as allowing for the different density between the lead and the uranium oxide pellets.

The units tested in Japan had a simulated 8X8 fuel assembly and weights representing a second fuel assembly in each test unit. The weight and dimensions of the mockup fuel approximated the weight of the fuel to be shipped in the container.

Details of the prototypes used in the drop testing can be found in Sections 2.7, 2.12.2, and 2.12.3.

The damage caused by the test was evaluated in each of the affected sections: Chapter 3.0, Chapter 4.0, and Chapter 6.0. Both the inner and outer lids stayed in place, although they were damaged. The IC holding frame was deformed but restrained the IC. Due to the end drop there was some plastic deformation of the fuel, but it was well within the limits of the criticality evaluation. After the testing, the fuel rods passed a helium leakage rate test demonstrating containment.

#### **2.12.2.2 Certification Test Unit**

The RAJ-II test packages were fabricated identically to the configuration depicted in the packaging general arrangement drawing found in Section 1.3.1. The CTU is identical to the production RAJ-II packages except for minor differences:

1. For ease in documentation/evaluation, tape and marker were used for reference markings during testing.
2. Minor amounts of the internal foam cushioning material were cut out to accommodate added weight in the fuel cavity.
3. Weight was added to the exterior of the package to allow the test units to be at the maximum allowed package weight.

The fuel assemblies were represented by a mockup fuel assembly. Lead rods inside the cladding replaced the fuel pellets. The fuel rods were seal welded using the same techniques used on the production fuel rods. A composite fuel assembly was used to represent the second fuel assembly. Steel tubes represented the ends with added steel for correct weight. The center section was made up of a mockup fuel assembly similar to the full-size mockup fuel assembly. The mockup of the fuel approximated the stiffness of the fuel and added no extra strength to the center section of the package that would potentially be damaged by the puncture test. See Figure 2-17 through Figure 2-23 for container and mockup fuel preparation. Weight was added to the fuel assembly cavity by placing lead sheeting on the side of the fuel where normally there is foam. The lead weighing 143 pounds represented the weight of the water channels that could be shipped with some fuel assemblies. The lead plate was cut into strips that were not over half the height of the fuel assemblies to ensure that there was no support or protection added to the fuel during any of the tests. The mass of the payload was split between each side of the IC to maintain the design center of gravity. The total weight of the CTUs is provided in Table 2-10. The added weight in the contents represents the maximum payload weight including the fuel, fuel assembly fittings and packing material that could be required in the future. The honeycomb was constructed of paper which has equivalent critical characteristics and shock absorbing abilities as the alternative aluminum construction.

For CTU 1 that was dropped lid down for a 30-foot slap down event and a 1 m oblique puncture event, the weight was added between the bolster boards at each end. The added weight

representing the difference between the actual tare weights of the package and the maximum allowed tare weight consisted of two ½-inch carbon steel plates. For CTU 1, these were held in place by the bolster and brackets attached to the bolster with lag bolts. See Figure 2-24. These plates were taken off CTU 1 and placed on the opposite end of CTU 2 for the end drop. See Figure 2-25.

**Table 2-10 Test Unit Weights**

<b>Property</b>	<b>CTU 1</b>		<b>CTU 2</b>	
<b>Unit of Measure</b>	<b>kg</b>	<b>lb</b>	<b>kg</b>	<b>lb</b>
<b>As Fabricated</b>	849	1,872	848	1,869
<b>Max. Fabricated</b>	930	2,050	930	2,050
<b>Added</b>	81.7	180	81.7	180
<b>Content</b>	684	1,508	685	1,510
<b>Measured Drop</b>	1,614	3,558	1,611	3,552
<b>Approximate Attaching Frame</b>	2.3	5.1	11.3	24.9
<b>Approximate Drop</b>	1,616	3,562	1,622	3,576

### 2.12.2.3 Test Orientations

Three certification tests were performed. Two tests were performed on CTU 1, a 9 m (30 ft) slap-down on the lid and a 1 m (40 in) oblique puncture test on the lid. A 9 m (30 ft) end drop was performed on CTU 2.

The 9 m (30 ft) drop on the lid was designed to provide maximum acceleration to the end of the fuel as well as maximize the crush of the package for criticality evaluation purposes. The top down orientation was chosen because the lid contains the least material. The lid down orientation was also chosen because on previous tests horizontal lid down tests had maximized the crush and had resulted in the failure of the retaining bolts on the frame holding the IC. As discussed in Section 2.7.1.4, the drop orientation was at 15 degrees with the horizontal. See Figure 2-26.

The 1 m (40 in) puncture test was performed on CTU 1 with the lid down after the 9 m (30 ft) slap-down test. The package was oriented at a 25 degree angle to maximize the possibility of the corner of the puncture bar penetrating the OC and maximizing the damage to the IC and fuel. The puncture bar was aligned over the center of gravity of the package. See Figure 2-27 and Figure 2-28.

CTU 2 was dropped 9 m (30 ft) with its lower end down. The purpose of this orientation was to maximize the damage to the fuel. The lower end was chosen because it is the most rigid end of the fuel assembly. The expansion springs outside the cladding tubes are on the upper end. See Figure 2-29.

#### **2.12.2.4 Test Performance**

Testing was performed at the National Transportation Research Center in Oak Ridge, Tennessee. The CTUs were shipped to the facility fully assembled. Only the additional tare weight as described in Section 2.12.2.2 was added at the test facility. Tests were performed on the packages prior to them being transported to the Framatome-ANP facility at Lynchburg, Virginia. At Lynchburg the packages were disassembled and examined, and the fuel rods were helium leak tested.

The slapdown test at 15 degrees to horizontal demonstrated the ability of the OC to protect the fuel and the IC. The energy absorbing capabilities of the package allowed the package to deform and limited the secondary impact to less than the primary impact. See Figure 2-30 and Figure 2-31. This test resulted in deformation inside the package. See Figure 2-37 and Figure 2-38. The crush of the paper honeycomb was limited by the stiffening plates in the lid. See Figure 2-39. The IC lid was deformed as well. Neither the lid bolts on either container nor the bolts on the IC clamping device failed. The frame did bend over 3 cm. The fuel rods, although slightly deformed due to the test and the added weight in the fuel cavity, were not damaged. See Figure 2-40. The added weight placed between the bolster timbers caused a slight deformation of the bottom wall of the outer package in the local area of the weights.

The puncture test was performed with the lid down at a 25-degree angle from horizontal (see Figure 2-27 and Figure 2-28). The puncture pin was bolted with three bolts to the drop pad. The puncture pin struck the lid over the CG of the package after the package had undergone the slap-down test. The pin did not penetrate the outer lid. The outer lid was deformed inward until it came in contact with the IC. This was confirmed by a slight mark on the IC lid. The pin appears to have bounced because there are two indentations very close together which could have been caused by the outer lid bottoming out against the IC lid. See Figure 2-32 and Figure 2-33. No significant internal package or fuel damage appeared to be attributable to the pin puncture test.

The 9 m (30 ft) end drop test was performed on CTU 2 with the bottom end down. There was little exterior damage to the OC. See Figure 2-34, Figure 2-35, and Figure 2-36. Extensive damage occurred to the inside of the IC as the fuel assemblies and the added weight impacted the interior of the IC. The rigid end fitting of the assembly crushed the wood located at the end of the package. Although some welds broke, the bottom end of the package remained in place. The fuel rods partially came out of the end fitting. The fuel assemblies bent to the side. See Figure 2-41, Figure 2-42, and Figure 2-43.

The mockup fuel assemblies from both CTU 1 and CTU 2 were helium leak tested. The fuel rods from CTU 1 were found to meet the leak tight requirements of having a leak rate less than  $1 \times 10^{-7}$  atm-cc/s. The fuel rods from CTU 2 were found to have a helium leak rate of  $5.5 \times 10^{-6}$  atm-cc/s. This is within the allowable leakage for the fuel as shown in Chapter 4.0.

#### **2.12.2.5 Test Summaries**

Two 9 m (30 ft) drops and one oblique puncture pin test were performed on two CTUs. The packages retained the fuel assemblies and protected the fuel. Mockup fuel rods from both

NEDO-33869 Revision 11  
Non-Proprietary Information

certification units were leak tested after the drop tests and were determined to have maintained containment. The tests are summarized in Table 2-11.

**Table 2-11    Testing Summary**

<b>Test</b>	<b>CTU</b>	<b>Orientation with Horizontal</b>	<b>Exterior Damage</b>	<b>Interior Damage</b>	<b>Fuel</b>
9 m (30 ft) lid down  Free Drop	1	15°	Minor deformation on both ends.	No bolts broken on the frame or the lids. Significant deformation to IC and internal clamp frame. Reduction of spacing between outside of package and fuel to about 4 inches.	Minimal damage to the fuel assemblies. Some twist to the assembly. No real damage to the fuel rods. The fuel was demonstrated to have a leak rate of less than $1 \times 10^{-7}$ atm-cc/s after the testing.
1 m (40 in) lid down over CG  Puncture	1	25°	Did not penetrate outer wall	Outer wall contacted IC. Figure 2-40 through Figure 2-43 show some damage to the IC, however, this damage is conservatively modeled in the HAC criticality analyses in Chapter 6.0 and is not sufficient to allow fuel to leak from the container.	The fuel appeared not to be affected by this test. Passed helium leak test.
9 m (30 ft) lower end  Free Drop	2	90°	Localized damage on impact end.	Major crushing of the wood at the end of the inner package and breaking of the inner wall of the IC on the impacted end. The outer wall was damaged but did not fail completely.	Fuel was bent and separated from end fittings. Fuel spacers were damaged. Fuel rods had no significant damage. Fuel bending was influenced by the movement of the weight added to the fuel cavity. Observation of deviation from nominal rod-to-rod pitch was localized to the lower 1,626 mm (64 in) of the bundle. Post drop leak test giving a helium leak rate of $5.5 \times 10^{-6}$ atm-cc/s demonstrated that containment had been maintained.



**Figure 2-17 Inner Container Being Prepared to Receive Mockup Fuel and Added Weight**

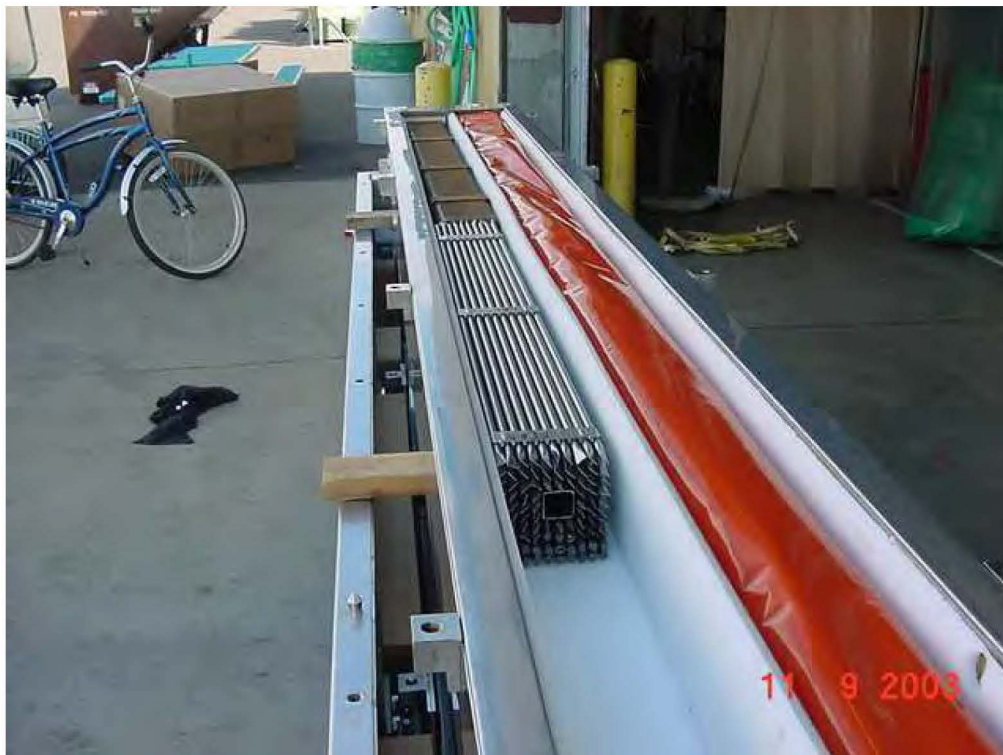


**Figure 2-18 Partial Fuel Assemblies in CTU 1**

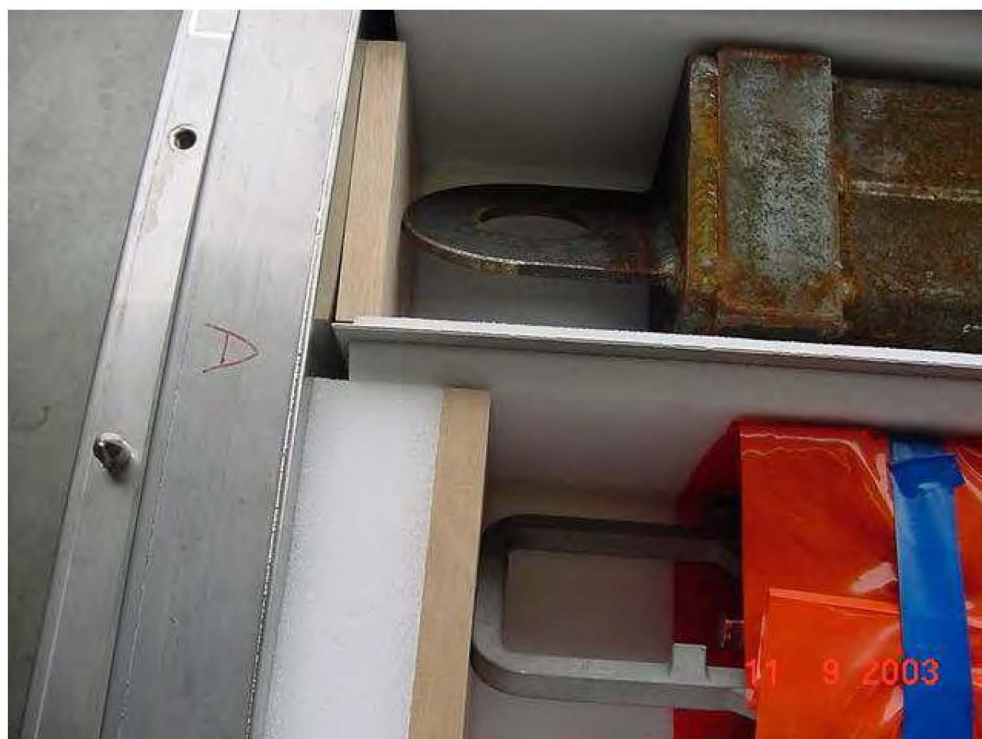


**Figure 2-19 Top End Fittings on Fuel in CTU 1**





**Figure 2-20 Contents of CTU 2**



**Figure 2-21 Outer Container without Inner Container**



**Figure 2-22 Inner Container Secured in Outer Container**



**Figure 2-23 CTU 2 Prior to Testing**





**Figure 2-24 Addition of Tare Weight to CTU 1**



**Figure 2-25 Addition of Tare Weight to CTU 2**



**Figure 2-26 CTU 1 Positioned for 15° 9 m (30 ft) Slap-Down Drop**



**Figure 2-27 Alignment for Oblique Puncture**





**Figure 2-28 Position for Puncture Test**



**Figure 2-29 Position for End Drop**



**Figure 2-30 Primary Impact End Slap-Down Damage**



**Figure 2-31 Secondary Impact End Damage**



**Figure 2-32 Puncture Damage**



**Figure 2-33 Close Up of Puncture Damage**



**Figure 2-34 End Impact**



**Figure 2-35 Damage from End Impact (Bottom and Side)**





**Figure 2-36 End Impact Damage (Top and Side)**



**Figure 2-37 Damage Inside Outer Container to CTU 1**



**Figure 2-38 Internal Damage to Outer Container CTU 1**



**Figure 2-39 Lid Crush on CTU 1**



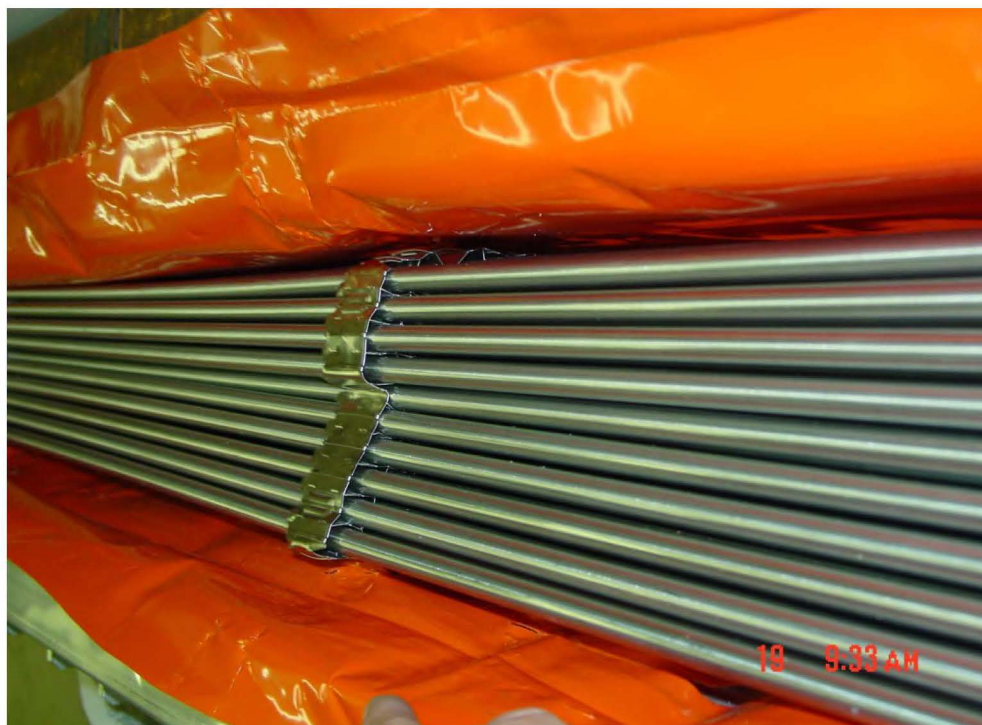


**Figure 2-40 Damage to Fuel in CTU 1**

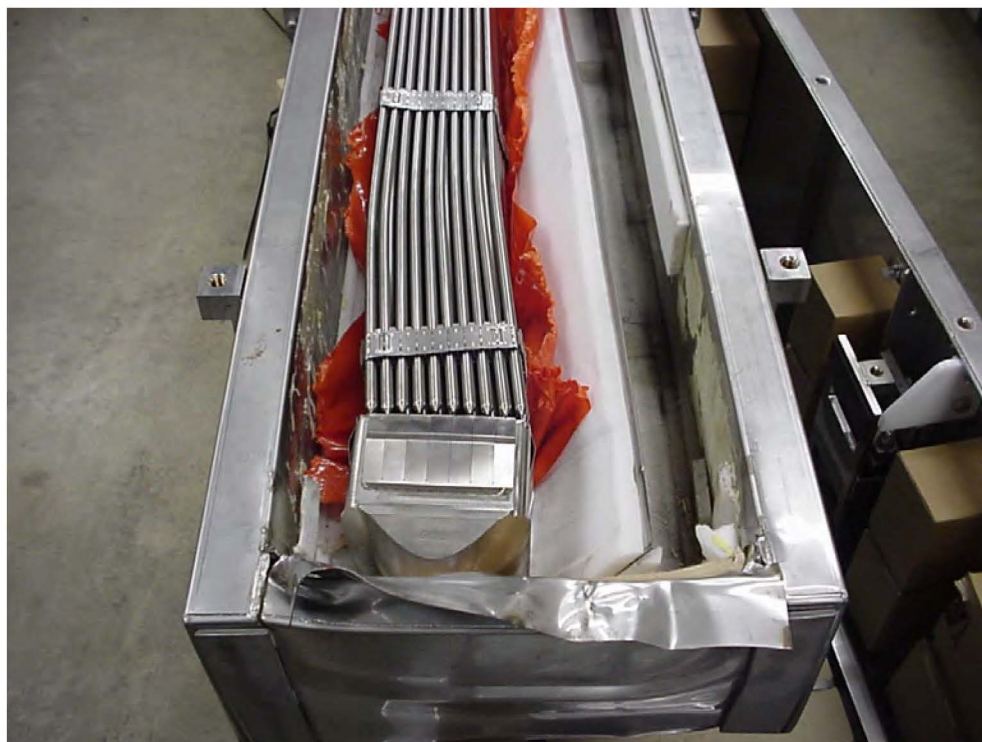


**Figure 2-41 Internal Damage to CTU 2**



**Figure 2-42 Fuel Damage CTU 2**

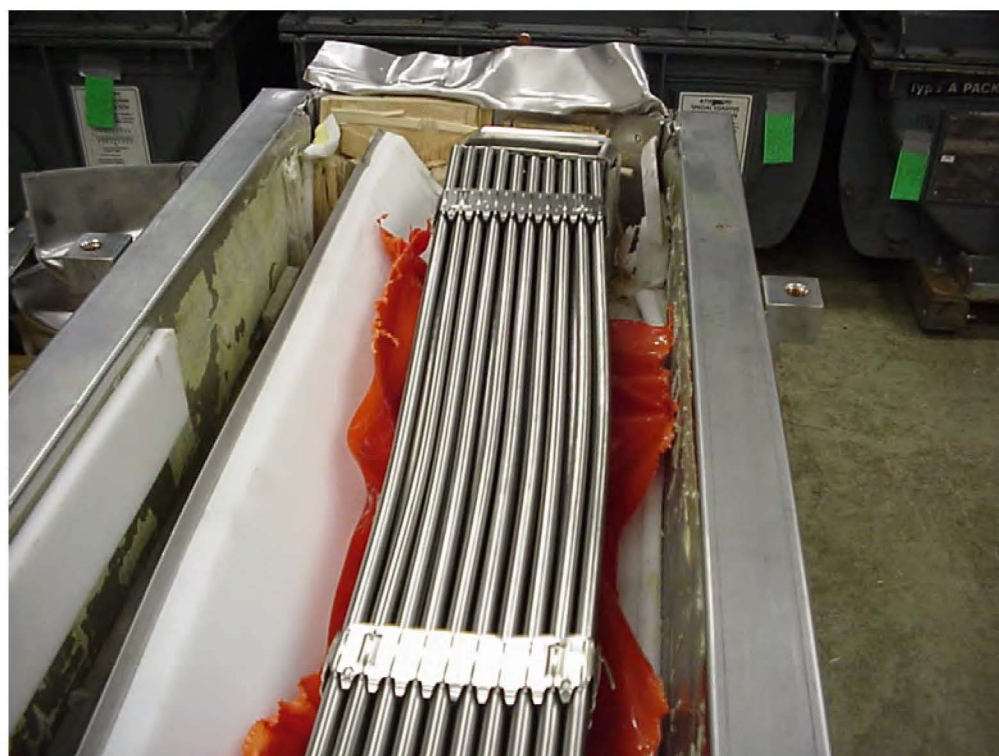


**Figure 2-43 Fuel Prior to Leak Testing CTU 2**

### **2.12.3 GNF-J Certification Tests**

NCT and HAC certification testing of the RAJ-II package was also performed by GNF-J as part of obtaining a Type A(F) package certificate of compliance (Reference 2-22) in Japan. For the U.S. testing, the GNF-J certification tests were utilized to determine the worst-case test orientations for the certification tests identified in Section 2.12.2. This section summarizes the GNF-J RAJ-II certification tests.

#### **2.12.3.1 Certification Test Units**

Two CTUs were utilized for the GNF-J RAJ-II tests. Each CTU was fabricated in accordance with the packaging general arrangement drawings found in Section 1.3.1, with the following exceptions:

1. The lateral wood bolsters on each end were not installed. Elimination of these wood bolsters is conservative for the free drops.
2. Maximum content weight was 560 kg (1,235 lb), which results in a maximum package weight of 1,490 kg (3,285 lb). This weight reduction is less than 8% lower than the maximum gross weight of the RAJ-II package and will result in higher impact forces. The small difference in weight will have an insignificant effect on the free drop response of the package and/or fuel assembly.

One simulated fuel assembly and one dummy weight were utilized in each CTU to simulate the payload contents. Accelerometers were installed on the CTUs to measure and record each free drop impact. No accelerometers were used for the puncture drop tests.

#### **2.12.3.2 Test Orientations**

Because the RAJ-II package relies on the fuel cladding as the containment boundary, free drop and puncture drop orientations that could damage the fuel cladding and potentially breach the containment boundary were included in the test series. In addition, orientations that could damage the package and/or the fuel assemblies such that an unsafe criticality geometry would exist were included in the test series.

Free drop orientations that could result in this type of damage include:

1. Vertical drop on the package end – maximizes axial impact acceleration on a fuel assembly, potentially buckling and failing the fuel cladding (containment boundary).
2. Horizontal drop of the package – maximizes lateral impact acceleration on a fuel assembly, potentially bending and failing the fuel cladding (containment boundary).
3. CG-over-upper end bottom corner of the package – maximizes deformation of the OC.

All of these orientations were included in the free drop test series of the package.

Puncture test orientations that could potentially breach the containment boundary (cladding) include:

1. Horizontal puncture by drop onto the center of the package – maximizes puncture impact onto fuel pins and potentially shearing and failure of the fuel cladding (containment boundary).
2. Vertical puncture by drop onto the end of the package – maximizes puncture impact onto the fuel assembly.

Because of the end internal structure and wood dunnage in the OC, the puncture drop on the end will not result in any significant deformation of the fuel assembly or the IC. Therefore, this puncture drop orientation is bounded by the horizontal puncture drop on the center of the package.

The free drop tests included NCT drops of 0.3 m (1 ft) and 1.2 m (4 ft) prior to performing the 9 m (30 ft) HAC free drop on each CTU. The horizontal puncture drop test was only performed on CTU 2J.

Two certification test series were performed. Three free drop tests were performed on CTU 1J, and three free drop and one puncture drop tests were performed on CTU 2J. The test series for each CTU is summarized in Table 2-12. All drop tests were performed at ambient temperature.

### **2.12.3.3 Test Performance**

Free drop and puncture testing was performed at two test facilities in Japan. At one facility, the drop pad consisted of a 32 mm (1.26 in) thick steel plate that was embedded in a 1 m (40 in) thick concrete and steel support structure, with an overall length of 8 m (26 ft). The other drop pad consisted of a 50 mm (1.97 in) thick  $\times$  5 m (16.4 ft)  $\times$  5 m (16.4 ft) steel plate that was embedded in a 450 mm (12 in) thick  $\times$  8.5 m (27.9 ft) wide concrete and steel structure. The mass of each drop pad constituted an essentially unyielding surface for the CTUs, which weighed approximately 1,490 kg (3,285 lb).

#### **2.12.3.3.1 CTU 1J**

CTU 1J was tested for a total of six free drop tests at heights of 0.3 m (1 ft), 1.2 m (4 ft), and 9 m (30 ft). Figure 2-44 through Figure 2-49 sequentially photo-document the CTU 1J tests.

The maximum resultant accumulated deformation, ~163 mm (~6 in) occurred in the OC body corner. This orientation resulted in the maximum impact acceleration of 203g. No failure of the cladding (containment boundary) occurred from this test series.

#### **2.12.3.3.2 CTU 2J**

The testing of CTU 2J focused on free drop orientations not addressed by the CTU 1J tests. In addition, a HAC puncture drop test and HAC thermal test were performed. A total of three free drop tests at heights of 0.3 m (1 ft), 1.2 m (4 ft), and 9 m (30 ft) were performed. Figure 2-50 and Figure 2-51 sequentially photo-document the CTU 2J tests.

The maximum resultant accumulated deformation, ~163 mm (~6 in) occurred in the OC body corner. This orientation resulted in the maximum impact acceleration of 146g. No failure of the cladding (containment boundary) occurred from this test series.

#### **2.12.3.4 Test Summaries**

Two 0.3 m (1 ft), four 1.2 m (4 ft), three 9 m (30 ft) free drops, one 1 m (40 in) puncture drop, and one HAC thermal test were performed on two CTUs. The packages retained the fuel assemblies and protected the fuel. There was no visual damage or loss of fuel pellets from the simulated fuel assemblies from both CTUs. A summary of the test results is provided in Table 2-13.

**Table 2-12 GNF-J CTU Test Series Summary**

CTU	Drop Height, m (ft)	Test Description	Purpose
1J	0.3 (1)	Free drop, CG-over-upper end bottom corner	Normal operation impact on OC body corner.
	1.2 (4)	NCT free drop, CG-over-upper end bottom corner	Impart initial deformation in same orientation as subsequent HAC free drop
		NCT free drop, horizontal on OC lid	Impart initial deformation in same orientation as planned HAC free drop
		NCT free drop, vertical, bottom end	Impart initial deformation in same orientation as subsequent HAC free drop
	9 (30)	HAC free drop, CG-over-end bottom corner	Maximize OC body deformation; potentially fail fuel rod and breach cladding.
		HAC free drop, vertical, bottom end	Maximize axial impact loads on fuel assemblies, potentially buckle fuel rod and breach cladding.
2J	0.3 (1)	Free drop, CG-over-lid corner	Normal operation impact on OC lid/body corner interface.
	1.2 (4)	NCT free drop, horizontal on lid	Impart initial deformation in same orientation as subsequent HAC free drop
	9 (30)	HAC free drop, horizontal on lid	Maximize lateral impact loads on fuel assemblies, potentially breaching cladding.
	1 (3.3)	HAC puncture drop, horizontal on OC lid	Impact directly on HAC free drop damage; attempt to rupture fuel cladding.
	N/A	HAC thermal test	Demonstrate thermal performance of package.



**Table 2-13 GNF-J CTU Test Series Results**

CTU	Drop Height, m (ft)	Test Description	Result
1J	0.3 (1)	Free drop, CG-over-upper end bottom corner	Combined deformation of ~40 mm (~1.6 in) of bottom corner.
	1.2 (4)	NCT free drop, CG-over-upper end bottom corner	
		NCT free drop, horizontal on OC lid	No significant deformation.
		NCT free drop, vertical, bottom end	Impacted end deformed ~3.9 mm (~0.2 in).
	9 (30)	HAC free drop, CG-over-upper end bottom corner	Impacted OC bottom corner deformed ~163 mm (~6 in), OC lid corner ~101 mm (~4 in). Maximum acceleration of 203g.
		HAC free drop, vertical, bottom end	IC body/lid deformed ~2 - 81 mm (~0.08 - 3 in) in length, U-shaped lifting bar on fuel assembly bent due to contact with wood end dunnage. Maximum acceleration of 58g.
2J	0.3 (1)	Free drop, CG-over-lid corner	Combined deformation of ~2.9 mm (~0.1 in) of lid corner.
	1.2 (4)	NCT free drop, horizontal on lid	
	9 (30)	HAC free drop, horizontal on lid	Impacted side deformed ~2 - 19 mm (~0.08 -0.8 in), localized weld failure of OC lid flange/OC lid sheet interface, no failure of OC lid bolts. Maximum acceleration of 146g.
	1 (3.3)	HAC puncture drop, horizontal on OC lid	~100 mm deep × ~2,000 mm (~4 in × ~79 in) wide indentation in OC lid, no breach of OC lid sheet.
	N/A	HAC thermal test	No failure of simulated fuel assembly cladding.



**Figure 2-44 CTU 1 J 9-m CG-Over-Upper End Bottom Corner Free Drop: View of Impacted Corner**

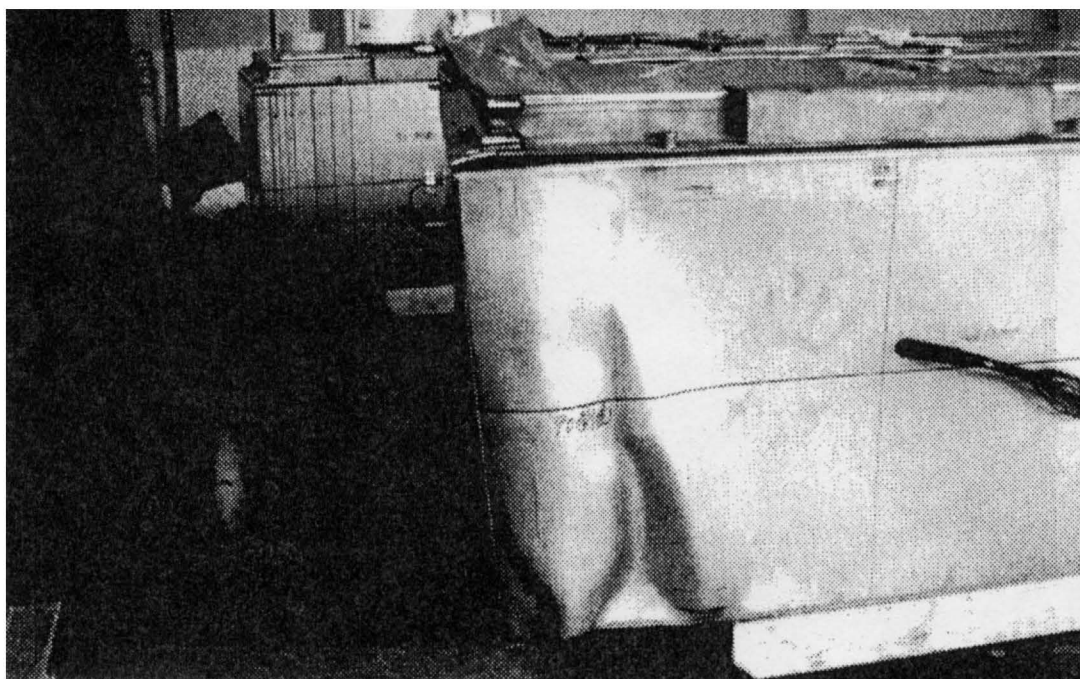


**Figure 2-45 CTU 1J 9-m CG-Over-Upper End Bottom Corner Free Drop: View of Opposite Corner**

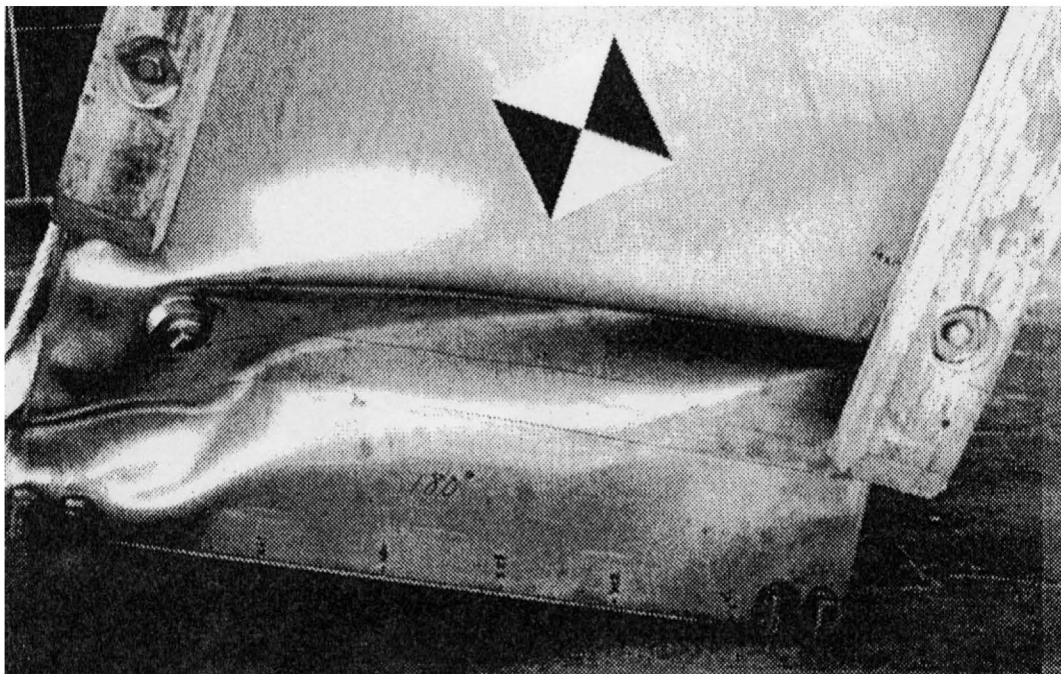


**Figure 2-46 CTU 1J 9-m CG-Over-Upper End Bottom Corner Free Drop: View of Bottom**

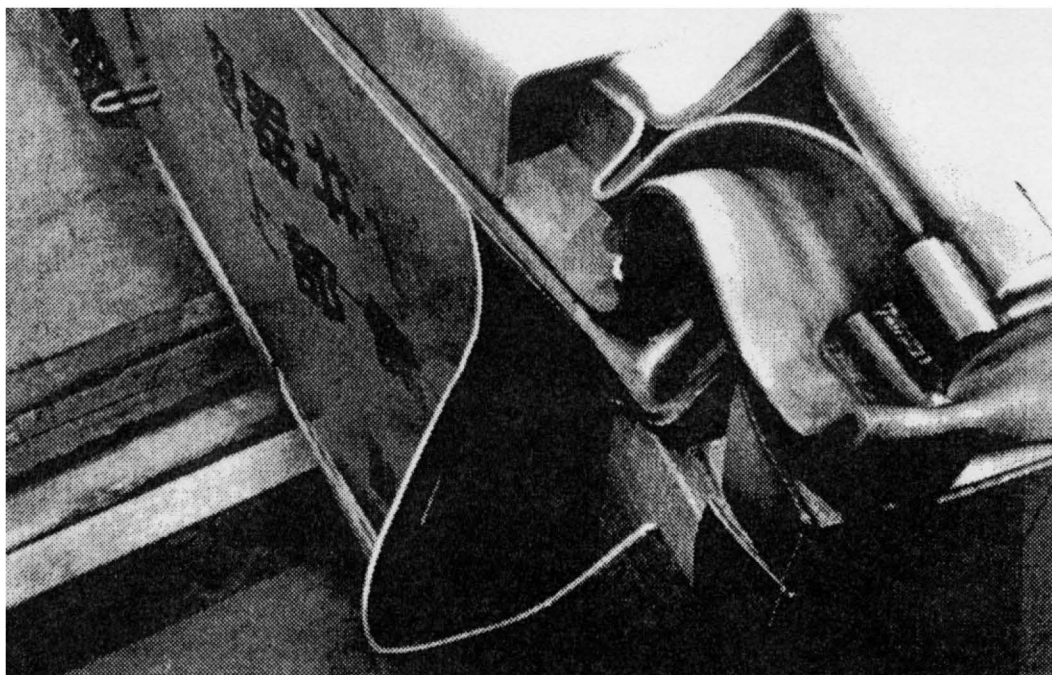


**Figure 2-47 CTU 1J 9-m CG-Over-Upper End Bottom Corner Free Drop: Close-Up View of Top Corner**

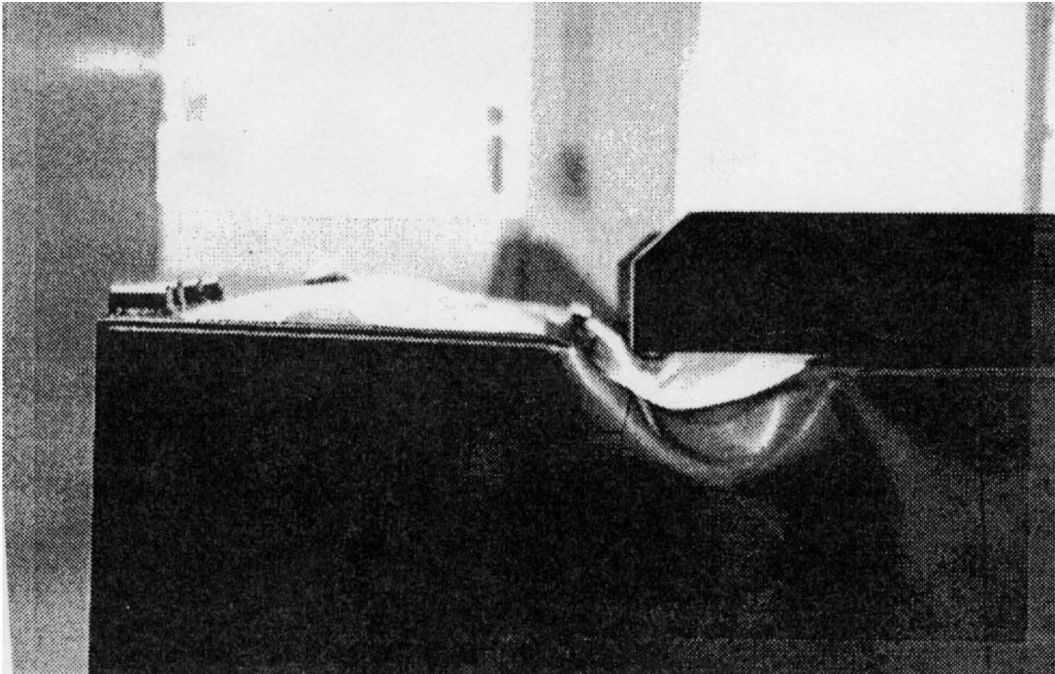


**Figure 2-48 CTU 1J 9-m Vertical End Drop: Close-Up Side View of Bottom Damage**

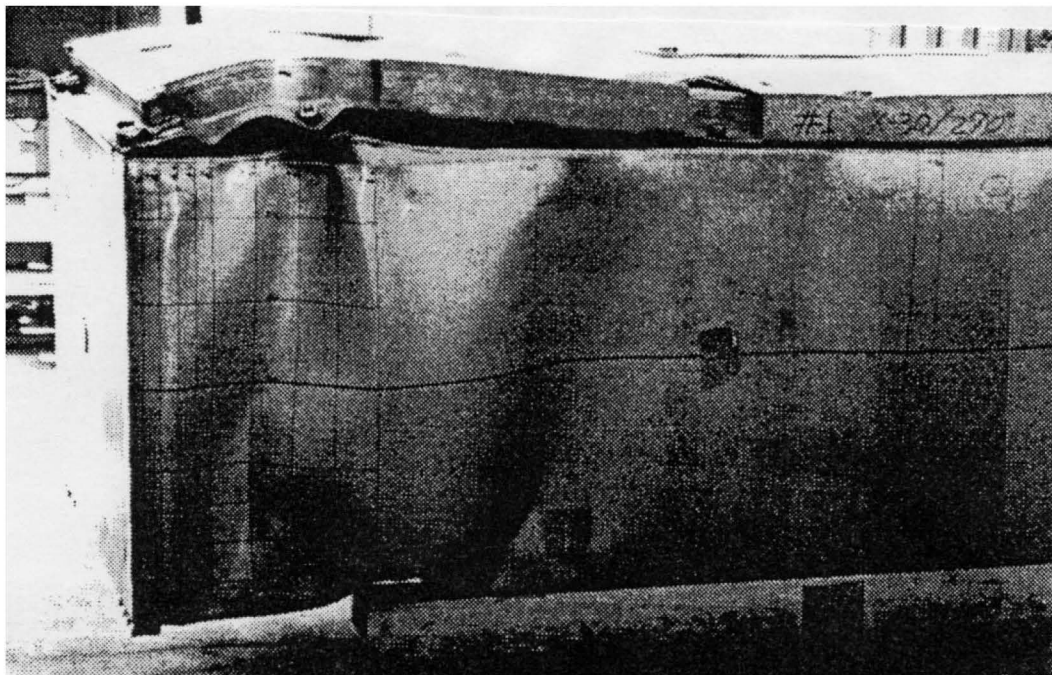


**Figure 2-49 CTU 1J 9-m Vertical End Drop: Overall View of Damage**



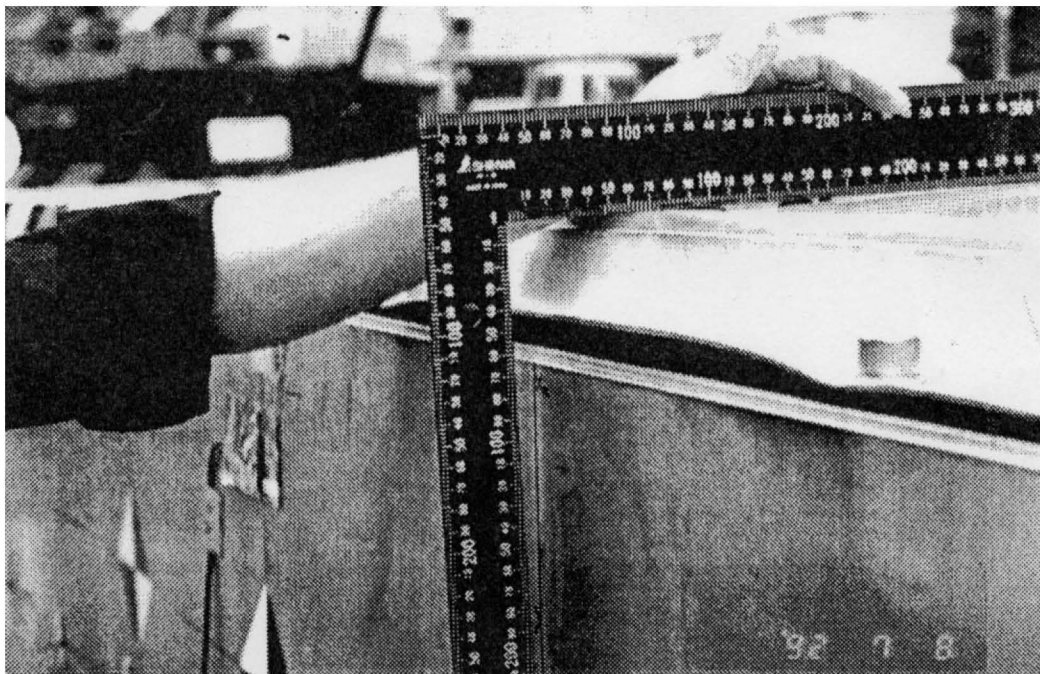


**Figure 2-50 CTU 2J 9-m Horizontal Free Drop: Close-Up Side View of Damage**

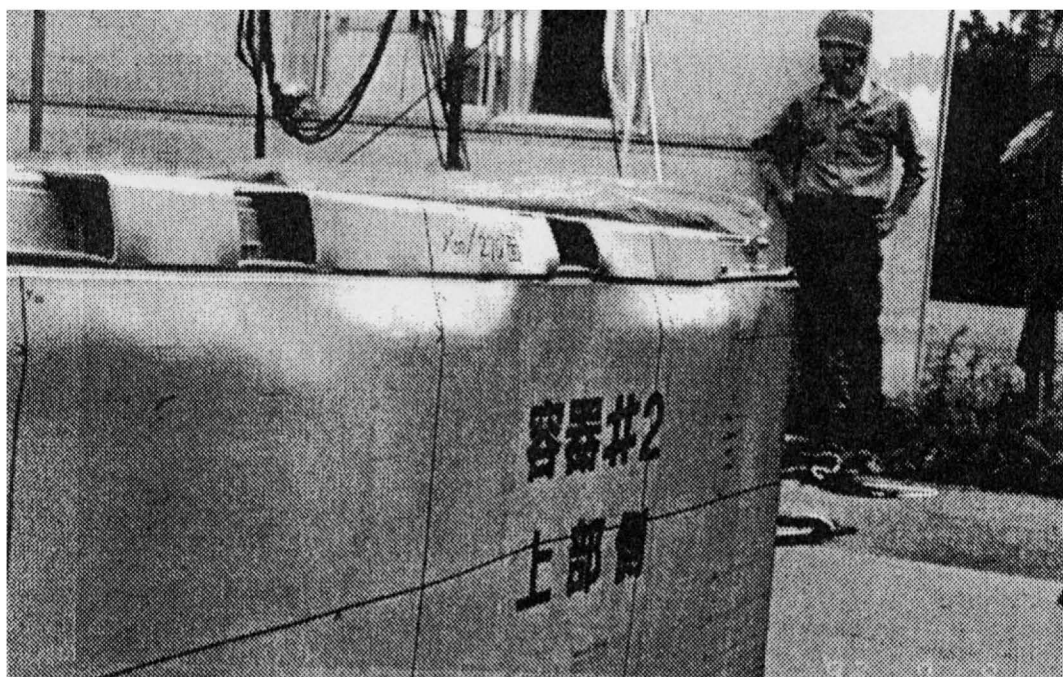


**Figure 2-51 CTU 2J 9-m Horizontal Free Drop: Overall Side View of Damage**

#### 2.12.4 Outer Container Gasket Sealing Capability

The OC for the RAJ-II packaging utilizes a 5 mm thick  $\times$  40 mm wide  $\times$  11,360 mm long, 50 shore durometer, solid natural rubber gasket. As shown in Section 1.3.1, the gasket is attached to the flange of the OC lid. The OC lid is secured to the OC body by twenty-four (24) M14  $\times$  2, Type 304 stainless steel bolts, which are tightened to wrench tight or as defined in user procedures. Because a tightening torque is not specified, the maximum bolt tension will be based on the minimum yield strength of the stainless steel.

The maximum force,  $F_b$ , in each lid bolt will be:

$$F_b = S_y (A_t)$$

where:  $S_y$  = Minimum yield strength = 206.8 MPa (30.0 ksi) (See Table 2-2)

$A_t$  = Tensile area for M14  $\times$  2 bolt = 115 mm<sup>2</sup> (0.1783 in<sup>2</sup>)

Substituting these values into the above equation yields a bolt force of 23,782 N (5,349 lbf). The total compressive force applied to the gasket,  $F_{\text{gasket}}$ , is then:

$$F_{\text{gasket}} = (24)F_b = (24)(23,782) = 570,768 \text{ N (128,376 lb}_f\text{)}$$

For the applied bolt force, the gasket compressive area,  $A_{\text{gasket}}$ , is  $40 \times 11,360 = 454,400 \text{ mm}^2$  (704.3 in<sup>2</sup>). Conservatively neglecting any deflection of the 4 mm thick lid flange between the lid bolts, the resultant compressive stress on the gasket is then:

$$\sigma_{\text{gasket}} = \frac{570,768}{454,400} = 1.256 \text{ MPa (182 psi)}$$

The shape factor,  $s$ , for the 5  $\times$  40 gasket is:

$$s = \frac{\text{One Load Area}}{\text{Total Free Area}} = \frac{\text{Width}}{2(\text{thickness})} = \frac{40}{10} = 4.0$$

From Figure 5-12 of Reference 2-23, the percent compressive deflection of the 50-durometer gasket with  $s = 4.0$  at 182 psi compressive stress is approximately 3%, or 0.15 mm (0.006 in), which is minimal.

To determine whether the gasket is compressed with the applied bolt force, the compression modulus and the linear spring rate for the gasket is computed. From Equation 3-7 of Reference 2-23, the linear spring rate,  $K_L$ , for the rubber gasket is:

$$K_L = \frac{E_c(A)}{h}$$

where:  $E_c$  = Compression modulus

$A$  = Compression area of gasket = 454,400 mm<sup>2</sup> (704.3 in<sup>2</sup>)

$h$  = height of gasket = 5 mm (0.197 in)

The compression modulus is extracted from Figure 5-20 of Reference 2-23 for a shape factor “s” of 4.0 and an approximate compression of 3% for the 50 durometer gasket. From this figure, the compression modulus is interpolated to be 6,912 psi (47.7 MPa). The linear spring rate of the gasket is then:

$$K_L = \frac{6,912(704)}{0.197} = 24.7 \times 10^6 \text{ lb}_f/\text{in} \quad (4.33 \times 10^6 \text{ N/mm})$$

To compress the gasket 0.15 mm (0.006 in), the required force in the bolts is:

$$\begin{aligned} 24F_{\text{bolt}} &= K_L \Delta = 24.7 \times 10^6 (0.006) = 148,200 \text{ lb}_f \quad (659,266 \text{ N}) \\ \Rightarrow F_{\text{bolt}} &= 6,175 \text{ lb}_f \quad (27,648 \text{ N}) \end{aligned}$$

Because the resultant bolt force required to compress the gasket 3% is greater than the yield strength of the lid bolts, the gasket will not be compressed to the estimated 3% compression.

To determine the estimated gasket compression with the maximum lid bolt force at yield strength (23,782 N [5,349 lb<sub>f</sub>]), the linear spring rate will be computed for zero compression and then compared to the applied maximum force. From Figure 5-20 of Reference 2-23 for a shape factor “s” of 4.0, the compression modulus at zero compression will be:

$$E_c = 9,000(0.75) = 6,750 \text{ psi} \quad (46.5 \text{ MPa})$$

For zero compression and this compression modulus, the linear spring rate is:

$$K_L = \frac{6,750(704)}{0.197} = 24.1 \times 10^6 \text{ lb}_f/\text{in} \quad (4.23 \times 10^6 \text{ N/mm})$$

The resultant deformation of the gasket for this spring rate with the maximum bolt force is:

$$\Delta_{\text{gasket}} = \frac{24(F_{\text{bolt}})}{K_L} = \frac{24(23,782)}{4.23 \times 10^6} = 0.135 \text{ mm} \quad (0.005 \text{ in})$$

This deformation is approximately a 2.7% compression of the gasket. Prototypic seal testing in support of the TRUPACT-II package (Reference 2-24) has demonstrated that a pressure seal requires a minimum of 10% – 12% compression. Section 3.6, *Squeeze*, of the Parker O-ring Handbook (Reference 2-25) states that “*The minimum squeeze for all seals, regardless of cross-section should be about 0.2 mm (0.007 in). The reason is that with a very light squeeze almost all elastomers quickly take 100% compression set.*” Based on these test results and the recommendations of Parker, the outer lid gasket will not form a pressure retaining seal.

### **3.0 THERMAL EVALUATION**

This chapter provides an evaluation of the package to protect the fuel during varying thermal conditions.

#### **3.1 DESCRIPTION OF THERMAL DESIGN**

The RAJ-II package is designed to provide thermal protection, as described in Subpart F of 10 CFR 71, for transport of unirradiated BWR fuel assemblies, BWR fuel rods, CANDU fuel rods, and PWR fuel rods with negligible decay heat. Compliance with 10 CFR 71 Subpart F is demonstrated in the following subsections. The RAJ-II protects the fuel through the use of an inner and outer container that restricts exposure of the fuel to heat loads. The insulated inner container further restricts the heat input to the fuel through its insulation. The fuel requires very little thermal protection because similar BWR fuels have been tested and maintained containment up to 800°C, while various non-BWR fuel types (PWR and CANDU) have been analyzed to maintain containment up to 765°C.

Given negligible decay heat, the thermal loads on the package in Section 3.3 come solely from the environment in the form of solar radiation for Normal Conditions of Transport (NCT), and in Section 3.4 the thermal loads on the package come from a half-hour, 800°C (1,475°F) fire for Hypothetical Accident Conditions (HAC).

Specific ambient temperatures and solar heat loads are considered in the package thermal evaluations. Ambient temperatures ranging from -40°C to 38°C (-40°F to 100°F) are considered for NCT. The HAC fire event considers an ambient temperature of 38°C (100°F), with solar heat loading (insolation) before and after the HAC half-hour fire event.

Details and assumptions used in the analytical thermal models are described with the thermal evaluations.

##### **3.1.1 Design Features**

The primary features that affect the thermal performance of the package are: 1) the materials of construction, 2) the inner and outer containers, and 3) the thermal insulation of the inner container. The stainless sheet metal construction of the structural components of the inner and outer containers influences the maximum temperatures under normal conditions. The material also ensures structural stability under the HAC as well as provides some protection to the fuel. Likewise, the zirconium alloy cladding has also been proven to be stable at the high temperatures potentially seen during the HAC.

The multi walled construction of the single walled outer container and the double walled inner container reduces the heat transfer as well as provides additional stability. The multi walled construction also reduces the opportunity for the fire in the accident conditions to impinge directly on the fuel. The thermal insulation also greatly reduces the heat transfer to the fuel from external sources. The insulation consists of alumina silicate within the walls of the inner container, plus the use of wood on the ends that both provide some insulation as well as shock absorbing capabilities.



### 3.1.2 Content's Decay Heat

Because the contents are unirradiated fuel, the decay heat is insignificant ( $< 1$  Watt).

### 3.1.3 Summary Tables of Temperatures

Because the decay heat load is negligible, the maximum NCT temperature of the inner container exterior is 215°F (102°C, 375 K) and the maximum of the inner container interior is 171°F (77°C, 350 K). The maximum HAC temperature of 1,198°F (648°C, 921 K) occurs at the inner surface of the inner container at the end of the fire. These temperatures are based on the paper honeycomb material due to the combustible energy provided by the paper material, making it the most conservative for the full thermal analysis of NCT followed by HAC. With conservatism, these analyses demonstrate that the RAJ-II package provides adequate thermal protection for the fuel rods and will maintain the maximum fuel rod temperature well below the BWR fuel rod cladding rupture temperature of 800+°C, and various non-BWR fuel types (PWR and CANDU) cladding rupture temperature of 765°C under all transportation conditions. Table 3-8 and Table 3-6 summarize the temperatures of various packaging components during NCT and HAC; respectively and are based on the paper honeycomb material.

### 3.1.4 Summary Tables of Maximum Pressures

The maximum pressure within the containment, the fuel rods, during NCT is 1.33 MPa absolute (193 psia) and 3.0 MPa absolute (435 psia) for BWR and non-BWR fuel types (PWR and CANDU) respectively. The maximum pressure during the HAC is 3.50 MPa absolute (508 psia) and 7.89 MPa absolute (1,144 psia) for BWR and non-BWR fuel types (PWR and CANDU) respectively. Table 3-1 summarizes the maximum pressures of the various fuel types.

**Table 3-1 Summary of Maximum Pressures**

Fuel Rod Type	Maximum Absolute Pressure	
	NCT	HAC
BWR	1.33 MPa (193 psia)	3.50 MPa (508 psia)
Non-BWR (PWR & CANDU)	3.0 MPa (435 psia)	7.89 MPa (1,144 psia)

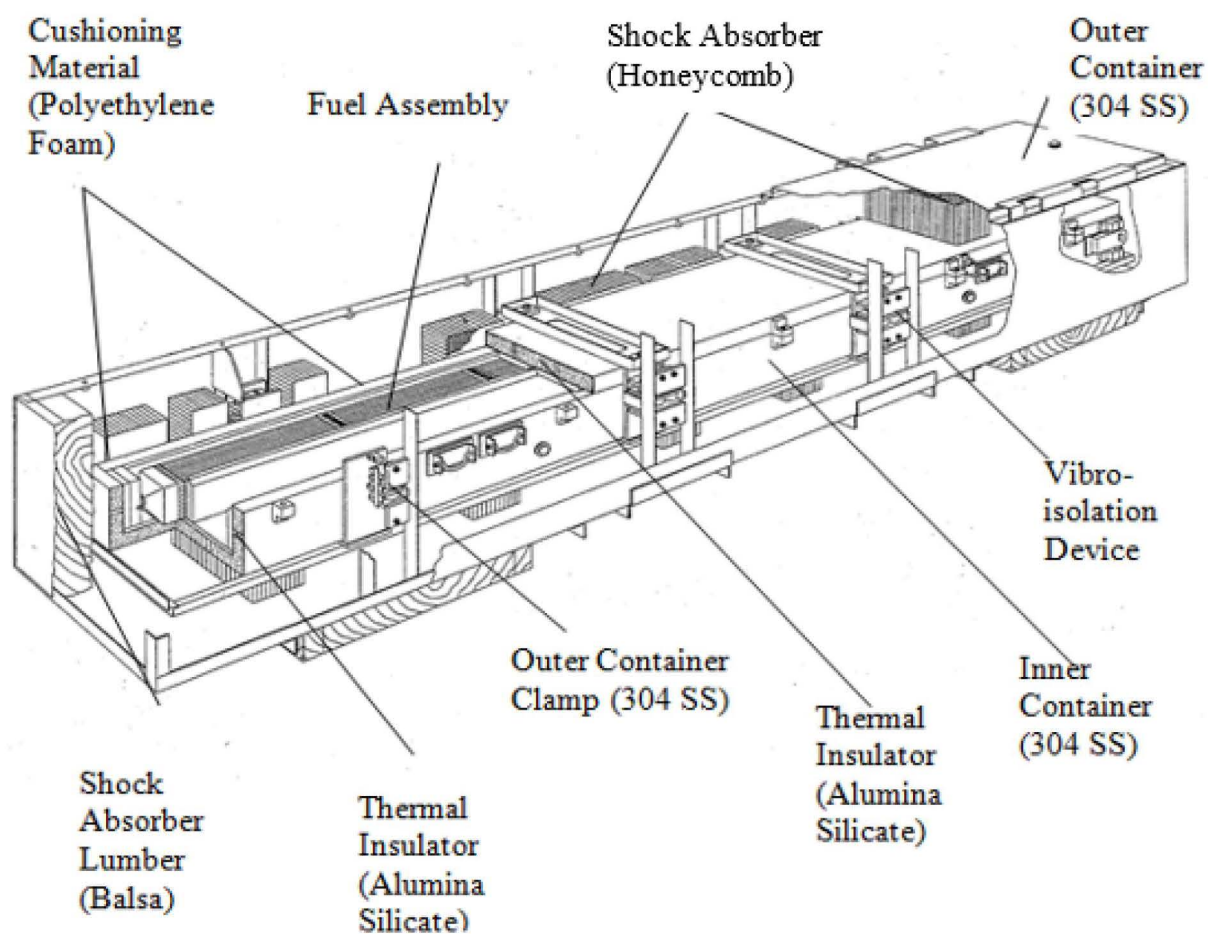


**Figure 3-1 Overall View of RAJ-II Package**

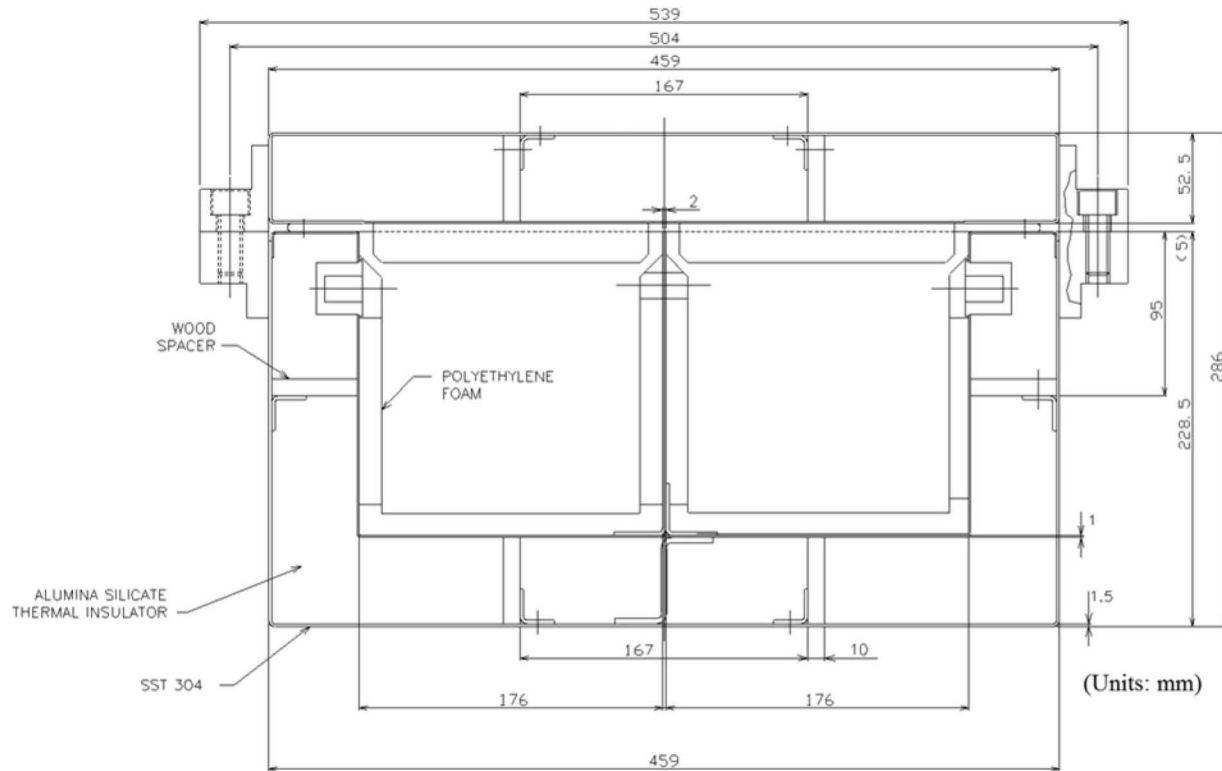


**Figure 3-2 Transverse Cross-Sectional View of the Inner Container**

## **3.2 MATERIAL PROPERTIES AND COMPONENT SPECIFICATIONS**

### **3.2.1 Material Properties**

The RAJ-II inner container is constructed primarily of Series 300 stainless steel, wood, and alumina silicate insulation. The void spaces within the inner container are filled with air at atmospheric pressure. The outer container is constructed of Series 300 stainless steel, wood, and honeycomb constructed of resin impregnated paper or aluminum. The thermal properties of the principal materials used in the thermal evaluations are presented in Table 3-2 and Table 3-3. Where necessary, the properties are presented as functions of temperature. Note that only properties for materials that constitute a significant heat transfer path are defined. A general view of the package is depicted in Figure 3-1. A sketch of the inner container transversal cross-section with the dimensions used in the calculation is presented in Figure 3-2.

For the alumina silicate, maximum values are specified because the maximum conductivity is the controlling parameter. This is because there is no significant decay heat in the payload and the only consideration is the material's ability to repel the rate of heat transfer to the fuel during the fire event.

**Table 3-2      Material Properties for Structural / Thermal Components**

Material	Temperature (K)	Thermal Conductivity (W/m-K)	Specific Heat (J/kg-K)	Density (kg/m <sup>3</sup> )	Notes
Wood	300	0.240	2,800	500	①
Series 300 Stainless Steel	300	15	477	7,900	②
	400	17	515		
	500	18	539		
	600	20	557		
	800	23	582		
	1,000	25	611		
Alumina Silicate Insulation	673	≤0.105	1,046 (Nominal)	250 (Nominal)	③
	873	≤0.151			
	1,073	≤0.198			④
	1,273	≤0.267			④

**Notes:**

- ① The material specified for the wood spacers. The properties have been placed with typical values for generic softwood.
- ② Reference 3-1, p.809, 811, 812, and 820.
- ③ The values shown are based on published data for Unifrax Duraboard LD (Reference 3-2) and include compensation for the possible variation in test data; see discussion in Section 3.2.1.
- ④ Values at temperatures higher than 1,000 K are linearly extrapolated.

**Table 3-3 Material Properties for Air**

<b>Temperature (K)</b>	<b>Thermal Conductivity (W/m-K)</b>	<b>Density (kg/m<sup>3</sup>)</b>	<b>Specific Heat (J/kg-K)</b>	<b>Coefficient of Kinematic Viscosity(m<sup>2</sup>/s)</b>	<b>Prandtl Pr (-)</b>
300	0.0267	1.177	1005	15.66 E-06	0.69
310	0.0274	1.141	1005	16.54 E-06	0.69
320	0.0281	1.106	1006	17.44 E-06	0.69
330	0.0287	1.073	1006	18.37 E-06	0.69
340	0.0294	1.042	1007	19.32 E-06	0.69
350	0.030	1.012	1007	20.30 E-06	0.69
360	0.0306	0.983	1007	21.30 E-06	0.69
370	0.0313	0.956	1008	22.32 E-06	0.69
380	0.0319	0.931	1008	23.36 E-06	0.69
390	0.0325	0.906	1009	24.42 E-06	0.69
400	0.0331	0.883	1009	25.50 E-06	0.69
500	0.0389	0.706	1017	37.30 E-06	0.69
600	0.0447	0.589	1038	50.50 E-06	0.69
700	0.0503	0.507	1065	65.15 E-06	0.70
800	0.0559	0.442	1089	81.20 E-06	0.70
900	0.0616	0.392	1111	98.60 E-06	0.70
1000	0.0672	0.354	1130	117.3 E-06	0.70

Source: Reference 3-1, p.824

### 3.2.2 Component Specifications

The configuration of the fuel is reliant on the integrity of the Inner Container (IC) structure. The Series 300 stainless steel and alumina silicate insulation in the RAJ-II package are not sensitive to temperatures within the range of -40°C to 800°C (-40°F to 1,475°F) that spans the NCT and HAC environment. Wood is used as dunnage and as part of the inner package wall in the RAJ-II package. Before potentially decomposing in the HAC fire, the wood would insulate portions of the inner container from exposure to the flames. However, the HAC transient thermal analyses presented herein conservatively neglects the wood's insulating effect, and instead assumes that all of the wood is consumed in the fire generating heat for all of its total mass. The lower melting point temperature of the inner container structural and packing materials are summarized in Table 3-4.

The temperature limit for all BWR fuel rods shipped in the RAJ-II package is greater than 800°C (1,472°F), based on the pressure evaluation provided in Section 3.4.3.2. The temperature limit for all non-BWR fuel rod types (PWR and CANDU) shipped in the RAJ-II package is greater than 765°C (1,409°F), based on the pressure evaluation provided in Section 3.4.3.2.

**Table 3-4 IC Structural and Packing Materials Melting Points**

<b>Material</b>	<b>Lower Melting Point Temperature</b>
Series 300 Stainless Steel	1,400°C (2,550°F)
Alumina Silicate	1,800°C (3,272°F)
Polymer Based Packing Materials	100°C (212°F)
Zirconium	1,850°C (3,362°F)
Uranium Dioxide	2,800°C (5,072°F)

### 3.3 THERMAL EVALUATION UNDER NORMAL CONDITIONS OF TRANSPORT

This section presents the results of the thermal analysis of the RAJ-II package for the NCT specified in 10 CFR 71.71. The maximum temperature of the inner container for the NCT is used as input (initial conditions) in the HAC (fire event) analysis. The NCT thermal conditions are evaluated by closed form calculations.

#### 3.3.1 Heat and Cold

Per 10 CFR 71.71(c)(1), the maximum environmental temperature is 100°F (311 K), and per 10 CFR 71.71(c)(2), the minimum environmental temperature is -40°F (233 K).

Given the negligible decay heat of the fuel assembly, the thermal loads on the RAJ-II package come solely from the environment in the form of solar radiation for NCT as prescribed by 10 CFR 71.71(c)(1). As such, the solar heat input into the package is 800 g·cal/cm<sup>2</sup> for horizontal surfaces and 200 g·cal/cm<sup>2</sup> for vertical surfaces for a varying insolation over a 24-hour period.

##### 3.3.1.1 Maximum Temperatures

For the analysis, the applied insolation is modeled transiently as sinusoidal over a 24-hour period, except when the sine function is negative (the insolation level is set to zero). The timing of the sine wave is set to achieve its peak at 12:00 PM and peak value of the curve is adjusted to ensure that the total energy delivered matched the regulatory values (800 g·cal/cm<sup>2</sup> for horizontal surfaces, 200 g·cal/cm<sup>2</sup> for vertical surfaces). As such, the total energy delivered in one day by the sine wave model is given by:

$$\int_{6 \text{ hr}}^{18 \text{ hr}} Q_{\text{peak}} \cdot \sin(\pi \cdot t / 12 \text{ hr} - \pi / 2) \cdot dt = Q_{\text{peak}} \cdot (24 \text{ hr} / \pi) \quad (1)$$

Using the expression above for the peak rate of insolation, the peak rates for top and side insolation may be calculated as follows:

$$\text{Top Surface: } Q_{\text{peak}} = 800 \text{ cal/cm}^2 \cdot \frac{\pi}{24 \text{ hr}} \cdot \frac{4.1868 \text{ J}}{\text{cal}} \cdot \frac{10^4 \text{ cm}^2}{\text{m}^2} \cdot \frac{\text{hr}}{3600 \text{ s}} = 1,218 \text{ W/m}^2 \quad (2)$$

$$\text{Side Surface: } Q_{\text{peak}} = 200 \text{ cal/cm}^2 \cdot \frac{\pi}{24 \text{ hr}} \cdot \frac{4.1868 \text{ J}}{\text{cal}} \cdot \frac{10^4 \text{ cm}^2}{\text{m}^2} \cdot \frac{\text{hr}}{3600 \text{ s}} = 305 \text{ W/m}^2 \quad (3)$$

Assuming a one-dimensional model where the 800 g·cal/cm<sup>2</sup> is applied to the outside of the thinnest part of the package, the maximum NCT temperature on the inside surface of the inner container, as calculated in Section 3.5.3, is 350 K (77°C, 171°F).

Given negligible decay heat, the maximum accessible surface temperature of the RAJ-II package in the shade is the maximum environment temperature of 38°C (100°F), which is less than the 50°C (122°F) limit established in 10 CFR 71.43(g) for a non-exclusive use shipment.

### 3.3.1.2 Minimum Temperatures

The minimum environmental temperature that the RAJ-II package will be subjected to is -40°C (-40°F), per 10 CFR 71.71(c)(2). Given the negligible decay heat load, the minimum temperature of the RAJ-II package is -40°C (-40°F).

### 3.3.2 Maximum Normal Operating Pressure

The RAJ-II package is intended to transport unirradiated: BWR fuel assemblies, BWR fuel rods, CANDU fuel rods, and PWR fuel rods. The fuel rods are pressurized with helium at ambient temperature (20°C, 293 K) prior to sealing. BWR fuel rods are pressurized with helium to a maximum pressure of 1.1145 MPa absolute (162 psia) at ambient temperature. The Maximum Normal Operating Pressure (MNOP) at the maximum normal temperature (77°C, 350 K) is:

$$\text{MNOP}_{\text{BWR}} = P_1 \cdot T_{\text{max}} / T_{\text{ambient}} = 1.1145 \cdot 350 / 293 = 1.33 \text{ MPa abs. (193 psia)} \quad (4)$$

For non-BWR fuel rod types (PWR and CANDU), the PWR fuel rods have the highest internal helium fill pressure of 2.51 MPa absolute (364 psia) at room temperature (20°C, 293 K). Hence, the MNOP at the maximum normal temperature (77°C, 350 K) is:

$$\text{MNOP}_{\text{non-BWR}} = P_1 \cdot T_{\text{max}} / T_{\text{ambient}} = 2.51 \cdot 350 / 293 = 3.0 \text{ MPa abs. (435 psia)} \quad (5)$$

The MNOPs are conservative as the maximum fuel rod temperature is taken as the maximum temperature on the inside surface of the inner container and neglects the pipe container used for non-BWR loose fuel rod types. Because there is no significant decay heat and the fuel composition is stable, the MNOP is not expected to change over a one-year time period.

## 3.4 THERMAL EVALUATION UNDER HYPOTHETICAL ACCIDENT CONDITIONS

This section presents the results of the thermal analysis of the RAJ-II package for the HAC specified in 10 CFR 71.73(c)(4).

For the purposes of the HAC fire analysis, the outer container of the RAJ-II package is conservatively assumed to not be present during the fire. This allows the outer surface of the inner container to be fully exposed to the fire event. The wood spacers used in the inner container are conservatively assumed to combust completely. By ignoring the outer container and applying the fire environment directly to the inner container, the predicted temperature of the fuel rods is bounded. To provide a conservative estimate of the worst-case fuel rod temperature, the fuel assembly, rods, pipe container, and the corresponding thermal masses are not explicitly modeled as well as the polyethylene foam shock absorber. The maximum fuel rod temperature is conservatively derived from the maximum temperature of the inside surface of the inner stainless

steel wall and neglects the pipe container used for non-BWR loose fuel rod types. The analysis, considering the insulation and multi-layers of packaging, is very conservative because as discussed in Section 3.1, the bare BWR fuel has been demonstrated to maintain integrity when exposed to temperatures that equal those found in the HAC. Likewise, the various non-BWR fuel types (PWR and CANDU) have been analyzed to maintain containment up to a temperature of 765°C for 30 minutes.

Thermal performance of the RAJ-II package is evaluated analytically using a Two-Dimensional (2-D) model that represents a transversal cross-section of the inner container (Figure 3-2) in the region containing the metallic and wood spacers. The 2-D inner container finite element model was developed using the ANSYS computer code (Reference 3-3). ANSYS is a comprehensive thermal, structural, and fluid flow analysis package. It is a finite element analysis code capable of solving steady state and transient thermal analysis problems. Heat transfer via a combination of conduction, radiation, and convection can be modeled.

The solid entities were modeled in the present analysis with PLANE55 2-D elements, and the radiation was modeled using the AUX12 Radiation Matrix method. The developed ANSYS input file is included as Section 3.5.2.

The initial temperature distribution in the inner container prior to the HAC fire event is a uniform 375 K, conservatively corresponding to the outer surface temperature of the inner container per the normal condition calculations presented in Section 3.5.3.

### **3.4.1 Initial Conditions**

The environmental conditions preceding and succeeding the fire consist of an ambient temperature of 38°C (311 K) and insolation per the normal condition thermal analysis. The solar absorptivity coefficient of the outer surface has been increased for the post-fire period to one to include changes due to charring of the surfaces during the fire event.

### **3.4.2 Fire Test Conditions**

The HAC fire event is specified per 10 CFR 71.73(c)(4) as a half-hour, 800°C (1,073 K) fire with forced convection. For the purpose of calculation, the value of the package surface absorptivity coefficient (0.8) is selected as the highest value between the actual value of the surface (0.42) and a value of 0.8 as specified in 10 CFR 71.73(c)(4).

A value of 1.0 for the emissivity of the flame for the fire condition is used in the calculation. The rationale for this is that 1.0 maximizes the heating of the package. This value exceeds the minimum value of 0.9 specified in 10 CFR 71.73(c)(4).

To model the combustion of the wood, the wood elements of the model are given a heat generation rate based on the high heat value of Western Hemlock of 3,630 Btu/lb ( $8.442 \times 10^6$  J/kg) from Reference 3-4, Section 7, Table 9. It is conservatively assumed that the entire mass of the wood will burn. Moreover, the wood will burn across its thinnest section from opposite faces. Using data burn rate data for redwood which has approximately the same density as hemlock (Reference 3-4), each face will burn 5 mm at a minimum rate of 0.543 mm/min (Reference 3-5) resulting in a 9.2-minute time of combustion. This conservatively results in the longest burn time



for the hemlock, and the greatest effect on temperature. The resulting heat generation rate in the wood spacers is equal to:

$$\dot{Q} = (8.442 \cdot 10^6 \text{ J/kg}) \cdot (500 \text{ kg/m}^3) / (9.2 \cdot 60 \text{ sec}) = 7.63 \cdot 10^6 \text{ W/m}^3 \quad (6)$$

#### 3.4.2.1 Heat Transfer Coefficient during the Fire Event

During a HAC hydrocarbon fire, the heating gases surrounding the package will achieve velocities sufficient to induce forced convection on the surface of the package. Peak velocities measured in the vicinity of the surfaces were under 10 m/s (Reference 3-6).

The heat transfer coefficient takes the form (Reference 3-7, p. 369):

$$h = k/D \cdot C \cdot (u \cdot D/\nu)^m \cdot \text{Pr}^{1/3} \quad (7)$$

Where:

D: average width of the cross-section of the inner container (0.373 m)

k: thermal conductivity of the fluid

$\nu$ : kinematic viscosity of the fluid

u: free stream velocity

C, m: constants that depend on the Reynolds number ( $\text{Re} = u \cdot D/\nu$ )

Pr: Prandtl number for the fluid

The property values of k,  $\nu$ , and Pr are evaluated at the film temperature, which is defined as the mean of the wall and free stream fluid temperatures. At the start of the fire the wall temperature is 375 K (101.7°C, 215°F) and the stream fluid temperature is 1,073 K (1,475°F). The film temperature is therefore 710.5 K, and the property values for air at this temperature (interpolated from Table 3-3) are  $k=0.0509 \text{ W/m} \cdot \text{K}$ ,  $\nu=66.84 \cdot 10^{-6} \text{ m}^2/\text{s}$ , and  $\text{Pr}=0.70$ . Assuming a maximum stream velocity of 10 m/s this yields a Reynolds number of  $55.8 \cdot 10^3$ . At this value of Re, the constants C and n are 0.102 and 0.675 respectively (Reference 3-7, Table 7.3).

$$h = 0.0509/0.373 \cdot 0.102 \cdot [10 \cdot 0.373 / (66.84 \cdot 10^{-6})]^{0.675} \cdot 0.70^{1/3} = 19.8 \text{ W/m}^2 \cdot \text{K} \quad (8)$$

A value of  $19.8 \text{ W/m}^2 \cdot \text{K}$  was conservatively used in the analysis of the regulatory fire.

#### 3.4.2.2 Heat Transfer Coefficient during Post-Fire Period

During the post-fire period of the HAC, it is conservatively assumed that there is negligible wind, and that heat is transferred from the inner container to the environment via natural convection. Natural heat transfer coefficients from the outer surface of the inner container are calculated as follows.

Reference 3-7 recommends the following correlations for the Nusselt number (Nu) describing natural convection heat transfer to air from heated vertical and horizontal surfaces:

Vertical heated surfaces (Reference 3-7, p. 493):

$$\text{Nu} = \left\{ 0.825 + 0.387 \cdot (\text{Gr} \cdot \text{Pr})^{1/6} / [1 + (0.492/\text{Pr})^{9/16}]^{8/27} \right\}^2 \quad (9)$$

For the entire range of  $Ra = Gr \cdot Pr$

Where:

Nu:	Nusselt number
Gr:	Grashof number
Pr:	Prandtl number
Ra:	Rayleigh number

Horizontal heated surfaces facing upward (Reference 3-7, p.498):

$$Nu = 0.54 \cdot (Gr \cdot Pr)^{1/4} \quad \text{for } (10^4 < Gr \cdot Pr < 10^7) \quad (10)$$

$$Nu = 0.15 \cdot (Gr \cdot Pr)^{1/3} \quad \text{for } (10^7 < Gr \cdot Pr < 10^{11}) \quad (11)$$

and, for horizontal heated surfaces facing downward:

$$Nu = 0.27(Gr \cdot Pr)^{1/4} \quad \text{for } (10^5 < Gr \cdot Pr < 10^{10}) \quad (12)$$

The correlations for the horizontal surfaces are calculated using a characteristic length defined by the relation  $L=A/P$ , where A is the horizontal surface area and P is the perimeter (Reference 3-7, p. 498). The calculated characteristic length for the horizontal surfaces of the inner container is  $L=0.209$  m ( $A=2.14812$  m<sup>2</sup> and  $P=10.278$  m).

The convective heat transfer coefficients in Table 3-5 are calculated using Eq. (9), (10), (11), and (12). The corresponding characteristic length used in calculating the Nusselt number for each surface is also used in calculating the heat transfer coefficient. The thermal properties of air have been evaluated at the mean film temperature ( $T_f = (T_s + T_{\text{ambient}}) / 2$ ).

The effects of solar radiation are included during the post-fire period by specifying the equivalent heat flow for each node of the surfaces exposed to fire for an additional 3.5 hours (i.e., the fire starts at the time of the peak temperature in the inner container (8 hours after sunrise) and is 0.5 hours in duration). This results in an additional 3.5 hours of solar insolation. Using the peak rates calculated in Section 3.3.1.1, the nodal heat flows at 2:30 PM are equal to:

$$\dot{q}_{\text{top}} = 1,218 \text{ W/m}^2 \cdot \{\sin[\pi \cdot (6+8.5)/12 - \pi/2]\} \cdot 0.459 \text{ m} / (155-1) = 2.88 \text{ W/m} \quad (13)$$

$$\dot{q}_{\text{side}} = 305 \text{ W/m}^2 \cdot \{\sin[\pi \cdot (6+8.5)/12 - \pi/2]\} \cdot 0.281 \text{ m} / (99-1) = 0.69 \text{ W/m} \quad (14)$$

where 0.459 m is the width of the inner container, 0.281 m is its height, and the model is 155 nodes in width by 99 nodes in height. For the remaining 3.5 hours of solar insolation, these heat fluxes are conservatively applied as bounding constant values rather than varying with time.

The solar absorptivity coefficient of the outer surface is conservatively assumed to be one. The duration of the post-fire period has been extended to 12.5 hours to investigate the cool-down of the inner container.

### 3.4.3 Maximum Temperatures and Pressure

#### 3.4.3.1 Maximum Temperatures

Representative plots of the isotherms at various points in time over the course of the HAC fire scenario are depicted in Figure 3-4 through Figure 3-7. The peak fuel rod temperature, which conservatively neglects the presence of the Outer Container (OC) and is assumed to be the same as the inner wall temperature of the package, is illustrated in Figure 3-3 and tabulated in Table 3-6. The temperature reaches its maximum point of 648°C (921 K, 1,198°F) at the end of the fire (1,800 seconds after the start of the fire). This peak temperature occurs at the top corners of the inner wall.

The maximum temperature even when applied to the fuel directly is well below the maximum temperature the fuel can withstand. Testing was performed for a range of BWR fuel rods of different diameter, clad thickness, and internal pressure. In these tests, the fuel rods were heated to various temperatures from 700°C to 900°C for periods of over one hour to determine the rupture temperature and pressure of the fuel. It was found that the BWR, fuel cladding maintained containment at 800°C, the upper HAC temperature range. PWR and CANDU fuel rods with no thermal protection have been analyzed to maintain containment up to a temperature of 765°C for 30 minutes.

#### 3.4.3.2 Maximum Internal Pressure

The maximum pressure for a fuel rod is a function of the initial helium fill pressure. As the fuel rod is heated, the pressure within the cladding increases. The fuel is conservatively evaluated at the maximum temperature of the inner wall of the inner container seen during the HAC thermal event of 648°C, and neglects the pipe container used for non-BWR fuel rod types (PWR and CANDU). The maximum pressure of the containment cladding is determined by applying the ideal gas law. The subsequent sections demonstrate the maximum internal pressure for various fuel types.

##### 3.4.3.2.1 Maximum Internal Pressure: BWR

Similar BWR fuel rods with similar initial pressures have been heated in an oven to over 800°C for over an hour without failures (Reference 3-8). The fuel that was tested in the oven was pressurized with [ ] absolute ([ ]) of helium. When tested to 850°C, some fuel ruptures were observed, but rupture did not occur at 800°C when held at this temperature for one hour. At 800°C (1,073 K), the equivalent fuel rod pressure defines the allowable pressure as:

$$P_{\text{allowable}} = P_1 \cdot T_{\text{allowable}}/T_{\text{ambient}} = [ ] \quad (15)$$

The maximum temperature of the inner wall of the inner container demonstrated during the HAC event is 648°C, as reported in Section 3.4.3.1. At 648°C (921 K), the equivalent maximum fuel rod pressure is [ ] and below the [ ] allowable pressure.

$$P_{\text{max}} = P_1 \cdot T_{\text{max}}/T_{\text{ambient}} = [ ] \quad (16)$$

### 3.4.3.2.2 Maximum Internal Pressure: Non-BWR

The non-BWR fuel types intended for shipment in the RAJ-II package are CANDU and PWR fuel rods. PWR fuel rods are pressurized to a higher magnitude, as compared to CANDU fuel rods which are pressurized to near atmospheric conditions. The maximum helium fill pressure for a PWR fuel rod is 2.51 MPa absolute (364 psia) and has been analyzed to maintain containment up to a temperature of 765°C for 30 minutes. At 765°C (1,038 K), the equivalent fuel rod pressure defines the allowable pressure as:

$$P_{\text{allowable}} = P_1 \cdot T_{\text{allowable}} / T_{\text{ambient}} = 2.51 \cdot 1,038 / 293 = 8.89 \text{ MPa abs. (1,290 psia)} \quad (17)$$

The maximum temperature of the inner wall of the inner container demonstrated during the HAC event is 648°C, as reported in Section 3.4.3.1, and conservatively neglects the pipe container used for non-BWR loose fuel rod types. At 648°C (921 K), the equivalent maximum fuel rod pressure is 7.89 MPa absolute (1,144 psia) and below the 8.89 MPa absolute (1,290 psia) allowable pressure.

$$P_{\text{max}} = P_1 \cdot T_{\text{max}} / T_{\text{ambient}} = 2.51 \cdot 921 / 293 = 7.89 \text{ MPa abs. (1,144 psia)} \quad (18)$$

### 3.4.4 Maximum Thermal Stress

The RAJ-II package is primarily constructed of the same material, light stainless steel sheet metal, and thus is not subjected to significant thermal stresses. The package is constructed so that there is no significant constraint on any component as it heats up and cools down. The fuel rods are allowed to expand in the package. The fuel within the cladding is also designed to expand without interfering with the cladding (see Sections 2.6 and 2.7).

The maximum thermal stress is the hoop stress of the fuel rod produced by the differential pressure across the thickness of the containment cladding. The subsequent sections demonstrate the maximum stress of the various fuel types do not exceed their allowable stress. Limitations are placed on the fuel rod cladding inner radius to thickness ratio to ensure the fuel cladding and closure welds maintain containment during a HAC event.

#### 3.4.4.1 Maximum Thermal Stress: BWR

The BWR fuel rods that were tested in the oven had a cladding inner radius to thickness ratio ( $r/t$ ) of  $[[ \quad ]]$ . When the fuel rods were tested to 850°C, some fuel ruptures were observed, but rupture did not occur at 800°C when held at this temperature for one hour. The stress at 800°C is used as the conservative BWR fuel rod cladding stress allowable.

$$\sigma_{\text{allowable}} = P_{\text{allowable}} \cdot r/t = [[ \quad ]] = 31.1 \text{ MPa (4,514 psi)} \quad (19)$$

The maximum thermal stress of all BWR fuel types shipped in the RAJ-II is limited to 31.1 MPa (4,514 psi). The maximum temperature of the inner wall of the inner container demonstrated during the HAC event is 648°C, as reported in Section 3.4.3.1. The thermal stress criterion, for all BWR fuel types shipped in the RAJ-II, is defined in Eq. (20) and corresponds to the maximum cladding exposure temperature of 648°C (921 K).

$$r/t|_{\text{BWR}} \cdot (P_f \cdot 921 / 293 - P_a) \leq 31.1 \text{ MPa (4,514 psi)} \quad (20)$$

Where:

$r/t _{\text{BWR}}$	BWR fuel rod type cladding inner radius to thickness ratio
$P_f$	absolute helium fill pressure, MPa absolute (psia)
$P_a$	atmospheric pressure, 0.101325 MPa (14.6959 psi)

#### 3.4.4.2 Maximum Thermal Stress: non-BWR

The non-BWR fuel types intended for shipment in the RAJ-II package are CANDU and PWR fuel rods. The various non-BWR fuel types have been analyzed to maintain containment up to a temperature of 765°C for 30 minutes, and with a corresponding maximum hoop stress of 56.3 MPa (8,166 psi). This is taken as the allowable stress for all non-BWR fuel rod types shipped in the RAJ-II package.

$$\sigma_{\text{allowable}} = 56.3 \text{ MPa (8,166 psi)} \quad (21)$$

The maximum thermal stress of all non-BWR fuel rod types shipped in the RAJ-II is limited to 56.3 MPa (8,166 psi). The maximum temperature of the inner wall of the inner container demonstrated during the HAC event is 648°C, as reported in Section 3.4.3.1. This is conservative as the HAC thermal analysis neglects the pipe container used for non-BWR loose fuel rod types. The thermal stress criterion, for all non-BWR fuel types shipped in the RAJ-II, is defined in Eq. (22) and corresponds to the maximum cladding exposure temperature of 648°C (921 K).

$$r/t|_{\text{non-BWR}} \cdot (P_f \cdot 921/293 - P_a) \leq 56.3 \text{ MPa (8,166 psi)} \quad (22)$$

Where:

$r/t _{\text{non-BWR}}$	non-BWR fuel rod type cladding inner radius to thickness ratio
$P_f$	absolute helium fill pressure, MPa absolute (psia)
$P_a$	atmospheric pressure, 0.101325 MPa (14.6959 psi)

#### 3.4.5 Accident Conditions for Fissile Material Packages for Air Transport

Approval for air transport is not requested for the RAJ-II.

**Table 3-5 Convection Coefficients for Post-Fire Analysis (Paper Honeycomb)**

<b>T<sub>s</sub> (Surface Temperature)</b>		<b>T<sub>ambient</sub></b>		<b>h (Vertical Surface)</b>	<b>h (Horizontal Surface Facing Upward)</b>	<b>h (Horizontal Surface Facing Downward)</b>
<b>°F</b>	<b>K</b>	<b>°F</b>	<b>K</b>	<b>(W/m<sup>2</sup>·K)</b>	<b>(W/m<sup>2</sup>·K)</b>	<b>(W/m<sup>2</sup>·K)</b>
150	338.71	100	311	4.68	5.19	2.34
200	366.48	100	311	5.61	6.34	2.74
250	394.26	100	311	6.18	7.05	2.99
300	422.04	100	311	6.60	7.55	3.17
350	449.82	100	311	6.90	7.92	3.30
400	477.59	100	311	7.13	8.18	3.41
600	588.71	100	311	7.64	8.74	3.67
900	755.37	100	311	8.00	9.07	3.89
1,375	1,019.26	100	311	8.25	9.17	4.09

**Table 3-6 Calculated Temperatures for Different Positions on the Walls of the Inner Container (Paper Honeycomb)**

<b>Time</b>	<b>Inner Wall Temperature (Top Right Corner)</b>	<b>Inner Wall Temperature (Bottom)</b>	<b>Inner Wall Temperature (Top)</b>	<b>Outer Wall Temperature</b>
<b>sec</b>	<b>K</b>	<b>K</b>	<b>K</b>	<b>K</b>
0.1	375	375	375	377
911	750	667	546	1,062
1,800	921	821	696	1,067
1,900	918	823	710	807
2,000	905	817	723	686
2,200	868	797	742	583
2,600	803	761	760	509
3,268	723	715	758	463
4,280	639	662	727	437
27,973	354	335	369	378
45,000	349	324	358	377

NEDO-33869 Revision 11  
Non-Proprietary Information

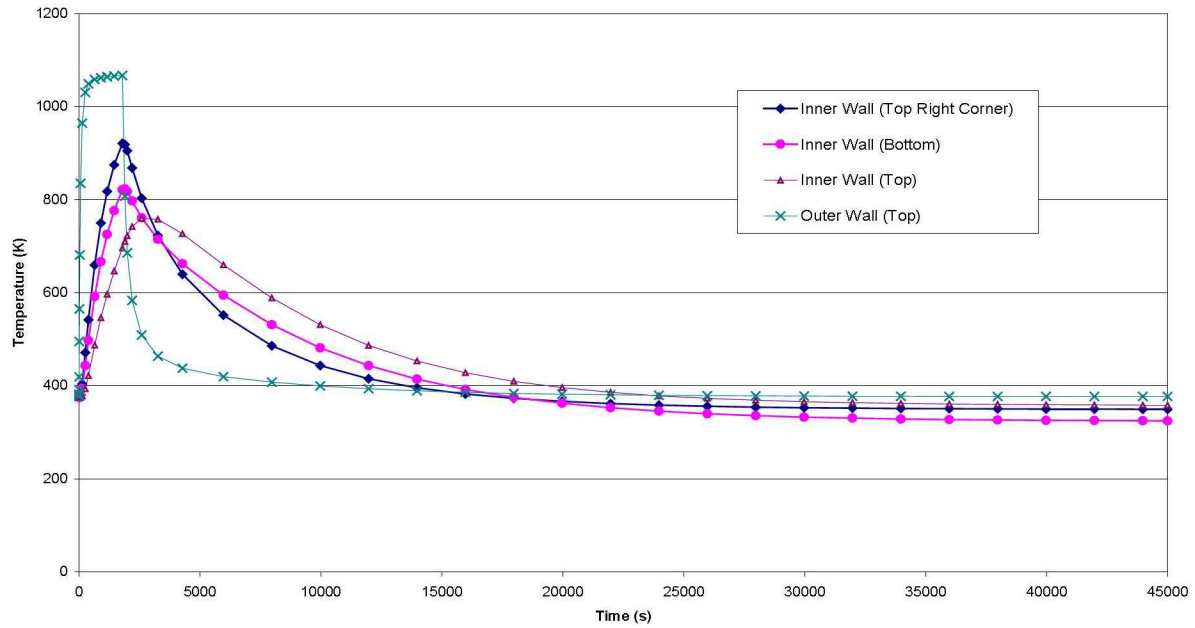


**Figure 3-3** Calculated Temperature Evolution During HAC Transient

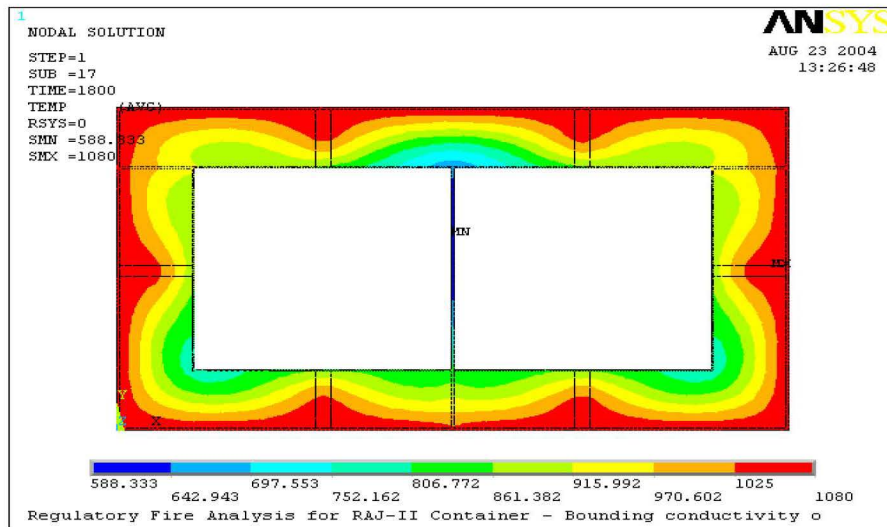


**Figure 3-4** Calculated Isotherms at the End of Fire Phase (1,800 s)

NEDO-33869 Revision 11  
Non-Proprietary Information

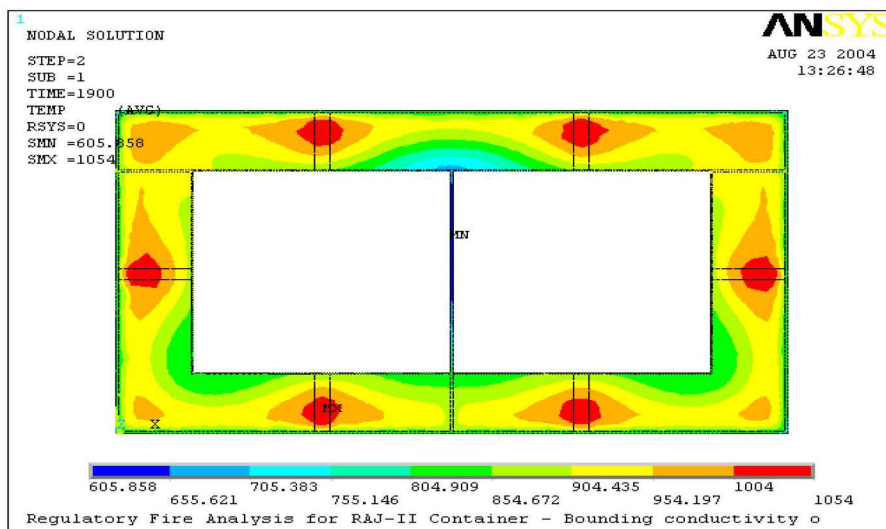


Figure 3-5 Calculated Isotherms at 100 s After the End of Fire

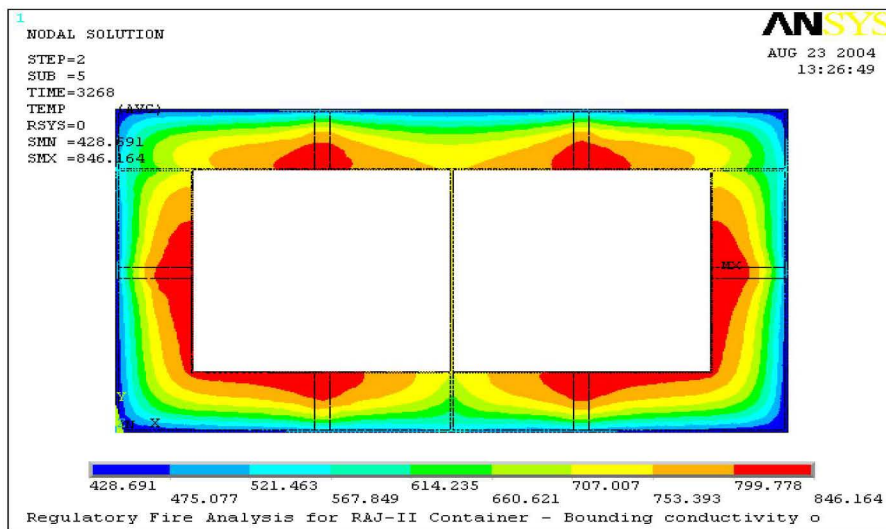


Figure 3-6 Calculated Isotherms at 1,468 s After the End of Fire



NEDO-33869 Revision 11  
Non-Proprietary Information

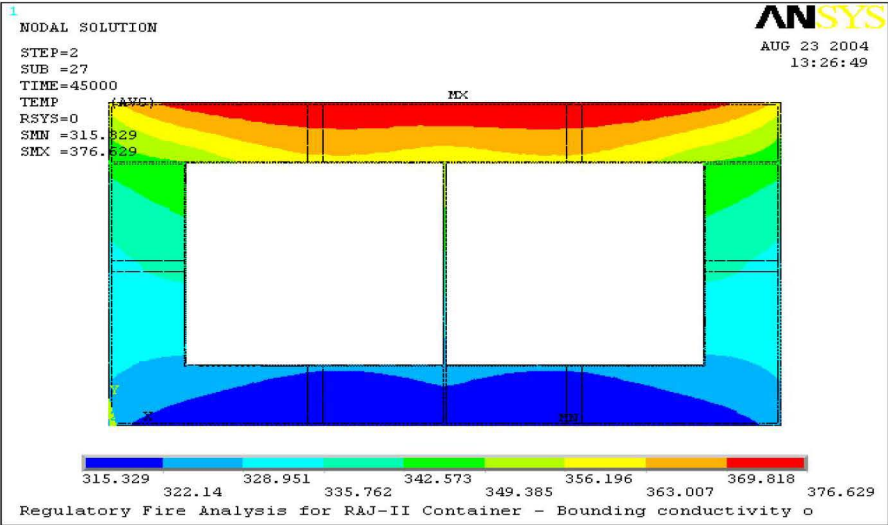


Figure 3-7 Calculated Isotherms at 12 hr After the End of Fire

### **3.5 APPENDIX**

#### **3.5.1 References**

- 3-1. Mills, A.F., Heat Transfer, Irwin, Inc., Homewood, Illinois, 1992.
- 3-2. “Pactec Specification: Regarding Global Nuclear Fuel Specification for Alumina Silicate for use in the RAJ-II Shipping container,” Unifrax Corporation, 6/3/04.
- 3-3. ANSYS Finite Element Computer Code, Version 5.6, ANSYS, Inc., 2000.
- 3-4. Standard Handbook for Mechanical Engineers, Baumeister, Marks, McGraw Hill book company, Seventh edition.
- 3-5. Tran, H. C., and White, R. H., Burning Rate of Solid Wood Measured in a Heat Release Calorimeter, Fire and Materials, Vol. 16, pp 197-206,1992.
- 3-6. McCaffery, B.J., Purely Buoyant Diffusion Flames – Some Experimental Results, Report PB80-112113, U.S. National Bureau of Standards, Washington, D.C., 1979.
- 3-7. Incropera, F.P., Dewitt, D.P., Fundamentals of Heat and Mass Transfer, John Wiley and Sons, Inc., New York, New York, 19966.
- 3-8. GNF-2 Fuel Rod Response to An Abnormal Transportation Event (proprietary)(30 Minute Fire).
- 3-9. Handbook of Heat Transfer, Warren M. Rohsenow, James P. Hartnett, McGraw Hill book company.
- 3-10. Thermal Properties of Paper, PTN149, Charles Green, Webster New York, 2002 (<http://www.frontiernet.net/~charmar/>).

### 3.5.2 ANSYS Input File Listing

#### Listing of the ANSYS Input File (file: model\_fl\_heat.inp)

<pre> fini /clear /filnam,model_fl_heat, /outp,model_fl_heatout,out /PREP7 /TITLE, Regulatory Fire Analysis for RAJ-II Container - Bounding conductivity of Alumina /UNITS,SI /SHOW,JPEG !* !*set element types !* ET,1,PLANE55,1 ET,2,LINK32 ET,3,MATRIX50,1 !* !* define keypoints !* K,1,0,0,0, K,2,0.459,0,0, K,3,0,0.0015,0, K,4,0.0015,0.0015,0, K,5,0.136,0.0015,0, K,6,0.146,0.0015,0, K,7,0.2285,0.0015,0, K,8,0.2305,0.0015,0, K,9,0.313,0.0015,0, K,10,0.323,0.0015,0, K,11,0.4575,0.0015,0, K,12,0.459,0.0015,0, K,13,0.0015,0.0515,0, K,14,0.0515,0.0515,0, K,15,0.136,0.0515,0, K,16,0.146,0.0515,0, K,17,0.2285,0.0515,0, K,18,0.2305,0.0515,0, K,19,0.313,0.0515,0, K,20,0.323,0.0515,0, K,21,0.4075,0.0515,0, K,22,0.4575,0.0515,0, K,23,0.0515,0.0525,0, K,24,0.0525,0.0525,0, K,25,0.2285,0.0525,0, K,26,0.2305,0.0525,0, K,27,0.4065,0.0525,0, K,28,0.4075,0.0525,0, K,29,0.0525,0.0705,0, K,30,0.0705,0.0705,0, K,31,0.2105,0.0705,0, K,32,0.2285,0.0705,0, K,33,0.2305,0.0705,0, K,34,0.2485,0.0705,0, </pre>	<pre> K,35,0.3885,0.0705,0, K,36,0.4065,0.0705,0, K,37,0.0015,0.1335,0, K,38,0.0515,0.1335,0, K,39,0.4075,0.1335,0, K,40,0.4575,0.1335,0, K,41,0.0015,0.1435,0, K,42,0.0515,0.1435,0, K,43,0.4075,0.1435,0, K,44,0.4575,0.1435,0, K,45,0.0705,0.1975,0, K,46,0.2105,0.1975,0, K,47,0.2485,0.1975,0, K,48,0.3885,0.1975,0, K,49,0.0525,0.2155,0, K,50,0.060,0.2115,0, K,51,0.066,0.2055,0, K,52,0.2175,0.2055,0, K,53,0.2235,0.2115,0, K,54,0.2285,0.2155,0, K,55,0.2305,0.2155,0, K,56,0.2355,0.2115,0, K,57,0.2415,0.2055,0, K,58,0.393,0.2055,0, K,59,0.399,0.2115,0, K,60,0.4065,0.2155,0, K,61,0.,0.2275,0, K,62,0.0015,0.2275,0, K,63,0.0515,0.2275,0, K,64,0.0525,0.2275,0, K,65,0.4065,0.2275,0, K,66,0.4075,0.2275,0, K,67,0.4575,0.2275,0, K,68,0.459,0.2275,0, K,69,0.,0.2285,0, K,70,0.0525,0.2285,0, K,71,0.06,0.2285,0, K,72,0.2235,0.2285,0, K,73,0.2285,0.2285,0, K,74,0.2305,0.2285,0, K,75,0.2355,0.2285,0, K,76,0.399,0.2285,0, K,77,0.4065,0.2285,0, K,78,0.459,0.2285,0, K,79,0.,0.2295,0, K,80,0.0015,0.2295,0, K,81,0.136,0.2295,0, K,82,0.146,0.2295,0, K,83,0.313,0.2295,0, K,84,0.323,0.2295,0, K,85,0.4575,0.2295,0, K,86,0.459,0.2295,0, </pre>
---	--

NEDO-33869 Revision 11  
Non-Proprietary Information

K,87,0.,0.2795,0,	FLST,2,12,3
K,88,0.0015,0.2795,0,	FITEM,2,1
K,89,0.136,0.2795,0,	FITEM,2,2
K,90,0.146,0.2795,0,	FITEM,2,12
K,91,0.313,0.2795,0,	FITEM,2,11
K,92,0.323,0.2795,0,	FITEM,2,10
K,93,0.4575,0.2795,0,	FITEM,2,9
K,94,0.459,0.2795,0,	FITEM,2,8
K,95,0.,0.281,0,	FITEM,2,7
K,96,0.459,0.281,0,	FITEM,2,6
SAVE	FITEM,2,5
!* !* define material properties	FITEM,2,4
!* !* !* STAINLESS STEEL (SS304)	FITEM,2,3
!* MP,DENS,1,7900	FITEM,2,4
MPTEMP,1,300,400,500,600,800,1000	FITEM,2,13
MPDATA,kxx,1,1,15,17,18,20,23,25	FITEM,2,37
MPDATA,c,1,1,477,515,539,557,582,611	FITEM,2,41
!* !* THERMAL INSULATOR	FITEM,2,62
!* MP,DENS,2,260	FITEM,2,61
MP,C,2,1046	A,P51X
MPTEMP	FLST,2,5,3
MPTEMP,1,673,873,1073,1273	FITEM,2,4
MPDATA,KXX,2,1,0.105,0.151,0.198,0.267 !MAX	FITEM,2,5
VALUES	FITEM,2,15
!* !* !* WOOD (generic softwood)	FITEM,2,14
!* UIMP,3,EX, , , ,	FITEM,2,13
UIMP,3,NUXY, , , ,	A,P51X
UIMP,3,ALPX, , , ,	FLST,2,4,3
UIMP,3,REFT, , , ,	FITEM,2,6
UIMP,3,MU, , , ,	FITEM,2,7
UIMP,3,DAMP, , , ,	FITEM,2,17
UIMP,3,DENS, , ,500,	FITEM,2,16
UIMP,3,KXX, , ,0.24,	A,P51X
UIMP,3,C, , ,2800,	FLST,2,4,3
UIMP,3,ENTH, , , ,	FITEM,2,7
UIMP,3,HF, , , ,	FITEM,2,8
UIMP,3,EMIS, , , ,	FITEM,2,18
UIMP,3,QRATE, , , ,	FITEM,2,17
UIMP,3,VISC, , , ,	A,P51X
UIMP,3,SONC, , , ,	FLST,2,4,3
UIMP,3,MURX, , , ,	FITEM,2,8
UIMP,3,MGXX, , , ,	FITEM,2,9
UIMP,3,RSVX, , , ,	FITEM,2,19
UIMP,3,PERX, , , ,	FITEM,2,18
!* !* define areas	A,P51X
!* 	FLST,2,4,3
	FITEM,2,9

NEDO-33869 Revision 11  
Non-Proprietary Information

FITEM,2,10	FITEM,2,33
FITEM,2,20	FITEM,2,55
FITEM,2,19	FITEM,2,74
A,P51X	FITEM,2,73
FLST,2,5,3	FITEM,2,54
FITEM,2,10	FITEM,2,32
FITEM,2,11	A,P51X
FITEM,2,22	FLST,2,8,3
FITEM,2,21	FITEM,2,27
FITEM,2,20	FITEM,2,28
A,P51X	FITEM,2,39
FLST,2,7,3	FITEM,2,43
FITEM,2,11	FITEM,2,66
FITEM,2,12	FITEM,2,65
FITEM,2,68	FITEM,2,60
FITEM,2,67	FITEM,2,36
FITEM,2,44	A,P51X
FITEM,2,40	FLST,2,5,3
FITEM,2,22	FITEM,2,21
A,P51X	FITEM,2,22
FLST,2,5,3	FITEM,2,40
FITEM,2,13	FITEM,2,39
FITEM,2,14	FITEM,2,28
FITEM,2,23	A,P51X
FITEM,2,38	FLST,2,4,3
FITEM,2,37	FITEM,2,37
A,P51X	FITEM,2,38
FLST,2,8,3	FITEM,2,42
FITEM,2,23	FITEM,2,41
FITEM,2,24	A,P51X
FITEM,2,29	FLST,2,4,3
FITEM,2,49	FITEM,2,39
FITEM,2,64	FITEM,2,40
FITEM,2,63	FITEM,2,44
FITEM,2,42	FITEM,2,43
FITEM,2,38	A,P51X
A,P51X	FLST,2,4,3
FLST,2,14,3	FITEM,2,41
FITEM,2,14	FITEM,2,42
FITEM,2,15	FITEM,2,63
FITEM,2,16	FITEM,2,62
FITEM,2,17	A,P51X
FITEM,2,18	FLST,2,4,3
FITEM,2,19	FITEM,2,43
FITEM,2,20	FITEM,2,44
FITEM,2,21	FITEM,2,67
FITEM,2,28	FITEM,2,66
FITEM,2,27	A,P51X
FITEM,2,26	SAVE
FITEM,2,25	FLST,2,6,3
FITEM,2,24	FITEM,2,61
FITEM,2,23	FITEM,2,62
A,P51X	FITEM,2,63
FLST,2,8,3	FITEM,2,64
FITEM,2,25	FITEM,2,70
FITEM,2,26	FITEM,2,69

NEDO-33869 Revision 11  
Non-Proprietary Information

A,P51X	FITEM,2,92
FLST,2,6,3	FITEM,2,91
FITEM,2,65	A,P51X
FITEM,2,66	FLST,2,4,3
FITEM,2,67	FITEM,2,84
FITEM,2,68	FITEM,2,85
FITEM,2,78	FITEM,2,93
FITEM,2,77	FITEM,2,92
A,P51X	A,P51X
FLST,2,18,3	FLST,2,4,3
FITEM,2,69	FITEM,2,85
FITEM,2,70	FITEM,2,86
FITEM,2,71	FITEM,2,94
FITEM,2,72	FITEM,2,93
FITEM,2,73	A,P51X
FITEM,2,74	SAVE
FITEM,2,75	FLST,2,10,3
FITEM,2,76	FITEM,2,87
FITEM,2,77	FITEM,2,88
FITEM,2,78	FITEM,2,89
FITEM,2,86	FITEM,2,90
FITEM,2,85	FITEM,2,91
FITEM,2,84	FITEM,2,92
FITEM,2,83	FITEM,2,93
FITEM,2,82	FITEM,2,94
FITEM,2,81	FITEM,2,96
FITEM,2,80	FITEM,2,95
FITEM,2,79	A,P51X
A,P51X	SAVE
FLST,2,4,3	!* !* glue all areas !* FLST,2,31,5,ORDE,2 FITEM,2,1 FITEM,2,-31 AGLUE,P51X !* /PNUM,KP,0 /PNUM,LINE,0 /PNUM,AREA,1 /PNUM,VOLU,0 /PNUM,NODE,0 /PNUM,TABN,0 /PNUM,SVAL,0 /NUMBER,0 !* /PNUM,ELEM,0 /REPLOT !* APLOT FLST,5,14,5,ORDE,10 FITEM,5,1 FITEM,5,-2 FITEM,5,6 FITEM,5,10 FITEM,5,12
FITEM,2,79	
FITEM,2,80	
FITEM,2,88	
FITEM,2,87	
A,P51X	
FLST,2,4,3	
FITEM,2,80	
FITEM,2,81	
FITEM,2,89	
FITEM,2,88	
A,P51X	
FLST,2,4,3	
FITEM,2,81	
FITEM,2,82	
FITEM,2,90	
FITEM,2,89	
A,P51X	
FLST,2,4,3	
FITEM,2,82	
FITEM,2,83	
FITEM,2,91	
FITEM,2,90	
A,P51X	
FLST,2,4,3	
FITEM,2,83	
FITEM,2,84	

NEDO-33869 Revision 11  
Non-Proprietary Information

FITEM,5,-15	ASEL, , , P51X
FITEM,5,21	CM,_Y1,AREA
FITEM,5,-24	CMSEL,S,_Y
FITEM,5,30	!*
FITEM,5,-31	CMSEL,S,_Y1
ASEL,S, , P51X	AATT, 2, , 1, 0
/REPLOT	CMSEL,S,_Y
FLST,5,14,5,ORDE,10	CMDELE,_Y
FITEM,5,1	CMDELE,_Y1
FITEM,5,-2	!*
FITEM,5,6	ALLSEL,ALL
FITEM,5,10	FLST,5,6,5,ORDE,6
FITEM,5,12	FITEM,5,4
FITEM,5,-15	FITEM,5,8
FITEM,5,21	FITEM,5,17
FITEM,5,-24	FITEM,5,-18
FITEM,5,30	FITEM,5,26
FITEM,5,-31	FITEM,5,28
CM,_Y,AREA	ASEL,S, , P51X
ASEL, , , P51X	FLST,5,6,5,ORDE,6
CM,_Y1,AREA	FITEM,5,4
CMSEL,S,_Y	FITEM,5,8
!*	FITEM,5,17
CMSEL,S,_Y1	FITEM,5,-18
AATT, 1, , 1, 0	FITEM,5,26
CMSEL,S,_Y	FITEM,5,28
CMDELE,_Y	CM,_Y,AREA
CMDELE,_Y1	ASEL, , , P51X
!*	CM,_Y1,AREA
ALLSEL,ALL	CMSEL,S,_Y
FLST,5,11,5,ORDE,11	!*
FITEM,5,3	CMSEL,S,_Y1
FITEM,5,5	AATT, 3, , 1, 0
FITEM,5,7	CMSEL,S,_Y
FITEM,5,9	CMDELE,_Y
FITEM,5,11	CMDELE,_Y1
FITEM,5,16	!*
FITEM,5,19	ALLSEL,ALL
FITEM,5,-20	SAVE
FITEM,5,25	!*
FITEM,5,27	!* mesh the areas
FITEM,5,29	!*
ASEL,S, , P51X	ALLSEL,ALL
FLST,5,11,5,ORDE,11	APLOT
FITEM,5,3	SMRT,10
FITEM,5,5	FLST,5,31,5,ORDE,2
FITEM,5,7	FITEM,5,1
FITEM,5,9	FITEM,5,-31
FITEM,5,11	CM,_Y,AREA
FITEM,5,16	ASEL, , , P51X
FITEM,5,19	CM,_Y1,AREA
FITEM,5,-20	CHKMSH,'AREA'
FITEM,5,25	CMSEL,S,_Y
FITEM,5,27	!*
FITEM,5,29	AMESH,_Y1
CM,_Y,AREA	!*

NEDO-33869 Revision 11  
Non-Proprietary Information

<pre> CMDELE,_Y CMDELE,_Y1 CMDELE,_Y2 !* /PNUM,KP,0 /PNUM,LINE,0 /PNUM,AREA,0 /PNUM,VOLU,0 /PNUM,NODE,0 /PNUM,TABN,0 /PNUM,SVAL,0 /NUMBER,0 !* /PNUM,MAT,1 /REPLOT ALLSEL,ALL !* select nodes on the outer surfaces NSEL,S,LOC,X,0.,0.0001 NSEL,A,LOC,X,0.4589,0.459 NSEL,A,LOC,Y,0.,0.0001 NSEL,A,LOC,Y,0.2809,0.281 !* define element for outer surface !* TYPE, 2 MAT, 1 NPLOT esurf !* !* create space node N,50000,0.3,0.5,0.,, !* select the nodes and elements that !* make up the radiation surfaces ESEL,S,TYPE,,2 NSLE,R NSEL,S,LOC,X,0.,0.0001 NSEL,A,LOC,X,0.4589,0.459 NSEL,A,LOC,Y,0.,0.0001 NSEL,A,LOC,Y,0.2809,0.281 ESLN,R NSEL,a,node,,50000 FINISH !* define radiation matrix /AUX12 EMIS,1,0.8, STEF,5.67e-08, GEOM,1,0, SPACE,50000, !* VTYPE,0,20, MPRINT,0 WRITE,rad !* ALLSEL,ALL FINISH /PREP7 !* </pre>	<pre> !* TYPE, 3 MAT, 1 REAL, ESYS, 0 SECNUM, TSHAP,LINE !* SE,rad, , ,0.0001, ESEL,S,TYPE,,2 EDELE,ALL SAVE !* Define effective heat transfer coefficients for !* post-fire (vert-20,horiz-up-25, horiz-down-35) MPTEMP MPTEMP,1,338.71,366.48,394.26,422.04,449.82,47 7.59, MPTEMP,7,588.71,755.37,1019.26, MPDATA,HF,20,1,4.68,5.61,6.18,6.60,6.90,7.13, MPDATA,HF,20,7,7.64,8.00,8.25, MPDATA,HF,25,1,5.19,6.34,7.05,7.55,7.92,8.18, MPDATA,HF,25,7,8.74,9.07,9.17, MPDATA,HF,35,1,2.34,2.74,2.99,3.17,3.30,3.41, MPDATA,HF,35,7,3.67,3.89,4.09, MPLIST SAVE FINISH /SOLU !* setup convection coefficients for fire case ALLSEL,ALL NSEL,S,LOC,X,0.,0.0001 NSEL,A,LOC,X,0.4589,0.459 NSEL,A,LOC,Y,0.,0.0001 NSEL,A,LOC,Y,0.2809,0.281 SF,ALL,CONV,19.8,1073 NSEL,ALL !***** ***** !* Test Heat Generation modelling wood burning ASEL,S,MAT,,3 ESLA,S /GO !* *DIM,burning,TABLE,5,1,0,TIME !* BFE,ALL,HGEN, , %burning% !* !*****BFA,ALL,HGEN, %burning% *SET,BURNING(1,0,1) , 0.0 *SET,BURNING(2,0,1) , 0.1 *SET,BURNING(3,0,1) , 0.2 *SET,BURNING(4,0,1) , 552.2 *SET,BURNING(5,0,1) , 552.3 *SET,BURNING(1,1,1) , 0.0 *SET,BURNING(2,1,1) , 0.0 *SET,BURNING(3,1,1) , 7.63e6 </pre>
---	--



NEDO-33869 Revision 11  
Non-Proprietary Information

<pre> *SET,BURNING(4,1,1) , 7.63e6 *SET,BURNING(5,1,1) , 0.0 ALLSEL,ALL SAVE !***** ***** D,50000,TEMP, 1073 !***** ***** TUNIF,375,          !REVISED FOR NEW NCT NUMBER (IC OUTER SHELL) !***** ***** SAVE !* !* set up run parameters for fire case !* ANTYPE,4 !* TRNOPT,FULL LUMPM,0 !* TIME,1800 AUTOTS,-1 DELTIM,0.1,0.1,600,1 KBC,1 !* TSRES,ERASE !* OUTRES,ALL,ALL, !* LSWRITE,2, !* !* change boundary conditions for post fire case !* ALLSEL,ALL NSSEL,S,LOC,X,0.000,0.0001 NSSEL,A,LOC,X,0.4589,0.459 SF,ALL,CONV,-20, 311 ALLSEL,ALL NSSEL,S,LOC,Y,0.0,0.0001 SF,ALL,CONV,-35, 311 ALLSEL,ALL NSSEL,S,LOC,Y,0.2809,0.281 SF,ALL,CONV,-25, 311 ALLSEL,ALL D,50000,TEMP,311 !* !* apply solar heat flux !* ALLSEL,ALL !* select vertical lines and nodes on the left side nsel,s,loc,x,0 !FLST,5,4,4,ORDE,4 !FITEM,5,18 !FITEM,5,76 </pre>	<pre> !FITEM,5,94 !FITEM,5,97 !LSEL,S, , P51X !NSLL,S,1 !FLST,2,97,1,ORDE,9 !FITEM,2,12 !FITEM,2,17 !FITEM,2,56 !FITEM,2,70 !FITEM,2,72 !FITEM,2,447 !FITEM,2,-521 !FITEM,2,2039 !FITEM,2,-2055 /GO !* F,all,HEAT,0.69 ALLSEL,ALL !* select lines and nodes on the right side nsel,s,loc,x,.459,.460 !FLST,5,4,4,ORDE,4 !FITEM,5,35 !FITEM,5,77 !FITEM,5,86 !FITEM,5,108 !LSEL,S, , P51X !NSLL,S,1 !FLST,2,97,1,ORDE,9 !FITEM,2,3 !FITEM,2,27 !FITEM,2,57 !FITEM,2,63 !FITEM,2,78 !FITEM,2,795 !FITEM,2,-869 !FITEM,2,2240 !FITEM,2,-2256 !/GO !* F,all,HEAT,0.69 !* select nodes on upper surface ALLSEL,ALL NSSEL,S,LOC,Y,0.2809,0.281 !FLST,2,155,1,ORDE,4 !FITEM,2,79 !FITEM,2,-80 !FITEM,2,2257 !FITEM,2,-2409 !/GO !* F,all,HEAT,2.88 ALLSEL,ALL !* set up run parameters for post fire TIME,14400 !was 9000 AUTOTS,-1 DELTIM,0.5,0.1,2000,1 </pre>
---	---

NEDO-33869 Revision 11  
Non-Proprietary Information

<pre> KBC,1 !* TSRE S,ERASE !* TINTP,0.005, , ,-1,0.5,-1 !* OUTRES,ALL,ALL, TIME,45000 DELTIM,100,10,2000,1 LSWRITE,3, SAVE FINISH /SOLU /STATUS,SOLU LSSOLVE,2,3,1 FINISH SAVE /POST26 !* !* plot temperature evolution at specified nodes !* !* !* inner wall, top right corner NSOL,2,58,TEMP, ,inn_wtr !* !* !* inner wall, bottom mid position NSOL,3,1185,TEMP, ,inn_wbm !* !* !* inner wall, top mid position NSOL,4,1720,TEMP, ,inn_wtm !* !* !* outer wall, top mid position NSOL,5,2333,TEMP, ,out_wtm !* !* PLVAR,2,3,4,5,,, , , , PRVAR,2,3,4,5,,, FINISH !* plot isotherms at certain moments in time /POST1 SET,LIST,2 SET, , ,1, , , ,17, /EFACE,1 !* PLNSOL,TEMP, ,0, FINISH /POST1 SET, , ,1, , , ,18, /EFACE,1 !* PLNSOL,TEMP, ,0, SET, , ,1, , , ,20, /EFACE,1 </pre>	<pre> !* PLNSOL,TEMP, ,0, SET, , ,1, , , ,22, /EFACE,1 !* PLNSOL,TEMP, ,0, SET, , ,1, , , ,30, /EFACE,1 !* PLNSOL,TEMP, ,0, SET, , ,1, , , ,43, /EFACE,1 !* PLNSOL,TEMP, ,0, SET,PREVIOUS FINISH !*****NEW allsel /post1 Tmax=0 TimeMAX=0 nmax=0 nsel,s,loc,x,0.0525,.4065, nsel,r,loc,y,0.0525,.2285, !nsel,u,loc,y,0.053,.2280 nplot *GET, ncount, NODE, 0, count cm,icnodes,node set,1,1 *do,t,1,46 tmaxn=0 cmsel,s,icnodes *do,i,1,ncount nodei=node(0,0,0) *get,tempi,node,nodei,temp *if,tempi,gt,tmaxn,then tmaxn=tempi nmaxn=nodei *endif nsel,u,,,nodei *enddo *if,tmaxn,gt,tmax,then tmax=tmaxn nmax=nmaxn *GET,timemax, ACTIVE, 0, set, time *endif set,next *enddo tmax=tmax nmax=nmax timemax=timemax allsel /show,term /post1, ! Reverse Video /rgb,index,100,100,100,0 </pre>
--	--

NEDO-33869 Revision 11  
Non-Proprietary Information

```
/rgb,index,80,80,80,13
/rgb,index,60,60,60,14
/rgb,index,0,0,0,15
set,1,17
plnsol,temp
/image,save,fig3-4(1800),wmf
set,2,1
/replot
/image,save,fig3-5(1900),wmf
set,2,5
/replot
/image,save,fig3-6(3268),wmf
set,last
/replot
/image,save,fig3-7(45000),wmf
!*****NEW
! /EXIT,ALL
```

### 3.5.3 NCT Transient Analysis

The NCT transient analysis uses a one-dimensional model of the vertical face of the packaging (thinner part of the packaging) as illustrated in Figure 3-8.

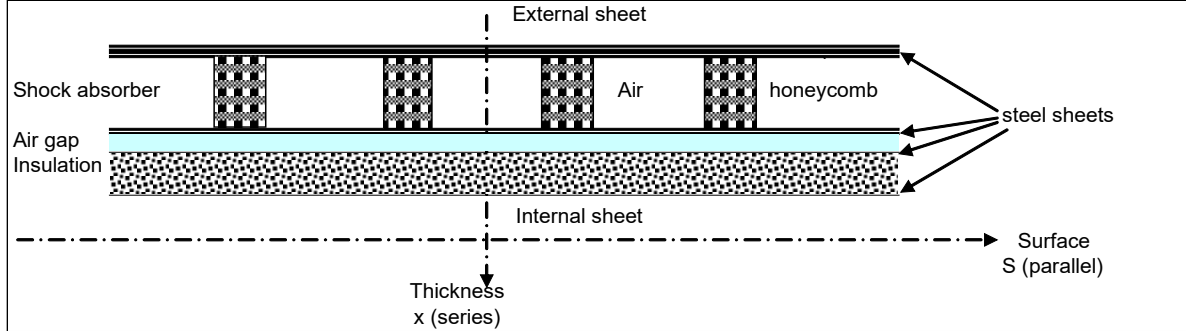


**Figure 3-8 Vertical Face Model**

The heat flux is set as a sine wave function:

$$Q = \pi/2 \cdot 800 \cdot \sin(\omega\theta) \quad 0 < (\omega\theta) < \pi \quad (23)$$

$$Q = 0 \quad \pi < (\omega\theta) < 2\pi \quad (24)$$

With:

$$Q = \text{heat energy in g-cal/cm}^2$$

$$\omega = 2\pi / 24 \text{ pulsation}$$

$$\theta = \text{time in hours}$$

Note that the peak value of  $(\pi/2 \cdot 800)$  complies with 10 CFR 71.71(c)(1), conservatively assuming the highest value of 800 g-cal/cm<sup>2</sup> for the insulation.

$$\int_0^{24 \text{ hours}} Q d\theta = 800 \text{ g-cal/cm}^2 \quad (25)$$

Assuming that at each time step the external surface of the package achieves steady-state conditions, the energy balance between the solar heat load and the convection and radiation exchanges (see Section 3.3.1.1) results in a time dependent solution for the external surface temperature.

The result is shown in the Figure 3-9 (blue curve) and is close to a sine wave function. Indeed, when calculating the energy balance equation, it appears that the convection term represents 65% of the exchange, and the radiation term 35%. As the convection term is linearly proportional to the external temperature, this curve is nearly proportional to the solar heat load.

Assume that the external temperature is a sine function with respect to time as follows (and as shown in Figure 3-9):

$$T_s = T_{\text{avg}} + T^+ \sin(\omega\theta) \quad (26)$$

With:

$$T_{avg} = 420 \text{ K} \quad (\text{maximum value of the blue curve})$$

$$T^+ = 420 - 311 = 109 \text{ K}$$

The system is thus modeled as a one-dimensional model of conduction, with a sinusoidal wave temperature on the external surface as a boundary condition.

Using Eq. (4-22) of Reference 3-9, the heat equation through a layer of material leads to a temperature of:

$$T(x,\theta) = T_{avg} + T^+ \exp(-Lx/d) \sin[L(2LFo - x/d)] \quad (27)$$

Using the reference's notation, it becomes:

$$T(x,\theta) = T_{avg} + T^+ \exp[-(\omega/2\alpha)^{1/2}x] \sin[\omega\theta - (\omega/2\alpha)^{1/2}x] \quad (28)$$

With:

$\alpha = K / \rho C = \text{thermal diffusivity,}$

$K = \text{conductivity of material,}$

$\rho = \text{density of material,}$

$C = \text{specific heat of the material,}$

$x = \text{thickness thru the material.}$

Through each layer of material “i” in the RAJ-II packaging, the temperature of the external surface is so decreased by a factor  $\eta$  and lagged by a factor  $\phi$ :

$$\eta_i = \exp[-(\omega/2\alpha_i)^{1/2}x_i] \quad (29)$$

$$\phi_i = (\omega/2\alpha_i)^{1/2}x_i \quad (30)$$

Table 3-7 summarizes the material properties for each component layer through the thickness of the model.

### Equivalent Properties of Material

The thermal properties ( $K$ ,  $\rho$ ,  $C$ ) of a material equivalent to materials of a system are following the rules:

$$\text{Materials in series } K = \frac{e_T}{\sum_i \frac{e_i}{K_i}}$$

$$\text{Materials in parallel } K = \frac{1}{S_T} \sum_i S_i K_i$$

$$\text{Materials in series } \rho C = \frac{\sum_i \rho_i C_i e_i}{e_T}$$

$$\text{Materials in parallel } \rho C = \frac{\sum_i \rho_i C_i S_i}{S_T}$$

The maximum temperature within the inner container resulting from solving the one-dimensional model occurs at ten hours into the cycle and is equal to 350 K. The maximum temperature on the

NEDO-33869 Revision 11  
Non-Proprietary Information

outer surface of the inner container occurs at 8 hours and is equal to 375K. Temperatures are summarized in Table 3-8.

**Table 3-7 Material Properties**

Component	Material	Thickness x (m)	Surface S (m)	Conductivity K (W/m-K)	Density r (kg/m <sup>3</sup> )	Specific Heat C (J/kg-K)	Diffusivity a (m <sup>2</sup> /s)
OC Outer Sheet	steel	0.004	-	15	7900	477	3.981E-06
Honeycomb <sup>①</sup>	paper	-	0.084 <sup>①</sup>	0.13595	700 <sup>①</sup>	1531 <sup>①</sup>	3.932E-07
	air	-	0.916 <sup>①</sup>	0.0267	1.177	1005	
Shock Absorbers	honeycomb	0.108	0.64	0.0359	60	1522	1.737E-06
	air		3.186	0.0267	1.177	1005	
OC Inner Sheet	steel	0.001	-	15	7900	477	3.981E-06
Air Gap	air	0.01	-	0.0267	1.177	1005	2.257E-05
IC Outer Sheet	steel	0.0015	-	15	7900	477	3.981E-06
IC Insulation	alumina	0.048	-	0.09	250	1046	3.442E-07
IC Inner Sheet	steel	0.001	-	15	7900	477	3.981E-06

**Notes:**

- ① The honeycomb is assumed to be a combination of paper and air in a parallel system (see below). The proportion of paper and air is determined by the ratio of the densities:

$$\text{Honeycomb density} = 60 \text{ kg/m}^3$$

$$\text{Paper density} = 700 \text{ kg/m}^3 \quad 8.4\%$$

$$\text{Air density} = 1.177 \text{ kg/m}^3 \quad 91.6\%$$

Thermal properties of resin impregnated kraft paper (density, conductivity, specific heat) are conservatively assumed to correspond to that of ordinary paper according to Reference 3-10.

Note: Although the honeycomb can be constructed of aluminum which is more conductive than paper, the paper honeycomb is the most conservative material for the entire thermal analysis due to paper's combustive properties during HAC. Aluminum is not included in this thermal analysis since paper is the most conservative for the full thermal analysis.

**Table 3-8 NCT Temperatures Through the Package Thickness (Paper Honeycomb)**

Time (hour)	Surface Temp Sine Wave Ts (K)	T thru OC Outer Shell (K)	T thru Honeycomb & Air (K)	T thru OC Inner Steel (K)	T thru Air Gap (K)	T thru IC Outer Shell (K)	T thru Alumina Silicate (K)
0	311	311	311	311	311	311	311
0.5	325	324	311	311	311	311	311
1	339	338	311	311	311	311	311
1.5	353	351	311	311	311	311	311
2	366	364	312	312	311	311	311
2.5	377	376	321	320	320	319	311
3	388	386	329	329	328	327	311
3.5	397	396	337	337	336	335	311
4	405	404	345	345	343	343	312
4.5	412	410	352	352	350	350	317
5	416	415	358	358	357	356	322
5.5	419	418	364	364	362	362	327
6	420	419	368	368	367	367	332
6.5	419	418	372	372	371	370	336
7	416	415	375	375	373	373	340
7.5	412	411	376	376	375	375	343
8	405	405	377	376	376	375	346
8.5	397	397	376	376	375	375	348
9	388	388	374	374	373	373	349
9.5	377	378	371	371	371	371	350
10	366	366	367	367	367	367	350
10.5	353	353	362	362	362	362	350
11	339	340	357	357	357	357	349
11.5	325	326	350	350	350	350	347
12	311	312	343	343	343	343	344
12.5	311	311	335	335	336	336	342
13	311	311	327	327	328	328	338
13.5	311	311	318	319	319	320	334
14	311	311	311	311	311	311	330
14.5	311	311	311	311	311	311	325
15	311	311	311	311	311	311	320
15.5	311	311	311	311	311	311	315
16	311	311	311	311	311	311	311
16.5	311	311	311	311	311	311	311

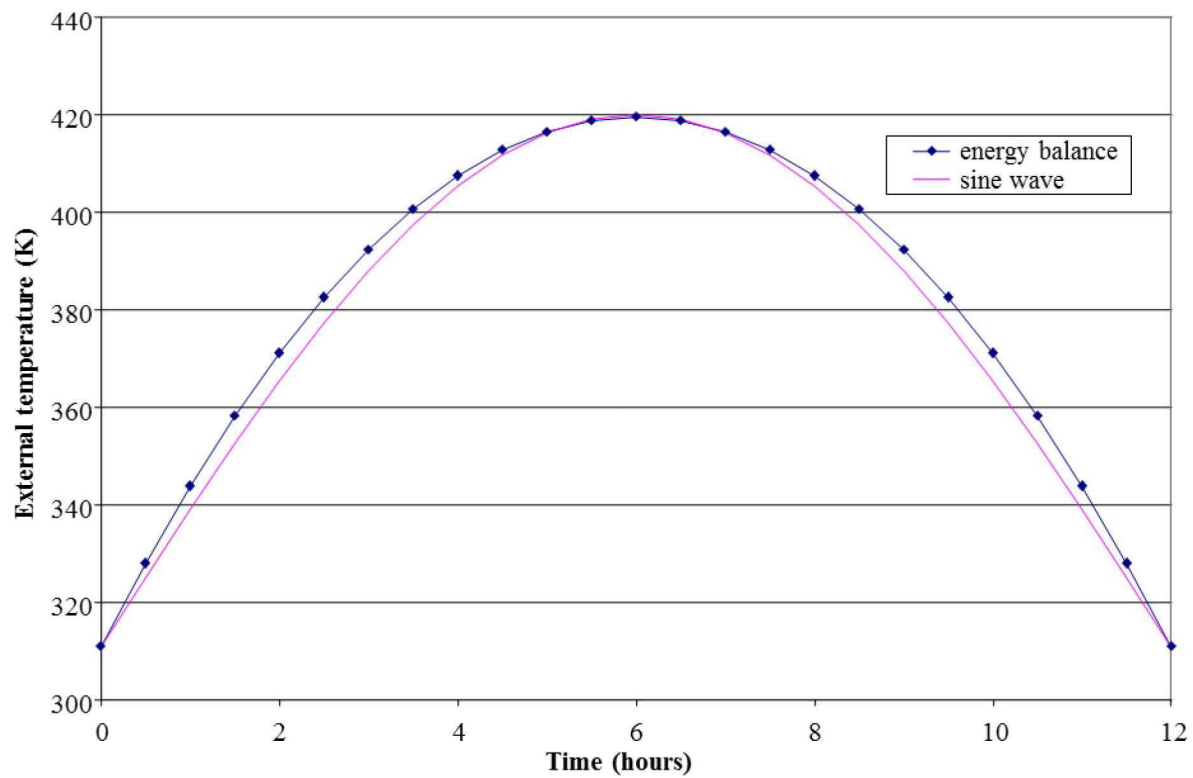


**Figure 3-9 Comparison Between Energy Equation Solution with a Sine Wave Equation**



## **4.0 CONTAINMENT**

### **4.1 DESCRIPTION OF THE CONTAINMENT SYSTEM**

The RAJ-II package containment boundary is the fuel rod cladding and welded end plugs. The package is designed to transport low enriched or reprocessed uranium nuclear reactor fuel assemblies (with or without a channel) and fuel rods. The radioactive material is bound in ceramic pellets, sintered at a temperature greater than 1,600°C, with very limited solubility and minimal propensity to suspend in air. The material is sealed inside zirconium alloy or stainless steel cladding to form the fuel rod, and there are no penetrations in the fuel cladding when shipped.

The fuel is pressurized with helium prior to sealing. The fuel is designed to withstand the rigorous operating environment of a nuclear reactor and is leak tested to demonstrate that it is leaktight ( $\leq 1 \times 10^{-7}$  ref-cc/s) per American National Standards Institute (ANSI) N14.5, Reference 4-1 or accepted alternate method. The package is shipped as Type B(F) based on the most limiting allowable content.

The Type B(F) package is constructed and prepared for shipment so that there is no loss or dispersal of the radioactive contents, no significant increase in external surface radiation levels, and no substantial reduction in the effectiveness of the packaging during Normal Conditions of Transport (NCT). Chapter 6.0 demonstrates that the package remains subcritical under normal and Hypothetical Accident Conditions (HAC). Because the fuel cladding and welded end plugs are the containment boundary, there are no other closure devices such as lids, seals, cover plates, positive fastening devices, vents or valves.

Throughout this chapter, calculations are presented specifically for the GNF 10x10 fuel assembly content, as this is the content subjected to certification testing. The 10x10 fuel assembly content was selected for certification testing because the 8x8, 9x9, and loose Boiling Water Reactor (BWR) rod content have a lower maximum weight bounded by the 10x10 fuel assembly content. The 10x10 fuel assembly content was also selected because the Uranium Carbide (UC) and Pressurized Water Reactor (PWR) loose rod content must be further confined within a 5-inch stainless steel pipe inside the inner container.

## 4.2 CONTAINMENT UNDER NORMAL CONDITIONS OF TRANSPORT

The RAJ-II package is constructed and prepared for shipment so that there is no loss or dispersal of the radioactive contents, no significant increase in external surface radiation levels, and no substantial reduction in the effectiveness of the packaging during NCT. The nature of the contained radioactive material and the structural integrity of the fuel rod cladding including the closure welds are such that there is no release of radioactivity predicted under NCT. However, the allowable release rate and associated allowable leak rate for NCT are calculated assuming 15% of the ceramic pellet material converts to an aerosol mixture.

The pressurization seen by the containment boundary during NCT is far below the reactor operating conditions, and the leak tightness of the rod is judged to not be impacted under NCT. Furthermore, the allowable release rate of less than  $10^{-6}$  A2 in a period of an hour, per 10 CFR 71.51(a)(1), is calculated in the following sections, and post HAC drop test leak test results bound the allowable rate (see Section 4.5.1.3 for details). Therefore, the containment boundary is demonstrated to be acceptable for NCT.

The maximum fuel rod conditions assumed for NCT are: [[  
]]. These values bound the NCT conditions for the BWR fuel rod type as summarized in Table 3-1.

### 4.3 CONTAINMENT UNDER HYPOTHETICAL ACCIDENT CONDITIONS

The sintered pellet form of the radioactive material and the integrity of the fuel rod cladding are such that there will be no substantial release of radioactivity under HAC. However, the allowable release rate and associated allowable leak rate for HAC are calculated assuming 100% of the ceramic pellet material converts to an aerosol mixture.

Three HAC certification tests were performed to assess containment integrity: one thermal test and two drop tests. Of these tests, two displayed no change in meeting the requirements of leaktight, while one measured a post drop leak rate of  $5.5 \times 10^{-6}$  ref-cc/s. As such, this leak rate is considered the worst case result and used for containment safety demonstration purposes.

The containment requirement of 10 CFR 71.51(a)(2), requiring no escape of other radioactive material exceeding a total amount of  $A_2$  in one week, is calculated in the following sections. Post-HAC drop test leak test results, discussed above, bound the calculated allowable rate (see Section 4.5.1.4 for details). Therefore, the containment boundary is demonstrated to be acceptable for HAC.

The allowable fuel rod conditions for HAC are assumed as: [[  
]]. These values bound the HAC allowable conditions for the BWR fuel rod type as summarized in Section 3.4.3.2.1.

#### **4.4 LEAKAGE RATE TESTS FOR TYPE B PACKAGES**

During manufacturing, the fuel is leak tested to demonstrate that it is leaktight ( $<1 \times 10^{-7}$  ref-cc/s per ANSI N14.5 (Reference 4-1) or accepted alternate method). There are no leak rate requirements for the inner and outer packaging. The fabrication leakage rate test satisfies the requirement for the pre-shipment leakage rate test, and there are no maintenance or periodic leak rate tests for the fuel. Leak rate tests performed for HAC are summarized in Section 4.3, and these results are used in further sections for comparison to the calculated leak rates of NCT and HAC.

## 4.5 APPENDIX

### 4.5.1 Determination of Allowable Leak Rates

This section calculates the package A<sub>2</sub> effective, activity concentration limits, allowable NCT release and leak rates, and allowable HAC release and leak rates for the 10x10 fuel assembly content.

#### 4.5.1.1 Calculation of Package A<sub>2</sub> Effective

In order to determine the package allowable leak rate, the A<sub>2</sub> effective of the content mixture is first determined. The A<sub>2</sub> effective is based on the maximum amount of radioactive material shipped in a 10x10 fuel assembly, comprised of reprocessed uranium in solid form as ceramic uranium dioxide that is enriched to no more than 5.0 wt% U-235 for LEU fuel and 8.0 wt% U-235 for LEU+ fuel for the purposes of this report. The package is assumed to have two assemblies, each with 100 rods. The uranium and other nuclides in the fuel are considered to be dispersible solids that have homogenous distribution.

The total activity is calculated for a package payload of two assemblies containing 550 kg UO<sub>2</sub> (484 kg U) with a nuclide specification for enriched reprocessed fuel. Table 4-1 summarizes the maximum radionuclide concentration from American Society for Testing and Materials (ASTM) Specification C996-20 (Reference 4-2) with specific alpha emitting isotopes defined based on allowable fuel composition. While not considered a maximum concentration listed in Table 4-1, the U-238 concentration is assumed as the remainder of the uranium concentration.

**Table 4-1 RAJ-II Content Radionuclide Maximum Concentrations for 5.0 wt% U-235**

Radionuclide	Maximum Content
U-232	0.050 µg/g U
U-234	2,000 µg/g U
U-235	50,000 µg/g U
U-236	25,000 µg/g U
Tc-99	5 µg/g U
Np-237	1.66 µg/g U
Pu-238	0.0000620 µg/g U
Pu-239	0.00304 µg/g U
Pu-240	0.00304 µg/g U
Gamma Emitters	4.4x10 <sup>5</sup> MeV Bq/kg U

Table 4-2 summarizes the maximum radionuclide concentration for 8.0 wt% U-235. Only the U-235 and remainder U-238 concentrations are impacted. Although not considered a maximum concentration, the U-238 concentration is assumed as the remainder of the uranium concentration.

**Table 4-2      RAJ-II Content Radionuclide Maximum Concentrations for 8.0 wt% U-235**

<b>Radionuclide</b>	<b>Maximum Content</b>
U-232	0.050 µg/g U
U-234	2,000 µg/g U
U-235	80,000 µg/g U
U-236	25,000 µg/g U
Tc-99	5 µg/g U
Np-237	1.66 µg/g U
Pu-238	0.0000620 µg/g U
Pu-239	0.00304 µg/g U
Pu-240	0.00304 µg/g U
Gamma Emitters	4.4x10 <sup>5</sup> MeV Bq/kg U

The A<sub>2</sub> and specific activity of each radionuclide, taken from 10 CFR 71 Appendix A, Table A-1, are shown in Table 4-3. Gamma emitter A<sub>2</sub> values are taken from 10 CFR 71 Appendix A, Table A-3, while the specific activity values are calculated based on note instructions applied to Table 4-3. Based on the concentration of each radionuclide, the mass is calculated. The mass is then used to determine the total activity of each radionuclide.



**Table 4-3 RAJ-II Content Radionuclide A<sub>2</sub>, Specific Activity, Mass, and Activity**

Radionuclide	A <sub>2</sub> (TBq)	A <sub>2</sub> (Ci)	Specific Activity		Mass	Activity	
			(TBq/g)	(Ci/g)	(g)	(TBq)	(Ci)
U-232	1.0x10 <sup>-3</sup>	2.7x10 <sup>-2</sup>	8.3x10 <sup>-1</sup>	2.2x10 <sup>1</sup>	2.42x10 <sup>-2</sup>	2.01x10 <sup>-2</sup>	5.32x10 <sup>-1</sup>
U-234	6.0x10 <sup>-3</sup>	1.6x10 <sup>-1</sup>	2.3x10 <sup>-4</sup>	6.2x10 <sup>-3</sup>	9.68x10 <sup>2</sup>	2.23x10 <sup>-1</sup>	6.00x10 <sup>0</sup>
U-235 at 5% U-235 at 8% U-235	Unlimited	Unlimited	8.0x10 <sup>-8</sup>	2.2x10 <sup>-6</sup>	2.42x10 <sup>4</sup> 3.87x10 <sup>4</sup>	1.94x10 <sup>-3</sup> 3.10x10 <sup>-3</sup>	5.32 x10 <sup>-2</sup> 8.52x10 <sup>-2</sup>
U-236	6.0x10 <sup>-3</sup>	1.6x10 <sup>-1</sup>	2.4x10 <sup>-6</sup>	6.5x10 <sup>-5</sup>	1.21x10 <sup>4</sup>	2.90 x10 <sup>-2</sup>	7.87x10 <sup>-1</sup>
U-238 at 5% U-235 at 8% U-235	Unlimited	Unlimited	1.2x10 <sup>-8</sup>	3.4x10 <sup>-7</sup>	4.47x10 <sup>5</sup> 4.32x10 <sup>5</sup>	5.36x10 <sup>-3</sup> 5.19x10 <sup>-3</sup>	1.52x10 <sup>-1</sup> 1.47x10 <sup>-1</sup>
Tc-99	9.0x10 <sup>-1</sup>	2.4x10 <sup>1</sup>	6.3x10 <sup>-4</sup>	1.7x10 <sup>-2</sup>	2.42x10 <sup>0</sup>	1.52x10 <sup>-3</sup>	4.11x10 <sup>-2</sup>
Np-237	2.0x10 <sup>-3</sup>	5.4x10 <sup>-2</sup>	2.6x10 <sup>-5</sup>	7.1x10 <sup>-4</sup>	8.03x10 <sup>-1</sup>	2.09x10 <sup>-5</sup>	5.70x10 <sup>-4</sup>
Pu-238	1.0x10 <sup>-3</sup>	2.7x10 <sup>-2</sup>	6.3x10 <sup>-1</sup>	1.7 x10 <sup>1</sup>	3.00x10 <sup>-5</sup>	1.89x10 <sup>-5</sup>	5.10x10 <sup>-4</sup>
Pu-239	1.0x10 <sup>-3</sup>	2.7x10 <sup>-2</sup>	2.3x10 <sup>-3</sup>	6.2x10 <sup>-2</sup>	1.47x10 <sup>-3</sup>	3.38x10 <sup>-6</sup>	9.12x10 <sup>-5</sup>
Pu-240	1.0x10 <sup>-3</sup>	2.7x10 <sup>-2</sup>	8.4x10 <sup>-3</sup>	2.3x10 <sup>-1</sup>	1.47x10 <sup>-3</sup>	1.24x10 <sup>-5</sup>	3.38x10 <sup>-4</sup>
Gamma Emitter*	2.0x10 <sup>-2</sup>	5.4x10 <sup>-1</sup>	8.5x10 <sup>-9</sup>	2.3x10 <sup>-7</sup>	-----	4.11x10 <sup>-3</sup>	1.11x10 <sup>-1</sup>
<b>Total Activity</b>							
<b>at 5% U-235</b>						2.85x10 <sup>-1</sup>	7.68x10 <sup>0</sup>
<b>at 8% U-235</b>						2.86x10 <sup>-1</sup>	7.71x10 <sup>0</sup>

**\*Note:** The mean gamma energy per disintegration for the gamma emitters measured by the standard test method for gamma energy emission from fission product ranges from 0.0518 to 0.766 (ASTM C1295-15, Reference 4-3). The gamma energy production specification for reprocessed enriched uranium (4.4 x10<sup>5</sup> MeV Bq/kgU) is divided by the lowest mean gamma energy (0.0518 MeV) to conservatively estimate the specific activity of the gamma emitters.

The method for calculating the A<sub>2</sub> value for normal form material mixtures of radionuclides is found in Appendix A, Section IV(d) of 10 CFR 71.

The package A<sub>2</sub> effective is derived as follows: 
$$X_m = \frac{1}{\sum_i \frac{f(i)}{X(i)}}$$

where,

- f(i) is the fraction of activity or activity concentration of each radionuclide in the mixture, found by
  - Calculating the activity a(i) of each radionuclide in the mixture
  - Summing to get the total activity A(i) of the mixture
  - Dividing the activity of each radionuclide by the total activity to get f(i)
- X(i) is the appropriate value of A<sub>2</sub> for each radionuclide, found in the regulations
- X<sub>m</sub> is the derived value of A<sub>2</sub> in the case of a mixture

**Table 4-4 A<sub>2</sub> Effective for RAJ-II Content Mixture for 5.0 wt% U-235**

Radionuclide	Fraction of Activity f(i) (TBq case only)	f(i)/A <sub>2</sub> (i)	
		1/TBq	1/Ci
U-232	7.05x10 <sup>-2</sup>	7.05x10 <sup>1</sup>	2.57x10 <sup>0</sup>
U-234	7.82x10 <sup>-1</sup>	1.30x10 <sup>2</sup>	4.88x10 <sup>0</sup>
U-235	6.80x10 <sup>-3</sup>	0.00x10 <sup>0</sup>	0.00x10 <sup>0</sup>
U-236	1.02x10 <sup>-1</sup>	1.70x10 <sup>1</sup>	6.40x10 <sup>-1</sup>
U-238	1.88x10 <sup>-2</sup>	0.00x10 <sup>0</sup>	0.00x10 <sup>0</sup>
Tc-99	5.35x10 <sup>-3</sup>	5.95x10 <sup>-3</sup>	2.23x10 <sup>-4</sup>
Np-237	7.34x10 <sup>-5</sup>	3.67x10 <sup>-2</sup>	1.38x10 <sup>-3</sup>
Pu-238	6.64x10 <sup>-5</sup>	6.64x10 <sup>-2</sup>	2.46x10 <sup>-3</sup>
Pu-239	1.19x10 <sup>-5</sup>	1.19x10 <sup>-2</sup>	4.40x10 <sup>-4</sup>
Pu-240	4.34x10 <sup>-5</sup>	4.34x10 <sup>-2</sup>	1.63x10 <sup>-3</sup>
Gamma Emitter	1.44x10 <sup>-2</sup>	7.22x10 <sup>-1</sup>	2.68x10 <sup>-2</sup>
Totals	-----	2.19x10 <sup>2</sup>	8.13x10 <sup>0</sup>

The A<sub>2</sub> effective for the RAJ-II package with 5.0 wt% U-235 contents, which is the inverse of the total listed in Table 4-4, is 4.57x10<sup>-3</sup> TBq or 0.123 Ci.

**Table 4-5 A<sub>2</sub> Effective for RAJ-II Content Mixture for 8.0 wt% U-235**

Radionuclide	Fraction of Activity f(i) (TBq case only)	f(i)/A <sub>2</sub> (i)	
		1/TBq	1/Ci
U-232	7.03x10 <sup>-2</sup>	7.03x10 <sup>1</sup>	2.56x10 <sup>0</sup>
U-234	7.79x10 <sup>-1</sup>	1.30x10 <sup>2</sup>	4.87x10 <sup>0</sup>
U-235	1.08x10 <sup>-2</sup>	0.00x10 <sup>0</sup>	0.00x10 <sup>0</sup>
U-236	1.02x10 <sup>-1</sup>	1.69x10 <sup>1</sup>	6.38x10 <sup>-1</sup>
U-238	1.82x10 <sup>-2</sup>	0.00x10 <sup>0</sup>	0.00x10 <sup>0</sup>
Tc-99	5.34x10 <sup>-3</sup>	5.93x10 <sup>-3</sup>	2.22x10 <sup>-4</sup>
Np-237	7.31x10 <sup>-5</sup>	3.66 x10 <sup>-2</sup>	1.37x10 <sup>-3</sup>
Pu-238	6.62x10 <sup>-5</sup>	6.62x10 <sup>-2</sup>	2.45x10 <sup>-3</sup>
Pu-239	1.18x10 <sup>-5</sup>	1.18x10 <sup>-2</sup>	4.38x10 <sup>-4</sup>
Pu-240	4.33x10 <sup>-5</sup>	4.33x10 <sup>-2</sup>	1.63x10 <sup>-3</sup>
Gamma Emitter	1.44x10 <sup>-2</sup>	7.19x10 <sup>-1</sup>	2.67x10 <sup>-2</sup>
Totals	-----	2.18x10 <sup>2</sup>	8.10x10 <sup>0</sup>

The A<sub>2</sub> effective for the RAJ-II package with 8.0 wt% U-235 contents, which is the inverse of the total listed in Table 4-5, is 4.59x10<sup>-3</sup> TBq or 0.124 Ci.



#### 4.5.1.2 Calculation of Package Activity Concentration Limits

Standard methods described in Reference 4-1 are applied to determine the package release rate limits.

Based on the calculated total activity, the specific activity of the package material is calculated and results in the same value for both 5.0 wt% and 8.0 wt% U-235 contents:

$$S_{A, 5\%U-235} = \frac{7.68 Ci}{550 kg UO_2} = 1.40 \times 10^{-5} \frac{Ci}{gUO_2}$$

$$S_{A, 8\%U-235} = \frac{7.71 Ci}{550 kg UO_2} = 1.40 \times 10^{-5} \frac{Ci}{gUO_2}$$

Releasable airborne materials can originate from the radionuclides within the individual fuel rods. The contribution of the fuel to the overall release rate largely depends on its initial pre-transport condition and on subsequent fuel rod response to transportation events. Loose radioactive particles may originate from spallation of material from the surface of the fuel pellets during NCT. The uranium oxide pellets may further fracture and crumble during HAC. These conditions tend to cause the fuel pellets inside the fuel rod to produce a powder aerosol in the helium fill gas. To estimate the source terms under NCT and HAC, an assumption is made that a portion of the fuel rod inventory is fine fuel particles. For NCT, 15% of the material is assumed to become fine fuel particles, while for HAC, 100% of the material is assumed to become fine fuel particles, per NUREG/CR-6487 (Reference 4-4). A reasonable bounding value for the mass density of a powder aerosol is  $9 \times 10^{-6}$  g/cc, per NUREG/CR-6487 (Reference 4-4).

The releasable activity concentration of the package is:

$$C = S_A \times \rho$$

where,

$C$  is the releasable activity concentration inside the package  $\left(\frac{Ci}{cc}\right)$

$S_A$  is the specific activity of the fines in the fuel  $\left(\frac{Ci}{gUO_2}\right)$

$\rho$  is the aerosol mass density  $\left(\frac{g}{cc}\right)$

The package release activity concentrations for both 5.0 wt% and 8.0 wt% U-235 are:

$$C_N = 1.40 \times 10^{-5} \frac{Ci}{gUO_2} \times 9 \times 10^{-6} \frac{g}{cc} \times 15\% = 1.89 \times 10^{-11} \frac{Ci}{cc}$$

$$C_A = 1.40 \times 10^{-5} \frac{Ci}{gUO_2} \times 9 \times 10^{-6} \frac{g}{cc} \times 100\% = 1.26 \times 10^{-10} \frac{Ci}{cc}$$

#### 4.5.1.3 Calculation of NCT Release and Leak Rates

As previously stated in Section 4.2, the following conditions apply for 10x10 fuel assemblies. The maximum conditions for NCT are assumed as: [[ ]].

NEDO-33869 Revision 11  
Non-Proprietary Information

The maximum allowed release rate of the RAJ-II during NCT in units of curies per second assuming a time-averaged constant flow rate is, according to 10 CFR 71.51(a)(1):

$$R_{N, 5\%U-235} = A_2 \times 10^{-6} \text{ per hour} = \frac{A_2 \times 2.78 \times 10^{-10}}{s} = \frac{0.123 \text{ Ci} \times 2.78 \times 10^{-10}}{s}$$

$$= 3.42 \times 10^{-11} \text{ Ci/s}$$

$$R_{N, 8\%U-235} = A_2 \times 10^{-6} \text{ per hour} = \frac{A_2 \times 2.78 \times 10^{-10}}{s} = \frac{0.124 \text{ Ci} \times 2.78 \times 10^{-10}}{s}$$

$$= 3.43 \times 10^{-11} \text{ Ci/s}$$

As previously calculated in Section 4.5.1.2, the activity concentration is applied to calculate the allowable leak rate which resulted in the same value for both 5.0 wt% and 8.0 wt% U-235.

$$C_N = 1.89 \times 10^{-11} \frac{\text{Ci}}{\text{cc}}$$

Therefore, the allowed leak rate for the package is calculated as:

$$L_N = R_N \div C_N$$

$$= 1.82 \text{ cc/s for 5.00 wt\% and 8.00 wt\% U-235}$$

where,

$C_N$  is the curies per unit volume of the releasable radioactive material within the containment vessel for normal conditions of transport (Ci/cc).

$L_N$  is the time-averaged volumetric gas flow rate for normal conditions of transport (cc/s), and

$R_N$  is the release rate for normal conditions of transport (Ci/s).

Because this is the total allowable leak rate for the package applying to two fuel assemblies, and the containment boundary of the package is a single fuel rod, the allowable leak rate is divided by the total maximum number of rods permitted in two 10x10 fuel bundles (200 rods).

$$L_{N,rod} = (1.82 \text{ cc/s}) \div 200 = 9.08 \times 10^{-3} \text{ cc/s}$$

From this allowable leak rate, the leak hole diameter is determined based on NCT conditions, based on the following equations.

$$L_u = (F_c + F_m)(P_u - P_d) \left( \frac{P_a}{P_u} \right)$$

$$F_c = \frac{[2.49 \times 10^6 D^4]}{a \times \mu}$$

$$F_m = \frac{\left[ 3.81 \times 10^3 D^3 \sqrt{\frac{T}{M}} \right]}{a \times P_a}$$

where,

$L_u$  is the volumetric flow rate of gas at average stream pressure, cc/s

a	is leakage hole length, cm
D	is leakage hole diameter, cm
F <sub>c</sub>	is coefficient of continuum flow conductance per unit pressure, cc/atm s
F <sub>m</sub>	is coefficient of free molecular flow conductance per unit pressure, cc/atm s
M	is molecular weight, g/mol
P <sub>u</sub>	is fluid upstream pressure, atm absolute
P <sub>d</sub>	is fluid downstream pressure, atm absolute
P <sub>a</sub>	is average stream pressure = 1/2 (P <sub>u</sub> +P <sub>d</sub> ), atm absolute
T	is fluid absolute temperature, K
μ	is fluid viscosity, cP (centipoises)

The conditions for this calculation are:

The leak path is also assumed to be the length of the minimum fuel rod cladding thickness, with helium as the medium.

[[  
]] a (10x10 fuel rod cladding minimum thickness) = 0.038 cm / [[  
]], and

The correlation for the coefficient of dynamic viscosity for helium is

$$\mu = 3.674 \times 10^{-7} T^{0.7} \text{ kg/m} \times \text{s} = 3.674 \times 10^{-4} T^{0.7} \text{ cP}$$

D is determined to be 0.000818 cm for both 5.0 wt% and 8.0 wt% U-235 contents.

The reference air leak rate of a fuel rod, based on the calculated hole diameter, is determined based on the following parameters:

$$a = 0.038 \text{ cm} / T = 298 \text{ K} / \mu(\text{air}, 298 \text{ K}) = 0.0186 \text{ cP} / P_u = 1 \text{ atm} / P_d = 0.01 \text{ atm} / M = 29 \text{ g/mol} / P_a = 0.505 \text{ atm}$$

$$L_{NCT \text{ Ref, rod allowable}} = 9.63 \times 10^{-4} \text{ ref} - \text{cc/s}$$

This fuel rod allowable leak rates for 5.0 wt% and 8.0 wt% U-235 at NCT is greater than the qualification leak rate ( $L_{HAC \text{ Ref, bundle actual}}$ ) measured for an entire bundle at HAC.

$$L_{HAC \text{ Ref, bundle actual}} = 5.5 \times 10^{-6} \text{ ref} - \text{cc/s}$$

Therefore, the containment release rate requirement for NCT is satisfied.

#### 4.5.1.4 Calculation of HAC Release and Leak Rate

As previously stated in Section 4.3, the following conditions apply for 10x10 fuel assemblies. The maximum conditions for HAC are assumed as: [[  
]]].

The maximum allowed release rate of the RAJ-II during HAC in units of curies per second assuming a time-averaged constant flow rate, as defined in 10 CFR 71.51(a)(2), is:

$$R_A = \frac{A_2}{\text{week}} = \frac{A_2}{\text{week}} \times \frac{1 \text{ week}}{6.048 \times 10^5 \text{ s}} = A_2 \times 1.65 \times 10^{-6} / \text{second}$$

$$R_{A,5\% \text{ U-235}} = \frac{(A_2 \times 1.65 \times 10^{-6})}{\text{second}} = \frac{(0.123 \text{ Ci} \times 1.65 \times 10^{-6})}{\text{second}} = 2.03 \times 10^{-7} \text{ Ci/s}$$

$$R_{A,8\% \text{ U-235}} = \frac{(A_2 \times 1.65 \times 10^{-6})}{\text{second}} = \frac{(0.124 \text{ Ci} \times 1.65 \times 10^{-6})}{\text{second}} = 2.04 \times 10^{-7} \text{ Ci/s}$$

As previously calculated in Section 4.5.1.2, the activity concentration is applied to calculate the allowable leak rate.

$$C_A = 1.26 \times 10^{-10} \frac{\text{Ci}}{\text{cc}}$$

Therefore, the allowed leak rate for the package is calculated as:

$$L_A = R_A \div C_A$$

$$L_A = 1.62 \times 10^3 \text{ cc/s for both 5.0 wt\% and 8.0 wt\% U-235.}$$

where,

$C_A$  is the curies per unit volume of the releasable radioactive material within the containment vessel accident transport conditions (Ci/cc).

$L_A$  is the time-averaged volumetric gas flow rate for accident transport conditions (cc/s), and

$R_A$  is the release rate for accident transport conditions (Ci/s).

Because the total allowable leak rate for the package applies to two fuel assemblies, and the containment boundary of the package is a single fuel rod, the allowable leak rate is divided by the total maximum number of rods permitted in two 10x10 fuel bundles (200 rods).

$$L_{A,rod} = (1.62 \times 10^3 \text{ cm}^3/\text{s}) \div 200 = 8.09 \text{ cc/s for both 5.0 wt\% and 8.0 wt\% U-235}$$

From this allowable leak rate, the leak hole diameter is determined based on HAC conditions, based on the following equations.

$$L_u = (F_c + F_m)(P_u - P_d) \left( \frac{P_a}{P_u} \right)$$

$$F_c = \frac{[2.49 \times 10^6 D^4]}{a \times \mu}$$

$$F_m = \frac{\left[ 3.81 \times 10^3 D^3 \sqrt{\frac{T}{M}} \right]}{a \times P_a}$$

where,

$L_u$  is the volumetric flow rate of gas at average stream pressure, cc/s

$a$  is leakage hole length, cm

$D$  is leakage hole diameter, cm

$F_c$  is coefficient of continuum flow conductance per unit pressure, cc/atm s

NEDO-33869 Revision 11  
Non-Proprietary Information

$F_m$	is coefficient of free molecular flow conductance per unit pressure, cc/atm s
$M$	is molecular weight, g/mol
$P_u$	is fluid upstream pressure, atm absolute
$P_d$	is fluid downstream pressure, atm absolute
$P_a$	is average stream pressure = $1/2 (P_u + P_d)$ , atm absolute
$T$	is fluid absolute temperature, K
$\mu$	is fluid viscosity, cP (centipoises)

The conditions for this calculation are:

The leak path is also assumed to be the length of the minimum fuel rod cladding thickness, with helium as the medium.

$$\left[ \frac{F_m}{P_u - P_d} \right] / a \text{ (fuel rod cladding minimum thickness)} = 0.038 \text{ cm} / \left[ \frac{F_m}{P_u - P_d} \right], \text{ and}$$

The correlation for the coefficient of dynamic viscosity for helium is

$$\mu = 3.674 \times 10^{-7} T^{0.7} \text{ kg/m} \times \text{s} = 3.674 \times 10^{-4} T^{0.7} \text{ cP}$$

$D$  is determined to be 0.00414 cm for both 5.0 wt% and 8.0 wt% U-235.

The reference air leak rate for a fuel rod, based on the calculated hole diameter is determined based on the following parameters:

$$a = 0.038 \text{ cm} / T = 298 \text{ K} / \mu(\text{air}, 298 \text{ K}) = 0.0186 \text{ cP} / P_u = 1 \text{ atm} / P_d = 0.01 \text{ atm} / M = 29 \text{ g/mol} / P_a = 0.505 \text{ atm}$$

$$L_{HAC \text{ Ref, rod allowable}} = 5.40 \times 10^{-1} \text{ ref} - \text{cc/s for both 5.0 wt\% and 8.0 wt\% U-235}$$

This fuel rod allowable leak rate at HAC for both 5.0 wt% and 8.0 wt% U-235 contents is greater than the qualification leak rate ( $L_{HAC \text{ Ref, bundle actual}}$ ) measured for an entire bundle at HAC.

$$L_{HAC \text{ Ref, bundle actual}} = 5.5 \times 10^{-6} \text{ ref} - \text{cc/s}$$

Therefore, the containment release rate requirement for HAC is satisfied.

#### 4.5.2 Summary

The worst case HAC leak rate for an entire 10x10 bundle was measured to be less than the allowable leak rate of a single fuel rod for NCT and HAC. Thus, the safety of the RAJ-II package containment boundary is demonstrated.

#### 4.5.3 References

- 4-1 ANSI N14.5-1997, "Leakage Tests on Packages for Shipment – for Radioactive Materials."
- 4-2 ASTM C996-20, "Standard Specification for Uranium Hexafluoride Enriched to Less than 5% U235."
- 4-3 ASTM C1295-15, "Standard Test Method for Gamma Energy Emission from Fission and Decay Products in Uranium Hexafluoride and Uranyl Nitrate Solution."
- 4-4 NUREG/CR-6487, "Containment Analysis for Type B Packages Use to Transport Various Contents," October 1996.

## **5.0 SHIELDING EVALUATION**

This chapter describes the RAJ-II shielding analysis and demonstrates compliance with the external radiation requirements of 10 CFR 71 under Normal Conditions of Transport (NCT) and Hypothetical Accident Conditions (HAC).

### **5.1 DESCRIPTION OF THE SHIELDING DESIGN**

#### **5.1.1 Design Features**

The contents transported by the RAJ-II are unirradiated fuel which does not emit significant gamma or neutron radiation. Hence the RAJ-II package does not have design features to specifically provide shielding.

The RAJ-II package provides positioning of the radiation sources within the inner container to provide distance to the package surface. Only attenuation in select stainless steel components of the inner container is modeled to determine the gamma dose rates in addition to the uranium of the fuel. No materials are modeled for the neutron dose rate. The general package description is provided in Section 1.2 and Section 6.1.1.1.

#### **5.1.2 Summary Table of Maximum Radiation Levels**

Prior to shipping, direct measurements of the dose rates are performed. The measurements are used to confirm compliance to the NCT dose rate limits established by 10 CFR 71.47(a). The packages are labeled with the Transport Index (TI) based on these measurements.

Because there is no shielding provided by the package, there is no shielding change during the HAC. Therefore, the higher dose rate allowed by 10 CFR 71.51(a)(2) will be met.

Nevertheless, the dose rates are calculated based on conservative assumptions and simplified models to demonstrate compliance with the requirements of 10 CFR 71. Table 5-1 shows that all dose rate requirements are met.

**Table 5-1 Summary Table of External Radiation Levels**

Transport Condition		Package Surface mSv/hr (mrem/hr)			1 meter from Package Surface mSv/hr (mrem/hr)		
		Top	Side	Ends	Top/Bottom	Side	Ends
N C T	Gamma	0.030 (3.0)	0.019 (1.9)	0.0017 (0.17)	0.0068 (0.68)	0.0037 (0.37)	0.00032 (0.032)
	Neutron	0.0049 (0.49)	0.0048 (0.48)	0.00080 (0.080)	0.00091 (0.091)	0.00083 (0.083)	0.00026 (0.026)
	Total	0.035 (3.5)	0.024 (2.4)	0.0025 (0.25)	0.008 (0.8)	0.005 (0.5)	0.001 (0.1)
	10 CFR 71.47(a) Limit	2 (200)	2 (200)	2 (200)	0.10 (10)*	0.10 (10)*	0.10 (10)*
* Transport index may not exceed 10.							
H A C	Gamma	--	--	--	0.0066 (0.66)	0.0037 (0.37)	0.00032 (0.032)
	Neutron	--	--	--	0.00091 (0.091)	0.00083 (0.083)	0.00027 (0.027)
	Total	--	--	--	0.0075 (0.75)	0.0045 (0.45)	0.00059 (0.059)
	10 CFR 71.51(a)(2) Limit	N/A	N/A	N/A	10 (1000)	10 (1000)	10 (1000)



## 5.2 SOURCE SPECIFICATION

The RAJ-II maximum isotopic mass specified in Table 4-2 shows that the contents may contain uranium, neptunium, and plutonium isotopes which decay by alpha emission. Contents may include technitium-99 which decays by beta emission. Alpha and beta particles have a short range and are not significant contributors to external dose rates.

### 5.2.1 Gamma Source

The gamma source from gamma emitting isotopes other than actinides present in either the commercial grade uranium or enriched reprocessed uranium is defined in American Society for Testing and Materials (ASTM) C996-20 (Reference 5-1). The maximum concentration of gamma emitters is  $4.4\text{E}+05$  MeV/s/kgU. Section 1.2.2.6 indicates that the maximum uranium payload is 484 kg. ASTM C1295-15 (Reference 5-2) provides the fission product nuclides whose gamma energy is to be measured to demonstrate compliance with ASTM C996-20. These nuclides and the measured gamma energy peaks are provided in Table 1 of ASTM C1295-15. The highest energy gamma is 0.7658 MeV (niobium-95) and the lowest is 2.736 keV (protactinium-231). Conservatively, the gamma source term from gamma emitters uses the highest energy gamma which results in a source strength of  $2.78\text{E}+08$   $\gamma/\text{s}$ .

The spectrum and source strength of the gammas emitted due to the decay of the actinides are determined using ORIGEN2 Version 2.1 (Reference 5-3). This includes gammas emitted from all decay modes, such as alpha or spontaneous fission, for all the actinides, in addition to the contribution from Bremsstrahlung due to slowing down of beta particles in the fuel, albeit a small effect on the gamma dose rate. The gamma source strength from actinides is  $3.893\text{E}+10$   $\gamma/\text{s}$ .

The spectrum from the ORIGEN2 output is provided in Table 5-2, except the contribution from the gamma emitters is added to the 0.70-1.0 MeV bin from the actinides, which conservatively results in a mean value of 0.85 MeV. The neutron-induced gammas are neglected. This gamma spectrum is used for both NCT and HAC.

**Table 5-2      Gamma Source Term**

<b>Mean Energy (MeV)</b>	<b>Lower Bound (MeV)</b>	<b>Upper Bound (MeV)</b>	<b>Intensity (γ/s)</b>
1.00E-02	1.00E-03 <sup>a</sup>	2.00E-02	3.61E+10
2.50E-02	2.00E-02	3.00E-02	2.41E+06
3.75E-02	3.00E-02	4.50E-02	2.84E+06
5.75E-02	4.50E-02	7.00E-02	2.88E+08
8.50E-02	7.00E-02	1.00E-01	2.46E+08
1.25E-01	1.00E-01	1.50E-01	5.84E+08
2.25E-01	1.50E-01	3.00E-01	1.69E+09
3.75E-01	3.00E-01	4.50E-01	4.78E+06
5.75E-01	4.50E-01	7.00E-01	3.13E+05
8.50E-01 <sup>b</sup>	7.00E-01	1.00E+00	2.78E+08
1.25E+00	1.00E+00	1.50E+00	5.86E+03
1.75E+00	1.50E+00	2.00E+00	2.87E+03
2.25E+00	2.00E+00	2.50E+00	1.65E+03
2.75E+00	2.50E+00	3.00E+00	9.46E+02
3.50E+00	3.00E+00	4.00E+00	8.35E+02
5.00E+00	4.00E+00	6.00E+00	3.53E+02
7.00E+00	6.00E+00	8.00E+00	3.99E+01
9.50E+00	8.00E+00	1.10E+01	4.54E+00
<b>Total</b>			<b>3.76E+10</b>

a. Lower bound from ORIGEN2 is 0.0 MeV. The lower bound for this bin is conservatively set to 1.00E-03 MeV.

b. Includes 2.78E+08 γ/s from gamma emitters.

### 5.2.2 Neutron Source

The neutron source strength from spontaneous fission and alpha-n events is determined using ORIGEN2 Version 2.1 as 9.77E+03 n/s. The main contributors to the spontaneous fission neutron source are U-238, U-236 and U-235, totaling 5.56E+03 n/s. The main contributors to the alpha-n source are U-234, U-232, U-236, U-238, and U-235, totaling 4.21E+03 n/s.

To account for subcritical multiplication, the total neutron source term determined from ORIGEN2 is increased by a factor of  $20 = 1/(1-k_{\text{eff}}) = 1/(1-0.95)$ , consistent with the guidance provided in NUREG-6802 (Reference 5-4). This is conservative because the system multiplication for a single package, when moderated by water, is demonstrated to be less than 0.95 in Table 6-3.

The Watt spectrum is used to approximate the neutron spectrum, using the default coefficients provided in the MCNP (Reference 5-5) code, with a total neutron source strength of 1.95E+05 n/s. The energy distribution,  $p(E)$ , is given by the equation below.

$$p(E) = \exp\left(-\frac{E}{0.965\text{MeV}}\right) \sinh\left(\frac{2.29}{\text{MeV}}E\right)^{1/2}$$

## 5.3 SHIELDING MODEL

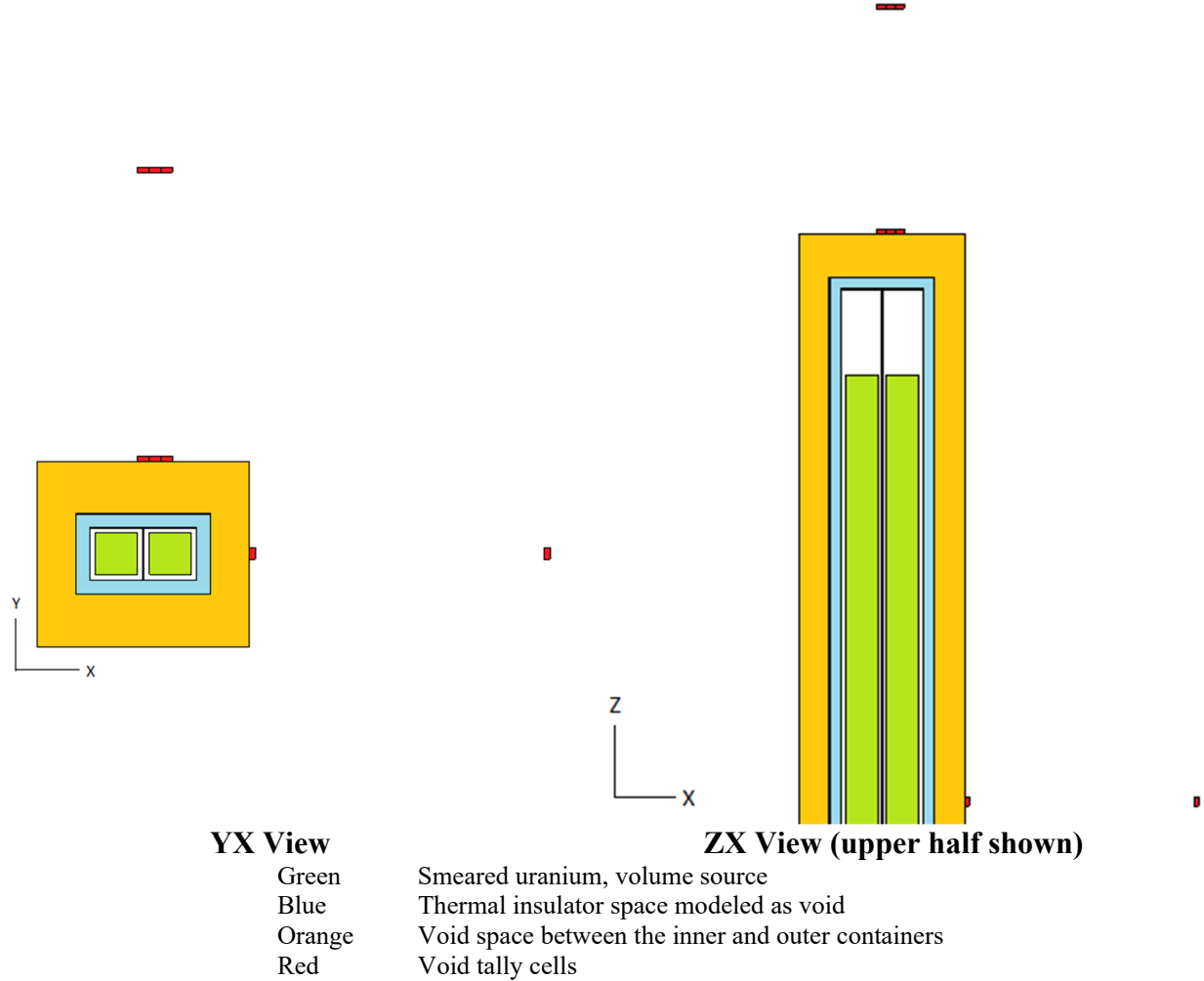
### 5.3.1 Configuration of Source and Shielding

Only the stainless steel sheets of the inner container are modeled, including the outer shell, the inner shell and the divider plate between the fuel compartments; the alumina silicate thermal insulator and the polyethylene cushioning foam are modeled as void. The distance provided by the outer container is maintained but the stainless steel sheet of the outer container is modeled as void. The stainless steel sheet thicknesses are provided in Table 6-7 and account for dimensional tolerances. The dimensions of the outer container and inner container are shown in Figure 6-1, Figure 6-2, and Figure 6-3 for NCT, and Figure 6-6, Figure 6-7, and Figure 6-8 for HAC. The difference between the NCT and HAC models is the package dimensions.

For both NCT and HAC, the source is modeled as two volumetric sources centered within the fuel compartments, with uranium density of  $3.10 \text{ g/cm}^3$ . The shielding provided by other fuel assembly and package components is conservatively neglected. The volumetric source preserves the total uranium mass because fuel rod integrity is maintained under NCT and HAC. The position of the volume source is not extensively analyzed because minimal credit for the package materials is included in the models.

The neutron models do not credit any materials, only the distances provided by the package. This approach accounts for any additional contribution to the total dose rate due to neutron-induced gammas.

Several small tally cells are placed at the top and ends of the package to capture the maximum dose rate: 4 cm x 4 cm, 2 cm thick. The top tallies are centered axially, and the end tallies are centered in the y-direction. The first tally cell of the top and ends is centered in the x-direction. Due to geometry, the maximum dose rate location on the side of the package is at the central elevation of the source, centered axially. A depiction of the model is shown in Figure 5-1.



Note: the inner container stainless steel sheets and fuel compartment divider are included in the shielding model.

**Figure 5-1 MCNP Model and Tally Locations**

### 5.3.2 Material Properties

The materials modeled include the stainless steel of the inner container. The specific type of stainless steel used does not affect the shielding evaluation. Therefore, consistent with the criticality evaluation, stainless steel 304 is used in the gamma models. The material composition is provided in Table 6-8.

The maximum uranium payload of 484 kg is smeared over the total compartment volume using the minimum active fuel length of 381 cm ( $7.80\text{E}+04 \text{ cm}^3$ ), resulting in a uranium density of  $3.10 \text{ g/cm}^3$ .

## 5.4 SHIELDING EVALUATION

### 5.4.1 Methods

ORIGEN2 Version 2.1 (Reference 5-3) with the default DECAY and GXUO2BRM libraries (RSICC CCC-371) is used for the gamma and neutron source terms. ORIGEN is a versatile point depletion and decay computer code for use in simulating nuclear fuel cycles and calculating the nuclide compositions of materials contained therein. ORIGEN uses a matrix exponential method to solve a large system of coupled, linear, first-order ordinary differential equations with constant coefficients. ORIGEN is only used to obtain the source term due to decay of the actinides because fuel depletion is not necessary.

MCNP5 Version 1.30 (Reference 5-5) with ENDF/B-VII.0 libraries (RSICC CCC-810) is used for the shielding analysis. MCNP is a general-purpose, continuous-energy, generalized-geometry, time-dependent, coupled neutron/photon/electron Monte Carlo transport code. MCNP was used in either photon only transport mode or neutron only transport mode to calculate external dose rates.

Geometric splitting is used for the top and side gamma dose rates, and weight windows are used for the end gamma dose rates, in addition to source directional bias. Variance reduction is not needed for the neutron dose rates.

### 5.4.2 Input and Output Data

The MCNP input and output files are provided separately. The key RAJ-II dimensions used in the shielding models are similar to those used in Chapter 6 and are listed in Table 5-3. The outputs show that all tallies pass all of the MCNP statistical checks.

**Table 5-3      Shielding Model Input Parameters**

<b>Description</b>	<b>Value (cm)</b>
NCT, Outer Container Width (X)	71.93
NCT, Outer Container Height (Y)	64.15
NCT, Outer Container Length (Z)	506.73
NCT, Inner Container Width (X)	45.88
NCT, Inner Container Height (Y)	28.05
NCT, Inner Container Length (Z)	467.16
HAC, Outer Container Width (X)	71.93
HAC, Outer Container Height (Y)	61.75
HAC, Outer Container Length (Z)	502.03
HAC, Inner Container Width (X)	45.88
HAC, Inner Container Height (Y)	28.05
HAC, Inner Container Length (Z)	459.06
Alumina Silicate Thickness (X/Y/Z)	4.8
Cushioning Foam Thickness (X/Y)	1.8
Inner Container Outer Shell Thickness (X/Y/Z)	0.14
Inner Container Inner Shell Thickness (X/Y/Z)	0.087
Fuel Compartment Divider Thickness (X/Y)	0.175

### 5.4.3 Flux-to-Dose Rate Conversion

The American National Standards Institute (ANSI)/American Nuclear Society (ANS)-6.1.1-1977 flux-to-dose rate conversion factors (Reference 5-6) used in this evaluation are provided in Table 5-4 and Table 5-5.

**Table 5-4      Gamma Flux-to-Dose Rate Conversion Factors (ANSI/ANS-6.1.1 1977)**

<b>Gamma Energy (MeV)</b>	<b>Conversion Factor (mrem/hr)/(<math>\gamma/\text{cm}^2\text{-s}</math>)</b>
1.00E-02	3.96E-03
3.00E-02	5.82E-04
5.00E-02	2.90E-04
7.00E-02	2.58E-04
1.00E-01	2.83E-04
1.50E-01	3.79E-04
2.00E-01	5.01E-04
2.50E-01	6.31E-04
3.00E-01	7.59E-04
3.50E-01	8.78E-04
4.00E-01	9.85E-04
4.50E-01	1.08E-03
5.00E-01	1.17E-03
5.50E-01	1.27E-03
6.00E-01	1.36E-03
6.50E-01	1.44E-03
7.00E-01	1.52E-03
8.00E-01	1.68E-03
1.00E+00	1.98E-03
1.40E+00	2.51E-03
1.80E+00	2.99E-03
2.20E+00	3.42E-03
2.60E+00	3.82E-03
2.80E+00	4.01E-03
3.25E+00	4.41E-03
3.75E+00	4.83E-03
4.25E+00	5.23E-03
4.75E+00	5.60E-03
5.00E+00	5.80E-03
5.25E+00	6.01E-03
5.75E+00	6.37E-03
6.25E+00	6.74E-03
6.75E+00	7.11E-03
7.50E+00	7.66E-03
9.00E+00	8.77E-03
1.10E+01	1.03E-02

<b>Gamma Energy (MeV)</b>	<b>Conversion Factor (mrem/hr)/(γ/cm<sup>2</sup>-s)</b>
1.30E+01	1.18E-02
1.50E+01	1.33E-02

**Table 5-5 Neutron Flux-to-Dose Rate Conversion Factors (ANSI/ANS-6.1.1 1977)**

<b>Neutron Energy (MeV)</b>	<b>Conversion Factor (mrem/hr)/(n/cm<sup>2</sup>-s)</b>
2.50E-08	3.67E-03
1.00E-07	3.67E-03
1.00E-06	4.46E-03
1.00E-05	4.54E-03
1.00E-04	4.18E-03
1.00E-03	3.76E-03
1.00E-02	3.56E-03
1.00E-01	2.17E-02
5.00E-01	9.26E-02
1.00E+00	1.32E-01
2.50E+00	1.25E-01
5.00E+00	1.56E-01
7.00E+00	1.47E-01
1.00E+01	1.47E-01
1.40E+01	2.08E-01
2.00E+01	2.27E-01

#### 5.4.4 External Radiation Levels

The approximations in the source terms include assigning the gamma emitter spectrum to the energy bin of the highest observed gamma energy emitted, neglecting the neutron-induced gammas, scaling the neutron source term to account for the subcritical multiplication, and using the Watt fission spectrum to approximate the neutron spectrum. Because the model only credits the uranium mass and RAJ-II materials such as inner container stainless steel sheets, the approximations used in the source terms are acceptable. However, due to these approximations and other geometric modeling simplifications, an additional safety factor of 1.2 is applied to the dose rate results provided in Table 5-1, which includes a  $2\sigma$  statistical uncertainty. Table 5-1 shows that the neutron contribution to the total dose rate is negligible. The results demonstrate that even though the shielding evaluation uses a conservative approach and simplified models, there is at least 92% margin to the regulatory limits stated in 10 CFR 71 with the limiting result being one meter from the top of the package surface under NCT.

## 5.5 REFERENCES

- 5-1 “Standard Specification for Uranium Hexafluoride Enriched to Less than 5%  $^{235}\text{U}$ ,” ASTM C996-20, American Society for Testing and Materials.
- 5-2 “Standard Test Method for Gamma Energy Emission from Fission and Decay Products in Uranium Hexafluoride and Uranyl Nitrate Solution,” ASTM C1295-15, American Society for Testing and Materials.
- 5-3 A.G. Croff, “A User’s Manual for the ORIGEN2 Computer Code,” ORNL/TM-7175, Oak Ridge National Laboratory, July 1980.
- 5-4 “Recommendations for Shielding Evaluations for Transport and Storage Packages,” NUREG/CR-6802, U.S. Nuclear Regulatory Commission, May 2003.
- 5-5 “MCNP – A General Monte Carlo N-Particle Transport Code, Version 5,” LA-UR-03-1987, Los Alamos National Laboratory, October 2005.
- 5-6 “Neutron and Gamma-Ray Flux-to-Dose Rate Factors,” ANSI/ANS-6.1.1-1977, American Nuclear Society, 1977.



## **6.0 CRITICALITY EVALUATION**

### **6.1 DESCRIPTION OF CRITICALITY DESIGN**

A criticality safety analysis is performed to demonstrate the performance of the RAJ-II package. The RAJ-II meets applicable International Atomic Energy Agency (IAEA) and 10 CFR 71 requirements for a Type B fissile material shipping container, transporting heterogeneous enriched uranium to a maximum of 5.0 weight percent (wt%) U-235, Low Enriched Uranium (LEU) fuel, or 8.0 wt% U-235, LEU Plus (LEU+) fuel, as specified in Table 6-1 and Table 6-2. Unless otherwise stated, the figures and tables presented apply to LEU fuel. To ensure criticality safety for the addition of GNF 10x10 LEU+ fuel, scoping calculations were performed. Generally, the conclusions and trends for LEU fuel hold true for LEU+ fuel and therefore remain unchanged in writing. Additions to parameters and results applying to LEU+ fuel are included in the relevant sections.

The RAJ-II package design features a stainless steel inner container positioned inside an outer stainless steel container by four evenly spaced stainless steel fixture assemblies. The fixture assemblies cradle the inner container and prevent horizontal or vertical movement. The inner container has two fuel assembly transport compartments, aligned side-by-side and separated by a stainless steel divider. Each transport compartment is lined with polyethylene cushioning foam in which the fuel assemblies rest. Additional container details are described in Section 1.2. Material manufacturing tolerances are presented in the general arrangement drawings in Section 1.3.1 and summarized in Table 6-7.

Water exclusion from the inner container is not required for this package design. The inner container is analyzed in both undamaged and damaged package arrays under optimal moderation conditions and is demonstrated to be safe under Normal Conditions of Transport (NCT) and Hypothetical Accident Condition (HAC) testing.

The uranium transported in the RAJ-II package is in the form of fuel rods. The criticality analysis for the RAJ-II package is performed at the applicable maximum enrichment in uranium dioxide (UO<sub>2</sub>) or uranium carbide (UC) fuel pellets contained in zirconium alloy or stainless steel cladding. The fuel rods may be arranged in 8x8, 9x9, or 10x10 square lattice arrays at fixed center-to-center spacing (i.e., rod pitch). Sensitivity analyses are performed by varying fuel parameters (i.e., rod pitch, clad inner diameter (ID), clad outer diameter (OD), pellet OD, fuel orientation, polyethylene packing material mass, gadolinia-urania (UO<sub>2</sub>-Gd<sub>2</sub>O<sub>3</sub>) loading, and moderator density) to obtain the most reactive configuration. The most reactive configuration is modeled for each authorized payload to demonstrate safety and to validate the fuel parameter ranges specified as loading criteria.

Fuel rods may also be transported loose with no fixed center-to-center spacing, strapped together in a close packed configuration, or inside a 5-inch diameter stainless steel pipe or protective case.

Table 6-1 and Table 6-2 summarize the fuel loading criteria for the RAJ-II package.

NEDO-33869 Revision 11  
Non-Proprietary Information

**Table 6-1 RAJ-II Fuel Assembly Loading Criteria**

Parameter	Units	Type	Type	Type	Type
Fuel Assembly Type	Rods	8x8	9x9	FANP 10x10	GNF 10x10
UO <sub>2</sub> Density (% Theoretical)		≤ 98%	≤ 98%	≤ 98%	≤ 98%
Number of Water Rods	#	0, 2x2	0, 2-2x2 off-center diagonal, 3x3	0, 2-2x2 off-center diagonal, 3x3	0, 2-2x2 off-center diagonal, 3x3, 1-axially varying centered
Number of Fuel Rods	#	60 - 64	72 - 81	91 - 100	91 - 100
Fuel Rod OD	cm	≥ 1.176	≥ 1.093	≥ 1.000	≥ 1.010
Fuel Pellet OD	cm	≤ 1.05	≤ 0.96	≤ 0.895	≤ 0.895
Cladding Type		Zirconium Alloy	Zirconium Alloy	Zirconium Alloy	Zirconium Alloy
Cladding ID	cm	≤ 1.10	≤ 1.02	≤ 0.933	≤ 0.934
Cladding Thickness	cm	≥ 0.038	≥ 0.036	≥ 0.033	≥ 0.038
Active Fuel Length	cm	≤ 381	≤ 381	≤ 385	≤ 385
Fuel Rod Pitch	cm	≤ 1.692	≤ 1.51	≤ 1.350	≤ 1.363
U-235 Pellet Enrichment	wt%	≤ 5.0	≤ 5.0	≤ 5.0	≤ 8.0
Lattice Average Enrichment	wt%	≤ 5.0	≤ 5.0	≤ 5.0	≤ 8.0
Channel Thickness <sup>a</sup>	cm	0.17 – 0.3048	0.17 – 0.3048	0.17 – 0.3048	Any
Part Length Fuel Rods	#	None	≤ 12	≤ 14	≤ 16
Minimum Gadolinia Requirements Lattice Average Enrichment (CSI=1.0) <sup>b</sup>	# @ wt% Gd <sub>2</sub> O <sub>3</sub>				
≤ 5.0 wt% U-235		7 @ 2 wt%	10 @ 2 wt%	12 @ 2 wt%	12 @ 2 wt%
≤ 4.9 wt% U-235		7 @ 2 wt%	10 @ 2 wt%	12 @ 2 wt%	11 @ 2 wt%
≤ 4.7 wt% U-235		6 @ 2 wt%	8 @ 2 wt%	12 @ 2 wt%	11 @ 2 wt%
≤ 4.6 wt% U-235		6 @ 2 wt%	8 @ 2 wt%	10 @ 2 wt%	10 @ 2 wt%
≤ 4.5 wt% U-235		6 @ 2 wt%	8 @ 2 wt%	10 @ 2 wt%	9 @ 2 wt%
≤ 4.3 wt% U-235		6 @ 2 wt%	8 @ 2 wt%	9 @ 2 wt%	9 @ 2 wt%
≤ 4.2 wt% U-235		6 @ 2 wt%	6 @ 2 wt%	8 @ 2 wt%	8 @ 2 wt%
≤ 4.1 wt% U-235		4 @ 2 wt%	6 @ 2 wt%	8 @ 2 wt%	8 @ 2 wt%
≤ 3.9 wt% U-235		4 @ 2 wt%	6 @ 2 wt%	6 @ 2 wt%	7 @ 2 wt%
≤ 3.8 wt% U-235		4 @ 2 wt%	4 @ 2 wt%	6 @ 2 wt%	7 @ 2 wt%
≤ 3.7 wt% U-235		2 @ 2 wt%	4 @ 2 wt%	6 @ 2 wt%	6 @ 2 wt%
≤ 3.6 wt% U-235		2 @ 2 wt%	4 @ 2 wt%	4 @ 2 wt%	5 @ 2 wt%
≤ 3.4 wt% U-235		2 @ 2 wt%	2 @ 2 wt%	4 @ 2 wt%	4 @ 2 wt%
≤ 3.3 wt% U-235		2 @ 2 wt%	2 @ 2 wt%	2 @ 2 wt%	3 @ 2 wt%
≤ 3.2 wt% U-235		2 @ 2 wt%	2 @ 2 wt%	2 @ 2 wt%	2 @ 2 wt%
≤ 3.1 wt% U-235		None	2 @ 2 wt%	2 @ 2 wt%	1 @ 2 wt%
≤ 2.9 wt% U-235		None	None	None	None

NEDO-33869 Revision 11  
Non-Proprietary Information

Parameter	Units	Type	Type	Type	Type
Fuel Assembly Type	Rods	8x8	9x9	FANP 10x10	GNF 10x10
Minimum Gadolinia Requirements Lattice Average Enrichment (CSI=1.6) <sup>b</sup>	# @ wt% Gd <sub>2</sub> O <sub>3</sub>				
≤ 8.0 wt% U-235		N/A	N/A	N/A	22 @ 2 wt%
≤ 7.9 wt% U-235		N/A	N/A	N/A	21 @ 2 wt%
≤ 7.6 wt% U-235		N/A	N/A	N/A	20 @ 2 wt%
≤ 7.3 wt% U-235		N/A	N/A	N/A	19 @ 2 wt%
≤ 7.0 wt% U-235		N/A	N/A	N/A	18 @ 2 wt%
≤ 6.7 wt% U-235		N/A	N/A	N/A	17 @ 2 wt%
≤ 6.5 wt% U-235		N/A	N/A	N/A	16 @ 2 wt%
≤ 6.3 wt% U-235		N/A	N/A	N/A	15 @ 2 wt%
≤ 6.0 wt% U-235		N/A	N/A	N/A	14 @ 2 wt%
≤ 5.8 wt% U-235		N/A	N/A	N/A	13 @ 2 wt%
≤ 5.5 wt% U-235		N/A	N/A	N/A	12 @ 2 wt%
≤ 5.0 wt% U-235 to ≤ 3.3 wt% U-235 ≤ 3.2 wt% U-235 ≤ 3.1 wt% U-235 ≤ 2.9 wt% U-235		Same as CSI=1.0 Requirements			Same as CSI=1.0 Requirements None None None
Polyethylene Equivalent Mass per Assembly <sup>c</sup>	kg	≤ 11	≤ 11	≤ 10.2	≤ 10.2

- a. Transport with or without channels is acceptable
- b. Required gadolinia rods must be distributed symmetrically about the major diagonal. Minimum required number of gadolinia rods applies for full-length rod locations, excluding the lattice peripheral locations. Additional gadolinia rods in other locations are allowed as long as the minimum is met. After seven (7) gadolinia rods there must be at least one gadolinia rod in at least two out of the four quadrants of the fuel rod array.
- c. Polyethylene equivalent mass (refer to Section 6.3.2.2)

Cylindrical Boiling Water Reactor (BWR) fuel rods containing UO<sub>2</sub>, enriched to 5.0 wt% or 8.0 wt% U-235, are analyzed within the RAJ-II inner container in a 5-inch stainless steel pipe, freely loose, in a protective case, or strapped together. Cylindrical Pressurized Water Reactor (PWR) fuel rods containing UO<sub>2</sub> or Canada Deuterium-Uranium (CANDU) fuel rods containing UC, enriched to 5.0 wt% U-235, are analyzed within the RAJ-II inner container in a 5-inch stainless steel pipe. The fuel rod loading criteria, determined from the criticality evaluation for the RAJ-II package, are shown in Table 6-2. Section 6.7.1 provides a discussion regarding the unlimited amount of polyethylene packing materials for the BWR UO<sub>2</sub> contents. Section 6.7.3 describes the basis for the polyethylene mass limits for the UC and generic PWR contents.

NEDO-33869 Revision 11  
Non-Proprietary Information

**Table 6-2 RAJ-II Fuel Rod Loading Criteria**

Parameter	Type					
Fuel Assembly Type	8x8 (UO <sub>2</sub> )	9x9 (UO <sub>2</sub> )	10x10 (UO <sub>2</sub> )	CANDU-14 (UC)	CANDU-25 (UC)	Generic PWR (UO <sub>2</sub> )
Fuel Density (% Theoretical)	≤ 98%	≤ 98%	≤ 98%	≤ 97%	≤ 97%	≤ 100%
Fuel Rod OD (cm)	≥ 1.10	≥ 1.02	≥ 1.00	≥ 1.340	≥ 0.996	≥ 1.118
Fuel Pellet OD (cm)	≤ 1.05	≤ 0.96	≤ 0.90	≤ 1.254	≤ 0.950	≤ 0.98
Cladding Type	Zirc. Alloy			Zirc. Alloy or SS		
Cladding ID (cm)	≤ 1.10	≤ 1.02	≤ 1.00	≤ 1.267	≤ 0.951	≤ 1.004
Cladding Thickness (cm)	≥ 0.00			≥ 0.00		
Active Fuel Length (cm)	≤ 381	≤ 381	≤ 385	≤ 47.752	≤ 40.013	≤ 450
U-235 Pellet Enrichment (wt%)	≤ 5.0		≤ 8.0	≤ 5.0		
Average Fuel Rod Enrichment (wt%)	≤ 5.0		≤ 8.0	≤ 5.0		
Polyethylene Equivalent Mass <sup>a</sup> per Compartment <sup>b</sup> (kg)	Protective Sleeves: Unlimited			Protective Sleeves: ≤ 2.3		
	Within SS Pipe: Unlimited		Within SS Pipe: Unlimited / ≤ 32.1	Within SS Pipe: Unlimited	Within SS Pipe: ≤ 27.5	
	All Other Packing Materials: Unlimited			All Other Packing Materials: Unlimited		
Reference Density for Polyethylene Equivalent Mass <sup>a</sup> Calculation <sup>b</sup> (g/cm <sup>3</sup> )	Protective Sleeves: 0.925 All Other Packing Materials: 0.08			Protective Sleeves: 1.005 All Other Packing Materials: 0.70		
Loose Rod Configuration	Maximum Number of Rods per Compartment based on the Maximum Active Fuel Length					
Freely Loose	≤ 25	≤ 25	≤ 25	N/A	N/A	N/A
Packed in 5-inch SS Pipe or Protective Case <sup>c</sup>	≤ 22	≤ 26	≤ 30	≤ 695 <sup>d,e</sup>	≤ 1458 <sup>d,e</sup>	≤ 105 <sup>d</sup>
Strapped Together	≤ 25	≤ 25	≤ 25	N/A	N/A	N/A

a. Polyethylene equivalent mass for packing materials (refer to Section 6.3.2.2).

b. Polyethylene packing materials examples: protective sleeves, end caps, and cushioning foam.

c. Protective case consists of stainless steel (SS) box with lid.

d. Only in 5-inch stainless steel pipes. Including partial rods: in reality, applying dense packing of congruent rods in the pipe will result in maximum number rods that can physically fit within the pipe to be less than the number provided in the table above.

e. Allows for dense loading of the relatively short UC rods axially along the length of the component.

f. General Note: Total mass of payload contents not to exceed 684 kg, as well as maximum U payload of 484 kg U.

## **6.1.1 Design Features**

### **6.1.1.1 Packaging**

A general discussion of the RAJ-II package design is provided in Section 1.2. A detailed set of licensing drawings for the RAJ-II package is provided in Section 1.3.1. Components important to criticality safety are described below.

The RAJ-II is comprised of two primary components: 1) an inner stainless steel container, and 2) an outer stainless steel container.

The inner stainless steel container is 468.6 cm (184.49 in) in length, 45.9 cm (18.07 in) in width, and 28.6 cm (11.26 in) in height. The fuel rods are located inside one of two compartments within the inner container. The compartments are fabricated from 18-gauge (0.1 cm thick) stainless steel, 456.7 cm (179.8 in) in length and 17.6 cm (6.93 in) in width and height. Each compartment is lined with polyethylene foam with a nominal thickness of 1.8 cm (0.71 in) and separated from each other by the compartment walls; the nominal polyethylene foam thickness is 2.3 cm (0.91 in) on the lid. A 5 cm (1.97 in) thick alumina silicate fiber surrounds the compartments to provide thermal insulation, and a 16-gauge (0.15 cm thick) stainless steel sheet surrounds the insulator. The inner container lid consists of an alumina silicate layer encased in a 16-gauge (0.15 cm thick) stainless steel sheet. The lid width and length are consistent with the inner container and the overall height is 5.25 cm (2.07 in).

The outer container is 506.8 cm (199.53 in) in length, 72.0 cm (28.35 in) in width, and 64.2 cm (25.28 in) in height (with the skids attached the height is 74.2 cm (29.21 in)). The inner container is held rigidly within the outer stainless steel container by four evenly spaced stainless steel hold-down sections. Shock absorbers, fabricated from a phenol impregnated cardboard material, are placed at six locations above and below the inner container, and ten locations on either side of the inner container. The wall for the outer container is fabricated from 14-gauge (0.2 cm thick) stainless steel.

### **6.1.2 Summary Table of Criticality Evaluation**

Table 6-3 lists the bounding cases evaluated for a given set of conditions. The cases include NCT and HAC for fuel assembly transport single package, fuel assembly transport package array, fuel rod transport single package, and fuel rod transport package array. The Upper Subcritical Limit (USL) provided in Table 6-3 is described in Section 6.10.

**Table 6-3 Criticality Evaluation Summary**

Case	Bounding Fuel Type	$k_{eff}$	$\sigma$	$k_{eff} + 2\sigma$	USL
Fuel Assembly Single Package NCT	GNF 10x10 LEU with worst case fuel parameters, 12, 2.0 wt% Gd <sub>2</sub> O <sub>3</sub> fuel rods, and 16 part length fuel rods	0.7045	0.0002	0.7051	0.9340
Fuel Assembly Single Package HAC	GNF 10x10 LEU with worst case fuel parameters, 12, 2.0 wt% Gd <sub>2</sub> O <sub>3</sub> fuel rods, and 16 part length fuel rods	0.7090	0.0003	0.7095	0.9340
Fuel Assembly Package Array NCT	GNF 10x10 LEU with worst case fuel parameters, 12, 2.0 wt% Gd <sub>2</sub> O <sub>3</sub> fuel rods, and 16 part length fuel rods	0.8116	0.0003	0.8122	0.9340
Fuel Assembly Package Array HAC	GNF 10x10 LEU with worst case fuel parameters, 12, 2.0 wt% Gd <sub>2</sub> O <sub>3</sub> fuel rods, and 16 part length fuel rods	0.9295	0.0003	0.9300	0.9340
Fuel Rod Single Package HAC	CANDU - 14 fuel rods with worst case fuel parameters	0.6549	0.0008	0.6565	0.9213
Fuel Rod Package Array NCT	CANDU - 25 fuel rods with worst case fuel parameters	0.9023	0.0007	0.9037	0.9213
Fuel Rod Package Array HAC	CANDU - 25 fuel rods with worst case fuel parameters	0.9116	0.0007	0.9131	0.9213
Fuel Assembly Single Package NCT	GNF 10x10 LEU+ with worst case fuel parameters, 22, 2.0 wt% Gd <sub>2</sub> O <sub>3</sub> fuel rods, and 16 part length fuel rods	0.7223	0.0003	0.7229	0.9340
Fuel Assembly Single Package HAC	GNF 10x10 LEU+ with worst case fuel parameters, 22, 2.0 wt% Gd <sub>2</sub> O <sub>3</sub> fuel rods, and 16 part length fuel rods	0.7207	0.0003	0.7214	0.9340
Fuel Assembly Package Array NCT	GNF 10x10 LEU+ with worst case fuel parameters, 22, 2.0 wt% Gd <sub>2</sub> O <sub>3</sub> fuel rods, and 16 part length fuel rods	0.8728	0.0003	0.8733	0.9340
Fuel Assembly Package Array HAC	GNF 10x10 LEU+ with worst case fuel parameters, 22, 2.0 wt% Gd <sub>2</sub> O <sub>3</sub> fuel rods, and 16 part length fuel rods	0.9235	0.0003	0.9241	0.9340
Fuel Rod Single Package NCT	GNF 10x10 LEU+ - 25 fuel rods with worst case fuel parameters	0.6860	0.0003	0.6865	0.9340
Fuel Rod Single Package HAC	GNF 10x10 LEU+ - 25 fuel rods with worst case fuel parameters	0.6795	0.0003	0.6800	0.9340
Fuel Rod Package Array NCT	GNF 10x10 LEU+ - 25 fuel rods with worst case fuel parameters	0.6859	0.0003	0.6865	0.9340
Fuel Rod Package Array HAC	GNF 10x10 LEU+ - 25 fuel rods with worst case fuel parameters	0.9100	0.0002	0.9105	0.9340

The LEU fuel rod single package HAC result is expected to bound the LEU fuel rod single package NCT result; therefore, the result for fuel rod single package NCT is not provided.

A comparison between the nominal fuel parameters and the worst case fuel parameters used in the criticality evaluation is shown in Table 6-4.

**Table 6-4      Nominal vs. Worst Case Fuel Parameters for the RAJ-II Criticality Analysis**

<b>Case</b>	<b>Fuel Rod Pitch (cm)</b>	<b>Clad Outer Diameter (cm)</b>	<b>Clad Inner Diameter (cm)</b>	<b>Pellet Outer Diameter (cm)</b>	<b>Pellet Theoretical Density</b>
<b>FANP 10x10</b>					
Nominal	1.284, 1.2954	1.010, 1.033	0.9020, 0.9217	0.8682, 0.8882	< 98%
Worst Case Modeled for Fuel Assembly Transport	1.350	1.000	0.9330	0.895	98%
Worst Case Modeled for Fuel Rod Transport	1.350	1.000	1.000	0.900	98%
<b>GNF 10x10</b>					
Nominal	[[ ]]	1.019, [[ ]]	0.9322, [[ ]]	0.8941, [[ ]]	< 98%
Worst Case Modeled for Fuel Assembly Transport	1.363	1.010	0.9338	0.895	98%
Worst Case Modeled for Fuel Rod Transport	1.350	1.000	1.000	0.900	98%
<b>FANP 9x9</b>					
Nominal	1.4478	1.095, 1.0998	0.968, 0.9601	0.94, 0.9398	< 98%
Worst Case Modeled for Fuel Assembly Transport	1.510	1.093	1.020	0.960	98%
Worst Case Modeled for Fuel Rod Transport	1.510	1.020	1.020	0.960	98%
<b>GNF 9x9</b>					
Nominal	1.438	1.110	0.983	0.955	< 98%
Worst Case Modeled for Fuel Assembly Transport	1.510	1.093	1.020	0.960	98%
Worst Case Modeled for Fuel Rod Transport	1.510	1.020	1.020	0.960	98%
<b>GNF 8x8</b>					
Nominal	1.6256	1.2192	1.072	1.044	< 98%
Worst Case Modeled for Fuel Assembly Transport	1.6923	1.176	1.100	1.050	98%
Worst Case Modeled for Fuel Rod Transport	1.6923	1.100	1.100	1.050	98%

### 6.1.3 Criticality Safety Index

For the RAJ-II, undamaged packages have been analyzed in 21x3x24 arrays and damaged packages have been analyzed in 10x1x10 arrays for LEU fuel and 8x1x8 arrays for LEU+ fuel. Pursuant to 10 CFR 71.59, the number of packages “N” in a 2N array that are subjected to the tests specified in 10 CFR 71.73, or in a 5N array for undamaged packages is used to determine the Criticality Safety Index (CSI). The CSI is determined by dividing the number 50 by the most limiting value of “N” as specified in 10 CFR 71.59.

For the RAJ-II package containing fuel assemblies enriched up to 5.0 wt%, the criticality analysis demonstrates safety for 5N=1,512 (undamaged, NCT) and 2N=100 (damaged, HAC) packages. The corresponding CSI for criticality control is given by  $CSI = 50/N$ . Because 5N=1,512 and 2N=100, it follows that the more restrictive N = 50 and  $CSI = 50/50 = 1.0$  for fuel assemblies enriched up to 5.0 wt%.

For the RAJ-II package containing fuel assemblies enriched up to 8.0 wt%, the criticality analysis demonstrates safety for 5N=1,512 (undamaged, NCT) and 2N=64 (damaged, HAC) packages. The corresponding CSI for criticality control is given by  $CSI = 50/N$ . Because 5N=1,512 and 2N=64, it follows that the more restrictive N = 32 and  $CSI = 50/32 = 1.56$ , or 1.6 rounded up for fuel assemblies enriched up to 8.0 wt%.

For the RAJ-II package containing fuel rods enriched up to 8.0 wt% under HAC, the contents of 2N=64 (8x1x8 array), RAJ-II damaged packages are demonstrated to remain subcritical. For criticality control purposes  $CSI = 50/32 = 1.56$ , or 1.6 rounded up (Reference 6-1).



## 6.2 FISSILE MATERIAL CONTENTS

The RAJ-II is used to transport  $\text{UO}_2$  conforming to the requirements stated in Section 6.1, Tables 6-1, 6-2 and 6-3. The uranium isotopic distribution considered in the models used for the criticality safety demonstration is shown in Table 6-5.

**Table 6-5      Uranium Isotopic Distribution**

<b>Isotope</b>	<b>Modeled wt%, LEU fuel</b>	<b>Modeled wt%, LEU+ fuel</b>
U-235	5.0	8.0
U-238	95.0	92.0

The criticality analysis conservatively demonstrates safety for  $\text{UO}_2$  pellets within cylindrical zirconium alloy tubes, arranged in 8x8, 9x9, or 10x10 square assembly lattices. Cylindrical fuel rods containing  $\text{UO}_2$  are also conservatively demonstrated to be safe within the RAJ-II package in a 5-inch stainless steel pipe, freely loose, in a protective case, or strapped together. The fuel loadings that are demonstrated to be safe in the RAJ-II are specified in Tables 6-1, 6-2 and 6-3.

## 6.3 GENERAL CONSIDERATIONS

Models generated for single package and package arrays under NCT and HAC are described in the following sections.

### 6.3.1 Model Configuration

#### 6.3.1.1 RAJ-II Package Single Package Model

The single package models are enveloped with a 30.48 cm layer of full density water for reflection.

##### 6.3.1.1.1 Single Package NCT Model

The RAJ-II outer container dimensions are shown in Figure 6-1. The inner container dimensions are shown in Figure 6-2, and the cross-sectional dimensions of both the inner container and the outer container are shown in Figure 6-3. Calculations performed with the package array HAC model determine all other modeling parameters for the single package NCT model, such as modeling the polyethylene foam at a thickness of 1.28 cm or 1.14 cm for LEU+ fuel (see Section 6.3.4.11).

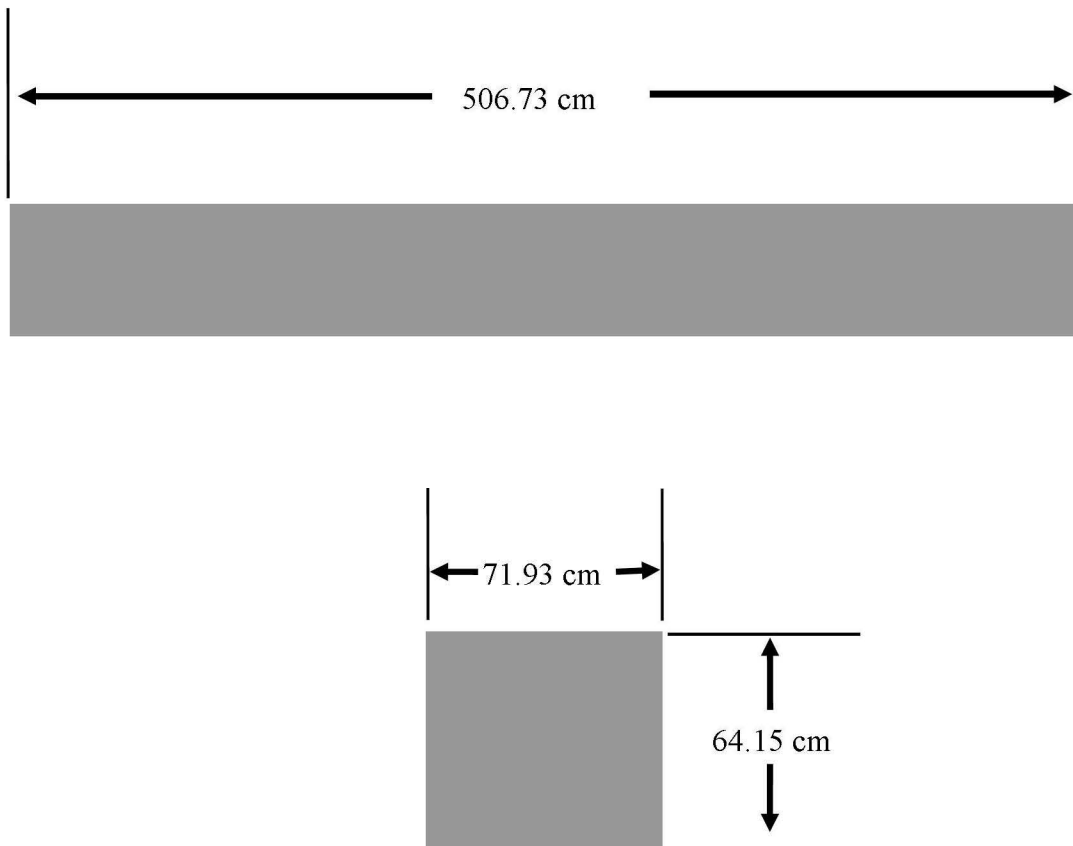
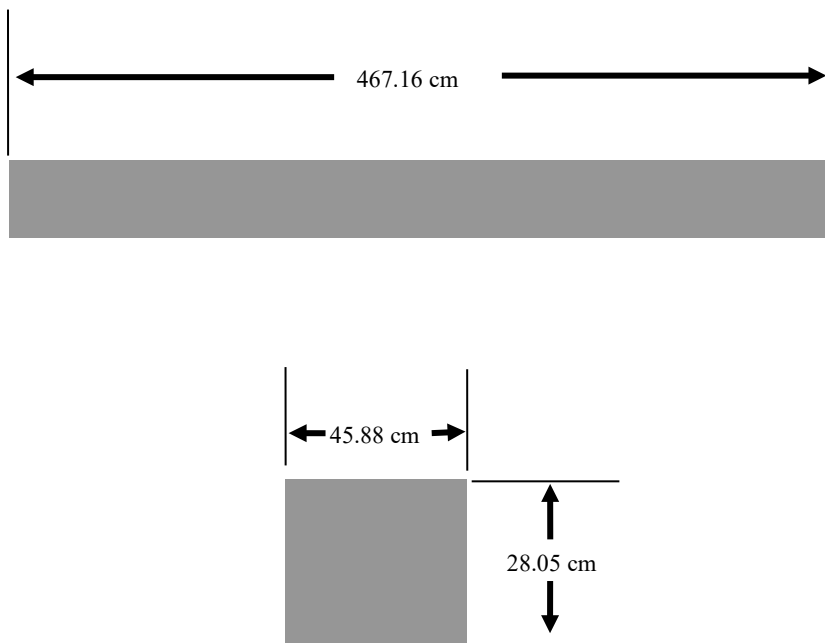
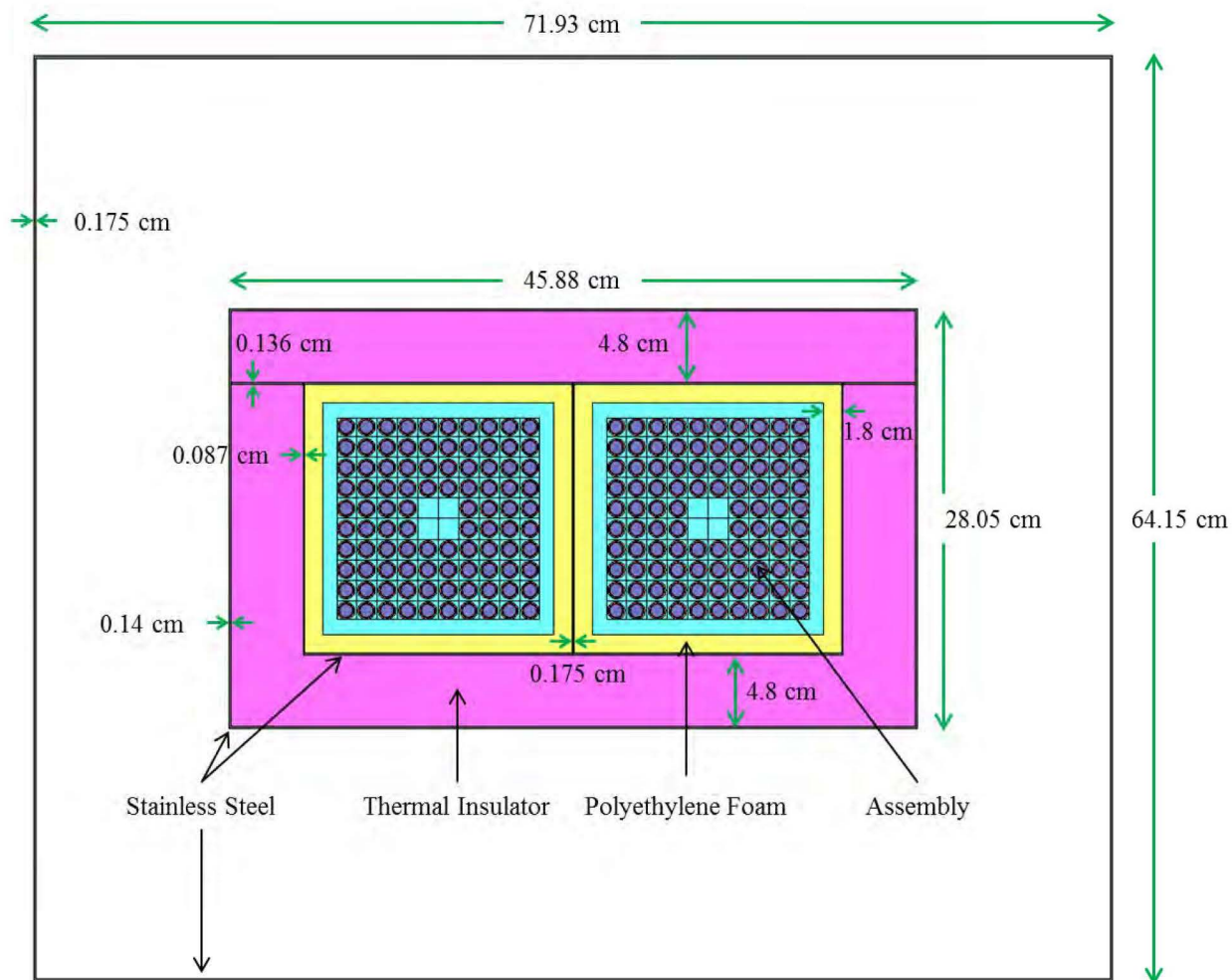


Figure 6-1 RAJ-II Outer Container NCT Model



**Figure 6-2 RAJ-II Inner Container NCT Model**



**Figure 6-3 RAJ-II Container Cross-Section NCT Model**

#### 6.3.1.1.2 Single Package HAC Model

The RAJ-II HAC model inner container dimensions are shown in Figure 6-7 and Figure 6-8. It is lined with polyethylene foam having a density of up to  $0.08 \text{ g/cm}^3$ . A sensitivity study was performed changing the density of the polyethylene foam. The change in system reactivity due to the change in polyethylene foam density is statistically insignificant. The polyethylene foam is assumed to burn away for the HAC single package model (as this is the most reactive configuration).

The inner container has alumina silicate thermal insulation between the inner and outer walls. The alumina silicate insulation is assumed to remain in place because scoping calculations proved it to provide a more reactive configuration (Table 6-19). The alumina silicate density is approximately  $0.25 \text{ g/cm}^3$ . No credit is taken for any of the structural steel between the inner and outer containers. The honeycomb shock absorbers, located between the inner and outer containers, are not explicitly modeled. Instead, water is placed in the space between the inner and outer containers, and its density is varied from  $0.0 - 1.0 \text{ g/cm}^3$ . The honeycomb shock absorbers have a density between  $0.04$  and  $0.08 \text{ g/cm}^3$ . The hydrogen number densities for water ( $1.0 \text{ g/cm}^3$ ) and for the honeycomb shock absorber ( $0.08 \text{ g/cm}^3$ ) are  $6.687 \times 10^{-2}$  and  $2.973 \times 10^{-3}$  atoms/b-cm, respectively. Considering optimal water density between the inner and outer containers accounts for the reflecting and thermalizing effects of the honeycomb shock absorbers.

The container deformation modeled for the RAJ-II HAC model includes the damage incurred from the 9-meter drop onto an unyielding surface as well as conservative factors. The RAJ-II inner container length is conservatively reduced by 8.1 cm (compared to NCT) to bound the damage incurred from the 9-meter drop onto an unyielding surface. The fuel assemblies rest against the polyethylene foam in a fixed position. The fuel assemblies are assumed to freely move within the respective compartment resulting in a worst case orientation. The rubber vibro-isolating devices are also assumed to melt when exposed to an external fire, allowing the inner container to shift downward about 2.54 cm. However, scoping calculations reveal no increase in reactivity by moving the inner container; therefore, the inner container is centered within the outer container as shown in Figure 6-8. The inner container horizontal position within the outer container remains the same as the NCT model because the stainless steel fixture assemblies remained intact following the 9-meter drop. Full density water that provides more moderation capability is assumed to flood the RAJ-II inner container fuel compartment.

The outer container dimensions are shown in Figure 6-6 and Figure 6-8. The outer container provides protection for the inner container and additional separation between fuel assemblies in adjacent containers. The outer container length is reduced by 4.7 cm (compared to NCT) to bound the damage sustained from a 9-meter drop onto an unyielding surface. In addition, the outer container height is reduced by 2.4 cm to bound the damage sustained during the 9-meter drop (Reference 6-2). The reduction in length for the inner and outer containers, the reduction in height for the outer container, the absence of polyethylene foam, the presence of the insulation, and the fuel assembly freedom of movement are consistent with the physical condition of the RAJ-II package after being subjected to the tests specified in 10 CFR 71.

Calculations performed with the package array HAC model determine the fuel assembly modeling for the single package HAC model. No fuel assembly structures outside the active length of the rod are represented in the models, with the exception of the fuel assembly channel. The fuel assembly structures outside the active fuel length, other than the fuel assembly channel, are composed of materials that absorb neutrons by radiative capture; therefore, neglecting them is conservative. In addition, no grids within the rod active length are represented. The internal grid structure displaces water from between the fuel rods, decreasing the Hydrogen to Fissile Material (H/X) ratio. Because the fuel assemblies are undermoderated, decreasing the H/X ratio decreases system reactivity. Therefore, it is conservative to neglect the internal grid structure in modeling the RAJ-II package. The maximum pellet enrichment and maximum fuel lattice average enrichment is 5.0 wt% U-235 or 8.0 wt% for LEU+ fuel. The gadolinium content of any gadolinia-urania fuel rods is modeled to be 75% of the minimum value specified in Table 6-1. The fuel assemblies are modeled inside the inner container, in one of seven orientations shown in Figure 6-9 through Figure 6-15. The worst case orientation is chosen for each fuel assembly design considered for transport and used in subsequent calculations.

Based on the fuel damage sustained in the RAJ-II package drop test (Reference 6-2), both reduction in fuel rod pitch and increase in fuel rod pitch was observed. Fuel damage sustained during the 9-meter (30 foot) drop test is simulated as a change in fuel rod pitch conservatively applied to the full axial length of each fuel assembly considered for transport. The change in rod pitch for the fuel designs considered for transport is discussed in Section 2.7.1.1. Both un-channeled (Figure 6-9 through Figure 6-15) and channeled fuel assemblies (Figure 6-16) are considered in the worst case orientation, subjected to the worst case fuel damage, and the most reactive configuration is chosen for subsequent calculations.

The fuel damage sustained during the 9-meter drop test is bounded by performing a fuel parameter sensitivity study and creating a worst case fuel assembly for each fuel design. The sensitivity study results determine the fuel parameter ranges for the fuel assembly loading criteria shown in Table 6-1. The ranges are broad enough to accommodate future fuel assembly design changes. The fuel rod pitch, fuel pellet OD, fuel rod clad ID and OD, fuel rod number, and part length fuel rod number are varied independently in the package array HAC calculations. Reactivity effects are investigated, and the worst case is identified for each parameter perturbation. To validate the ranges for worst case fuel parameter combinations (e.g., worst case pellet OD, clad OD, clad ID) within the same assembly, a worst case fuel assembly is created for each fuel design considered for transport in the RAJ-II package, by choosing each parameter value that provides the highest system reactivity. Calculations performed with the worst case fuel assemblies validate the parameter ranges to be used as fuel acceptance criteria.

The GNF 10x10 LEU and LEU+ designs are used for the RAJ-II single package HAC model because they are determined to be the most reactive assembly in the package array HAC fuel parameter studies. The GNF 10x10 LEU assembly contains fuel enriched to 5.0 wt% U-235, twelve 2 wt% gadolinia-urania fuel rods, and sixteen part length fuel rods, and the GNF 10x10 LEU+ assembly contains fuel enriched to 8.0 wt% U-235, twenty-two 2 wt% gadolinia-urania fuel

rods, and sixteen part length fuel rods. Additional worst case fuel parameters are presented in Table 6-4.

Packing materials such as polyethylene inserts (cluster separators) are positioned between fuel rods at various locations along the axis of the fuel assembly to avoid stressing the axial grids during transportation. Two types of inserts, shown in Figure 6-4 and Figure 6-5, are considered for use with the RAJ-II package. Because the polyethylene cluster separators provide a higher volume-averaged density polyethylene inventory, they are chosen for the RAJ-II criticality analysis. Other types of inserts are acceptable provided that their polyethylene inventory is within the limits established in Table 6-1.

In the HAC model, the polyethylene cluster separators are assumed to melt when subjected to the tests specified in 10 CFR 71. The polyethylene is assumed to uniformly coat the fuel rods in each fuel assembly forming a cylindrical layer of polyethylene around each fuel rod. Different coating thicknesses are investigated in the package array HAC calculations, and a polyethylene mass limit is developed for each fuel assembly type considered for transport. The RAJ-II single package model contains GNF 10x10 worst case fuel assemblies with 10.2 kg of polyethylene per assembly. The polyethylene is modeled as a cylindrical layer wrapped around the fuel rod cladding.

Reference 6-3 describes a sensitivity study performed for the limiting GNF 10x10 design to confirm that modeling the polyethylene uniformly distributed around each fuel rod as a wrap is more conservative than explicit modeling of the geometry of the cluster separator. The study shows that at the optimum moderation condition the  $k_{\text{eff}}$  value from the rod wrap model is larger than that from the explicit cluster separator model. Hence, the rod wrap model is a simple and conservative approach for modeling the packing components under HAC.

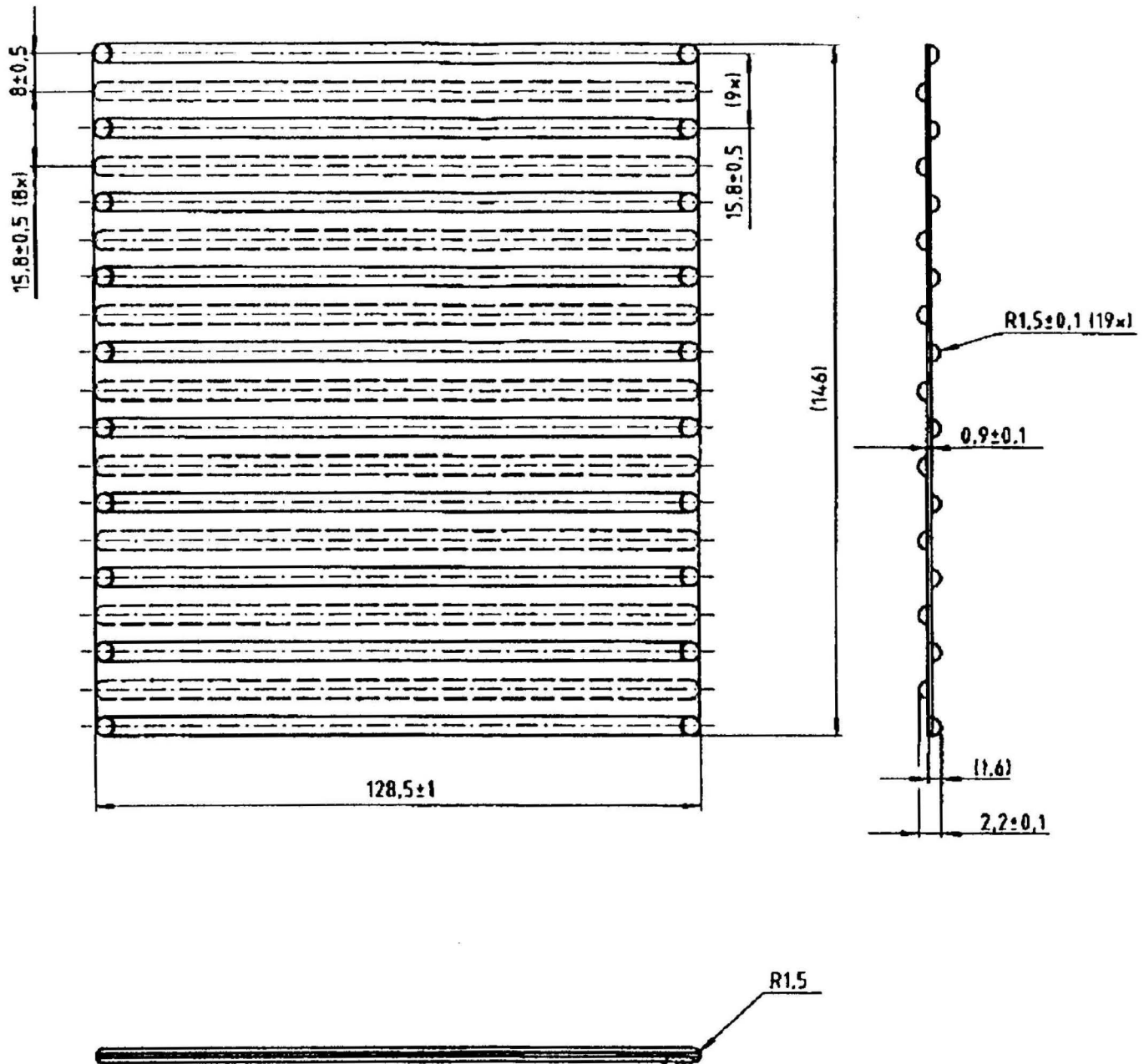
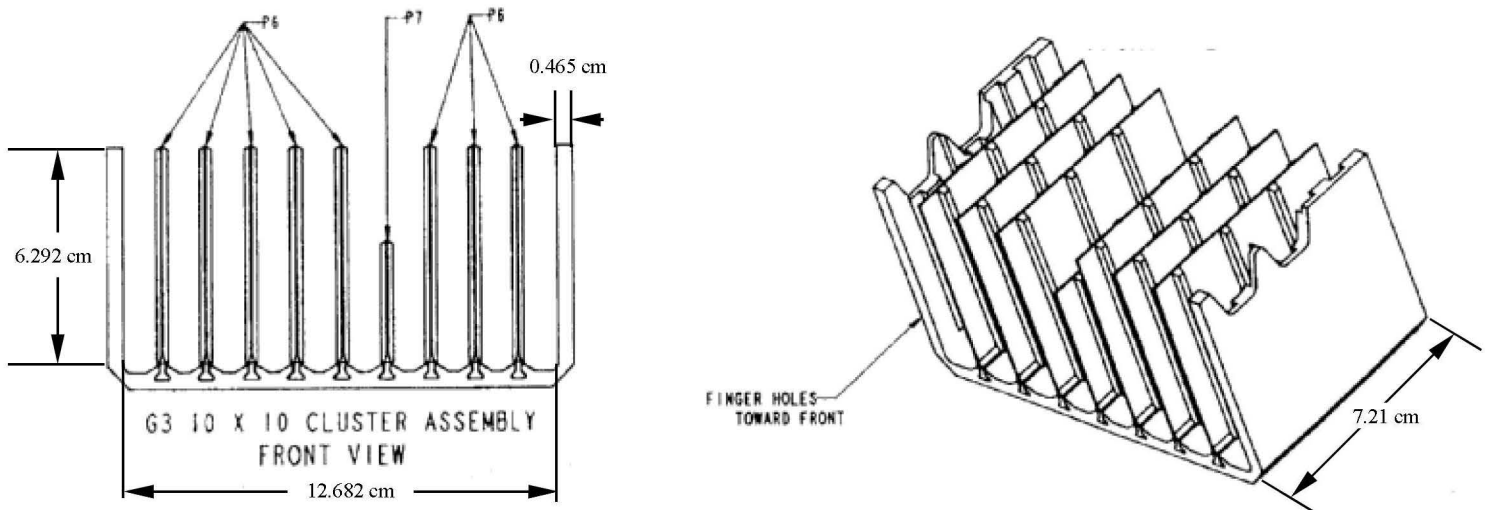


Figure 6-4 Polyethylene Insert (FANP Design)





**Figure 6-5 Polyethylene Cluster Separator Assembly (GNF Design)**

### 6.3.1.2 Package Array Models

#### 6.3.1.2.1 Package Array NCT Model

The RAJ-II package array NCT model consists of a 21x3x24 array of containers, surrounded by a 30.48 cm layer of full density water for reflection. The container array (inner and outer containers) is fully flooded with water at a density sufficient for optimum moderation. The container and fuel model in the array are those discussed in Section 6.3.1.1.1.

#### 6.3.1.2.2 Package Array HAC Model

The RAJ-II package array HAC model consists of either a 14x2x16, 10x1x10, or 8x1x8 array of containers, surrounded by a 30.48 cm layer of full density water for reflection. The 14x2x16 array (Sections 6.3.4.1 – 6.3.4.10) is initially used under the assumption that the polyethylene foam, on which the fuel assemblies rest, completely burns away during a fire. The 10x1x10 and 8x1x8 arrays (Sections 6.3.4.11 – 6.3.4.13) account for the possibility of incomplete polyethylene foam burn following a fire. A polyethylene foam thickness of 1.28 cm, or 1.14 cm for LEU+ fuel, is used for the final demonstration of criticality safety (see Section 6.3.4.11). The presence of polyethylene foam allows increased neutron leakage from the inner container fuel compartment and promotes increased neutron interaction among containers in the array. The inner container fuel compartment space not occupied by the polyethylene foam is fully flooded with water at a density sufficient for optimum moderation. The container array has no interspersed water between packages in the array and no water in the outer container. These moderator conditions optimize the interaction between packages in the array. The remaining HAC model container and fuel details are those discussed in Section 6.3.1.1.2.

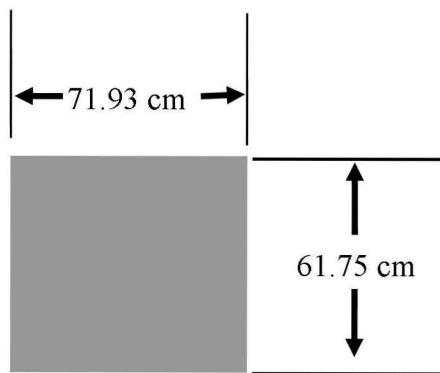
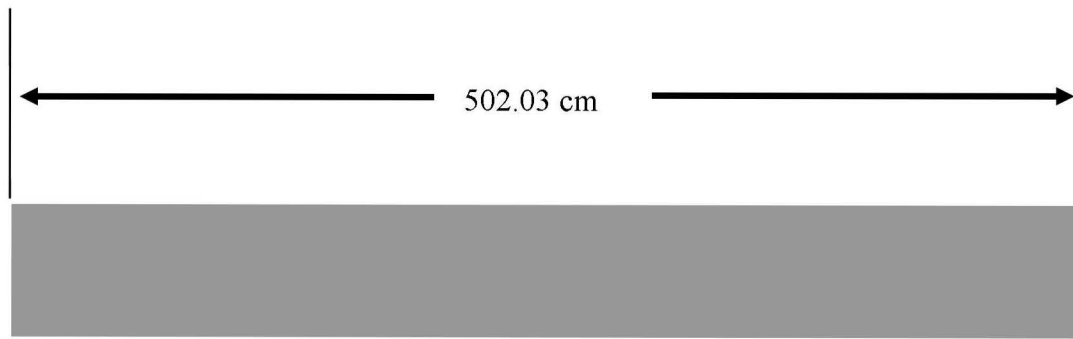


**Figure 6-6 RAJ-II Outer Container HAC Model**

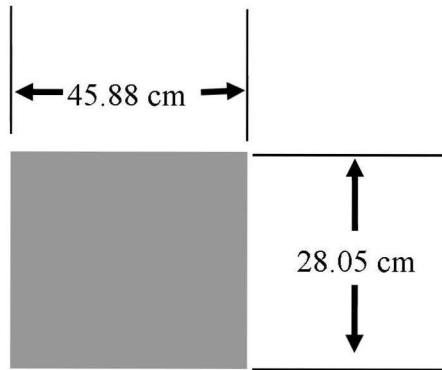
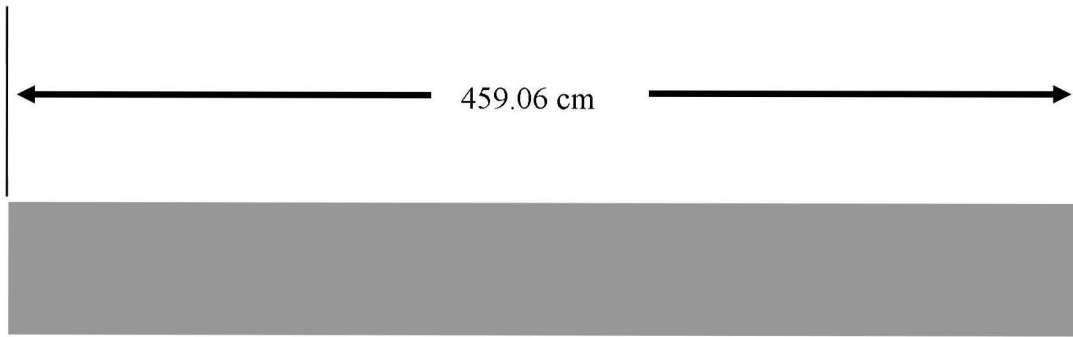


**Figure 6-7 RAJ-II Inner Container HAC Model**

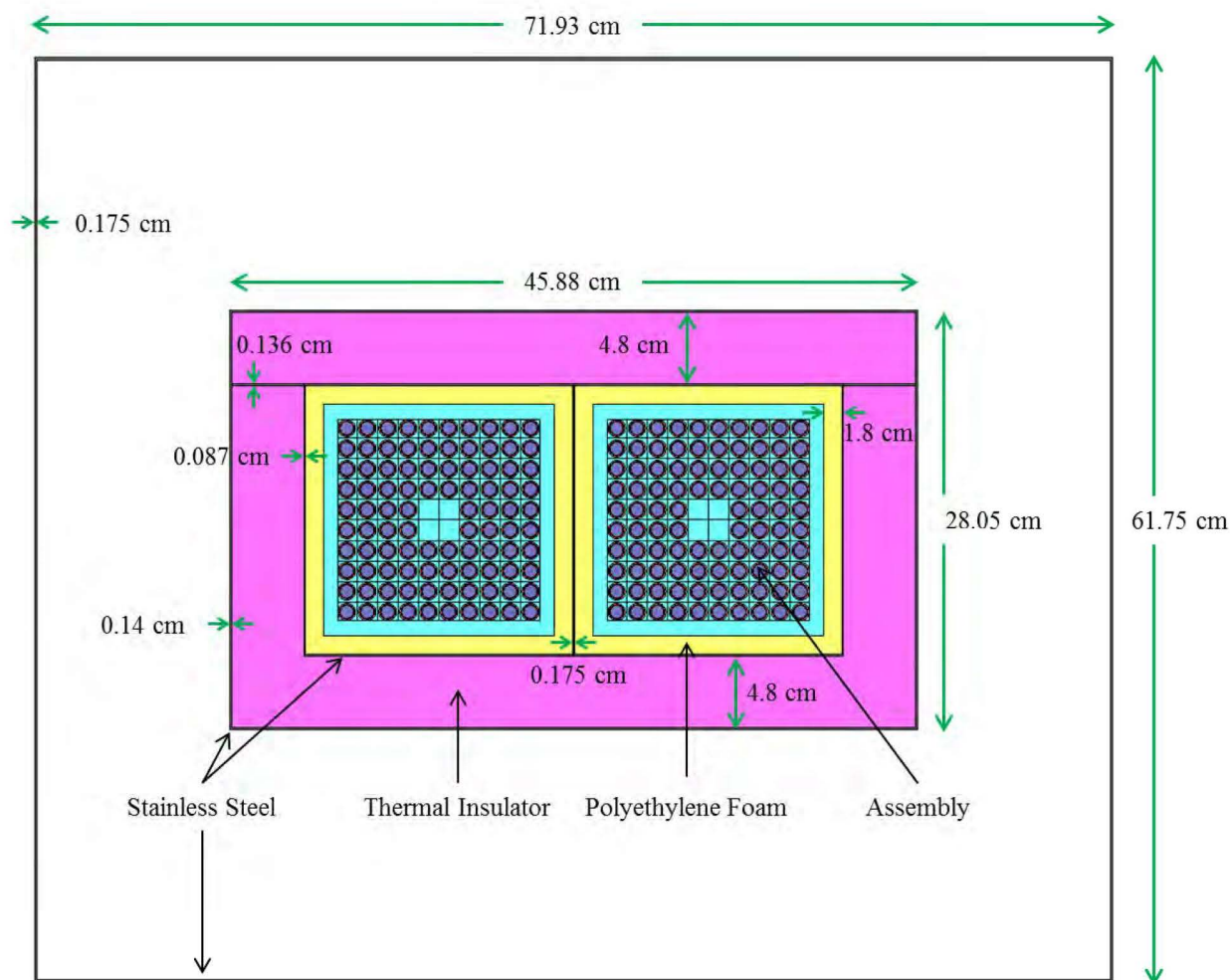


**Figure 6-8 RAJ-II Cross-Section HAC Model**

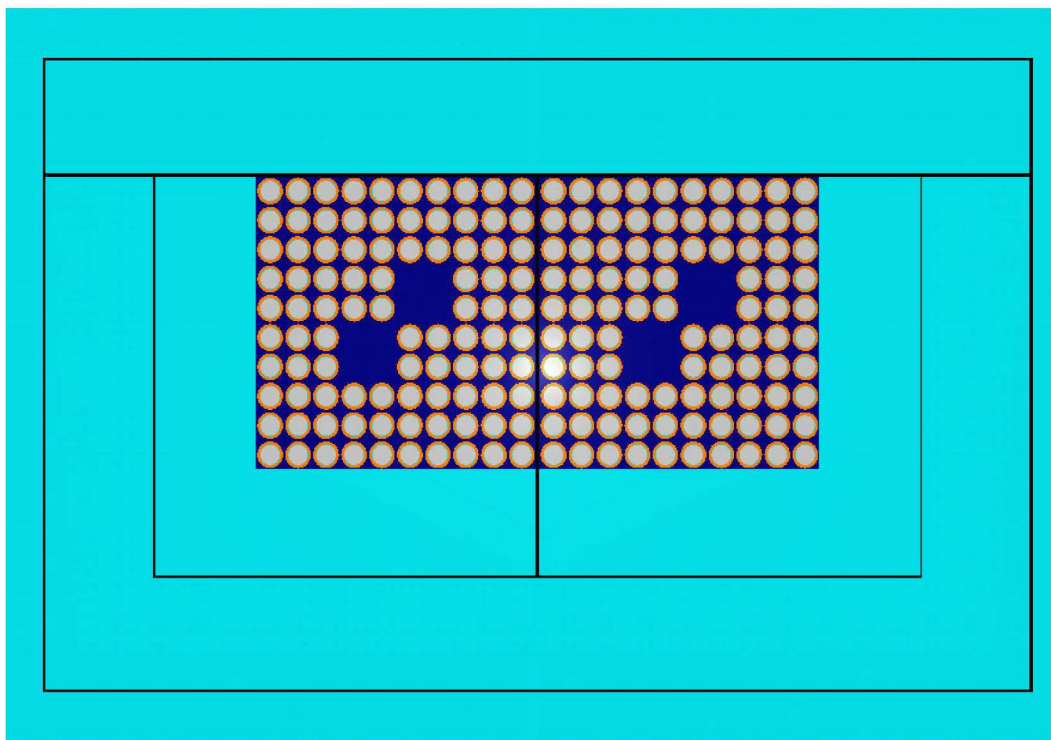


**Figure 6-9 RAJ-II HAC Model with Fuel Assembly Orientation 1**

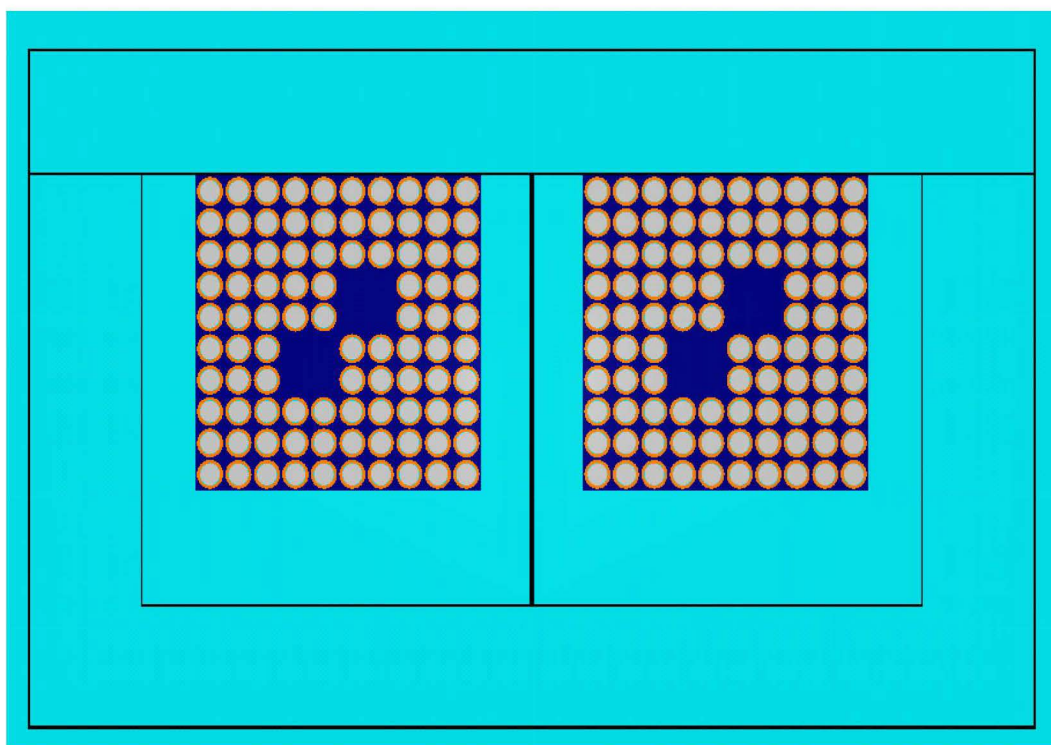


**Figure 6-10 RAJ-II HAC Model with Fuel Assembly Orientation 2**

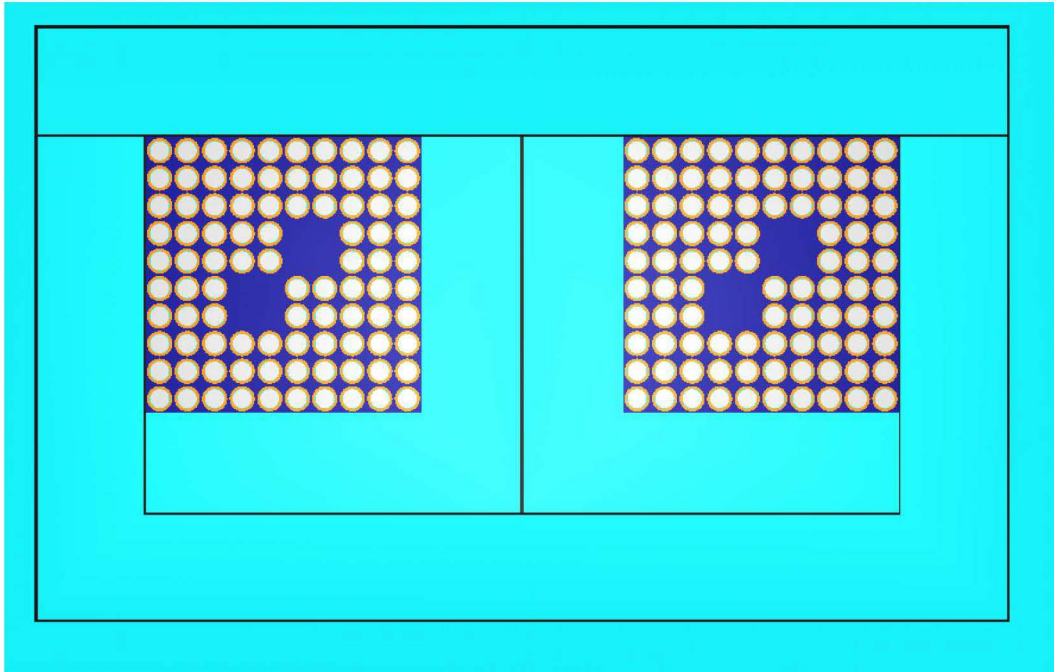


**Figure 6-11 RAJ-II HAC Model with Fuel Assembly Orientation 3**

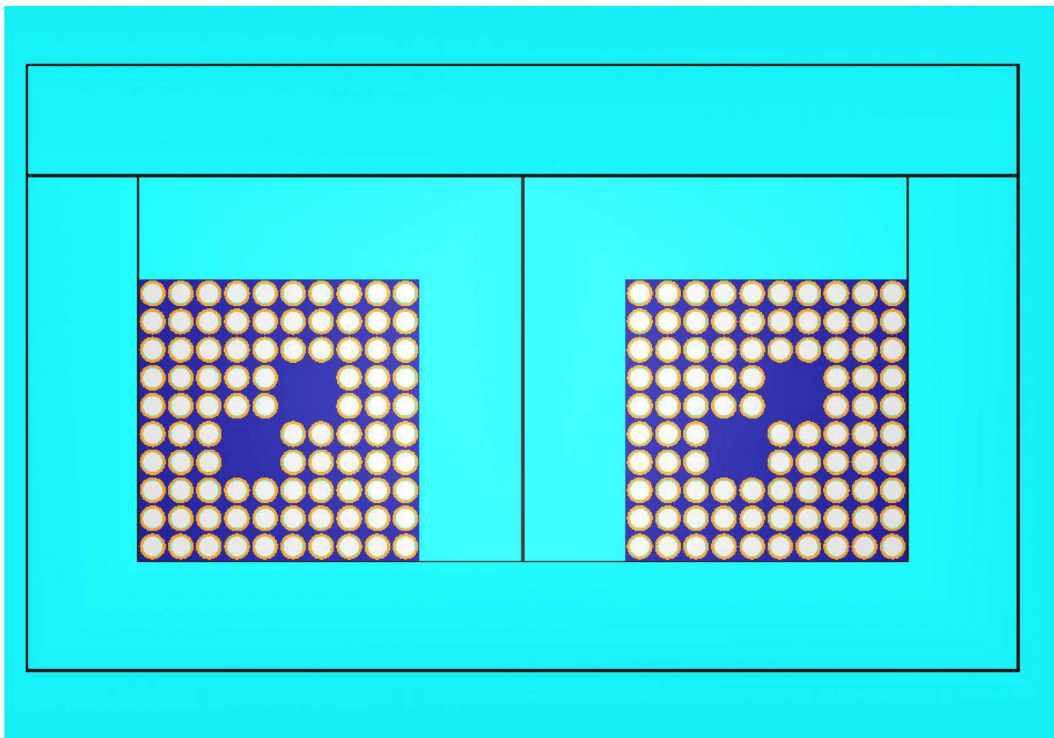


**Figure 6-12 RAJ-II HAC Model with Fuel Assembly Orientation 4**



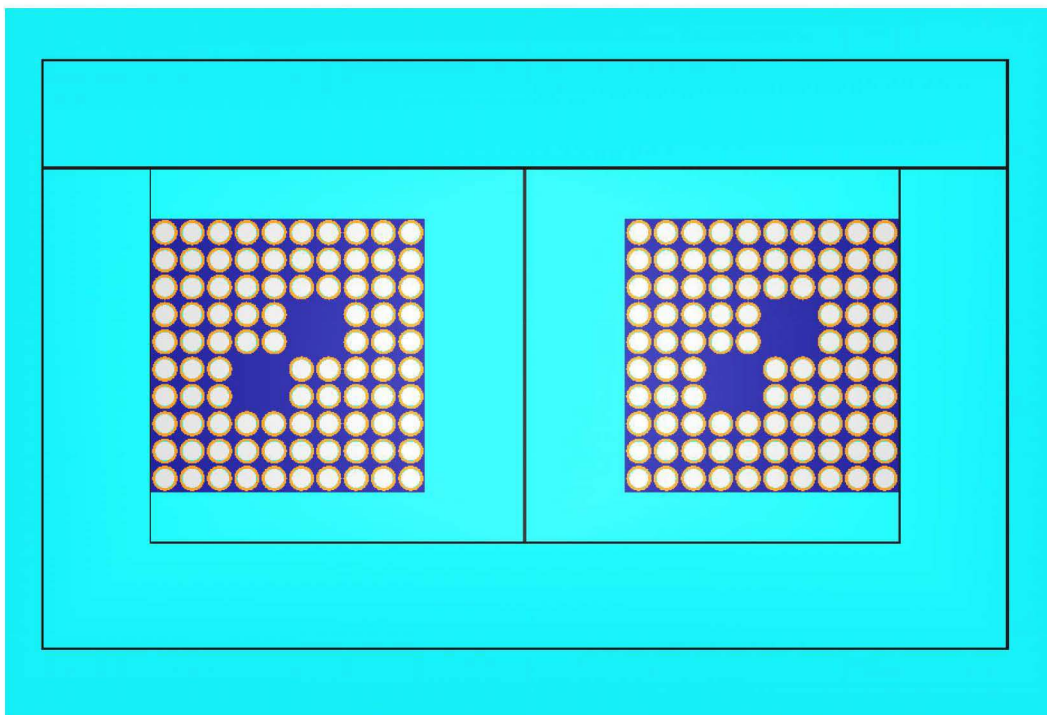


**Figure 6-13 RAJ-II HAC Model with Fuel Assembly Orientation 5**

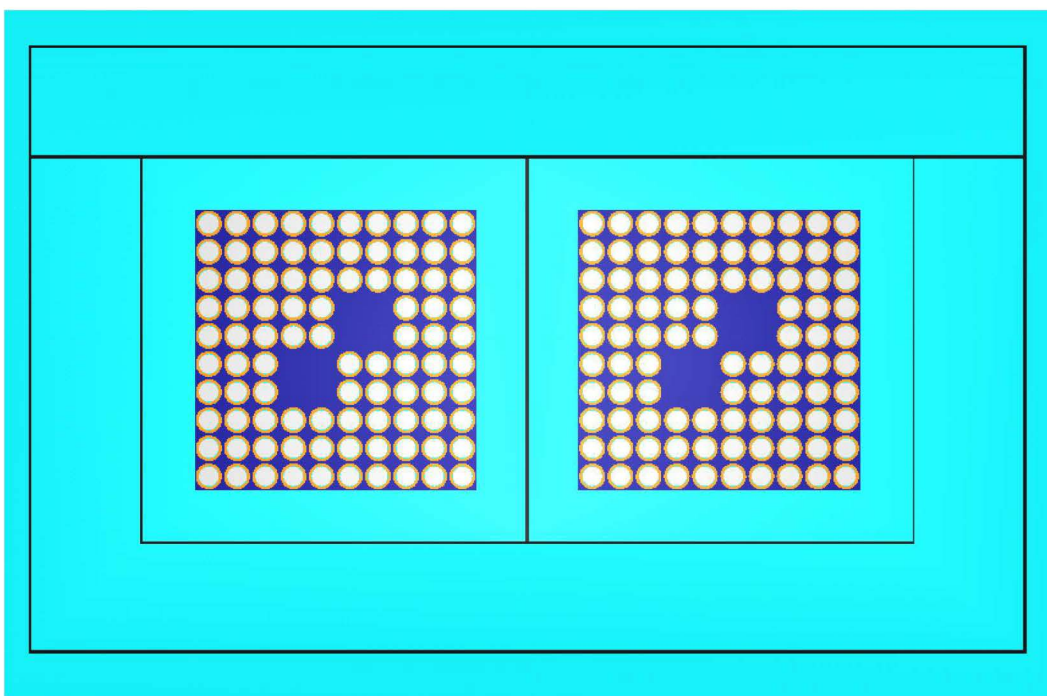


**Figure 6-14 RAJ-II HAC Model with Fuel Assembly Orientation 6**

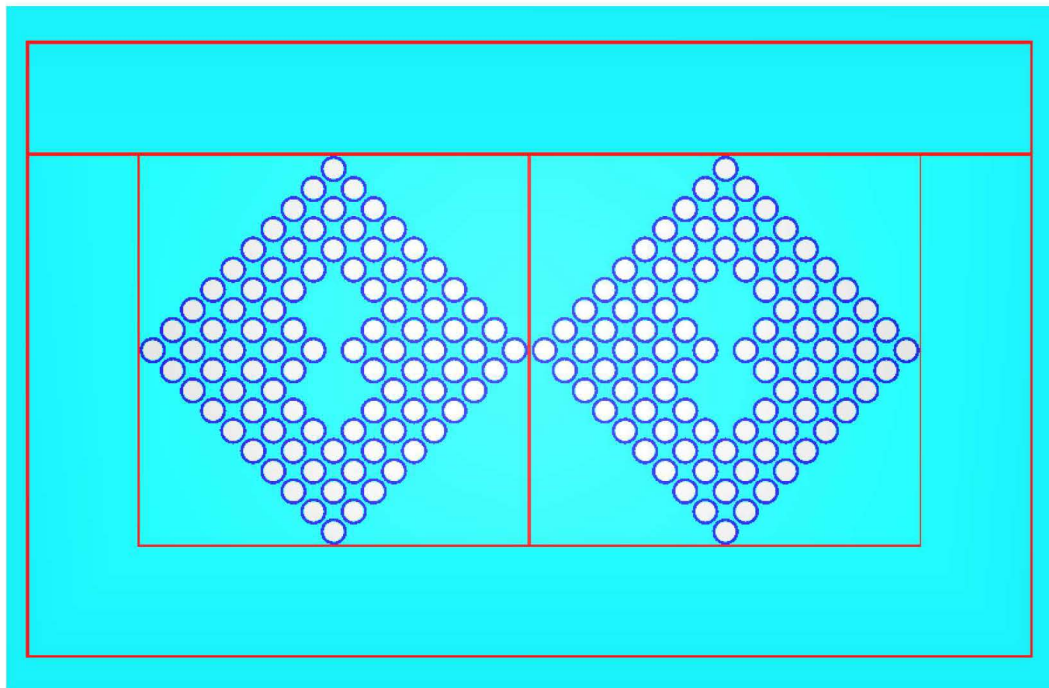


**Figure 6-15 RAJ-II HAC Model with Fuel Assembly Orientation 7**

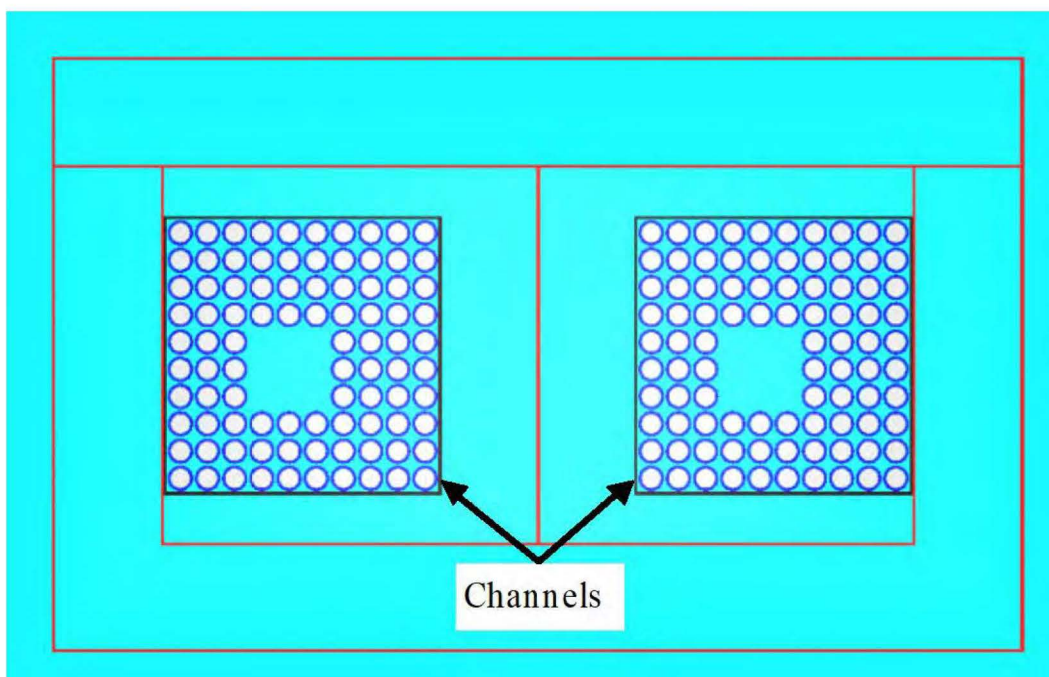


**Figure 6-16 RAJ-II HAC Model with Channels**



### 6.3.1.3 RAJ-II Fuel Rod Transport Model

The RAJ-II fuel rod transport models are developed for single packages and package arrays under NCT and HAC. Cylindrical BWR fuel rods containing  $\text{UO}_2$ , enriched to 5.0 wt% or 8.0 wt% U-235, are modeled freely loose, strapped together, or in a 5-inch stainless steel pipe or protective case. Cylindrical fuel rods containing UC or generic PWR  $\text{UO}_2$ , enriched to 5.0 wt% U-235, are modeled in a 5-inch stainless steel pipe or protective case.

The analysis is also applicable to UC or  $\text{UO}_2$  fuel rods with  $\text{Gd}_2\text{O}_3$  or boron, provided that the maximum enrichment and dimensional limits are met because the presence of neutron absorbers in the fuel rods will result in a reduction in the applicable neutron multiplication factors. The same applies to fuel rods clad with stainless steel because stainless steel (with the same or greater clad thickness) is a better neutron absorber than Zircaloy.

#### 6.3.1.3.1 RAJ-II Single Package Fuel Rod Transport NCT Model

The RAJ-II single package NCT model described in Section 6.3.1.1.1 is used for the single package fuel rod transport models.

The BWR  $\text{UO}_2$  fuel rods are modeled inside the inner container, flush with the polyethylene foam. A 0.0152 cm thick polyethylene layer is modeled around each fuel rod to simulate any protective material present.

The worst case fuel rod parameters are shown in Table 6-6.

**Table 6-6 RAJ-II Fuel Rod Transport Model Fuel Parameters**

Fuel Rod Type	Pellet OD (cm)	Fuel Rod ID (cm)	Fuel Rod OD (cm)	Fuel Rod Length (cm)
10x10 $\text{UO}_2$	0.90	1.00	1.00	385
9 x 9 $\text{UO}_2$	0.96	1.02	1.02	381
8 x 8 $\text{UO}_2$	1.05	1.10	1.10	381
CANDU-14 UC	1.254	1.267	1.34	450
CANDU-25 UC	0.95	0.951	0.996	450
Generic PWR $\text{UO}_2$	0.98	1.004	1.118	450

Calculations performed with the fuel rod transport package array HAC model determine the fuel modeling for the fuel rod transport single package NCT model. The RAJ-II fuel rod transport, single package NCT model is shown in Figure 6-17. As shown in Table 6-6, the fuel rod cladding is not modeled for the BWR  $\text{UO}_2$  fuel rods (8x8, 9x9, and 10x10). Although the cladding material is removed, the fuel rod external boundary is maintained (i.e., pellet clad gap to fuel rod OD is maintained, polyethylene coating applied to fuel rod OD region).

For transport of UC and generic PWR  $\text{UO}_2$  fuel rods, the single package HAC result is expected to bound the fuel rod single package NCT result; therefore, result for fuel rod single package NCT is not provided.

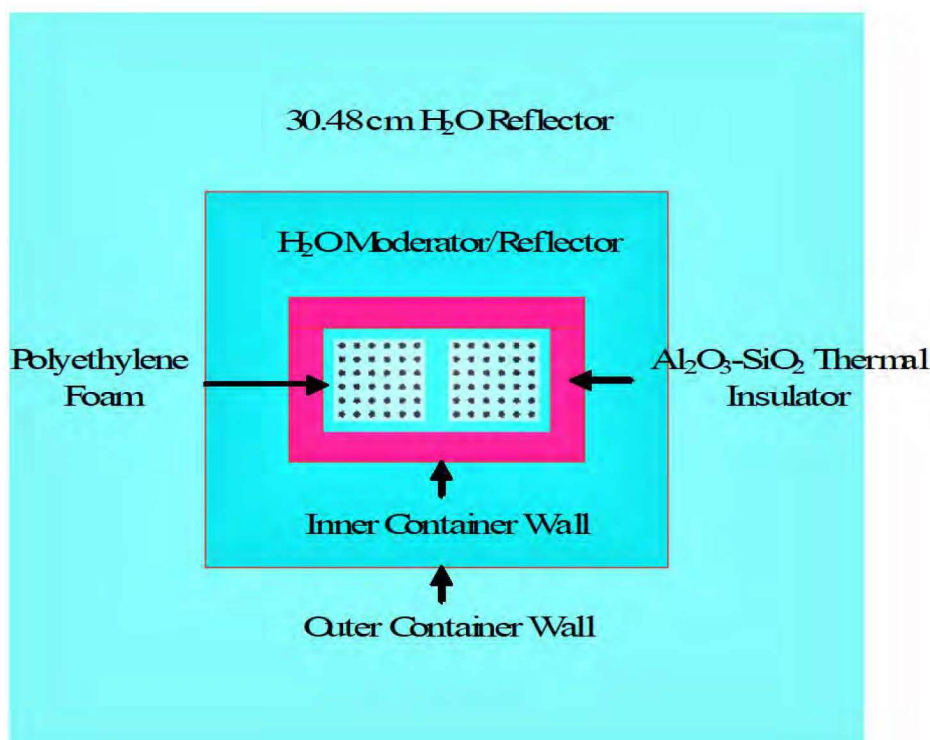


**Figure 6-17 RAJ-II BWR UO<sub>2</sub> Fuel Rod Transport Single Package NCT Model**

#### **6.3.1.3.2 RAJ-II Single Package Fuel Rod Transport HAC Model**

The RAJ-II single package HAC model described in Section 6.3.1.1.2 is used for the single package BWR UO<sub>2</sub> fuel rod transport models. The fuel rods are modeled as filling the inner container fuel compartment because the polyethylene foam is removed due to the HAC. The calculations performed with the fuel rod transport package array HAC model in Section 6.3.1.3.4 determine the fuel modeling for the fuel rod transport single package HAC model. The RAJ-II BWR UO<sub>2</sub> fuel rod transport single package HAC model is shown in Figure 6-18.

Additional analysis is performed for Atomic Energy of Canada Limited's (ACEL's) CANDU UC and generic PWR UO<sub>2</sub> fuel rods inside the 5-inch stainless steel pipe (Reference 6-1). The fuel rods are modeled inside a 5-inch stainless steel pipe placed in the inner container, without polyethylene foam because the pitch sensitivity studies identify the optimal Water to Fuel (W/F) ratio. Unlike the BWR UO<sub>2</sub> fuel rod model, the UC and generic PWR UO<sub>2</sub> rod model includes the material of the 5-inch stainless steel pipe. A 0.0381 cm thick high density (1.005 g/cm<sup>3</sup>) polyethylene layer is modeled around each fuel rod to simulate any protective material present. Each UC rod (CANDU-14 and CANDU-25) has a much shorter active fuel length (47.752 cm and 40.013 cm, respectively) than the value listed in Table 6-6, but a length of 450 cm is used to simulate dense packing of congruent rods in the transport component (5-inch stainless steel pipe or protective case). The space inside the 5-inch pipe surrounding the fuel rods as well as inside the inner and outer container has full density water because studies show this to be the optimal moderator condition. The single package is surrounded by 30.48 cm of full density water for

reflection. The RAJ-II UC and generic PWR  $\text{UO}_2$  fuel rod transport single package HAC model is shown in Figure 6-19.

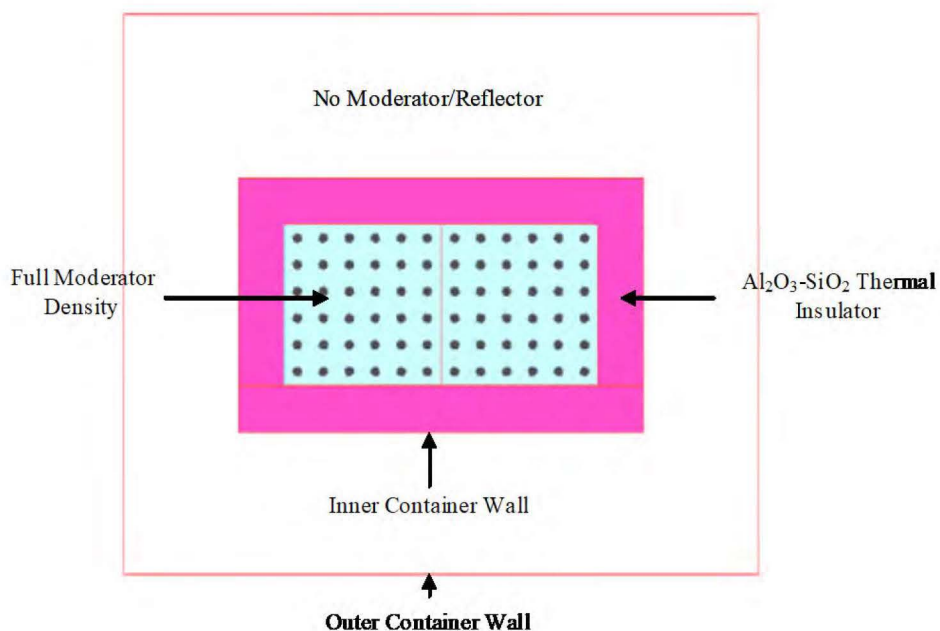


**Figure 6-18 RAJ-II BWR  $\text{UO}_2$  Fuel Rod Transport Single Package HAC Model**

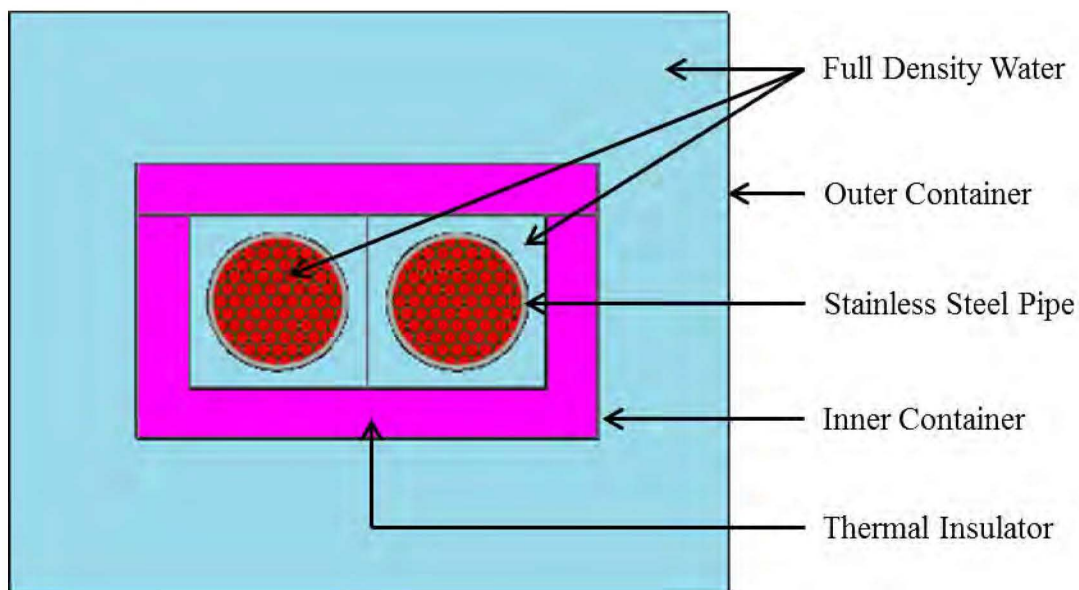


**Figure 6-19 RAJ-II UC and Generic PWR  $\text{UO}_2$  Fuel Rod Transport Single Package HAC Model**

#### 6.3.1.3.3 RAJ-II Package Array Fuel Rod Transport NCT Model

The RAJ-II package array NCT model described in Section 6.3.1.2.1 is used for the package array NCT BWR UO<sub>2</sub> fuel rod transport models. Calculations performed with the fuel rod transport package array HAC model determine the fuel modeling for the fuel rod transport package array NCT model. A portion of the RAJ-II fuel rod transport 21x3x24 package array NCT model is shown in Figure 6-20.

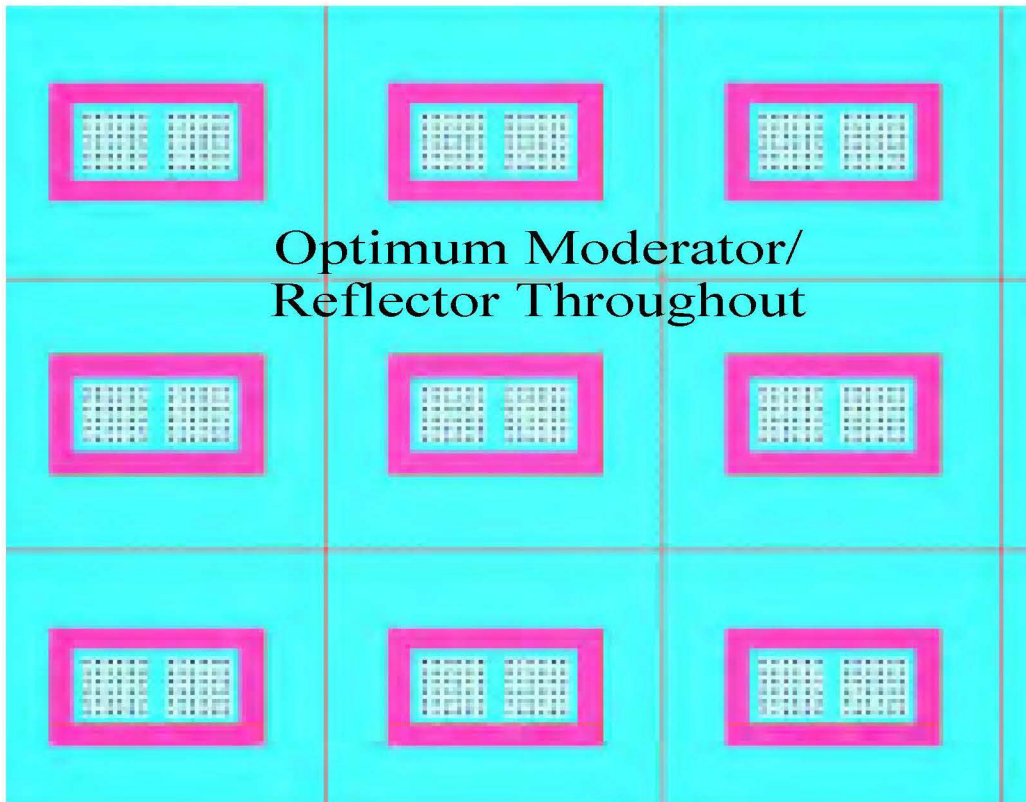


**Figure 6-20 RAJ-II BWR UO<sub>2</sub> Fuel Rod Transport Package Array NCT Model**

#### 6.3.1.3.4 RAJ-II Package Array Fuel Rod Transport HAC Model

The RAJ-II package array HAC model described in Section 6.3.1.2.2 is used for the package array HAC fuel rod transport models.

The fuel rods are modeled filling the inner container for HAC. For BWR UO<sub>2</sub> rods a 0.0152 cm thick polyethylene layer is modeled around each fuel rod to simulate any protective material present. Worst case fuel rod parameters determined from the package array HAC parameter sensitivity analyses (Section 6.3.1.2.2) are used for the fuel rod transport models. The worst case fuel rod parameters are shown in Table 6-6. The GNF 8x8 and GNF 10x10 LEU+ worst case fuel rod designs are determined to be the most reactive BWR UO<sub>2</sub> fuel rods in the fuel rod transport package array HAC pitch sensitivity studies. As shown in Table 6-6, the BWR UO<sub>2</sub> fuel rod (8x8, 9x9, and 10x10) cladding is not modeled. Although the cladding material is removed, the fuel rod



external boundary is maintained (i.e., pellet clad gap to fuel rod OD is maintained and a polyethylene coating is applied to fuel rod OD region).

Calculations are conducted to investigate transporting freely loose fuel rods, fuel rods strapped together, and fuel rods inside a 5-inch stainless steel pipe within each RAJ-II shipping compartment. A fuel rod pitch sensitivity study is conducted for each fuel rod type to determine the number of fuel rods that can be transported in a loose configuration within the RAJ-II fuel compartment. For convenience, a square pitch array is used to conduct the sensitivity study because scoping calculations showed no statistically significant difference in system reactivity between square and triangular pitch arrays for the freely loose configuration. The pitch sensitivity study results in the minimum and maximum allowable fuel rod quantity for shipping rods in a loose configuration. The loose rod analysis is used to bound a fuel rod shipment in which fuel rods are strapped or bundled together.

A fuel rod pitch sensitivity analysis is also performed to determine the fuel rod quantity that may be transported inside a 5-inch stainless steel pipe. Triangular pitch fuel rod arrays are used to find the maximum allowable quantity. A triangular pitch fuel rod array is used for the sensitivity study because scoping calculations showed it to result in higher system reactivity than a square pitch rod array inside a 5-inch stainless steel pipe. The stainless steel material is conservatively neglected when performing the calculations; therefore, any container with a volume equivalent to or less than the 5-inch stainless steel pipe is acceptable for fuel rod transport, as long as the fuel rod quantity is limited to that for the pipe.

The GNF 8x8 and GNF 10x10 LEU+ worst case fuel rod designs are used for the RAJ-II fuel rod transport models because they are determined to be the most reactive BWR UO<sub>2</sub> fuel rods in the pitch sensitivity studies. A portion of the RAJ-II BWR UO<sub>2</sub> fuel rod transport package array HAC model is shown in Figure 6-21.

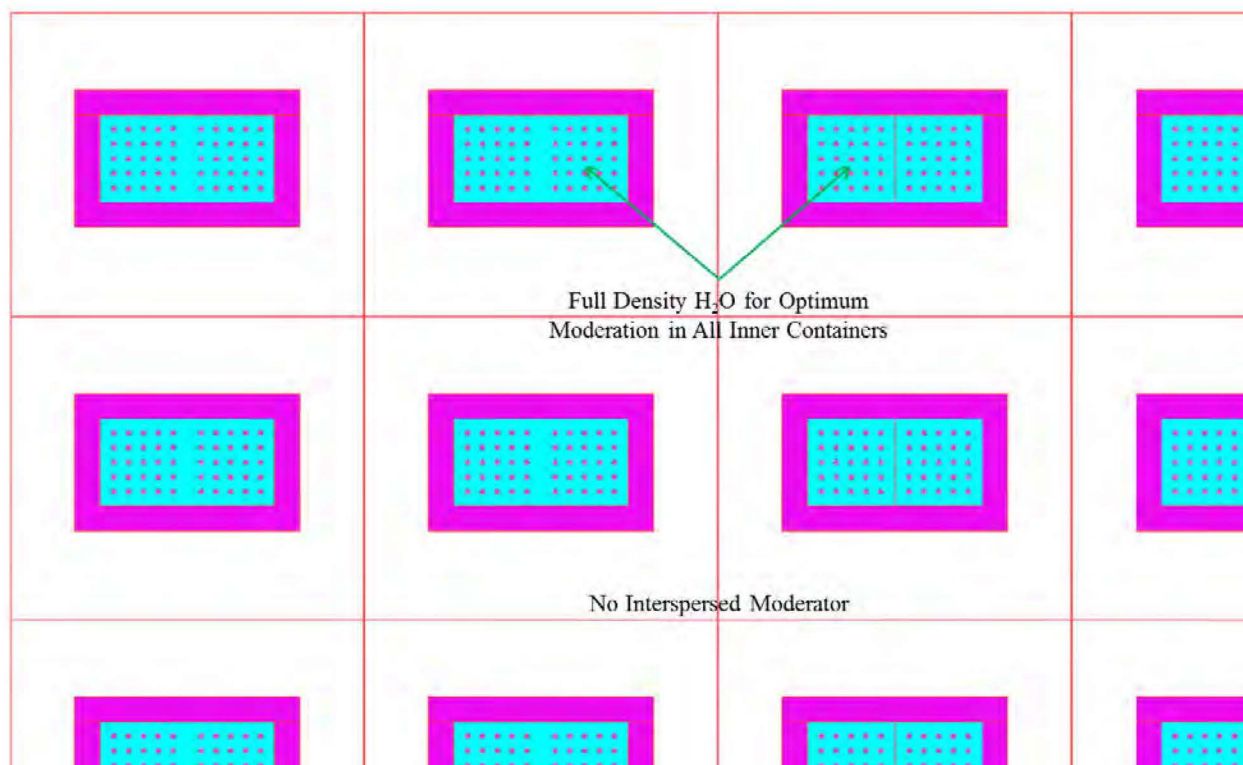


**Figure 6-21 RAJ-II BWR UO<sub>2</sub> Fuel Rod Transport Package Array HAC Model**

The package array HAC model for UC and generic PWR UO<sub>2</sub> fuel rods inside a 5-inch stainless steel pipe is at the optimal W/F ratio with an array size of 8x1x8. The space inside the 5-inch pipe has full density water, while the remaining space inside the inner and outer container (interspersed) is void because studies show this to be the optimal moderator condition for package arrays. The package array is surrounded by 30.48 cm of full density water for reflection. Other aspects of the model are described in Section 6.3.1.3.2. The RAJ-II UC and generic PWR UO<sub>2</sub> fuel rod transport package array HAC model is shown in Figure 6-22.

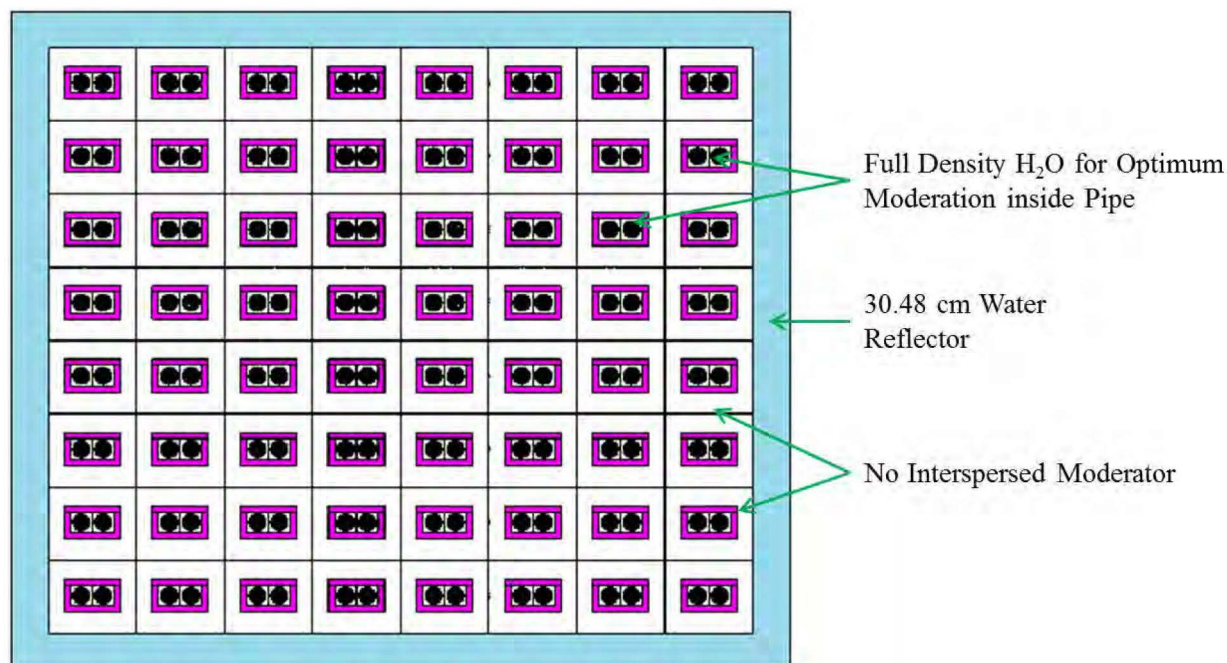


**Figure 6-22 RAJ-II UC and Generic PWR UO<sub>2</sub> Fuel Rod Transport Package Array HAC Model**

### 6.3.2 Material Properties

#### 6.3.2.1 Material Tolerances

Table 6-7 provides sheet metal thickness dimensional tolerance from American Society for Testing and Materials (ASTM) A240 (Reference 6-4) and ASTM A480 (Reference 6-5) (the former refers to the latter for specific tolerances). The table also provides the thicknesses used in the damaged and undamaged container models.

**Table 6-7 Dimensional Tolerances**

Stainless Steel Sheet Gauge	Nominal Thickness (mm)	Permissible Variations* (mm)	Model Thickness Used (in) [cm] (Description)
2 mm	2.00 mm	± 0.18	0.0689 [0.175] (outer container wall)
1.5 mm	1.50 mm	± 0.15	0.0551 [0.14] (inner container wall)
1.0 mm	1.00 mm	± 0.13	0.0343 [0.087] (inner container fuel assembly compartments)

\* Table A1.2 of Reference 6-4.

### 6.3.2.2 MATERIAL SPECIFICATIONS

Table 6-8 contains the material compositions for the RAJ-II package. The UO<sub>2</sub> stack density is taken as 98% of theoretical. The presence of Gd<sub>2</sub>O<sub>3</sub> in the UO<sub>2</sub>-Gd<sub>2</sub>O<sub>3</sub> pellet reduces the density from 10.74 to 10.67 g/cm<sup>3</sup>.

**Table 6-8 Material Specifications for the RAJ-II**

Material	Density (g/cm <sup>3</sup> )	Constituent	Atomic Density (atoms/b-cm)
U(5.0)O <sub>2</sub> 98% Theoretical Density	10.74	U-235 U-238 O	1.2129x10 <sup>-3</sup> 2.2754x10 <sup>-2</sup> 4.7933x10 <sup>-2</sup>
U(8.0)O <sub>2</sub> 98% Theoretical Density	10.74	U-235 U-238 O	1.94051x10 <sup>-3</sup> 2.20340x10 <sup>-2</sup> 4.79491x10 <sup>-2</sup>
U(5.0)O <sub>2</sub> -Gd <sub>2</sub> O <sub>3</sub> 98% Theoretical Density 2 wt% Gd <sub>2</sub> O <sub>3</sub> (75% credit for Gd)	10.67	U-235 U-238 O Gd-152 Gd-154 Gd-155 Gd-156 Gd-157 Gd-158 Gd-160	1.2129x10 <sup>-3</sup> 2.2754x10 <sup>-2</sup> 5.0743x10 <sup>-2</sup> 1.0600x10 <sup>-6</sup> 1.1554x10 <sup>-5</sup> 7.8440x10 <sup>-5</sup> 1.0849x10 <sup>-4</sup> 8.2945x10 <sup>-5</sup> 1.3165x10 <sup>-4</sup> 1.1586x10 <sup>-4</sup>
U(8.0)O <sub>2</sub> -Gd <sub>2</sub> O <sub>3</sub> 98% Theoretical Density 2 wt% Gd <sub>2</sub> O <sub>3</sub> (75% credit for Gd)	10.67	U-235 U-238 O Gd-152 Gd-154 Gd-155 Gd-156 Gd-157 Gd-158 Gd-160	1.94051x10 <sup>-3</sup> 2.20340x10 <sup>-2</sup> 5.07591x10 <sup>-2</sup> 1.0600x10 <sup>-6</sup> 1.1554x10 <sup>-5</sup> 7.8440x10 <sup>-5</sup> 1.0849x10 <sup>-4</sup> 8.2945x10 <sup>-5</sup> 1.3165x10 <sup>-4</sup> 1.1586x10 <sup>-4</sup>
Zirconium	6.49	Zr	4.2844x10 <sup>-2</sup>
Stainless Steel 304 <sup>a</sup>	7.94	Fe Cr Ni Mn Si C P	5.8546x10 <sup>-2</sup> 1.7472x10 <sup>-2</sup> 7.7401x10 <sup>-3</sup> 1.7407x10 <sup>-3</sup> 1.7025x10 <sup>-3</sup> 3.1849x10 <sup>-4</sup> 6.9469x10 <sup>-5</sup>
Polyethylene Foam	0.08 (≤ 0.05 – 0.075)	C H	3.4348x10 <sup>-3</sup> 6.8695x10 <sup>-3</sup>
Low Density Polyethylene (LDPE) Insert	0.925	C H	3.9745x10 <sup>-2</sup> 7.9490x10 <sup>-2</sup>
Polyethylene Cluster Assembly Packing Materials	0.995	C H	4.2720x10 <sup>-2</sup> 8.5440x10 <sup>-2</sup>
Alumina Silicate [Al <sub>2</sub> O <sub>3</sub> (49%)-SiO <sub>2</sub> (51%)]	0.25	Al Si O	1.4474x10 <sup>-3</sup> 1.2782x10 <sup>-3</sup> 4.7274x10 <sup>-3</sup>



NEDO-33869 Revision 11  
Non-Proprietary Information

Material	Density (g/cm <sup>3</sup> )	Constituent	Atomic Density (atoms/b-cm)
Paper Honeycomb C <sub>6</sub> H <sub>10</sub> O <sub>5</sub>	0.04 – 0.08	C	1.7840x10 <sup>-3</sup>
		H	2.9733x10 <sup>-3</sup>
		O	1.4867x10 <sup>-3</sup>
Full Density Water	1.0	H	6.6873x10 <sup>-2</sup>
		O	3.3437x10 <sup>-2</sup>

- a. Structural materials are made of 300 series stainless steel. The specific type used in the criticality analysis is statistically insignificant.

Polyethylene inserts or polyethylene cluster separators are positioned between fuel rods at various locations along the axis of the fuel assembly to avoid stressing the axial grids during transportation. The inserts are shown in Figure 6-4 while the separators are shown in Figure 6-5.

The following provides an example of calculating the volume-averaged density of the packing materials which includes the inserts or cluster separators and a polyethylene bag (see Section 7.1.2). The LDPE insert has a 0.925 g/cm<sup>3</sup> density and an approximate volume of 25 cm<sup>3</sup>. Therefore, a 10x10 assembly with 9 polyethylene inserts has a 225 cm<sup>3</sup> total LDPE volume required for one location along the fuel assembly.

GNF designs the cluster separators based on the geometry of the assembly. The cluster separator design yielding the highest volume averaged density is for the GNF 10x10 fuel. There are 50 cluster separators (25 axial locations) and one polyethylene bag per assembly. The cluster separator is composed of LDPE (0.925 g/cm<sup>3</sup>) fingers and a High Density Polyethylene (HDPE, 1.045 g/cm<sup>3</sup>) holder. The LDPE fingers (10x10) occupy an approximate total volume of 1906 cm<sup>3</sup>, while the HDPE holders have an approximate total volume of 3141 cm<sup>3</sup>. The polyethylene bag is composed of LDPE and has a volume of approximately 346 cm<sup>3</sup>. A volume average density of 0.995 g/cm<sup>3</sup> is calculated for the polyethylene packing materials.

The RAJ-II criticality calculations use the 10x10 cluster separator characteristics for the fuel types investigated. However, the polyethylene characteristics are only used to establish a polyethylene mass limit so that an accurate measurement of polyethylene characteristics by the user is unnecessary. Other plastics with equivalent hydrogen mass limits are acceptable. The following equation can be used to determine the equivalent plastic mass for material *i*.

$$M_{eq,i} = M_r \left( \frac{\rho_r w_{r,H}}{\rho_i w_{i,H}} \right)$$

where,

- $M_r$  = reference polyethylene mass, kg
- $\rho_r$  = reference polyethylene mixture density, g/cm<sup>3</sup>
- $w_{r,H}$  = mass fraction of hydrogen in the reference polyethylene mixture
- $\rho_i$  = polyethylene mixture density of material *i*, g/cm<sup>3</sup>
- $w_{i,H}$  = mass fraction of hydrogen in material *i*

As an example to determine the equivalent plastic mass using the assembly packing materials as the reference:

$$M_{eq,i} = 10.2 \left( \frac{0.995 \times 0.144}{\rho_i w_{i,H}} \right) = \left( \frac{1.46}{\rho_i w_{i,H}} \right)$$

The fuel parameters used in the RAJ-II NCT model are shown in Table 6-9. Each fuel type considered for transport in the RAJ-II is limited to the maximum polyethylene equivalent mass specified in Table 6-1. The polyethylene of the packing materials is modeled as a cylindrical layer wrapped around the fuel rod clad. The thickness of the polyethylene wrap is dependent on the number and dimensions of the fuel rod and is provided in Table 6-10 for the limiting GNF 10x10 design. Additional detailed description of the limiting GNF 10x10 design is provided in Reference 6-3.

**Table 6-9 RAJ-II NCT Model Fuel Parameters**

Fuel Assembly	Fuel Rod Outer Radius (cm)	Number of Fuel Rods	Fuel Rod Pitch (cm)	Fuel Rod Length (cm)	Polyethylene Surrounding Fuel (cm <sup>3</sup> )	Number of Part Length Fuel Rods
GNF 10x10	0.505	[[ ]]	1.363	385	10,251	16

**Table 6-10 RAJ-II NCT Model Fuel Parameters for Determining the Polyethylene Wrap Dimensions**

Fuel Assembly	Number of Full Length Rods	Number/Length of Part Length Fuel Rods	Polyethylene Volume (cm <sup>3</sup> )	Polyethylene Radius (cm)
GNF 10x10	[[ ]]	Short: [[ ]] Long: [[ ]]	10,251	0.593

In the HAC model, the polyethylene inserts are assumed to melt when subjected to the tests specified in 10 CFR 71. The polyethylene is assumed to uniformly coat the fuel rods in each fuel assembly forming a cylindrical layer of polyethylene around each fuel rod. Different coating thicknesses are investigated, and a maximum thickness is determined to set a polyethylene mass limit for each fuel assembly type considered for transport. The fuel assembly parameters used to calculate the polyethylene mass limits are shown in Table 6-11. For the fuel parameter sensitivity study and the worst case fuel assembly models, the polyethylene is smeared into the fuel rod cladding to accommodate the limitations in the lattice cell modeling for cross-section processing in SCALE (KENO V.a). A visual representation of the smeared clad/polyethylene mixture compared to a discrete treatment is shown in Figure 6-23. The polyethylene mass and the volume fractions of polyethylene and zirconium clad for each fuel assembly analyzed are shown in Table 6-12. The volume fractions in Table 6-12 are entered into the model input standard composition specification area. Mixtures representing the polyethylene inserts between fuel rods are created

using the compositions specified, and used in the KENO V.a calculation. The mixtures are also used in the lattice cell description to provide the lump shape and dimensions for resonance cross-section processing, the lattice corrections for cross-section processing, and the information necessary to create cell-weighted cross-sections.

With the use of KENO-VI and continuous energy cross-sections, the smearing of the polyethylene packing materials with the fuel rod cladding is not necessary for the calculations reported for the limiting GNF 10x10 assemblies shown in Table 6-3.

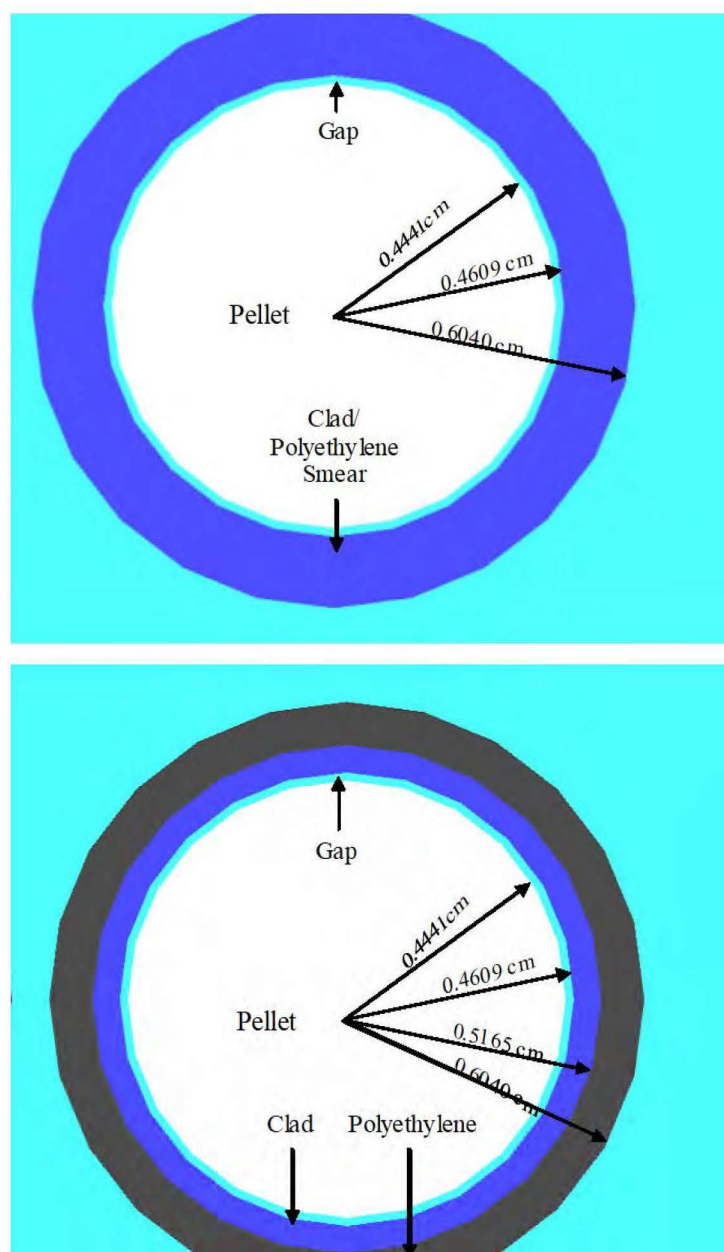


**Figure 6-23 Visual Representation of the Clad/Polyethylene Smeared Mixture versus Discrete Modeling**

**Table 6-11 Fuel Assembly Parameters for Polyethylene Mass Calculations**

Fuel Assembly Design	Fuel Rod Outer Radius (cm)	Number of Fuel Rods	Fuel Rod Pitch (cm)	Fuel Rod Length (cm)	Fuel Rod Inner Radius (cm)
ATRIUM 10x10	0.5165	91	1.284	383.54	0.4609
GNF 10x10	0.50927	92	[[ ]]	381	0.46609
Framatome 9x9	0.54991	72	1.4478	381	0.48006
GNF 9x9	0.55499	74	1.43764	381	0.49149
GNF 8x8	0.6096	60	1.6256	381	0.53594

**Table 6-12 Polyethylene Mass and Volume Fraction Calculations**

Radius (cm)	Thickness (cm)	Total Poly Volume <sup>a</sup> (cm <sup>3</sup> )	Total Poly Mass <sup>b</sup> (g)	Volume <sub>poly</sub> Per Fuel Rod <sup>c</sup> (cm <sup>3</sup> )	Volume <sub>clad</sub> Per Fuel Rod <sup>d</sup> (cm <sup>3</sup> )	Vf <sub>clad</sub> <sup>e</sup>	Vf <sub>poly</sub> <sup>f</sup>
<b>Two ATRIUM 10x10 Fuel Assemblies</b>							
0.51650	0.00000	0	0	0.00	65.47985	1.00000	0.00000
0.56504	0.04854	11512.03	10924.92	63.25	65.47985	0.50865	0.49135
0.59071	0.07421	18019.18	17100.20	99.01	65.47985	0.39809	0.60191
0.60395	0.08745	21487	20391.16	118.06	65.47985	0.35676	0.64324
0.61369	0.08000	24087.04	22858.60	132.35	65.47985	0.33100	0.66900
0.62343	0.10693	26729.6	25366.39	146.87	65.47985	0.30836	0.69164
0.63317	0.11667	29414.68	27914.53	161.62	65.47985	0.28833	0.71167
<b>Two GNF 10x10 Fuel Assemblies</b>							
0.50927	0.00000	0	0	0.00	50.41067	1.00000	0.00000
0.55824	0.04897	11512.03	10924.92	62.57	50.41067	0.44621	0.55379
0.59086	0.08159	19768.04	18759.87	107.43	50.41067	0.31937	0.68063
0.59743	0.08816	21487	20391.16	116.78	50.41067	0.30152	0.69848
0.60723	0.09796	24087.04	22858.6	130.91	50.41067	0.27802	0.72198
0.61703	0.10776	26729.6	25366.39	145.27	50.41067	0.25762	0.74238
0.62683	0.11756	29414.68	27914.53	159.86	50.41067	0.23974	0.76026
<b>Two Framatome 9x9 Fuel Assemblies</b>							
0.5499	0.0000	0	0	0.00	86.11243	1.00000	0.00000
0.6470	0.0971	20021.07	19000	139.04	86.11243	0.38247	0.61753
0.6610	0.1111	23182.3	22000	160.99	86.11243	0.34849	0.65151
0.6702	0.1203	25289.78	24000	175.62	86.11243	0.32901	0.67099
0.6792	0.1293	27397.26	26000	190.26	86.11243	0.31158	0.68842
0.6882	0.1383	29504.74	28000	204.89	86.11243	0.29591	0.70409
0.6970	0.1471	31612.22	30000	219.53	86.11243	0.28174	0.71826
<b>Two GNF 9x9 Fuel Assemblies</b>							
0.55499	0.00000	0	0	0.00	79.53889	1.00000	0.00000
0.65344	0.09845	21074.82	20000	142.40	79.53889	0.35839	0.64161
0.66248	0.10749	23182.3	22000	156.64	79.53889	0.33678	0.66322
0.67140	0.11641	25289.78	24000	170.88	79.53889	0.31763	0.68237
0.68020	0.12521	27397.26	26000	185.12	79.53889	0.30054	0.69946
0.68889	0.13390	29504.74	28000	199.36	79.53889	0.28519	0.71481

NEDO-33869 Revision 11  
Non-Proprietary Information

Radius (cm)	Thickness (cm)	Total Poly Volume <sup>a</sup> (cm <sup>3</sup> )	Total Poly Mass <sup>b</sup> (g)	Volume <sub>poly</sub> Per Fuel Rod <sup>c</sup> (cm <sup>3</sup> )	Volume <sub>clad</sub> Per Fuel Rod <sup>d</sup> (cm <sup>3</sup> )	Vf <sub>clad</sub> <sup>e</sup>	Vf <sub>poly</sub> <sup>f</sup>
0.69747	0.14248	31612.22	30000	213.60	79.53889	0.27134	0.72866
<b>Two GNF 8x8 Fuel Assemblies</b>							
0.60960	0.00000	0	0	0.00	100.9989	1.00000	0.00000
0.71484	0.10524	20021.07	19000	166.84	100.9989	0.37709	0.62291
0.73008	0.12048	23182.3	22000	193.19	100.9989	0.34332	0.65668
0.74006	0.13046	25289.78	24000	210.75	100.9989	0.32398	0.67602
0.74990	0.14030	27397.26	26000	228.31	100.9989	0.30670	0.69330
0.75962	0.15002	29504.74	28000	245.87	100.9989	0.29117	0.70883
0.76922	0.15962	31612.22	30000	263.44	100.9989	0.27714	0.72286

The following example calculations are for two Atrium 10x10 assemblies with a total 21,487 cm<sup>3</sup> polyethylene volume:

- a) Total Polyethylene Volume = (Total Fuel Rod Number)x(2 Fuel Assemblies)x(Polyethylene Area)x(Fuel Rod Length)

$$Volume = (91 \text{ fuel rods})(2 \text{ fuel assemblies}) \left\{ (\pi) \left[ (0.60395 \text{ cm})^2 - (0.5165 \text{ cm})^2 \right] \right\} (383.54 \text{ cm}) = 21487 \text{ cm}^3$$

- b) Total Polyethylene Mass = (Total Polyethylene Volume)x(Polyethylene Density)

$$Mass = \left( 21487 \text{ cm}^3 \right) \left( 0.949 \frac{\text{g}}{\text{cm}^3} \right) = 20391.16 \text{ g}$$

- c) Polyethylene Volume per Fuel Rod = Total Polyethylene Volume/Total Fuel Rod Number

$$\frac{Volume_{poly}}{FuelRod} = \frac{21487 \text{ cm}^3}{(91 \text{ fuel rods})(2 \text{ fuel assemblies})} = 118.06 \text{ cm}^3$$

- d) Clad Volume per Fuel Rod = [(Fuel Rod Area to Outer Clad)-(Fuel Rod Area to Inner Clad)]x Fuel Rod Length

$$\frac{Volume_{clad}}{FuelRod} = (\pi) \left[ (0.5165 \text{ cm})^2 - (0.4609 \text{ cm})^2 \right] (383.54 \text{ cm}) = 65.48 \text{ cm}^3$$

- e) Clad Volume Fraction = Clad Volume/Total Clad and Polyethylene Volumes

$$VF_{clad} = 65.48 \text{ cm}^3 / \left[ (118.06 \text{ cm}^3) + (65.48 \text{ cm}^3) \right] = 0.35676$$

- f) Polyethylene Volume Fraction = Polyethylene Volume/ Total Clad and Polyethylene Volumes

$$VF_{poly} = 118.06 \text{ cm}^3 / \left[ (118.06 \text{ cm}^3) + (65.48 \text{ cm}^3) \right] = 0.64323$$

### 6.3.3 Computer Codes and Cross-Section Libraries

The calculational methodology employed in the analyses is based on that embodied in SCALE-PC (Version 4.4a), as documented in Reference 6-6. The neutron cross-section library employed in the analyses and the supporting validation analyses was the 44 group ENDF/B-V library distributed with Version 4.4a of the SCALE package. Each case was run using the CSAS25 sequence of codes (i.e., BONAMI, NITAWL, and KENO V.a). For each case, 400 generations with 2,500 neutrons per generation were run to ensure proper behavior about the mean value. The methodology and results of the validation of SCALE 4.4a on the PC is outlined in Section 6.10, and results in a USL that is the basis for comparison to ensure subcriticality.

For the performance of the UC and generic PWR loose rod provision analysis (Reference 6-1), the GEMER Monte Carlo code was used. GEMER is the evolution of Geometry Enhanced MERIT by combining the neutron transport physics of the MERIT Monte Carlo code and the initial geometry features of the KENO-IV Monte Carlo code systems, as well as by enhancing geometry and

graphics capabilities. The MERIT code is based on the Battelle Northwest Laboratory's BMC code and is characterized by its explicit treatment of resolved resonance in material cross section set. Functionally, the GEMER Monte Carlo code is similar in analytic capability to other industry recognized codes such as KENO Va. or MCNP.

Cross sections in GEMER are currently processed from the ENDF/B-IV library in multigroup and resonance parameter formats. Cross-sections are prepared in the 190 energy group format and those in the resonance energy range have the form of resonance parameters. The resonance parameters describe the cross sections in the resonance range and Monte Carlo sampling in this range is done from resonance kernels rather than from broad group cross sections (i.e., explicit treatment of resolved resonance's using a single level Breit-Wigner equation at each collision in the resonance energy range). Thus, there is a single unique cross section set associated with each available isotope and dependence is not placed on Dancoff (flux shadowing) correction factors or effective scattering cross sections. This treatment of cross-sections with explicit resonance parameters is especially suited to the analysis of uranium compounds in the form of heterogeneous accumulations, lattices, or systems containing nuclear poisons.

Thermal scattering of hydrogen is represented by the Hayward Kernel  $S(\alpha, \beta)$  data in the ENDF/B-IV library. The types of reactions considered in the GEMER Monte Carlo calculation are fission, capture, elastic, inelastic, and (n, 2n) reactions; absorption is implicitly treated by applying the non-absorption probability to neutron weights on each collision. As part of the solutions, GEMER produces eigenvalue, micro- and macro-group fluxes, reaction rates, cross sections, and neutron balance by isotopes.

Since Revision 9 of the RAJ-II Safety Analysis Report (SAR), the limiting GNF 10x10 calculations are performed using SCALE (Version 6.1) with KENO-VI Monte Carlo code using continuous energy ENDF/B-VII cross-section libraries. The methodology and results of the validation of KENO-VI are outlined in Section 6.10 and the USL is the basis for comparison to ensure subcriticality. Material specifications for the KENO-VI models are described in Table 6-8 and all polyethylene is represented using the 'poly(H<sub>2</sub>O)' standard composition.

#### **6.3.4 Demonstration of Maximum Reactivity**

The objectives for the RAJ-II analysis are to demonstrate package criticality safety and determine fuel loading criteria. To accomplish these objectives, calculations are performed to determine the most reactive fuel configuration inside the RAJ-II assembly compartments. Once the fuel configuration is determined, moderator and reflector conditions are investigated. Finally, package orientation (for arrays) is examined. When the worst case fuel configuration, moderator/reflector conditions, and package orientation are found, the single package and package array calculations under both NCT and HAC are performed.

Revision 9 of the RAJ-II SAR extends the fuel parameter ranges of the GNF 10x10 design, and Revision 11 of the RAJ-II SAR extends the enrichment range of the GNF 10x10 design. Depending on the intent and conclusions of the sensitivity studies described in this section, only the affected parameters were revisited to ensure the most bounding GNF 10x10 fuel parameters are identified.

Scoping calculations with enrichments up to 8.0 wt% U-235 were utilized to support existing conclusions presented in this SAR, or to update parameters and results where applicable.

#### **6.3.4.1 Fuel Assembly Orientation Study (2N=448)**

The package array dimensions for the fuel assembly orientation are 14x2x16 (width x depth x height). Initial calculations are performed to find the worst case fuel assembly orientation inside each RAJ-II fuel compartment. Nominal fuel assembly dimensions are used for these initial calculations (Table 6-4). Note that in all cases with cladding, zirconium is used to conservatively represent any zirconium alloy. The package array HAC model described in Section 6.3.1.2.2 is used and the fuel assembly orientations depicted in Figure 6-9 through Figure 6-15 are applied. In addition, a polyethylene coating covers each fuel rod in the assembly, the fuel assembly is unchanneled, and the moderator density is 1.0 g/cm<sup>3</sup> in the RAJ-II inner container fuel region. The polyethylene foam is assumed to burn away, alumina silicate thermal insulator envelopes the inner container, and no water is in either the outer container or between packages in the array. The results of the calculations are shown in Table 6-13. Based on the results in Table 6-13, assembly orientation 6 is bounding for all designs. Therefore, orientation 6 with the assembly centered in each fuel compartment is used in the remaining design calculations. It is also noted that most results in Table 6-13 exceed the 0.94254 USL. For this reason, gadolinia-urania fuel rods are added to the fuel assemblies to provide reactivity hold-down.



**Table 6-13 RAJ-II Array HAC Fuel Assembly Orientation**

Fuel Assembly	Interspersed Moderator Density (g/cm <sup>3</sup> )	Polyethylene Mass Per Assembly (kg)	Assembly Orientation	k <sub>eff</sub>	σ	k <sub>eff</sub> + 2σ
FANP 10x10	0.0	10.2	1	0.9375	0.0010	0.9395
FANP 10x10	0.0	10.2	2	0.9529	0.0008	0.9545
FANP 10x10	0.0	10.2	3	0.8973	0.0008	0.8989
FANP 10x10	0.0	10.2	4	0.8965	0.0010	0.8985
FANP 10x10	0.0	10.2	5	0.9248	0.0010	0.9268
FANP 10x10	0.0	10.2	6	0.9741	0.0009	<b>0.9759</b>
FANP 10x10	0.0	10.2	7	0.9486	0.0009	0.9504
GNF 10x10	0.0	10.2	1	0.9586	0.0010	0.9606
GNF 10x10	0.0	10.2	2	0.9721	0.0009	0.9739
GNF 10x10	0.0	10.2	3	0.9184	0.0008	0.9200
GNF 10x10	0.0	10.2	4	0.9183	0.0009	0.9201
GNF 10x10	0.0	10.2	5	0.9431	0.0008	0.9447
GNF 10x10	0.0	10.2	6	0.9909	0.0010	<b>0.9929</b>
GNF 10x10	0.0	10.2	7	0.9652	0.0008	0.9668
FANP 9x9 <sup>a</sup>	0.0	11	1	0.9486	0.0009	0.9504
FANP 9x9	0.0	11	2	0.9559	0.0009	0.9577
FANP 9x9	0.0	11	3	0.9052	0.0008	0.9068
FANP 9x9	0.0	11	4	0.9056	0.0008	0.9072
FANP 9x9	0.0	11	5	0.9293	0.0010	0.9313
FANP 9x9	0.0	11	6	0.9791	0.0008	<b>0.9807</b>
FANP 9x9	0.0	11	7	0.9362	0.0009	0.9380
GNF 9x9	0.0	11	1	0.9491	0.0008	0.9507
GNF 9x9	0.0	11	2	0.9577	0.0008	0.9593
GNF 9x9	0.0	11	3	0.9051	0.0008	0.9067
GNF 9x9	0.0	11	4	0.9042	0.0009	0.9060
GNF 9x9	0.0	11	5	0.9287	0.0009	0.9305
GNF 9x9	0.0	11	6	0.9787	0.0008	<b>0.9803</b>
GNF 9x9	0.0	11	7	0.9556	0.0008	0.9572
GNF 8x8	0.0	11	1	0.9506	0.0009	0.9524
GNF 8x8	0.0	11	2	0.9563	0.0008	0.9579
GNF 8x8	0.0	11	3	0.9048	0.0008	0.9064
GNF 8x8	0.0	11	4	0.9052	0.0009	0.9070
GNF 8x8	0.0	11	5	0.9299	0.0009	0.9317
GNF 8x8	0.0	11	6	0.9764	0.0008	<b>0.9780</b>
GNF 8x8	0.0	11	7	0.9554	0.0009	0.9572

- a. The Framatome D-lattice 9x9 assembly was modeled. However, the results presented here are applicable to the C-lattice as well
- b. Limiting case shown in bold

#### 6.3.4.2 Fuel Assembly Gadolinia Rod Study (2N=448)

Fuel assemblies with lattice average U-235 enrichments up to 8.0 wt% are qualified for transport in the RAJ-II package by crediting the gadolinia-urania fuel rods present in the assembly. The gadolinia-urania fuel rods decrease system reactivity such that the  $k_{\text{eff}} + 2\sigma$  remain below the 0.94254 USL. The gadolinium content of each gadolinia-urania fuel rod is limited to 75% of the value specified in Table 6-1. Scoping studies are performed using numerous gadolinia-urania fuel rod placement patterns in the orientation 6 models, from the fuel assembly orientation study, to find the pattern that yields the highest reactivity for each fuel assembly type. Of the patterns investigated, three patterns that produce the highest reactivity for each fuel assembly type are shown in Figure 6-26 through Figure 6-28. The calculations are performed using optimum moderator conditions. The results for the 14x2x16 RAJ-II array transporting 10x10, 9x9, or 8x8 fuel assemblies with gadolinia-urania fuel rods arranged in the patterns shown in Figure 6-26 through Figure 6-28 are listed in Table 6-14. As shown in Table 6-14, the gadolinia-urania fuel rods hold the system reactivity below the 0.94254 USL. Based on the gadolinia-urania fuel rod pattern optimization calculations:

- Gadolinia-urania fuel rod Pattern G is selected for future Framatome Advanced Nuclear Power (FANP) 10x10 fuel assembly sensitivity calculations,
- Gadolinia-urania fuel rod Pattern B is selected for future GNF 10x10 fuel assembly sensitivity calculations,
- Gadolinia-urania fuel rod Pattern A is selected for future FANP and GNF 9x9 fuel assembly sensitivity calculations,
- Gadolinia-urania fuel rod Pattern I is selected for future GNF 8x8 fuel assembly sensitivity calculations.

Note that Pattern B for the GNF 10x10 was selected for the remaining sensitivity studies described in Section 6.3.4. This GNF 10x10 contains two 2x2 off center diagonal water rods. Additional analysis using KENO-VI with continuous energy ENDF/B-VII library is performed to determine the limiting gadolinia-urania fuel rod pattern for the GNF 10x10 designs with a single axially varying water rod centrally located within the fuel rod array, with sixteen part length fuel rods. The analysis uses a systematic approach to identify the least gadolinia reactivity worth locations [[ ]] within the assembly.

The fuel rod [[ ]] is a measure of rod importance in contributing to the package system reactivity. Therefore, the fractional rod [[ ]] distribution in a fuel assembly is the best indicator showing the relative effect of each rod to the system reactivity. A lower fractional rod [[ ]] means less gadolinia reactivity worth in that rod location. [[ ]]

]]

The model used for this study is an infinite array of RAJ-II packages with fuel parameters given in Table 6-1, at 5.0 wt% or 8.0 wt% U-235, with optimum moderator conditions (flooded inner container and voided outer container). The gadolinia rod locations are chosen based on the following constraints:

1. The gadolinia rods must be distributed symmetrically about the major diagonal of the fuel rod lattice.
2. The gadolinia rods are not allowed to be in the peripheral locations.
3. The gadolinia rods must be placed in full-length rod locations.
4. After seven (7) gadolinia rods there must be at least one (1) gadolinia rod in at least two (2) out of the four (4) quadrants of the fuel rod array. The quadrant definition is shown in Figure 6-24.

[[

]]

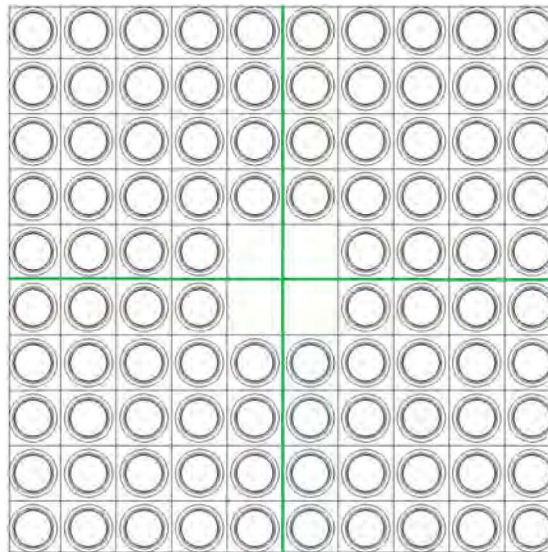


**Figure 6-24 Quadrants of a 10x10 Lattice**

Because the two adjacent fuel assemblies in the container are tightly coupled in terms of neutronics, [[ ]] to ensure that the most bounding gadolinia loading within the package is identified. The resulting bounding gadolinia rod distribution pattern for GNF 10x10 designs for each required number of gadolinia rods as the two assemblies are placed within the RAJ-II inner container is shown in Figure 6-25.

To confirm that the GNF 10x10 designs used in this study are limiting, other fuel designs were analyzed using the as-designed part length rod configurations without any gadolinia rods to compare the relative reactivity. These designs include 8x8, 9x9, and 10x10 (both GNF and FANP products); the 10x10 designs have various water rod geometries such as two 2x2 off-center diagonal and 3x3, and also includes a different number of part length rods between 8 and 14. The

study confirmed that the GNF 10x10 designs have the highest reactivity and determine the RAJ-II package CSI.

The bounding gadolinia rod distribution pattern maximizes the package system reactivity. The actual locations of gadolinia rods in the as-designed fuel assemblies are more evenly distributed and therefore lead to lower reactivity than the bounding gadolinia rod distribution pattern identified by this study.

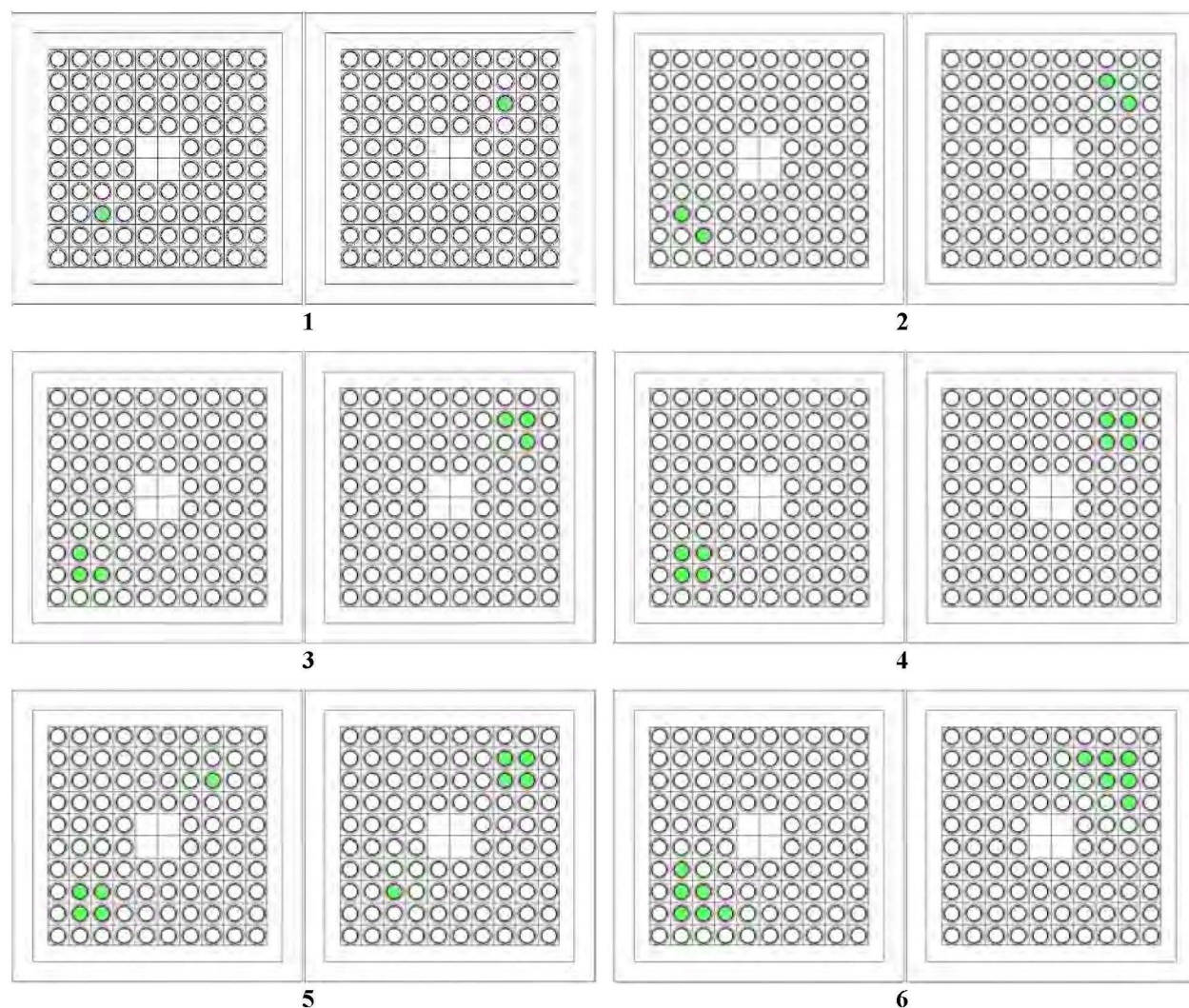


**Figure 6-25 Gadolinia-Urania Fuel Rod Loading Pattern for GNF 10x10**



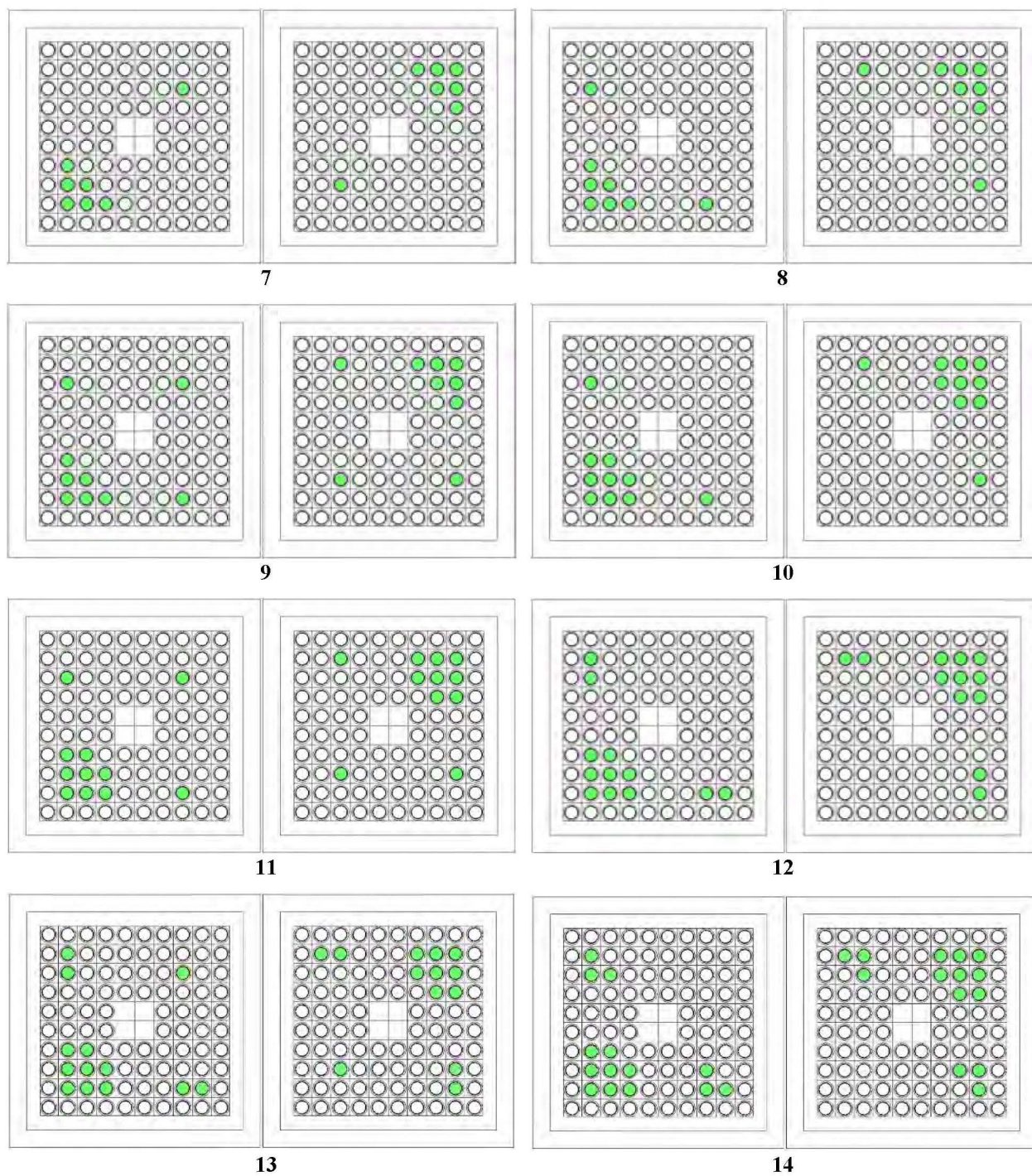


**Figure 6-25 Gadolinia-Urania Fuel Rod Loading Pattern for GNF 10x10 (Continued)**



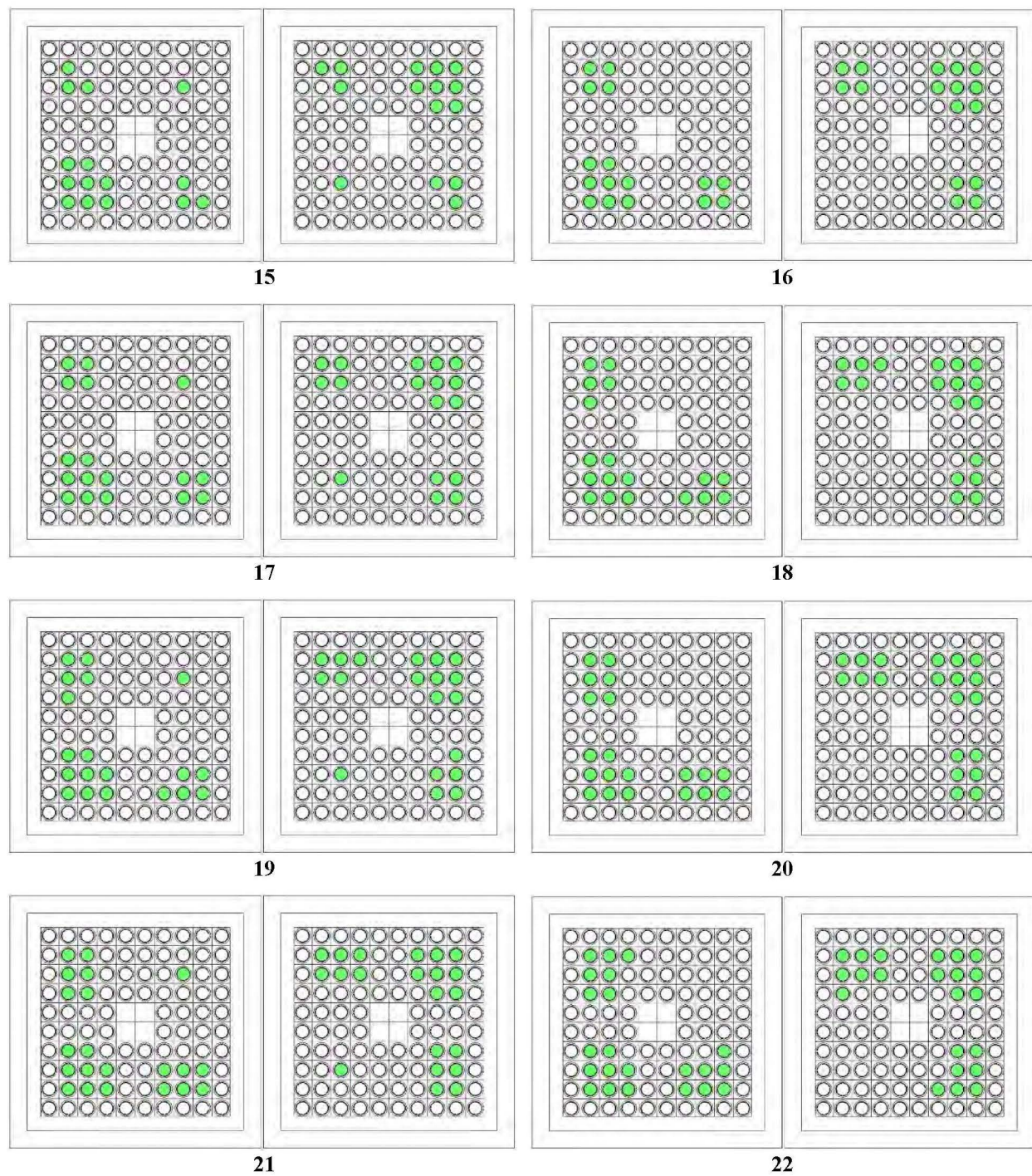


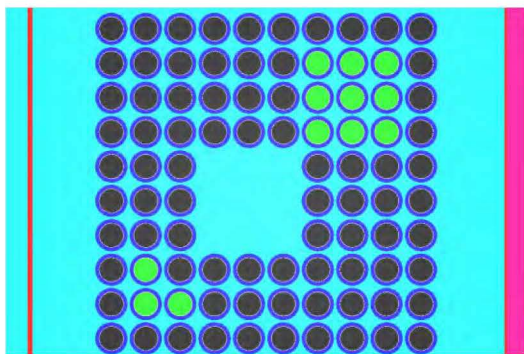
**Figure 6-25 Gadolinia-Urania Fuel Rod Loading Pattern for GNF 10x10 (Continued)**

**Table 6-14 RAJ-II Shipping Container 14x2x16 Array with Gadolinia-Urania Fuel Rods**

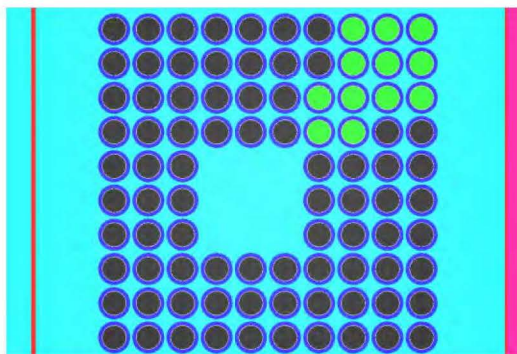
Assembly Type	Pattern Designation	U-235 Enrich (wt%)	Gad Rod #	Pitch (cm)	Pellet Diameter (cm)	Clad ID (cm)	Clad OD (cm)	k <sub>eff</sub>	σ	k <sub>eff</sub> + 2σ
FANP 10x10	B	5.0	12	1.284	0.8882	0.9218	1.033	0.8716	0.0008	0.8732
FANP 10x10	F	5.0	12	1.284	0.8882	0.9218	1.033	0.8699	0.0008	0.8715
FANP 10x10	G	5.0	12	1.284	0.8882	0.9218	1.033	0.8732	0.0008	<b>0.8748</b>
GNF 10x10	B	5.0	12	1.2954	0.8941	0.9322	1.019	0.8886	0.0008	<b>0.8902</b>
GNF 10x10	G	5.0	12	1.2954	0.8941	0.9322	1.019	0.8871	0.0008	0.8887
GNF 10x10	H	5.0	12	1.2954	0.8941	0.9322	1.019	0.8880	0.0009	0.8898
FANP 9x9	A	5.0	10	1.4478	0.9398	0.9601	1.099	0.8644	0.0007	<b>0.8658</b>
FANP 9x9	B	5.0	10	1.4478	0.9398	0.9601	1.099	0.8605	0.0008	0.8621
FANP 9x9	E	5.0	10	1.4478	0.9398	0.9601	1.099	0.8354	0.0009	0.8372
GNF 9x9	A	5.0	10	1.4376	0.9550	0.9830	1.110	0.8579	0.0008	<b>0.8596</b>
GNF 9x9	B	5.0	10	1.4376	0.9550	0.9830	1.110	0.8572	0.0008	0.8588
GNF 9x9	F	5.0	10	1.4376	0.9550	0.9830	1.110	0.8524	0.0009	0.8540
GNF 8x8	E	5.0	7	1.6256	1.0439	1.0719	1.219	0.8779	0.0009	0.8797
GNF 8x8	G	5.0	7	1.6256	1.0439	1.0719	1.219	0.8726	0.0008	0.8742
GNF 8x8	I	5.0	7	1.6256	1.0439	1.0719	1.219	0.8800	0.0009	<b>0.8818</b>

a. Limiting case(s) shown in bold

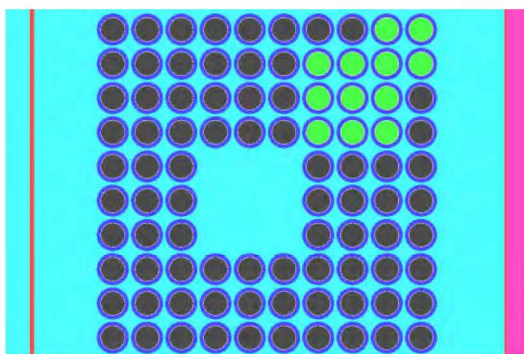




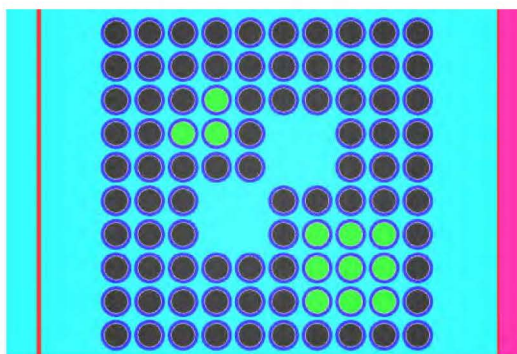
FANP 10x10 5.0 wt%  $^{235}\text{U}$ , Pattern B



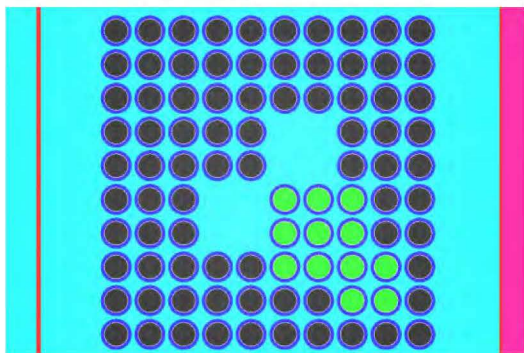
FANP 10x10 5.0 wt%  $^{235}\text{U}$ , Pattern F



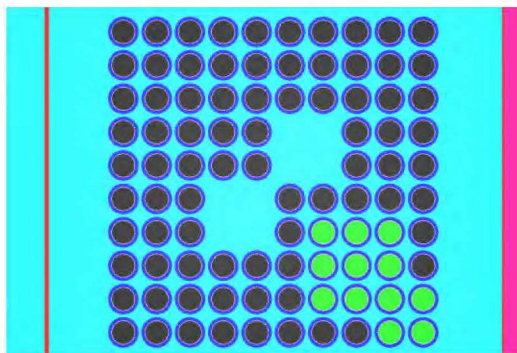
FANP 10x10 5.0 wt%  $^{235}\text{U}$ , Pattern G



GNF 10x10 5.0 wt%  $^{235}\text{U}$ , Pattern B



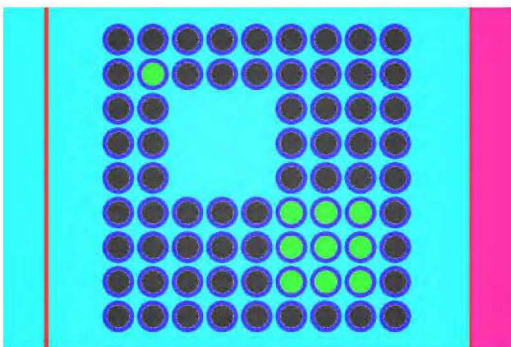
GNF 10x10 5.0 wt%  $^{235}\text{U}$ , Pattern G



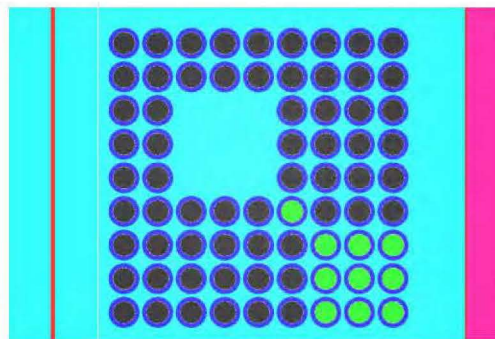
GNF 10x10 5.0 wt%  $^{235}\text{U}$ , Pattern H

Figure 6-26 Gadolinia-Urania Fuel Rod Placement Pattern for 10x10 Fuel Assemblies at 5.0 wt%  $^{235}\text{U}$

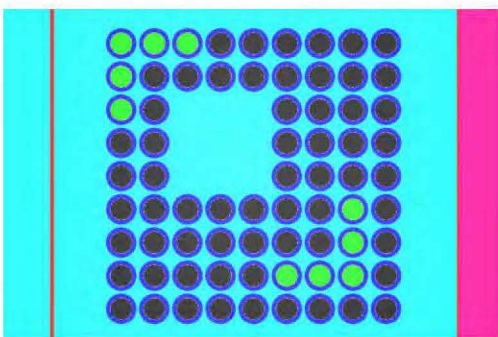




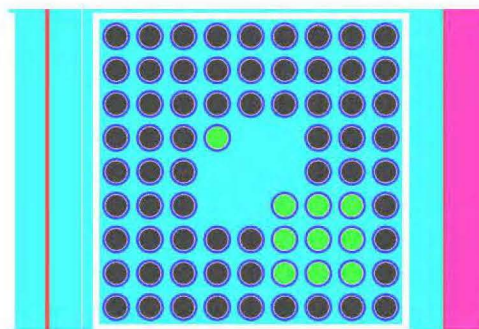
FANP 9x9 5.0 wt%  $^{235}\text{U}$ , Pattern A



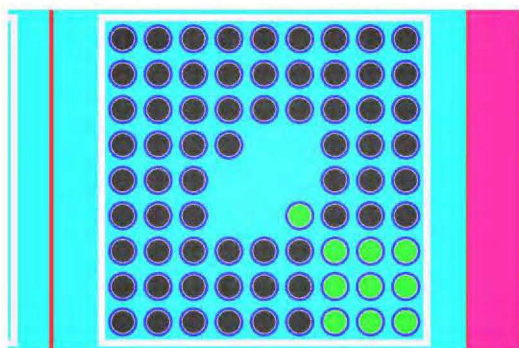
FANP 9x9 5.0 wt%  $^{235}\text{U}$ , Pattern B



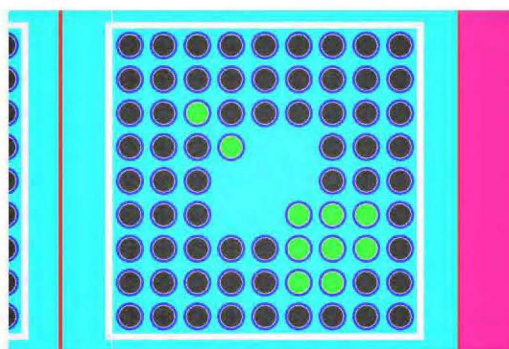
FANP 9x9 5.0 wt%  $^{235}\text{U}$ , Pattern E



GNF 9x9 5.0 wt%  $^{235}\text{U}$ , Pattern A

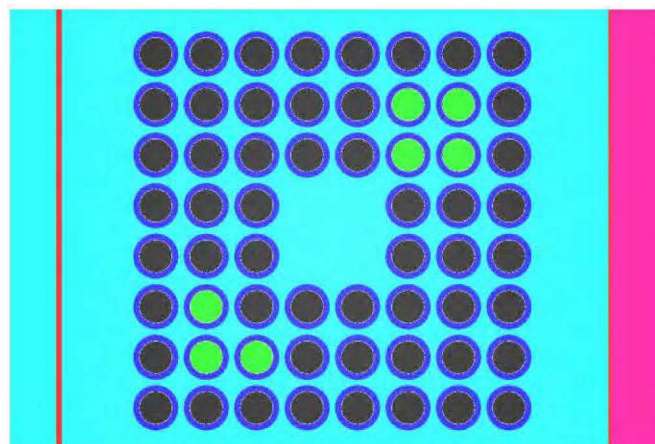


GNF 9x9 5.0 wt%  $^{235}\text{U}$ , Pattern B

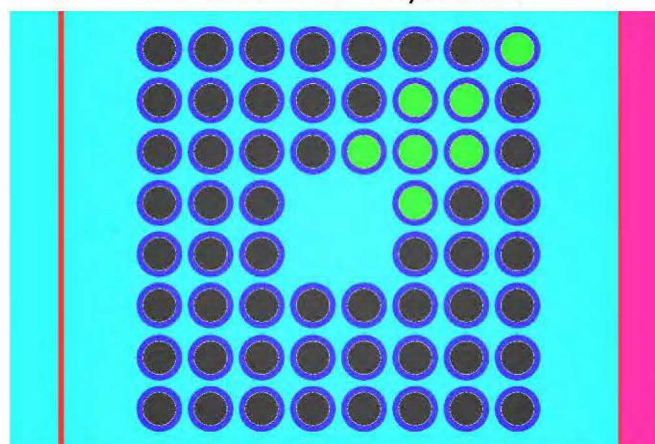


GNF 9x9 5.0 wt%  $^{235}\text{U}$ , Pattern F

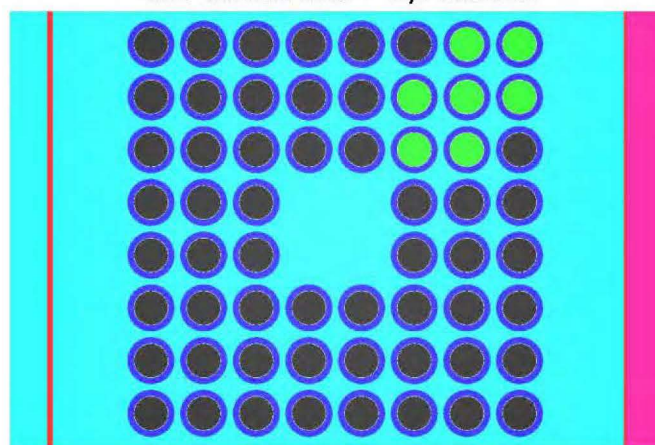
Figure 6-27 Gadolinia-Urania Fuel Rod Placement Pattern for 9x9 Fuel Assemblies at 5.0 wt%  $^{235}\text{U}$



GNF 8x8 5.0 wt%  $^{235}\text{U}$ , Pattern E



GNF 8x8 5.0 wt%  $^{235}\text{U}$ , Pattern G



GNF 8x8 5.0 wt%  $^{235}\text{U}$ , Pattern I

**Figure 6-28 Gadolinia-Urania Fuel Rod Placement Pattern for 8x8 Fuel Assemblies at 5.0 wt%  $^{235}\text{U}$**

### 6.3.4.3 Fuel Assembly Channel Study (2N=448)

A calculation is performed to determine if the presence of channels around the fuel assembly increases system reactivity. The orientation 6 models with the gadolina-urania fuel rod patterns from the previous studies are used and a zirconium channel is placed around each assembly as shown in Figure 6-16. The channel thickness is varied from 0.17 cm to 0.3048 cm and the effect on reactivity is assessed. The fuel assembly channel is located in the reflector region for each fuel assembly. It has no effect on the assembly H/X ratio because it is not located within the fuel envelope. Therefore, removing it would not have the same effect on system reactivity as removing the internal grid structure. The results are shown in Table 6-15. Comparing the results in Table 6-15 and Table 6-14 indicates reactivity increases with the presence of channels due to increased neutron leakage from the inner fuel compartment, resulting in increased neutron interaction among containers in the array. Therefore, channels will be included in subsequent calculations.

**Table 6-15 RAJ-II Sensitivity Analysis for Channeled Fuel Assemblies**

Assembly Type	Channel Thickness (cm)	Poly Mass per Assembly (kg)	Pitch (cm)	Pellet Diameter (cm)	Clad ID (cm)	Clad OD (cm)	$k_{eff}$	$\sigma$	$k_{eff} + 2\sigma$
FANP 10x10	0.1700	10.2	1.284	0.8882	0.9218	1.033	0.8801	0.0008	0.8817
FANP 10x10	0.2032	10.2	1.284	0.8882	0.9218	1.033	0.8786	0.0008	0.8802
FANP 10x10	0.2540	10.2	1.284	0.8882	0.9218	1.033	0.8815	0.0009	<b>0.8833</b>
FANP 10x10	0.3048	10.2	1.284	0.8882	0.9218	1.033	0.8810	0.0008	0.8826
GNF 10x10	0.1700	10.2	1.2954	0.8941	0.9322	1.019	0.8922	0.0009	0.8940
GNF 10x10	0.2032	10.2	1.2954	0.8941	0.9322	1.019	0.8948	0.0008	0.8964
GNF 10x10	0.2540	10.2	1.2954	0.8941	0.9322	1.019	0.8947	0.0008	0.8963
GNF 10x10	0.3048	10.2	1.2954	0.8941	0.9322	1.019	0.8953	0.0008	<b>0.8969</b>
FANP 9x9	0.1700	11	1.4478	0.9398	0.9601	1.0998	0.8719	0.0009	0.8737
FANP 9x9	0.2032	11	1.4478	0.9398	0.9601	1.0998	0.8724	0.0009	0.8742
FANP 9x9	0.2540	11	1.4478	0.9398	0.9601	1.0998	0.8739	0.0008	0.8756
FANP 9x9	0.3048	11	1.4478	0.9398	0.9601	1.0998	0.8755	0.0009	<b>0.8773</b>
GNF 9x9	0.1700	11	1.4376	0.9550	0.9830	1.11	0.8626	0.0009	0.8644
GNF 9x9	0.2032	11	1.4376	0.9550	0.9830	1.11	0.8651	0.0009	0.8669
GNF 9x9	0.2540	11	1.4376	0.9550	0.9830	1.11	0.8654	0.0010	<b>0.8674</b>
GNF 9x9	0.3048	11	1.4376	0.9550	0.9830	1.11	0.8659	0.0008	0.8676
GNF 8x8	0.1700	11	1.6256	1.0439	1.0719	1.2192	0.8834	0.0010	0.8854
GNF 8x8	0.2032	11	1.6256	1.0439	1.0719	1.2192	0.8857	0.0008	0.8873
GNF 8x8	0.2540	11	1.6256	1.0439	1.0719	1.2192	0.8884	0.0009	0.8902
GNF 8x8	0.3048	11	1.6256	1.0439	1.0719	1.2192	0.8900	0.0009	<b>0.8918</b>

a. Limiting case(s) shown in bold

#### 6.3.4.4 Polyethylene Mass Study (2N=448)

The effect that polyethylene mass has on reactivity for each fuel assembly design is considered for transport in the RAJ-II package. The results of the previous sensitivity studies are taken into consideration for the polyethylene mass study. The worst case channeled (0.3048 cm thick channels) models, used in the previous study, are used for the polyethylene mass study. The polyethylene and clad volume fractions, shown in Table 6-12, are used in the model material description to represent the polyethylene and clad mixture. They are also used in the lattice cell description for resonance cross-section processing. The polyethylene coating thickness around the fuel rods is varied, and the effect on reactivity is determined. The results of the calculations, Table 6-28, are displayed in Figure 6-29. Although the polyethylene addition increases reactivity, the increase is gradual with a linear trend, and the resulting system  $k_{eff}$  remains subcritical. Based on the results in Figure 6-29:

- a polyethylene mass of 10.2 kg/assembly (20.4 kg/container) is chosen for further FANP and GNF 10x10 calculations,
- an 11 kg/assembly (22 kg/container) polyethylene mass is selected for subsequent FANP 9x9, GNF 9x9, and GNF 8x8 fuel assembly calculations.

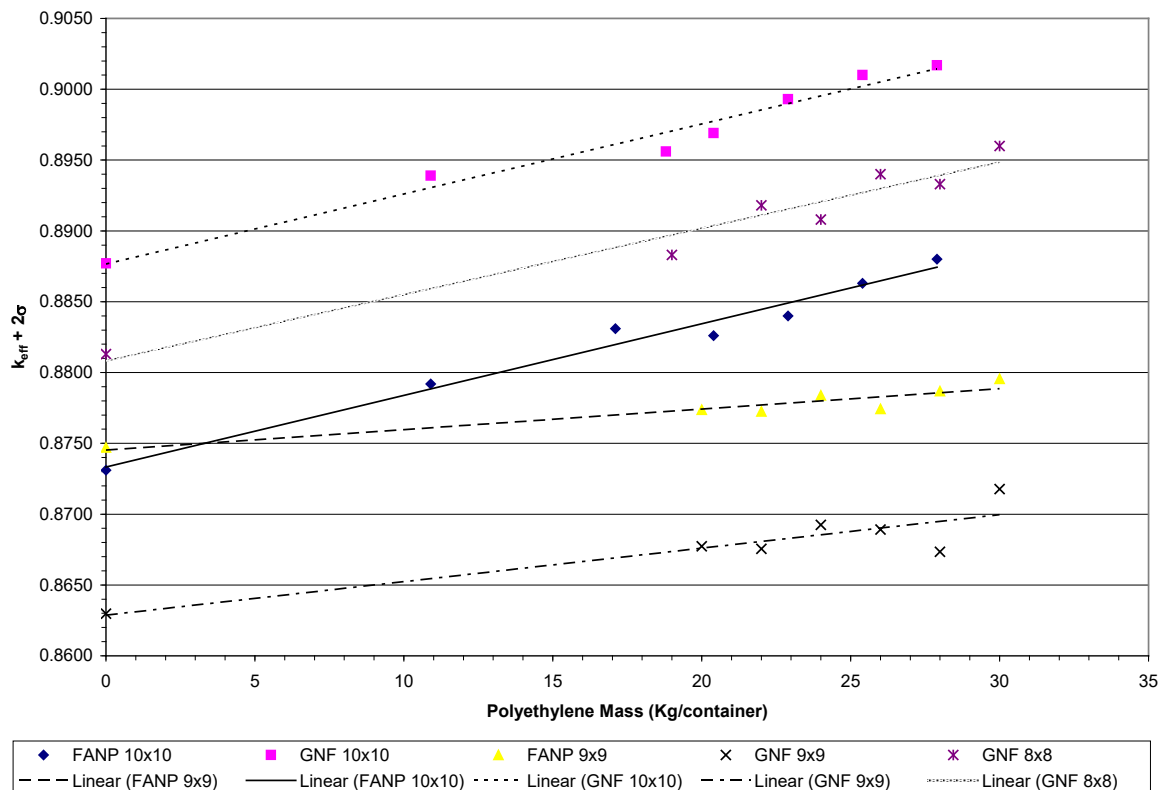


**Figure 6-29 RAJ-II Array HAC Polyethylene Sensitivity**

#### 6.3.4.5 Fuel Rod Pitch Sensitivity Study (2N=448)

A fuel rod pitch sensitivity study is conducted using the worst case models from the polyethylene sensitivity study. The minimum fuel rod pitch is chosen to be at the point that the polyethylene coating on adjacent fuel rods contact. The maximum fuel rod pitch is chosen to bound the damage sustained during the 9 meter drop. The change in rod pitch for the fuel designs considered for transport is discussed in Section 2.7.1.1. The results are shown in Figure 6-30. Based on the results in Figure 6-30, the fuel assemblies are under-moderated such that increasing the pitch increases system reactivity, with a trend that is approximately linear. Based on the pitch sensitivity calculations (Table 6-29):

- a 1.350 cm fuel rod pitch is selected as the value for FANP and GNF 10x10 pitch range used in subsequent sensitivity studies (however, for the limiting GNF 10x10 results presented in Sections 6.4, 6.5, and 6.6 a rod pitch of 1.363 cm is used),
- a 1.510 cm fuel rod pitch is selected as the upper limit for FANP and GNF 9x9 pitch range,
- a 1.6923 cm fuel rod pitch is selected as the upper limit for GNF 8x8 pitch range.

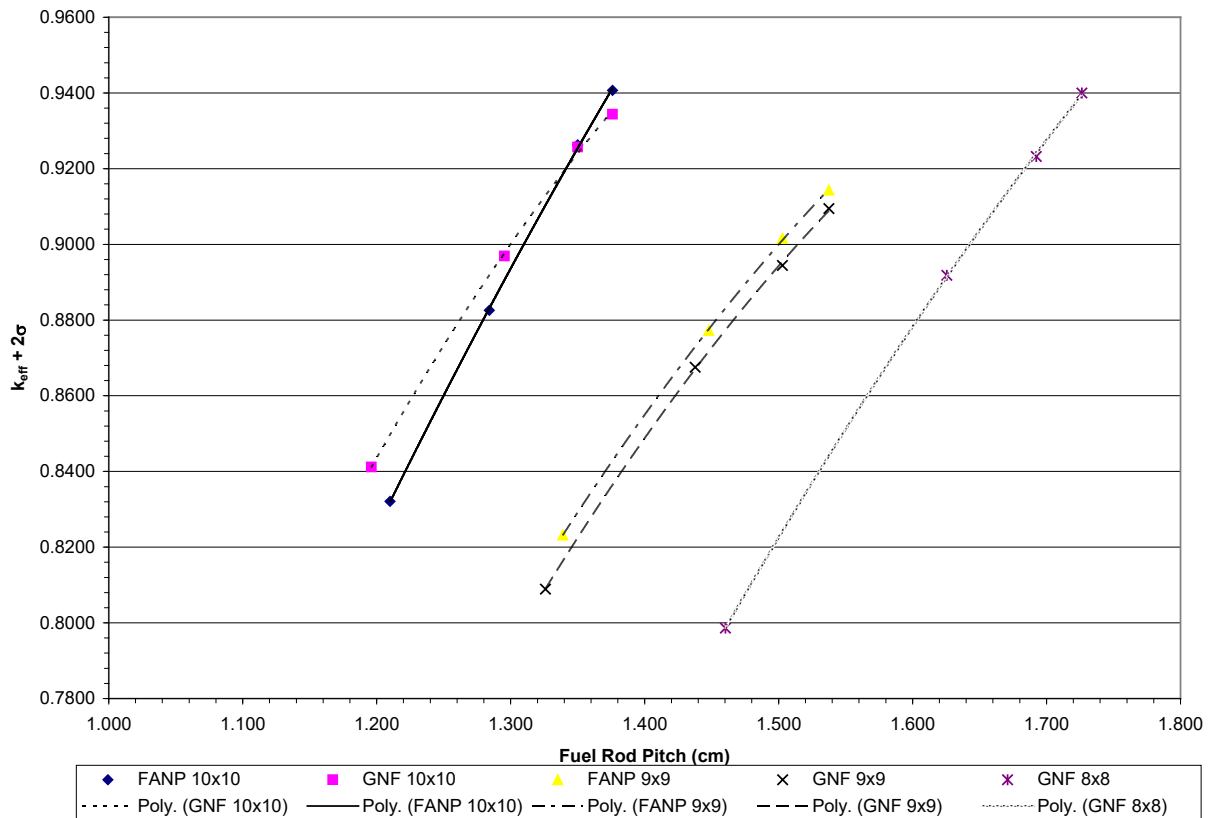


**Figure 6-30 RAJ-II Fuel Rod Pitch Sensitivity Study**



#### 6.3.4.6 Fuel Pellet Diameter Sensitivity Study (2N=448)

With a polyethylene quantity chosen, the worst case orientation known, the channeled fuel effect assessed, and the gadolinia-urania fuel rod patterns identified, a fuel pellet diameter sensitivity study is conducted. For the pellet diameter sensitivity study, the package array HAC model described in Section 6.3.1.2.2 is used for the study, fuel assembly orientation 6 is selected based on the results in Table 6-13, the maximum polyethylene amount for each fuel assembly design is chosen, the gadolinia-urania rod pattern is selected from the sensitivity study in Section 6.3.4.2, the inner container fuel compartment is maintained at optimum density water, an alumina silicate thermal insulator envelopes the inner container fuel compartment, and water is removed from the outer container and between packages in the array. The results are shown in Figure 6-31. The results in Figure 6-31 demonstrate that reactivity increases as pellet diameter is increased, and the trend is linear. Pellet diameters of 0.895 cm for the FANP and GNF 10x10 designs, 0.96 cm for the Framatome and GNF 9x9 designs, and 1.05 cm for the GNF 8x8 design are found acceptable as the upper bounds for the fuel assembly design pellet ranges (Table 6-29).

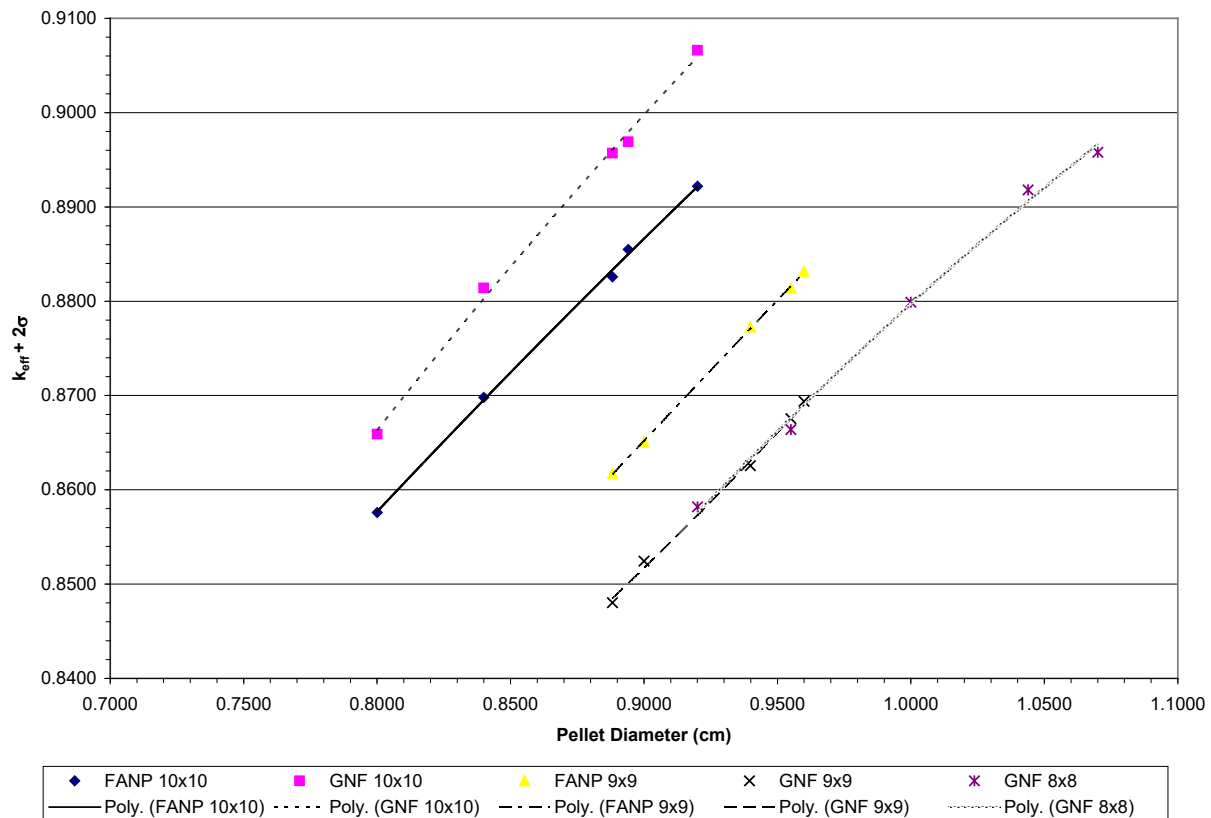


Figure 6-31 RAJ-II Array HAC Pellet Diameter Sensitivity Study

#### 6.3.4.7 Fuel Rod Clad Thickness Sensitivity Study (2N=448)

Two sets of calculations are performed to assess the reactivity sensitivity to changes in cladding thickness. For the clad thickness sensitivity studies, the package array HAC model described in Section 6.3.1.2.2 is used for the study, fuel assembly orientation 6 is selected based on the results in Table 6-13, the maximum polyethylene amount for each fuel assembly design is chosen, the gadolinia-urania rod pattern is selected from the sensitivity study in Section 6.3.4.2, the inner container fuel compartment is maintained at optimum density moderation, an alumina silicate thermal insulator envelopes the inner container fuel compartment, and water is removed from the outer container and between packages in the array. For the first set of calculations, the inner clad diameter is adjusted to determine the effect on reactivity while the outer clad diameter is fixed at its nominal value shown in Table 6-4. The minimum value for the parameter search range is the pellet OD, while the maximum value for the range is the clad OD. The second set of calculations involves adjustments to the outer clad diameter while the inner clad diameter is held at its nominal value shown in Table 6-4. Figure 6-32 displays the results for the inner clad diameter sensitivity calculations, and Figure 6-33 shows the results for the outer clad diameter sensitivity study. Both sets of results demonstrate that a decrease in the clad thickness results in an increase in system reactivity. The results also indicate that reactivity increases as the clad OD is decreased and increases as the clad ID is increased. Based on these results and fabrication constraints (Table 6-31 and Table 6-32):

- a 0.933 cm upper bound clad ID, and a 1.00 cm lower bound clad OD are selected for the FANP and GNF 10x10 parameter ranges for downstream sensitivity studies,
- a 1.02 cm upper bound clad ID, and a 1.09 cm lower bound clad OD are selected for the FANP and GNF 9x9 parameter ranges,
- a 1.10 cm upper bound clad ID, and a 1.17 cm lower bound clad OD are selected for the GNF 8x8 parameter range.

NEDO-33869 Revision 11  
Non-Proprietary Information

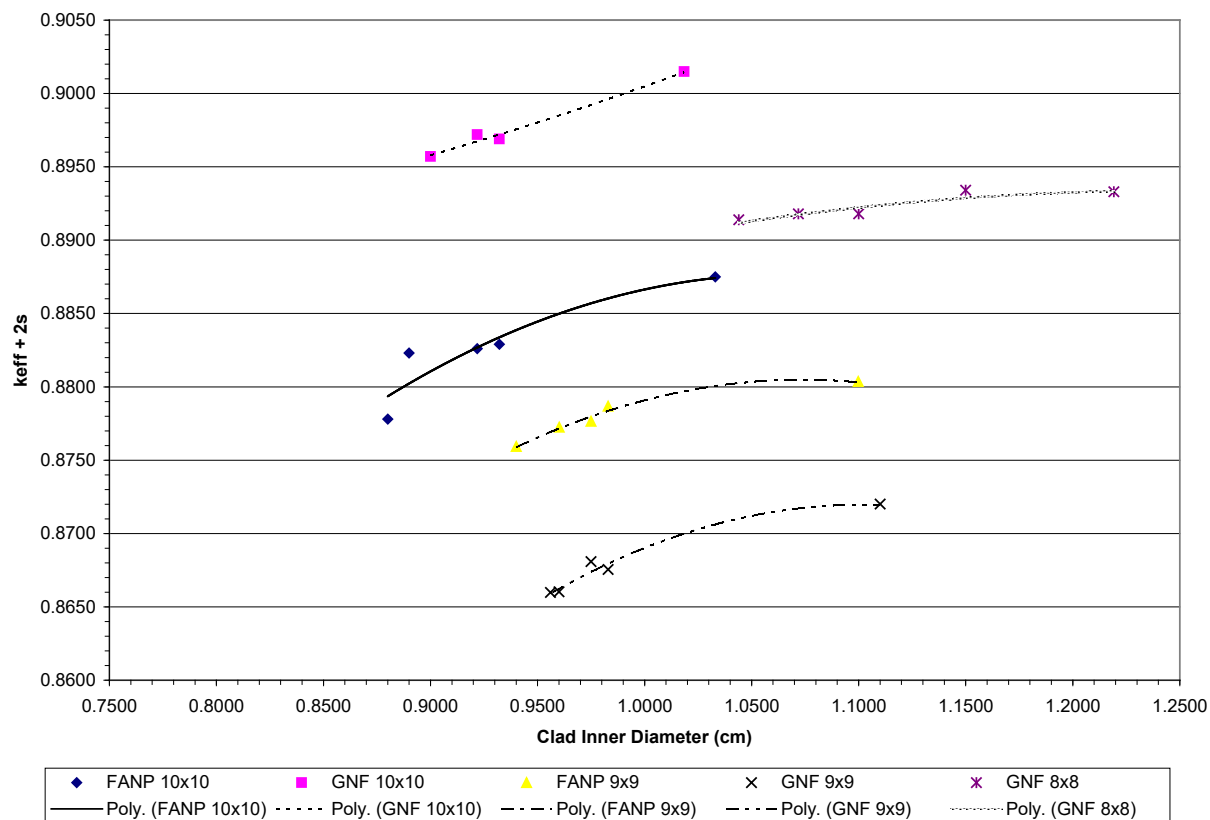


**Figure 6-32 RAJ-II Array HAC Fuel Rod Clad ID Sensitivity Study**



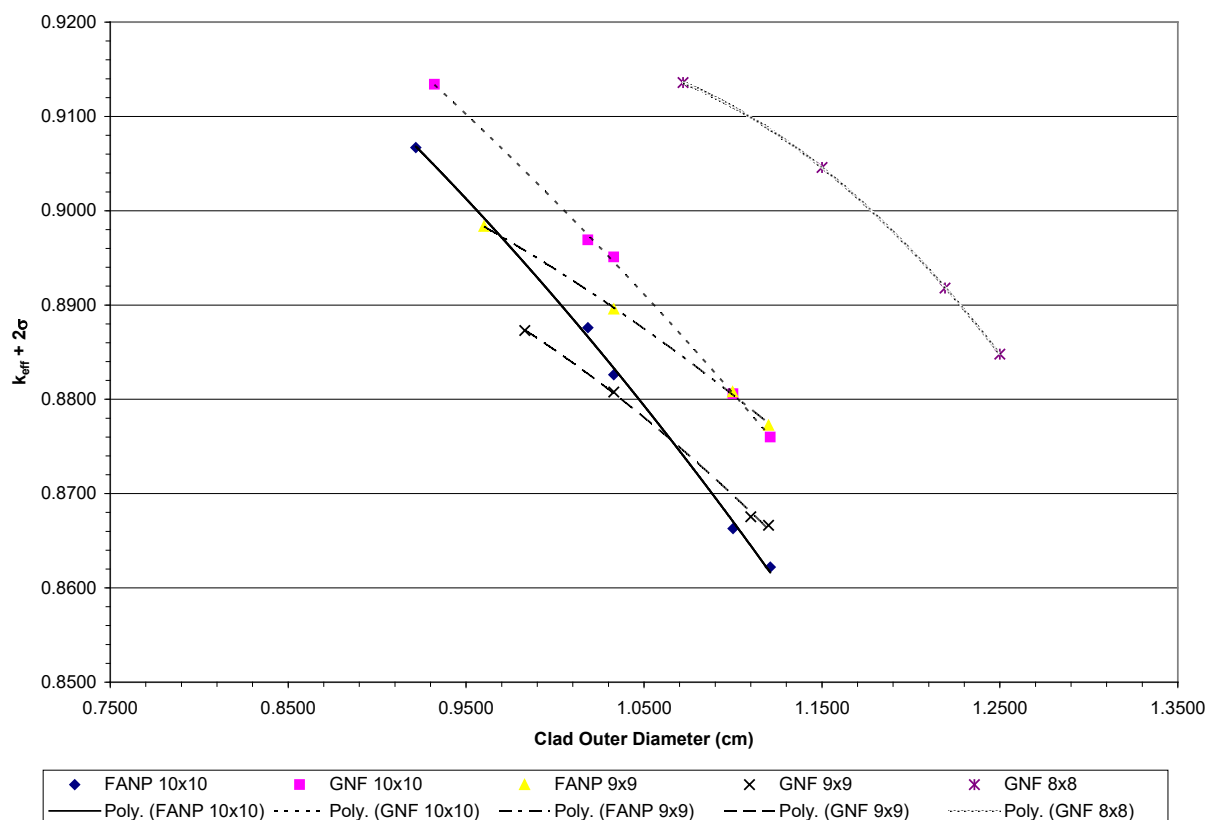


**Figure 6-33 RAJ-II Array HAC Fuel Rod Clad OD Sensitivity Study**

#### 6.3.4.8 Worst Case Parameter Fuel Designs (2N=448)

The previous calculations have varied single parameters and assessed the effect on reactivity. Because the ranges investigated are to be a part of the fuel loading criteria, an assessment must be made for more than one parameter change at a time. To validate the parameter ranges selected to appear in the fuel loading criteria, a fuel design is developed by assembling the worst case parameters for each design considered for transport in the RAJ-II package. Table 6-16 contains the worst case parameters for each design. The worst case models from the clad ID and OD sensitivity study are used to conduct the worst case fuel parameter study. The polyethylene is smeared into the fuel rod cladding to accommodate the limitations in the lattice cell modeling for cross-section processing in SCALE. A search for the worst case gadolinia-urania fuel rod pattern is also conducted to validate the worst case fuel design. Numerous patterns were investigated for each fuel assembly with the worst case fuel parameters determined from the sensitivity studies. Of the patterns investigated, three patterns that produce the highest reactivity for each fuel assembly type are shown in Figure 6-26 to Figure 6-28. Additional calculations are performed to investigate the number of gadolinia-urania fuel rods needed based on fuel assembly U-235 enrichment. For each fuel assembly U-235 enrichment, a gadolinia-urania fuel rod pattern optimization study is conducted. The three patterns that produce the highest reactivity for each fuel assembly based on U-235 enrichment are shown in Figure 6-34 to Figure 6-36. All results are listed in Table 6-16 and are below the USL of 0.94254. Based on the results listed in Table 6-16,

all worst case fuel assembly designs result in maximum system reactivities that are within the statistical uncertainty of one another and criticality safety can be assured based on the meeting the required number of gadolinia-urania rods specified in Table 6-1.

The results for GNF 10x10 in Table 6-16 contain two 2x2 off center diagonal water rods (rod pitch of 1.350 cm). Additional analysis using KENO-VI with continuous energy ENDF/B-VII library is performed to determine the limiting gadolinia-urania fuel rod pattern for a GNF 10x10 design with a single axially varying water rod centrally located within the fuel rod array, with sixteen part length fuel rods, and the approach is described in Section 6.3.4.2. The gadolinia loading patterns shown in Figure 6-25 are applicable to any lattice average enrichment because the reactivity effect of the gadolinia loading is only geometry dependent. The results for the limiting GNF 10x10 design (single axially varying water rod centrally located within the fuel rod array, with sixteen part length fuel rods at 1.363 cm rod pitch) at various enrichments based on the HAC package array model described in Section 6.6.1 are added to the bottom of Table 6-16. As noted in Section 6.6.2, the presence of the channel at various channel thicknesses has either a statistically insignificant or slightly negative effect on the system reactivity; therefore, the cases for the limiting GNF 10x10 do not include the channel. Additionally, Section 6.3.4.11 indicates that optimal polyethylene foam thickness is lower than the nominal foam thickness. In Table 6-16, the cases for the limiting GNF 10x10 LEU use a foam thickness of 1.28 cm, and the cases for the limiting GNF 10x10 LEU+ use a foam thickness of 1.14 cm. (see Section 6.3.4.11 for the foam thickness justification). These cases are below the USL (0.9340).

**Table 6-16 RAJ-II Array HAC Worst Case Parameter Fuel Designs**

Assembly Type	Gadolinia -Urania Fuel Rod Number	<sup>235</sup> U Enrichment (wt%)	Poly Mass per Assembly (kg)	Pitch (cm)	Pellet Diameter (cm)	Clad ID (cm)	Clad OD (cm)	k <sub>eff</sub>	σ	k <sub>eff</sub> + 2σ <sup>a</sup>
FANP 10x10	12	5.0	10.2	1.350	0.895	0.933	1.00	0.9368	0.0008	0.9384
FANP 10x10	10	4.6	10.2	1.350	0.895	0.933	1.00	0.9360	0.0009	0.9378
FANP 10x10	9	4.3	10.2	1.350	0.895	0.933	1.00	0.9325	0.0010	0.9345
FANP 10x10	8	4.2	10.2	1.350	0.895	0.933	1.00	0.9366	0.0009	<b>0.9384</b>
FANP 10x10	6	3.9	10.2	1.350	0.895	0.933	1.00	0.9353	0.0007	0.9367
FANP 10x10	4	3.6	10.2	1.350	0.895	0.933	1.00	0.9341	0.0009	0.9359
FANP 10x10	2	3.3	10.2	1.350	0.895	0.933	1.00	0.9305	0.0009	0.9323
FANP 10x10	0	2.9	10.2	1.350	0.895	0.933	1.00	0.9274	0.0008	0.9290
GNF 10x10	12	5.0	10.2	1.350	0.895	0.933	1.00	0.9393	0.0008	0.9409
GNF 10x10	10	4.6	10.2	1.350	0.895	0.933	1.00	0.9349	0.0010	0.9369
GNF 10x10	9	4.3	10.2	1.350	0.895	0.933	1.00	0.9346	0.0008	0.9362
GNF 10x10	8	4.2	10.2	1.350	0.895	0.933	1.00	0.9395	0.0009	<b>0.9413</b>
GNF 10x10	6	3.9	10.2	1.350	0.895	0.933	1.00	0.9377	0.0009	0.9395
GNF 10x10	4	3.6	10.2	1.350	0.895	0.933	1.00	0.9370	0.0008	0.9386
GNF 10x10	2	3.3	10.2	1.350	0.895	0.933	1.00	0.9344	0.0009	0.9362
GNF 10x10	0	2.9	10.2	1.350	0.895	0.933	1.00	0.9317	0.0007	0.9331
FANP 9x9	10	5.0	11	1.510	0.96	1.02	1.09	0.9191	0.0008	0.9207
FANP 9x9	8	4.7	11	1.510	0.96	1.02	1.09	0.9294	0.0008	<b>0.9310</b>
FANP 9x9	6	4.2	11	1.510	0.96	1.02	1.09	0.9242	0.0010	0.9262

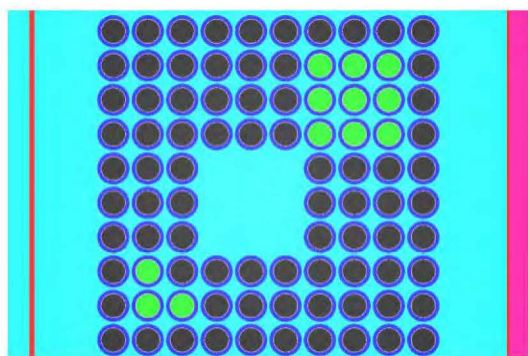
NEDO-33869 Revision 11  
Non-Proprietary Information

Assembly Type	Gadolinia -Urania Fuel Rod Number	<sup>235</sup> U Enrichment (wt%)	Poly Mass per Assembly (kg)	Pitch (cm)	Pellet Diameter (cm)	Clad ID (cm)	Clad OD (cm)	k <sub>eff</sub>	σ	k <sub>eff</sub> + 2σ <sup>a</sup>
FANP 9x9	4	3.8	11	1.510	0.96	1.02	1.09	0.9264	0.0007	0.9278
FANP 9x9	2	3.5	11	1.510	0.96	1.02	1.09	0.9257	0.0007	0.9271
FANP 9x9	0	3.0	11	1.510	0.96	1.02	1.09	0.9214	0.0008	0.9230
GNF 9x9	10	5.0	11	1.510	0.96	1.02	1.09	0.9151	0.0008	0.9167
GNF 9x9	8	4.8	11	1.510	0.96	1.02	1.09	0.9368	0.0009	<b>0.9386</b>
GNF 9x9	6	4.2	11	1.510	0.96	1.02	1.09	0.9294	0.0009	0.9312
GNF 9x9	4	3.8	11	1.510	0.96	1.02	1.09	0.9333	0.0007	0.9347
GNF 9x9	2	3.5	11	1.510	0.96	1.02	1.09	0.9311	0.0008	0.9327
GNF 9x9	0	3.0	11	1.510	0.96	1.02	1.09	0.9290	0.0008	0.9306
GNF 8x8	7	5.0	11	1.6923	1.05	1.10	1.17	0.9356	0.0008	<b>0.9372</b>
GNF 8x8	6	4.7	11	1.6923	1.05	1.10	1.17	0.9323	0.0009	0.9341
GNF 8x8	4	4.1	11	1.6923	1.05	1.10	1.17	0.9305	0.0008	0.9321
GNF 8x8	2	3.7	11	1.6923	1.05	1.10	1.17	0.9321	0.0008	0.9337
GNF 8x8	0	3.1	11	1.6923	1.05	1.10	1.17	0.9311	0.0008	0.9327
GNF 10x10 <sup>b</sup>	12	5.0	10.2	1.363	0.895	0.934	1.010	0.9295	0.0003	0.9300
GNF 10x10 <sup>b</sup>	11	4.9	10.2	1.363	0.895	0.934	1.010	0.9299	0.0003	0.9306
GNF 10x10 <sup>b</sup>	10	4.6	10.2	1.363	0.895	0.934	1.010	0.9320	0.0003	<b>0.9326</b>
GNF 10x10 <sup>b</sup>	9	4.5	10.2	1.363	0.895	0.934	1.010	0.9274	0.0003	0.9280
GNF 10x10 <sup>b</sup>	8	4.2	10.2	1.363	0.895	0.934	1.010	0.9285	0.0003	0.9290
GNF 10x10 <sup>b</sup>	7	3.9	10.2	1.363	0.895	0.934	1.010	0.9214	0.0003	0.9220
GNF 10x10 <sup>b</sup>	6	3.7	10.2	1.363	0.895	0.934	1.010	0.9271	0.0003	0.9276
GNF 10x10 <sup>b</sup>	5	3.6	10.2	1.363	0.895	0.934	1.010	0.9221	0.0003	0.9227
GNF 10x10 <sup>b</sup>	4	3.4	10.2	1.363	0.895	0.934	1.010	0.9270	0.0003	0.9276
GNF 10x10 <sup>b</sup>	3	3.3	10.2	1.363	0.895	0.934	1.010	0.9279	0.0002	0.9284
GNF 10x10 <sup>b</sup>	2	3.2	10.2	1.363	0.895	0.934	1.010	0.9276	0.0003	0.9282
GNF 10x10 <sup>b</sup>	1	3.1	10.2	1.363	0.895	0.934	1.010	0.9310	0.0002	0.9315
GNF 10x10 <sup>b</sup>	0	2.9	10.2	1.363	0.895	0.934	1.010	0.9302	0.0002	0.9307
GNF 10x10 <sup>c</sup>	22	8.0	10.2	1.363	0.895	0.934	1.010	0.9242	0.0003	0.9248
GNF 10x10 <sup>c</sup>	21	7.9	10.2	1.363	0.895	0.934	1.010	0.9280	0.0003	0.9286
GNF 10x10 <sup>c</sup>	20	7.6	10.2	1.363	0.895	0.934	1.010	0.9309	0.0003	0.9315
GNF 10x10 <sup>c</sup>	19	7.3	10.2	1.363	0.895	0.934	1.010	0.9262	0.0003	0.9268
GNF 10x10 <sup>c</sup>	18	7.0	10.2	1.363	0.895	0.934	1.010	0.9295	0.0003	0.9301
GNF 10x10 <sup>c</sup>	17	6.7	10.2	1.363	0.895	0.934	1.010	0.9229	0.0003	0.9235
GNF 10x10 <sup>c</sup>	16	6.5	10.2	1.363	0.895	0.934	1.010	0.9307	0.0003	0.9313
GNF 10x10 <sup>c</sup>	15	6.3	10.2	1.363	0.895	0.934	1.010	0.9259	0.0003	0.9265
GNF 10x10 <sup>c</sup>	14	6.0	10.2	1.363	0.895	0.934	1.010	0.9291	0.0003	0.9297
GNF 10x10 <sup>c</sup>	13	5.8	10.2	1.363	0.895	0.934	1.010	0.9270	0.0003	0.9276
GNF 10x10 <sup>c</sup>	12	5.5	10.2	1.363	0.895	0.934	1.010	0.9302	0.0003	0.9308
GNF 10x10 <sup>c</sup>	0	3.2	10.2	1.363	0.895	0.934	1.010	0.9317	0.0003	<b>0.9323</b>

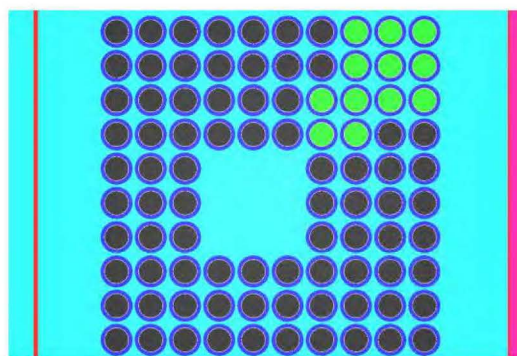
a. Limiting case(s) shown in bold

b. Cases do not include fuel channel, HAC package array (10x1x10), optimal moderation, polyethylene foam thickness of 1.28 cm (see Section 6.3.4.11)

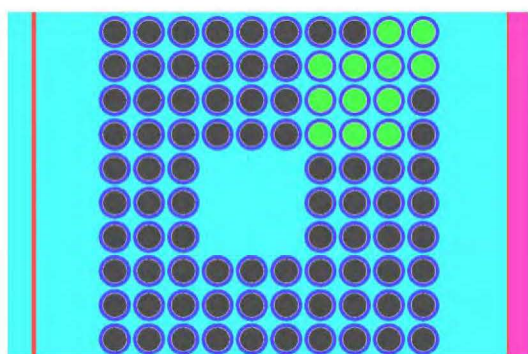
c. Cases do not include fuel channel, HAC package array (8x1x8), optimal moderation, polyethylene foam thickness of 1.14 cm (see Section 6.3.4.11)



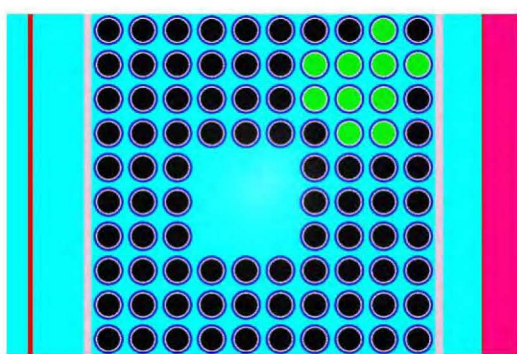
FANP 10x10 5.0 wt%  $^{235}\text{U}$ , Pattern B



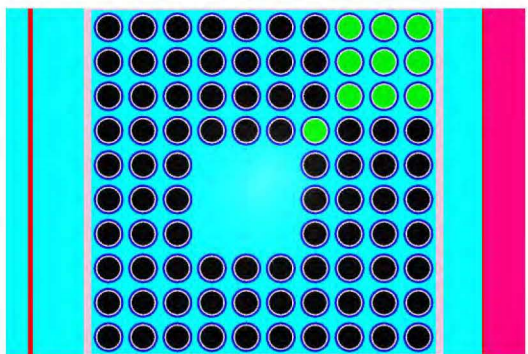
FANP 10x10 5.0 wt%  $^{235}\text{U}$ , Pattern F



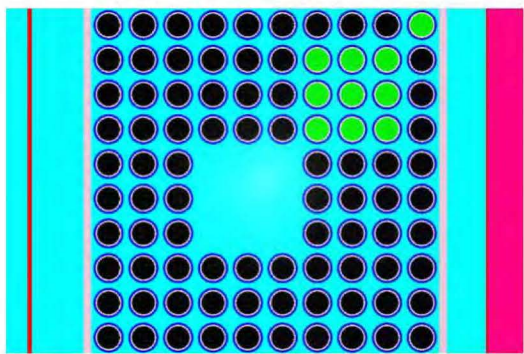
FANP 10x10 5.0 wt%  $^{235}\text{U}$ , Pattern G



FANP 10x10 4.6 wt%  $^{235}\text{U}$ , Pattern E



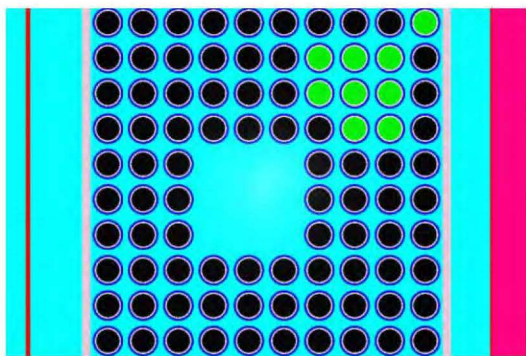
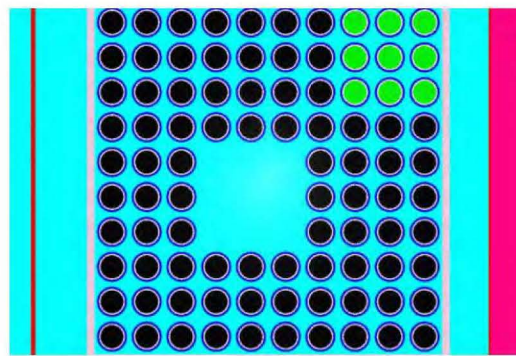
FANP 10x10 4.6 wt%  $^{235}\text{U}$ , Pattern F



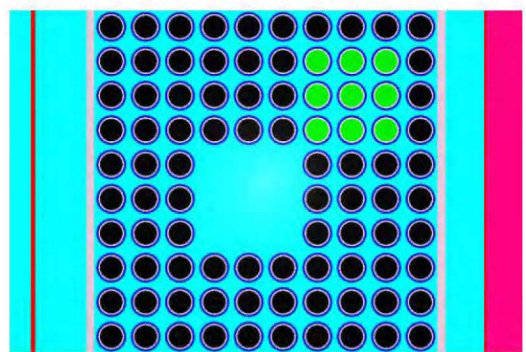
FANP 10x10 4.6 wt%  $^{235}\text{U}$ , Pattern G

Figure 6-34 Gadolinia-Urania Fuel Rod Placement Pattern for 10x10 Fuel Assemblies

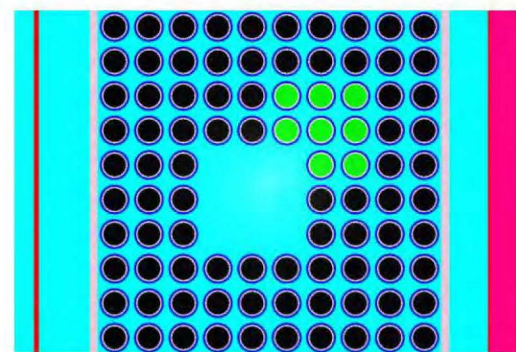
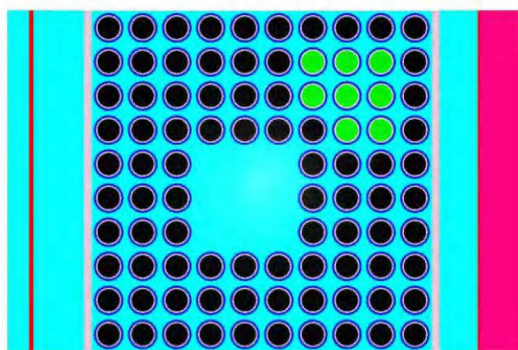
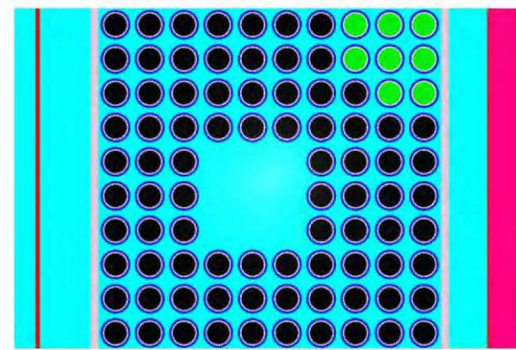


FANP 10x10 4.3 wt%  $^{235}\text{U}$ , Pattern E

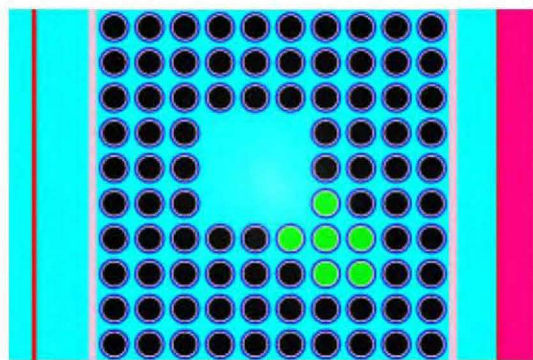
**FANP 10x10 4.3 wt%  $^{235}\text{U}$ , Pattern F**



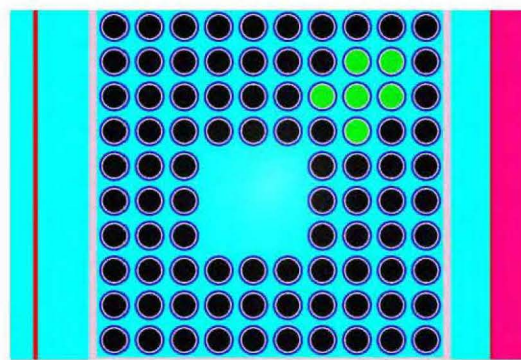
FANP 10x10 4.3 wt%  $^{235}\text{U}$ , Pattern G

FANP 10x10 4.2 wt% <sup>235</sup>U, Pattern DFANP 10x10 4.2 wt%  $^{235}\text{U}$ , Pattern EFANP 10x10 4.2 wt% <sup>235</sup>U, Pattern F

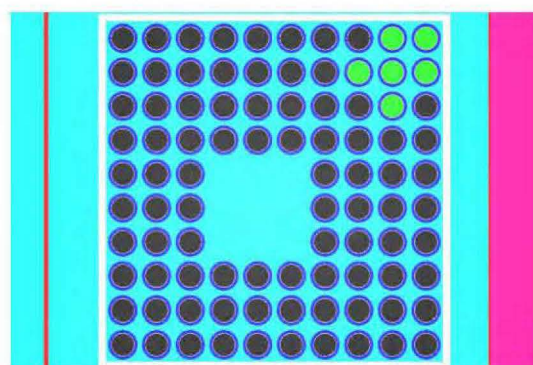
**Figure 6-34 Gadolinia-Urania Fuel Rod Placement Pattern for 10x10 Fuel Assemblies  
(Continued)**



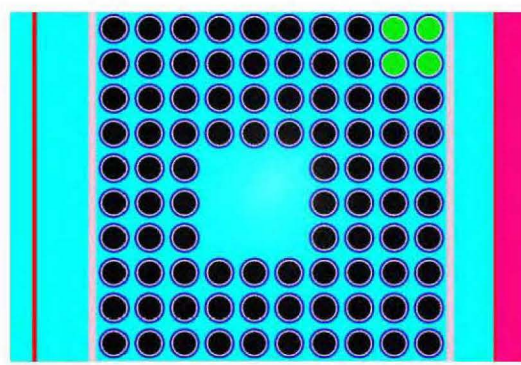
FANP 10x10 3.9 wt%  $^{235}\text{U}$ , Pattern E



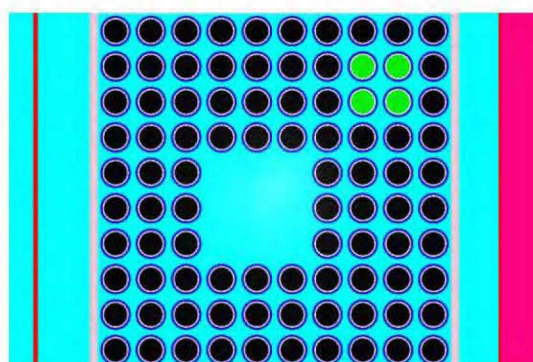
FANP 10x10 3.9 wt%  $^{235}\text{U}$ , Pattern F



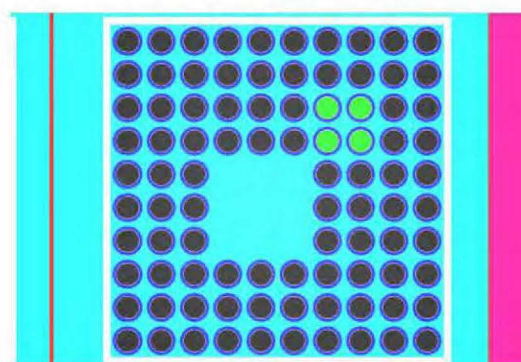
FANP 10x10 3.9 wt%  $^{235}\text{U}$ , Pattern G



FANP 10x10 3.6 wt%  $^{235}\text{U}$ , Pattern H



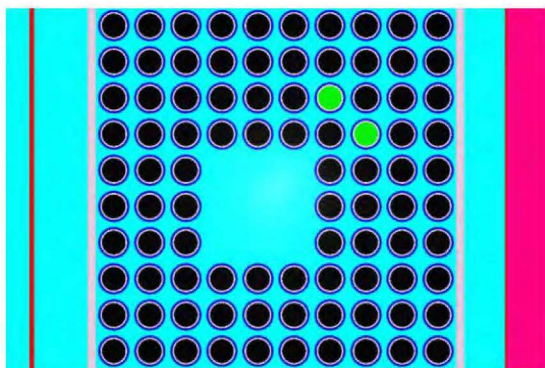
FANP 10x10 3.6 wt%  $^{235}\text{U}$ , Pattern I



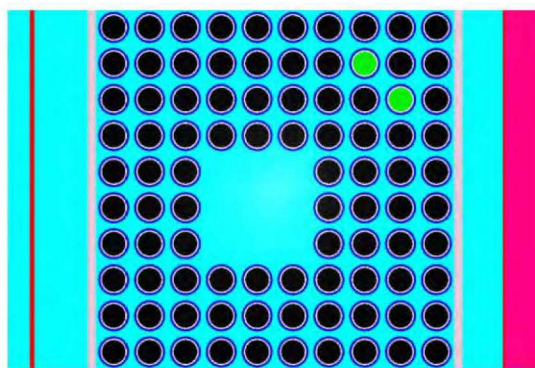
FANP 10x10 3.6 wt%  $^{235}\text{U}$ , Pattern J

Figure 6-34 Gadolinia-Urania Fuel Rod Placement Pattern for 10x10 Fuel Assemblies  
(Continued)

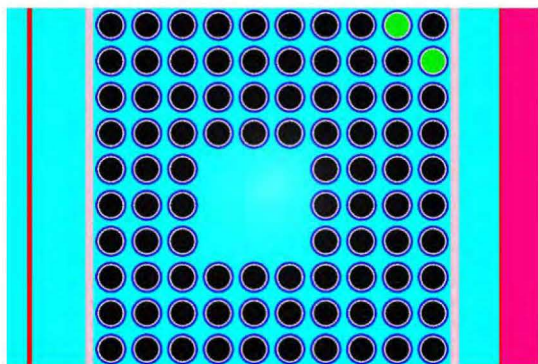




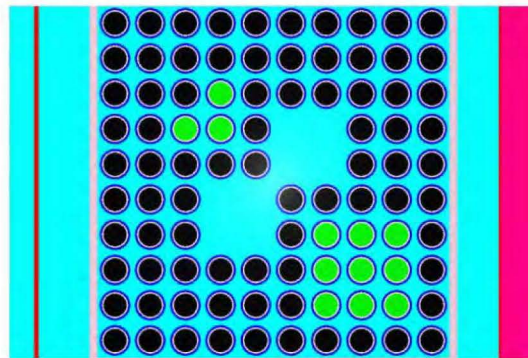
FANP 10x10 3.3 w1%  $^{235}\text{U}$ , Pattern F



FANP 10x10 3.3 w1%  $^{235}\text{U}$ , Pattern G

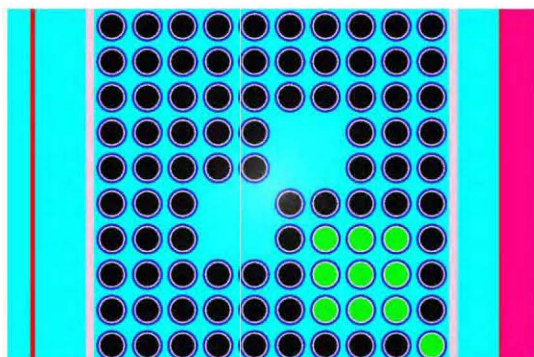


FANP 10x10 3.3 w1%  $^{235}\text{U}$ , Pattern H

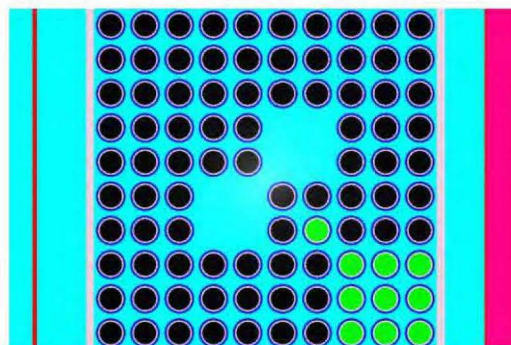


GNF 10x10 5.0 w1%  $^{235}\text{U}$ , Pattern B

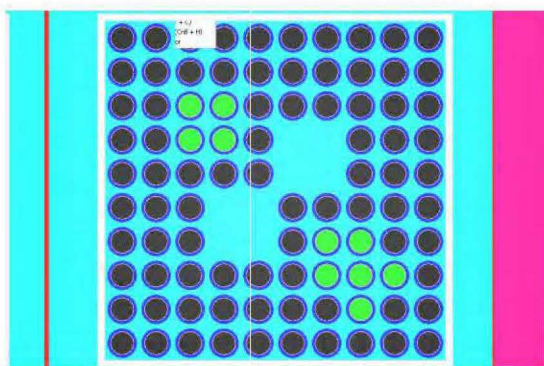
**Figure 6-34 Gadolinia-Urania Fuel Rod Placement Pattern for 10x10 Fuel Assemblies  
(Continued)**



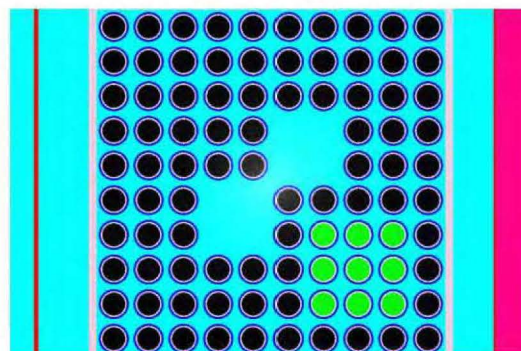
GNF 10x10 4.6 wt%  $^{235}\text{U}$ , Pattern F



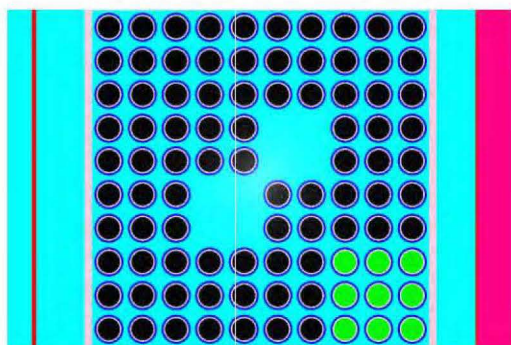
GNF 10x10 4.6 wt%  $^{235}\text{U}$ , Pattern G



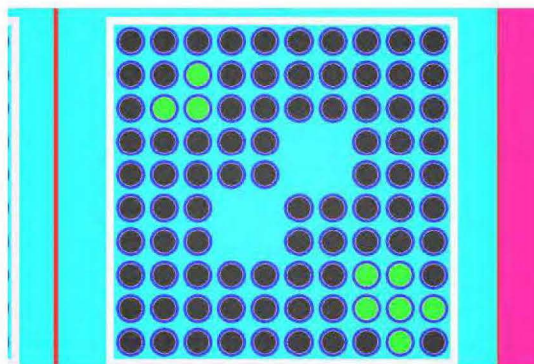
GNF 10x10 4.6 wt%  $^{235}\text{U}$ , Pattern I



GNF 10x10 4.3 wt%  $^{235}\text{U}$ , Pattern F



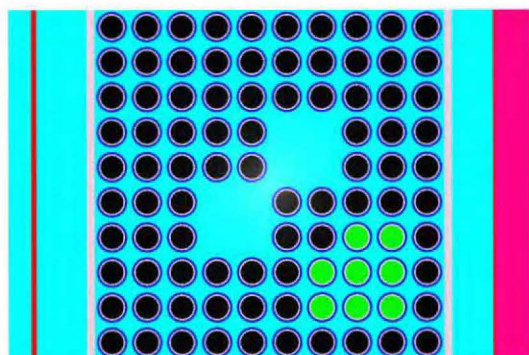
GNF 10x10 4.3 wt%  $^{235}\text{U}$ , Pattern G



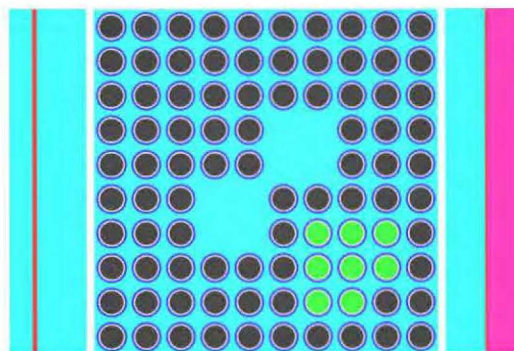
GNF 10x10 4.3 wt%  $^{235}\text{U}$ , Pattern J

**Figure 6-34 Gadolinia-Urania Fuel Rod Placement Pattern for 10x10 Fuel Assemblies (Continued)**

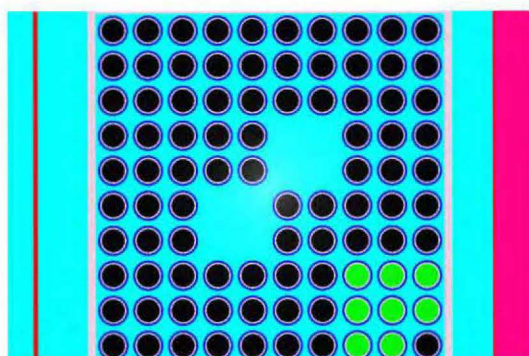




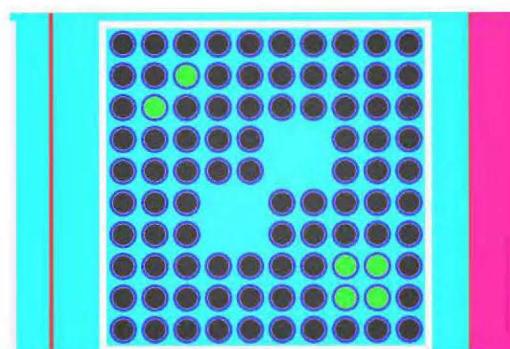
GNF 10x10 4.2 wt%  $^{235}\text{U}$ , Pattern F



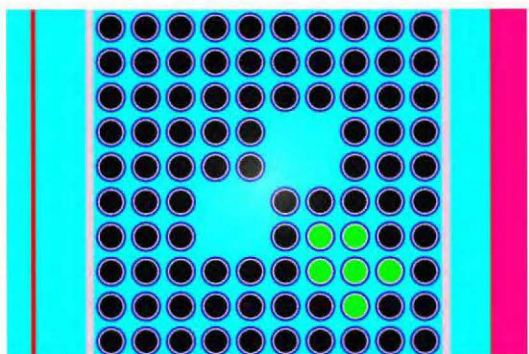
GNF 10x10 4.2 wt%  $^{235}\text{U}$ , Pattern I



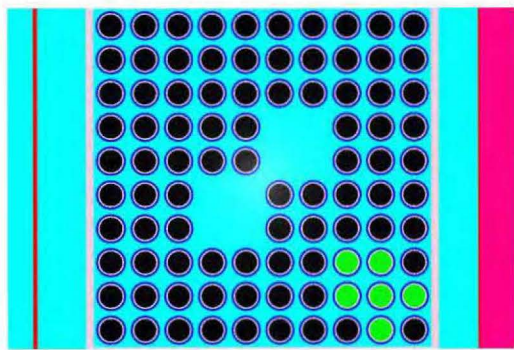
GNF 10x10 4.2 wt%  $^{235}\text{U}$ , Pattern J



GNF 10x10 3.9 wt%  $^{235}\text{U}$ , Pattern G

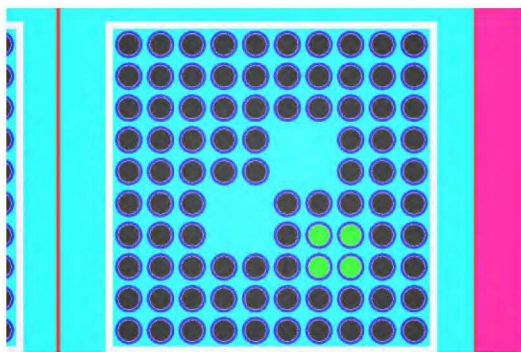


GNF 10x10 3.9 wt%  $^{235}\text{U}$ , Pattern J

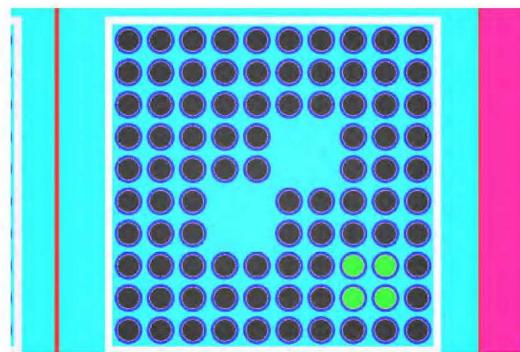


GNF 10x10 3.9 wt%  $^{235}\text{U}$ , Pattern K

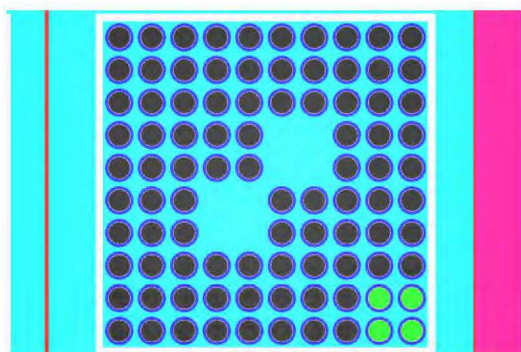
Figure 6-34 Gadolinia-Urania Fuel Rod Placement Pattern for 10x10 Fuel Assemblies  
(Continued)



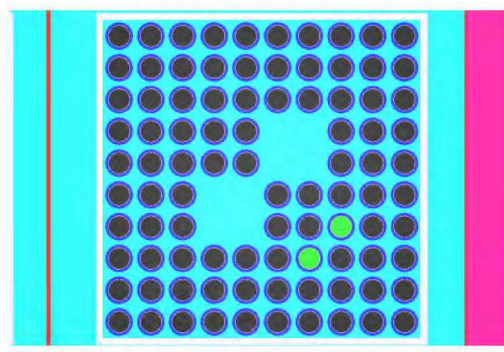
GNF 10x10 3.6 wt%  $^{235}\text{U}$ , Pattern F



GNF 10x10 3.6 wt%  $^{235}\text{U}$ , Pattern G



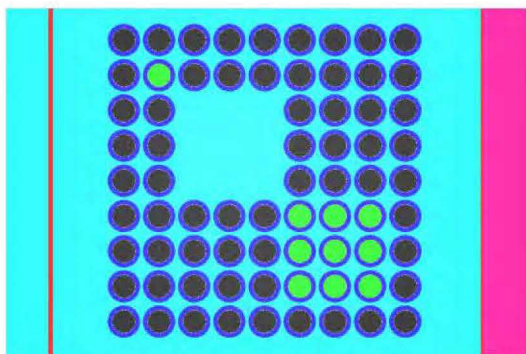
GNF 10x10 3.6 wt%  $^{235}\text{U}$ , Pattern H



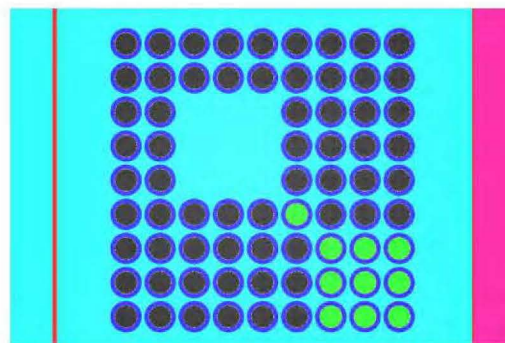
GNF 10x10 3.3 wt%  $^{235}\text{U}$ , Pattern A

**Figure 6-34 Gadolinia-Urania Fuel Rod Placement Pattern for 10x10 Fuel Assemblies  
(Continued)**

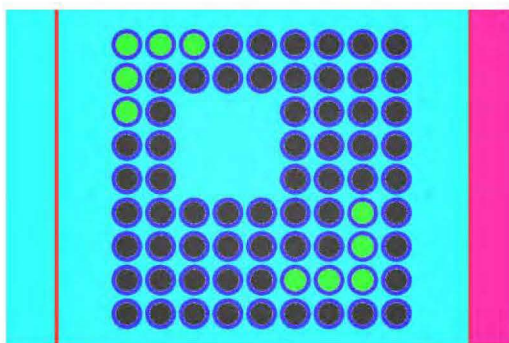




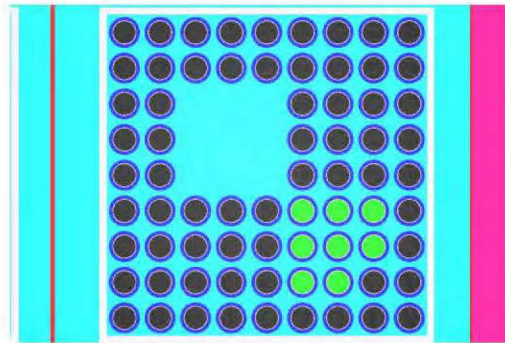
FANP 9x9 5.0 wt%  $^{235}\text{U}$ , Pattern A



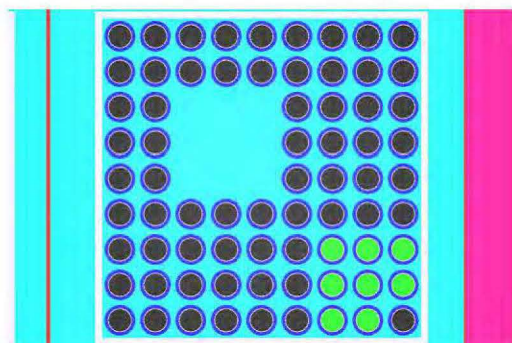
FANP 9x9 5.0 wt%  $^{235}\text{U}$ , Pattern B



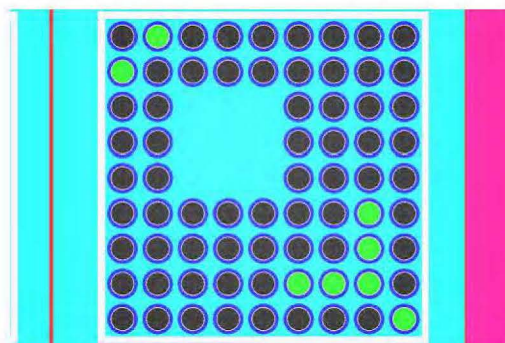
FANP 9x9 5.0 wt%  $^{235}\text{U}$ , Pattern E



FANP 9x9 4.7 wt%  $^{235}\text{U}$ , Pattern A

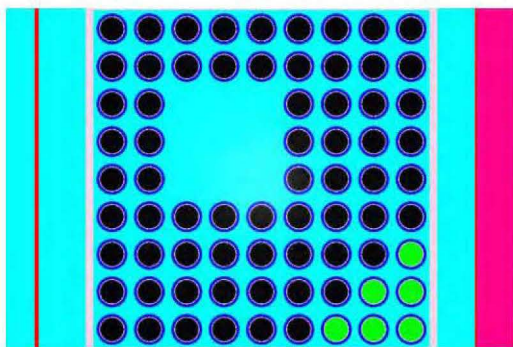


FANP 9x9 4.7 wt%  $^{235}\text{U}$ , Pattern B

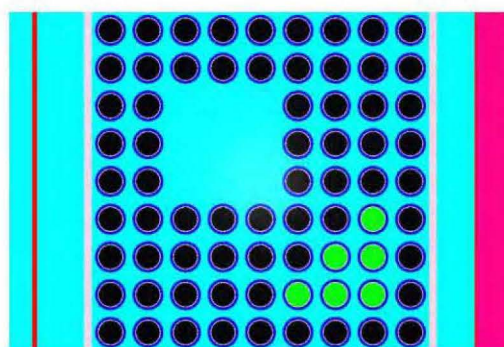


FANP 9x9 4.7 wt%  $^{235}\text{U}$ , Pattern E

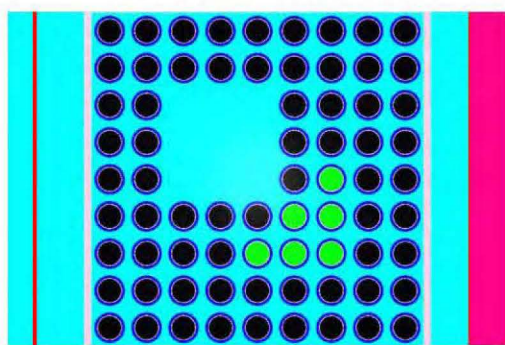
Figure 6-35 Gadolinia-Urania Fuel Rod Placement Pattern for 9x9 Fuel Assemblies



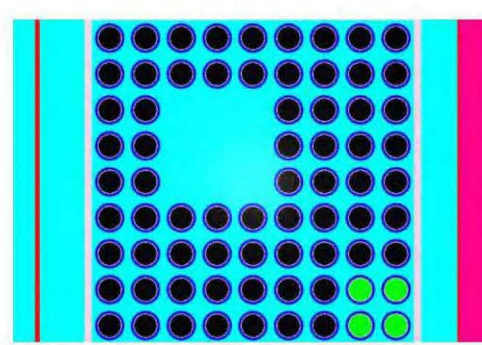
FANP 9x9 4.2 wt% U-235, Pattern A



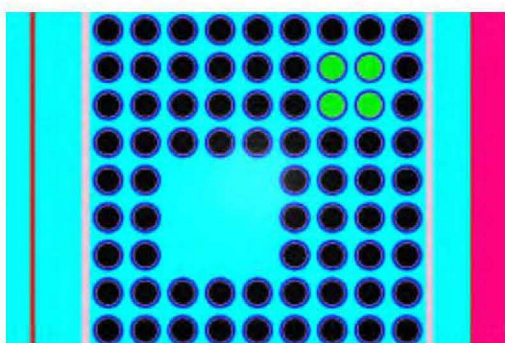
FANP 9x9 4.2 wt% U-235, Pattern B



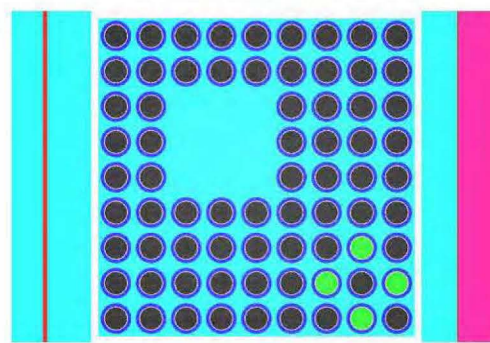
FANP 9x9 4.2 wt% U-235, Pattern C



FANP 9x9 3.8 wt% U-235, Pattern A



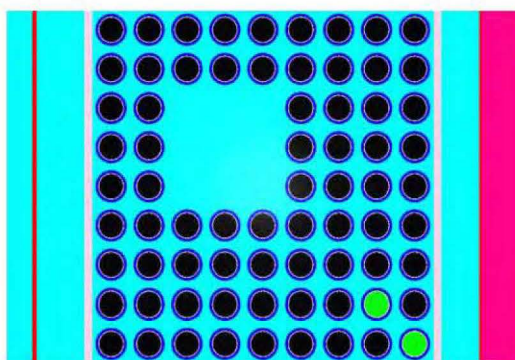
FANP 9x9 3.8 wt% U-235, Pattern B



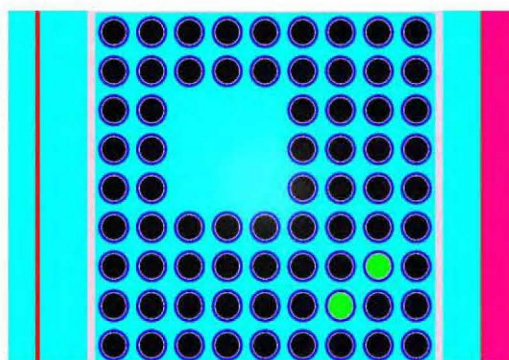
FANP 9x9 3.8 wt% U-235, Pattern F

Figure 6-35 Gadolinia-Urania Fuel Rod Placement Pattern for 9x9 Fuel Assemblies  
(Continued)

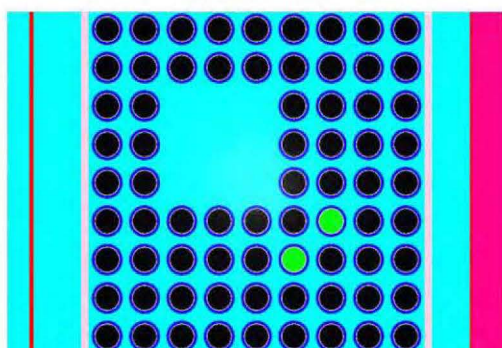




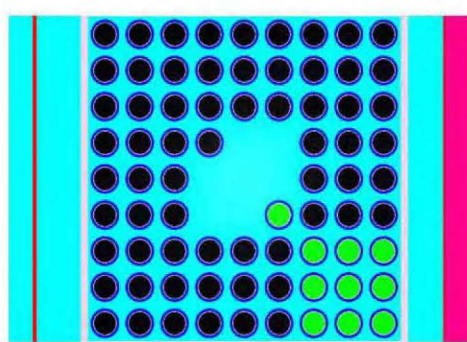
FANP 9x9 3.5 wt% U-235, Pattern B



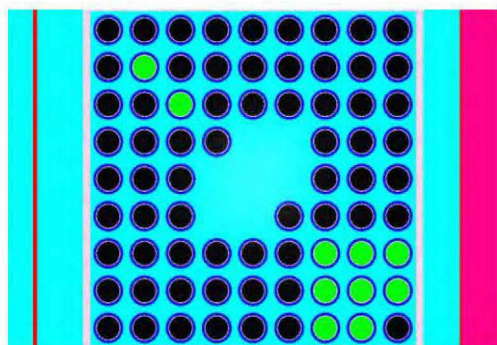
FANP 9x9 3.5 wt% U-235, Pattern C



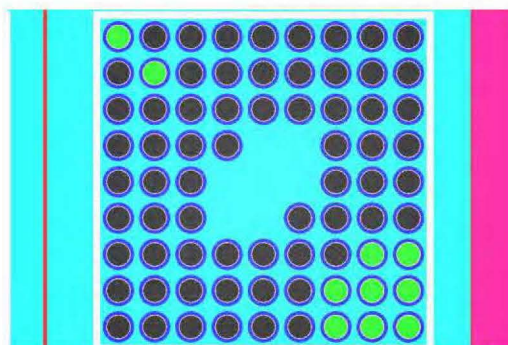
FANP 9x9 3.5 wt% U-235, Pattern D



GNF 9x9 5.0 wt% U-235, Pattern B

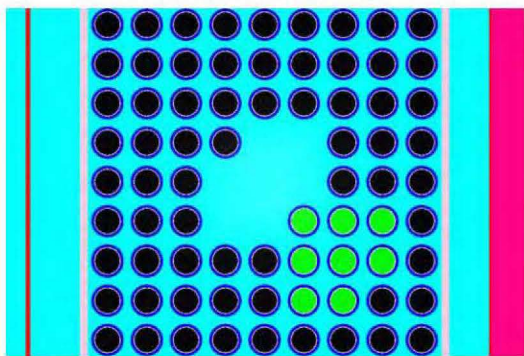


GNF 9x9 5.0 wt% U-235, Pattern G

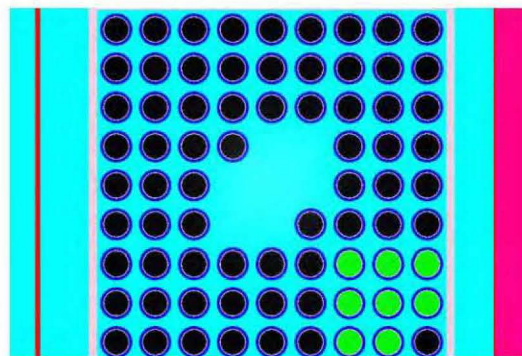


GNF 9x9 5.0 wt% U-235, Pattern H

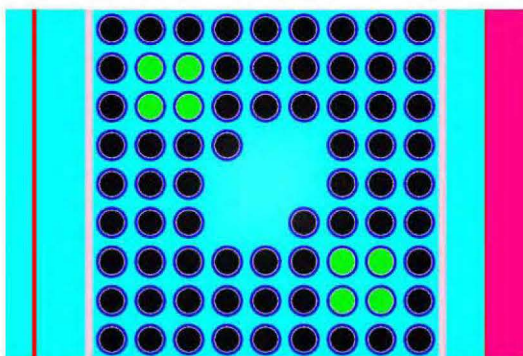
Figure 6-35 Gadolinia-Urania Fuel Rod Placement Pattern for 9x9 Fuel Assemblies  
(Continued)



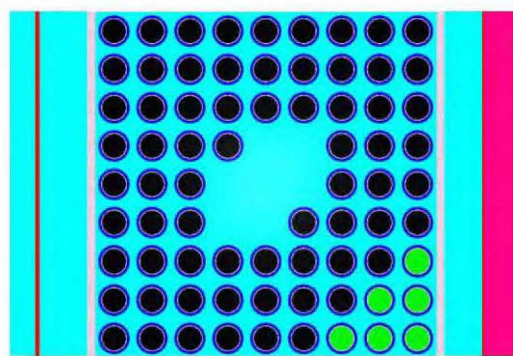
GNF 9x9 4.8 wt% U-235, Pattern A



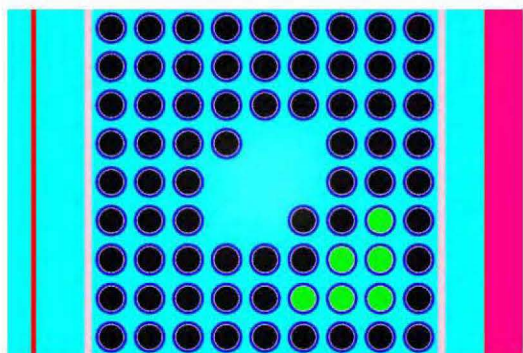
GNF 9x9 4.8 wt% U-235, Pattern B



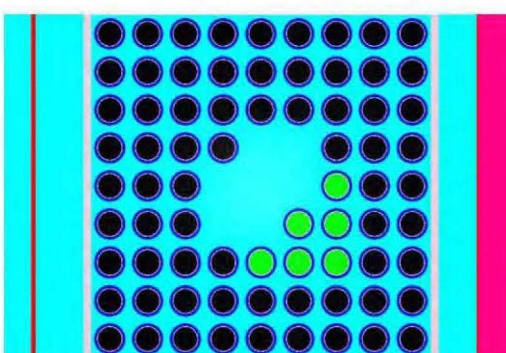
GNF 9x9 4.8 wt% U-235, Pattern H



GNF 9x9 4.2 wt% U-235, Pattern A



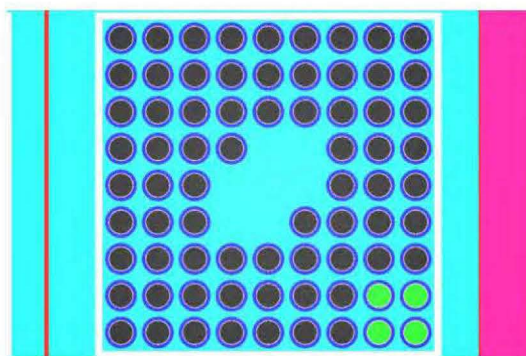
GNF 9x9 4.2 wt% U-235, Pattern B



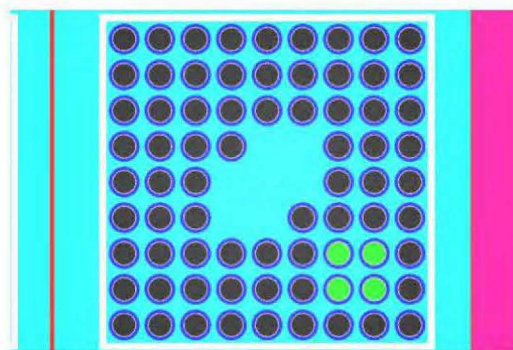
GNF 9x9 4.2 wt% U-235, Pattern C

Figure 6-35 Gadolinia-Urania Fuel Rod Placement Pattern for 9x9 Fuel Assemblies  
(Continued)

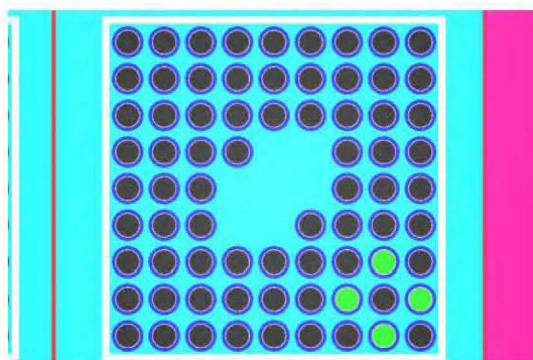




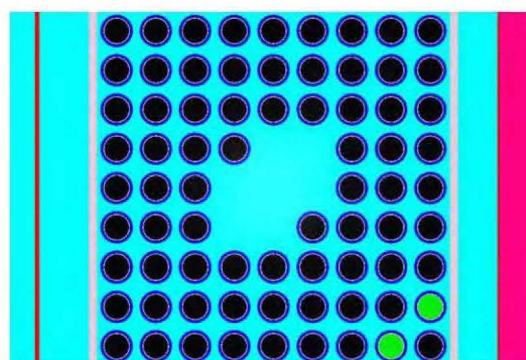
GNF 9x9 3.8 wt%  $^{235}\text{U}$ , Pattern A



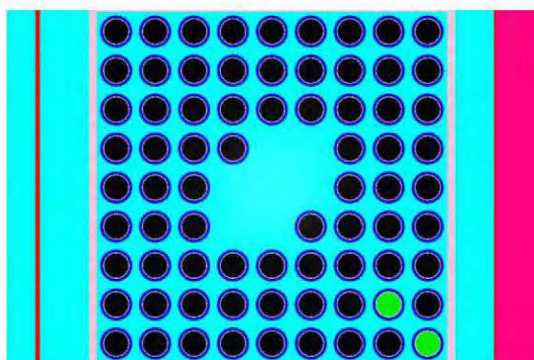
GNF 9x9 3.8 wt%  $^{235}\text{U}$ , Pattern B



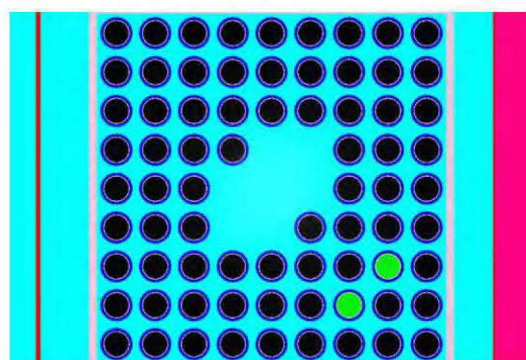
GNF 9x9 3.8 wt%  $^{235}\text{U}$ , Pattern F



GNF 9x9 3.5 wt%  $^{235}\text{U}$ , Pattern A

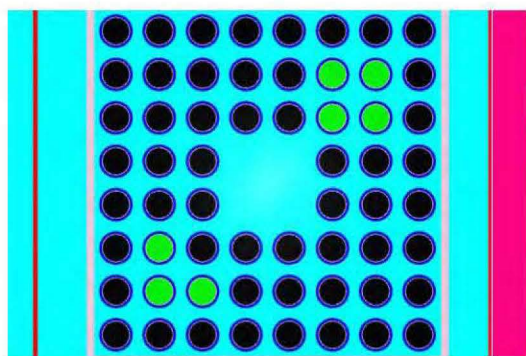


GNF 9x9 3.5 wt%  $^{235}\text{U}$ , Pattern B

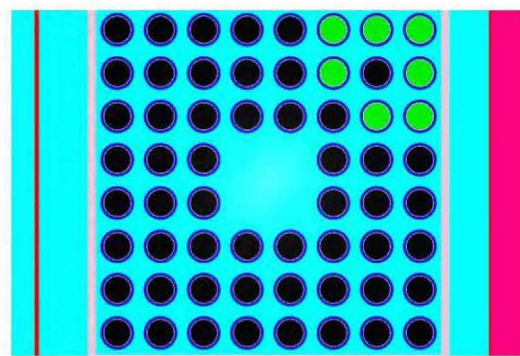


GNF 3.5 wt%  $^{235}\text{U}$ , Pattern C

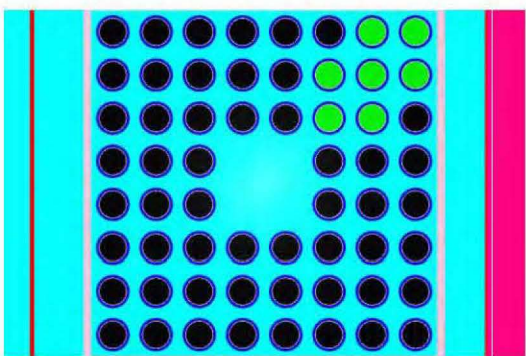
Figure 6-35 Gadolinia-Urania Fuel Rod Placement Pattern for 9x9 Fuel Assemblies  
(Continued)



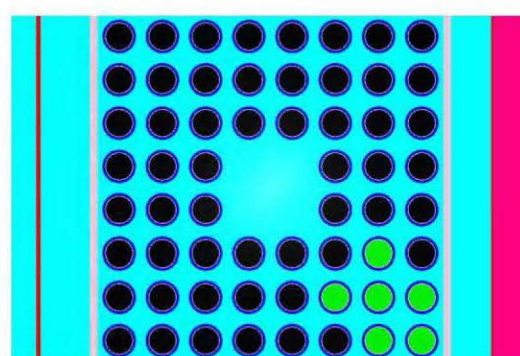
GNF 8x8 5.0 wt%  $^{235}\text{U}$ , Pattern E



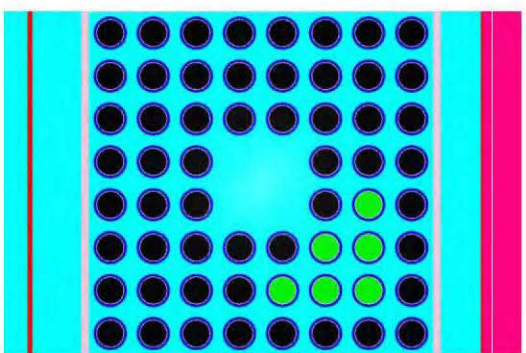
GNF 8x8 5.0 wt%  $^{235}\text{U}$ , Pattern H



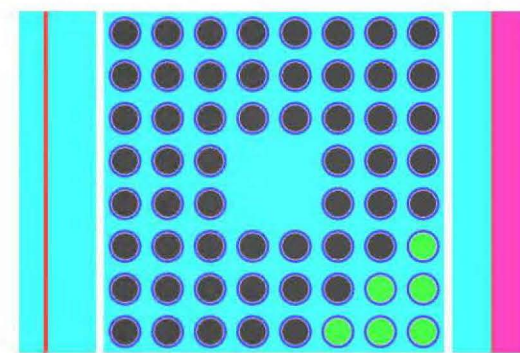
GNF 8x8 5.0 wt%  $^{235}\text{U}$ , Pattern I



GNF 8x8 4.7 wt%  $^{235}\text{U}$ , Pattern B



GNF 8x8 4.7 wt%  $^{235}\text{U}$ , Pattern C



GNF 8x8 4.7 wt%  $^{235}\text{U}$ , Pattern D

Figure 6-36 Gadolinia-Urania Fuel Rod Placement Pattern for 8x8 Fuel Assemblies



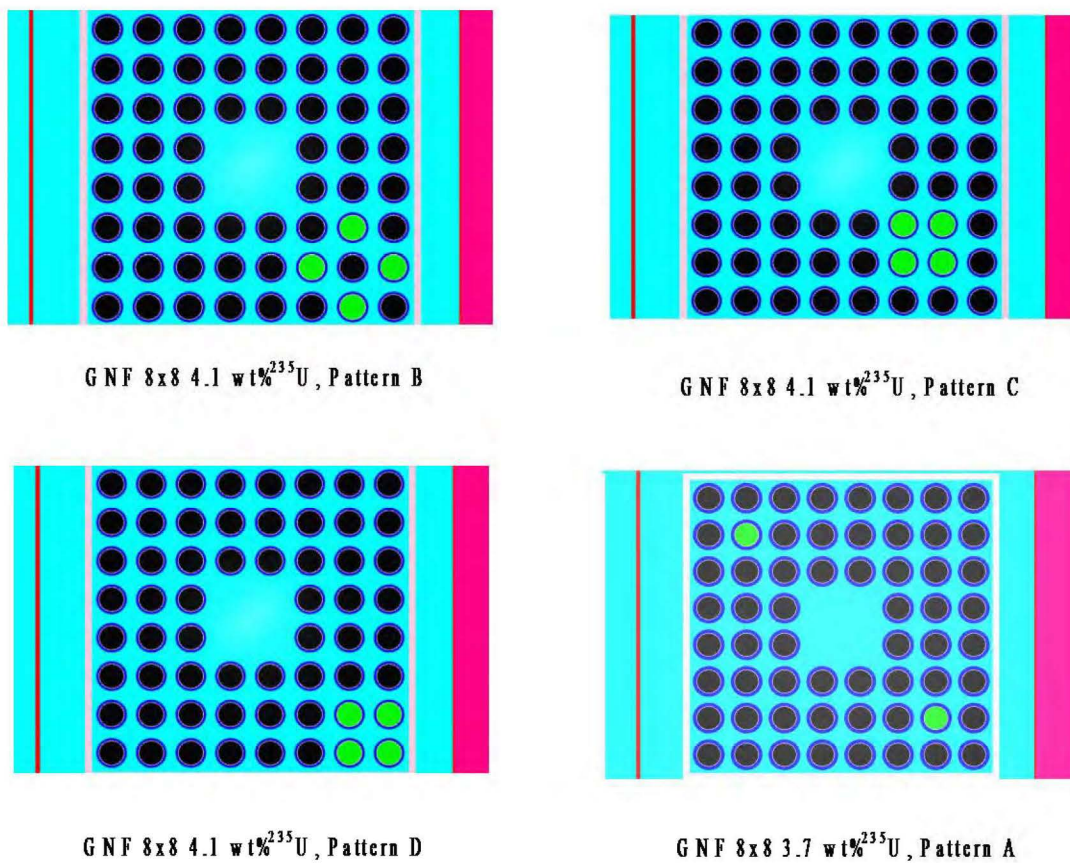


**Figure 6-36 Gadolinia-Urania Fuel Rod Placement Pattern for 8x8 Fuel Assemblies  
(Continued)**

#### 6.3.4.9 Part Length Fuel Rod Study (2N=448)

The FANP 10x10, FANP 9x9, GNF 10x10, and GNF 9x9 worst case designs are used to investigate the effect that part length fuel rods have on system reactivity. The worst case part length fuel rod patterns identified by performing scoping studies for the 10x10 designs are shown in Figure 6-37 and Figure 6-38. The worst case part length fuel rod patterns identified by performing scoping studies for the 9x9 designs are shown in Figure 6-39 and Figure 6-40. The fuel rod lengths for the part length rods are half that of the normal rod, and calculations showed that reducing the length further decreases system reactivity. To maintain the same amount of polyethylene when the part length rods are inserted, the polyethylene is redistributed to all rods in the assembly. The worst case models from the moderator density sensitivity study are used to conduct the part length fuel rod study, and the worst case fuel parameters listed in Table 6-16 are utilized. The part length fuel rod study results are contained in Table 6-17. All results for the FANP 9x9, the FANP 10x10, and the GNF 9x9 are below the USL of 0.94254. Several cases for the GNF 10x10 fuel design are above the USL of 0.94254. Therefore, an increased clad thickness is investigated for the 10x10 designs to reduce the system reactivity; these cases are included at the end of Table 6-17. The increased clad thickness for the 10x10 designs reduce system reactivity, and all 10x10 results are below the USL of 0.94254. Comparing the results in Table 6-17 with those in Table 6-16 reveals the system reactivity remains about the same for the 9x9 fuel assembly designs with part length fuel rods. The FANP 10x10 and GNF 10x10 fuel designs are more reactive with the part length fuel rod configuration. Based on the results in Table 6-16 and Table 6-17.

- The maximum system reactivity with FANP 10x10 fuel assemblies having part length fuel rods and gadolinia-urania fuel is statistically greater than the maximum system reactivity with FANP 10x10 fuel assemblies having gadolinia-urania fuel and no part length fuel rods. The configuration that yields the highest  $k_{\text{eff}} + 2\sigma$  consists of fuel assemblies with a lattice average enrichment of 5.0 wt% U-235, 12 gadolinia-urania fuel rods enriched to 2.0 wt% gadolinia arranged in Pattern G, and 10 part length fuel rods. With the clad thickness for the fuel assemblies increased from 0.0335 cm to 0.0381 cm, the  $k_{\text{eff}} + 2\sigma$  for this configuration is 0.9394.
- The maximum system reactivity with GNF 10x10 fuel assemblies having part length fuel rods and gadolinia-urania fuel is statistically greater than the maximum system reactivity with GNF 10x10 fuel assemblies having gadolinia-urania fuel and no part length fuel rods. The configuration that yields the highest  $k_{\text{eff}} + 2\sigma$  consists of fuel assemblies with a lattice average enrichment of 5.0 wt% U-235, 12 gadolinia-urania fuel rods enriched to 2.0 wt% gadolinia arranged in Pattern H, and 12 part length fuel rods. With the clad thickness for the fuel assemblies increased from 0.0335 cm to 0.0381 cm, the  $k_{\text{eff}} + 2\sigma$  for this configuration is 0.9418.
- Based on fuel parameter changes made to the 10x10 designs to lower reactivity, a 0.9338 cm upper bound clad ID, and a 1.01 cm lower bound clad OD are established for the GNF 10x10 parameter ranges. The 0.9330 cm upper bound clad ID and 1.00 cm lower bound clad OD may still be used for the FANP 10x10 design because the fuel assembly with this configuration remained below the USL of 0.94254.

NEDO-33869 Revision 11  
Non-Proprietary Information

- The most reactive FANP 9x9 configuration consists of fuel assemblies with a lattice average enrichment of 4.7 wt% U-235 and 8 gadolinia-urania fuel rods enriched to 2.0 wt% gadolinia arranged in Pattern A and 8 part length rods. The  $k_{\text{eff}} + 2\sigma$  for this configuration is 0.9303.
- The most reactive GNF 9x9 configuration consists of fuel assemblies with a lattice average enrichment of 4.7 wt% U-235 and 8 gadolinia-urania fuel rods enriched to 2.0 wt% gadolinia arranged in Pattern B and 8 part length fuel rods. The  $k_{\text{eff}} + 2\sigma$  for this configuration is 0.9407.
- The most reactive GNF 8x8 configuration consists of fuel assemblies with a lattice average enrichment of 5.0 wt% U-235, 7 gadolinia-urania fuel rods enriched to 2.0 wt% gadolinia arranged in Pattern I, and no part length fuel rods. The  $k_{\text{eff}} + 2\sigma$  for this configuration is 0.9372 (Table 6-16). The GNF 8x8 fuel assembly is not evaluated for part length fuel rods.

The GNF 10x10 assembly is chosen as the overall bounding fuel type because the  $k_{\text{eff}} + 2\sigma$  is among the largest numerical values; however, the system reactivity of the 10x10, and 9x9 worst case fuel assembly designs in the 14x2x16 RAJ-II package array, as presented in Table 6-16, are statistically indistinguishable.

The results presented in Table 6-17 are for GNF 10x10 designs with two 2x2 off center diagonal water rods and up to fourteen part length fuel rods. To confirm that the GNF 10x10 design is the limiting design, various fuel designs were analyzed with KENO-VI and continuous energy ENDF/B-VII library using the as-designed part length rod configurations without any gadolinia rods to compare the relative reactivity. These designs include 8x8, 9x9, and 10x10 (both GNF and FANP products); the 10x10 designs have various water rod geometries such as a single axially varying water rod centrally located within the fuel rod array, two 2x2 off-center diagonal and 3x3, and also includes different number of part length rods between 8 and 16. The KENO-VI results for each assembly type are provided in Table 6-18. Table 6-18 results are based on the parameters listed in Table 6-1 using rod pitch of 1.350 cm. The part length rod locations for various GNF 10x10 designs are provided in Reference 6-3, which confirms that the limiting GNF 10x10 design is the one with a single axially varying water rod centrally located within the fuel rod array and sixteen part length rods.

**Table 6-17 RAJ-II Array HAC Part Length Fuel Rod Calculations**

Assembly Type	Number of Part Length Rods	Gadolinia -Urania Fuel Rod Number	<sup>235</sup> U Enrichment (wt%)	Pitch (cm)	Pellet Diameter (cm)	Clad ID (cm)	Clad OD (cm)	k <sub>eff</sub>	σ	k <sub>eff</sub> + 2σ
FANP 10x10	8	0	2.9	1.350	0.895	0.933	1.00	0.9228	0.0008	0.9244
FANP 10x10	8	2	3.3	1.350	0.895	0.933	1.00	0.9282	0.0008	0.9298
FANP 10x10	8	4	3.6	1.350	0.895	0.933	1.00	0.9332	0.0008	0.9348
FANP 10x10	8	6	3.9	1.350	0.895	0.933	1.00	0.9327	0.0008	0.9343
FANP 10x10	8	8	4.2	1.350	0.895	0.933	1.00	0.9367	0.0008	0.9383
FANP 10x10	8	9	4.3	1.350	0.895	0.933	1.00	0.9282	0.0008	0.9298
FANP 10x10	8	10	4.6	1.350	0.895	0.933	1.00	0.9363	0.0009	0.9381
FANP 10x10	8	12	5.0	1.350	0.895	0.933	1.00	0.9403	0.0008	<b>0.9419</b>
FANP 10x10	10	0	2.9	1.350	0.895	0.933	1.00	0.9224	0.0008	0.9240
FANP 10x10	10	2	3.3	1.350	0.895	0.933	1.00	0.9283	0.0008	0.9299
FANP 10x10	10	4	3.6	1.350	0.895	0.933	1.00	0.9330	0.0007	0.9344
FANP 10x10	10	6	3.9	1.350	0.895	0.933	1.00	0.9333	0.0008	0.9349
FANP 10x10	10	8	4.2	1.350	0.895	0.933	1.00	0.9367	0.0008	0.9383
FANP 10x10	10	9	4.3	1.350	0.895	0.933	1.00	0.9301	0.0008	0.9317
FANP 10x10	10	10	4.6	1.350	0.895	0.933	1.00	0.9379	0.0009	0.9397
FANP 10x10	10	12	5.0	1.350	0.895	0.933	1.00	0.9399	0.0008	<b>0.9415</b>
FANP 10x10	12	0	2.9	1.350	0.895	0.933	1.00	0.9234	0.0008	0.9250
FANP 10x10	12	2	3.3	1.350	0.895	0.933	1.00	0.9281	0.0008	0.9297
FANP 10x10	12	4	3.6	1.350	0.895	0.933	1.00	0.9329	0.0008	0.9345
FANP 10x10	12	6	3.9	1.350	0.895	0.933	1.00	0.9319	0.0008	0.9335
FANP 10x10	12	8	4.2	1.350	0.895	0.933	1.00	0.9356	0.0008	0.9372
FANP 10x10	12	9	4.3	1.350	0.895	0.933	1.00	0.9294	0.0007	0.9308
FANP 10x10	12	10	4.6	1.350	0.895	0.933	1.00	0.9371	0.0008	0.9387
FANP 10x10	12	12	5.0	1.350	0.895	0.933	1.00	0.9404	0.0009	<b>0.9422</b>
FANP 10x10	14	0	2.9	1.350	0.895	0.933	1.00	0.9225	0.0008	0.9241
FANP 10x10	14	2	3.3	1.350	0.895	0.933	1.00	0.9274	0.0008	0.9290
FANP 10x10	14	4	3.6	1.350	0.895	0.933	1.00	0.9326	0.0009	0.9344
FANP 10x10	14	6	3.9	1.350	0.895	0.933	1.00	0.9313	0.0008	0.9329
FANP 10x10	14	8	4.2	1.350	0.895	0.933	1.00	0.9348	0.0010	0.9368
FANP 10x10	14	9	4.3	1.350	0.895	0.933	1.00	0.9310	0.0008	0.9326
FANP 10x10	14	10	4.6	1.350	0.895	0.933	1.00	0.9371	0.0008	0.9387
FANP 10x10	14	12	5.0	1.350	0.895	0.933	1.00	0.9393	0.0009	<b>0.9411</b>
GNF 10x10	8	0	2.9	1.350	0.895	0.933	1.00	0.9321	0.0007	0.9335
GNF 10x10	8	2	3.3	1.350	0.895	0.933	1.00	0.9327	0.0007	0.9341
GNF 10x10	8	4	3.6	1.350	0.895	0.933	1.00	0.9395	0.0010	0.9415
GNF 10x10	8	6	3.9	1.350	0.895	0.933	1.00	0.9367	0.0008	0.9383
GNF 10x10	8	8	4.2	1.350	0.895	0.933	1.00	0.9402	0.0008	<b>0.9418</b>
GNF 10x10	8	9	4.3	1.350	0.895	0.933	1.00	0.9369	0.0009	0.9387
GNF 10x10	8	10	4.6	1.350	0.895	0.933	1.00	0.9376	0.0009	0.9394
GNF 10x10	8	12	5.0	1.350	0.895	0.933	1.00	0.9386	0.0010	0.9406
GNF 10x10	10	0	2.9	1.350	0.895	0.933	1.00	0.9300	0.0008	0.9316
GNF 10x10	10	2	3.3	1.350	0.895	0.933	1.00	0.9319	0.0008	0.9335
GNF 10x10	10	4	3.6	1.350	0.895	0.933	1.00	0.9380	0.0009	0.9398
GNF 10x10	10	6	3.9	1.350	0.895	0.933	1.00	0.9347	0.0008	0.9363

**Table 6-17 RAJ-II Array HAC Part Length Fuel Rod Calculations**

Assembly Type	Number of Part Length Rods	Gadolinia -Urania Fuel Rod Number	<sup>235</sup> U Enrichment (wt%)	Pitch (cm)	Pellet Diameter (cm)	Clad ID (cm)	Clad OD (cm)	k <sub>eff</sub>	σ	k <sub>eff</sub> + 2σ
GNF 10x10	10	8	4.2	1.350	0.895	0.933	1.00	0.9419	0.0010	<b>0.9439</b>
GNF 10x10	10	9	4.3	1.350	0.895	0.933	1.00	0.9374	0.0008	0.9390
GNF 10x10	10	10	4.6	1.350	0.895	0.933	1.00	0.9385	0.0009	0.9403
GNF 10x10	10	12	5.0	1.350	0.895	0.933	1.00	0.9412	0.0008	0.9428
GNF 10x10	12	0	2.9	1.350	0.895	0.933	1.00	0.9300	0.0007	0.9314
GNF 10x10	12	2	3.3	1.350	0.895	0.933	1.00	0.9316	0.0007	0.9330
GNF 10x10	12	4	3.6	1.350	0.895	0.933	1.00	0.9377	0.0009	0.9395
GNF 10x10	12	6	3.9	1.350	0.895	0.933	1.00	0.9352	0.0008	0.9368
GNF 10x10	12	8	4.2	1.350	0.895	0.933	1.00	0.9408	0.0009	0.9426
GNF 10x10	12	9	4.3	1.350	0.895	0.933	1.00	0.9374	0.0008	0.9390
GNF 10x10	12	10	4.6	1.350	0.895	0.933	1.00	0.9406	0.0009	0.9424
GNF 10x10	12	12	5.0	1.350	0.895	0.933	1.00	0.9415	0.0008	<b>0.9431</b>
GNF 10x10	14	0	2.9	1.350	0.895	0.933	1.00	0.9277	0.0008	0.9293
GNF 10x10	14	2	3.3	1.350	0.895	0.933	1.00	0.9305	0.0008	0.9321
GNF 10x10	14	4	3.6	1.350	0.895	0.933	1.00	0.9374	0.0009	0.9392
GNF 10x10	14	6	3.9	1.350	0.895	0.933	1.00	0.9347	0.0008	0.9363
GNF 10x10	14	8	4.2	1.350	0.895	0.933	1.00	0.9401	0.0009	<b>0.9419</b>
GNF 10x10	14	9	4.3	1.350	0.895	0.933	1.00	0.9370	0.0009	0.9388
GNF 10x10	14	10	4.6	1.350	0.895	0.933	1.00	0.9381	0.0009	0.9399
GNF 10x10	14	12	5.0	1.350	0.895	0.933	1.00	0.9401	0.0008	0.9417
FANP 9x9	8	0	3.0	1.510	0.96	1.02	1.09	0.9168	0.0008	0.9184
FANP 9x9	8	2	3.5	1.510	0.96	1.02	1.09	0.9219	0.0008	0.9235
FANP 9x9	8	4	3.8	1.510	0.96	1.02	1.09	0.9234	0.0009	0.9252
FANP 9x9	8	6	4.2	1.510	0.96	1.02	1.09	0.9227	0.0007	0.9241
FANP 9x9	8	8	4.7	1.510	0.96	1.02	1.09	0.9287	0.0008	<b>0.9303</b>
FANP 9x9	8	10	5.0	1.510	0.96	1.02	1.09	0.9165	0.0008	0.9181
FANP 9x9	10	0	3.0	1.510	0.96	1.02	1.09	0.9139	0.0008	0.9155
FANP 9x9	10	2	3.5	1.510	0.96	1.02	1.09	0.9195	0.0008	0.9211
FANP 9x9	10	4	3.8	1.510	0.96	1.02	1.09	0.9189	0.0008	0.9205
FANP 9x9	10	6	4.2	1.510	0.96	1.02	1.09	0.9208	0.0008	0.9224
FANP 9x9	10	8	4.7	1.510	0.96	1.02	1.09	0.9256	0.0009	<b>0.9274</b>
FANP 9x9	10	10	5.0	1.510	0.96	1.02	1.09	0.9135	0.0009	0.9153
FANP 9x9	12	0	3.0	1.510	0.96	1.02	1.09	0.9100	0.0007	0.9114
FANP 9x9	12	2	3.5	1.510	0.96	1.02	1.09	0.9155	0.0007	0.9169
FANP 9x9	12	4	3.8	1.510	0.96	1.02	1.09	0.9168	0.0008	0.9184
FANP 9x9	12	6	4.2	1.510	0.96	1.02	1.09	0.9147	0.0007	0.9161
FANP 9x9	12	8	4.7	1.510	0.96	1.02	1.09	0.9208	0.0008	<b>0.9224</b>
FANP 9x9	12	10	5.0	1.510	0.96	1.02	1.09	0.9087	0.0009	0.9105
GNF 9x9	8	0	3.0	1.510	0.96	1.02	1.09	0.9261	0.0008	0.9277
GNF 9x9	8	2	3.5	1.510	0.96	1.02	1.09	0.9311	0.0008	0.9327
GNF 9x9	8	4	3.8	1.510	0.96	1.02	1.09	0.9303	0.0008	0.9319
GNF 9x9	8	6	4.2	1.510	0.96	1.02	1.09	0.9293	0.0008	0.9309
GNF 9x9	8	8	4.7	1.510	0.96	1.02	1.09	0.9391	0.0008	<b>0.9407</b>
GNF 9x9	8	10	5.0	1.510	0.96	1.02	1.09	0.9140	0.0008	0.9156

**Table 6-17 RAJ-II Array HAC Part Length Fuel Rod Calculations**

Assembly Type	Number of Part Length Rods	Gadolinia -Urania Fuel Rod Number	<sup>235</sup> U Enrichment (wt%)	Pitch (cm)	Pellet Diameter (cm)	Clad ID (cm)	Clad OD (cm)	k <sub>eff</sub>	σ	k <sub>eff</sub> + 2σ
GNF 9x9	10	0	3.0	1.510	0.96	1.02	1.09	0.9249	0.0009	0.9267
GNF 9x9	10	2	3.5	1.510	0.96	1.02	1.09	0.9315	0.0008	0.9331
GNF 9x9	10	4	3.8	1.510	0.96	1.02	1.09	0.9287	0.0008	0.9303
GNF 9x9	10	6	4.2	1.510	0.96	1.02	1.09	0.9297	0.0009	0.9315
GNF 9x9	10	8	4.7	1.510	0.96	1.02	1.09	0.9377	0.0008	<b>0.9393</b>
GNF 9x9	10	10	5.0	1.510	0.96	1.02	1.09	0.9048	0.0008	0.9064
GNF 9x9	12	0	3.0	1.510	0.96	1.02	1.09	0.9235	0.0008	0.9251
GNF 9x9	12	2	3.5	1.510	0.96	1.02	1.09	0.9294	0.0009	0.9312
GNF 9x9	12	4	3.8	1.510	0.96	1.02	1.09	0.9288	0.0009	0.9306
GNF 9x9	12	6	4.2	1.510	0.96	1.02	1.09	0.9263	0.0008	0.9279
GNF 9x9	12	8	4.7	1.510	0.96	1.02	1.09	0.9370	0.0009	<b>0.9388</b>
GNF 9x9	12	10	5.0	1.510	0.96	1.02	1.09	0.9056	0.0008	0.9072
FANP 10x10	8	0	2.9	1.350	0.895	0.9338	1.01	0.9203	0.0008	0.9219
FANP 10x10	8	2	3.3	1.350	0.895	0.9338	1.01	0.9150	0.0008	0.9166
FANP 10x10	8	4	3.6	1.350	0.895	0.9338	1.01	0.9290	0.0008	0.9306
FANP 10x10	8	6	3.9	1.350	0.895	0.9338	1.01	0.9303	0.0008	0.9319
FANP 10x10	8	8	4.2	1.350	0.895	0.9338	1.01	0.9292	0.0008	0.9308
FANP 10x10	8	9	4.3	1.350	0.895	0.9338	1.01	0.9293	0.0008	0.9309
FANP 10x10	8	10	4.6	1.350	0.895	0.9338	1.01	0.9335	0.0008	0.9351
FANP 10x10	8	12	5.0	1.350	0.895	0.9338	1.01	0.9353	0.0009	<b>0.9371</b>
FANP 10x10	10	0	2.9	1.350	0.895	0.9338	1.01	0.9218	0.0008	0.9234
FANP 10x10	10	2	3.3	1.350	0.895	0.9338	1.01	0.9265	0.0008	0.9281
FANP 10x10	10	4	3.6	1.350	0.895	0.9338	1.01	0.9320	0.0008	0.9336
FANP 10x10	10	6	3.9	1.350	0.895	0.9338	1.01	0.9311	0.0008	0.9327
FANP 10x10	10	8	4.2	1.350	0.895	0.9338	1.01	0.9345	0.0008	0.9361
FANP 10x10	10	9	4.3	1.350	0.895	0.9338	1.01	0.9296	0.0009	0.9314
FANP 10x10	10	10	4.6	1.350	0.895	0.9338	1.01	0.9369	0.0009	0.9387
FANP 10x10	10	12	5.0	1.350	0.895	0.9338	1.01	0.9376	0.0009	<b>0.9394</b>
FANP 10x10	12	0	2.9	1.350	0.895	0.9338	1.01	0.9216	0.0008	0.9232
FANP 10x10	12	2	3.3	1.350	0.895	0.9338	1.01	0.9256	0.0008	0.9272
FANP 10x10	12	4	3.6	1.350	0.895	0.9338	1.01	0.9314	0.0009	0.9332
FANP 10x10	12	6	3.9	1.350	0.895	0.9338	1.01	0.9319	0.0007	0.9333
FANP 10x10	12	8	4.2	1.350	0.895	0.9338	1.01	0.9345	0.0008	0.9361
FANP 10x10	12	9	4.3	1.350	0.895	0.9338	1.01	0.9277	0.0008	0.9293
FANP 10x10	12	10	4.6	1.350	0.895	0.9338	1.01	0.9347	0.0009	0.9365
FANP 10x10	12	12	5.0	1.350	0.895	0.9338	1.01	0.9370	0.0009	<b>0.9388</b>
FANP 10x10	14	0	2.9	1.350	0.895	0.9338	1.01	0.9207	0.0008	0.9223
FANP 10x10	14	2	3.3	1.350	0.895	0.9338	1.01	0.9247	0.0009	0.9265
FANP 10x10	14	4	3.6	1.350	0.895	0.9338	1.01	0.9291	0.0008	0.9307
FANP 10x10	14	6	3.9	1.350	0.895	0.9338	1.01	0.9301	0.0009	0.9319
FANP 10x10	14	8	4.2	1.350	0.895	0.9338	1.01	0.9324	0.0008	0.9340
FANP 10x10	14	9	4.3	1.350	0.895	0.9338	1.01	0.9293	0.0008	0.9309
FANP 10x10	14	10	4.6	1.350	0.895	0.9338	1.01	0.9352	0.0008	0.9368
FANP 10x10	14	12	5.0	1.350	0.895	0.9338	1.01	0.9370	0.0009	<b>0.9388</b>

**Table 6-17 RAJ-II Array HAC Part Length Fuel Rod Calculations**

Assembly Type	Number of Part Length Rods	Gadolinia -Urania Fuel Rod Number	<sup>235</sup> U Enrichment (wt%)	Pitch (cm)	Pellet Diameter (cm)	Clad ID (cm)	Clad OD (cm)	k <sub>eff</sub>	σ	k <sub>eff</sub> + 2σ
GNF 10x10	8	0	2.9	1.350	0.895	0.9338	1.01	0.9292	0.0008	0.9308
GNF 10x10	8	2	3.3	1.350	0.895	0.9338	1.01	0.9296	0.0009	0.9314
GNF 10x10	8	4	3.6	1.350	0.895	0.9338	1.01	0.9357	0.0010	0.9377
GNF 10x10	8	6	3.9	1.350	0.895	0.9338	1.01	0.9354	0.0009	0.9372
GNF 10x10	8	8	4.2	1.350	0.895	0.9338	1.01	0.9399	0.0008	<b>0.9415</b>
GNF 10x10	8	9	4.3	1.350	0.895	0.9338	1.01	0.9346	0.0010	0.9366
GNF 10x10	8	10	4.6	1.350	0.895	0.9338	1.01	0.9376	0.0009	0.9394
GNF 10x10	8	12	5.0	1.350	0.895	0.9338	1.01	0.9375	0.0008	0.9391
GNF 10x10	10	0	2.9	1.350	0.895	0.9338	1.01	0.9292	0.0008	0.9308
GNF 10x10	10	2	3.3	1.350	0.895	0.9338	1.01	0.9296	0.0008	0.9312
GNF 10x10	10	4	3.6	1.350	0.895	0.9338	1.01	0.9371	0.0008	0.9387
GNF 10x10	10	6	3.9	1.350	0.895	0.9338	1.01	0.9370	0.0008	0.9386
GNF 10x10	10	8	4.2	1.350	0.895	0.9338	1.01	0.9372	0.0008	0.9388
GNF 10x10	10	9	4.3	1.350	0.895	0.9338	1.01	0.9363	0.0009	0.9381
GNF 10x10	10	10	4.6	1.350	0.895	0.9338	1.01	0.9345	0.0009	0.9363
GNF 10x10	10	12	5.0	1.350	0.895	0.9338	1.01	0.9375	0.0008	<b>0.9391</b>
GNF 10x10	12	0	2.9	1.350	0.895	0.9338	1.01	0.9276	0.0008	0.9292
GNF 10x10	12	2	3.3	1.350	0.895	0.9338	1.01	0.9309	0.0008	0.9325
GNF 10x10	12	4	3.6	1.350	0.895	0.9338	1.01	0.9373	0.0009	0.9391
GNF 10x10	12	6	3.9	1.350	0.895	0.9338	1.01	0.9347	0.0009	0.9365
GNF 10x10	12	8	4.2	1.350	0.895	0.9338	1.01	0.9374	0.0009	0.9392
GNF 10x10	12	9	4.3	1.350	0.895	0.9338	1.01	0.9333	0.0009	0.9351
GNF 10x10	12	10	4.6	1.350	0.895	0.9338	1.01	0.9378	0.0008	0.9394
GNF 10x10	12	12	5.0	1.350	0.895	0.9338	1.01	0.9404	0.0007	<b>0.9418</b>
GNF 10x10	14	0	2.9	1.350	0.895	0.9338	1.01	0.9261	0.0008	0.9277
GNF 10x10	14	2	3.3	1.350	0.895	0.9338	1.01	0.9299	0.0008	0.9315
GNF 10x10	14	4	3.6	1.350	0.895	0.9338	1.01	0.9345	0.0008	0.9361
GNF 10x10	14	6	3.9	1.350	0.895	0.9338	1.01	0.9351	0.0009	0.9369
GNF 10x10	14	8	4.2	1.350	0.895	0.9338	1.01	0.9376	0.0009	0.9394
GNF 10x10	14	9	4.3	1.350	0.895	0.9338	1.01	0.9353	0.0008	0.9369
GNF 10x10	14	10	4.6	1.350	0.895	0.9338	1.01	0.9368	0.0009	0.9386
GNF 10x10	14	12	5.0	1.350	0.895	0.9338	1.01	0.9398	0.0008	<b>0.9414</b>

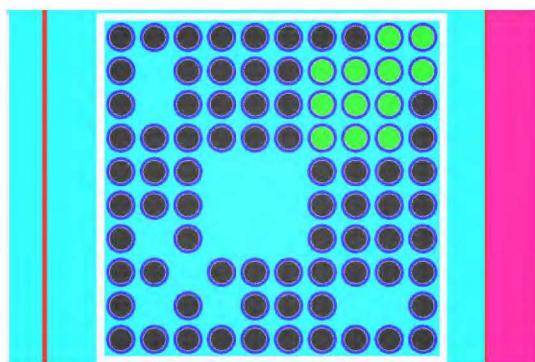
a. Limiting case(s) shown in bold

**Table 6-18     Relative Reactivity of Fuel Designs with As-Built Part Length Rod Locations**

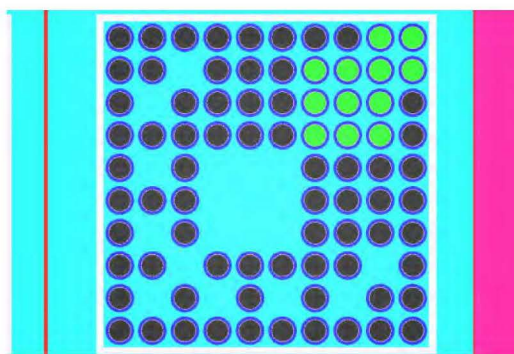
<b>Fuel Assembly Type</b>	<b>Water Rod Designs</b>	<b>Number of Part Length Rods</b>	<b><math>\Delta k^a</math></b>	<b><math>\Delta k/\sigma_{\Delta k}</math></b>
GNF 10X10	2-2x2 off-center diagonal 1-axially varying centered	$\leq 16$	0.0000	0
FANP 10X10	3x3	$\leq 12$	-0.0033	-7
GNF 9X9	2-2x2 off-center diagonal	8	-0.0094	-19
GNF 8X8	0 2x2	0	-0.0098	-20

- a. Difference in reactivity of the specific design yielding the maximum system reactivity in each fuel type for an infinite array of RAJ-II packages.

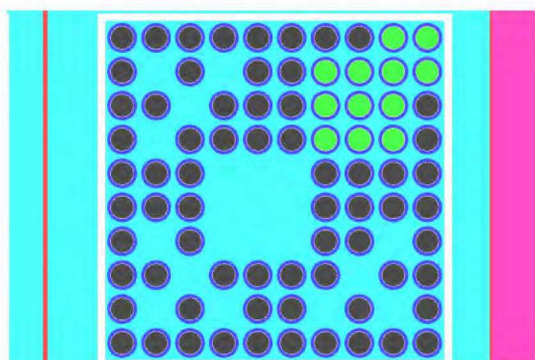




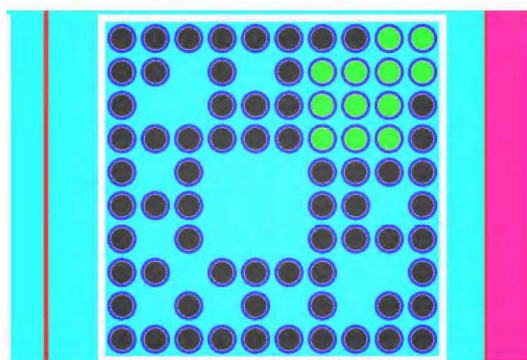
FANP 10x10 5.0 wt%  $^{235}\text{U}$ , 8 Part Length Rods



FANP 10x10 5.0 wt%  $^{235}\text{U}$ , 10 Part Length Rods

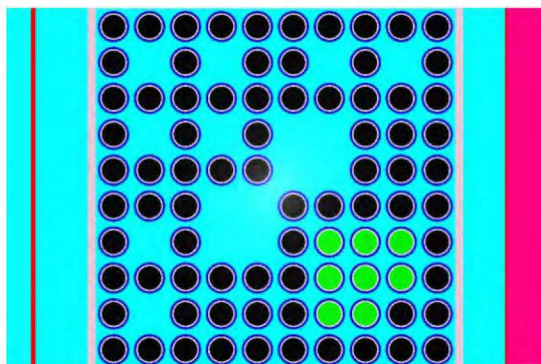


FANP 10x10 5.0 wt%  $^{235}\text{U}$ , 12 Part Length Rods

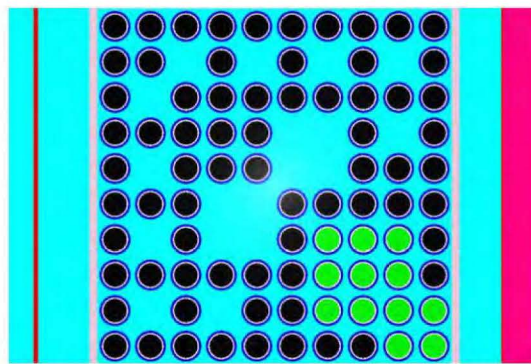


FANP 10x10 5.0 wt%  $^{235}\text{U}$ , 14 Part Length Rods

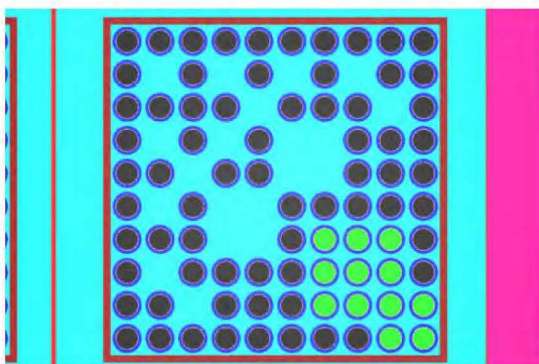
**Figure 6-37 FANP 10x10 Worst Case Fuel Parameters Model with Part Length Fuel Rods**



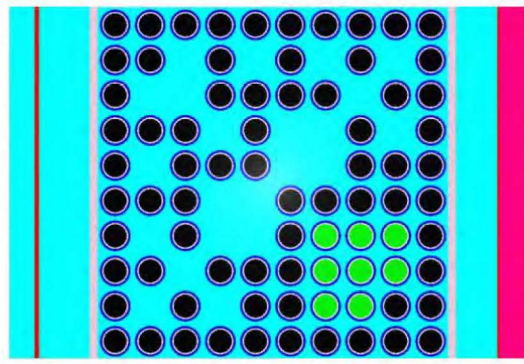
GNF 10x10 4.2 wt%  $^{235}\text{U}$ , 8 Part Length Rods



GNF 10x10 5.0 wt%  $^{235}\text{U}$ , 10 Part Length Rods

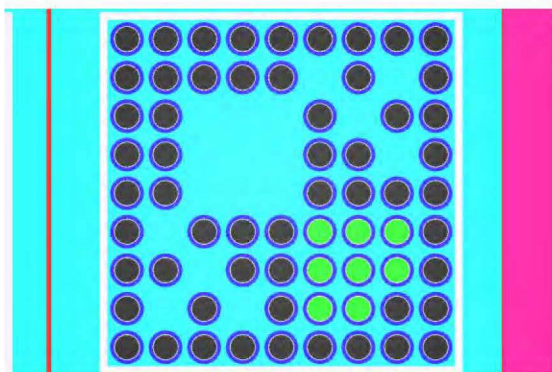


GNF 10x10 5.0 wt%  $^{235}\text{U}$ , 12 Part Length Rods

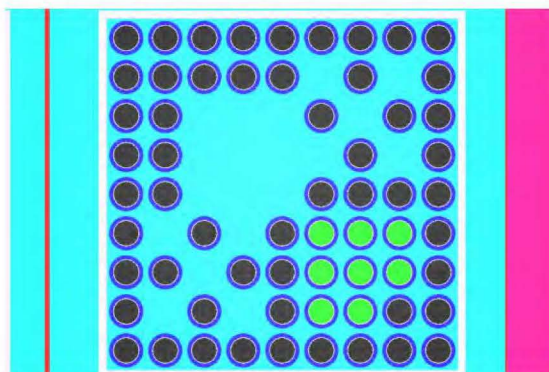


GNF 10x10 4.2 wt%  $^{235}\text{U}$ , 14 Part Length Rods

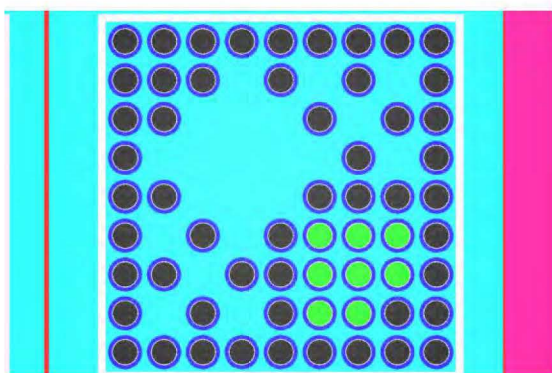
Figure 6-38 GNF 10x10 Worst Case Fuel Parameters Model with Part Length Fuel Rods



FANP 9x9 4.7 wt%  $^{235}\text{U}$ , 8 Part Length Rods



FANP 9x9 4.7 wt%  $^{235}\text{U}$ , 10 Part Length Rods



FANP 9x9 4.7 wt%  $^{235}\text{U}$ , 12 Part Length Rods

**Figure 6-39 FANP 9x9 Worst Case Fuel Parameters Model with Part Length Fuel Rods**



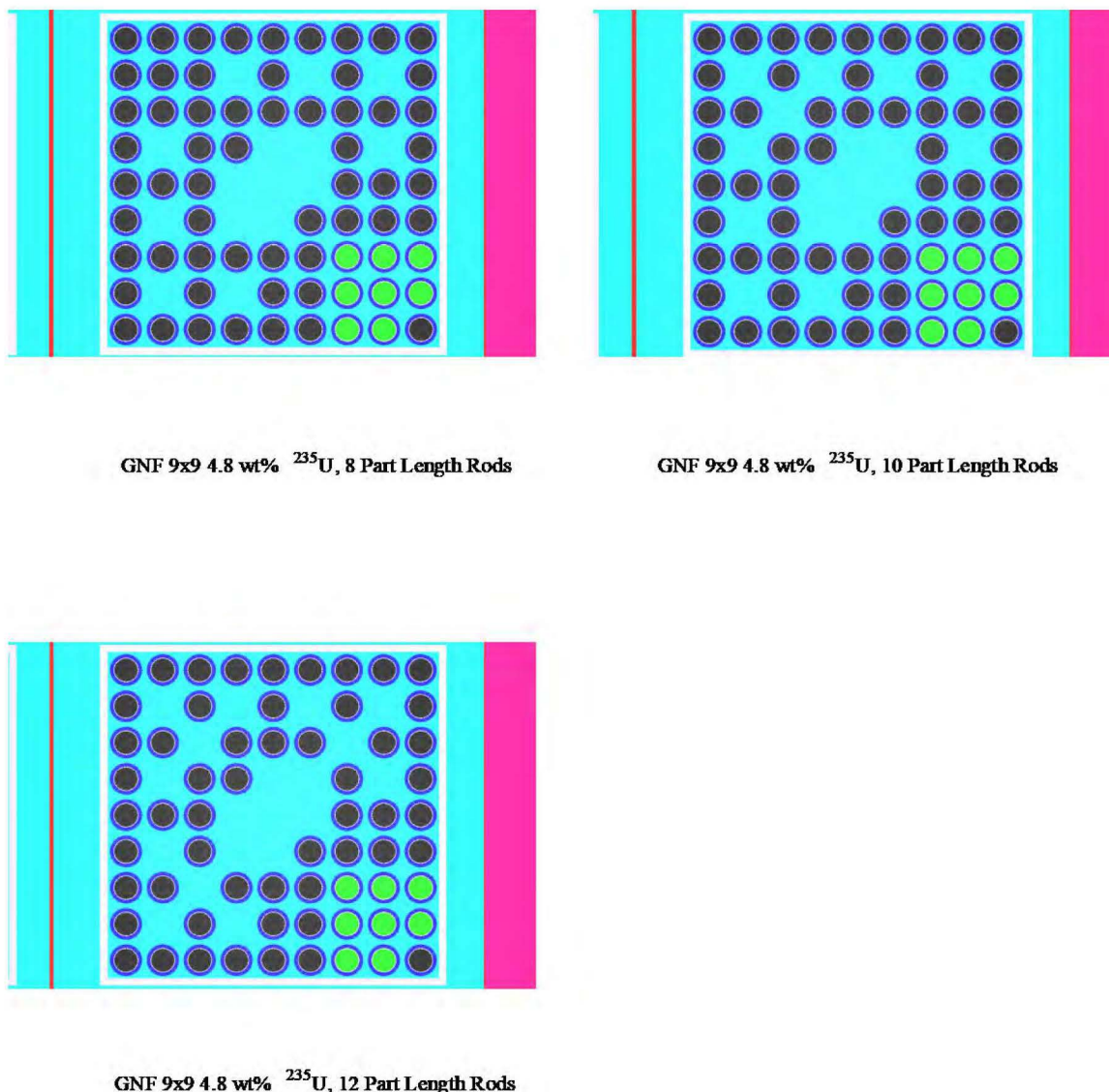


**Figure 6-40 GNF 9x9 Worst Case Fuel Parameters Model with Part Length Fuel Rods**

#### 6.3.4.10 Moderator Density Study (2N=448)

The worst case design from Table 6-17 is used to conduct a moderator density sensitivity analysis. The GNF 10x10 fuel assembly is chosen for the study because it resulted in the highest reactivity in Table 6-17. Previous calculations demonstrated the worst case condition for maximum reactivity is a configuration in which there is no moderator between the RAJ-II packages. The moderator density study is conducted by varying the moderator density inside the inner container fuel compartment. The outer region of the inner container is filled with the alumina silicate thermal insulating material. The results of the moderator density study, Table 6-32, are shown in Figure 6-41. As shown in Figure 6-41, all cases peak at full moderator density. Therefore, a moderator density of  $1.0 \text{ g/cm}^3$  is chosen as the worst case moderator condition for the RAJ-II inner container fuel compartment.

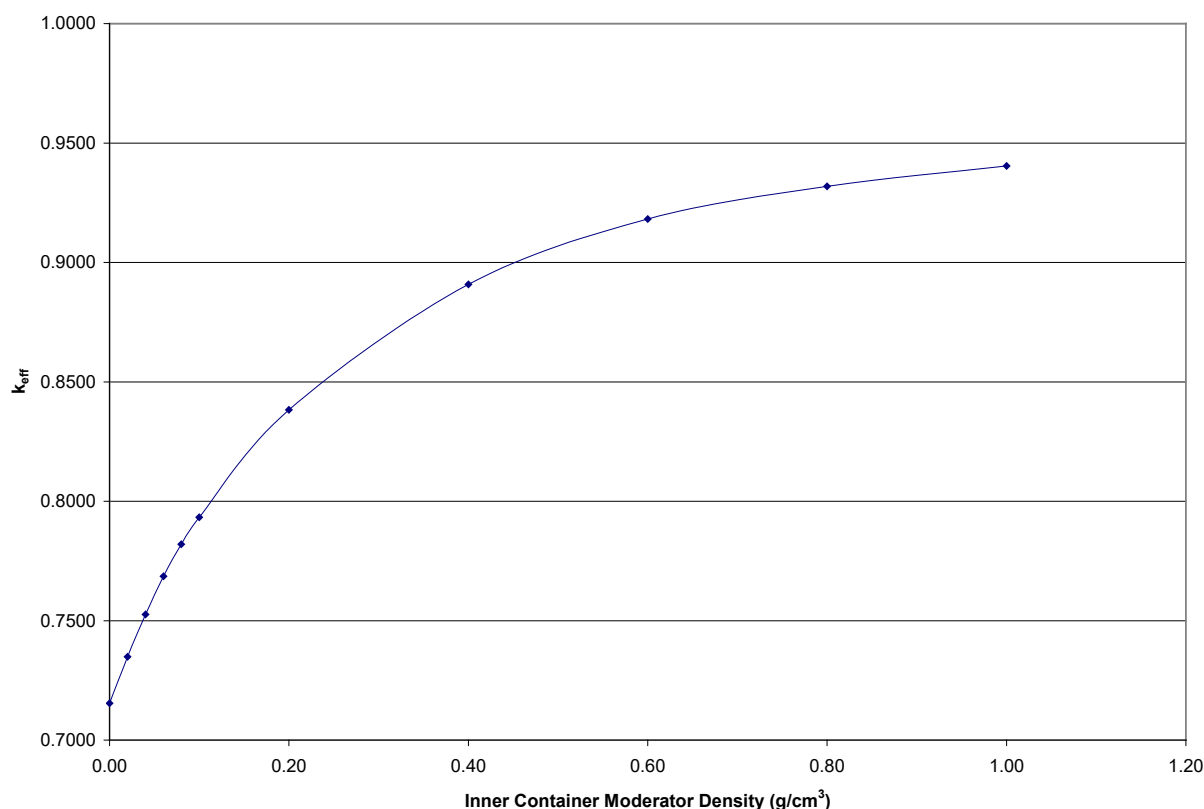


**Figure 6-41 Moderator Density Sensitivity Study for the RAJ-II HAC Worst Case Parameter Fuel Design**

#### 6.3.4.11 Material Distribution Reactivity Study

The sensitivity studies in this section were performed using KENO-VI with continuous energy ENDF/B-VII cross-section library. Therefore, the USL is 0.9340.

A study is performed to determine the worst packing material distribution within the RAJ-II inner container. The material normally present around the inner container fuel compartment is a thermal insulator consisting of alumina silicate. The material normally lining the inner container fuel compartment is polyethylene foam material which has a density in the range 0.05 – 0.075 g/cm<sup>3</sup>; a density of 0.08 g/cm<sup>3</sup> is used.

The first part of the material distribution study investigates replacing the alumina silicate alternately with full density water and void while the inner container fuel compartment is filled with full density water. The limiting GNF 10x10 fuel assembly is chosen for the study because it resulted in the highest reactivity in Table 6-18. In addition, the worst case RAJ-II model is used in a 10x1x10 (2N=100) array and an 8x1x8 (2N=64) array for LEU+ fuel. The results are shown in Table 6-19. Table 6-19 shows that the most reactive condition is achieved with the alumina silicate thermal insulator in place. Therefore, the alumina silicate thermal insulator will remain a part of the worst case RAJ-II model.

The second part of the material distribution study investigates placing the polyethylene foam material in its proper location within the RAJ-II fuel assembly compartment. In the models used for the majority of the sensitivity studies the polyethylene foam was assumed to burn away in the fire that also melted the polyethylene packing materials. It is extremely unlikely that this configuration would exist post thermal excursion. The polyethylene foam would be as susceptible to the fire as the polyethylene packing materials. However, the incomplete foam burn is considered in this study for conservatism. The limiting GNF 10x10 fuel assembly is chosen for the study because it resulted in the highest reactivity in Table 6-18. The RAJ-II model is used is a 10x1x10 (2N=100) array and an 8x1x8 (2N=64) array for LEU+ fuel. For simplicity, the full thickness of polyethylene foam will be maintained for the remaining RAJ-II sensitivity calculations in Section 6.3.4. The demonstration of criticality safety for various enrichment bands for the limiting GNF 10x10 design (bottom of Table 6-16) use a foam thickness 1.28 cm and 1.14 cm for LEU+ fuel. Several enrichment/gadolinia cases with less margin to the USL were chosen to confirm that the USL is met at optimum foam thickness. The results shown in Figure 6-42 and Table 6-16 demonstrate that all cases are below the USL. The difference in system reactivity using a foam thickness of 1.28 cm compared to the optimum foam thickness (determined from Figure 6-42) is statically insignificant; the maximum difference is less than  $3\sigma$ . Therefore, a polyethylene foam thickness of 1.28 cm and 1.14 cm for LEU+ fuel is used in the final demonstration of criticality safety for the results reported in Sections 6.4, 6.5, and 6.6.

**Table 6-19     RAJ-II Inner Container Thermal Insulator Region and Polyethylene Foam Material Study**

<b>Fuel Type</b>	<b>Array Size</b>	<b>Inner Container Foam Space</b>	<b>Insulator Space Fill</b>	<b>k<sub>eff</sub></b>	<b><math>\sigma</math></b>	<b>k<sub>eff</sub> + 2 <math>\sigma</math></b>
GNF 10x10	10x1x10 (2N=100)	Water	Thermal Ins.	0.8974	0.0003	0.8980
GNF 10x10	10x1x10 (2N=100)	Water	Water	0.7929	0.0002	0.7934
GNF 10x10	10x1x10 (2N=100)	Water	None	0.8944	0.0003	0.8950

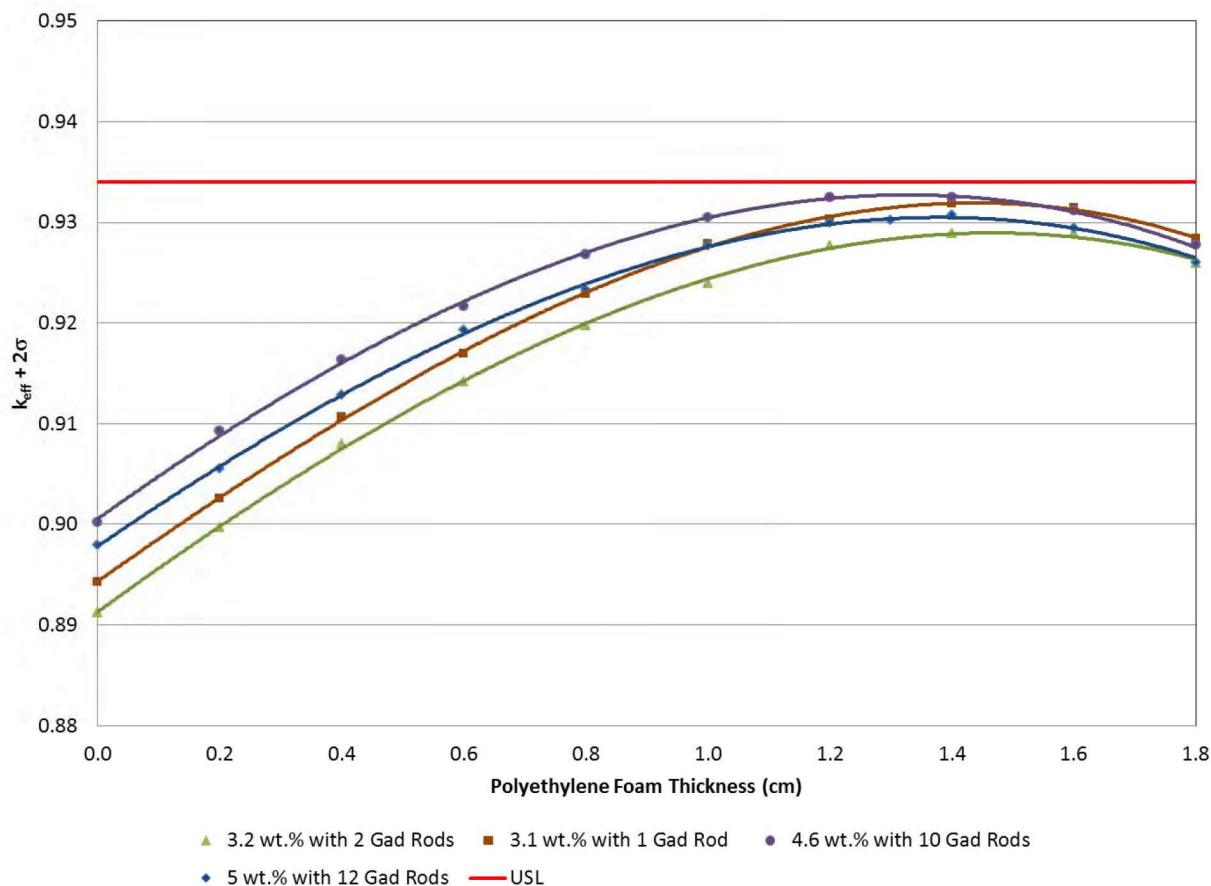


**Figure 6-42 Polyethylene Foam Thickness Sensitivity Study, HAC 10x1x10 (2N=100)**

#### 6.3.4.12 Inner Container Partial Flooding Study (2N=100)

Calculations are run in which the fuel assembly rows are partially filled within the RAJ-II inner fuel compartment as shown in Figure 6-43. The GNF 10x10 fuel assembly is chosen for the analysis because it produced the highest reactivity in Table 6-17. The RAJ-II HAC model from the polyethylene foam study is used with an array size of 10x1x10 (2N=100). The results are shown in Table 6-20. As shown in Table 6-20, the most reactive condition exists when water fully covers each fuel assembly. Therefore, the inner container fuel compartment will be fully flooded with water in the worst case RAJ-II model.

**Table 6-20 RAJ-II Inner Container Partially Filled with Moderator**

<b>Fuel Type</b>	<b>Fuel Rows Filled</b>	<b>Moderator Density (g/cm<sup>3</sup>)</b>	<b>k<sub>eff</sub></b>	<b>σ</b>	<b>k<sub>eff</sub> + 2σ<sup>a</sup></b>
GNF 10x10	1	1.00	0.6643	0.0007	0.6657
GNF 10x10	3	1.00	0.7678	0.0009	0.7696
GNF 10x10	5	1.00	0.8653	0.0008	0.8669
GNF 10x10	7	1.00	0.9212	0.0008	0.9228
GNF 10x10	9	1.00	0.9355	0.0009	0.9373
GNF 10x10	10	1.00	0.9378	0.0009	<b>0.9396</b>

a. Limiting case shown in bold



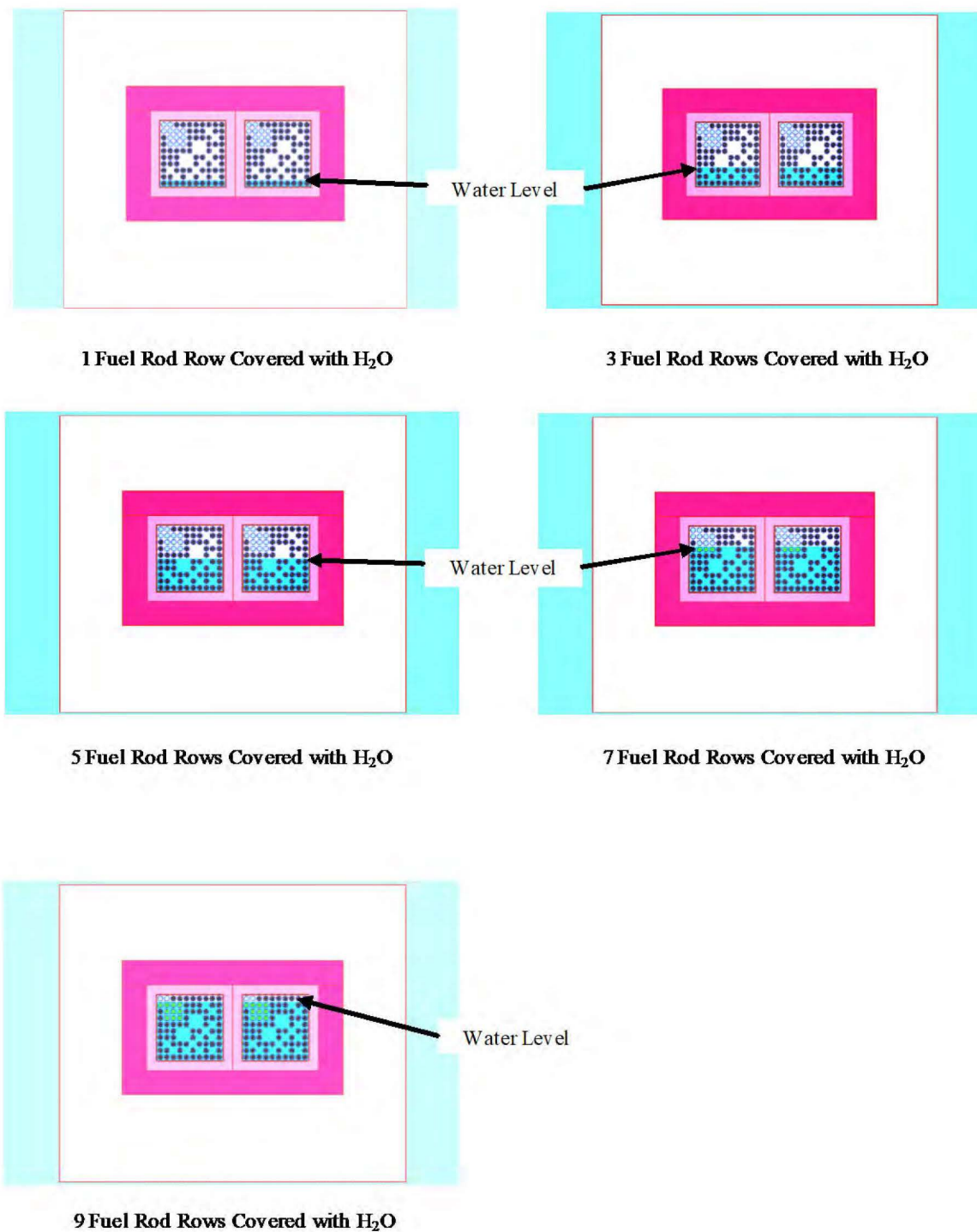


**Figure 6-43 RAJ-II Inner Container Fuel Compartment Flooding Cases**

### 6.3.4.13 RAJ-II Package Spacing Study (2N=100)

Calculations performed previously assume the RAJ-II packages are resting next to one another with no spacing between them. A container pitch sensitivity study is conducted to determine if reactivity increases as containers are moved away from one another. The HAC model used in the inner container partial flooding study is used for the pitch sensitivity study with an array size of 10x1x10 (2N=100). The GNF 10x10 fuel assemblies with an average lattice enrichment of 5.0 wt% U-235, 12 gadolinia-urania fuel rods enriched to 2.0 wt% gadolinia, and 12 part length fuel rods is used. The edge-to-edge separation is increased from 0 to 10 cm and an effect on reactivity is observed. The results in Table 6-21 show a decrease in reactivity with increased spacing between containers. Therefore, the most reactive container configuration occurs when there is minimum spacing between containers.

**Table 6-21 RAJ-II Array Spacing Sensitivity Study**

Assembly Type	Interspersed Moderator Density (g/cm <sup>3</sup> )	Container Pitch (cm)	Pitch (cm)	Pellet Diameter (cm)	Clad ID (cm)	Clad OD (cm)	k <sub>eff</sub>	σ	k <sub>eff</sub> + 2σ <sup>a</sup>
GNF 10x10	0.0	71.926	1.350	0.895	0.9338	1.01	0.9378	0.0009	<b>0.9396</b>
GNF 10x10	0.0	74.426	1.350	0.895	0.9338	1.01	0.9259	0.0009	0.9277
GNF 10x10	0.0	76.926	1.350	0.895	0.9338	1.01	0.9122	0.0008	0.9138
GNF 10x10	0.0	81.926	1.350	0.895	0.9338	1.01	0.8865	0.0008	0.8881

a. Limiting case shown in bold

### 6.3.4.14 Other Considerations

The analysis approach for demonstrating the criticality safety of the RAJ-II package transporting fuel assemblies which meets the requirements provided in Table 6-1 models the assemblies as:

- The enrichment has a uniform distribution to represent the lattice averaged enrichment, where the as-built assemblies would have varying enrichment in each fuel rod. In addition, the models use a uniform axial enrichment distribution, where the as-built assemblies could have axially varying enrichment.
- The analyses presented in Sections 6.4, 6.5, and 6.6 for the limiting GNF 10x10 use the as-built part length rod configuration for both NCT and HAC. Consideration for the applicability of this analysis approach is provided below.
- The polyethylene of the packing materials is modeled as an annular wrap around the fuel rod. This approach is conservative.

#### 6.3.4.14.1 Enrichment Distribution

A sensitivity study was performed to assess the reactivity effect of radial (rod-wise) enrichment distribution. The system reactivity of the four non-uniform distribution cases is used to compare

to a uniform enrichment distribution case. All cases resulted in the same lattice average enrichment of 4.5 wt%. The study assessed the effect of loading the maximum enrichment fuel rods (5.0 wt%) in the peripheral locations compared to central locations of the fuel rod array. Three of the four non-uniform enrichment cases resulted in lower reactivity than the uniform enrichment case. One case resulted in a  $\Delta k/\sigma_{\Delta k}$  of 0.39, which is statistically insignificant. Therefore, average enrichment can be used in the demonstration of maximum reactivity.

A sensitivity study was performed on a similar package to evaluate the effect of axial enrichment distribution. A uniform axial enrichment, single lattice case was first used to determine the required number of gadolinia-bearing rods so that the system reactivity is below the USL for each enrichment band. Three multiple lattice cases with various combinations of single lattice enrichment zones (4.70 wt% and 2.80 wt%) were analyzed; each enrichment zone contains the required number and loading of gadolinia-bearing rods as the single lattice case. The system reactivity of the multiple lattice cases are bounded by the more limiting of the single lattice cases by more than  $4\sigma$ . Therefore, the most limiting single lattice in an assembly with multiple lattices can be used to ensure criticality safety of the package array.

#### **6.3.4.14.2 Part Length Rod Configuration**

GNF fuel assembly designs [[

]] which prevent the standard full length fuel rods from separating during a drop event. Therefore, random sliding of the full length rods causing the rods to separate from the tie plates does not occur as a result of the HAC drop sequence. The location of part length rods for each fuel design type does not change. [[

]] Under HAC, the rod relative location is assured by the mechanical design of the assembly; therefore, the criticality analysis considering the as-built part length rod locations appropriately captures the package system reactivity.

#### **6.3.4.14.3 Model for Polyethylene Packing Materials**

A sensitivity study explicitly modeled the cluster separators being inserted along the entire active fuel length within the fuel assembly in the RAJ-II HAC package arrays. At optimum moderation, modeling of the polyethylene packing materials (cluster separators and protective sheathing) as a uniform annular wrap over each fuel rod is more reactive than the explicit model. This analysis is described in detail in Reference 6-3. Hence, the rod wrap model is a conservative approach for modeling the packing components under HAC.

## 6.4 SINGLE PACKAGE EVALUATION

The analyses in this section were performed using KENO-VI with a continuous energy ENDF/B-VII cross-section library. Therefore, the USL is 0.9340.

Based on the sensitivity studies performed in Section 6.3.4, the single package and package array NCT and HAC calculations are performed using the most reactive fuel assembly design which is the GNF 10x10. Various GNF 10x10 designs were analyzed using the as-built part length rod locations and the limiting gadolinia loading patterns. The GNF design with a single axially varying water rod centrally located within the fuel rod array and sixteen part length fuel rods bounds all other 10x10 designs. An average lattice enrichment of 5.0 wt% U-235, twelve 2.0 wt% gadolinia fuel rods (or 8.0 wt% U-235, twenty-two 2.0 wt% gadolinia fuel rods), with the patterns shown in Figure 6-25 are used for the analyses in this section.

### 6.4.1 Configuration

The single package model described in Section 6.3.1.1 is used to demonstrate criticality safety of the RAJ-II package using the worst case fuel design. The GNF 10x10 at an average lattice enrichment of 5.0 wt% U-235, twelve 2.0 wt% gadolinia fuel rods (or 8.0 wt% U-235, twenty-two 2.0 wt% gadolinia fuel rods), and 16 part length fuel rods are used for the NCT and HAC evaluations. A moderator density study is conducted under both NCT and HAC. In the HAC study, the water density in the inner package is varied while the outer container remains void. For NCT, the moderator density is uniformly varied. A 30.48 cm thick water reflector surrounds all sides of the NCT and HAC single package.

The polyethylene foam remains in place for the NCT single package configuration, but the polyethylene foam is removed from the HAC single package configuration. Removing the polyethylene foam in the HAC single package model decreases neutron leakage which increases reactivity for a single container.

### 6.4.2 Results

The results for the single package NCT evaluation are displayed in Figure 6-44. The results for the single package HAC evaluation are shown in Figure 6-45. The results in the figures indicate reactivity for the single package increases with increasing moderator density. The highest  $k_{\text{eff}}$  is achieved for both cases at full density moderation in the inner container. In both cases, the  $k_{\text{eff}}$  remains far below the USL of 0.9340. The maximum  $k_{\text{eff}} + 2\sigma$  values are provided in Table 6-34 and Table 6-35 for the single package NCT and HAC cases, respectively. Therefore, criticality safety is established for the single package RAJ-II.

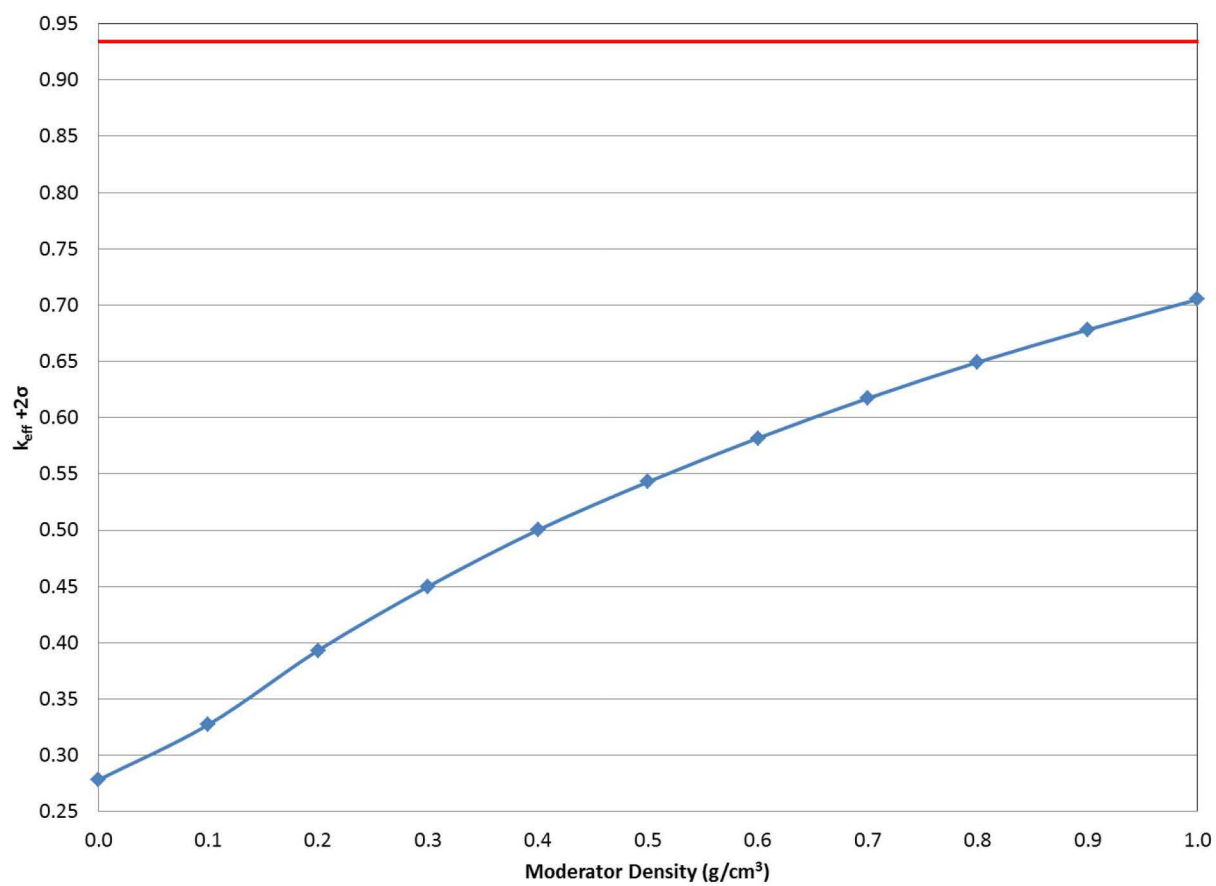


**Figure 6-44 RAJ-II Single Package NCT Results**

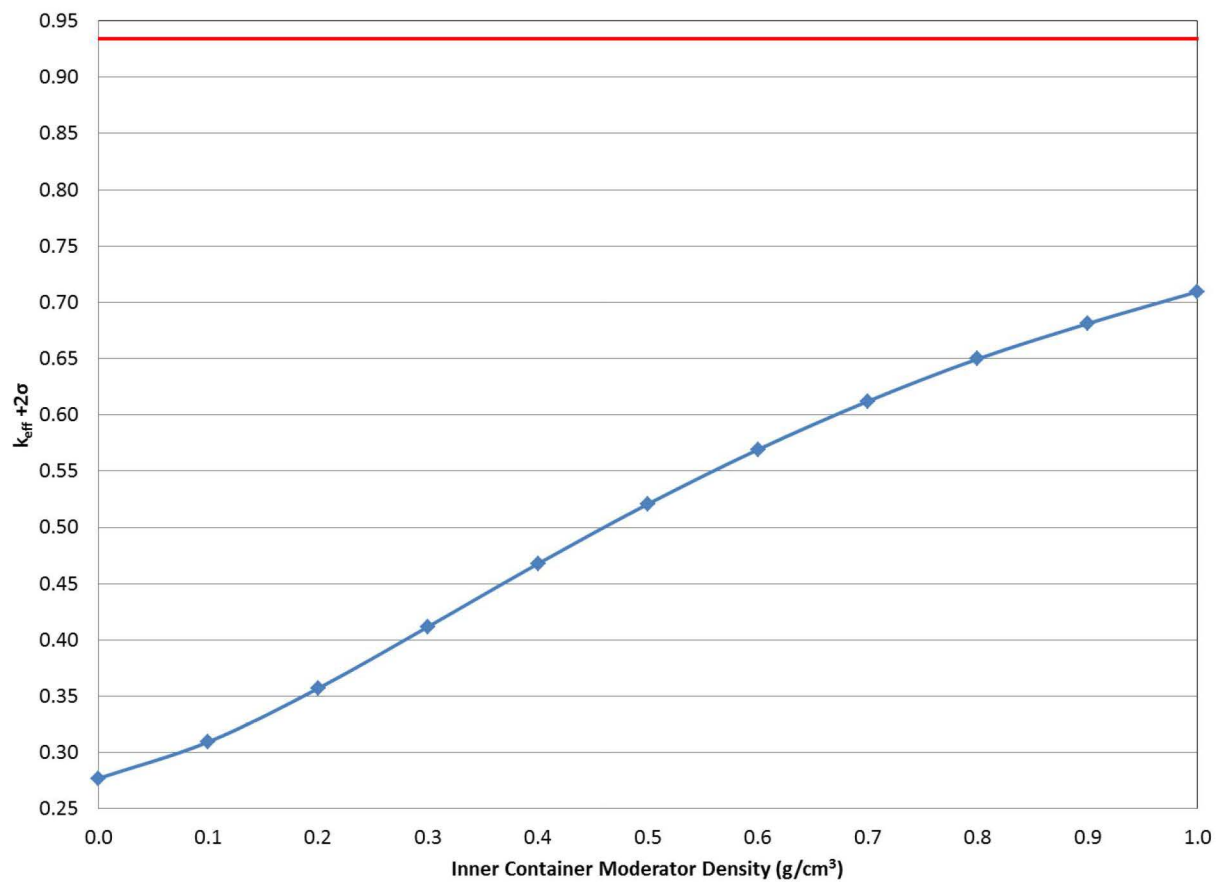


**Figure 6-45 RAJ-II Single Package HAC Results**

## 6.5 EVALUATION OF PACKAGE ARRAYS UNDER NCT

The analyses in this section were performed using KENO-VI with continuous energy ENDF/B-VII cross-section library. Therefore, the USL is 0.9340.

### 6.5.1 Configuration

The package array NCT model described in Section 6.3.1.2.1 is used to demonstrate criticality safety of the RAJ-II package using the GNF 10x10 worst case fuel design at an average lattice enrichment of 5.0 wt% U-235, twelve 2.0 wt% gadolinia fuel rods (or 8.0 wt% U-235, twenty-two 2.0 wt% gadolinia fuel rods), and 16 part length fuel rods. The calculation using the NCT model involves a moderator density sensitivity study. In the model, the moderator density is uniformly varied and the system reactivity is observed.

### 6.5.2 Results

The results of the package array NCT model calculations are shown in Figure 6-46. The reactivity peaks with no moderator present. A decreasing trend continues until the moderator density reaches 0.3 g/cm<sup>3</sup> at which point reactivity increases almost linearly to full water density. The maximum  $k_{eff} + 2\sigma$  is provided in Table 6-36, which is below the USL of 0.9340. Therefore, criticality safety of the RAJ-II package is demonstrated under NCT.

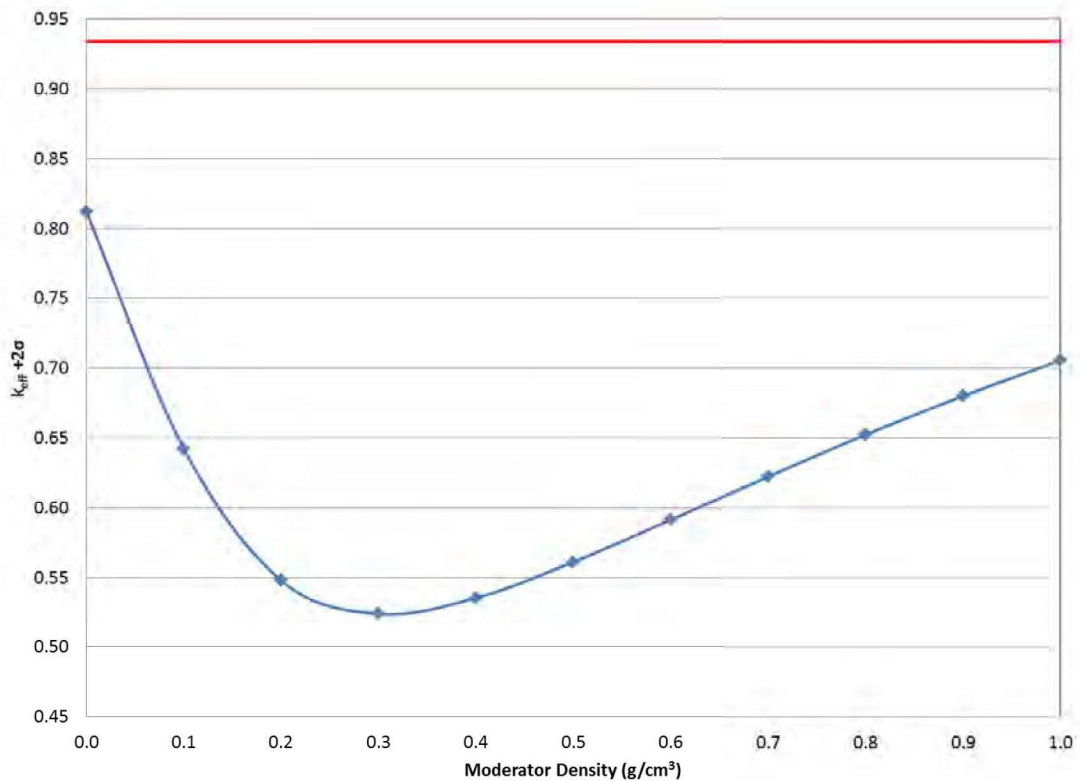


Figure 6-46 RAJ-II Package Array Under NCT Results

## 6.6 PACKAGE ARRAYS UNDER HAC

The analyses in this section were performed using KENO-VI with continuous energy ENDF/B-VII cross-section library. Therefore, the USL is 0.9340.

### 6.6.1 Configuration

The package array HAC model described in Section 6.3.1.2.2 is used to demonstrate criticality safety of a 10x1x10 array (2N=100) of RAJ-II packages using the GNF 10x10 worst case fuel design at an average lattice enrichment of 5.0 wt% U-235, twelve 2.0 wt% gadolinia fuel rods (or 8.0 wt% U-235, twenty-two 2.0 wt% gadolinia fuel rods), and 16 part length fuel rods. The calculation using the HAC model involves a moderator density sensitivity study. In the first study, no moderator is present in the outer container while the moderator density inside the inner container is varied. In the second study the moderator in the inner container is at full density while the moderator density inside the outer container is varied. The polyethylene foam inside the inner container fuel compartment is modeled at a thickness of 1.28 cm for LEU or 1.14 cm for LEU+ (see Section 6.3.4.11).

### 6.6.2 Results

The results of the package array (2N=10x1x10=100 array) HAC model calculations are shown in Figure 6-47 for the reactivity change with the change in moderator density in the inner container. The system reactivity begins at its lowest value and increases with increasing moderator density. This trend highlights the neutronics of the system. Initially, no moderator, other than the polyethylene surrounding the fuel rods, is present to thermalize neutrons that enter the inner container. As the inner container moderator density increases, higher energy neutrons pass into adjacent containers and thermalize in the vicinity of the fuel creating a more reactive situation. The maximum  $k_{eff} + 2\sigma$  for the package array HAC case is provided in Table 6-36 which is below the USL of 0.9340. Figure 6-48 confirms that void in the outer container is most reactive (data provided in Table 6-38). Therefore, criticality safety of the RAJ-II is demonstrated for the package array under HAC.



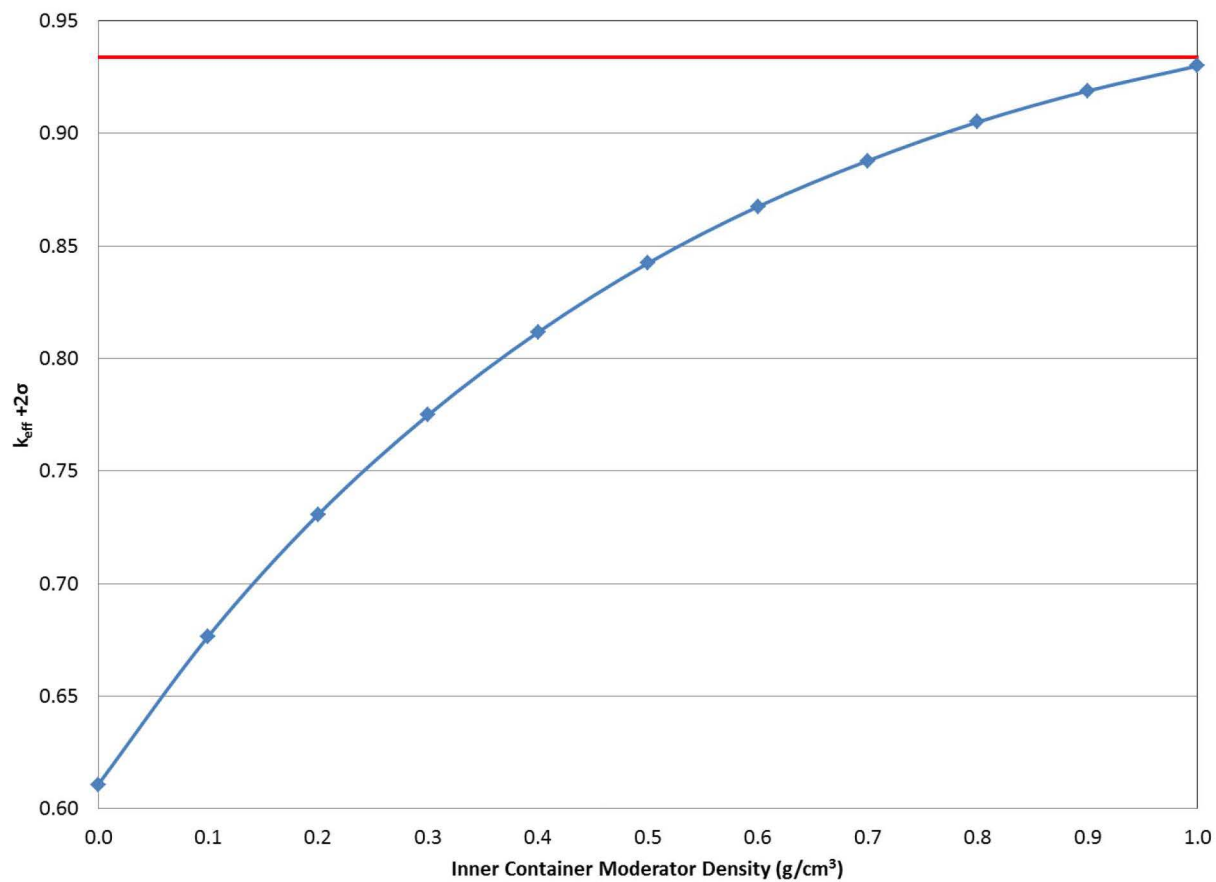


**Figure 6-47 RAJ-II Package Array HAC Results, Inner Container Moderation Study**

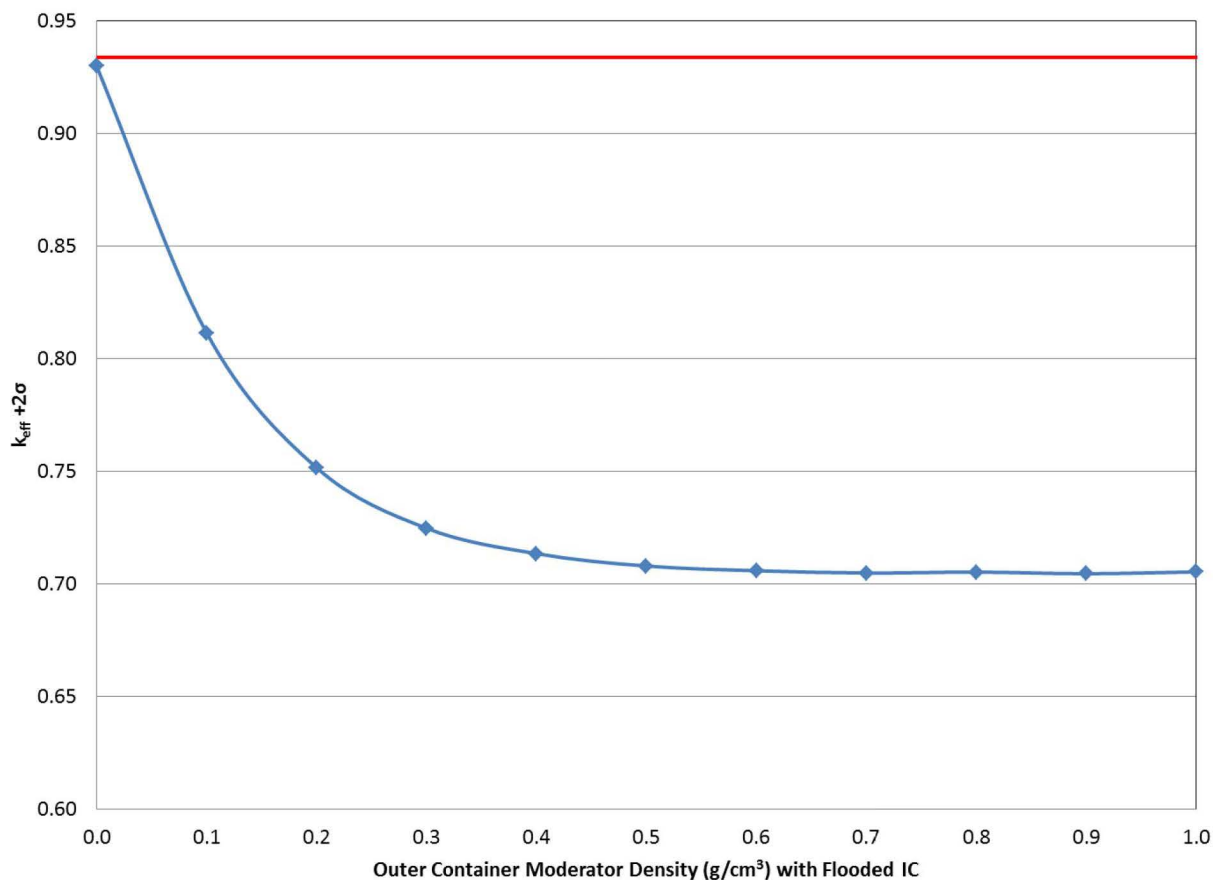


**Figure 6-48 RAJ-II Package Array HAC Results, Outer Container Moderation Study**

The results of the HAC package array shown in Figure 6-47 and Figure 6-48 do not include the fuel channel. As shown in Table 6-22 and Table 6-23, the presence of the channel at various channel thicknesses has either a statistically insignificant or slightly negative effect on the system reactivity; therefore, not modeling the channel is acceptable. This is because the models are already optimized in terms of the inter-package neutron interactions by identifying the optimum foam thickness and the optimum moderator conditions.

**Table 6-22 HAC Channel Sensitivity (10x1x10) for LEU Fuel**

Channel Thickness (cm)	$k_{eff}$	$\sigma$	$k_{eff} + 2\sigma$
[[	0.9292	0.0003	0.9298
]]	0.9300	0.0003	0.9305
No Channel	0.9295	0.0003	0.9300

**Table 6-23    HAC Channel Sensitivity (8x1x8) for LEU+ Fuel**

Channel Thickness (cm)	$k_{eff}$	$\sigma$	$k_{eff} + 2\sigma$
[[	0.9218	0.0003	0.9224
]]	0.9232	0.0004	0.9240
No Channel	0.9242	0.0003	0.9248

#### 6.6.2.1    Pu-239 Effect on Reactivity for the RAJ-II Package Array HAC

The fuel scheduled for transport in the RAJ-II could have a small Pu-239 content; therefore, the effect on the RAJ-II package HAC reactivity is investigated. The maximum plutonium concentration ( $3.04 \times 10^{-9}$  gPu-239/gU) listed in Table 1-3 of the SAR is added to the package array HAC model (10x1x10 array). The results showed no statistically significant difference between the cases with and without plutonium; the change in reactivity with and without Pu-239 is 0.0010 delta-k which is within  $2\sigma$  of the statistical uncertainty. Therefore, the plutonium is justifiably neglected in the RAJ-II evaluation.

## **6.7 Fuel Rod Transport in the RAJ-II**

Studies are conducted to allow transport of UO<sub>2</sub> fuel rods in the RAJ-II package. Several configurations are investigated including: freely loose fuel rods, fuel rods strapped together, and fuel rods contained in 5-inch stainless steel pipe/protective case. The model uses the 10x10, 9x9, or 8x8 worst case fuel rod designs developed in Section 6.3.4 for the BWR UO<sub>2</sub> rods. A 6-mil (0.0152 cm) layer of polyethylene encircles each fuel rod in the model to bound protective packing material that may be used for fuel rod transport.

Section 6.3.1.3.4 describes the model for the transport of UC and generic PWR UO<sub>2</sub> fuel rods inside the 5-inch stainless steel pipe.

### **6.7.1 Freely Loose Fuel Rod Study**

The package array model under HAC is used for fuel rod calculations in the RAJ-II because it was demonstrated to be more reactive than the NCT package array model. The worst case fuel rods are arranged in a square pitch array inside each RAJ-II transport compartment. Scoping studies indicated little difference between the square and triangular pitch array, therefore the square pitch array is chosen for convenience. The inner container is filled with full density water and the outer container has no water, which facilitates leakage of neutrons into neighboring containers. The fuel rod pitch is varied, and the results are illustrated in Figure 6-49 and corresponding calculational data are listed in Table 6-24. The results demonstrate that a fully loaded inner compartment in which the rods are all in contact with each other is a supercritical configuration. As a result, a maximum fuel rod quantity to ensure subcriticality is established for the loose configuration, as shown in Table 6-2. The 8x8 rod design is limiting for LEU fuel as shown in Figure 6-49 and Table 6-24.

With the introduction of the LEU+ fuel type, the calculations described above are repeated with 25 freely loose rods in each transport compartment of the RAJ-II container for both the HAC and NCT array configurations. Unless otherwise stated, the results and trends hold true for the single package NCT and HAC evaluations with LEU+ fuel.

NEDO-33869 Revision 11  
Non-Proprietary Information

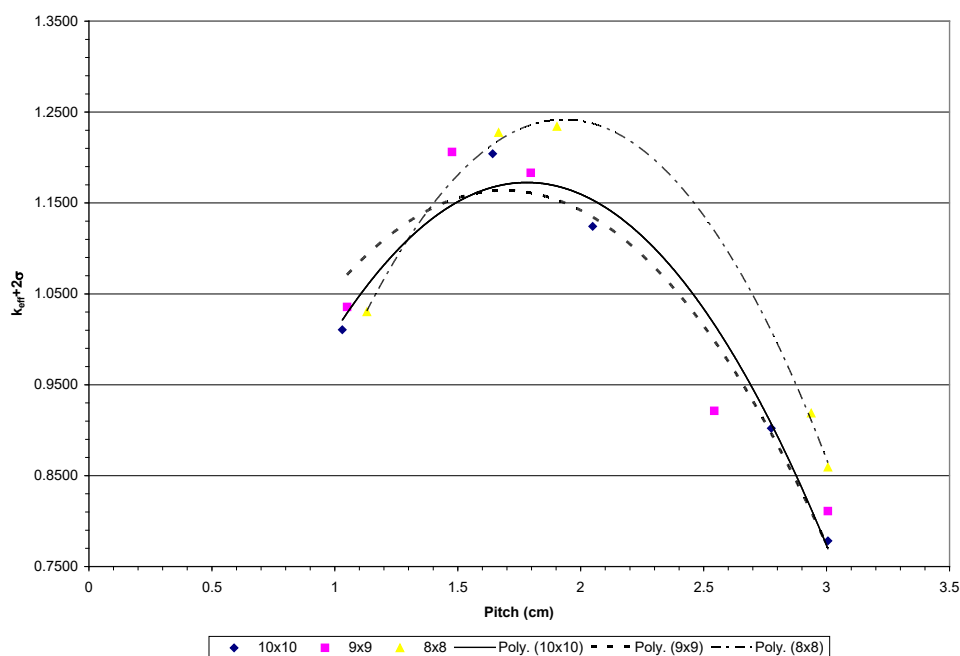


Figure 6-49 BWR UO<sub>2</sub> Fuel Rod Pitch Sensitivity Study

Table 6-24 BWR UO<sub>2</sub> Fuel Rod Pitch Sensitivity Study Results

Fuel Rod Type	Fuel Rod Pitch (cm)	No. of Fuel Rods	Fuel Pellet OD (cm)	Clad ID & OD (cm)	k <sub>eff</sub>	σ	k <sub>eff</sub> + 2σ <sup>a</sup>
10x10	1.0305	289	0.90	1.00	1.0092	0.0007	1.0106
10x10	1.6416	100	0.90	1.00	1.2024	0.0009	<b>1.2042</b>
10x10	2.0484	64	0.90	1.00	1.1224	0.0009	1.1242
10x10	2.7754	34	0.90	1.00	0.9005	0.0008	0.9021
10x10	3.0056	25	0.90	1.00	0.7769	0.0007	0.7783
10x10 LEU+	2.0000	25	0.90	1.00	0.8082	0.0003	0.8088
10x10 LEU+	2.5000	25	0.90	1.00	0.8928	0.0003	0.8934
10x10 LEU+	2.7500	25	0.90	1.00	0.9084	0.0002	0.9088
10x10 LEU+	2.8000	25	0.90	1.00	0.9094	0.0003	<b>0.9100</b>
10x10 LEU+	2.8500	25	0.90	1.00	0.9091	0.0003	0.9097
9x9	1.0505	256	0.96	1.02	1.0341	0.0007	1.0355
9x9	1.4770	121	0.96	1.02	1.2045	0.0008	<b>1.2061</b>
9x9	1.7972	81	0.96	1.02	1.1816	0.0008	1.1832
9x9	2.5432	34	0.96	1.02	0.9196	0.0008	0.9212
9x9	3.0056	25	0.96	1.02	0.8096	0.0007	0.8110
8x8	1.1305	225	1.05	1.10	1.0288	0.0007	1.0302
8x8	1.6662	100	1.05	1.10	1.2259	0.0008	1.2275
8x8	1.9035	81	1.05	1.10	1.2328	0.0007	<b>1.2342</b>
8x8	2.9370	30	1.05	1.10	0.9172	0.0008	0.9188
8x8	3.0056	25	1.05	1.10	0.8577	0.0008	0.8593

a. Limiting case(s) shown in bold

The results in Table 6-24 are based on calculations performed with full water density inside the inner container. It appears the maximum fuel rod quantity allowable for the 10x10 and 9x9 fuel rods should be 34, while that for the 8x8 fuel rods should be 30. However, the rod configurations at full moderator densities represent an overmoderated condition in which reactivity peaks at a reduced moderator density. Therefore, calculations are performed with 25 fuel rods in each transport compartment for each fuel rod type, and the moderator density inside the inner container is varied from 0.4 g/cm<sup>3</sup> to 1.0 g/cm<sup>3</sup> to investigate the possibility that reactivity peaks at a lower moderator density. The results of these calculations are shown in Table 6-25. The peak reactivity for all the LEU fuel rod types occurs at a moderator density of 0.6 g/cm<sup>3</sup> and at a moderator density of 1.0 g/cm<sup>3</sup> for LEU+ fuel. All results are below the USL of 0.94254, or 0.9340 for LEU+ fuel. Therefore, criticality safety for loose fuel rod transport with a maximum of 25 rods in each transport compartment is demonstrated.

**Table 6-25 BWR UO<sub>2</sub> Fuel Rod Maximum Quantity at Reduced Moderator Densities**

Fuel Rod Type	Fuel Rod Pitch (cm)	No. of Fuel Rods	Inner Container Moderator Density (g/cm <sup>3</sup> )	Fuel Pellet OD (cm)	Clad ID & OD (cm)	k <sub>eff</sub>	σ	k <sub>eff</sub> + 2σ <sup>a</sup>
10x10 LEU	3.0056	25	0.40	0.90	1.00	0.7875	0.0009	0.7893
10x10 LEU	3.0056	25	0.60	0.90	1.00	0.8113	0.0008	<b>0.8129</b>
10x10 LEU	3.0056	25	0.80	0.90	1.00	0.8012	0.0007	0.8026
10x10 LEU	3.0056	25	1.00	0.90	1.00	0.7769	0.0007	0.7783
10x10 LEU+	2.8000	25	0.40	0.90	1.00	0.7710	0.0003	0.7716
10x10 LEU+	2.8000	25	0.60	0.90	1.00	0.8578	0.0003	0.8584
10x10 LEU+	2.8000	25	0.80	0.90	1.00	0.8977	0.0003	0.8983
10x10 LEU+	2.8000	25	1.00	0.90	1.00	0.9094	0.0003	<b>0.9100</b>
9x9	3.0056	25	0.40	0.96	1.02	0.8128	0.0008	0.8144
9x9	3.0056	25	0.60	0.96	1.02	0.8404	0.0008	<b>0.8420</b>
9x9	3.0056	25	0.80	0.96	1.02	0.8321	0.0008	0.8337
9x9	3.0056	25	1.00	0.96	1.02	0.8096	0.0007	0.8110
8x8	3.0056	25	0.40	1.05	1.10	0.8529	0.0008	0.8545
8x8	3.0056	25	0.60	1.05	1.10	0.8832	0.0008	<b>0.8848</b>
8x8	3.0056	25	0.80	1.05	1.10	0.8799	0.0009	0.8817
8x8	3.0056	25	1.00	1.05	1.10	0.8577	0.0008	0.8593

a. Limiting case(s) shown in bold

Two additional sensitivities studies were performed to determine whether the BWR loose rods should be limited in the amount of hydrogenous packing materials using 25 8x8 freely loose rods in a 10x1x10 HAC array. First, the thickness of polyethylene wrap around the fuel rods is increased keeping the pitch constant, and second the rods are expanded to the inner container steel wall (4.18 cm pitch) and filled with polyethylene of varying densities. Both studies show that the limiting configuration of optimal water moderation bounds configurations with additional polyethylene packing materials. Therefore, limits on the mass of packing materials such as polyethylene sleeves, end caps, or cushioning foam is not required to maintain criticality safety.

### **6.7.2 Fuel Rods Strapped Together**

Based on the results in the previous calculation, there is no advantage to strapping fuel rods together because close packed rods do not guarantee subcriticality. The straps holding the fuel rods together in the bundle may fail during an accident, and the rods could move about the transport compartment without restraint. Therefore, the maximum number of fuel rods allowable in each RAJ-II fuel compartment when fuel rods are strapped together is 25 for all types.

### **6.7.3 Fuel Rods Transported in 5-Inch Stainless Steel Pipe**

A fuel rod pitch sensitivity study is conducted for the transport of fuel rods inside 5-inch stainless steel pipe, residing in the RAJ-II fuel compartment. The package array model under HAC is used for fuel rod calculations in the RAJ-II package because it was demonstrated to be more reactive than the NCT package array model. The GNF UO<sub>2</sub> 10x10, GNF 9x9, GNF 8x8, the UC and generic PWR worst case fuel rod designs are used for the study. Because the 5-inch stainless steel pipe presents a more difficult volume to accommodate rods in a square pitch, a triangular pitch array is used for the rod configuration. The pipe's stainless steel wall is also neglected for conservatism. The fuel rod configuration inside the pipe is shown in Figure 6-50 for the GNF 8x8 UO<sub>2</sub> fuel rods. The volume inside the pipe is filled with water at a density sufficient for optimum moderation. The inner fuel compartment volume outside the pipe is modeled with no material present to maximize neutron interaction among packages in the array.

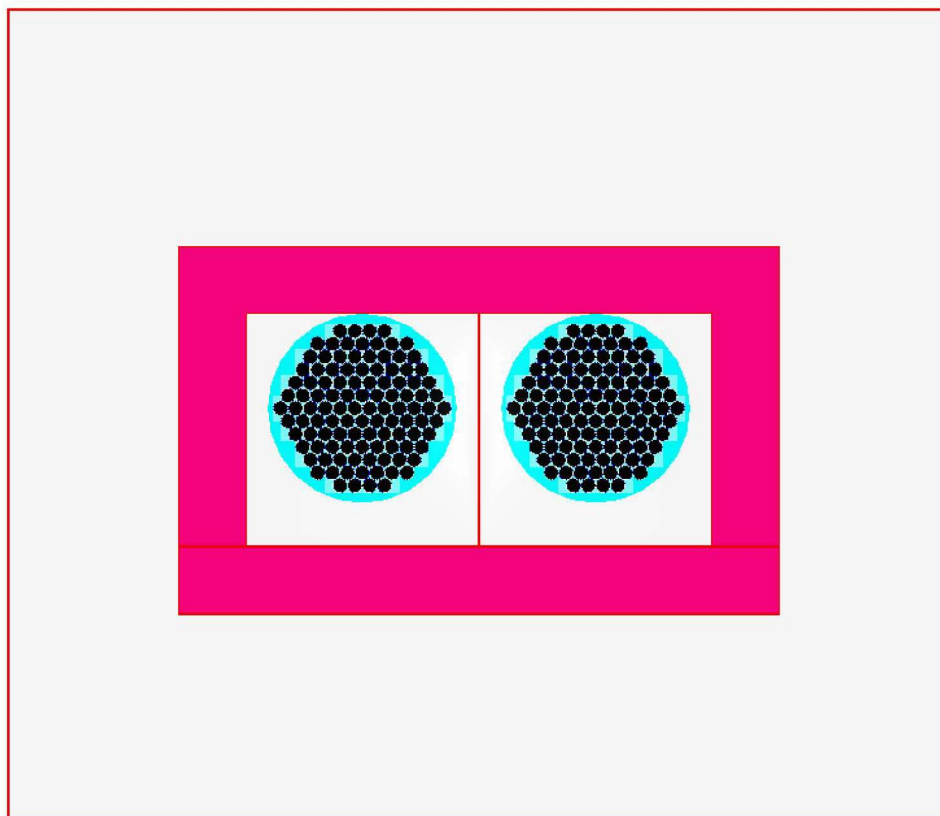


**Figure 6-50 RAJ-II with BWR UO<sub>2</sub> Fuel Rods in 5-Inch Stainless Steel Pipes for Transport**

The results for fuel rod transport in a stainless steel pipe within the RAJ-II package for the LEU UO<sub>2</sub> rod designs are displayed in Figure 6-51. As shown in Figure 6-51, optimum peaks are formed above the USL of 0.94254. Therefore, the stainless steel pipe may be used to ship a limited number of fuel rods. The maximum number of 10x10 LEU fuel rods that may be transported in the stainless steel pipe is 30. The maximum number of 9x9 fuel rods that may be transported in the stainless steel pipe is 26. The maximum number of 8x8 fuel rods that may be transported in the stainless steel pipe is 22. The  $k_{\text{eff}} + 2\sigma$  values (Table 6-39) for different UO<sub>2</sub> LEU fuel rod types with the appropriate fuel rod quantity are below the USL of 0.94254. Therefore, criticality safety is demonstrated for BWR UO<sub>2</sub> LEU fuel rod transport inside a 5-inch stainless steel pipe within the RAJ-II package.

Similar sensitivity studies are performed for GNF 10x10 LEU+ fuel rods. The most limiting  $k_{\text{eff}} + 2\sigma$  value is 0.9143 and is subject to one restriction. The polyethylene equivalent mass inside of the pipe per container is 32.1 kg and the reference density for polyethylene equivalent mass calculation is 0.80 g/cm<sup>3</sup>. Therefore, the criticality safety of transporting loose rods in a 5-inch stainless steel pipe the RAJ-II is confirmed for transporting up to 30 freely loose 10x10 BWR UO<sub>2</sub> LEU+ fuel rods.

The optimum peak for the 10x10 LEU fuel rods is greater than that for the 9x9 or 8x8 fuel rods in the stainless steel pipe. However, the reactivity peak for the 8x8 fuel rods in the loose rod study



is greater than that for the 10x10 fuel rods in the stainless steel pipe. Therefore, the GNF 8x8 and GNF 10x10 LEU+ fuel rod designs are chosen as the worst case BWR UO<sub>2</sub> rod types.

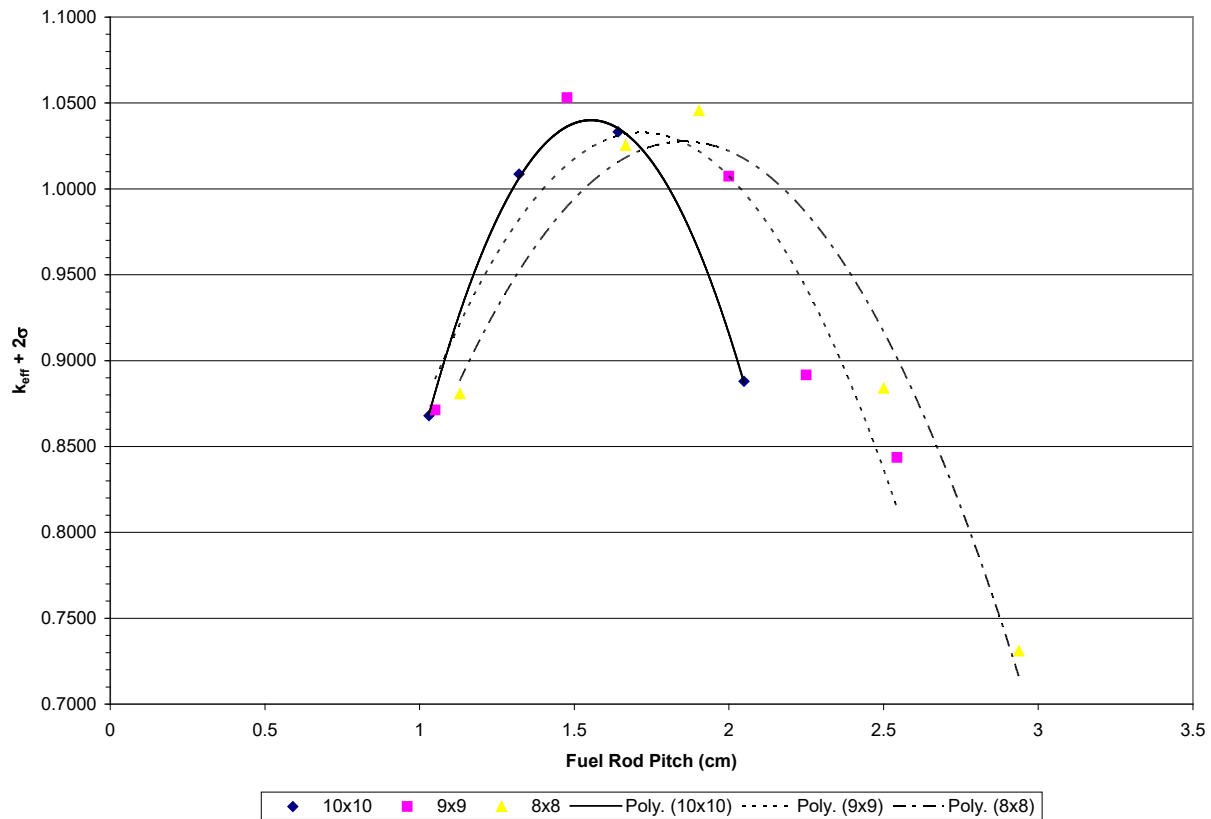


**Figure 6-51 RAJ-II BWR UO<sub>2</sub> Fuel Rod Transport in Stainless Steel Pipe**

For the UC and generic PWR UO<sub>2</sub> fuel rod transport, three different fuel rods have been considered in this analysis, as designated by the labels CANDU-14, CANDU-25, and PWR. The CANDU-14 and CANDU-25 types are those corresponding to the fuel rods in typical CANDU 14 element and 25 element fuel bundle assemblies (Table 6-2). The PWR type is that corresponding to generic PWR fuel rods.

The optimum condition for interspersed water in the package arrays of damaged containers is based on results from a 5-high horizontally infinite array of damaged containers by independently varying the W/F ratios inside the product containers and the interspersed water outside. The results confirm that the optimum interspersed water is 0.0 g/cm<sup>3</sup> because the fuel region inside the pipes is already fully moderated by the water and plastic sleeving surrounding the fuel rods. The W/F ratio was also varied using the single package HAC analysis and both confirmed the optimum W/F ratio for each rod type.

Two sensitivities studies were performed to determine whether the UC and generic PWR UO<sub>2</sub> fuel rod should be limited in the amount of hydrogenous packing materials using CANDU-25 (the limiting of the 3 content types) at the optimum pitch in an 8x1x8 HAC array, while maintaining a 0.0381 cm (15 mils) thick polyethylene sleeving. First, the space within the pipe is filled with

polyethylene of varying densities while the inner container (outside the pipe) and the outer container are voided. Second, the space within the pipe is filled with full density water while the inner container is filled with polyethylene of varying densities and the outer container is voided. Consistent with moderation studies, the inner container voided is most reactive; therefore, limits on mass of packing materials are not required to maintain criticality safety. Within the pipe, moderation studies show that the pipe flooded with full density water is most reactive; therefore, the mass of the polyethylene packing materials is limited to 27.5 kg per compartment. This limit is equivalent to the pipe filled with polyethylene foam at a density of  $0.70 \text{ g/cm}^3$  with CANDU-25 rods at optimum pitch (1.8 cm). Polyethylene with a density of  $0.70 \text{ g/cm}^3$  has a hydrogen atom density slightly less than full density water. The polyethylene sleeving is not included in this mass limit.

#### **6.7.4 Fuel Rods Transported in Stainless Steel Protective Case**

The fuel rod pitch sensitivity study conducted for the transport of fuel rods inside the 5-inch stainless steel pipe described in Section 6.7.3 bounds the transport of fuel rods in the protective case. The protective case cross-section is 89 mm (3.50 inches) by 80 mm (3.15 inches). Based on this small cross-sectional area, the total number of fuel rods that will fit in the protective case is less than the total for the 5-inch pipe. Based on the calculations for the stainless steel pipe, the maximum number of 10x10 fuel rods that may be transported in the protective case is 30, the maximum number of 9x9 fuel rods that may be transported in the protective case is 26, the maximum number of 8x8 fuel rods that may be transported in the protective case is 22.

#### **6.7.5 Single Package Fuel Rod Transport Evaluation**

##### **6.7.5.1 Configuration**

The single package model described in Section 6.3.1.1 is used to demonstrate criticality safety of the RAJ-II package using the worst case fuel design. The single package is evaluated under both NCT and HAC. For transport of BWR  $\text{UO}_2$  rods the evaluation consists of a moderator density sensitivity study. For the NCT model, the moderator density is uniformly varied. In contrast, the moderator density is fixed in the outer container for the HAC model, and the moderator in the inner container is varied. Based on the results in Table 6-24 and Table 6-25, the GNF 8x8 and GNF 10x10 LEU+ worst case fuel rod designs are used for the study because they produced the highest reactivity peak among the BWR  $\text{UO}_2$  fuel rod designs.

For transport of UC and generic PWR  $\text{UO}_2$  rods, the optimum W/F ratio is used to demonstrate criticality safety for single packages. Due to the design of the RAJ-II, the HAC results bound the NCT results. Therefore, single package HAC results are presented.

##### **6.7.5.2 Results**

The results for the single package BWR  $\text{UO}_2$  loose fuel rod NCT evaluation are displayed in Figure 6-52. The results for the single package BWR  $\text{UO}_2$  LEU loose fuel rod HAC evaluation are shown in Figure 6-53. The results in the figures indicate reactivity for the single package increases with increasing moderator density. The highest  $k_{\text{eff}}$  is achieved for both cases at full density moderation. In both cases, the  $k_{\text{eff}}$  remains far below the USL of 0.94254. The LEU fuel maximum  $k_{\text{eff}} + 2\sigma$

for the single package NCT case is 0.6381 (Table 6-40), and the maximum  $k_{\text{eff}} + 2\sigma$  for the single package HAC case is 0.6548 (Table 6-41). Therefore, criticality safety is established for the single package RAJ-II transporting BWR UO<sub>2</sub> loose fuel rods.

The results for the single package UC and generic PWR UO<sub>2</sub> fuel rod HAC evaluation are displayed in Figure 6-54. The maximum  $k_{\text{eff}} + 2\sigma$  for the single package HAC case is 0.6565 and remains far below the USL of 0.9213. Therefore, criticality safety is established for the single package RAJ-II transporting UC and generic PWR UO<sub>2</sub> fuel rods inside a 5-inch stainless steel pipe.

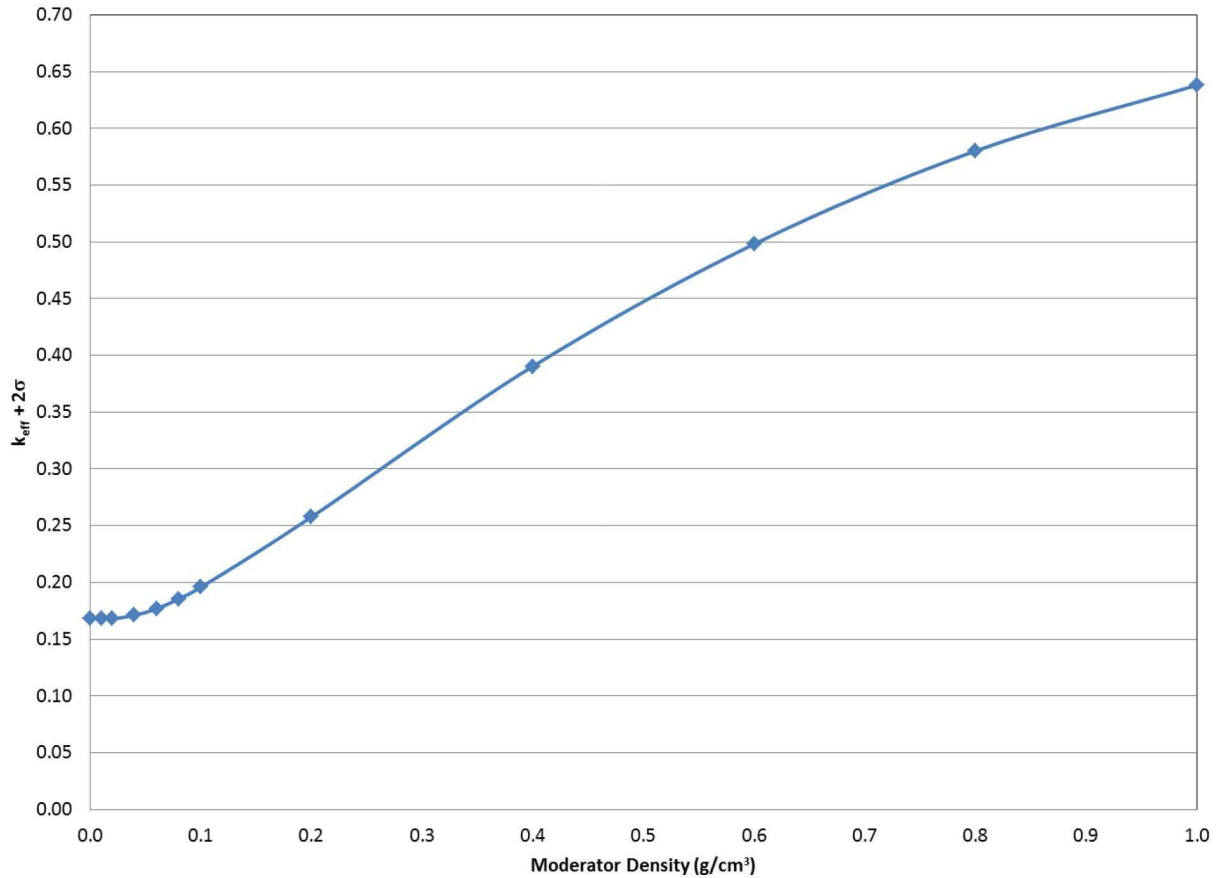


**Figure 6-52 RAJ-II BWR UO<sub>2</sub> Fuel Rod Single Package Under NCT**

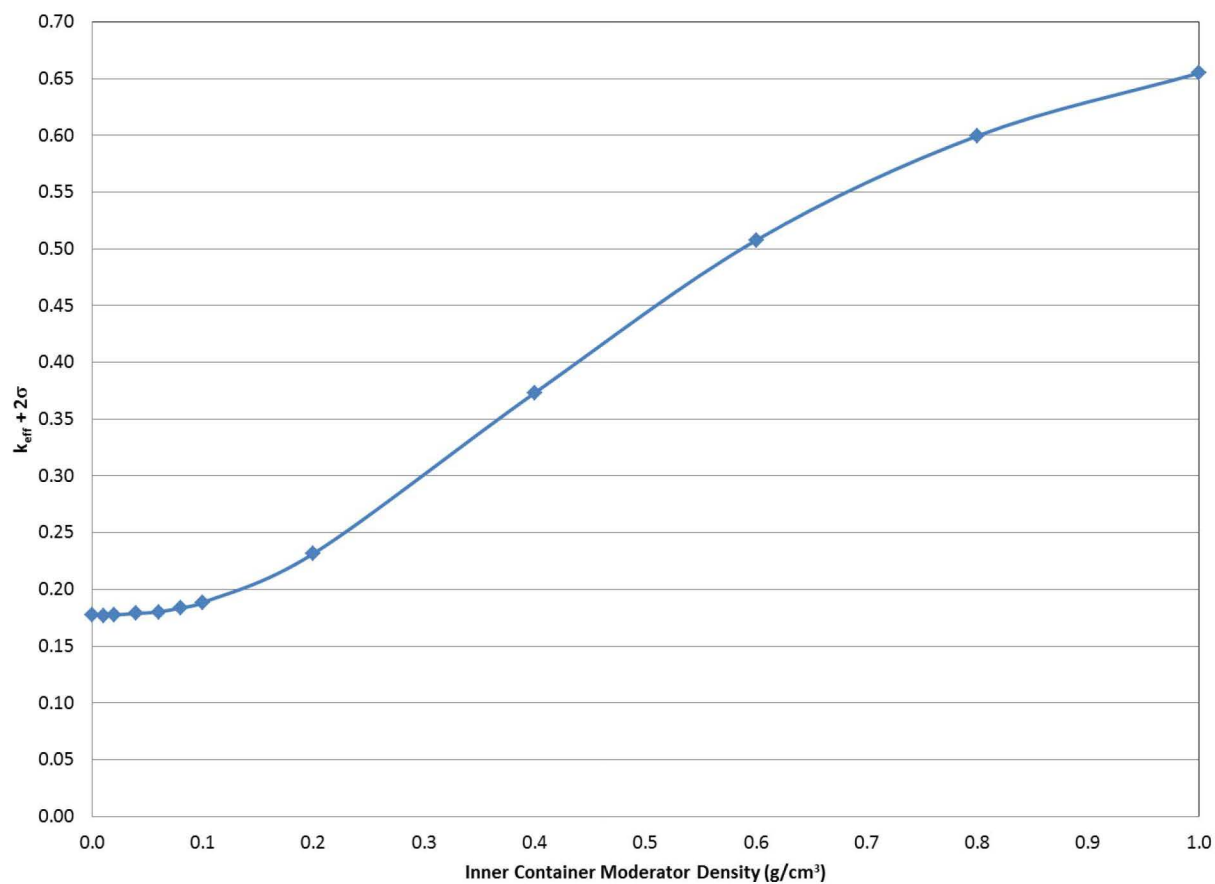


**Figure 6-53 RAJ-II BWR UO<sub>2</sub> Fuel Rod Transport Single Package HAC**

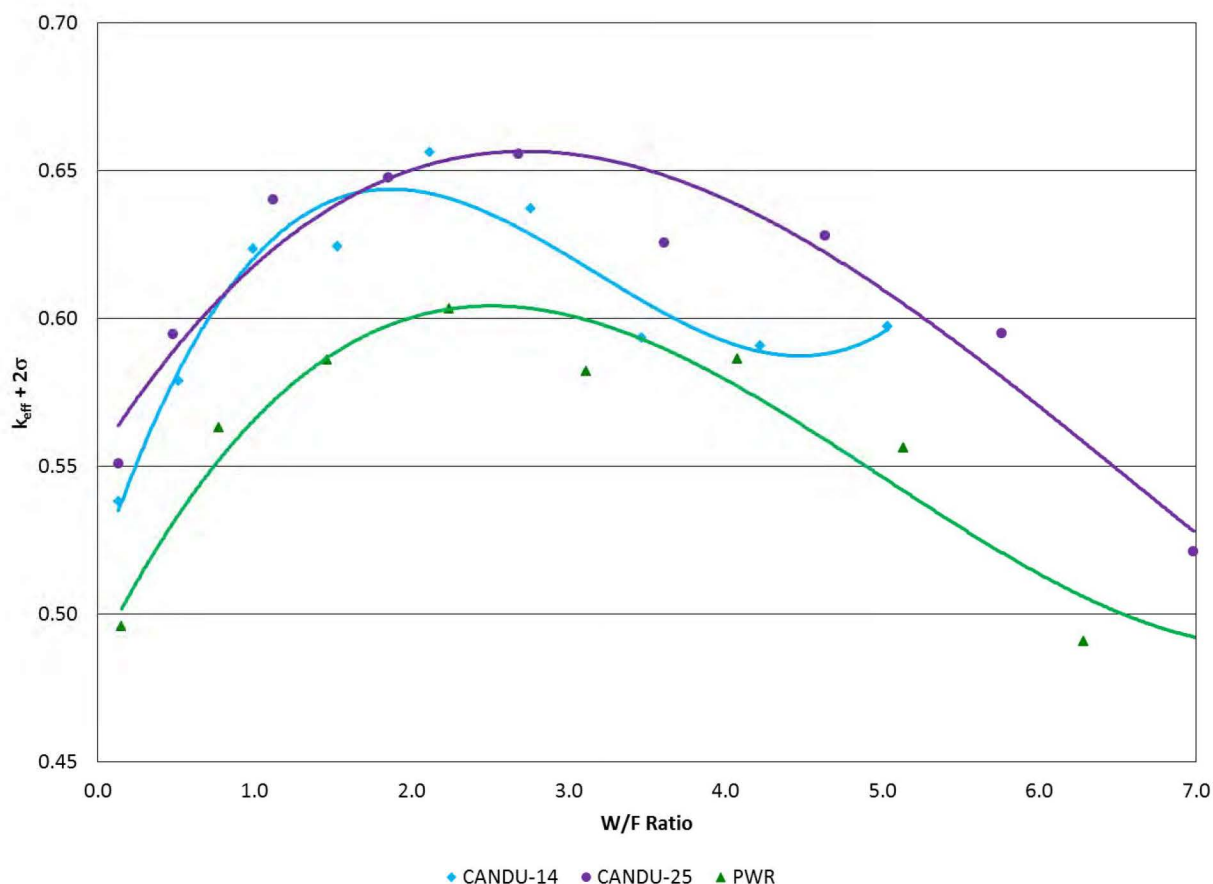


**Figure 6-54 RAJ-II UC and Generic PWR UO<sub>2</sub> Fuel Rod Transport Single Package HAC**

### 6.7.6 Evaluation of Package Arrays with Fuel Rods Under NCT

The package array NCT model described in Section 6.3.1.2.1 is used to demonstrate criticality safety of the RAJ-II package when transporting fuel rods. Based on the results in Table 6-24 and Table 6-25, the GNF 8x8 and GNF 10x10 LEU+ worst case fuel rod designs are used for the study because they produced the highest reactivity peak among the BWR UO<sub>2</sub> fuel rod designs. The calculation using the package array NCT model for fuel rod transport involves a moderator density sensitivity study. In the model, the moderator density is uniformly varied, and the system reactivity is observed.

For transport of UC and generic PWR rods, the optimum W/F ratio is used to demonstrate criticality safety under NCT. A 5-high horizontally infinite array of damaged RAJ-II packages is analyzed. This configuration bounds the results for a 5-high horizontally infinite array of undamaged RAJ-II packages. Regardless, due to the design of the RAJ-II, the HAC package array results determine the package CSI.

#### 6.7.6.1 Results

The results of the package array BWR UO<sub>2</sub> fuel rod transport NCT model calculations are shown in Figure 6-55. As shown, the reactivity initially increases then decreases as the moderator density increases until a density of ~0.4 g/cm<sup>3</sup> is reached, then it increases essentially linearly until full density is reached. The maximum  $k_{\text{eff}} + 2\sigma$  obtained is 0.6381 (Table 6-42) which is below the USL of 0.94254. Therefore, criticality safety of the RAJ-II package with BWR UO<sub>2</sub> fuel rods is demonstrated under NCT.

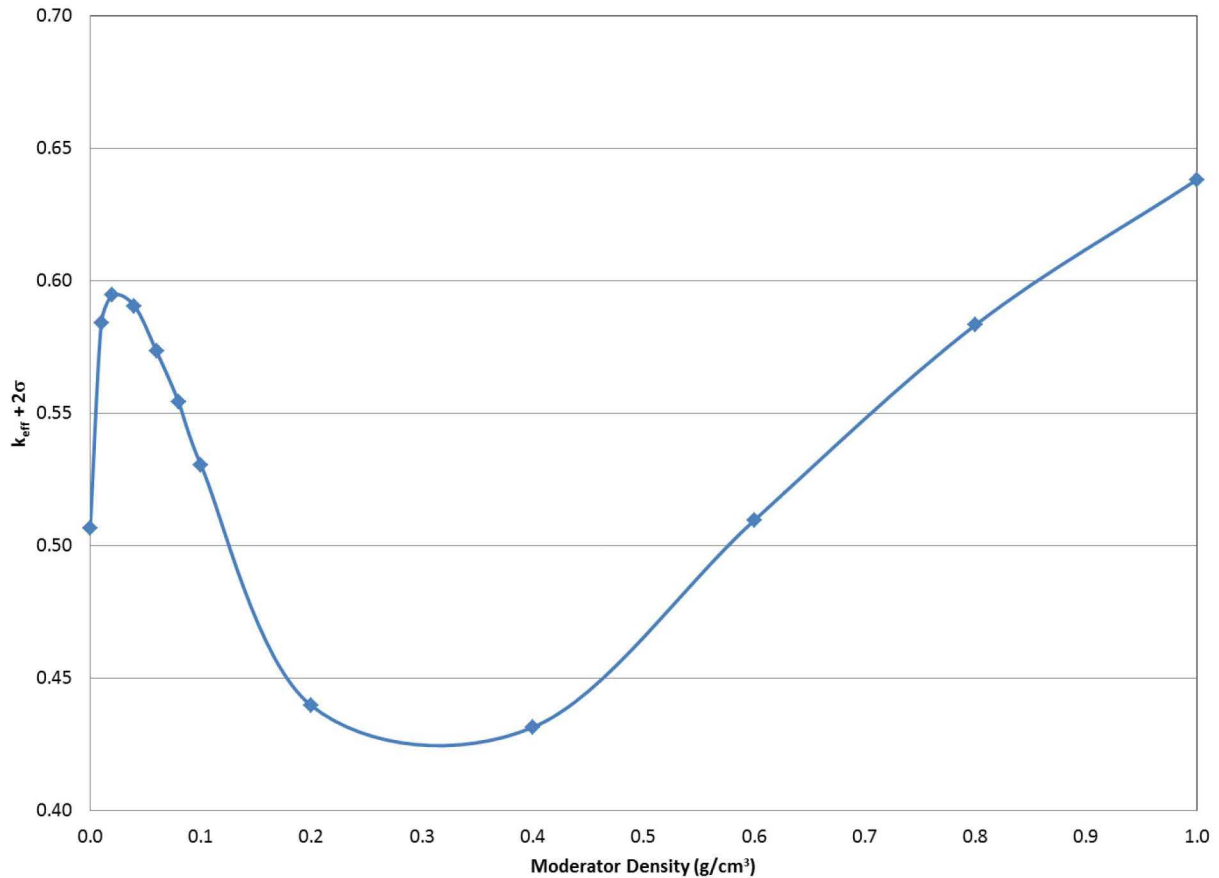


**Figure 6-55 RAJ-II Package Array Under NCT with BWR UO<sub>2</sub> Loose Fuel Rods**

The results of the UC and generic PWR UO<sub>2</sub> fuel rod transported in a 5-inch stainless steel pipe, configured in an array which is horizontally infinite, using package HAC dimensions, bounding the package array NCT results, are shown in Figure 6-56. The maximum  $k_{\text{eff}} + 2\sigma$  obtained is 0.9037 which is below the USL of 0.9213. Therefore, criticality safety of the RAJ-II package with UC and generic PWR UO<sub>2</sub> fuel rods is demonstrated under NCT.

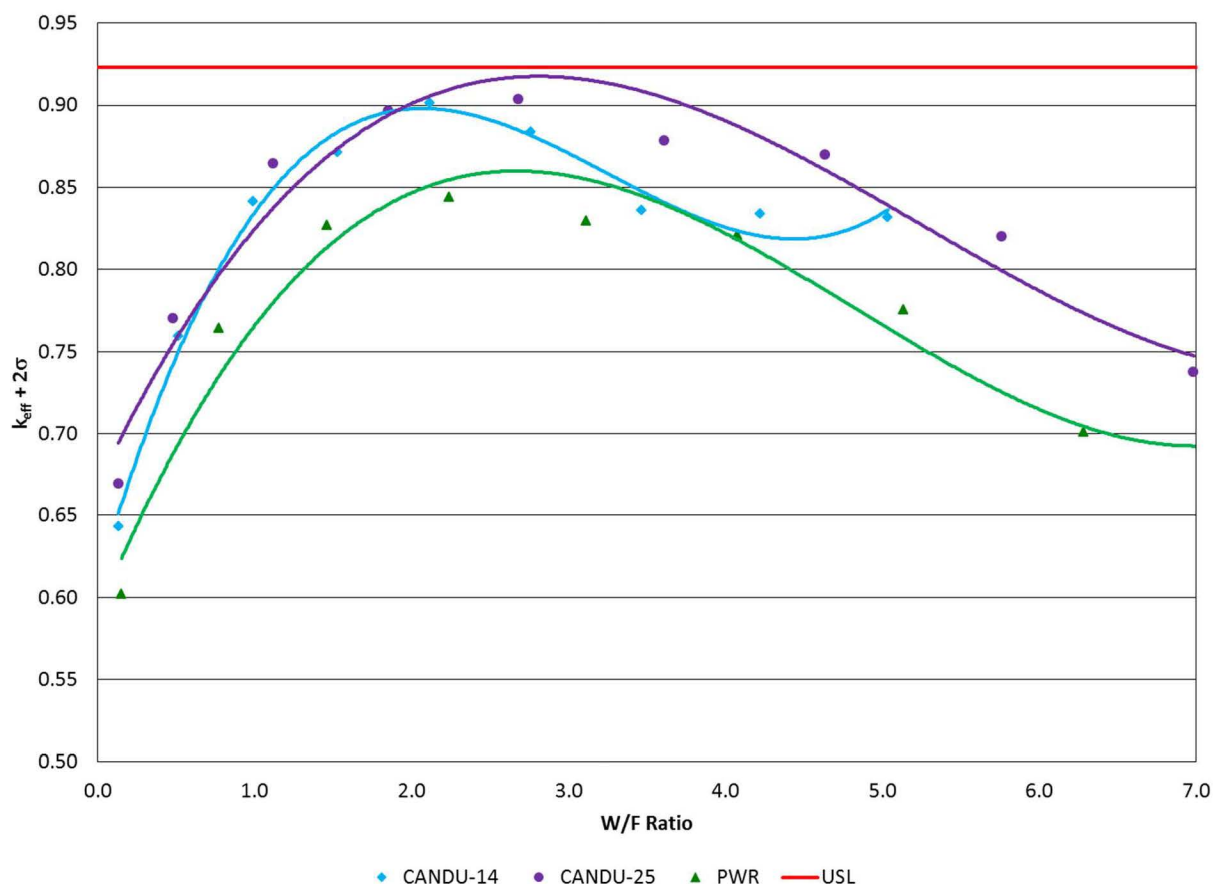


**Figure 6-56 RAJ-II Package Array Bounding NCT with UC and Generic PWR UO<sub>2</sub> Loose Fuel Rods**

### 6.7.7 Fuel Rod Transport Package Arrays Under HAC

The package array HAC model described in Section 6.3.1.2.2 is used to demonstrate criticality safety of a 10x1x10 array (2N=100) of RAJ-II packages when transporting BWR UO<sub>2</sub> loose fuel rods. Based on the results in Table 6-24 and Table 6-25, the GNF 8x8 and GNF 10x10 LEU+ worst case fuel rod designs are used for the study because they produced the highest reactivity peak among the BWR UO<sub>2</sub> fuel rod designs. The calculation using the HAC model involves a moderator density sensitivity study. In the study, there is no interspersed moderator, and the moderator density inside the inner container is varied. The polyethylene foam lines the inner container fuel compartment because the configuration resulted in the most reactive conditions.

For UC and generic PWR rods the optimum W/F ratio is used in the final demonstration of criticality safety. Because the HAC package array size is 8x1x8, this array size determines the package CSI for fuel rod transport.

#### 6.7.7.1 Results

The results using KENO-VI with continuous-energy ENDF/B-VII cross-section library of the BWR UO<sub>2</sub> package array HAC model calculations are shown in Figure 6-57. The reactivity begins



at its lowest value and increases with increasing internal moderator density until a maximum is reached at a density of 1.0 g/cm<sup>3</sup>. The maximum  $k_{\text{eff}} + 2\sigma$  for the package array fuel rod transport HAC case is 0.8738 (Table 6-43), which is below the USL of 0.9340. Therefore, criticality safety of the RAJ-II is demonstrated for the package array under HAC when BWR UO<sub>2</sub> fuel rods are being transported.

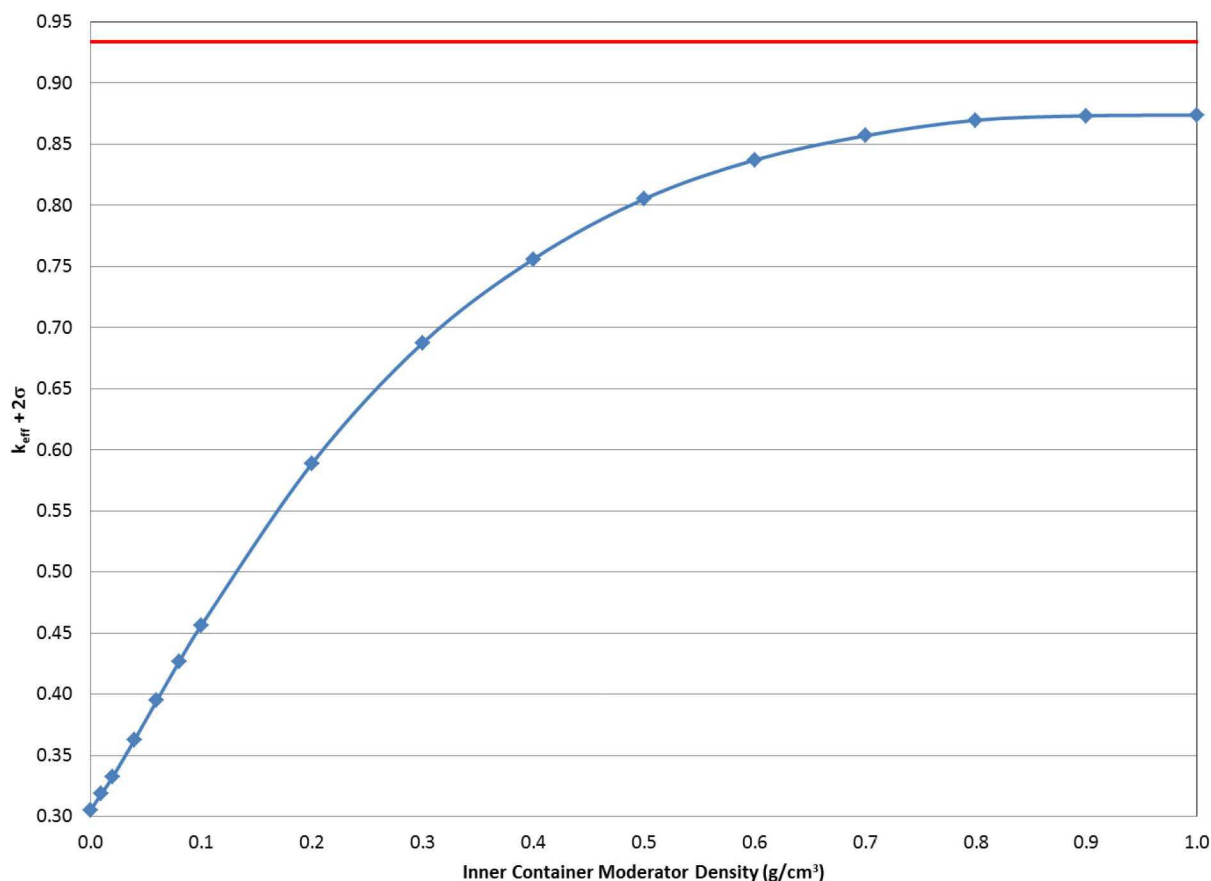


**Figure 6-57 RAJ-II BWR UO<sub>2</sub> LEU Fuel Rod Transport Under HAC**

Results for the 8x1x8 array of damaged RAJ-II packages with the optimum W/F ratio inside a 5-inch stainless steel pipe with UC or generic PWR fuel rods, with full density water inside the pipes, and without interspersed water outside the pipes, are reported in Table 6-26. The maximum  $k_{\text{eff}} + 2\sigma$  for 8x1x8 array of RAJ-II packages is 0.9131 (below the USL of 0.9213) which occurs for loose CANDU-25 UC fuel rods at a W/F ratio of 2.68. This result also bounds the  $k_{\text{eff}}$  values of the CANDU-14 UC fuel rod and generic PWR UO<sub>2</sub> designs.

As shown in Figure 6-54 and Figure 6-56, the optimum W/F ratios are identified for each fuel rod type. This was done by changing the fuel rod pitch within the package, thereby changing the number of fuel rods within the pipe. The lowest W/F ratio corresponds to the configuration where the fuel rods are densely packed within the pipe; Figure 6-19 shows that a lattice of fuel rods is modeled within the confines of the pipe, and some of the rods are only partially modeled. The total number of rods densely packed within the pipe, including the partially modeled rods is 74,



130, and 105 for CANDU-14, CANDU-25, and generic PWR UO<sub>2</sub> rods, respectively. Because the criticality analysis demonstrates safety for a large range of W/F ratios, including the optimum, any number of fuel rods is demonstrated to be safe, and the UC and generic PWR UO<sub>2</sub> fuel rod transport shipments are only limited by the physical dimensions of the 5-inch stainless steel pipe or protective case and the CSI. The UC rods are modeled with an active fuel length of 450 cm even though actual active lengths are significantly shorter (see Table 6-2). Therefore, the maximum number of UC fuel rods which can be loaded is set to 695 and 1458 for CANDU-14 and CANDU-25, respectively.

**Table 6-26 Results for 8x1x8 HAC Array of Containers with Fuel Rods in Stainless Steel Pipe**

Type of Rod	W/F Ratio	k <sub>eff</sub>	σ	k <sub>eff</sub> + 2σ
CANDU-14 (UC)	2.12	0.9079	0.0008	0.9095
CANDU-25 (UC)	2.68	0.9116	0.0007	<b>0.9131</b>
PWR (UO <sub>2</sub> )	2.24	0.8548	0.0007	0.8563

## **6.8 FISSILE MATERIAL PACKAGES FOR AIR TRANSPORT**

This package is not intended for the air transport of fissile material.

## **6.9 CONCLUSION**

Based on the calculations that have been documented, the RAJ-II package is qualified to transport UO<sub>2</sub> fuel assemblies, including 10x10, 9x9, and 8x8 BWR designs, in accordance with the criticality safety requirements of the IAEA and 10 CFR 71. The fuel assemblies may be channeled or un-channeled. The calculations demonstrate a damaged 10x1x10 array for LEU fuel, a damaged 8x1x8 array for LEU+ fuel, or a 21x3x24 array of un-damaged packages remains subcritical with optimum interspersed moderation. The 10x10 fuel assemblies may be transported with 8, 10, 12, 14, or 16 part length fuel rods, and 9x9 fuel assemblies may be transported with 8, 10 and 12 part length fuel rods.

In addition, the calculations demonstrate UO<sub>2</sub> fuel rods may be packaged within the RAJ-II inner container freely loose, inside a 5-inch stainless steel pipe or protective case, or strapped together. The fuel rods may consist of BWR UO<sub>2</sub> 10x10 LEU or LEU+, 9x9, or 8x8, CANDU UC or generic PWR UO<sub>2</sub> fuel rod designs.

## 6.10 BENCHMARK EVALUATIONS

### 6.10.1 SCALE 4.4a and GEMER

#### 6.10.1.1 Applicability of Benchmark Experiments

The criticality calculation method is validated by comparison with critical experiment data which is sufficiently diverse to establish that the method bias and uncertainty will apply to conditions considered in the RAJ-II criticality analysis. A set of 27 critical experiments are analyzed using SCALE-PC to demonstrate its applicability to criticality analysis and to establish a set of USLs that define acceptance criteria. Benchmark experiments are selected with compositions, configurations, and nuclear characteristics that are comparable to those encountered in the RAJ-II package loaded with fuel as described in Table 6-1. The critical experiments are described in detail in References 6-7 through 6-14 and summarized in Section 6.11.10.

The critical experiments consisted of water moderated, oxide fuel arrays in square lattices. Fourteen experiments were 15x8 fuel rod lattices, with 4.31 wt% U-235 enrichment, and different absorber plates in the water gaps between rods. The absorber plates include aluminum, Type 304L stainless steel, Type 304L stainless steel with various boron enrichments, Zircaloy-4, and Boral™. Thirteen experiments were 15x15 fuel rod lattices using multiple enrichments, no absorbers between rod clusters, and gadolinium absorber integral to the fuel in most cases (9 cases). The lattice arrays in these experiments had enrichments of 2.46, 2.73, 2.74, 2.75, 2.76, 2.77, or 2.78 wt% U-235. Comparison with these experiments demonstrates the applicability of the criticality calculation method.

#### 6.10.1.2 Bias Determination

A set of USL is determined using the results from the 27 critical experiments and USL Method 1, Confidence Band with Administrative Margin, described in Section 4.0 of NUREG/CR-6361 (Reference 6-15). The USL Method 1 applies a statistical calculation of the method bias and its uncertainty plus an administrative margin ( $\Delta k=0.05$ ) to a linear fit of the critical experiment benchmark data. The USLs are determined as a function of the critical experiment system parameters; enrichment, W/F ratio, H/X ratio, pin pitch, Energy of the Average Lethargy causing Fission (EALF), and the Average Energy Group causing Fission (AFG).

- The following equation is determined for the USL as a function of enrichment:

$$USL = 0.9388 + (8.6824 \times 10^{-4})x \quad \text{for all } x$$

*The variance of the equation fit is  $3.6827 \times 10^{-6}$ . The applicable range for enrichment is  $2.46 \leq x \leq 4.31$ .*

- The following equation is determined for the USL as a function of water-to-fuel ratio:

$$USL = 0.9398 + (6.6864 \times 10^{-4})x \quad \text{for all } x$$

*The variance of the equation fit is  $3.8188 \times 10^{-6}$ . The applicable range for water-to-fuel ratio is  $1.8714 \leq x \leq 3.8832$ .*

- The following equation is determined for the USL as a function of hydrogen-to-U-235:

$$\text{USL} = 0.9380 + (1.4976 \times 10^{-5})x \quad \text{for all } x$$

*The variance of the equation fit is  $4.1692 \times 10^{-6}$ . The applicable range for hydrogen-to-U-235 ratio is  $200.56 \leq x \leq 255.92$ .*

- The following equation is determined for the USL as a function of pin pitch:

$$\text{USL} = 0.9387 + (1.4894 \times 10^{-3})x \quad \text{for all } x$$

*The variance of the equation fit is  $3.7993 \times 10^{-6}$ . The applicable range for pin pitch is  $1.6358 \leq x \leq 2.54$ .*

- The following equation is determined for the USL as a function of average energy of the lethargy causing fission:

$$\text{USL} = 0.9423 - (3.8725 \times 10^{-3})x \quad \text{for all } x$$

*The variance of the equation fit is  $4.1339 \times 10^{-6}$ . The applicable range for average energy of the lethargy causing fission is  $0.1127 \leq x \leq 0.3645$ .*

- The following equation is determined for the USL as a function of the average energy group causing fission:

$$\text{USL} = 0.9281 + (3.9834 \times 10^{-4})x \quad \text{for all } x$$

*The variance of the equation fit is  $4.0641 \times 10^{-6}$ . The applicable range for the average energy group causing fission is  $32.89 \leq x \leq 35.77$ .*

Of the preceding equations, the USL as a function of enrichment is the best correlated to the data because the variance of the equation fit is the smallest. Therefore, the USL as a function of enrichment is used to determine a minimum USL for each fuel assembly type considered for use with the RAJ-II package (Table 6-1). Figure 6-58 shows the USL as a function of enrichment. USL values are calculated as a function of enrichment for each candidate fuel design. All candidate fuel designs have the same maximum enrichment of 5.0 wt% U-235. Although the 5.0 wt% U-235 enrichment falls outside the range of applicability, American National Standards Institute (ANSI)/American Nuclear Society (ANS)-8.1 (Reference 6-16) allows the range of applicability to be extended beyond the range of conditions represented by the benchmarks, as long as that extrapolation is not large. As outlined in Reference 6-15,  $k(x)-w(x)$  is used to extend the USL curve beyond the range of applicability.

Figure 6-58 displays the USL curve extrapolation using  $k(x)-w(x)$ ; the extrapolated USL value corresponding to the 5.0 wt% U-235 enrichment is 0.94323. Because the extrapolated value results in a higher USL than the maximum enrichment within the range of applicability would produce, the USL corresponding to the 4.31 wt% U-235 enrichment is conservatively selected. Therefore, the USL for the RAJ-II package is 0.94254 when SCALE 4.4a and 44 group ENDF/B-V library is used.

The following equation is used to develop the  $k_{\text{eff}}$  for the transportation of fuel in the RAJ-II package:

$$k_{\text{eff}} = k_{\text{case}} + 2\sigma$$

where:

$k_{case}$  = KENO V.a  $k_{eff}$  for a particular case of interest

$\sigma$  = uncertainty in calculated KENO V.a  $k_{eff}$  for a particular case of interest

The  $k_{eff}$  for each container configuration analyzed in the RAJ-II criticality analysis is compared to the minimum USL (0.94254) to ensure subcriticality.

The GEMER program has been validated (Reference 6-17) against experiments that have uranium form, chemical composition and moderation/reflection conditions similar to those of this application. For low-enriched  $UO_2$  lattice systems without poison, the calculational bias and bias uncertainty of GEMER is given by (Reference 6-1):

$$b = -0.0187$$

A minimum margin of subcriticality is applied as:

$$\Delta k_m = 0.05$$

Because the GEMER validation benchmarks for heterogeneous  $UO_2$  systems do not include UC fuel types in the Area of Applicability (AOA), an additional margin  $k_{AOA} = 0.01$  will be applied for loose UC rods because no UC critical benchmarks are currently available.

Therefore,

$$\text{For } UO_2 \text{ Rods: } USL = 1 + b - \Delta k_m = 1 + (-0.0187) - 0.05 = 0.9313$$

$$\text{For UC Rods: } USL = 1 + b - \Delta k_m - \Delta k_{AOA} = 1 + (-0.0187) - 0.05 - 0.01 = 0.9213$$

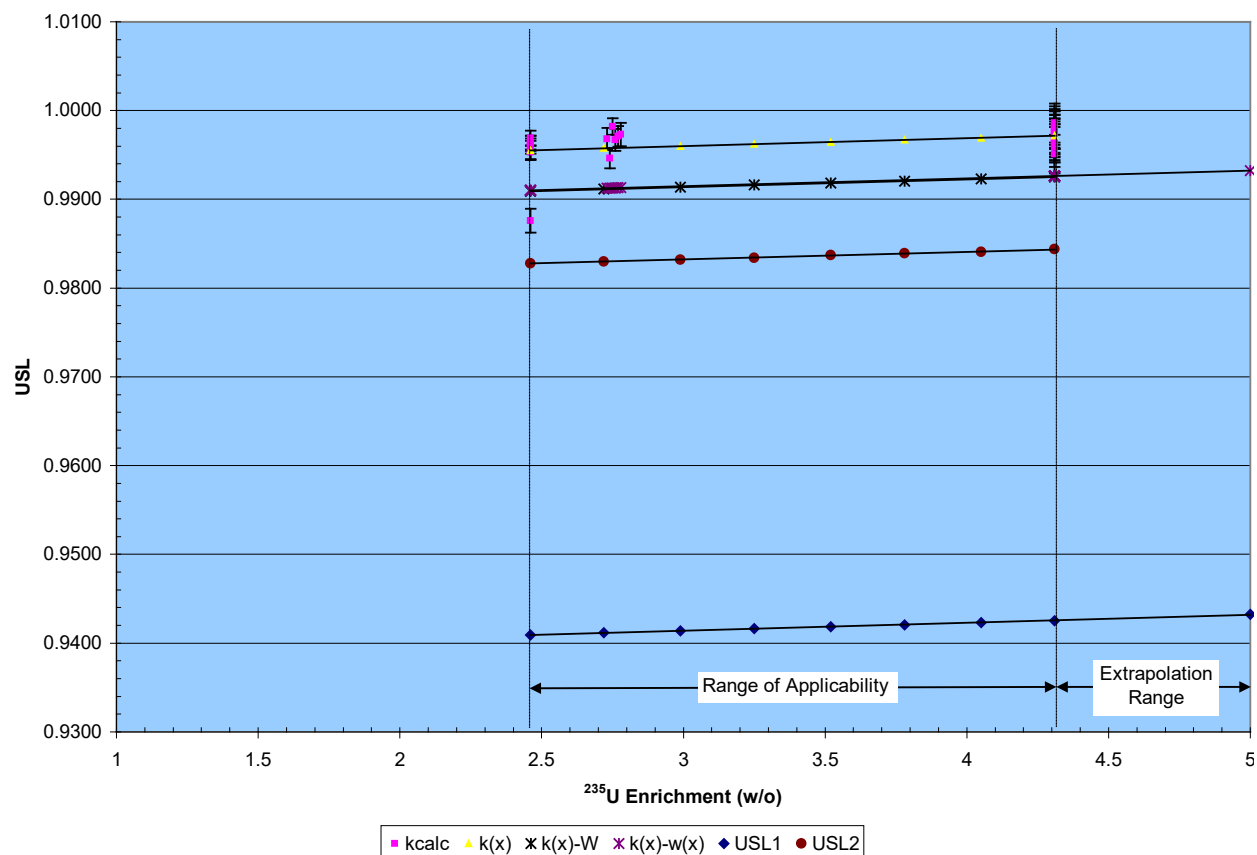


**Figure 6-58 USL as a Function of Enrichment**

## 6.10.2 KENO-VI

The results reported in Sections 6.4, 6.5 and 6.6 are performed using KENO-VI (part of the SCALE 6.1 analysis package, Reference 6-18) with continuous-energy ENDF/B-VII cross-section library. Critical experiments were selected to represent the materials and geometry of the package.

### 6.10.2.1 Applicability of Benchmark Experiments

To evaluate the performance of KENO-VI and cross-section libraries for Low-Enriched Uranium (LEU) heterogeneous compound systems with similarity to the package configurations, 16 benchmark experiments, consisting of 70 critical configurations without neutron poisons and 5 critical configurations with  $\text{UO}_2\text{-Gd}_2\text{O}_3$  rods, are selected from References 6-19 through 6-22.

Most of these critical experiments are low-enriched Light Water Reactor (LWR) lattices and span a range of moderation and fuel pin arrangements that are applicable in evaluating LWR fuel storage and transport. The AOA for LEU heterogeneous compound systems with gadolinia is defined by the key parameters for the critical benchmark experiments, as shown in Table 6-27.

**Table 6-27    AOA – LEU Heterogeneous Systems with Gadolinia**

Parameters	Critical Benchmarks	Area of Applicability
Fissile Material	Uranium	Uranium
Chemical Form	U, UO <sub>2</sub>	U, U <sub>y</sub> O <sub>x</sub> (x/y ≥ 2)
Enrichment (wt% U-235)	[[            ]]	[[            ]]
Physical Form	Solid Compound, Metal	Solid Compound, Metal
Moderator (in fuel region)	H <sub>2</sub> O, UO <sub>2</sub> F <sub>2</sub>	H <sub>2</sub> O, UO <sub>2</sub> F <sub>2</sub>
Physical Form	Solution	Solution
Moderation Ratio (H/U-235)	[[            ]]	[[            ]]
Reflector (in fuel region)	H <sub>2</sub> O, UO <sub>2</sub> F <sub>2</sub> , Depleted U, Steel, Pb, Plexiglas	H <sub>2</sub> O, UO <sub>2</sub> F <sub>2</sub> , Depleted U, Steel, Pb, Polymers
Physical Form	Solution, Solid	Solution, Solid
Absorber (in fuel region)	Gd	Gd
Neutron Energy Spectrum	Thermal	Thermal

#### 6.10.2.2 Bias Determination

Due to the limited availability of benchmark experiments with gadolinium (Gd), a 3-step method is used to determine the bias:

1. Determine the bias from 70 critical configurations without neutron poisons.
2. Evaluate the effect of Gd on the bias established from 70 critical configurations without Gd by including 5 critical configurations containing UO<sub>2</sub>-Gd<sub>2</sub>O<sub>3</sub> rods.
3. Determine an Additional Margin to Subcriticality (AMS) based on a similarity analysis between the RAJ-II package containing GNF2 fuel assemblies with UO<sub>2</sub>-Gd<sub>2</sub>O<sub>3</sub> rods and 5 critical experiments with UO<sub>2</sub>-Gd<sub>2</sub>O<sub>3</sub>.

The bias is a statistical average determined based on a group of selected critical experiments. The bias uncertainty is established as a statistical interval at a specified confidence level by a statistical analysis of the variation of bias around this average. The bias must be either negative or zero (a bias calculated in this manner to be positive is taken to be zero). A margin of subcriticality of 0.05 is applied in all package criticality safety evaluations. Single-Sided Lower Tolerance Limit (SSLTL) is used to determine the bias and bias uncertainty because there are no trends apparent in the calculated  $k_{eff}$  from the selected critical experiments. The calculated  $k_{eff}$  values from the benchmarks are normally distributed. The 95% of confidence level and at least 95% of population are used in the bias determination.

Sixteen benchmark experiments, consisting of a total of 70 critical configurations, are used to determine the bias and bias uncertainty for AOA of LEU heterogeneous compound systems without neutron poisons. An additional five critical configurations containing UO<sub>2</sub>-Gd<sub>2</sub>O<sub>3</sub> rods (configurations labeled as BW1810 from Reference 6-20) are added to the 70 critical

configurations without neutron poisons to evaluate the effect of Gd to the bias. The results show that there is no significant effect on the bias and bias uncertainty by adding five Gd critical configurations to the 70 critical configurations without Gd.

Due to the limitation in the number and the diversity of critical experiments containing gadolinium, TSUNAMI-3D-K6 is used to provide quantitative justifications for the coverage of the critical experiments without Gd for the intended KENO-VI application involving Gd to determine whether an AMS is needed. TSUNAMI-3D-K6 is used to calculate the sensitivity of  $k_{\text{eff}}$  to each constituent cross-section data component used in the criticality safety analysis. The sensitivity data is coupled with cross-section uncertainty data, in the form of multigroup covariance matrices, to produce an uncertainty in  $k_{\text{eff}}$  due to uncertainties in the underlying nuclear data.

Five BW1810 critical configurations are compared to the following RAJ-II package cases for the similarity and coverage analysis using two different GNF 10x10 assembly designs. TSUNAMI reports the suggested AMS for each case. For conservatism, the maximum AMS among all the cases is chosen to determine the USL for the KENO-VI criticality safety analyses of the RAJ-II package containing GNF 10x10 fuel assemblies with  $\text{UO}_2\text{-Gd}_2\text{O}_3$  rods.

The USL can be determined from the following equation when using KENO-VI with continuous-energy ENDF/B-VII cross-section library:

$$\text{USL} = 1 + b - \Delta k_b - \Delta k_m - \Delta k_{\text{AMS}} = 0.9340$$

where,

<b>b</b>	= the bias	[[	]]
<b><math>\Delta k_b</math></b>	= the bias uncertainty	[[	]]
<b><math>\Delta k_m</math></b>	= the margin of subcriticality		0.0500
<b><math>\Delta k_{\text{AMS}}</math></b>	= additional margin to subcriticality	[[	]]

NEDO-33869 Revision 11  
Non-Proprietary Information

## 6.11 APPENDIX

### 6.11.1 Single Package NCT Input

```
=CSAS25          PARM=SIZE=500000
RAJ-II CONTAINER, HAC, NO INTERSPERSED H2O, 100% INNER H2O DENSITY, 5.0 W/O
235U, 12 PART LENGTH RODS, 12 GAD RODS, SINGLE PACKAGE
44GROUPNDF5      LATTICECELL
UO2              1  DEN=10.74      1.0  293 92235 5.0 92238 95.0  END
ZR              2  1.00              293              END
H2O             3  1.00              293              END
ARBMUO2         10.74 2 1 1 1 92000 1
                                   8016 2 4 0.97840 293 92235 5.0
                                   92238 95.0  END
ARBMGD2O3       7.407 2 0 1 1 64000 2
                                   8016 3 4 0.02160 293              END
H2O             5  1.00              293              END
SS304           6  1.00              293              END
POLYETHYLENE    7  DEN=0.080000 1.0  293              END
POLYETHYLENE    8  DEN=0.949 0.25405 293              END
H2O             8  DEN=1.00 0.74595 293              END
H2O             9  1.00              293              END
ARBMAL2O3       0.25 2 0 1 0 13027 2 8016 3 10 0.49  END
ARBMSIO2        0.25 2 0 1 0 14000 1 8016 2 10 0.51  END
ZR             11 1.00              293              END
END COMP
SQUAREPITCH 1.3500 0.8950 1 8 1.01000 2 0.9338 0  END
MORE DATA
RES=4 CYLINDER 0.4475  DAN(4)=2.3197146E-01
END MORE DATA
RAJ-II CONTAINER, HAC, NO INTERSPERSED H2O, 100% INNER H2O DENSITY, 5.0 W/O
235U, 12 GAD RODS, SINGLE PACKAGE
READ PARM TME=400 GEN=400 NPG=2500 NSK=50 NUB=YES RUN=YES END PARM
READ GEOM

UNIT 1
COM=!CONTAINER INNER BOX!
'DEFINE GEOMETRY FOR SEPARATOR PLATE BETWEEN ASSEMBLY COMPARTMENTS
CUBOID 6 1 2P0.0875 2P228.34 2P8.829
'DEFINE REGION FOR ASSEMBLY COMPARTMENTS WITHIN INNER BOX
CUBOID 9 1 2P17.713 2P228.34 2P8.829
'INSERT FOAM POLYETHYLENE
HOLE 4 -8.9003 0.00 0.00
HOLE 5 8.9003 0.00 0.00
'DEFINE WALLS FOR ASSEMBLY COMPARTMENTS WITHIN INNER BOX
CUBOID 6 1 2P17.800 2P228.34 8.829 -8.9165
'DEFINE REGION OUTSIDE THE WALLS OF THE ASSEMBLY COMPARTMENTS
CUBOID 10 1 2P22.798 2P228.34 8.829 -13.839
'DEFINE THE INNER WALLS OF THE BOX ENDS
CUBOID 6 1 2P22.798 2P228.48 8.829 -13.979
'DEFINE INNER CORE OF BOX ENDS
CUBOID 10 1 2P22.798 2P233.44 8.829 -13.979
'DEFINE OUTER WALLS OF THE INNER BOX
CUBOID 6 1 2P22.938 2P233.58 8.829 -13.979
```



NEDO-33869 Revision 11  
Non-Proprietary Information

```
UNIT 2
COM=!INNER BOX LID!
'DEFINE INNER CORE OF INNER BOX LID
CUBOID    10 1  2P22.798    2P233.44    2P2.48
'DEFINE WALLS FOR INNER BOX LID
CUBOID     6 1  2P22.938    2P233.58    2P2.62

UNIT 3
COM=!INNER BOX WITH ENDS AND LID!
ARRAY 1 3*0

UNIT 4
COM=!FOAM POLYETHYLENE FOR LEFT ASSEMBLY COMPARTMENT!
CUBOID     9 1  2P7.055    2P228.34    2P7.055
HOLE       70      -6.7500  -192.50  -6.750
'FOAM POLYETHYLENE FOR ASSEMBLY COMPARTMENTS
CUBOID     7 1  2P8.8126    2P228.34    2P8.829

UNIT 5
COM=!FOAM POLYETHYLENE FOR RIGHT ASSEMBLY COMPARTMENT!
CUBOID     9 1  2P7.055    2P228.34    2P7.055
HOLE       70      -6.7500  -192.50  -6.750
'FOAM POLYETHYLENE FOR ASSEMBLY COMPARTMENT
CUBOID     7 1  2P8.8126    2P228.34    2P8.829

UNIT 10
COM=!5 W/O FUEL PINS W/O GAD!
'DEFINE THE FUEL PELLET
YCYLINDER 1  1    0.4475    192.5  0
'DEFINE THE PELLET-CLAD GAP
YCYLINDER 0  1    0.4669    192.5  0
'DEFINE THE FUEL ROD CLADDING/POLY
YCYLINDER 2  1    0.5050    192.5  0
'DEFINE THE FUEL ROD PITCH FILLED WITH POLYETHYLENE
CUBOID     8 1  2P0.6750    192.5  0  2P0.6750

UNIT 20
COM=!SPACE WITHIN FUEL ASSEMBLY LATTICE!
CUBOID     8 1  2P0.6750    192.5  0  2P0.6750

UNIT 40
COM=!5 W/O FUEL PINS W (2.0 WT% X 0.75) GAD!
'DEFINE THE FUEL PELLET
YCYLINDER 4  1    0.4475    192.5  0
'DEFINE THE PELLET-CLAD GAP
YCYLINDER 0  1    0.4669    192.5  0
'DEFINE THE FUEL ROD CLADDING/POLY
YCYLINDER 2  1    0.5050    192.5  0
'DEFINE THE FUEL ROD PITCH FILLED WITH POLYETHYLENE
CUBOID     8 1  2P0.6750    192.5  0  2P0.6750

UNIT 50
COM=!LOWER HALF FUEL ASSEMBLY WITH CLUSTER SEPARATOR!
ARRAY 2 3*0

UNIT 60
```

NEDO-33869 Revision 11  
Non-Proprietary Information

COM=!UPPER HALF FUEL ASSEMBLY WITH CLUSTER SEPARATOR!  
ARRAY 3 3\*0

UNIT 70  
COM=!COMPLETE FUEL ASSEMBLY!  
ARRAY 4 3\*0  
REFLECTOR 11 1 2R0.3048 2R0.0 2R0.3048 1

GLOBAL  
UNIT 400  
COM=!OUTER CONTAINER BODY AND LID!  
'DEFINE INNER REGION OF THE OUTER CONTAINER  
CUBOID 3 1 2P35.788 2P253.188 2P31.900  
'INNER CONTAINER PLACEMENT WITHIN OUTER CONTAINER  
HOLE 3 -22.938 -233.58 -14.024  
'DEFINE WALLS OF THE OUTER CONTAINER AND LID  
CUBOID 6 1 2P35.963 2P253.363 2P32.075

'GLOBAL  
'UNIT 500  
'ARRAY 10 3\*0  
REFLECTOR 5 1 6R30.48 1  
END GEOM

READ ARRAY  
ARA=1 NUX=1 NUY=1 NUZ=2  
FILL 1 2  
END FILL  
ARA=2 NUX=10 NUY=1 NUZ=10  
FILL 10 10 10 10 10 10 10 10 10 40 40  
10 10 20 10 10 10 40 40 40 40  
10 20 10 10 10 10 40 40 40 10  
10 10 10 20 20 10 40 40 40 10  
10 20 10 20 20 10 10 10 10 10  
10 10 20 10 10 20 20 10 10 10  
10 20 10 20 10 20 20 10 10 10  
10 10 10 10 20 10 10 10 20 10  
10 20 10 20 10 20 10 20 10 10  
10 10 10 10 10 10 10 10 10 10

END FILL  
ARA=3 NUX=10 NUY=1 NUZ=10  
FILL 10 10 10 10 10 10 10 10 10 40 40  
10 10 10 10 10 10 40 40 40 40  
10 10 10 10 10 10 40 40 40 10  
10 10 10 20 20 10 40 40 40 10  
10 10 10 20 20 10 10 10 10 10  
10 10 10 10 10 20 20 10 10 10  
10 10 10 10 10 20 20 10 10 10  
10 10 10 10 10 10 10 10 10 10  
10 10 10 10 10 10 10 10 10 10  
10 10 10 10 10 10 10 10 10

END FILL  
ARA=4 NUX=1 NUY=2 NUZ=1  
FILL 50 60  
END FILL  
ARA=10 NUX=21 NUY=3 NUZ=24

NEDO-33869 Revision 11  
Non-Proprietary Information

FILL F400  
END FILL  
END ARRAY

READ BNDS ALL=VACUUM  
END BNDS  
END DATA  
END

NEDO-33869 Revision 11  
Non-Proprietary Information

### 6.11.2 Single Package HAC Input

```
=CSAS25          PARM=SIZE=500000
RAJ-II CONTAINER, HAC, 12 PART LENGTH RODS, 12 GAD RODS, 1.350 CM PITCH,
PATTERN H, SINGLE PACKAGE
44GROUPNDF5      LATTICECELL
UO2              1  DEN=10.74 1.0 293 92235 5.0 92238 95.0      END
ZR              2              0.26380 293                      END
POLYETHYLENE     2  DEN=0.949 0.73620 293                      END
H2O              3  0.01 293                                    END
ARBMUO2          10.74 2 1 1 1 92000 1
                                   8016 2 4 0.97840 293 92235 5.0
                                   92238 95.0 END
ARBMGD2O3        7.407 2 0 1 1 64000 2
                                   8016 3 4 0.02160 293          END
H2O              5  1.00 293                                    END
SS304            6  1.00 293                                    END
H2O              7  1.00 293                                    END
H2O              8  1.00 293                                    END
ZR              9  1.00 293                                    END
ARBMAL2O3        0.25 2 0 1 0 13027 2 8016 3 10 0.49          END
ARBMSIO2         0.25 2 0 1 0 14000 1 8016 2 10 0.51          END
END COMP
SQUAREPITCH 1.3500 0.8950 1 7 1.19720 2 0.9338 0            END
MORE DATA
RES=4 CYLINDER 0.4475 DAN(4)=2.2023524E-01
END MORE DATA
RAJ-II CONTAINER, HAC, 12 PART LENGTH RODS, 12 GAD RODS, 1.350 CM PITCH,
PATTERN H, SINGLE PACKAGE
READ PARM TME=400 GEN=400 NPG=2500 NSK=50 NUB=YES RUN=YES END PARM
READ GEOM

UNIT 1
COM=!CONTAINER INNER BOX!
'DEFINE GEOMETRY FOR SEPARATOR PLATE BETWEEN ASSEMBLY COMPARTMENTS
CUBOID 6 1 2P0.0875 225.20 -228.34 2P8.829
'DEFINE REGION FOR ASSEMBLY COMPARTMENTS WITHIN INNER BOX
CUBOID 7 1 2P17.713 225.20 -228.34 2P8.829
'PLACE THE FUEL ASSEMBLIES INSIDE INNER BOX
HOLE 70 -15.290 -192.50 -6.477
HOLE 70 2.336 -192.50 -6.477
'DEFINE WALLS FOR ASSEMBLY COMPARTMENTS WITHIN INNER BOX
CUBOID 6 1 2P17.800 225.20 -228.34 8.829 -8.9165
'DEFINE REGION OUTSIDE THE WALLS OF THE ASSEMBLY COMPARTMENTS
CUBOID 10 1 2P22.798 225.20 -228.34 8.829 -13.839
'DEFINE THE INNER WALLS OF THE BOX ENDS
CUBOID 6 1 2P22.798 225.34 -228.48 8.829 -13.979
'DEFINE INNER CORE OF BOX ENDS -8.1CM IN Y FOR TOTAL DEFORMATION
CUBOID 10 1 2P22.798 225.34 -233.44 8.829 -13.979
'DEFINE OUTER WALLS OF THE INNER BOX -8.1CM IN Y FOR TOTAL DEFORMATION
CUBOID 6 1 2P22.938 225.48 -233.58 8.829 -13.979

UNIT 2
COM=!INNER BOX LID!
'DEFINE INNER CORE OF INNER BOX LID -8.1CM IN Y FOR TOTAL DEFORMATION
```

NEDO-33869 Revision 11  
Non-Proprietary Information

```
CUBOID      10 1  2P22.798    2P229.39    2P2.48
'DEFINE WALLS FOR INNER BOX LID -8.1CM IN Y FOR TOTAL DEFORMATION
CUBOID       6 1  2P22.938    2P229.53    2P2.62
```

```
UNIT 3
COM=!INNER BOX WITH ENDS AND LID!
ARRAY 1 3*0
```

```
UNIT 10
COM=!5 W/O FUEL PINS W/O GAD!
'DEFINE THE FUEL PELLET
YCYLINDER 1  1    0.4475    192.5  0
'DEFINE THE PELLET-CLAD GAP
YCYLINDER 0  1    0.4669    192.5  0
'DEFINE THE FUEL ROD CLADDING/POLY
YCYLINDER 2  1    0.5986    192.5  0
'DEFINE THE FUEL ROD PITCH FILLED WITH POLYETHYLENE
CUBOID      7 1  2P0.6750    192.5  0  2P0.6750
```

```
UNIT 20
COM=!SPACE WITHIN FUEL ASSEMBLY LATTICE!
CUBOID      7 1  2P0.6750    192.5  0  2P0.6750
```

```
UNIT 30
COM=!ARRAY FOR COMPLETE FUEL ASSEMBLY!
ARRAY 2 3*0
REFLECTOR 9  1  2R0.3048 2R0.0  2R0.3048  1
```

```
UNIT 40
COM=!5 W/O FUEL PINS W (2.0 WT% X 0.75) GAD!
'DEFINE THE FUEL PELLET
YCYLINDER 4  1    0.4475    192.5  0
'DEFINE THE PELLET-CLAD GAP
YCYLINDER 0  1    0.4669    192.5  0
'DEFINE THE FUEL ROD CLADDING/POLY
YCYLINDER 2  1    0.5986    192.5  0
'DEFINE THE FUEL ROD PITCH FILLED WITH POLYETHYLENE
CUBOID      7 1  2P0.6750    192.5  0  2P0.6750
```

```
UNIT 50
COM=!LOWER HALF FUEL ASSEMBLY WITH CLUSTER SEPARATOR!
ARRAY 2 3*0
```

```
UNIT 60
COM=!UPPER HALF FUEL ASSEMBLY WITH CLUSTER SEPARATOR!
ARRAY 3 3*0
```

```
UNIT 70
COM=!COMPLETE FUEL ASSEMBLY!
ARRAY 4 3*0
REFLECTOR 9  1  2R0.3048 2R0.0  2R0.3048  1
```

```
GLOBAL
UNIT 400
COM=!OUTER CONTAINER BODY AND LID!
'DEFINE INNER REGION OF THE OUTER CONTAINER
```

NEDO-33869 Revision 11  
Non-Proprietary Information

```
'MINUS 4.7CM IN Y AND -2.4CM IN Z FOR TOTAL DEFORMATION
CUBOID    0  1    2P35.788  247.960  -253.190  29.500  -31.900
'INNER CONTAINER PLACEMENT WITHIN OUTER CONTAINER
HOLE 3      -22.938      -229.53      -14.024
'DEFINE WALLS OF THE OUTER CONTAINER AND LID
CUBOID     6  1    2P35.963  248.135  -253.365  29.675  -32.075
```

```
'GLOBAL
'UNIT 500
'ARRAY 10 3*0
REFLECTOR  5  1   6R30.48  1
END GEOM
```

```
READ ARRAY
ARA=1 NUX=1 NUY=1 NUZ=2
FILL 1 2
END FILL
ARA=2 NUX=10 NUY=1 NUZ=10
FILL 10 10 10 10 10 10 10 10 10 10 40 40
      10 10 20 10 10 10 10 40 40 40 40
      10 20 10 10 10 10 10 40 40 40 10
      10 10 10 20 20 10 40 40 40 10
      10 20 10 20 20 10 10 10 10 10
      10 10 20 10 10 20 20 10 10 10
      10 20 10 20 10 20 20 10 10 10
      10 10 10 10 20 10 10 10 20 10
      10 20 10 20 10 20 10 20 10 10
      10 10 10 10 10 10 10 10 10 10
```

```
END FILL
ARA=3 NUX=10 NUY=1 NUZ=10
FILL 10 10 10 10 10 10 10 10 10 40 40
      10 10 10 10 10 10 10 40 40 40 40
      10 10 10 10 10 10 10 40 40 40 10
      10 10 10 20 20 10 40 40 40 10
      10 10 10 20 20 10 10 10 10 10
      10 10 10 10 10 20 20 10 10 10
      10 10 10 10 10 20 20 10 10 10
      10 10 10 10 10 10 10 10 10 10
      10 10 10 10 10 10 10 10 10 10
      10 10 10 10 10 10 10 10 10
```

```
END FILL
ARA=4 NUX=1 NUY=2 NUZ=1
FILL 50 60
END FILL
END ARRAY
```

```
READ BNDS ALL=VACUUM
END BNDS
END DATA
END
```

NEDO-33869 Revision 11  
Non-Proprietary Information

### 6.11.3 Package Array NCT Input

```
=CSAS25          PARM=SIZE=500000
RAJ-II CONTAINER, HAC, NO INTERSPERSED H2O, 100% INNER H2O DENSITY, 5.0 W/O
235U, 12 PART LENGTH RODS, 12 GAD RODS, 21 X 3 X 24 ARRAY
44GROUPNDF5      LATTICECELL
UO2              1  DEN=10.74      1.0  293 92235 5.0 92238 95.0  END
ZR              2  1.00              293  END
H2O             3  1.00              293  END
ARBMUO2         10.74 2 1 1 1 92000 1
                                   8016 2 4 0.97840 293 92235 5.0
                                   92238 95.0  END

ARBMGD2O3       7.407 2 0 1 1 64000 2
                                   8016 3 4 0.02160 293  END
H2O             5  1.00              293  END
SS304           6  1.00              293  END
POLYETHYLENE    7  DEN=0.080000 1.0  293  END
POLYETHYLENE    8  DEN=0.949 0.25405 293  END
H2O             8  DEN=1.00 0.74595 293  END
H2O            9  1.00              293  END
ARBMAL2O3       0.25 2 0 1 0 13027 2 8016 3 10 0.49  END
ARBMSIO2        0.25 2 0 1 0 14000 1 8016 2 10 0.51  END
ZR             11 1.00              293  END
END COMP
SQUAREPITCH 1.3500 0.8950 1 8 1.01000 2 0.9338 0  END
MORE DATA
RES=4 CYLINDER 0.4475  DAN(4)=2.3197146E-01
END MORE DATA
RAJ-II CONTAINER, HAC, NO INTERSPERSED H2O, 100% INNER H2O DENSITY, 5.0 W/O
235U, 12 GAD RODS, 21 X 3 X 24 ARRAY
READ PARM TME=400 GEN=400 NPG=2500 NSK=50 NUB=YES RUN=YES END PARM
READ GEOM
```

```
UNIT 1
COM=!CONTAINER INNER BOX!
'DEFINE GEOMETRY FOR SEPARATOR PLATE BETWEEN ASSEMBLY COMPARTMENTS
CUBOID 6 1 2P0.0875 2P228.34 2P8.829
'DEFINE REGION FOR ASSEMBLY COMPARTMENTS WITHIN INNER BOX
CUBOID 9 1 2P17.713 2P228.34 2P8.829
'INSERT FOAM POLYETHYLENE
HOLE 4 -8.9003 0.00 0.00
HOLE 5 8.9003 0.00 0.00
'DEFINE WALLS FOR ASSEMBLY COMPARTMENTS WITHIN INNER BOX
CUBOID 6 1 2P17.800 2P228.34 8.829 -8.9165
'DEFINE REGION OUTSIDE THE WALLS OF THE ASSEMBLY COMPARTMENTS
CUBOID 10 1 2P22.798 2P228.34 8.829 -13.839
'DEFINE THE INNER WALLS OF THE BOX ENDS
CUBOID 6 1 2P22.798 2P228.48 8.829 -13.979
'DEFINE INNER CORE OF BOX ENDS
CUBOID 10 1 2P22.798 2P233.44 8.829 -13.979
'DEFINE OUTER WALLS OF THE INNER BOX
CUBOID 6 1 2P22.938 2P233.58 8.829 -13.979
```

```
UNIT 2
COM=!INNER BOX LID!
```

NEDO-33869 Revision 11  
Non-Proprietary Information

```
'DEFINE INNER CORE OF INNER BOX LID
CUBOID    10 1  2P22.798    2P233.44    2P2.48
'DEFINE WALLS FOR INNER BOX LID
CUBOID     6 1  2P22.938    2P233.58    2P2.62

UNIT 3
COM=!INNER BOX WITH ENDS AND LID!
ARRAY 1 3*0

UNIT 4
COM=!FOAM POLYETHYLENE FOR LEFT ASSEMBLY COMPARTMENT!
CUBOID     9 1  2P7.055    2P228.34    2P7.055
HOLE       70      -6.7500  -192.50  -6.750
'FOAM POLYETHYLENE FOR ASSEMBLY COMPARTMENTS
CUBOID     7 1  2P8.8126    2P228.34    2P8.829

UNIT 5
COM=!FOAM POLYETHYLENE FOR RIGHT ASSEMBLY COMPARTMENT!
CUBOID     9 1  2P7.055    2P228.34    2P7.055
HOLE       70      -6.7500  -192.50  -6.750
'FOAM POLYETHYLENE FOR ASSEMBLY COMPARTMENT
CUBOID     7 1  2P8.8126    2P228.34    2P8.829

UNIT 10
COM=!5 W/O FUEL PINS W/O GAD!
'DEFINE THE FUEL PELLET
YCYLINDER 1  1    0.4475    192.5  0
'DEFINE THE PELLET-CLAD GAP
YCYLINDER 0  1    0.4669    192.5  0
'DEFINE THE FUEL ROD CLADDING/POLY
YCYLINDER 2  1    0.5050    192.5  0
'DEFINE THE FUEL ROD PITCH FILLED WITH POLYETHYLENE
CUBOID     8 1  2P0.6750    192.5  0  2P0.6750

UNIT 20
COM=!SPACE WITHIN FUEL ASSEMBLY LATTICE!
CUBOID     8 1  2P0.6750    192.5  0  2P0.6750

UNIT 40
COM=!5 W/O FUEL PINS W (2.0 WT% X 0.75) GAD!
'DEFINE THE FUEL PELLET
YCYLINDER 4  1    0.4475    192.5  0
'DEFINE THE PELLET-CLAD GAP
YCYLINDER 0  1    0.4669    192.5  0
'DEFINE THE FUEL ROD CLADDING/POLY
YCYLINDER 2  1    0.5050    192.5  0
'DEFINE THE FUEL ROD PITCH FILLED WITH POLYETHYLENE
CUBOID     8 1  2P0.6750    192.5  0  2P0.6750

UNIT 50
COM=!LOWER HALF FUEL ASSEMBLY WITH CLUSTER SEPARATOR!
ARRAY 2 3*0

UNIT 60
COM=!UPPER HALF FUEL ASSEMBLY WITH CLUSTER SEPARATOR!
ARRAY 3 3*0
```



NEDO-33869 Revision 11  
Non-Proprietary Information

```
UNIT 70
COM=!COMPLETE FUEL ASSEMBLY!
ARRAY 4 3*0
REFLECTOR 11 1 2R0.3048 2R0.0 2R0.3048 1

UNIT 400
COM=!OUTER CONTAINER BODY AND LID!
'DEFINE INNER REGION OF THE OUTER CONTAINER
CUBOID 3 1 2P35.788 2P253.188 2P31.900
'INNER CONTAINER PLACEMENT WITHIN OUTER CONTAINER
HOLE 3 -22.938 -233.58 -14.024
'DEFINE WALLS OF THE OUTER CONTAINER AND LID
CUBOID 6 1 2P35.963 2P253.363 2P32.075

GLOBAL
UNIT 500
ARRAY 10 3*0
REFLECTOR 5 1 6R30.48 1
END GEOM

READ ARRAY
ARA=1 NUX=1 NUY=1 NUZ=2
FILL 1 2
END FILL
ARA=2 NUX=10 NUY=1 NUZ=10
FILL 10 10 10 10 10 10 10 10 40 40
      10 10 20 10 10 10 40 40 40 40
      10 20 10 10 10 10 40 40 40 10
      10 10 10 20 20 10 40 40 40 10
      10 20 10 20 20 10 10 10 10 10
      10 10 20 10 10 20 20 10 10 10
      10 20 10 20 10 20 20 10 10 10
      10 10 10 10 20 10 10 10 20 10
      10 20 10 20 10 20 10 20 10 10
      10 10 10 10 10 10 10 10 10 10
END FILL
ARA=3 NUX=10 NUY=1 NUZ=10
FILL 10 10 10 10 10 10 10 10 40 40
      10 10 10 10 10 10 40 40 40 40
      10 10 10 10 10 10 40 40 40 10
      10 10 10 20 20 10 40 40 40 10
      10 10 10 20 20 10 10 10 10 10
      10 10 10 10 10 20 20 10 10 10
      10 10 10 10 10 20 20 10 10 10
      10 10 10 10 10 10 10 10 10 10
      10 10 10 10 10 10 10 10 10 10
      10 10 10 10 10 10 10 10 10 10
END FILL
ARA=4 NUX=1 NUY=2 NUZ=1
FILL 50 60
END FILL
ARA=10 NUX=21 NUY=3 NUZ=24
FILL F400
END FILL
END ARRAY
```

NEDO-33869 Revision 11  
Non-Proprietary Information

```
READ BNDS ALL=VACUUM  
END BNDS  
END DATA  
END
```

NEDO-33869 Revision 11  
Non-Proprietary Information

## 6.11.4 Package Array HAC Input

### 6.11.4.1 GNf 10x10

```
=CSAS25          PARM=SIZE=500000
RAJ-II CONTAINER, HAC, 100% H2O DENSITY, WORSTCASE, GNf 10x10, 10 X 1 X 10
ARRAY, 12 PART LENGTH RODS, 12 GAD RODS
44GROUPNDF5      LATTICECELL
UO2              1  DEN=10.74 1.0 293 92235 5.0 92238 95.0      END
ZR              2          0.26380 293                      END
POLYETHYLENE     2  DEN=0.949 0.73620 293                    END
H2O              3  0.01 293                                END
ARBMUO2          10.74 2 1 1 1 92000 1
                                   8016 2 4 0.97840 293 92235 5.0
                                   92238 95.0 END
ARBMGD2O3        7.407 2 0 1 1 64000 2
                                   8016 3 4 0.02160 293      END
H2O              5  1.00 293                                END
SS304           6  1.00 293                                END
H2O              7  1.00 293                                END
POLYETHYLENE     8  DEN=0.080000 1.0 293                    END
ZR              9  1.00 293                                END
ARBMAL2O3        0.25 2 0 1 0 13027 2 8016 3 10 0.49        END
ARBMSIO2         0.25 2 0 1 0 14000 1 8016 2 10 0.51        END
END COMP
SQUAREPITCH 1.3500 0.8950 1 7 1.19720 2 0.9338 0          END
MORE DATA
RES=4 CYLINDER 0.4475 DAN(4)=2.2023524E-01
END MORE DATA
RAJ-II CONTAINER, HAC, 100% H2O DENSITY, WORSTCASE, GNf 10x10, 10 X 1 X 10
ARRAY
READ PARM TME=400 GEN=400 NPG=2500 NSK=50 NUB=YES RUN=YES END PARM
READ GEOM

UNIT 1
COM=!CONTAINER INNER BOX!
'DEFINE GEOMETRY FOR SEPARATOR PLATE BETWEEN ASSEMBLY COMPARTMENTS
CUBOID 6 1 2P0.0875 225.20 -228.34 2P8.829
'DEFINE REGION FOR ASSEMBLY COMPARTMENTS WITHIN INNER BOX
CUBOID 7 1 2P17.713 225.20 -228.34 2P8.829
'INSERT FOAM POLYETHYLENE AND FUEL
HOLE 4 -8.9001 0.00 0.00
HOLE 5 8.9001 0.00 0.00
'DEFINE WALLS FOR ASSEMBLY COMPARTMENTS WITHIN INNER BOX
CUBOID 6 1 2P17.800 225.20 -228.34 8.829 -8.9165
'DEFINE REGION OUTSIDE THE WALLS OF THE ASSEMBLY COMPARTMENTS
CUBOID 10 1 2P22.798 225.20 -228.34 8.829 -13.839
'DEFINE THE INNER WALLS OF THE BOX ENDS
CUBOID 6 1 2P22.798 225.34 -228.48 8.829 -13.979
'DEFINE INNER CORE OF BOX ENDS -8.1CM IN Y FOR TOTAL DEFORMATION
CUBOID 10 1 2P22.798 225.34 -233.44 8.829 -13.979
'DEFINE OUTER WALLS OF THE INNER BOX -8.1CM IN Y FOR TOTAL DEFORMATION
CUBOID 6 1 2P22.938 225.48 -233.58 8.829 -13.979

UNIT 2
```

NEDO-33869 Revision 11  
Non-Proprietary Information

```
COM=!INNER BOX LID!
'DEFINE INNER CORE OF INNER BOX LID -8.1CM IN Y FOR TOTAL DEFORMATION
CUBOID    10 1  2P22.798    2P229.39    2P2.48
'DEFINE WALLS FOR INNER BOX LID -8.1CM IN Y FOR TOTAL DEFORMATION
CUBOID     6 1  2P22.938    2P229.53    2P2.62

UNIT 3
COM=!INNER BOX WITH ENDS AND LID!
ARRAY 1 3*0

UNIT 4
COM=!FOAM POLYETHYLENE FOR LEFT ASSEMBLY COMPARTMENT!
CUBOID     7 1  2P7.055    225.20   -228.34   2P7.055
HOLE       70      -6.7500 -192.50    -6.750
'FOAM POLYETHYLENE FOR ASSEMBLY COMPARTMENTS
CUBOID     8 1  2P8.8126   225.20   -228.34   2P8.829

UNIT 5
COM=!FOAM POLYETHYLENE FOR RIGHT ASSEMBLY COMPARTMENT!
CUBOID     7 1  2P7.055    225.20   -228.34   2P7.055
HOLE       70      -6.7500 -192.50    -6.750
'FOAM POLYETHYLENE FOR ASSEMBLY COMPARTMENT
CUBOID     8 1  2P8.8126   225.20   -228.34   2P8.829

UNIT 10
COM=!5 W/O FUEL PINS W/O GAD!
'DEFINE THE FUEL PELLET
YCYLINDER 1  1      0.4475   192.5    0
'DEFINE THE PELLET-CLAD GAP
YCYLINDER 0  1      0.4669   192.5    0
'DEFINE THE FUEL ROD CLADDING/POLY
YCYLINDER 2  1      0.5986   192.5    0
'DEFINE THE FUEL ROD PITCH FILLED WITH POLYETHYLENE
CUBOID     7 1  2P0.6750    192.5    0  2P0.6750

UNIT 20
COM=!SPACE WITHIN FUEL ASSEMBLY LATTICE!
CUBOID     7 1  2P0.6750    192.5    0  2P0.6750

UNIT 30
COM=!ARRAY FOR COMPLETE FUEL ASSEMBLY!
ARRAY 2 3*0
REFLECTOR 9  1  2R0.3048 2R0.0   2R0.3048   1

UNIT 40
COM=!5 W/O FUEL PINS W (2.0 WT% X 0.75) GAD!
'DEFINE THE FUEL PELLET
YCYLINDER 4  1      0.4475   192.5    0
'DEFINE THE PELLET-CLAD GAP
YCYLINDER 0  1      0.4669   192.5    0
'DEFINE THE FUEL ROD CLADDING/POLY
YCYLINDER 2  1      0.5986   192.5    0
'DEFINE THE FUEL ROD PITCH FILLED WITH POLYETHYLENE
CUBOID     7 1  2P0.6750    192.5    0  2P0.6750

UNIT 50
```

NEDO-33869 Revision 11  
Non-Proprietary Information

COM=!LOWER HALF FUEL ASSEMBLY WITH CLUSTER SEPARATOR!  
ARRAY 2 3\*0

UNIT 60  
COM=!UPPER HALF FUEL ASSEMBLY WITH CLUSTER SEPARATOR!  
ARRAY 3 3\*0

UNIT 70  
COM=!COMPLETE FUEL ASSEMBLY!  
ARRAY 4 3\*0  
REFLECTOR 9 1 2R0.3048 2R0.0 2R0.3048 1

UNIT 400  
COM=!OUTER CONTAINER BODY AND LID!  
'DEFINE INNER REGION OF THE OUTER CONTAINER  
'MINUS 4.7CM IN Y AND -2.4CM IN Z FOR TOTAL DEFORMATION  
CUBOID 0 1 2P35.788 247.960 -253.190 29.500 -31.900  
'INNER CONTAINER PLACEMENT WITHIN OUTER CONTAINER  
HOLE 3 -22.938 -229.53 -14.024  
'DEFINE WALLS OF THE OUTER CONTAINER AND LID  
CUBOID 6 1 2P35.963 248.135 -253.365 29.675 -32.075

GLOBAL  
UNIT 500  
ARRAY 10 3\*0  
REFLECTOR 5 1 6R30.48 1  
END GEOM

READ ARRAY  
ARA=1 NUX=1 NUY=1 NUZ=2  
FILL 1 2  
END FILL  
ARA=2 NUX=10 NUY=1 NUZ=10  
FILL 10 10 10 10 10 10 10 10 10 40 40  
10 10 20 10 10 10 40 40 40 40  
10 20 10 10 10 10 40 40 40 10  
10 10 10 20 20 10 40 40 40 10  
10 20 10 20 20 10 10 10 10 10  
10 10 20 10 10 20 20 10 10 10  
10 20 10 20 10 20 20 10 10 10  
10 10 10 10 20 10 10 10 20 10  
10 20 10 20 10 20 10 20 10 10  
10 10 10 10 10 10 10 10 10 10

END FILL  
ARA=3 NUX=10 NUY=1 NUZ=10  
FILL 10 10 10 10 10 10 10 10 10 40 40  
10 10 10 10 10 10 40 40 40 40  
10 10 10 10 10 10 40 40 40 10  
10 10 10 20 20 10 40 40 40 10  
10 10 10 20 20 10 10 10 10 10  
10 10 10 10 10 20 20 10 10 10  
10 10 10 10 10 20 20 10 10 10  
10 10 10 10 10 10 10 10 10 10  
10 10 10 10 10 10 10 10 10 10  
10 10 10 10 10 10 10 10 10 10

END FILL

NEDO-33869 Revision 11  
Non-Proprietary Information

```
ARA=4  NUX=1  NUY=2  NUZ=1  
FILL 50 60  
END FILL  
ARA=10 NUX=10 NUY=1 NUZ=10  
FILL F400  
END FILL  
END ARRAY  
  
READ BNDS ALL=VACUUM  
END BNDS  
END DATA  
END
```

NEDO-33869 Revision 11  
Non-Proprietary Information

### 6.11.5 Single Package Loose Rods NCT Input

```
=CSAS25                PARM=SIZE=500000
RAJ-II CONTAINER, 8, NCT, 100% H2O, 2.8150 CM PITCH, LOOSE FUEL RODS, SINGLE
PACKAGE
44GROUPNDF5                LATTICECELL
UO2            1    DEN=10.74      1.0    293 92235 5.0 92238 95.0    END
POLYETHYLENE   2    DEN=0.925      1.0    293                      END
H2O            3    1.00                      293                      END
UO2            4    DEN=10.4799   1.0    293 92235 3.25 92238 96.75  END
GD             4    DEN=0.17374   1.0    293                      END
O              4    DEN=0.026514  1.0    293                      END
H2O            5    1.00                      293                      END
SS304          6    1.00                      293                      END
H2O            8    1.00                      293                      END
H2O            9    1.00                      293                      END
ARBMAL2O3      0.25 2 0 1 0 13027 2 8016 3 10 0.49    END
ARBSIO2        0.25 2 0 1 0 14000 1 8016 2 10 0.51    END
ZR             11 1.00                      293                      END
END COMP
SQUAREPITCH 2.8150 1.0500 1 8 1.13048 2 1.100 0                      END
RAJ-II CONTAINER, 8, NCT, 100% H2O, 2.8150 CM PITCH, LOOSE FUEL RODS, SINGLE
PACKAGE
READ PARM TME=400 GEN=400 NPG=2500 NSK=50 NUB=YES END PARM
READ GEOM

UNIT 1
COM=!CONTAINER INNER BOX!
'DEFINE GEOMETRY FOR SEPARATOR PLATE BETWEEN ASSEMBLY COMPARTMENTS
CUBOID        6 1 2P0.0875 2P228.34 2P8.829
'DEFINE REGION FOR ASSEMBLY COMPARTMENTS WITHIN INNER BOX
CUBOID        3 1 2P17.713 2P228.34 2P8.829
'INSERT FOAM POLYETHYLENE
HOLE          4      -8.9003      0.00    0.00
HOLE          5      8.9003      0.00    0.00
'DEFINE WALLS FOR ASSEMBLY COMPARTMENTS WITHIN INNER BOX
CUBOID        6 1 2P17.800 2P228.34 8.829 -8.9165
'DEFINE REGION OUTSIDE THE WALLS OF THE ASSEMBLY COMPARTMENTS
CUBOID       10 1 2P22.798 2P228.34 8.829 -13.839
'DEFINE THE INNER WALLS OF THE BOX ENDS
CUBOID        6 1 2P22.798 2P228.48 8.829 -13.979
'DEFINE INNER CORE OF BOX ENDS
CUBOID       10 1 2P22.798 2P233.44 8.829 -13.979
'DEFINE OUTER WALLS OF THE INNER BOX
CUBOID        6 1 2P22.938 2P233.58 8.829 -13.979

UNIT 2
COM=!INNER BOX LID!
'DEFINE INNER CORE OF INNER BOX LID
CUBOID       10 1 2P22.798 2P233.44 2P2.48
'DEFINE WALLS FOR INNER BOX LID
CUBOID        6 1 2P22.938 2P233.58 2P2.62

UNIT 3
COM=!INNER BOX WITH ENDS AND LID!
```

NEDO-33869 Revision 11  
Non-Proprietary Information

ARRAY 1 3\*0

UNIT 4

COM=!FOAM POLYETHYLENE FOR LEFT ASSEMBLY COMPARTMENT!

CUBOID 3 1 2P7.0378 2P228.34 2P7.054

HOLE 30 -7.0376 -191.77 -7.0376

'FOAM POLYETHYLENE FOR ASSEMBLY COMPARTMENTS

CUBOID 7 1 2P8.8126 2P228.34 2P8.829

UNIT 5

COM=!FOAM POLYETHYLENE FOR RIGHT ASSEMBLY COMPARTMENT!

CUBOID 3 1 2P7.0378 2P228.34 2P7.054

HOLE 30 -7.0376 -191.77 -7.0376

'FOAM POLYETHYLENE FOR ASSEMBLY COMPARTMENT

CUBOID 7 1 2P8.8126 2P228.34 2P8.829

UNIT 10

COM=!5 W/O FUEL PINS W/O GAD!

'DEFINE THE FUEL PELLET

YCYLINDER 1 1 0.52500 381 0

'DEFINE THE PELLET-CLAD GAP

YCYLINDER 0 1 0.55000 381 0

'DEFINE THE FUEL ROD CLADDING

YCYLINDER 2 1 0.56524 381 0

'DEFINE THE FUEL ROD PITCH FILLED WITH WATER

CUBOID 8 1 2P1.40750 381 0 2P1.40750

UNIT 20

COM=!SPACE WITHIN FUEL ASSEMBLY LATTICE!

CUBOID 8 1 2P1.40750 381 0 2P1.40750

UNIT 30

COM=!ARRAY FOR COMPLETE FUEL ASSEMBLY!

ARRAY 2 3\*0

UNIT 400

COM=!OUTER CONTAINER BODY AND LID!

'DEFINE INNER REGION OF THE OUTER CONTAINER

CUBOID 3 1 2P35.788 2P253.188 2P31.900

'INNER CONTAINER PLACEMENT WITHIN OUTER CONTAINER

HOLE 3 -22.938 -233.58 -14.024

'DEFINE WALLS OF THE OUTER CONTAINER AND LID

CUBOID 6 1 2P35.963 2P253.363 2P32.075

GLOBAL

UNIT 500

ARRAY 10 3\*0

REFLECTOR 5 1 6R30.48 1

END GEOM

READ ARRAY

ARA=1 NUX=1 NUY=1 NUZ=2

FILL 1 2

END FILL

ARA=2 NUX=5 NUY=1 NUZ=5

FILL 10 10 10 10 10



NEDO-33869 Revision 11  
Non-Proprietary Information

```
      10 10 10 10 10
      10 10 10 10 10
      10 10 10 10 10
      10 10 10 10 10
END FILL
ARA=10 NUX=21 NUY=3  NUZ=24
FILL F400
END FILL
END ARRAY

READ BNDS ALL=VACUUM
END BNDS
END DATA
END
```

NEDO-33869 Revision 11  
Non-Proprietary Information

### 6.11.6 Single Package Loose Fuel Rods HAC Input

```
=CSAS25                PARM=SIZE=500000
RAJ-II CONTAINER, 8, HAC, 100% H2O, WORST CASE MODEL, 3.0056 CM PITCH, LOOSE
FUEL RODS, SINGLE PACKAGE
44GROUPNDF5            LATTICECELL
UO2                    1  DEN=10.74 1.0 293 92235 5.0 92238 95.0      END
POLYETHYLENE           2  DEN=0.925 1.0 293                        END
H2O                    3  1.00 293                                END
UO2                    4  DEN=10.4799 1.0 293 92235 3.25 92238 96.75 END
GD                    4  DEN=0.17374 1.0 293                      END
O                      4  DEN=0.026514 1.0 293                  END
H2O                    5  1.00 293                                END
SS304                  6  1.00 293                                END
H2O                    7  DEN=1.00 1.0 293                      END
H2O                    8  DEN=1.00 1.0 293                      END
ZR                     9  1.00 293                                END
ARBMAL2O3              0.25 2 0 1 0 13027 2 8016 3 10 0.49      END
ARBMSIO2               0.25 2 0 1 0 14000 1 8016 2 10 0.51      END
END COMP
SQUAREPITCH 3.0056 1.0500 1 8 1.13048 2 1.100 0              END
RAJ-II CONTAINER, 8, HAC, 100% H2O, WORST CASE MODEL, 3.0056 CM PITCH, LOOSE
FUEL RODS, SINGLE PACKAGE
READ PARM TME=400 GEN=400 NPG=2500 NSK=50 NUB=YES END PARM
READ GEOM
```

```
UNIT 1
COM=!CONTAINER INNER BOX!
'DEFINE GEOMETRY FOR SEPARATOR PLATE BETWEEN ASSEMBLY COMPARTMENTS
CUBOID 6 1 2P0.0875 225.20 -228.34 2P8.829
'DEFINE REGION FOR ASSEMBLY COMPARTMENTS WITHIN INNER BOX
CUBOID 7 1 2P17.713 225.20 -228.34 2P8.829
'PLACE THE FUEL ASSEMBLIES INSIDE INNER BOX
HOLE 30 -16.413 -190.50 -7.514
HOLE 30 1.386 -190.50 -7.514
'DEFINE WALLS FOR ASSEMBLY COMPARTMENTS WITHIN INNER BOX
CUBOID 6 1 2P17.800 225.20 -228.34 8.829 -8.9165
'DEFINE REGION OUTSIDE THE WALLS OF THE ASSEMBLY COMPARTMENTS
CUBOID 10 1 2P22.798 225.20 -228.34 8.829 -13.839
'DEFINE THE INNER WALLS OF THE BOX ENDS
CUBOID 6 1 2P22.798 225.34 -228.48 8.829 -13.979
'DEFINE INNER CORE OF BOX ENDS -8.1CM IN Y FOR TOTAL DEFORMATION
CUBOID 10 1 2P22.798 225.34 -233.44 8.829 -13.979
'DEFINE OUTER WALLS OF THE INNER BOX -8.1CM IN Y FOR TOTAL DEFORMATION
CUBOID 6 1 2P22.938 225.48 -233.58 8.829 -13.979
```

```
UNIT 2
COM=!INNER BOX LID!
'DEFINE INNER CORE OF INNER BOX LID -8.1CM IN Y FOR TOTAL DEFORMATION
CUBOID 10 1 2P22.798 2P229.39 2P2.48
'DEFINE WALLS FOR INNER BOX LID -8.1CM IN Y FOR TOTAL DEFORMATION
CUBOID 6 1 2P22.938 2P229.53 2P2.62
```

```
UNIT 3
COM=!INNER BOX WITH ENDS AND LID!
```

NEDO-33869 Revision 11  
Non-Proprietary Information

ARRAY 1 3\*0

UNIT 10

COM=!5 W/O FUEL PINS W/O GAD!

'DEFINE THE FUEL PELLET

YCYLINDER 1 1 0.52500 381 0

'DEFINE THE PELLET-CLAD GAP

YCYLINDER 0 1 0.55000 381 0

'DEFINE THE FUEL ROD CLADDING

YCYLINDER 2 1 0.56524 381 0

'DEFINE THE FUEL ROD PITCH FILLED WITH WATER

CUBOID 8 1 2P1.50280 381 0 2P1.50280

UNIT 20

COM=!SPACE WITHIN FUEL ASSEMBLY LATTICE!

CUBOID 8 1 2P1.50280 381 0 2P1.50280

UNIT 30

COM=!ARRAY FOR COMPLETE FUEL ASSEMBLY!

ARRAY 2 3\*0

GLOBAL

UNIT 400

COM=!OUTER CONTAINER BODY AND LID!

'DEFINE INNER REGION OF THE OUTER CONTAINER

'MINUS 4.7CM IN Y AND -2.4CM IN Z FOR TOTAL DEFORMATION

CUBOID 0 1 2P35.788 247.960 -253.190 29.500 -31.900

'INNER CONTAINER PLACEMENT WITHIN OUTER CONTAINER

HOLE 3 -22.938 -229.53 -14.024

'DEFINE WALLS OF THE OUTER CONTAINER AND LID

CUBOID 6 1 2P35.963 248.135 -253.365 29.675 -32.075

'GLOBAL

'UNIT 500

'ARRAY 10 3\*0

REFLECTOR 5 1 6R30.48 1

END GEOM

READ ARRAY

ARA=1 NUX=1 NUY=1 NUZ=2

FILL 1 2

END FILL

ARA=2 NUX=5 NUY=1 NUZ=5

FILL 10 10 10 10 10

10 10 10 10 10

10 10 10 10 10

10 10 10 10 10

10 10 10 10 10

END FILL

ARA=10 NUX=14 NUY=2 NUZ=16

FILL F400

END FILL

END ARRAY

READ BNDS ALL=VACUUM

END BNDS

END DATA

NEDO-33869 Revision 11  
Non-Proprietary Information

### 6.11.7 Package Array Loose Fuel Rods NCT Input

```
=CSAS25                      PARM=SIZE=500000
RAJ-II CONTAINER, 8, NCT, 100% H2O, 2.8150 CM PITCH, LOOSE FUEL RODS, 21 x 3
x 24
44GROUPNDF5                  LATTICECELL
UO2          1  DEN=10.74      1.0  293 92235 5.0 92238 95.0  END
POLYETHYLENE 2  DEN=0.925      1.0  293                      END
H2O          3  1.00          293                      END
UO2          4  DEN=10.4799    1.0  293 92235 3.25 92238 96.75 END
GD           4  DEN=0.17374    1.0  293                      END
O            4  DEN=0.026514   1.0  293                      END
H2O          5  1.00          293                      END
SS304        6  1.00          293                      END
POLYETHYLENE 7  DEN=0.067967   1.0  293                      END
H2O          8  1.00          293                      END
H2O          9  1.00          293                      END
ARBMAL2O3    0.25 2 0 1 0 13027 2 8016 3 10 0.49  END
ARBMSIO2     0.25 2 0 1 0 14000 1 8016 2 10 0.51  END
ZR           11 1.00          293                      END
END COMP
SQUAREPITCH 2.8150 1.0500 1 8 1.13048 2 1.100 0  END
RAJ-II CONTAINER, 8, NCT, 100% H2O, 2.8150 CM PITCH, LOOSE FUEL RODS, 21 x 3
x 24
READ PARM TME=400 GEN=400 NPG=2500 NSK=50 NUB=YES END PARM
READ GEOM

UNIT 1
COM=!CONTAINER INNER BOX!
'DEFINE GEOMETRY FOR SEPARATOR PLATE BETWEEN ASSEMBLY COMPARTMENTS
CUBOID      6  1  2P0.0875  2P228.34  2P8.829
'DEFINE REGION FOR ASSEMBLY COMPARTMENTS WITHIN INNER BOX
CUBOID      3  1  2P17.713  2P228.34  2P8.829
'INSERT FOAM POLYETHYLENE
HOLE        4      -8.9003      0.00  0.00
HOLE        5      8.9003      0.00  0.00
'DEFINE WALLS FOR ASSEMBLY COMPARTMENTS WITHIN INNER BOX
CUBOID      6  1  2P17.800  2P228.34  8.829 -8.9165
'DEFINE REGION OUTSIDE THE WALLS OF THE ASSEMBLY COMPARTMENTS
CUBOID     10  1  2P22.798  2P228.34  8.829 -13.839
'DEFINE THE INNER WALLS OF THE BOX ENDS
CUBOID      6  1  2P22.798  2P228.48  8.829 -13.979
'DEFINE INNER CORE OF BOX ENDS
CUBOID     10  1  2P22.798  2P233.44  8.829 -13.979
'DEFINE OUTER WALLS OF THE INNER BOX
CUBOID      6  1  2P22.938  2P233.58  8.829 -13.979

UNIT 2
COM=!INNER BOX LID!
'DEFINE INNER CORE OF INNER BOX LID
CUBOID     10  1  2P22.798  2P233.44  2P2.48
'DEFINE WALLS FOR INNER BOX LID
CUBOID      6  1  2P22.938  2P233.58  2P2.62

UNIT 3
```

NEDO-33869 Revision 11  
Non-Proprietary Information

COM=!INNER BOX WITH ENDS AND LID!  
ARRAY 1 3\*0

UNIT 4  
COM=!FOAM POLYETHYLENE FOR LEFT ASSEMBLY COMPARTMENT!  
CUBOID 3 1 2P7.0378 2P228.34 2P7.054  
HOLE 30 -7.0376 -191.77 -7.0376  
'FOAM POLYETHYLENE FOR ASSEMBLY COMPARTMENTS  
CUBOID 7 1 2P8.8126 2P228.34 2P8.829

UNIT 5  
COM=!FOAM POLYETHYLENE FOR RIGHT ASSEMBLY COMPARTMENT!  
CUBOID 3 1 2P7.0378 2P228.34 2P7.054  
HOLE 30 -7.0376 -191.77 -7.0376  
'FOAM POLYETHYLENE FOR ASSEMBLY COMPARTMENT  
CUBOID 7 1 2P8.8126 2P228.34 2P8.829

UNIT 10  
COM=!5 W/O FUEL PINS W/O GAD!  
'DEFINE THE FUEL PELLET  
YCYLINDER 1 1 0.52500 381 0  
'DEFINE THE PELLET-CLAD GAP  
YCYLINDER 0 1 0.55000 381 0  
'DEFINE THE FUEL ROD CLADDING  
YCYLINDER 2 1 0.56524 381 0  
'DEFINE THE FUEL ROD PITCH FILLED WITH WATER  
CUBOID 8 1 2P1.40750 381 0 2P1.40750

UNIT 20  
COM=!SPACE WITHIN FUEL ASSEMBLY LATTICE!  
CUBOID 8 1 2P1.40750 381 0 2P1.40750

UNIT 30  
COM=!ARRAY FOR COMPLETE FUEL ASSEMBLY!  
ARRAY 2 3\*0

UNIT 400  
COM=!OUTER CONTAINER BODY AND LID!  
'DEFINE INNER REGION OF THE OUTER CONTAINER  
CUBOID 3 1 2P35.788 2P253.188 2P31.900  
'INNER CONTAINER PLACEMENT WITHIN OUTER CONTAINER  
HOLE 3 -22.938 -233.58 -14.024  
'DEFINE WALLS OF THE OUTER CONTAINER AND LID  
CUBOID 6 1 2P35.963 2P253.363 2P32.075

GLOBAL  
UNIT 500  
ARRAY 10 3\*0  
REFLECTOR 5 1 6R30.48 1  
END GEOM

READ ARRAY  
ARA=1 NUX=1 NUY=1 NUZ=2  
FILL 1 2  
END FILL  
ARA=2 NUX=5 NUY=1 NUZ=5

NEDO-33869 Revision 11  
Non-Proprietary Information

```
FILL 10 10 10 10 10
      10 10 10 10 10
      10 10 10 10 10
      10 10 10 10 10
      10 10 10 10 10
END FILL
ARA=10 NUX=21 NUY=3  NUZ=24
FILL F400
END FILL
END ARRAY

READ BNDS ALL=VACUUM
END BNDS
END DATA
END
```

NEDO-33869 Revision 11  
Non-Proprietary Information

### 6.11.8 Package Array Loose Fuel Rods HAC Input

```
=CSAS25                PARM=SIZE=500000
RAJ-II CONTAINER, 8, HAC, 100% H2O, WORST CASE MODEL, 3.0056 CM PITCH, LOOSE
FUEL RODS, 10 X 1 X 10 ARRAY
44GROUPNDF5            LATTICECELL
UO2                    1  DEN=10.74 1.0 293 92235 5.0 92238 95.0      END
POLYETHYLENE          2  DEN=0.925 1.0 293                        END
H2O                   3  1.00 293                                END
H2O                   5  1.00 293                                END
SS304                 6  1.00 293                                END
POLYETHYLENE          7  DEN=0.08000 1.0 293                      END
H2O                   8  DEN=1.00 1.0 293                      END
ZR                    9  1.00 293                                END
ARBMAL2O3             0.25 2 0 1 0 13027 2 8016 3 10 0.49      END
ARBMSIO2              0.25 2 0 1 0 14000 1 8016 2 10 0.51      END
END COMP
SQUAREPITCH 3.0056 1.0500 1 8 1.13048 2 1.100 0              END
RAJ-II CONTAINER, 8, HAC, 100% H2O, WORST CASE MODEL, 3.0056 CM PITCH, LOOSE
FUEL RODS, 10 X 1 X 10 ARRAY
READ PARM TME=400 GEN=400 NPG=2500 NSK=50 NUB=YES END PARM
READ GEOM
```

```
UNIT 1
COM=!CONTAINER INNER BOX!
'DEFINE GEOMETRY FOR SEPARATOR PLATE BETWEEN ASSEMBLY COMPARTMENTS
CUBOID 6 1 2P0.0875 225.20 -228.34 2P8.829
'DEFINE REGION FOR ASSEMBLY COMPARTMENTS WITHIN INNER BOX
CUBOID 7 1 2P17.713 225.20 -228.34 2P8.829
'PLACE THE FUEL ASSEMBLIES INSIDE INNER BOX
HOLE 30 -15.913 -190.50 -7.014
HOLE 30 1.886 -190.50 -7.014
'DEFINE WALLS FOR ASSEMBLY COMPARTMENTS WITHIN INNER BOX
CUBOID 6 1 2P17.800 225.20 -228.34 8.829 -8.9165
'DEFINE REGION OUTSIDE THE WALLS OF THE ASSEMBLY COMPARTMENTS
CUBOID 10 1 2P22.798 225.20 -228.34 8.829 -13.839
'DEFINE THE INNER WALLS OF THE BOX ENDS
CUBOID 6 1 2P22.798 225.34 -228.48 8.829 -13.979
'DEFINE INNER CORE OF BOX ENDS -8.1CM IN Y FOR TOTAL DEFORMATION
CUBOID 10 1 2P22.798 225.34 -233.44 8.829 -13.979
'DEFINE OUTER WALLS OF THE INNER BOX -8.1CM IN Y FOR TOTAL DEFORMATION
CUBOID 6 1 2P22.938 225.48 -233.58 8.829 -13.979
```

```
UNIT 2
COM=!INNER BOX LID!
'DEFINE INNER CORE OF INNER BOX LID -8.1CM IN Y FOR TOTAL DEFORMATION
CUBOID 10 1 2P22.798 2P229.39 2P2.48
'DEFINE WALLS FOR INNER BOX LID -8.1CM IN Y FOR TOTAL DEFORMATION
CUBOID 6 1 2P22.938 2P229.53 2P2.62
```

```
UNIT 3
COM=!INNER BOX WITH ENDS AND LID!
ARRAY 1 3*0
```

```
UNIT 10
```

NEDO-33869 Revision 11  
Non-Proprietary Information

COM=!5 W/O FUEL PINS W/O GAD!

'DEFINE THE FUEL PELLET

YCYLINDER 1 1 0.52500 381 0

'DEFINE THE PELLET-CLAD GAP

YCYLINDER 0 1 0.55000 381 0

'DEFINE THE FUEL ROD CLADDING

YCYLINDER 2 1 0.56524 381 0

'DEFINE THE FUEL ROD PITCH FILLED WITH WATER

CUBOID 8 1 2P1.50280 381 0 2P1.50280

UNIT 20

COM=!SPACE WITHIN FUEL ASSEMBLY LATTICE!

CUBOID 8 1 2P1.50280 381 0 2P1.50280

UNIT 30

COM=!ARRAY FOR COMPLETE FUEL ASSEMBLY!

ARRAY 2 3\*0

UNIT 40

COM=!5 W/O FUEL PINS W/O GAD LEFT SIDE FOAM!

'DEFINE THE FUEL PELLET

YCYLINDER 1 1 0.52500 381 0

'DEFINE THE PELLET-CLAD GAP

YCYLINDER 0 1 0.55000 381 0

'DEFINE THE FUEL ROD CLADDING

YCYLINDER 2 1 0.56524 381 0

'DEFINE THE FUEL ROD PITCH FILLED WITH WATER

CUBOID 8 1 1.50280 -1.00280 381 0 2P1.50280

UNIT 46

COM=!5 W/O FUEL PINS W/O GAD LEFT SIDE TOP FOAM!

'DEFINE THE FUEL PELLET

YCYLINDER 1 1 0.52500 381 0

'DEFINE THE PELLET-CLAD GAP

YCYLINDER 0 1 0.55000 381 0

'DEFINE THE FUEL ROD CLADDING

YCYLINDER 2 1 0.56524 381 0

'DEFINE THE FUEL ROD PITCH FILLED WITH WATER

CUBOID 8 1 1.50280 -1.00280 381 0 1.00280 -1.50280

UNIT 47

COM=!5 W/O FUEL PINS W/O GAD LEFT SIDE BOTTOM FOAM!

'DEFINE THE FUEL PELLET

YCYLINDER 1 1 0.52500 381 0

'DEFINE THE PELLET-CLAD GAP

YCYLINDER 0 1 0.55000 381 0

'DEFINE THE FUEL ROD CLADDING

YCYLINDER 2 1 0.56524 381 0

'DEFINE THE FUEL ROD PITCH FILLED WITH WATER

CUBOID 8 1 1.50280 -1.00280 381 0 1.50280 -1.00280

UNIT 50

COM=!5 W/O FUEL PINS W/O GAD RIGHT SIDE FOAM!

'DEFINE THE FUEL PELLET

YCYLINDER 1 1 0.52500 381 0

'DEFINE THE PELLET-CLAD GAP



NEDO-33869 Revision 11  
Non-Proprietary Information

```

YCYLINDER 0 1 0.55000 381 0
'DEFINE THE FUEL ROD CLADDING
YCYLINDER 2 1 0.56524 381 0
'DEFINE THE FUEL ROD PITCH FILLED WITH WATER
CUBOID 8 1 1.00280 -1.50280 381 0 2P1.50280

```

UNIT 56

```

COM=!5 W/O FUEL PINS W/O GAD RIGHT SIDE TOP FOAM!
'DEFINE THE FUEL PELLET
YCYLINDER 1 1 0.52500 381 0
'DEFINE THE PELLET-CLAD GAP
YCYLINDER 0 1 0.55000 381 0
'DEFINE THE FUEL ROD CLADDING
YCYLINDER 2 1 0.56524 381 0
'DEFINE THE FUEL ROD PITCH FILLED WITH WATER
CUBOID 8 1 1.00280 -1.50280 381 0 1.00280 -1.50280

```

UNIT 57

```

COM=!5 W/O FUEL PINS W/O GAD RIGHT BOTTOM SIDE FOAM!
'DEFINE THE FUEL PELLET
YCYLINDER 1 1 0.52500 381 0
'DEFINE THE PELLET-CLAD GAP
YCYLINDER 0 1 0.55000 381 0
'DEFINE THE FUEL ROD CLADDING
YCYLINDER 2 1 0.56524 381 0
'DEFINE THE FUEL ROD PITCH FILLED WITH WATER
CUBOID 8 1 1.00280 -1.50280 381 0 1.50280 -1.00280

```

UNIT 60

```

COM=!5 W/O FUEL PINS W/O GAD TOP SIDE FOAM!
'DEFINE THE FUEL PELLET
YCYLINDER 1 1 0.52500 381 0
'DEFINE THE PELLET-CLAD GAP
YCYLINDER 0 1 0.55000 381 0
'DEFINE THE FUEL ROD CLADDING
YCYLINDER 2 1 0.56524 381 0
'DEFINE THE FUEL ROD PITCH FILLED WITH WATER
CUBOID 8 1 2P1.50280 381 0 1.00280 -1.50280

```

UNIT 70

```

COM=!5 W/O FUEL PINS W/O GAD BOTTOM SIDE FOAM!
'DEFINE THE FUEL PELLET
YCYLINDER 1 1 0.52500 381 0
'DEFINE THE PELLET-CLAD GAP
YCYLINDER 0 1 0.55000 381 0
'DEFINE THE FUEL ROD CLADDING
YCYLINDER 2 1 0.56524 381 0
'DEFINE THE FUEL ROD PITCH FILLED WITH WATER
CUBOID 8 1 2P1.50280 381 0 1.50280 -1.00280

```

UNIT 400

```

COM=!OUTER CONTAINER BODY AND LID!
'DEFINE INNER REGION OF THE OUTER CONTAINER
'MINUS 4.7CM IN Y AND -2.4CM IN Z FOR TOTAL DEFORMATION
CUBOID 0 1 2P35.788 247.960 -253.190 29.500 -31.900
'INNER CONTAINER PLACEMENT WITHIN OUTER CONTAINER

```

NEDO-33869 Revision 11  
Non-Proprietary Information

```
HOLE 3          -22.938      -229.53      -14.024
'DEFINE WALLS OF THE OUTER CONTAINER AND LID
CUBOID    6  1    2P35.963  248.135  -253.365  29.675  -32.075

GLOBAL
UNIT 500
ARRAY 10 3*0
REFLECTOR 5  1    6R30.48  1
END GEOM

READ ARRAY
ARA=1 NUX=1 NUY=1 NUZ=2
FILL 1 2
END FILL
ARA=2 NUX=5 NUY=1 NUZ=5
FILL 47 70 70 70 57
      40 10 10 10 50
      40 10 10 10 50
      40 10 10 10 50
      46 60 60 60 56
END FILL
ARA=10 NUX=10 NUY=1 NUZ=10
FILL F400
END FILL
END ARRAY

READ BNDS ALL=VACUUM
END BNDS
END DATA
END
```

### 6.11.9 Data Tables for Figures in Chapter 6

**Table 6-28 Data for Figure 6-29 RAJ-II Array HAC Polyethylene Sensitivity**

Output File Name	Case Description	Interspersed Moderator Density (g/cm <sup>3</sup> )	Polyethylene Mass (kg)	k <sub>eff</sub>	σ	k <sub>eff</sub> + 2σ
rajII_hac_a10_nointer spersedh2o_polyethyl enesensitivity_1.284c mpitch 14X2X16	Atrium 10XP+	0.00	0	0.8715	0.0008	0.8731
“	Atrium 10XP+	0.00	10.9	0.8774	0.0009	0.8792
“	Atrium 10XP+	0.00	17.1	0.8813	0.0009	0.8831
“	Atrium 10XP+	0.00	20.4	0.8810	0.0008	0.8826
“	Atrium 10XP+	0.00	22.9	0.8822	0.0009	0.8840
“	Atrium 10XP+	0.00	25.4	0.8847	0.0008	0.8863
“	Atrium 10XP+	0.00	27.9	0.8860	0.001	0.8880
rajII_hac_g10_nointer spersedh2o_polyethyl enesensitivity_pitch1. 2954cm 14X2X16	GNF 10 x 10	0.00	0	0.8863	0.0007	0.8877
“	GNF 10 x 10	0.00	10.9	0.8923	0.0008	0.8939
“	GNF 10 x 10	0.00	17.1	0.8940	0.0008	0.8956
“	GNF 10 x 10	0.00	20.4	0.8955	0.0007	0.8969
“	GNF 10 x 10	0.00	22.9	0.8975	0.0009	0.8993
“	GNF 10 x 10	0.00	25.4	0.8994	0.0008	0.9010
“	GNF 10 x 10	0.00	27.9	0.9001	0.0008	0.9017
rajII_hac_f9_10gadro ds_refassy_14x2x16_ polysens	FANP 9x9	0.00	0	0.8728	0.0009	0.8746
rajII_hac_f9_10gadro ds_refassy_14x2x16_ polysens	FANP 9x9	0.00	20	0.8756	0.0009	0.8774
rajII_hac_f9_10gadro ds_refassy_14x2x16_c hannels	FANP 9x9	0.00	22	0.8755	0.0009	0.8773
rajII_hac_f9_10gadro ds_refassy_14x2x16_ polysens	FANP 9x9	0.00	24	0.8769	0.0007	0.8783
rajII_hac_f9_10gadro ds_refassy_14x2x16_ polysens	FANP 9x9	0.00	26	0.8758	0.0008	0.8774
rajII_hac_f9_10gadro ds_refassy_14x2x16_ polysens	FANP 9x9	0.00	28	0.8766	0.0008	0.8782
rajII_hac_f9_10gadro ds_refassy_14x2x16_ polysens	FANP 9x9	0.00	30	0.8776	0.0009	0.8794
rajII_hac_g9_10gadro ds_refassy_14X2X16_ polysens	GNF 9x9	0.00	0	0.8612	0.0008	0.8628

NEDO-33869 Revision 11  
Non-Proprietary Information

Output File Name	Case Description	Interspersed Moderator Density (g/cm <sup>3</sup> )	Polyethylene Mass (kg)	k <sub>eff</sub>	σ	k <sub>eff</sub> + 2σ
rajII_hac_g9_10gadros_refassy_14X2X16_polysens	GNF 9x9	0.00	20	0.8661	0.0009	0.8679
rajII_hac_g9_10gadros_refassy_14X2X16_channels	GNF 9x9	0.00	22	0.8659	0.0008	0.8676
rajII_hac_g9_10gadros_refassy_14X2X16_polysens	GNF 9x9	0.00	24	0.8676	0.0007	0.8690
rajII_hac_g9_10gadros_refassy_14X2X16_polysens	GNF 9x9	0.00	26	0.8670	0.0009	0.8688
rajII_hac_g9_10gadros_refassy_14X2X16_polysens	GNF 9x9	0.00	28	0.8656	0.0009	0.8674
rajII_hac_g9_10gadros_refassy_14X2X16_polysens	GNF 9x9	0.00	30	0.8702	0.0008	0.8718
rajII_hac_g8_nointerspersedh2o_polyethylenesensitivity_1.6256cm_14X2X16	GNF 8x8	0.00	0	0.8795	0.0009	0.8813
“	GNF 8x8	0.00	19	0.8865	0.0009	0.8883
“	GNF 8x8	0.00	22	0.8900	0.0009	0.8918
“	GNF 8x8	0.00	24	0.8892	0.0008	0.8908
“	GNF 8x8	0.00	26	0.8924	0.0008	0.8940
“	GNF 8x8	0.00	28	0.8915	0.0009	0.8933
“	GNF 8x8	0.00	30	0.8942	0.0009	0.8960

NEDO-33869 Revision 11  
Non-Proprietary Information

**Table 6-29 Data for Figure 6-30 RAJ-II Fuel Rod Pitch Sensitivity Study**

Output File Name	Interspersed Moderator Density (g/cm <sup>3</sup> )	Polyethylene Mass (kg)	Pitch (cm)	k <sub>eff</sub>	σ	k <sub>eff</sub> + 2σ
rajII_hac_a10_nointerspersedh2o_pitchsensitivity_14X2X16	0.00	20.4	1.210	0.8301	0.0010	0.8321
“	0.00	20.4	1.284	0.8810	0.0008	0.8826
“	0.00	20.4	1.350	0.9245	0.0009	0.9263
“	0.00	20.4	1.376	0.9391	0.0008	0.9407
rajII_hac_g10_nointerspersedh2o_pitchsensitivity_14X2X16	0.00	20.4	1.1960	0.8394	0.0009	0.8412
“	0.00	20.4	1.2954	0.8955	0.0007	0.8969
“	0.00	20.4	1.350	0.9241	0.0008	0.9257
“	0.00	20.4	1.3760	0.9328	0.0008	0.9344
rajII_hac_f9_10gad rods_refassy_14x2x16_pitch	0.00	22	1.3389	0.8219	0.0008	0.8235
“	0.00	22	1.4478	0.8755	0.0009	0.8773
“	0.00	22	1.5028	0.8998	0.0008	0.9014
rajII_hac_f9_10gad rods_refassy_14x2x16_channels	0.00	22	1.5376	0.9126	0.0009	0.9144
rajII_hac_g9_10gad rods_refassy_14X2X16_pitchsens	0.00	22	1.3260	0.8073	0.0008	0.8089
“	0.00	22	1.4376	0.8659	0.0008	0.8676
“	0.00	22	1.5028	0.8929	0.0008	0.8944
rajII_hac_g9_10gad rods_refassy_14X2X16_channels	0.00	22	1.5376	0.9076	0.0009	0.9095
rajII_hac_g8_nointerspersedh2o_pitchsensitivity_14X2X16	0.00	22	1.4603	0.7968	0.0009	0.7986
“	0.00	22	1.6256	0.8900	0.0009	0.8918
“	0.00	22	1.6923	0.9216	0.0008	0.9232
“	0.00	22	1.7264	0.9384	0.0008	0.9400

**Table 6-30 Data for Figure 6-31 RAJ-II Array HAC Pellet Diameter Sensitivity Study**

Output File Name	Interspersed Moderator Density (g/cm <sup>3</sup> )	Pellet Diameter (cm)	k <sub>eff</sub>	σ	k <sub>eff</sub> + 2σ
rajII_hac_a10_nointers persedh2o_pelletodsens itivity 14X2X16	0	0.8000	0.8560	0.0008	0.8576
“	0	0.8400	0.8680	0.0009	0.8698
“	0	0.8882	0.8810	0.0008	0.8826
“	0	0.8941	0.8839	0.0008	0.8855
“	0	0.9200	0.8906	0.0008	0.8922
rajII_hac_g10_nointers persedh2o_pelletodsens itivity 14X2X16	0	0.8000	0.8641	0.0009	0.8659
“	0	0.8400	0.8796	0.0009	0.8814
“	0	0.8882	0.8941	0.0008	0.8957
“	0	0.8941	0.8955	0.0007	0.8969
“	0	0.9200	0.9050	0.0008	0.9066
rajII_hac_f9_10gadrod s_refassy_14x2x16_pell etod	0	0.8882	0.8600	0.0008	0.8616
“	0	0.9000	0.8633	0.0009	0.8651
rajII_hac_f9_10gadrod s_refassy_14x2x16_chan nels	0	0.9398	0.8755	0.0009	0.8773
rajII_hac_f9_10gadrod s_refassy_14x2x16_pell etod	0	0.9550	0.8799	0.0008	0.8815
“	0	0.9600	0.8817	0.0007	0.8831
rajII_hac_g9_10gadrod s_refassy_14X2X16_pe lletodsens	0	0.8882	0.8462	0.0008	0.8478
“	0	0.9000	0.8509	0.0009	0.8527
“	0	0.9398	0.8609	0.0008	0.8625
rajII_hac_g9_10gadrod s_refassy_14X2X16_ch annels	0	0.9550	0.8659	0.0008	0.8676
rajII_hac_g9_10gadrod s_refassy_14X2X16_pe lletodsens	0	0.9600	0.8678	0.0008	0.8694
rajII_hac_g8_nointersp ersedh2o_pelletodsensit ivity 14X2X16	0	0.9200	0.8566	0.0008	0.8582
“	0	0.9550	0.8648	0.0008	0.8664
“	0	1.0000	0.8783	0.0008	0.8799
“	0	1.0439	0.8900	0.0009	0.8918
“	0	1.0700	0.8940	0.0009	0.8958

**Table 6-31 Data for Figure 6-32 RAJ-II Array HAC Fuel Rod Clad ID Sensitivity Study**

Output File Name	Moderator Density (g/cm <sup>3</sup> )	Clad Inner Diameter (cm)	k <sub>eff</sub>	σ	k <sub>eff</sub> + 2σ
rajII_hac_a10_nointersperse dh2o_cladidsensitivity_14X 2X16	0	0.8800	0.8760	0.0009	0.8778
“	0	0.8900	0.8805	0.0009	0.8823
“	0	0.9218	0.8810	0.0008	0.8826
“	0	0.9322	0.8813	0.0008	0.8829
“	0	1.0330	0.8855	0.0010	0.8875
rajII_hac_g10_nointersperse dh2o_cladidsensitivity_14X 2X16 (clad OD = 1.019 cm)	0	0.9000	0.8937	0.0010	0.8957
“	0	0.9218	0.8956	0.0008	0.8972
“	0	0.9322	0.8955	0.0007	0.8969
“	0	1.0185	0.8999	0.0008	0.9015
rajII_hac_f9_10gad rods_ref assy 14x2x16 cladid	0	0.9400	0.8742	0.0009	0.8759
rajII_hac_f9_10gad rods_ref assy 14x2x16 channels	0	0.9601	0.8755	0.0009	0.8773
rajII_hac_f9_10gad rods_ref assy 14x2x16 cladid	0	0.9750	0.8760	0.0009	0.8777
“	0	0.9830	0.8768	0.0009	0.8786
“	0	1.0998	0.8789	0.0008	0.8804
rajII_hac_g9_10gad rods_ref assy 14X2X16 cladid	0	0.9560	0.8641	0.0008	0.8657
“	0	0.9600	0.8643	0.0008	0.8659
“	0	0.9750	0.8660	0.0009	0.8678
rajII_hac_g9_10gad rods_ref assy 14X2X16 channels	0	0.9830	0.8659	0.0008	0.8676
rajII_hac_g9_10gad rods_ref assy 14X2X16 cladid	0	1.1100	0.8702	0.0008	0.8718
rajII_hac_g8_nointerspersed h2o_cladidsensitivity_14X2 X16	0	1.0440	0.8894	0.001	0.8914
“	0	1.0719	0.8900	0.0009	0.8918
“	0	1.1000	0.8900	0.0009	0.8918
“	0	1.1500	0.8918	0.0008	0.8934
“	0	1.2192	0.8917	0.0008	0.8933

**Table 6-32 Data for Figure 6-33 RAJ-II Array HAC Fuel Rod Clad OD Sensitivity Study**

Output File Name	Moderator Density (g/cm <sup>3</sup> )	Clad Outer Diameter (cm)	k <sub>eff</sub>	σ	k <sub>eff</sub> + 2σ
rajII_hac_a10_nointersper sedh2o_cladodsensitivity_ 14X2X16	0	0.9218	0.9051	0.0008	0.9067
“	0	1.0185	0.8858	0.0009	0.8876
“	0	1.0330	0.8810	0.0008	0.8826
“	0	1.1000	0.8647	0.0008	0.8663
“	0	1.1210	0.8604	0.0009	0.8622
rajII_hac_g10_nointersper sedh2o_cladodsensitivity_ 14X2X16 (clad ID = 0.9322 cm)	0	0.9322	0.9118	0.0008	0.9134
“	0	1.0185	0.8955	0.0007	0.8969
“	0	1.0330	0.8935	0.0008	0.8951
“	0	1.1000	0.8790	0.0008	0.8806
“	0	1.1210	0.8742	0.0009	0.8760
rajII_hac_f9_10gad rods_r efassy_14x2x16_cladod	0	0.9601	0.8967	0.0008	0.8984
“	0	1.0330	0.8876	0.0008	0.8892
“	0	1.0998	0.8792	0.0008	0.8808
rajII_hac_f9_10gad rods_r efassy_14x2x16_channels	0	1.1200	0.8755	0.0009	0.8773
rajII_hac_g9_10gad rods_r efassy_14X2X16_cladod	0	0.9830	0.8857	0.0008	0.8873
“	0	1.0330	0.8791	0.0009	0.8809
rajII_hac_g9_10gad rods_r efassy_14X2X16_channel s	0	1.1100	0.8659	0.0008	0.8676
rajII_hac_g9_10gad rods_r efassy_14X2X16_cladod	0	1.1200	0.8644	0.0010	0.8664
rajII_hac_g8_nointerspers edh2o_cladodsensitivity_ 14X2X16	0	1.0719	0.9120	0.0008	0.9136
“	0	1.1500	0.9030	0.0008	0.9046
“	0	1.2192	0.8900	0.0009	0.8918
“	0	1.2500	0.8832	0.0008	0.8848



**Table 6-33 Data for Figure 6-41 Moderator Density Sensitivity Study for the RAJ-II  
HAC Worst Case Parameter Fuel Design**

Output File Name	Moderator Density (g/cm <sup>3</sup> )	Clad Inner Diameter (cm)	Clad Outer Diameter (cm)	k <sub>eff</sub>	σ	k <sub>eff</sub> + 2σ
rajII_hac_g10_worstcase_ moderatordensity_14X2X 16	0.00	0.9338	1.010	0.7154	0.0006	0.7166
“	0.02	0.9338	1.010	0.7349	0.0007	0.7363
“	0.04	0.9338	1.010	0.7526	0.0007	0.7540
“	0.06	0.9338	1.010	0.7686	0.0006	0.7698
“	0.08	0.9338	1.010	0.7820	0.0007	0.7834
“	0.10	0.9338	1.010	0.7933	0.0008	0.7949
“	0.20	0.9338	1.010	0.8383	0.0007	0.8397
“	0.40	0.9338	1.010	0.8908	0.0007	0.8922
“	0.60	0.9338	1.010	0.9182	0.0009	0.9200
“	0.80	0.9338	1.010	0.9319	0.0008	0.9335
“	1.00	0.9338	1.010	0.9404	0.0007	0.9418

**Table 6-34 Data for Figure 6-44 RAJ-II Single Package NCT Results with LEU Fuel**

<b>Fuel Assembly Type</b>	<b>Moderator Density (g/cm<sup>3</sup>)</b>	<b>Gadolinia Rod (#)</b>	<b>Pitch (cm)</b>	<b>Pellet OD (cm)</b>	<b>Clad Inner Diameter (cm)</b>	<b>Clad Outer Diameter (cm)</b>	<b>k<sub>eff</sub></b>	<b>σ</b>	<b>k<sub>eff</sub> + 2σ</b>
GNF 10x10	0.0	12	1.363	0.895	0.934	1.010	0.2777	0.0002	0.2781
GNF 10x10	0.1	12	1.363	0.895	0.934	1.010	0.3268	0.0002	0.3272
GNF 10x10	0.2	12	1.363	0.895	0.934	1.010	0.3928	0.0002	0.3932
GNF 10x10	0.3	12	1.363	0.895	0.934	1.010	0.4495	0.0002	0.4499
GNF 10x10	0.4	12	1.363	0.895	0.934	1.010	0.4996	0.0003	0.5002
GNF 10x10	0.5	12	1.363	0.895	0.934	1.010	0.5424	0.0002	0.5429
GNF 10x10	0.6	12	1.363	0.895	0.934	1.010	0.5813	0.0002	0.5818
GNF 10x10	0.7	12	1.363	0.895	0.934	1.010	0.6166	0.0003	0.6172
GNF 10x10	0.8	12	1.363	0.895	0.934	1.010	0.6487	0.0003	0.6493
GNF 10x10	0.9	12	1.363	0.895	0.934	1.010	0.6775	0.0003	0.6781
GNF 10x10	1.0	12	1.363	0.895	0.934	1.010	0.7045	0.0002	0.7051

**Table 6-35 Data for Figure 6-45 RAJ-II Single Package HAC Results with LEU Fuel**

<b>Fuel Assembly Type</b>	<b>Inner Container Moderator Density (g/cm<sup>3</sup>)</b>	<b>Gadolinia Rod (#)</b>	<b>Pitch (cm)</b>	<b>Pellet OD (cm)</b>	<b>Clad Inner Diameter (cm)</b>	<b>Clad Outer Diameter (cm)</b>	<b>k<sub>eff</sub></b>	<b>σ</b>	<b>k<sub>eff</sub> + 2σ</b>
GNF 10x10	0.0	12	1.363	0.895	0.934	1.010	0.2766	0.0002	0.2770
GNF 10x10	0.1	12	1.363	0.895	0.934	1.010	0.3090	0.0002	0.3094
GNF 10x10	0.2	12	1.363	0.895	0.934	1.010	0.3565	0.0002	0.3570
GNF 10x10	0.3	12	1.363	0.895	0.934	1.010	0.4114	0.0002	0.4118
GNF 10x10	0.4	12	1.363	0.895	0.934	1.010	0.4673	0.0002	0.4678
GNF 10x10	0.5	12	1.363	0.895	0.934	1.010	0.5203	0.0002	0.5208
GNF 10x10	0.6	12	1.363	0.895	0.934	1.010	0.5686	0.0002	0.5691
GNF 10x10	0.7	12	1.363	0.895	0.934	1.010	0.6115	0.0003	0.6121
GNF 10x10	0.8	12	1.363	0.895	0.934	1.010	0.6491	0.0003	0.6497
GNF 10x10	0.9	12	1.363	0.895	0.934	1.010	0.6805	0.0003	0.6811
GNF 10x10	1.0	12	1.363	0.895	0.934	1.010	0.7090	0.0003	0.7095

**Table 6-36 Data for Figure 6-46 RAJ-II Package Array Under NCT Results with LEU Fuel**

<b>Fuel Assembly Type</b>	<b>Moderator Density (g/cm<sup>3</sup>)</b>	<b>Gadolinia Rod (#)</b>	<b>Pitch (cm)</b>	<b>Pellet OD (cm)</b>	<b>Clad Inner Diameter (cm)</b>	<b>Clad Outer Diameter (cm)</b>	<b>k<sub>eff</sub></b>	<b>σ</b>	<b>k<sub>eff</sub> + 2σ</b>
GNF 10x10	0.0	12	1.363	0.895	0.934	1.010	0.8116	0.0003	0.8122
GNF 10x10	0.1	12	1.363	0.895	0.934	1.010	0.6419	0.0002	0.6424
GNF 10x10	0.2	12	1.363	0.895	0.934	1.010	0.5473	0.0003	0.5479
GNF 10x10	0.3	12	1.363	0.895	0.934	1.010	0.5236	0.0002	0.5241
GNF 10x10	0.4	12	1.363	0.895	0.934	1.010	0.5349	0.0002	0.5354
GNF 10x10	0.5	12	1.363	0.895	0.934	1.010	0.5606	0.0003	0.5612
GNF 10x10	0.6	12	1.363	0.895	0.934	1.010	0.5908	0.0003	0.5914
GNF 10x10	0.7	12	1.363	0.895	0.934	1.010	0.6217	0.0003	0.6223
GNF 10x10	0.8	12	1.363	0.895	0.934	1.010	0.6519	0.0003	0.6524
GNF 10x10	0.9	12	1.363	0.895	0.934	1.010	0.6795	0.0003	0.6800
GNF 10x10	1.0	12	1.363	0.895	0.934	1.010	0.7050	0.0003	0.7056

**Table 6-37 Data for Figure 6-47 RAJ-II Package Array HAC Results, Inner Container Moderation Study with LEU Fuel**

<b>Fuel Assembly Type</b>	<b>Inner Container Moderator Density (g/cm<sup>3</sup>)</b>	<b>Gadolinia Rods (#)</b>	<b>Pitch (cm)</b>	<b>Pellet OD (cm)</b>	<b>Clad Inner Diameter (cm)</b>	<b>Clad Outer Diameter (cm)</b>	<b>k<sub>eff</sub></b>	<b>σ</b>	<b>k<sub>eff</sub> + 2σ</b>
GNF 10x10	0.0	12	1.363	0.895	0.934	1.010	0.6103	0.0002	0.6108
GNF 10x10	0.1	12	1.363	0.895	0.934	1.010	0.6760	0.0002	0.6766
GNF 10x10	0.2	12	1.363	0.895	0.934	1.010	0.7300	0.0003	0.7307
GNF 10x10	0.3	12	1.363	0.895	0.934	1.010	0.7743	0.0003	0.7749
GNF 10x10	0.4	12	1.363	0.895	0.934	1.010	0.8112	0.0003	0.8117
GNF 10x10	0.5	12	1.363	0.895	0.934	1.010	0.8418	0.0003	0.8424
GNF 10x10	0.6	12	1.363	0.895	0.934	1.010	0.8668	0.0003	0.8675
GNF 10x10	0.7	12	1.363	0.895	0.934	1.010	0.8873	0.0003	0.8879
GNF 10x10	0.8	12	1.363	0.895	0.934	1.010	0.9046	0.0003	0.9051
GNF 10x10	0.9	12	1.363	0.895	0.934	1.010	0.9183	0.0003	0.9189
GNF 10x10	1.0	12	1.363	0.895	0.934	1.010	0.9295	0.0003	0.9300

**Table 6-38 Data for Figure 6-48 RAJ-II Package Array HAC Results, Outer Container Moderation Study with LEU Fuel**

Fuel Assembly Type	Outer Container Moderator Density (g/cm <sup>3</sup> )	Gadolinia Rods (#)	Pitch (cm)	Pellet OD (cm)	Clad Inner Diameter (cm)	Clad Outer Diameter (cm)	k <sub>eff</sub>	σ	k <sub>eff</sub> + 2σ
GNF 10x10	0.0	12	1.363	0.895	0.934	1.010	0.9295	0.0003	0.9300
GNF 10x10	0.1	12	1.363	0.895	0.934	1.010	0.8108	0.0003	0.8115
GNF 10x10	0.2	12	1.363	0.895	0.934	1.010	0.7510	0.0003	0.7516
GNF 10x10	0.3	12	1.363	0.895	0.934	1.010	0.7241	0.0003	0.7247
GNF 10x10	0.4	12	1.363	0.895	0.934	1.010	0.7128	0.0003	0.7134
GNF 10x10	0.5	12	1.363	0.895	0.934	1.010	0.7073	0.0003	0.7079
GNF 10x10	0.6	12	1.363	0.895	0.934	1.010	0.7052	0.0003	0.7058
GNF 10x10	0.7	12	1.363	0.895	0.934	1.010	0.7043	0.0002	0.7048
GNF 10x10	0.8	12	1.363	0.895	0.934	1.010	0.7046	0.0003	0.7052
GNF 10x10	0.9	12	1.363	0.895	0.934	1.010	0.7040	0.0002	0.7045
GNF 10x10	1.0	12	1.363	0.895	0.934	1.010	0.7048	0.0002	0.7053

**Table 6-39 Data for Figure 6-51 RAJ-II BWR UO<sub>2</sub> LEU Fuel Rod Transport in Stainless Steel Pipe**

Output File Name	Fuel Assembly Type	Interspersed Moderator Density (g/cm <sup>3</sup> )	Pitch (cm)	Fuel Rod (#)	Pellet OD (cm)	Clad Inner Diameter (cm)	Clad Outer Diameter (cm)	k <sub>eff</sub>	σ	k <sub>eff</sub> + 2σ
rajII_hac_8_worstcase_sspipe_14x2x16	8x8	1.000	1.1305	110	1.05	1.1000	1.1000	0.8793	0.0007	0.8807
“	8x8	1.000	1.6662	52	1.05	1.1000	1.1000	1.0235	0.0009	1.0253
“	8x8	1.000	1.9035	43	1.05	1.1000	1.1000	1.0440	0.0008	1.0456
rajII_hac_8_worstcase_sspipe_22fuelrods_14x2x16	8x8	1.000	2.5	22	1.05	1.1000	1.1000	0.8823	0.0008	0.8839
rajII_hac_8_worstcase_sspipe_14x2x16	8x8	1.000	2.937	14	1.05	1.1000	1.1000	0.7294	0.0008	0.7310
rajII_hac_9_worstcase_sspipe_14x2x16	9x9	1.000	1.0505	140	0.9600	1.0200	1.0200	0.8701	0.0006	0.8713
“	9x9	1.000	1.4770	72	0.9600	1.0200	1.0200	1.0515	0.0008	1.0531
“	9x9	1.000	2	38	0.9600	1.0200	1.0200	1.0056	0.0009	1.0074
rajII_hac_9_worstcase_sspipe_26fuelrods_14x2x16	9x9	1.000	2.25	26	0.9600	1.0200	1.0200	0.8900	0.0008	0.8916
rajII_hac_9_worstcase_sspipe_14x2x16	9x9	1.000	2.5432	22	0.9600	1.0200	1.0200	0.8416	0.0010	0.8436
rajII_hac_10_worstcase_sspipe_14x2x16	10x10	1.000	1.0305	144	0.9	1.000	1.000	0.8666	0.0007	0.8680
“	10x10	1.000	1.3213	84	0.9	1.000	1.000	1.0070	0.0008	1.0086
“	10x10	1.000	1.6416	56	0.9	1.000	1.000	1.0310	0.0011	1.0332
“	10x10	1.000	2.0484	30	0.9	1.000	1.000	0.8863	0.0008	0.8879

**Table 6-40 Data for Figure 6-52 RAJ-II BWR UO<sub>2</sub> LEU Fuel Rod Single Package Under NCT**

Output File Name	Fuel Assembly Type	Interspersed Moderator Density (g/cm <sup>3</sup> )	Pitch (cm)	Fuel Rod Number (#)	Pellet OD (cm)	Clad Inner Diameter (cm)	Clad Outer Diameter (cm)	k <sub>eff</sub>	σ	k <sub>eff</sub> + 2σ
rajII_normal_8_worstcasefuel_fuelrodtransport_moderatordensitysensitivity_singlepackage	8x8	0.00	2.815	25	1.05	1.1000	1.1000	0.1675	0.0004	0.1683
“	8x8	0.01	2.815	25	1.05	1.1000	1.1000	0.1675	0.0004	0.1683
“	8x8	0.02	2.815	25	1.05	1.1000	1.1000	0.1672	0.0004	0.1680
“	8x8	0.04	2.815	25	1.05	1.1000	1.1000	0.1702	0.0004	0.1710
“	8x8	0.06	2.815	25	1.05	1.1000	1.1000	0.1757	0.0005	0.1767
“	8x8	0.08	2.815	25	1.05	1.1000	1.1000	0.1845	0.0005	0.1855
“	8x8	0.10	2.815	25	1.05	1.1000	1.1000	0.1949	0.0004	0.1957
“	8x8	0.20	2.815	25	1.05	1.1000	1.1000	0.2567	0.0005	0.2577
“	8x8	0.40	2.815	25	1.05	1.1000	1.1000	0.3890	0.0007	0.3904
“	8x8	0.60	2.815	25	1.05	1.1000	1.1000	0.4967	0.0007	0.4981
“	8x8	0.80	2.815	25	1.05	1.1000	1.1000	0.5783	0.0009	0.5801
“	8x8	1.00	2.815	25	1.05	1.1000	1.1000	0.6365	0.0008	0.6381



**Table 6-41 Data for Figure 6-53 RAJ-II BWR UO<sub>2</sub> LEU Fuel Rod Transport Single Package HAC**

Output File Name	Fuel Assembly Type	Interspersed Moderator Density (g/cm <sup>3</sup> )	Pitch (cm)	Fuel Rod Number (#)	Pellet OD (cm)	Clad Inner Diameter (cm)	Clad Outer Diameter (cm)	k <sub>eff</sub>	σ	k <sub>eff</sub> + 2σ
rajII_hac_8_worstcase_fuelrod_transport_mode_ratordensitysensitivity_singlepackage	8x8	0.00	3.0056	25	1.05	1.1000	1.1000	0.1769	0.0004	0.1777
“	8x8	0.01	3.0056	25	1.05	1.1000	1.1000	0.1761	0.0004	0.1769
“	8x8	0.02	3.0056	25	1.05	1.1000	1.1000	0.1767	0.0004	0.1775
“	8x8	0.04	3.0056	25	1.05	1.1000	1.1000	0.1778	0.0005	0.1788
“	8x8	0.06	3.0056	25	1.05	1.1000	1.1000	0.1794	0.0004	0.1802
“	8x8	0.08	3.0056	25	1.05	1.1000	1.1000	0.1829	0.0004	0.1837
“	8x8	0.10	3.0056	25	1.05	1.1000	1.1000	0.1876	0.0004	0.1884
“	8x8	0.20	3.0056	25	1.05	1.1000	1.1000	0.2306	0.0005	0.2316
“	8x8	0.40	3.0056	25	1.05	1.1000	1.1000	0.3718	0.0007	0.3732
“	8x8	0.60	3.0056	25	1.05	1.1000	1.1000	0.5062	0.0007	0.5076
“	8x8	0.80	3.0056	25	1.05	1.1000	1.1000	0.5980	0.0008	0.5996
“	8x8	1.00	3.0056	25	1.05	1.1000	1.1000	0.6532	0.0008	0.6548

**Table 6-42 Data for Figure 6-55 RAJ-II Package Array Under NCT with BWR UO<sub>2</sub> LEU Loose Fuel Rods**

Output File Name	Fuel Assembly Type	Interspersed Moderator Density (g/cm <sup>3</sup> )	Pitch (cm)	Fuel Rod Number (#)	Pellet OD (cm)	Clad Inner Diameter (cm)	Clad Outer Diameter (cm)	k <sub>eff</sub>	σ	k <sub>eff</sub> + 2σ
rajII_normal_8_worstcasefuel_fuelrodtransport_moderator_densitysensitivity_21X3X24	8x8	0.00	2.815	25	1.05	1.1000	1.1000	0.5055	0.0006	0.5067
“	8x8	0.01	2.815	25	1.05	1.1000	1.1000	0.5827	0.0006	0.5839
“	8x8	0.02	2.815	25	1.05	1.1000	1.1000	0.5931	0.0007	0.5945
“	8x8	0.04	2.815	25	1.05	1.1000	1.1000	0.5891	0.0007	0.5905
“	8x8	0.06	2.815	25	1.05	1.1000	1.1000	0.5719	0.0007	0.5733
“	8x8	0.08	2.815	25	1.05	1.1000	1.1000	0.5523	0.0009	0.5541
“	8x8	0.10	2.815	25	1.05	1.1000	1.1000	0.5291	0.0007	0.5305
“	8x8	0.20	2.815	25	1.05	1.1000	1.1000	0.4383	0.0006	0.4395
“	8x8	0.40	2.815	25	1.05	1.1000	1.1000	0.4300	0.0007	0.4314
“	8x8	0.60	2.815	25	1.05	1.1000	1.1000	0.5079	0.0008	0.5095
“	8x8	0.80	2.815	25	1.05	1.1000	1.1000	0.5817	0.0008	0.5833
“	8x8	1.00	2.815	25	1.05	1.1000	1.1000	0.6365	0.0008	0.6381

**Table 6-43 Data for Figure 6-57 RAJ-II BWR UO<sub>2</sub> LEU Fuel Rod Transport Under HAC**

Fuel Assembly Type	Interspersed Moderator Density (g/cm <sup>3</sup> )	Pitch (cm)	Fuel Rod Number (#)	Pellet OD (cm)	Clad Inner Diameter (cm)	Clad Outer Diameter (cm)	k <sub>eff</sub>	σ	k <sub>eff</sub> + 2σ
8x8	0.00	3.0056	25	1.05	1.1000	1.1000	0.3040	0.0005	0.3051
8x8	0.01	3.0056	25	1.05	1.1000	1.1000	0.3175	0.0006	0.3187
8x8	0.02	3.0056	25	1.05	1.1000	1.1000	0.3311	0.0006	0.3323
8x8	0.04	3.0056	25	1.05	1.1000	1.1000	0.3618	0.0006	0.3630
8x8	0.06	3.0056	25	1.05	1.1000	1.1000	0.3934	0.0007	0.3949
8x8	0.08	3.0056	25	1.05	1.1000	1.1000	0.4249	0.0007	0.4264
8x8	0.10	3.0056	25	1.05	1.1000	1.1000	0.4548	0.0007	0.4562
8x8	0.20	3.0056	25	1.05	1.1000	1.1000	0.5869	0.0008	0.5886
8x8	0.20	3.0056	25	1.05	1.1000	1.1000	0.6856	0.0008	0.6872
8x8	0.40	3.0056	25	1.05	1.1000	1.1000	0.7542	0.0009	0.7559
8x8	0.20	3.0056	25	1.05	1.1000	1.1000	0.8031	0.0010	0.8051
8x8	0.60	3.0056	25	1.05	1.1000	1.1000	0.8352	0.0009	0.8370
8x8	0.20	3.0056	25	1.05	1.1000	1.1000	0.8550	0.0009	0.8569
8x8	0.80	3.0056	25	1.05	1.1000	1.1000	0.8676	0.0010	0.8696
8x8	0.20	3.0056	25	1.05	1.1000	1.1000	0.8714	0.0009	0.8732
8x8	1.00	3.0056	25	1.05	1.1000	1.1000	0.8720	0.0009	0.8738

### 6.11.10 Summary of Experiments

This document provides a summary of the experiments used in Reference 6-8 to determine the SCALE 4.4a bias. Trending data is either from the original experiments or calculated herein (i.e., Hydrogen-to-Uranium (H/U) values are added to the data). Note that in most cases the experimental  $k_{\text{eff}} \pm \sigma$  from Reference 6-8 does not have a reference. If data from the original experiment and/or data from the International Handbook of Evaluated Criticality Safety Benchmark Experiments (see Reference 6-8) provided these values, it was so noted or additional values provided.

The USL method of NUREG/CR-6361 (Reference 6-15) has the tacit assumption that the experimental  $k$  is 1.0000. Likewise, it does not account for the uncertainty in the experimental values; therefore, the procedure in NUREG/CR-6698, "Guide for Validation of Nuclear Criticality Safety Calculational Methodology," (Reference 6-23) is used. The document has the following definitions for the calculated values used for the bias evaluation:

$$k_{\text{norm}} = k_{\text{calc}}/k_{\text{exp}}$$

The normalized  $k_{\text{norm}}$  is used in the determination of the USL.

**Note:** The reference numbers quoted in the following sections are references listed in each section, rather than those listed in Section 6.12.

#### 6.11.10.1 Critical Configurations

##### 6.11.10.1.1 Water-Moderated U(4.31)O<sub>2</sub> Fuel Rods in 2.54-cm Square-Pitched Arrays

###### References:

1. "Critical Separation Between Subcritical Clusters of 4.29 Wt% U-235 Enriched UO<sub>2</sub> Rods in Water With Fixed Neutron Poisons," S.R. Bierman, B. M. Durst, E.D. Clayton, Battelle Pacific Northwest Laboratories, NUREG/CR-0073(PNL-2695).
2. "Water-Moderated U(4.31)O<sub>2</sub> Fuel Rods in 2.54-cm Square-Pitched Arrays," V.F. Dean, Evaluator, International Handbook of Evaluated Criticality Safety Benchmark Experiments," NEA/NSC/DOC(95)03, Sept 2001, Nuclear Energy Agency.
3. "Software Validation Document, EMF-2670, PC-SCALE 4.4a V&V," C.D. Manning, EMF-2670, Rev. 1, 11/26/2002, Framatome ANP.

Reference 3 uses the data from this set of experiments as part of a heterogeneous uranium oxide set of benchmark calculations. Table 6 of that reference provides some information on the experimental configuration and Tables 7 and 9 provide results for the 238 and 44 group Scale 4.4a cross-sections, respectively. Table 6-44 below provides a summary of the benchmark information from References 1 and 2. The rod and oxide dimensional and material information came from Reference 1. The enrichment quoted in Reference 1 was changed in Reference 2 due to a later chemical analysis of the fuel rods used in the experiment. Thus, the table uses the 4.31 value from Reference 2 rather than 4.29 quoted in Reference 1. The temperatures of the experiments were not included in Reference 1 and were not explicitly noted at the time of the experiment. The

NEDO-33869 Revision 11  
Non-Proprietary Information

authors of Reference 2 obtained log books from similar experiments at Pacific Northwest Laboratories (PNL) that showed temperatures ranging from ~18°C to ~25°C. From these data Reference 2 inferred an average value of ~22°C which is listed here. The value used in the calculations of Reference 3 is not currently known. The temperature value is used to calculate the hydrogen atom density and a deviation of a few degrees will not significantly change the results. The U and H atom densities used a value of Avogadro's number of 0.6022142E-24. The H/U value applies only to the fuel cluster. Table 6-45 shows the results of the benchmarks. Table 6-46 contains cases using cell-weighted models, 'x' added to case ID. These are included for completeness and should not be included in the normal benchmarking trending.

**Table 6-44 Summary of Information for Experiment**

Pellet OD, cm	1.2649	Enrichment, wt%	4.31 <sup>a</sup>	V <sub>H2O</sub> /V <sub>oxide</sub>	3.883228
Rod OD, cm	1.2827	Oxide Density, g/cm <sup>3</sup>	94.9	U-235 Atom Density	1.0125E-03
Rod OD, cm	1.4147	Temperature, °C	22 <sup>b</sup>	H Atom Density	0.066724
Rod Pitch, cm	2.54	Water Density, g/cm <sup>3</sup>	0.9978	H/U	255.92
Clad Material	Aluminum	Boron, ppm	0.0		

- a) Redefined from 4.29 in Reference 2 due to fuel evaluation after publication of Reference 1.
- b) Not defined in Reference 1, assumed in Reference 2 based upon inference from data notebooks of experiments.

**Table 6-45 Parameters for Benchmark Cases for SCALE 4.4a 44 Group Cross-Section Set**

Case ID <sup>c</sup>	Lattice <sup>a</sup>	Spacing <sup>a</sup> between clusters, cm		Experimental $k_{eff}$ and $\sigma$				SCALE 4.4a 44 Group Cross-Section Calculated $k_{eff}$ and $\sigma$				Absorber Plates in Water Gap
		Rod- rod	Cell- cell	$k_{eff}^b$	$\sigma^b$	$k_{eff}^c$	$\sigma^c$	$k_{eff}^d$	$\sigma^d$	AFG <sup>d</sup>	EALF <sup>d</sup> (ev)	
c004.out	15x8	11.72	10.62	1.0000	0.0020	0.9997	0.0020	0.9971	0.0008	35.772	0.112667	None
c005b.out	15x8	10.77	9.64	1.0000	0.0180	0.9997	0.0020	0.9960	0.0008	35.763	0.112942	0.625 cm Al plates
c006b.out	15x8	10.72	9.59	1.0000	0.0019	0.9997	0.0020	0.9960	0.0008	35.768	0.112841	0.625 cm Al plates
c007a.out	15x8	9.76	8.63	1.0000	0.0021	0.9997	0.0020	0.9966	0.0008	35.768	0.112705	0.302 cm SS 304L plates
c008b.out	15x8	9.22	8.09	1.0000	0.0021	0.9997	0.0020	0.9948	0.0008	35.755	0.113485	0.302 cm SS 304L plates
c009b.out	15x8	8.08	6.95	1.0000	0.0021	0.9997	0.0020	0.9963	0.0008	35.748	0.113698	0.298 cm 304L plates with 1.05 wt% B
c010b.out	15x8	6.60	5.47	1.0000	0.0021	0.9997	0.0020	0.9980	0.0008	35.728	0.114519	0.298 cm 304L plates with 1.05 wt% B
c011b.out	15x8	7.90	6.77	1.0000	0.0021	0.9997	0.0020	0.9983	0.0009	35.750	0.113450	0.298 cm 304L plates with 1.62 wt% B
c012b.out	15x8	5.76	4.63	1.0000	0.0021	0.9997	0.0020	0.9975	0.0007	35.729	0.114508	0.298 cm 304L plates with 1.62 wt% B
c013b.out	15x8	9.65	8.52	1.0000	0.0021	0.9997	0.0020	0.9956	0.001	35.768	0.112832	0.485 cm, SS 304L plates
c014b.out	15x8	8.58	7.45	1.0000	0.0021	0.9997	0.0020	0.9970	0.0009	35.745	0.113819	0.485 cm, SS 304L plates
c029b.out	15x8	10.90	9.77	1.0000	0.0021	0.9997	0.0020	0.9967	0.0008	35.770	0.112874	0.652 cm, Zircaloy-4 plates
c030b.out	15x8	10.86	9.73	1.0000	0.0021	0.9997	0.0020	0.9977	0.0009	35.767	0.112860	0.652 cm, Zircaloy-4 plates
c031b.out	15x8	7.672	6.55	1.0000	0.0021	0.9997	0.0020	0.9975	0.0008	35.727	0.114536	0.723 cm, Boral plates, 28.7 wt% B

- a) From Reference 1. The 'rod surface-to-rod' surface spacing is reported in Reference 1. Reference 2 (p. 9) provides the cell-to-cell spacing for selected experiments from Reference 1 as: (rod-rod) – (pitch) + (rod diameter). This formula was applied to all above values even though some 'rod-rod' may be 'array plate-to-plate'.
- b) Values from Reference 3, Table 6, p. 42. Source of  $\sigma$  values is not listed in this reference.
- c) Values from Reference 2, p. 23 based upon calculational uncertainties in parameters and assumptions in the benchmark models of the reference. Note that Reference 2 only includes 4 of the cases from Reference 1 listed above. Here it is assumed that the values listed above apply to all cases.
- d) From Reference 3, Table 9, p. 61 for 44 group cross-sections. Table 7 in this reference has values for 238 group cross-sections.

**Table 6-46 Parameters for Benchmark Cases for SCALE 4.4a 238 Group Cross-Section Set**

Case ID <sup>c</sup>	Lattice <sup>a</sup>	Cluster Spacing <sup>a</sup> , cm		Experimental $k_{eff}$ and $\sigma$				SCALE 4.4a 238 Group Cross-Section Calculated $k_{eff}$ and $\sigma$				Absorber Plates in Water Gap
		Rod-rod	Cell-cell	$k_{eff}^b$	$\sigma^b$	$k_{eff}^c$	$\sigma^c$	$k_{eff}^d$	$\sigma^d$	AFG <sup>d</sup>	EALF <sup>d</sup> (ev)	
c001x.out <sup>e</sup>	10x11.51	0.0	0.0	1.0000	0.0021	0.9997	0.0020	0.9987	0.0008	208.112	0.108721	--
c002x.out	8x16.37	0.0	0.0	1.0000	0.0021	0.9997	0.0020	0.9993	0.0008	208.157	0.108277	--
c003x.out	9x13.35	0.0	0.0	1.0000	0.0021	0.9997	0.0020	1.0015	0.0010	208.136	0.108496	--
c004.out	15x8	11.72	10.62	1.0000	0.0020	0.9997	0.0020	0.9930	0.0010	207.568	0.114058	None
c005b.out	15x8	10.77	9.64	1.0000	0.0180	0.9997	0.0020	0.9931	0.0008	207.550	0.114504	0.625 cm Al plates
c006b.out	15x8	10.72	9.59	1.0000	0.0019	0.9997	0.0020	0.9941	0.0009	207.508	0.114748	0.625 cm Al plates
c007a.out	15x8	9.76	8.63	1.0000	0.0021	0.9997	0.0020	0.9944	0.0008	207.547	0.114468	0.302 cm SS 304L plates
c007x.out	15x8	9.76	8.63	1.0000	0.0021	0.9997	0.0020	1.0010	0.0008	208.273	0.107285	0.302 cm SS 304L plates
c008b.out	15x8	9.22	8.09	1.0000	0.0021	0.9997	0.0020	0.9931	0.0007	207.487	0.114939	0.302 cm SS 304L plates
c008x.out	15x8	9.22	8.09	1.0000	0.0021	0.9997	0.0020	0.9981	0.0008	208.220	0.107758	0.302 cm SS 304L plates
c009b.out	15x8	8.08	6.95	1.0000	0.0021	0.9997	0.0020	0.9928	0.0008	207.472	0.114907	0.298 cm 304L plates with 1.05 wt% B
c010b.out	15x8	6.60	5.47	1.0000	0.0021	0.9997	0.0020	0.9952	0.0009	207.373	0.115896	0.298 cm 304L plates with 1.05 wt% B
c011b.out	15x8	7.90	6.77	1.0000	0.0021	0.9997	0.0020	0.9964	0.0008	207.507	0.114703	0.298 cm 304L plates with 1.62 wt% B
c012b.out	15x8	5.76	4.63	1.0000	0.0021	0.9997	0.0020	0.9938	0.0009	207.364	0.116224	0.298 cm 304L plates with 1.62 wt% B
c013b.out	15x8	9.65	8.52	1.0000	0.0021	0.9997	0.0020	0.9953	0.0008	207.495	0.114944	0.485 cm, SS 304L plates
c013x.out	15x8	9.65	8.52	1.0000	0.0021	0.9997	0.0020	1.0002	0.0009	208.270	0.107272	0.485 cm, SS 304L plates
c014b.out	15x8	8.58	7.45	1.0000	0.0021	0.9997	0.0020	0.9942	0.0009	207.484	0.115038	0.485 cm, SS 304L plates
c014x.out	15x8	8.580	7.45	1.0000	0.0021	0.9997	0.0020	1.0018	0.0008	208.211	0.107849	0.485 cm, SS 304L plates
c029b.out	15x8	10.90	9.77	1.0000	0.0021	0.9997	0.0020	0.9942	0.0008	207.549	0.114428	0.652 cm, Zircaloy-4 plates
c030b.out	15x8	10.86	9.73	1.0000	0.0021	0.9997	0.0020	0.9946	0.0008	207.508	0.114783	0.652 cm, Zircaloy-4 plates
c031b.out	15x8	7.672	6.55	1.0000	0.0021	0.9997	0.0020	0.9951	0.0008	207.387	0.115885	0.723 cm, Boral plates, 28.7 wt% B

- From Reference 1. The 'rod surface-to-rod' surface spacing is reported in Reference 1. Reference 2 (p. 9) provides the cell-to-cell spacing for selected experiments from Reference 1 as: (rod-rod) – (pitch) + (rod diameter). This formula was applied to all above values even though some 'rod-rod' may be 'array plate-to-plate'.
- Values from Reference 3, Table 6, p. 42. Source of  $\sigma$  values is not listed in this reference.
- Values from Reference 2, p. 23 based upon calculational uncertainties in parameters and assumptions in the benchmark models of the reference. Note that Reference 2 only includes 4 of the cases from Reference 1 listed above. Here it is assumed that the values listed above apply to all cases.
- From Reference 3, Table 9, p. 61 for 44 group cross-sections. Table 7 in this reference has values for 238 group cross-sections.
- From Reference 3, Table 6. The 'x' before '.out' means the case is a cell weighted model.

### 6.11.10.1.2 Urania Gadolinia Experiments

#### References:

4. FANP Doc: 32-5012895-00, "Validation Report – SCALEPC-44A Urania-Gadolinia Experiments," R.S. Harding.
5. "Urania Gadolinia: Nuclear Model Development and Critical Experiment Benchmark," L.W. Newman, Babcock & Wilcox for DOE, DOE/ET/34212-41, BAW-1910, April 1984.
6. "Development and Demonstration of An Advanced Extended-Burnup Fuel Assembly Design Incorporating Urania-Gadolinia," L.W. Newman, Babcock & Wilcox for DOE, DOE/ET/34212-41, BAW-1681-2, August 1982.

Reference 4 uses the experimental data from References 5 and 6 to construct benchmark cases for SCALE 4.4a. Table 6-47 summarizes the experimental configuration data that form the basis for the KENO V.a models. Table 6-49 provides trending parameters for this set of experiments. Table 6-48 lists the basis for the H/U values tabulated in Table 6-49. Table 6-50 provides the experimental and calculated results for the 44 and 238 group SCALE 4.4a cross-section sets from Reference 3.

**Table 6-47 Urania Gadolinia Experiment Summary<sup>a</sup>**

Parameter	Rod 1	Rod 2	Rod 3
U-235 wt%	4.02	2.459	1.944
Gadolinia Wt%	-	-	4
Pellet density <sup>b</sup> , g/cm <sup>3</sup>	9.46	10.218	10.328
Pellet OD, cm	1.1265	1.03	1.0296
Rod OD, cm	1.1265	1.044	1.0439
Rod OD, cm	1.2078	1.206	1.2065
Rod Pitch, cm	1.6358	1.6358	1.6358
Clad Material	SS	Al	Al
V <sub>fuel/cell</sub>	0.996654	0.833229	0.832582
V <sub>H2O/cell</sub>	1.530044	1.533399	1.532452
Water boron factor <sup>c</sup>	0.99928		
Temperature <sup>d</sup> , °C	22		
Water density, g/cm <sup>3</sup>	0.99777		

a) From Reference 4.

b) Based upon rod mass and fuel volume in rod.

c) A factor to correct water density from 25 °C to 20 °C. Boron ppm is based upon 25 °C measurements. See Reference 4, p. 9.

d) Not specified explicitly for this set of experiments. This value is inferred from temperature data in Reference 7.



NEDO-33869 Revision 11  
Non-Proprietary Information

**Table 6-48 Experimental Parameters for Calculating U-235 and H Atom Densities**

Case ID	Number of Different Type Rods in each Critical Configuration (Reference 1 Table 1))						Core Volume <sup>a</sup>		Atom Density <sup>a</sup>	
	2.46 wt%	4.02 wt%	1.94 wt% (Gd)	Water	Misc	Core Total	Fuel	Water	U-235	H
core01.out	4808	-	-	153	-	4961	4006.16	7765.83	5.67711E-04	0.066676
core03.out	4788	-	-	137	16	4941	3989.50	7692.42	5.67711E-04	0.066676
core05.out	4780	-	28	153	-	4961	4006.15	7765.90	5.67061E-04	0.066676
core5a.out	4776	-	32	153	-	4961	4006.14	7765.91	5.66968E-04	0.066676
core5b.out	4780	-	28	153	-	4961	4006.15	7765.90	5.67061E-04	0.066676
core08.out	4772	-	36	153	-	4961	4006.14	7765.92	5.66875E-04	0.066676
core10.out	4772	-	36	137	16	4961	4006.14	7723.11	5.66875E-04	0.066676
core12a.out	3920	888	-	153	-	4961	4151.29	7768.81	6.21492E-04	0.066676
core14.out	3920	860	28	153	-	4961	4146.69	7768.79	6.19146E-04	0.066676
core16.out	3920	852	36	153	-	4961	4145.38	7768.78	6.18475E-04	0.066676
core18.out	3676	944	-	180	-	4800	4003.79	7553.60	6.27210E-04	0.066676
core19.out	3676	928	16	180	-	4800	4001.17	7553.58	6.25815E-04	0.066676
core20.out	3676	912	32	180	-	4800	3998.54	7553.57	6.24420E-04	0.066676

a) Calculated values. Atom densities based upon Avogadro's number of 0.6022142E-24

NEDO-33869 Revision 11  
Non-Proprietary Information

**Table 6-49 Urania Gadolinia Critical Experiment Trending Data**

Case Name	Clad <sup>a</sup>	Lattice <sup>a</sup>	wt% 235 <sup>a</sup>	Boron, ppm <sup>a</sup>	Vh2o/Vfuel <sup>b</sup>	H/U <sup>b</sup>	k <sub>eff</sub> <sup>c</sup>	Sigma <sup>c</sup>	Rod Configurations <sup>a</sup>
core01.out	Al	15x15	2.46	1337.9	1.9385	227.67	1.0002	0.0005	0
core03.out	Al	15x15	2.46/1.94	1239.3	1.9282	226.46	1.0000	0.0006	20-4%Gd
core05.out	Al	15x15	2.46/1.94	1208.0	1.9385	227.93	0.9999	0.0006	28-4%Gd
core5a.out	Al	15x15	2.46/1.94	1191.3	1.9385	227.97	0.9999	0.0006	32-4%Gd
core5b.out	Al	15x15	2.46/1.94	1207.1	1.9385	227.93	0.9999	0.0006	28-4%Gd
core08.out	Al	15x15	2.46/1.94	1170.7	1.9385	228.01	1.0083	0.0012	36-4%Gd
core10.out	Al	15x15	2.46/1.94	1177.1	1.9278	226.75	1.0001	0.0009	36-4%Gd+3 void rods
core12a.out	SS/Al	15x15	4.02/2.46	1899.3	1.8714	200.77	1.0000	0.0007	4.02 inner/2.456 outer
core14.out	SS/Al	15x15	4.02/2.46/1.94	1653.8	1.8735	201.76	1.0030	0.0009	28-4%Gd
core16.out	SS/Al	15x15	4.02/2.46/1.94	1579.4	1.8741	202.04	1.0001	0.0010	36-4%Gd
core18.out	SS/Al	16x16	4.02/2.46	1776.8	1.8866	200.56	1.0002	0.0011	Combustion Engineering design with Large Guide Tubes
core19.out	SS/Al	16x16	4.02/2.46/1.94	1628.3	1.8878	201.14	1.0002	0.0010	16-4%Gd
core20.out	SS/Al	16x16	4.02/2.46/1.94	1499.0	1.8891	201.72	1.0002	0.0010	Zone + 32-4%

a) Reference 4.

b) Calculated values from Table 5 of Reference 4.

c) Reference 3, Table 6. The source of these values is not documented in the reference.

NEDO-33869 Revision 11  
Non-Proprietary Information

**Table 6-50 Urania Gadolinia Benchmark  $k_{eff}$  Data**

Case ID	Experimental $k_{eff}$ and $\sigma$		SCALE 4.4a 44 Group Cross-Section Calculated $k_{eff}$ and $\sigma$				SCALE 4.4a 238 Group Cross-Section Calculated $k_{eff}$ and $\sigma$			
	$k_{eff}^a$	$\sigma^a$	$k_{eff}^b$	$\sigma^b$	AFG <sup>b</sup>	EALF <sup>b</sup> (ev)	$k_{eff}^b$	$\sigma^b$	AFG <sup>b</sup>	EALF <sup>b</sup> (ev)
core01.out	1.0002	0.0005	0.9955	0.0006	33.8930	0.2530	0.9952	0.0007	197.6190	0.2567
core03.out	1.0000	0.0006	0.9963	0.0006	33.9190	0.2499	0.9943	0.0006	197.6810	0.2547
core05.out	0.9999	0.0006	0.9968	0.0006	33.9280	0.2493	0.9935	0.0006	197.6840	0.2543
core5a.out	0.9999	0.0006	0.9963	0.0005	33.9270	0.2494	0.9940	0.0006	197.6850	0.2547
core5b.out	0.9999	0.0006	0.9959	0.0006	33.9160	0.2504	0.9941	0.0007	197.6280	0.2558
core08.out	1.0083	0.0012	0.9958	0.0006	33.9200	0.2503	0.9928	0.0005	197.7470	0.2534
core10.out	1.0001	0.0009	0.9956	0.0006	33.9130	0.2512	0.9922	0.0007	197.6080	0.2562
core12a.out	1.0000	0.0007	0.9982	0.0006	32.8910	0.3644	0.9950	0.0006	193.1960	0.3697
core14.out	1.0030	0.0009	0.9976	0.0007	33.0670	0.3421	0.9942	0.0007	193.8910	0.3488
core16.out	1.0001	0.0010	0.9969	0.0007	33.1010	0.3376	0.9941	0.0007	194.1570	0.3412
core18.out	1.0002	0.0011	0.9975	0.0007	32.8960	0.3645	0.9950	0.0007	193.2390	0.3684
core19.out	1.0002	0.0010	0.9973	0.0006	33.0140	0.3489	0.9941	0.0007	193.6610	0.3553
core20.out	1.0002	0.0010	0.9969	0.0007	33.1050	0.3382	0.9950	0.0006	194.0850	0.3425

a) Values from Reference 3, Table 6, p. 42. Source of  $\sigma$  values is not documented in this reference.

b) From Reference 3, Table 9, p. 61 for 44 group cross-sections. Table 7 in this reference has values for 238 group cross-sections.

### 6.11.10.1.3 Critical Experiments Supporting Close Proximity Water Storage of Power Reactor Fuel

#### References:

7. FANP Doc. 32-5012896-00, "Validation Report – SCALEPC-44A Close Proximity Experiments," R.S. Harding.
8. "Critical Experiments Supporting Close Proximity Water Storage of Power Reactor Fuel," M.N. Baldwin, et al., BAW-1484-7, July 1979.

Reference 7 uses the experimental data from Reference 8 to construct benchmark cases for SCALE 4.4a. Table 6-51 summarizes the experimental configuration data that form the basis for the KENO V.a models. Table 6-52 provides trending parameters for this set of experiments. Table 6-53 provides the experimental and calculated results for the 44 and 238 group SCALE 4.4a cross-section sets from Reference 3.

**Table 6-51 Close Proximity Experiment Summary<sup>a</sup>**

U-235 wt%	2.459	Fuel Lattice	14x14
Pellet Density <sup>b</sup> , g/cm <sup>3</sup>	10.218	Clad Material	Al
Pellet OD, cm	1.030	V <sub>fuel</sub> /cell	0.8332
Rod OD, cm	1.044	V <sub>h2o</sub> /cell	1.5342
Rod OD, cm	1.206	V <sub>h2o</sub> /V <sub>f</sub>	1.8413
Rod Pitch, cm	1.636		

a) From Reference 7.

b) Based upon rod mass and fuel volume in rod.

**Table 6-52 Close Proximity Experiment Trending Data**

Case ID	Cluster Spacing <sup>a</sup> , cm	Temp <sup>a</sup> , °C	Boron <sup>a</sup> , ppm	Boron Factors <sup>b</sup>	Water density <sup>b</sup> , g/cm <sup>3</sup>	Atom Density <sup>c</sup>		H/U <sup>c</sup>	Absorbers <sup>a</sup>
						U-235	H		
ac1p1.out	--	21	0	0.999788	0.99799	5.6991E-04	0.066725	215.57	--
ac1p2.out	0.000	18.5	1037	1.000298	0.99850	5.6991E-04	0.066793	215.79	--
ac1p3.out	1.636	18	764	1.000392	0.99860	5.6991E-04	0.066806	215.83	H2O
ac1p4.out	1.636	17	0	1.000572	0.99878	5.6991E-04	0.066830	215.91	84 B4C pins/H2O
ac1p5.out	3.272	17.5	0	1.000483	0.99869	5.6991E-04	0.066818	215.87	64 B4C pins/H2O
ac1p6.out	3.272	17.5	0	1.000483	0.99869	5.6991E-04	0.066818	215.87	64 B4C pins/H2O
ac1p7.out	4.908	17.5	0	1.000483	0.99869	5.6991E-04	0.066818	215.87	34 B4C pins/H2O
ac1p8.out	4.908	17.5	0	1.000483	0.99869	5.6991E-04	0.066818	215.87	34 B4C pins/H2O
ac1p9.out	6.544	17.5	0	1.000483	0.99869	5.6991E-04	0.066818	215.87	H2O
ac1p10.out	6.544	24.5	143	0.998967	0.99718	5.6991E-04	0.066616	215.22	H2O
ac1p11a.out	1.636	25.5	510	0.999712	0.99692	5.6991E-04	0.066648	215.32	0.462 cm, SS 304/H2O
ac1p11b.out	1.636	26	514	0.998578	0.99992	5.6991E-04	0.066773	215.73	0.462 cm, SS 304/H2O
ac1p11c.out	1.636	25.5	501	0.999712	0.99692	5.6991E-04	0.066648	215.32	0.462 cm, SS 304/H2O
ac1p11d.out	1.636	25.5	493	0.998840	0.99692	5.6991E-04	0.066590	215.14	0.462 cm, SS 304/H2O
ac1p11e.out	1.636	25	474	0.999712	0.99404	5.6991E-04	0.066456	214.70	0.462 cm, SS 304/H2O
ac1p11f.out	1.636	25	462	0.998840	0.99404	5.6991E-04	0.066398	214.52	0.462 cm, SS 304/H2O
ac1p11g.out	1.636	25.5	432	0.999712	0.99992	5.6991E-04	0.066849	215.97	0.462 cm, SS 304/H2O
ac1p12.out	3.272	26	217	0.998578	0.99679	5.6991E-04	0.066564	215.05	0.462 cm, SS 304/H2O
ac1p13.out	1.636	20	15	1.000000	0.99821	5.6991E-04	0.066754	215.67	0.645 cm, BAl 1.614 wt% B/H2O
ac1p13a.out	1.636	17	28	1.000572	0.99878	5.6991E-04	0.066830	215.91	0.645 cm, BAl 1.614 wt% B/H2O
ac1p14.out	1.636	18	92	1.000392	0.99860	5.6991E-04	0.066806	215.83	0.645 cm, BAl 1.614 wt% B/H2O
ac1p15.out	1.636	18	395	1.000392	0.99860	5.6991E-04	0.066806	215.83	0.645 cm, BAl 1.614 wt% B/H2O
ac1p16.out	3.272	17.5	121	1.000483	0.99878	5.6991E-04	0.066824	215.89	0.645 cm, BAl 1.614 wt% B/H2O
ac1p17.out	1.636	17.5	487	1.000483	0.99878	5.6991E-04	0.066824	215.89	0.645 cm, BAl 1.614 wt% B/H2O
ac1p18.out	3.272	18	197	1.000392	0.99860	5.6991E-04	0.066806	215.83	0.645 cm, BAl 1.614 wt% B/H2O
ac1p19.out	1.636	17.5	634	1.000483	0.99878	5.6991E-04	0.066824	215.89	0.645 cm, BAl 1.614 wt% B/H2O
ac1p20.out	3.272	17.5	320	1.000483	0.99878	5.6991E-04	0.066824	215.89	0.645 cm, BAl 1.614 wt% B/H2O
ac1p21.out	6.544	16.5	72	1.000740	0.99992	5.6991E-04	0.066918	216.19	0.645 cm, BAl 1.614 wt% B/H2O

a) Reference 8.

b) Boron factors to correct water density from 25°C to 20°C. Boron ppm is based upon 25°C measurements. See Reference 7, Table 3.0-1, p. 46. Water density from standard tables.

c) Calculated values based upon Avogadro's number of 0.6022142E-24

NEDO-33869 Revision 11  
Non-Proprietary Information

**Table 6-53 Close Proximity Experiment  $k_{eff}$  Data**

Case ID	Experimental $k_{eff}$ and $\sigma$		SCALE 4.4a 44 Group Cross-Section Calculated $k_{eff}$ and $\sigma$				SCALE 4.4a 238 Group Cross-Section Calculated $k_{eff}$ and $\sigma$			
	$k_{eff}^a$	$\sigma^a$	$k_{eff}^b$	$\sigma^b$	AFG <sup>b</sup>	EALF <sup>b</sup> (ev)	$k_{eff}^b$	$\sigma^b$	AFG <sup>b</sup>	EALF <sup>b</sup> (ev)
acp1.out	1.0002	0.0005	0.9931	0.0008	34.8710	0.1712	0.9889	0.0009	201.9510	0.1761
acp2.out	1.0001	0.0005	0.9956	0.0008	33.9420	0.2484	0.9939	0.0008	197.6580	0.2540
acp3.out	1.0000	0.0006	0.9963	0.0006	34.5210	0.1960	0.9934	0.0007	200.5280	0.2002
acp4.out	0.9999	0.0006	0.9897	0.0008	34.6110	0.1910	0.9875	0.0008	200.7350	0.1946
acp5.out	1.0000	0.0007	0.9883	0.0008	34.9500	0.1662	0.9873	0.0008	202.4670	0.1689
acp6.out	1.0097	0.0012	0.9884	0.0007	34.8840	0.1716	0.9872	0.0007	201.9760	0.1760
acp7.out	0.9998	0.0009	0.9900	0.0007	35.2100	0.1496	0.9867	0.0008	203.6900	0.1527
acp8.out	1.0083	0.0012	0.9906	0.0008	35.1720	0.1526	0.9874	0.0007	203.3420	0.1573
acp9.out	1.0030	0.0009	0.9906	0.0006	35.3620	0.1411	0.9879	0.0007	204.4120	0.1438
acp10.out	1.0001	0.0009	0.9913	0.0007	35.2090	0.1494	0.9883	0.0008	203.7410	0.1528
acp11a.out	1.0000	0.0006	0.9955	0.0007	34.4600	0.2001	0.9919	0.0006	200.2820	0.2046
acp11b.out	1.0007	0.0007	0.9942	0.0007	34.4640	0.1997	0.9916	0.0009	200.2900	0.2043
acp11c.out	1.0007	0.0006	0.9943	0.0008	34.4550	0.2007	0.9915	0.0008	200.1800	0.2060
acp11d.out	1.0007	0.0006	0.9939	0.0006	34.4290	0.2035	0.9920	0.0009	200.1670	0.2063
acp11e.out	1.0007	0.0006	0.9952	0.0007	34.4350	0.2030	0.9918	0.0006	200.0830	0.2078
acp11f.out	1.0007	0.0006	0.9947	0.0008	34.4360	0.2033	0.9916	0.0006	200.0020	0.2089
acp11g.out	1.0007	0.0006	0.9941	0.0007	34.4200	0.2054	0.9908	0.0007	199.9760	0.2096
acp12.out	1.0000	0.0007	0.9911	0.0007	34.8740	0.1702	0.9889	0.0008	202.2960	0.1727
acp13.out	1.0000	0.0010	0.9922	0.0007	34.5220	0.1963	0.9906	0.0009	200.3490	0.2013
acp13a.out	1.0000	0.0010	0.9901	0.0008	34.5020	0.1979	0.9884	0.0007	200.2550	0.2031
acp14.out	1.0001	0.0010	0.9905	0.0007	34.4720	0.2005	0.9891	0.0009	200.1840	0.2045
acp15.out	0.9998	0.0016	0.9881	0.0008	34.4020	0.2057	0.9823	0.0007	199.8980	0.2102
acp16.out	1.0001	0.0006	0.9860	0.0007	34.8250	0.1737	0.9841	0.0007	202.0010	0.1769
acp17.out	1.0007	0.0019	0.9897	0.0007	34.3970	0.2061	0.9874	0.0007	199.9490	0.2097
acp18.out	1.0002	0.0011	0.9869	0.0007	34.8410	0.1728	0.9859	0.0008	202.0310	0.1759
acp19.out	1.0002	0.0010	0.9910	0.0007	34.4010	0.2052	0.9888	0.0006	199.9530	0.2096
acp20.out	1.0003	0.0011	0.9889	0.0006	34.8410	0.1726	0.9869	0.0008	202.0440	0.1758
acp21.out	0.9997	0.0013	0.9868	0.0008	35.1290	0.1544	0.9854	0.0007	203.3850	0.1570

a) Values from Reference 3, Table 6, p. 42. Generally obtained from Tables 8 and 9 of Reference 8; acp11 series of values not documented in Reference 3.

b) From Reference 3, Table 9, p. 61 for 44 group cross-sections. Table 7 in this reference has values for 238 group cross-sections.

#### 6.11.10.1.4 Critical Experiments Supporting Underwater Storage of Tightly Packed Configurations of Spent Fuel Pins

References:

9. FANP Doc. 32-5012897-00, "Validation Report – SCALEPC-44A Consolidation Experiments," R.S. Harding
10. "Critical Experiments Supporting Underwater Storage of Tightly Packed Configurations of Spent Fuel Pins," G.S. Hoovler, et al., BAW-1645-4, November, 1981.

Reference 9 uses the experimental data from Reference 10 to construct benchmark cases for SCALE 4.4a. Table 6-54 summarizes the experimental configuration data that form the basis for the KENO V.a models. Table 6-55 provides trending parameters for this set of experiments. Table 6-56 provides the experimental and calculated results for the 44 and 238 group SCALE 4.4a cross-section sets from Reference 3.

**Table 6-54 Tightly Packed Configuration Experiment Summary<sup>a</sup>**

U-235 wt%	2.459	Fuel Volume, cm <sup>3</sup>	0.833229
Pellet Density <sup>b</sup> , g/cm <sup>3</sup>	10.233	Pitch, cm	Vh20/Ffuel
U-235 atom density <sup>c</sup>	5.7075E-04	1.2093	0.149022
Pellet OD, cm	1.0300	1.2090	0.383292
Rod OD, cm	1.0440	1.4097	1.014058
Rod OD, cm	1.2060		
Clad Material	Al		

a) From Reference 9.

b) Based upon rod mass and fuel volume in rod, note this is the same 2.459 wt% fuel used in the previous 2 benchmark cases. The difference in densities has not been discussed.

c) Calculated values based upon Avogadro's number of 0.6022142E-24.

NEDO-33869 Revision 11  
Non-Proprietary Information

**Table 6-55    Tightly Packed Configuration Experiment Trending Data**

Case ID	Rod Pitch <sup>a</sup> , cm	Lattice <sup>a</sup>	Cluster Spacing <sup>a</sup> , cm	Temp <sup>a</sup> , °C	Boron <sup>a</sup> , ppm	Boron Factor <sup>b</sup>	Water density <sup>b</sup>	V <sub>h2o</sub> /V <sub>fuel</sub> <sup>c</sup>	H atom density <sub>1</sub> <sup>c</sup>	H/U <sub>1</sub> <sup>c</sup>
rcon01.out	1.2093	15x17 tria <sup>d</sup>	1.778x1.945	22.5	435	0.999451	0.99767	0.1490	0.066681	17.41
rcon02.out	1.2093	15x17 tria	1.778x1.945	23.5	426	0.999214	0.99742	0.1490	0.066648	17.40
rcon03.out	1.2093	15x17 tria	1.778x1.945	24.0	406	0.999091	0.99730	0.1490	0.066632	17.40
rcon04.out	1.2093	15x17 tria	1.778x1.945	22.5	383	0.999451	0.99767	0.1490	0.066681	17.41
rcon05.out	1.2093	15x17 tria	1.778x1.945	23.0	354	0.999334	0.99754	0.1490	0.066665	17.41
rcon06.out	1.2093	15x17 tria	1.778x1.945	23.0	335	0.999334	0.99754	0.1490	0.066665	17.41
rcon07.out	1.2093	15x17 tria	2.539x2.709	20.0	361	1.000000	0.99821	0.1490	0.066754	17.43
rcon09.out	1.2090	15x15 sq	1.7780	21.0	886	0.999788	0.99799	0.3833	0.066725	44.81
rcon10.out	1.2090	15x15 sq	1.7780	21.0	871	0.999788	0.99799	0.3833	0.066725	44.81
rcon11.out	1.2090	15x15 sq	1.7780	22.0	852	0.999566	0.99777	0.3833	0.066695	44.79
rcon12.out	1.2090	15x15 sq	1.7780	21.0	834	0.999788	0.99799	0.3833	0.066725	44.81
rcon13.out	1.2090	15x15 sq	1.7780	21.0	815	0.999788	0.99799	0.3833	0.066725	44.81
rcon14.out	1.2090	15x15 sq	1.7780	22.0	781	0.999566	0.99777	0.3833	0.066695	44.79
rcon15.out	1.2090	15x15 sq	1.7780	22.0	746	0.999566	0.99777	0.3833	0.066695	44.79
rcon16.out	1.4097	13x13 sq	1.7920	22.5	1156	0.999451	0.99767	1.0141	0.066681	118.47
rcon17.out	1.4097	13x13 sq	1.7920	22.5	1141	0.999451	0.99767	1.0141	0.066681	118.47
rcon18.out	1.4097	13x13 sq	1.7920	23.0	1123	0.999334	0.99754	1.0141	0.066665	118.44
rcon19.out	1.4097	13x13 sq	1.7920	23.0	1107	0.999334	0.99754	1.0141	0.066665	118.44
rcon20.out	1.4097	13x13 sq	1.7920	23.0	1093	0.999334	0.99754	1.0141	0.066665	118.44
rcon21.out	1.4097	13x13 sq	1.7920	23.0	1068	0.999334	0.99754	1.0141	0.066665	118.44
rcon28.out	1.4097	15x17 tria	3.807x2.976	18.5	121	1.000298	0.99850	1.0141	0.066793	17.44

- a) Reference 9.
- b) Boron factors to correct water density from 25°C to 20°C. Boron ppm is based upon 25 °C measurements. See Reference 10, Table 3.0-1, p. 46. Water density from standard tables.
- c) Calculated values based upon Avogadro's number of 0.6022142E-24.
- d) Triangular pitch for array.



NEDO-33869 Revision 11  
Non-Proprietary Information

**Table 6-56    Tightly Packed Configuration Experiment  $k_{eff}$  Data**

Case ID	Experimental $k_{eff}$ and $\sigma$		SCALE 4.4a 44 Group Cross-Section Calculated $k_{eff}$ and $\sigma$				SCALE 4.4a 238 Group Cross-Section Calculated $k_{eff}$ and $\sigma$			
	$k_{eff}^a$	$\sigma^a$	$k_{eff}^b$	$\sigma^b$	AFG <sup>b</sup>	EALF <sup>b</sup> (ev)	$k_{eff}^b$	$\sigma^b$	AFG <sup>b</sup>	EALF <sup>b</sup> (ev)
rcon01.out	1.0007	0.0006	0.9999	0.0008	28.9400	2.4011	0.9910	0.0007	170.1330	2.4368
rcon02.out	1.0007	0.0006	1.0009	0.0007	28.9020	2.4444	0.9909	0.0008	169.9770	2.4688
rcon03.out	1.0007	0.0006	0.9973	0.0008	28.8680	2.4872	0.9882	0.0007	169.6020	2.5454
rcon04.out	1.0007	0.0006	1.0008	0.0007	28.8990	2.4644	0.9899	0.0007	169.6960	2.5284
rcon05.out	1.0007	0.0006	0.9995	0.0008	28.8970	2.4706	0.9899	0.0008	169.6200	2.5435
rcon06.out	1.0007	0.0006	0.9980	0.0007	28.8900	2.4915	0.9906	0.0008	169.5520	2.5553
rcon07.out	1.0007	0.0006	0.9982	0.0008	29.8910	1.6259	0.9904	0.0008	175.2760	1.6431
rcon09.out	1.0007	0.0006	0.9977	0.0006	29.8930	1.4607	1.0092	0.0007	180.0400	1.1271
rcon10.out	1.0007	0.0006	0.9966	0.0008	29.8760	1.4759	0.9884	0.0006	176.1470	1.4891
rcon11.out	1.0007	0.0006	0.9959	0.0007	29.8450	1.4982	0.9909	0.0008	176.1150	1.4922
rcon12.out	1.0007	0.0006	0.9980	0.0008	29.8490	1.4979	0.9876	0.0007	175.8550	1.5240
rcon13.out	1.0007	0.0006	0.9969	0.0007	29.8430	1.5074	0.9897	0.0007	175.8220	1.5280
rcon14.out	1.0007	0.0006	0.9963	0.0007	29.8310	1.5207	0.9894	0.0007	175.7230	1.5402
rcon15.out	1.0007	0.0006	0.9975	0.0008	29.8450	1.5180	0.9915	0.0007	175.7200	1.5399
rcon16.out	1.0007	0.0006	0.9948	0.0007	32.7100	0.4216	0.9892	0.0007	175.7140	1.5415
rcon17.out	1.0007	0.0006	0.9952	0.0006	32.6820	0.4276	0.9894	0.0006	191.3680	0.4309
rcon18.out	1.0007	0.0006	0.9939	0.0006	32.6400	0.4370	0.9909	0.0007	191.2180	0.4360
rcon19.out	1.0007	0.0006	0.9965	0.0006	32.6540	0.4344	0.9897	0.0007	191.0430	0.4426
rcon20.out	1.0007	0.0006	0.9967	0.0007	32.6370	0.4391	0.9915	0.0007	190.9880	0.4447
rcon21.out	1.0007	0.0006	0.9959	0.0008	32.6220	0.4427	0.9903	0.0007	190.8780	0.4485
rcon28.out	1.0007	0.0006	0.9968	0.0008	31.0790	1.0062	0.9915	0.0008	190.7670	0.4529

a) Values from Reference 3, Table 6, p. 42. Source of value not documented in this reference.

b) From Reference 3, Table 9, p. 61 for 44 group cross-sections. Table 7 in this reference has values for 238 group cross-sections

#### 6.11.10.1.5 Reduced Density Moderation Between Fuel Clusters with 4.738 Wt% Fuel

##### References:

11. FANP Doc. 32-5012894-00, "Validation Report – SCALEPC-44A Dissolution Experiments," R.S. Harding.
12. "Dissolution and Storage Experimental Program with U[4.75]O<sub>2</sub> Rods," Transactions of the American Nuclear Society, Vol. 33, pg. 362.

Reference 11 uses the experimental data from Reference 12 to construct benchmark cases for SCALE 4.4a. Table 6-57 summarizes the experimental configuration data that form the basis for the KENO V.a models and provides trending parameters that are constant for the series of experiments. Table 6-58 provides trending parameters for this set of experiments. It also provides the experimental and calculated results for the 44 and 238 group SCALE 4.4a cross-section sets from Reference 3.

**Table 6-57     Reduced Density Moderation Experiments Summary and Trending Parameters<sup>a</sup>**

U-235 wt%	4.738	Temperature, °C	22
Pellet Density, g/cm <sup>3</sup>	10.38	Water density, g/cm <sup>3</sup>	0.99777
Pellet OD, cm	0.7900	Fuel Volume, cm <sup>3</sup>	0.49017
Rod OD, cm	0.8200	Water Volume, cm <sup>3</sup>	1.12852
Rod OD, cm	0.9400	V <sub>h2o</sub> /V <sub>fuel</sub>	2.30232
Rod Pitch, cm	1.3500	U-235 atom density <sup>b</sup>	1.1155E-03
Clad Material	Al alloy	H atom density <sup>b</sup>	0.066676
Lattice	18x18	H/U	1.3761E+02

a) From Reference 11.

b) Calculated values based upon Avogadro's number of 0.6022142E-24.

**Table 6-58 Reduced Density Moderation Experiments Trending Data and  $k_{eff}$  Data**

Case ID	Cluster Spacing <sup>a</sup> , cm	Spacing Material <sup>a</sup> [Material (density, g/cm <sup>3</sup> )]	Experimental $k_{eff}$ and $\sigma$		SCALE 4.4a 44 Group Cross-Section Calculated $k_{eff}$ and $\sigma$				SCALE 4.4a 238 Group Cross-Section Calculated $k_{eff}$ and $\sigma$			
			$k_{eff}^b$	$\sigma^b$	$k_{eff}^c$	$\sigma^c$	AFG <sup>c</sup>	EALF <sup>c</sup> (ev)	$k_{eff}^c$	$\sigma^c$	AFG <sup>c</sup>	EALF <sup>c</sup> (ev)
mdis01.out	0.0	-	1.0000	0.0014	0.9914	0.0008	33.5390	0.2824	0.9885	0.0010	195.994	0.2879
mdis02.out	2.5	H2O	1.0000	0.0014	0.9871	0.0009	33.6720	0.2644	0.9862	0.0008	196.836	0.2685
mdis03.out	2.5	Air/Box	1.0000	0.0014	0.9841	0.0011	33.6720	0.2647	0.9805	0.0008	196.750	0.2702
mdis04.out	2.5	Polysty(0.0323)/Box	1.0000	0.0014	0.9902	0.0008	33.8040	0.2514	0.9884	0.0008	197.439	0.2559
mdis05.out	2.5	Polyeth(0.2879)/Box	1.0000	0.0014	0.9908	0.0010	33.9160	0.2407	0.9891	0.0009	198.001	0.2442
mdis06.out	2.5	Polyeth(0.5540)/Box	1.0000	0.0014	1.0008	0.0010	34.0370	0.2295	0.9963	0.0008	198.539	0.2344
mdis07.out	2.5	H2O/Box	1.0000	0.0014	0.9917	0.0009	34.1100	0.2242	0.9886	0.0008	198.827	0.2288
mdis08.out	5.0	H2O	1.0000	0.0014	0.9873	0.0010	33.8000	0.2497	0.9840	0.0009	197.504	0.2545
mdis09.out	5.0	Air/Box	1.0000	0.0014	0.9869	0.0010	33.8110	0.2485	0.9861	0.0009	197.586	0.2524
mdis10.out	5.0	Polysty(0.0262)/Box	1.0000	0.0014	0.9938	0.0008	34.0940	0.2225	0.9912	0.0008	198.934	0.2267
mdis11.out	5.0	Polyeth(0.3335)/Box	1.0000	0.0014	1.0031	0.0010	34.3010	0.2048	0.9997	0.0008	200.018	0.2076
mdis12.out	5.0	Polyeth(0.5796)/Box	1.0000	0.0014	-	-	-	-	1.0027	0.0009	200.577	0.1984
mdis13.out	5.0	H2O/Box	1.0000	0.0014	0.9907	0.0008	34.4280	0.1951	0.9878	0.0008	200.547	0.1988
mdis14.out	10.0	H2O	1.0000	0.0014	0.9890	0.0008	33.9850	0.2294	0.9854	0.0009	198.552	0.2333
mdis15.out	10.0	Air/Box	1.0000	0.0014	0.9894	0.0009	34.0150	0.2266	0.9842	0.0008	198.647	0.2315
mdis16.out	10.0	Polysty(0.0288)/Box	1.0000	0.0014	1.0013	0.0008	34.4450	0.1907	0.9970	0.0009	200.792	0.1948
mdis17.out	10.0	Polyeth(0.3216)/Box	1.0000	0.0014	0.9985	0.0008	34.5970	0.1788	0.9951	0.0009	201.537	0.1831
mdis18.out	10.0	Polyeth(0.568)/Box	1.0000	0.0014	0.9965	0.0008	34.6430	0.1740	0.9923	0.0009	201.894	0.1774
mdis19.out	10.0	H2O/Box	1.0000	0.0014	0.9931	0.0009	34.6530	0.1737	0.9888	0.0008	201.908	0.1772

a) References 11 and 12.

b) Values from Reference 3, Table 6, p. 42. Source of value not documented in this reference.

c) From Reference 3, Table 9, p. 61 for 44 group cross-sections. Table 7 in this reference has values for 238 group cross-sections.

## 6.12 References

- 6-1. GE Energy Nuclear, "Criticality Safety Analysis – Shipment of Loose Rods in RAJ-II Shipping Container," Revision 1, November 2007.
- 6-2. Davis, J. K., "RAJ-II Shipping Container Test," Document Identifier 51-5032941-00, September 10, 2003.
- 6-3. Letter, Scott P. Murray (GNF) to Document Control Desk (NRC), "GNF-A Request for Letter Authorization to Use the RAJ-II Package," SPM 14-030, July 30, 2014.
- 6-4. American Society for Testing and Materials, ASTM A 240/A 240M, "Standard Specification for Chromium and Chromium-Nickel Stainless Steel Plate, Sheet, and Strip for Pressure Vessels and for General Applications."
- 6-5. American Society for Testing and Materials, ASTM A 480, "Standard Specification for General Requirements for Flat-Rolled Stainless and Heat-Resisting Steel Plate, Sheet, and Strip."
- 6-6. NRC, "SCALE Standardized Computer Analyses for Licensing Evaluation," NUREG/CR-2000 ORNL/NUREG/CSD-2, Volumes 1, 2, and 3.
- 6-7. NRC, "Critical Separation Between Subcritical Clusters of 4.29 Wt% U-235 Enriched UO<sub>2</sub> Rods in Water With Fixed Neutron Poisons," NUREG/CR-0073(PNL-2695).
- 6-8. Dean, V.F., Evaluator, "Water-Moderated U(4.31)O<sub>2</sub> Fuel Rods in 2.54-cm Square-Pitched Arrays," International Handbook of Evaluated Criticality Safety Benchmark Experiments," NEA/NSC/DOC(95)03, Sept 2001, Nuclear Energy Agency.
- 6-9. Newman, L.W., "Urania Gadolinia: Nuclear Model Development and Critical Experiment Benchmark," Babcock & Wilcox for DOE, DOE/ET/34212-41, BAW-1810, April 1984.
- 6-10. Newman, L.W., "Development and Demonstration of An Advanced Extended-Burnup Fuel Assembly Design Incorporating Urania-Gadolinia," Babcock & Wilcox for DOE, DOE/ET/34212-41, BAW-1681-2, August 1982.
- 6-11. Baldwin, M.N. et al., Critical Experiments Supporting Close Proximity Water Storage of Power Reactor Fuel, BAW-1484-7, July 1979.
- 6-12. Hovler, G.S. et al., Critical Experiments Supporting Underwater Storage of Tightly Packed Configurations of Spent Fuel Pins, BAW-1645-4, November, 1981.
- 6-13. Transactions of the American Nuclear Society, Dissolution and Storage Experimental Program with U[4.75]O<sub>2</sub> Rods, Volume 33, pg. 362.
- 6-14. Harding, R.S., Validation Report – SCALEPC-44A Consolidation Experiments, FANP Doc. 32-5012897-00.
- 6-15. NRC, "Criticality Benchmark Guide for Light-Water-Reactor Fuel in Transportation and Storage Packages," NUREG/CR-6361, ORNL/TM-13211, March 1997.

NEDO-33869 Revision 11  
Non-Proprietary Information

- 6-16. ANSI/ANS, "Nuclear Criticality Safety in Operations with Fissionable Materials Outside Reactors," ANSI/ANS-8.1-1998, September 1998.
- 6-17. GE Hitachi Nuclear Energy, "GEMER Monte Carlo Validation Report: RA-3/RAJ-II Shipping Containers," October 2007.
- 6-18. Scale: A Comprehensive Modeling and Simulation Suite for Nuclear Safety Analysis and Design, ORNL/TM-2005/39, Version 6.1, June 2011. (Available from Radiation Safety Information Computational Center at Oak Ridge National Laboratory as CCC-785).
- 6-19. "International Handbook of Evaluated Criticality Safety Benchmark Experiments," NEA/NSC/DOC(95)03, Nuclear Energy Agency (NEA) and Organisation for Economic Co-operation and Development (OECD), September 2005 Edition.
- 6-20. NRC, "Criticality Benchmark Guide for Light-Water-Reactor Fuel Transportation and Storage Packages," NUREG/CR-6361, ORNL/TM-13211, March 1997.
- 6-21. Parsons, "AVLIS Nuclear Criticality Safety Report, Appendix 3," USEC Atomic Vapor Laser Isotope Separation Project, 1997.
- 6-22. J. Hardy, D. Kline and J.J. Volpe, "A Study of Physics Parameters in Several Water Moderated Lattices of Slightly Enriched Natural Uranium," WAPD-TM-931, Bettis Atomic Power Laboratory, March 1970.
- 6-23. NRC, "Guide for Validation of Nuclear Criticality Safety Calculational Methodology," NUREG/CR-6698, January 2001.

## 7.0 PACKAGE OPERATIONS

This chapter provides general instructions for loading and unloading and operation of the RAJ-II package. Specific detailed procedures based on and consistent with this application are used for the operation of the package. These procedures are maintained by the user of the package and may provide additional detail regarding the handling and operation of the package. Due to the low specific activity and low abundance of gamma emitting radionuclides, dose rates from the contents of the package are minimal. As a result of the low dose rates, there are no special handling requirements for radiation protection.

### 7.1 PACKAGE LOADING

This section delineates the procedures for loading a payload into the RAJ-II packaging. Hereafter, reference to specific RAJ-II packaging drawings may be found in Section 1.3.1.

**Note:** The regulatory references provided, such as 49 CFR and 10 CFR, are the current requirements. If regulatory references change, the new references are applicable. This applies throughout this document.

#### 7.1.1 Preparation for Loading

Prior to loading the RAJ-II with fuel, the packaging is inspected to ensure that it is in unimpaired physical condition. The inspection looks for damage, dents, corrosion, and missing hardware. Acceptable conditions are defined by the drawings in Section 1.3.1 and described in Section 8.1. Acceptance criteria and detailed loading procedures derived from this application are also specified in user written procedures. These user procedures are specific to the authorized content of the package and incorporate the torques provided in Table 7-1.

Because the primary containment is the sealed fuel rod, radiation and contamination surveys are not required prior to loading. There is no required moderator, neutron absorbers or gaskets that require testing or inspection.

Defects that require repair shall be identified and addressed prior to shipping in accordance with approved procedures consistent with a quality program meeting the requirements of 10 CFR 71, Subpart H.

Verification that the primary containment (i.e., fuel rods) has been leak checked shall be performed prior to shipping.

**Table 7-1 Required Packaging Component Torques**

Component	Torque
Inner Container End Lid Bolts	wrench tight or as defined in user procedures
Inner Container Top Lid Bolts	wrench tight or as defined in user procedures
Hold Down Clamp Bolts	wrench tight or as defined in user procedures
Outer Container Top Lid Bolts	wrench tight or as defined in user procedures

#### **7.1.1.1 Outer Container Lid Removal**

1. Remove the lid bolts.
2. Attach slings to the four lid lift attachment points on the lid.
3. Remove the outer lid.

#### **7.1.1.2 Inner Container Removal**

1. Release the inner clamp by removing the eight clamp bolts.
2. Remove the inner container from the outer container and move it onto the packing table. Ensure that the inner container is lifted using the inner container handles and not the inner container lid handles.
3. Remove the bolts of the inner container lid and take the lid off.

#### **7.1.2 Loading of Contents**

##### **7.1.2.1 Loading Fuel Assemblies (With Channel) or Fuel Bundles (Without Channel)**

1. Clamp the inner container body to the packing table or up righting device and remove the end lid.
2. Ensure that the following preparation work for packing has been completed and is in compliance with polyethylene mass limits per Table 6-1, noting the mass of polyethylene cushioning foam for this configuration is not limited.
  - a. The separators have been inserted, as applicable.
  - b. The finger spring protectors have been attached, as applicable.
  - c. The foam has been put in place.
  - d. The fuel assemblies/bundles have been covered with poly bags, as applicable.
3. Stand the packing table upright. (The inner container body is fixed with clamps.)
4. Lift one fuel assembly/bundle and pack it in the inner container.
5. After packing one fuel assembly/bundle into the inner container, fit the securing fixtures of the fuel assembly/bundle. Then pack the other fuel assembly/bundle in the inner container, or recommended dunnage if only one cavity contains fuel. Care should be taken to distribute the payload in a safe manner.
6. Lower the packing table back to the horizontal position from the upright position.
7. Attach the end lid of the inner container, per the torque in Table 7-1.
8. Check to ensure that the fuel assemblies/bundles are packaged in the container properly.
9. Attach the inner container lid and tighten the bolts, per the torque in Table 7-1.
10. Place the inner container into the outer container.
11. Attach hold down clamps and tighten bolts, per the torque in Table 7-1.

12. Place the outer container lid on the package, and tighten the bolts, per the torque in Table 7-1.
13. Install tamper-indicating devices on the outer container ends.

#### **7.1.2.2 Loading Loose Fuel Rods in the Protective Case**

1. Fuel rods shall be loaded into protective case while either in the inner container or while removed from the inner container. All polyethylene packaging components shall be within mass limits per Section 6.1.
  - a. Insert poly endcap spacers over each end of the fuel rod endcap (optional).
  - b. Sleeve each fuel rod to be packed (optional). The ends of the sleeves should be closed in a manner such as knotting or taping with the excess polyethylene trimmed away.
  - c. Insert desired quantity of fuel rods in compliance with requirements in Table 6-2 (criticality requirements), Section 1.2.2.6 (payload mass requirements), and Chapter 4.0 (radioactive material content requirements). Fill any empty space with tubing or dunnage.
  - d. Place cushioning foam pads in protective case as needed to prevent sliding during shipment (optional).
  - e. Close the protective case and tighten bolts, wrench tight or as defined in user procedures.
2. After packing the protective case(s) into the inner container, fit the securing fixtures for the case.
3. Check to ensure that the protective case(s) are packaged in the container properly.
4. Follow Section 7.1.2.1 Steps 9 through 13.
5. It is allowable to ship one or two protective cases in an RAJ-II inner container. However, care should be taken to distribute the payload in a safe manner. When shipping only one case, the opposing cavity should be filled with dunnage, if deemed necessary.

#### **7.1.2.3 Loading Loose Fuel Rods in the Rod Pipe Container**

1. Fuel rods shall be loaded in the rod pipe container while removed from the inner container. All polyethylene packaging materials shall be within mass limits per Section 6.1.
  - a. Sleeve each fuel rod to be packed (optional). The ends of the sleeves should be closed in a manner such as knotting or taping with the excess polyethylene trimmed away.
  - b. Place a cushioning foam pad in the capped end of the rod pipe container (optional).
  - c. Insert desired quantity of fuel rods in compliance with requirements in Table 6-2 (criticality requirements), Section 1.2 (payload mass requirements), and Chapter 4.0 (radioactive material content requirements). Fill any empty space with tubing or dunnage.
  - d. Place cushioning foam pads against the fuel rod ends to block the fuel rods from sliding during shipment (optional).



- e. Close the rod pipe container and tighten bolts, wrench tight or as defined in user procedures. Approved anti-seize compound may be used on bolt threads.
2. Lift each rod pipe container and pack it in the inner container.
3. Check to ensure that the rod pipe container(s) are packaged in the inner container properly.
4. Follow Section 7.1.2.1 Steps 9 through 13.
5. It is allowable to ship one or two rod pipe containers in an RAJ-II inner container. However, care should be taken to distribute the payload in a safe manner. When shipping only one rod pipe container, opposing cavity should be filled with dunnage, as necessary for safe load distribution.

#### **7.1.2.4 Loading Loose or Clamped Fuel Rods**

1. A maximum of 25 fuel rods shall be loaded in each side of the inner container partition, as defined in Table 6-2. All polyethylene packaging materials shall be within mass limits per Section 6.1.
2. Sleeve each fuel rod to be packed (optional). The ends of the sleeves should be closed in a manner such as knotting or taping with the excess polyethylene trimmed away.
3. When only one fuel rod per side is to be packed, no clamps are required. Block the fuel rod in the lower corner of the container by evenly spacing 10 or more notched foam pads the length of the fuel rod.
4. When 2 to 25 fuel rods are to be packed per side of the inner container partition, banding with steel clamps is not required for criticality safety purposes. If fuel rods are banded, each cluster of fuel rods should be gathered with 10 or more clamps spaced evenly along the length of the fuel rods.
5. Place foam pads between the open clamps and the fuel rods.
6. Close and tighten the clamps so the foam surrounds the array of fuel rods. Tighten each clamp until the foam collapses slightly.
7. Place foam pads against the ends of the fuel rods, above the fuel rods and beside the fuel rods to block the fuel rods from moving during shipment.
8. Repeat the above steps for the other side of the inner container, if required.
9. Follow Section 7.1.2.1 Steps 9 through 13.
10. It is allowable to ship fuel rods in either or both sides of the partition in the RAJ-II inner container. However, care should be taken to distribute the payload in a safe manner. When using only one side of the RAJ-II inner container, opposing cavity should be filled with dunnage, if deemed necessary.

#### **7.1.3 Preparation for Transport**

Leak testing of the fuel rods (primary containment) is performed during the manufacturing process. Verification of successful leak testing is done prior to shipment. There are no surface

temperature measurements required for this package. The following steps may be performed in any sequence.

1. Complete the necessary shipping papers in accordance with Subpart C of 49 CFR 172.
2. Ensure that the RAJ-II package markings are in accordance with 10 CFR 71.85(c) and Subpart D of 49 CFR 172. Package labeling shall be in accordance with Subpart E of 49 CFR 172. Package placarding shall be in accordance with Subpart F of 49 CFR 172.
3. Survey the surface of the package for potential contamination and dose rates.
4. Transfer the package to the conveyance and secure using tie-downs secured to the package.

## **7.2 PACKAGE UNLOADING**

This section delineates the procedures for unloading a payload from the RAJ-II packaging. Hereafter, reference to specific RAJ-II packaging drawings may be found in Section 1.3.1.

### **7.2.1 Receipt of Package from Carrier**

In compliance with 10 CFR 20.1906, radiation and contamination surveys are performed upon receipt of the package and the packages are inspected for significant damage. There are no fission gases, coolants or solid contaminants to be removed and no special controls or precautions for handling and unloading.

After freeing the tie downs, the RAJ-II packaging is lifted from the carrier either by fork lift or by the use of lifting slings placed around the package. If lifted by forklift, the forks are placed at the designated lift locations, and the package is lifted. If slings lift the package, a sling is placed under each end of the package at the lifting angles that prevent the sling from sliding. Care should be taken to ensure that the slings are placed in the correct location depending on whether the package is loaded or empty.

### **7.2.2 Removal of Contents**

#### **7.2.2.1 Unloading Fuel Assemblies/Bundles**

1. Remove the outer container lid, the inner container lid, and the inner container from the outer container as described in Sections 7.1.1.1 and 7.1.1.2, using approved methods.
2. Clamp the inner container body to the packing table or up right device, and remove the end lid.
3. Stand the packaging table upright.
4. Attach the lifting device to the assembly/bundle and remove the securing fixture.
5. Lift one fuel assembly/bundle at a time from the package.
6. Repeat for the other assembly/bundle.

#### **7.2.2.2 Unloading Fuel Rods**

1. Remove the outer container lid, the inner container lid, and the inner container from the outer container as described in Sections 7.1.1.1 and 7.1.1.2, using approved methods.

2. The inner container may be removed from or remain in the outer container for removal of the rod container (protective case or pipe) or loose fuel rods.
3. Remove the rod container, if used, with approved methods.
4. Open the rod container if used to transport fuel rods.
5. Remove the fuel rods from the rod container or the inner container, unclamping banded fuel rods if applicable, per approved methods.

### **7.3 PREPARATION OF EMPTY PACKAGE FOR TRANSPORT**

Empty RAJ-II packages shall be prepared and transported per the requirements of 49 CFR 173.428. Prior to shipping as an empty RAJ-II, the packaging shall be surveyed to assure that contamination levels are less than the 49 CFR 173.433(a) limit. The RAJ-II shall be visually verified as being empty of radioactive contents. The packaging is inspected to assure that it is in an unimpaired condition and is securely closed so that there shall be no leakage of material under conditions normally incident to transportation.

Any labels previously applied in conformance with Subpart E of Part 172 are removed, obliterated, or covered and the “Empty” label prescribed in 49 CFR 172.450 is affixed to the packaging.

### **7.4 OTHER OPERATIONS**

Not applicable. There are no provisions for any special operational controls (e.g., route, weather, shipping time restrictions).

### **7.5 APPENDIX**

No additional information is required. Loading and unloading this package is a relatively simple and routine operation. The weights, contamination levels and radiation dose rates do not impose significant hazards or operations outside normal material handling.

## **8.0 ACCEPTANCE TESTS AND MAINTENANCE PROGRAM**

### **8.1 ACCEPTANCE TESTS**

Per the requirements of Subpart G of 10 CFR 71, this section discusses the inspections and tests to be performed prior to first use of the RAJ-II. The RAJ-II is manufactured under a Quality Assurance (QA) program meeting the requirements of 10 CFR 71 Subpart H.

#### **8.1.1 Visual Inspections and Measurements**

Prior to the first use of the RAJ-II for the shipment of licensed material, the RAJ-II shall be inspected to ensure that it is conspicuously and durably marked with its model number, serial number, gross weight and package identification number assigned by the NRC. Prior to applying the model number, it shall be determined that the RAJ-II was fabricated in accordance with the drawings referenced in the Nuclear Regulatory Commission (NRC) Certificate of Compliance.

General dimensions are shown on the drawings in Section 1.3.1. Data for these dimensions is recorded and verified in accordance with the QA program. Documentation of these measurements is compiled in a data pack. This data pack shall be checked for completeness for each RAJ-II as part of the acceptance program. Dimensions without tolerances may vary to ensure form, function and fit by the fabricator.

The RAJ-II is inspected to ensure that there are no missing parts (e.g., nuts, bolts, gaskets, plugs) or components, and that there is no shipping damage on receipt.

#### **8.1.2 Weld Examinations**

RAJ-II packaging materials of construction and welds shall be examined in accordance with requirements delineated on the drawings in Section 1.3.1, per the requirements of 10 CFR 71.85(a), and as defined in the manufacturing QA program.

The non-destructive examination personnel qualification and certification shall be in accordance with either American Society for Non-destructive Testing (ASNT) SNT-TC-1A, (recommended practice) or Japanese Society for Non-destructive Inspection (JSND) Japanese Industrial Standard (JIS) JIS Z 2305 latest revision (References 8-1 and 8-2, respectively).

#### **8.1.3 Structural and Pressure Tests**

The RAJ-II is not pressurized and is structurally the same as the test units. There are no additional structural or pressure tests required to comply with NRC regulations.

#### **8.1.4 Leakage Tests**

No leak tests of the packaging are required. The fuel rod weld joints are examined at the time of fuel fabrication and leak tested to ensure they are sealed. The welding and leak testing of fuel rods is performed during manufacturing using a qualified process. This process assures that the fuel is acceptable for use in a nuclear reactor core and is tightly controlled. The acceptable leak rate is less than  $1 \times 10^{-7}$  atm-cc/s. The inner and outer container are not relied on for containment, and do not require leak testing.

#### **8.1.5 Component and Material Tests**

The RAJ-II packaging does not contain gaskets that perform a safety function or pressure boundary, and as such, do not require testing. Neither the inner nor outer container lids are required to provide an air or water tight seal.

The packaging does not contain neutron absorbers that would require testing. Material testing or certification of Category A and B items for this container, as defined by NUREG/CR-6407 (Reference 8-3), shall demonstrate compliance to the properties found in Tables 2-2 and 2-3, and Section 1.3.1 licensing drawings, or to other properties that satisfactorily indicate compliance to the properties found in these tables and that are approved by the licensee.

#### **8.1.6 Shielding Tests**

The RAJ-II packaging does not contain shielding and therefore shielding tests are not required.

#### **8.1.7 Thermal Tests**

The alumina silicate thermal properties shall be assured by procuring this material with a certified pedigree that demonstrates compliance to the properties in Table 3-1. This procurement is done consistent with the QA program.

#### **8.1.8 Miscellaneous Tests**

There are no additional or miscellaneous tests required prior to the use of the RAJ-II packaging.

## **8.2 MAINTENANCE PROGRAM**

### **8.2.1 Structural and Pressure Tests**

Prior to each use of the RAJ-II, the packaging is visually inspected to assure that the packaging is not damaged and that the components are in place. The packaging is constructed primarily from stainless steel making it corrosion resistant. Because the packaging is not relied on for containment, there are no pressure test requirements for the inner or outer containers that comprise the packaging. Each fuel rod is leak checked and the results of the test are checked before shipment.

The RAJ-II packaging is maintained consistent with a 10 CFR 71 Subpart H QA program. Packaging that does not conform to the licensing drawings is removed from service until it is brought back into compliance. Repairs are performed in accordance with the approved procedures and consistent with the QA program.

### **8.2.2 Leakage Tests**

Containment is provided by the fuel rod. Each fuel rod is leak tested to assure it is either leak tight in compliance with American National Standards Institute (ANSI) N14.5 (Reference 8-4) or by an accepted alternate method. The leak testing assures each fuel rod has satisfactorily passed the leak rate requirements defined by 10 CFR 71.51. Neither the inner nor the outer container is credited with providing leak protection. Therefore, no leak test of the packaging is required.

### **8.2.3 Component and Material Tests**

There are no prescribed component tests or replacement requirements for the RAJ-II packaging. The packaging does not use neutron absorbers or shielding that would require testing or maintenance. Any replacement for Category A or B components, as defined in NUREG/CR-6407, shall meet the requirements defined in the licensing drawings and in Tables 2-2 and 2-3 by either testing or certification.

When any packaging component deviation is identified for a Category A or B component, the RAJ-II shall be removed from service, and the item(s) shall be identified as non-conforming material and dispositioned in accordance with written procedures under a QA program meeting 10 CFR 71, Subpart H.

### **8.2.4 Thermal Tests**

The alumina silicate thermal material is sealed within the stainless steel plates of the container wall. The packaging is visually inspected prior to use to assure that the alumina silicate is contained. No thermal testing is required.

### **8.2.5 Miscellaneous Tests**

There are no additional or miscellaneous tests required for the use of this packaging. The RAJ-II packaging shall be inspected prior to each use and maintained consistent with the licensing drawings. This inspection shall include examination for cleanliness and dryness, cracks, missing or cracked welds, excessive distortion, dents, bulges, scratches, damage to honeycomb, damage to gaskets, foreign material inside the box (e.g. bolts, washers, loose padding) and any other

NEDO-33869 Revision 11  
Non-Proprietary Information

conditions that may affect the safe use of the package. Questionable conditions shall be referred to a qualified inspector for evaluation and for recommendations concerning use, repair, or condemnation of the package. As noted on the drawings, localized deformation in the shell is permitted up to 25.4 mm, and the lids of both containers need not provide an air tight seal. The packaging is repaired and reworked in accordance with drawings found in Section 1.3.1 and under a QA program meeting 10 CFR 71 Subpart H.

Foam cushioning material shall be inspected prior to use of the packaging and repaired according to approved procedures.

Small dents, tears and rounding of corners on honeycomb materials are acceptable provided the volume of material missing or damaged is less than 10% of the original individual piece.

### **8.3 APPENDIX**

#### **8.3.1 References**

- 8-1 American Society for Non-destructive Testing, “ASNT Recommended Practice for Nondestructive Testing Personnel Qualification and Certification (SNT-TC-IA) and Its Use,” SNT-TC-1A, latest revision.
- 8-2 Japanese Standards Association, “Non-destructive testing – Qualification and certification of NDT Personnel,” JIS Z 2305, latest revision.
- 8-3 Nuclear Regulatory Commission, “Classification of Transportation Packaging and Dry Spent Fuel Storage System Components According to Importance to Safety,” NUREG/CR-6407, February 1996.
- 8-4 American National Standards Institute, “Radioactive Materials – Leakage Tests on Packages for Shipment,” ANSI N14.5 – 1997, February 5, 1998.